Material Applications in Future Automotive Structure. Volume II

Budd Co, Fort Washington, PA Technical Center

Prepared for

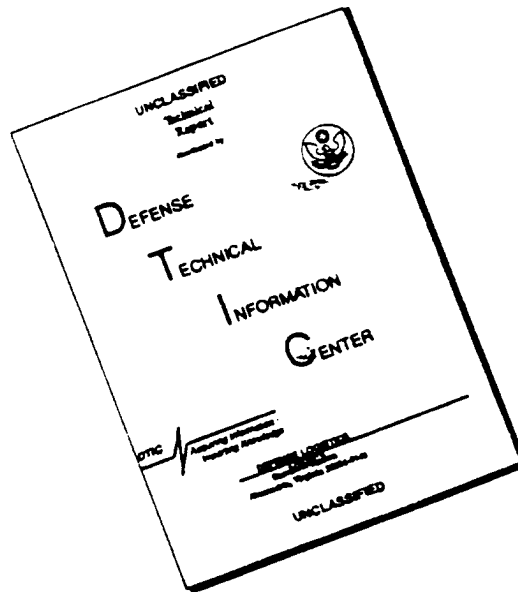National Highway Traffic Safety Administration, Washington, DC

Apr 79

DTIC QUALITY INSPECTED 1

19960313 005

PLASTEC 3181

DISCLAIMER NOTICE

THIS DOCUMENT IS BEST
QUALITY AVAILABLE. THE COPY
FURNISHED TO DTIC CONTAINED
A SIGNIFICANT NUMBER OF
PAGES WHICH DO NOT
REPRODUCE LEGIBLY.

MATERIAL APPLICATIONS IN FUTURE AUTOMOTIVE STRUCTURE
Volume II: Final Report

Herbert A. Jahnle

The Budd Company
Technical Center
375 Commerce Drive
Fort Washington, PA 19034

Contract No. DOT HS-6-01479
Contract Amt. $632,137

April 1979
FINAL REPORT

Prepared For

U.S. DEPARTMENT OF TRANSPORTATION
National Highway Traffic Safety Administration
Washington, D.C. 20590

1. Report No.	2. Government Accession No.	3. Recipient's Catalog No.
DOT HS 805 065		PB80-124845

4. Title and Subtitle	5. Report Date
MATERIAL APPLICATIONS IN FUTURE AUTOMOTIVE STRUCTURE Volume II: Final Report	April 1979
	6. Performing Organization Code

7. Author(s)	8. Performing Organization Report No.
Herbert A. Jahnle	TCR-0385

9. Performing Organization Name and Address	10. Work Unit No. (TRAIS)
The Budd Company Technical Center 375 Commerce Drive Fort Washington, PA 19034	11. Contract or Grant No. DOT-HS-6-01479

12. Sponsoring Agency Name and Address	13. Type of Report and Period Covered
Department of Transportation National Highway Traffic Safety Admin. 400 - 7th Street, S.W. Washington, D.C. 20590	Final Report 10/76-5/79
	14. Sponsoring Agency Code

15. Supplementary Notes

16. Abstract

Candidate materials which might be used in future automotive structure were selected. These included steels, aluminum alloys plastics and fiber reinforced composites. General materials property data, availability, manufacturability, cost and their effects on crashworthiness, durability and non damageability were evaluated. Three vehicle structures; body on frame, unibody and unibody van were investigated with the possible use of the candidate materials in mind. Finite element analysis and mass-spring modeling of the vehicle structures were completed to determine limits and boundaries of materials application. The existing structure with appropriate sectional properties were obtained from current production vehicles. New concepts were suggested using the candidate materials in several forms. Advantages, disadvantages, manufacturing costs and the general complexity of alternate applications were reviewed. Suggested typical weight savings which might evolve through the use of these materials were presented.

17. Key Words	18. Distribution Statement
Alternate materials, crashworthiness, durability, design and concepts, non damageability, weight reductions, cost, material availability, manufacturing, HSLA steels, aluminum alloys, composites.	Document is available through the National Technical Information Service. Springfield, Virginia 22161

19. Security Classif. (of this report)	20. Security Classif. (of this page)	22. Price
Unclassified	Unclassified	H22H01

Form DOT F 1700.7 (8-72)   Reproduction of completed page authorized

i

METRIC CONVERSION FACTORS

Approximate Conversions to Metric Measures

Symbol	When You Know	Multiply by	To Find	Symbol
		LENGTH		
in	inches	*2.5	centimeters	cm
ft	feet	30	centimeters	cm
yd	yards	0.9	meters	m
mi	miles	1.6	kilometers	km
		AREA		
in²	square inches	6.5	square centimeters	cm²
ft²	square feet	0.09	square meters	m²
yd²	square yards	0.8	square meters	m²
mi²	square miles	2.6	square kilometers	km²
	acres	0.4	hectares	ha
		MASS (weight)		
oz	ounces	28	grams	g
lb	pounds	0.45	kilograms	kg
	short tons (2000 lb)	0.9	tonnes	t
		VOLUME		
tsp	teaspoons	5	milliliters	ml
Tbsp	tablespoons	15	milliliters	ml
fl oz	fluid ounces	30	milliliters	ml
c	cups	0.24	liters	l
pt	pints	0.47	liters	l
qt	quarts	0.95	liters	l
gal	gallons	3.8	liters	l
ft³	cubic feet	0.03	cubic meters	m³
yd³	cubic yards	0.76	cubic meters	m³
		TEMPERATURE (exact)		
°F	Fahrenheit temperature	5/9 (after subtracting 32)	Celsius temperature	°C

*1 in = 2.54 (exactly). For other exact conversions and more detailed tables, see NBS Misc. Publ. 286, Units of Weights and Measures. Price $2.25, SD Catalog No. C13.10:286.

Approximate Conversions from Metric Measures

Symbol	When You Know	Multiply by	To Find	Symbol
		LENGTH		
mm	millimeters	0.04	inches	in
cm	centimeters	0.4	inches	in
m	meters	3.3	feet	ft
m	meters	1.1	yards	yd
km	kilometers	0.6	miles	mi
		AREA		
cm²	square centimeters	0.16	square inches	in²
m²	square meters	1.2	square yards	yd²
km²	square kilometers	0.4	square miles	mi²
ha	hectares (10,000 m²)	2.5	acres	
		MASS (weight)		
g	grams	0.035	ounces	oz
kg	kilograms	2.2	pounds	lb
t	tonnes (1000 kg)	1.1	short tons	
		VOLUME		
ml	milliliters	0.03	fluid ounces	fl oz
l	liters	2.1	pints	pt
l	liters	1.06	quarts	qt
l	liters	0.26	gallons	gal
m³	cubic meters	35	cubic feet	ft³
m³	cubic meters	1.3	cubic yards	yd³
		TEMPERATURE (exact)		
°C	Celsius temperature	9/5 (then add 32)	Fahrenheit temperature	°F

°F -40   0   32   80   98.6   120   160   200   212 °F
°C -40   -20   0   20   37   40   60   80   100 °C

PREFACE

Table of Contents

Preceding page blank

Table of Contents (Cont.)

Table of Contents (Cont.)

List of Figures

List of Figures (Cont.)

List of Tables

List of Tables (Cont.)

REFERENCES

1. A Second Iron Age Ahead?, Brian J. Skinner, _American Scientist_, Vol. 64, May-June, 1976.

2. _Americas Energy_, Dr. Ralph E. Lapp, Reddy Communications, Inc., Greenwich, Ct. 1976.

3. _Automotive Engineering_, SAE, Page 7, Vol. 84, Nov. 10, 1976.

4. _Automotive News, Market Data Book 1976_, Detroit, April 28, 1976.

5. _Automotive Engineering_, SAE, Page 44, Vol. 84, Nov. 12, 1976.

6. "An Assessment of Alternative Economic Stockpiling Policies", United States Congress, Office of Technology Assessment, Aug. 1976.

7. _Materials Engineering_, July, 1975, Page 45.

8. _Materials Engineering_, June, 1976, Page 26.

9. Data on Aluminum Alloy Properties and Characteristics for Automotive Applications, T9, The Aluminum Association, December, 1974.

10. Metals Handbook, Vol. 1, Properties and Selection of Metals, 8th edition, American Society for Metals.

11. 3M Company, Technical Data Bulletins, SP-250 and SP-313.

12. Hercules, Incorporated; Sales Literature.

13. DuPont de Nemours Co., Inc.; Sales Literature.

14. Military Handbook - 17A, Plastic for Aerospace Vehicles, Part 1, Reinforced Plastics, Department of Defense, Washington, D.C., January, 1971.

15. Budd Co., Technical Sales Literature (DSM 710, G-759).

16. PPG Industries, Sales Literature.

17. Carbon Fibers Add Muscle to Plastics, _Machine Design_, 2-7-74.

18. _Fortified Polymers_, Liquid Nitrogen Processing Corporation, Sales Literature.

Preceding page blank

REFERENCES (Cont.)

19. Technical Division, Automotive Market, Aluminum Company
       of America.

20. Materials Selector 77, Vol. 84, No. 6, Reinhold Publishing
       Company.

21. Amoco Chemicals Corporation 2626.

22. G.R.T.L. Company, AZDEL P-100 Stampable Sheet.

23. Materials Engineering, July, 1974, Page 26.

24. Metals – An Endangered Species?, J.K. Tien, R.M. Arona,
       R.W. Clark, Journal of Metals, December, 1976, Page 26.

25. Earth Resources, Brian J. Skinner, Prentice-Hall, Inc., 1976.

26. Metals Progress, September, 1974, Page 7.

27. Classification of Structures – Present Auto, G.L. McCafferty,
       J.M. Herring, Final Report PR 396, DOT-HS-257-2-514,
       May, 1973.

28. Iron Age, March 29, 1976, Page MP-9.

29. A Review of the Magnesium Situation in the Western Hemisphere,
       Joe Chapman, Light Metal Age, August, 1976, Page 16.

30. Glass Materials: 1974 – 1980, Richard F. Sperring, SAE 750344.

31. Handbook of Fiberglass and Advanced Plastics Composites,
       George Lubin, Van Nostran Reinhold Company, 1969.

32. Glass, Its Industrial Applications, Charles John Phillips,
       Reinhold Publishing Corporation, 1960.

33. Minerals Yearbook, 1973, Volume 1, Bureau of Mines NTIS
       PB-253655.

34. How Much Energy is Needed to Produce an Automobile?, J. G.
       McGowan, R. H. Kirchoff, Automotive Engineering,
       Vol. 80, No. 7, July, 1972.

35. Weight Saving Approaches through the Use of Fiber Glass –
       Reinforced Plastic, Eldon D. Trueman, SAE 750155.

36. Critical Point, Allen G. Gray, Metals Progress, October,
       1976, Page 29.

REFERENCES (Cont.)

37. What's Being Done About Steel Availability, Harry Chandler, Metals Progress, October, 1976, Page 37.

38. Father Hogan: Steel 1976 - 80, Metal Progress, October, 1976, Page 33.

39. ASM Seminar - Materials Availability, October 1976.

40. A Healthy Year for Aluminum, Cornell Maier, Light Metal Age, April, 1976, Page 14.

41. Coming: More Aluminum Sheet From Alcan, Fred L. Church, Modern Metals, April, 1976, Page 47.

42. Plastiscope 1, Modern Plastics, December, 1976, Page 10.

43. The Present and Future Demand - Supply Outlook for Thermosetting Plastics and a Forecast of Pricing Trends, Charles S. Stryker, Materials Show and Conference, ASM, Cleveland, Ohio, October 28, 1976.

44. General and Special Purposes Synthetic Elastomer Availability in the U.S.A., Cyrus L. Blackfan, Materials Show and Conference, ASM, Cleveland, Ohio, October 28, 1976.

45. Polypropylene: For Material Planners a Bright Price - Supply Outlook, Plastic World, August, 1976, Page 26.

46. Engineering Resins, Remarks, Roy W. McLeese, Second National Conference on Materials Availability, Cleveland, Ohio, October 28, 1976.

47. The Supply/Demand Outlook for Styrene Based Plastics, Second National Conference on Materials Availability, Cleveland, Ohio, October 28, 1976.

48. Materials Availability - Olifinics, J. J. Coughlan, Second National Conference on Materials Availability, Cleveland, Ohio, October 28, 1976.

49. Energy Use Patterns in Metallurgical and Non Metallic Mineral Processing, Battelle Columbus Laboratories, Prepared for Bureau of Mines, NTIS PB-245 759, June 27, 1975.

50. Energy Use Patterns in Metallurgical and Non Metallic Mineral Processing, Battelle Columbus Laboratories, Prepared for Bureau of Mines, NTIS PB-246 357, September 16, 1975.

51. Production Energies for Selected Feedstocks, Christopher Hill and Larry Teasley.

52. Energy Requirements for Environmental Control In the Iron and Steel Industry, Resource Planning Associates, Inc. for the U. S. Department of Commerce NTIS PB-249-960.

53. The Making, Shaping and Treating of Steel, United States Steel 1957, Page 308.

54. Facts and Figures of the Plastics Industry; The Society of the Plastics Industry, Inc., September 1976.

55. Oil and Gas Resources, Reserves and Productive Capacities, Federal Energy Administration, U. S. Department of Commerce, Vol. 1, October 1975, NTIS PB 246354.

56. Oil Picture Worse Than Three Years Ago, William P. Smith, New York Times Service, The Evening Bulletin, October 18, 1976.

57. How to Take on OPEC, Christopher D. Stone and Jack McNamara, The New York Times Magazine, December 12, 1976.

58. CBS News Almanac 1977, Hammond Almanac, Inc., 1976.

59. Review of Secondary and Tertiary Recovery of Crude Oil; Levin and Associates, Inc., Prepared for the Federal Energy Administration, June 1975 (NTIS PB-244970).

60. Statement on ERDA's R & D Program in Oil Shale, Dr. Phillip White for sub-committee on Minerals, Materials and Fuels, Senate Committee on Interior and Insular Affairs, 11/30/76.

61. Americas Energy, Dr. Ralph E. Lapp, Reddy Communications, Inc., 1976.

62. Energy Statistics, Annual Report, U. S. Department of Transportation, DOT-TSC-OST-76-30.

63. Bethlehem Steel, F. Laxar, E. Stephenson, J. Ferrigan, N. Griffing, L. Field and J. Omdahl.

64. Metals Handbook, ASM, 1948 Edition.

65. Impacts of Material Substitution in Automobile Manufacture on Resources Recovery, Volume 1, Results and Summary.

66. "Plastics v.s. Metal" Which as the Edge on the '80's? Auto Products, June 1975.

REFERENCES (Cont.)

67. SPI, "The Plastics Industry in Year 2000", April 1973.

68.   DuPont Study, May 1976.

69.   Letter from Mobay Chemical.

70.   Data from Shell Co.

71. Guha, Probirk, "Production Energy Determination of FRP
        Systems", PS-114, January 21, 1977.

72. Solving the Junk Vehicle Problem: A Guide for Program
        Development, CONSAD Research Corporation for the Motor
        Vehicle Manufacturers Association, July 31, 1975, NTIS-
        PB-255704.

73. Impacts of Material Substitution in Automobile Manufacture on
        Resource Recovery, Volume 1. Results and Summary, 1, R
        and T, prepared for Environmental Protection Agency,
        July 1976, NTIS- PB-257242.

74. Studies on Upgrading of Automotive Scrap by Vacuum Melting and
        Electroslag Remelting, Carlson, Schmidt, McCluskey, Owen,
        Hichtenberg and Shaw, Proceedings of the Fourth Mineral
        Waste Utilization Symposium, Chicago, Illinois, May 7-8,
        1974.

75. Resource Recovery and Waste Reduction, Third Report to Congress,
        Environmental Protection Agency, 1975, NTIS-PB-255141.

76. Aluminum Company of America, E. Gieselmann, Communication.

77. Modern Plastics, September 1975, Page 78.

78. Utilization of Municipal Refuse for Recovery of Energy and
        Other Resources, Earl K. Dille, IEEE.

79. The International Plastics Selector 1977, Cordura Publications,
        Inc., 1977.

80. J. Epel, Budd Company Plastics Research Center, Communication.

81. E. Gieselmann, Aluminum Company of America.

82. Calculated from data, Reed TES Save Your Barrells of Energy,
        Plastics Design and Processing, October 1974, Page 4.

83. Subcompact Automobile Crashworthiness Program, Minicars, Inc.,
        Department of Transportation, DOT-HS-113-3-746.

REFERENCES (Cont.)

84. A Study of Rigid Polyurethane Foam, Vito A. Grasso, Department of Transportation DOT-HS-5-01261, September, 1976.

85. Research Safety Vehicle Study, Minicars, Inc., The Budd Company, Department of Transportation DOT-HS-7-01552.

86. Feasibility Study of Plastic Automotive Structure, Herbert A. Jahnle, Department of Transportation DOT-HS-4-00929, NTIS-PB 248354, September, 1975.

87. Dent Resistance of Cold Rolled Low Carbon Steel Sheet, T. E. Johnson, Jr. and W. O. Schaffuit, SAE 730528, May 14-18, 1973.

88. Dynamic Denting of Autobody Panels, C. E. Burley, B. A. Niemeier and G. P. Koch, SAE 760165, February 23-27, 1976.

89. Denting Properties of Aluminum Autobody Components, C. E. Burley and B. A. Niemeier, SAE 770199, February 28, March 4, 1977.

90. J. W. Clark, Alcoa Research Laboratories.

91. F. Hull, Budd Company.

92. The Application of Elastomeric Buckling Columns in an Energy Management Bumper System, J. H. Tundermann, G. M. Larson and R. B. Anderson, SAE 750011, February 24-28, 1975.

93. Energy Absorption of High Strength Tubes Under Impact Crush Conditions, R. C. Van Kuren and J. E. Scott, SAE 770213, February 28 - March 4, 1977.

94. High Strain Rate Behavior of Some Hot and Cold Rolled Low Carbon Steels, SAE 760209, Ashok Saxena and David A. Chatfield, February 23 - 27, 1976.

95. Hexagonal Cell Structure Under Post - Buckling Axial Load, R. K. McFarland, Jr., AIAA Journal, Volume I, No. 6, June 1963, Page 1380.

96. The Development of Metal Honey Comb Energy Absorbing Elements, Technical Report No. 32-639, Jet Propulsion Laboratory, California Institute of Technology, July 24, 1964.

REFERENCES (Cont.)

97. Some Factors Affecting the Plastic Deformation of Sheet and
    Strip Steel and Their Relation to Deep Drawings Proper-
    ties, Winlock, J. and Lister, R. W. E., Transactions of
    The American Society for Metals, Vol. 25, 1938.

98. Energy Absorbing Characteristics of Vehicle Body Structure,
    Norimoto Aya and Kunikiro Takahaski, Bulletin of Japan,
    SAE, No. 7, 1976.

99. The Crippling Strength of Compression Elements, George Gerard,
    Journal of the Aeronautical Sciences, January, 1958.

100. Computer Simulation of Vehicle-to-Barrier Impact – A User's
     Guide, K. Lin, J. Augustitus and M. Kamal, GMR – 1943.

101. Lightweight Subcompact Vehicle Side Structure Program, Michael
     J. Pavlick, DOT-HS-7-01588.

102. Crashworthiness Report – Near Term Electric Vehicle, G. P.
     McCafferty, Budd Co. TCR-0440-1, Prepared for AiResearch
     Manufacturing Co., ERDA Contract EY-76-C-03-1213.

103. An Overall Design Approach to Improving Passenger Car Fuel
     Economy, Edward K. Harison, SAE 780132.

104. Should We Have A New Engine?: An Automobile Power Systems
     Evaluation, R. Rhoads Stevenson, August 1975,
     JPL SP 43-17 Library of Congress.

1.0 INTRODUCTION

The early 1970's has witnessed an intensified interest in materials and energy conservation. A number of recent social and economic factors have stimulated many studies by industry, institutions and the Federal Government. Conclusions reached, based on these studies, generally agree that there are serious shortages of some materials and energy sources and there will be associated high cost penalties in the future.

Metals can be classified as geochemically abundant or geochemically scarce.[1] These have been listed in Table 1 with the weight percent of each in the continental crust. The geochemically abundant materials are present either in localized concentrations or distributed in sufficient quantity in most rocks such that they can be concentrated for smelting. As the grade or weight percent of a metal in the rock decreases the energy required for concentration of the mineral increases. Naturally the richer, more readily recoverable deposits will be, or have been, consumed first.

Geochemically scarce materials are also available in concentrated ore deposits and dispersed in the rock crust. However, the concentration in the crust is so low that a much greater quantity of energy is needed to beneficiate these minerals to a useable form.

The energy used to recover a unit mass of a geochemically scarce and a geochemically abundant metal have been plotted schematically in Figure 1. This plot shows how the energy requirements continue to increase as the mineral concentration decreases. The discontinuity in the curve for the geochemically scarce metals is expected to occur at the end of the 20th century.[1]

Shifts in importing and exporting occur within each country as the rich ore deposits are found and depleted. The United States at present has, for example, considerable deposits of iron and aluminum. Iron and aluminum ores are imported however, because the cost of transporting and refining the imported ore is less than the cost of concentrating and refining American ore. As seen in Table 2, the United States currently imports 90% of its aluminum ore, bauxite, and 30% of its iron ore.

The major sources of energy used in the United States have been historically: wood, hydropower, coal, petroleum and natural gas. Unlike metals which can be reclaimed or recycled, once a fuel is consumed to produce heat or electricity it is gone forever. The rate of energy consumption increases yearly with increase in population and Gross National Product.

In the United States the rate of petroleum discovery has not been keeping up with the rate of consumption. This has necessitated an increasing dependence on foreign imports, Table 2. The United States production of petroleum liquids from 1920 to the present and

1

TABLE 1:   METALLIC ELEMENTS IN CONTINENTAL CRUST

Geochemically Abundant Elements	Weight Percent
Silicon	27.20
Aluminum	8.00
Iron	5.80
Calcium	5.06
Magnesium	2.77
Sodium	2.32
Potassium	1.68
Titanium	0.86
Manganese	0.10

Geochemically Scarce	Weight Percent
Copper	0.0058
Gold	0.0000002
Lead	0.0010
Mercury	0.0000002
Molybdenum	0.00012
Nickel	0.0072
Niobium	0.0020
Platinum	0.0000005
Silver	0.0000008
Tantatum	0.00024
Thorium	0.00058
Tin	0.00015
Tungsten	0.00010
Uranium	0.00016

Reference: 1

FIGURE 1   ENERGY USED TO RECOVER METALS

ENERGY USED / UNIT MASS RECOVERED →

METALS TRAPPED BY ATOMIC SUBSTITUTION

GEOCHEMICALLY
SCARCE METALS

METALS CONCENTRATED IN
SEPARATE ORE MINERALS

GEOCHEMICALLY
ABUNDANT METALS

GRADE (%) →
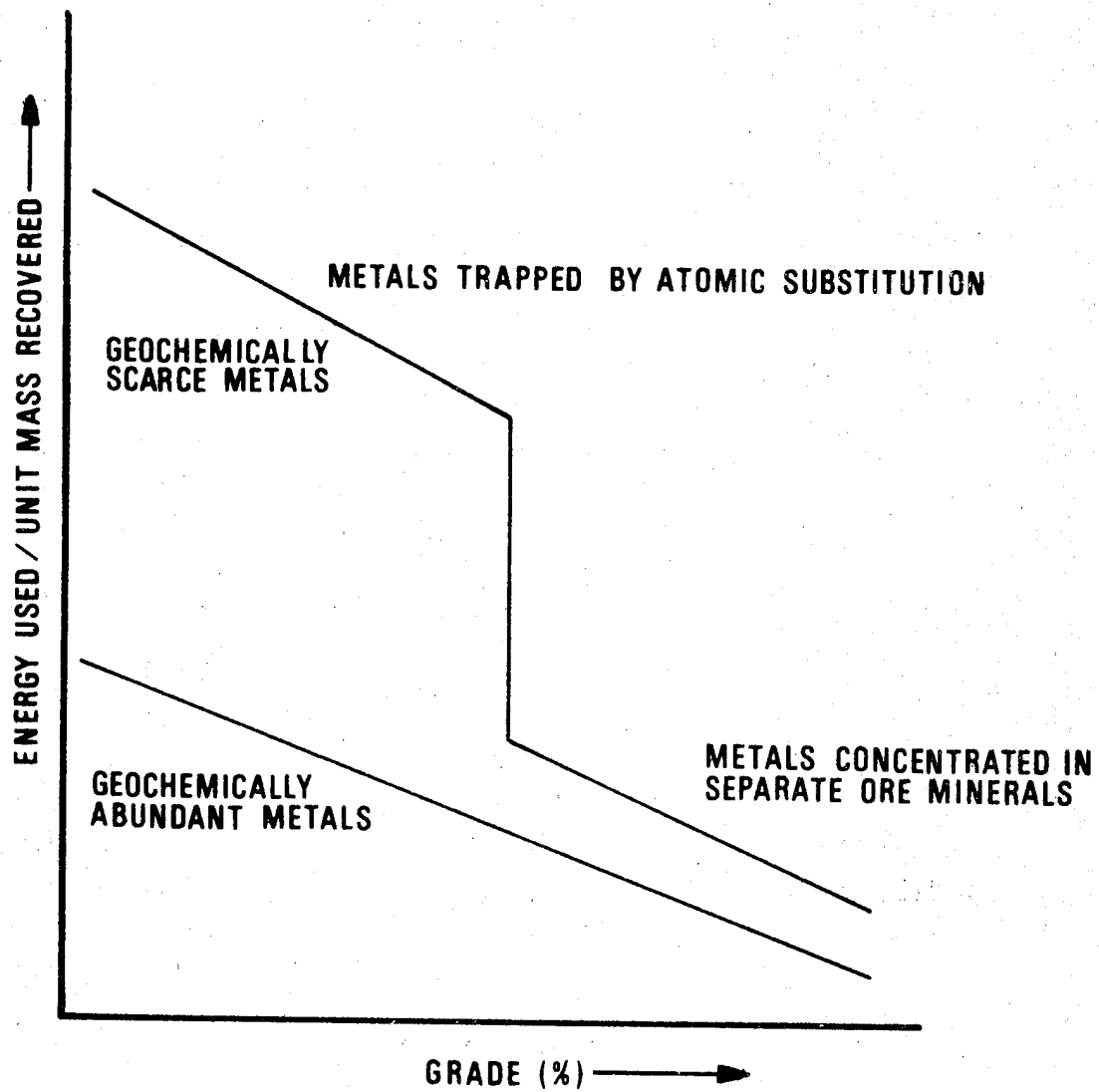
TABLE 2: U.S. IMPORT DEPENDENCE FOR SELECTED MATERIALS

MATERIAL	% IMPORTED	MAJOR IMPORT SOURCE
Chromite	100	U.S.S.R., South Africa, Turkey, Rhodesia
Bauxite	90	Jamaica, Surinam
Manganese	100	Brazil, Gabon, Australia
Rubber, Material	100	Indonesia, Malaysia
Petroleum	38	Venezuela, Canada, Nigeria, Iran
Fluorspar	90	Mexico
Nickel	90	Canada
Iron Ore	30	Canada, Venezuela, Brazil

Data represents conditions through the year 1974.

Reference: 6

projected to the year 2000 is shown in Figure 2. Obviously the dependence on imported petroleum liquids is expected to increase.

Transportation of all types combined, consumes approximately 25% of the total U.S. gross energy as shown for 1973 in Figure 3. Of this 25%, greater than 50% is consumed in the manufacturing and use of automobiles. It is estimated that 4250 Btu per passenger mile is consumed by automobiles based on 1975 data.[2]

The Federal Government requires that automoble efficiency in 1985 by equal to 27.5 mpg on a fleet average.[3] Using production data of the Ford Motor Company[4] for 1975 the total fleet weight was 6.67×10^9 pounds for 1.8×10^6 vehicles. The average fleet weight was 3705 pounds per vehicle. The EPA combined city-highway mileage rating for each vehicle was multiplied by the number of vehicles, summed and divided by 1.8×10^6 vehicles to obtain an average EPA rating of 21.4 mpg. This average rating was obtained by using the EPA values for manual transmissions for all vehicles where a value was listed. Using a 3705 pound average weight and 21.4 mpg average efficiency the average weight of a vehicle to obtain a 27.5 mpg efficiency was calculated to be 2880 pounds. The greater the percentage of vehicles with automatic transmissions that are sold the lower will be the target fleet average weight for 1985.

Fuel consumption on a vehicle fleet basis has been reviewed by the Federal Government's Energy Resources Council and summarized in "Automotive Engineering".[5] Various innovations were considered including structural weight, engines and drive trains. Using a changing mix of new and old cars a fuel consumption projection for the period of 1976 to 2000 was made, Figure 4. Vehicle weights used for these projections were based on projected vehicle weights shown in Table 3. It was recognized in this assessment that lower levels of occupant protection may result and no consideration was given to increased energy requirements that may be required in the application of new materials of construction to meet the target weights.

With the projected decrease in materials and energy supply (natural gas and petroleum) it appears necessary that the materials for future automobiles will change. The two primary goals should be:

1. Minimize energy consumption
2. Minimize material consumption

Both of these goals could be met by reducing the average vehicle weight. A reduction in weight does not however guarantee a reduction in energy consumed. Each material has an associated energy of recovery and for manufacturing which must be factored into the total energy consumption.

FIGURE 2 U.S. PRODUCTION OF PETROLEUM LIQUIDS
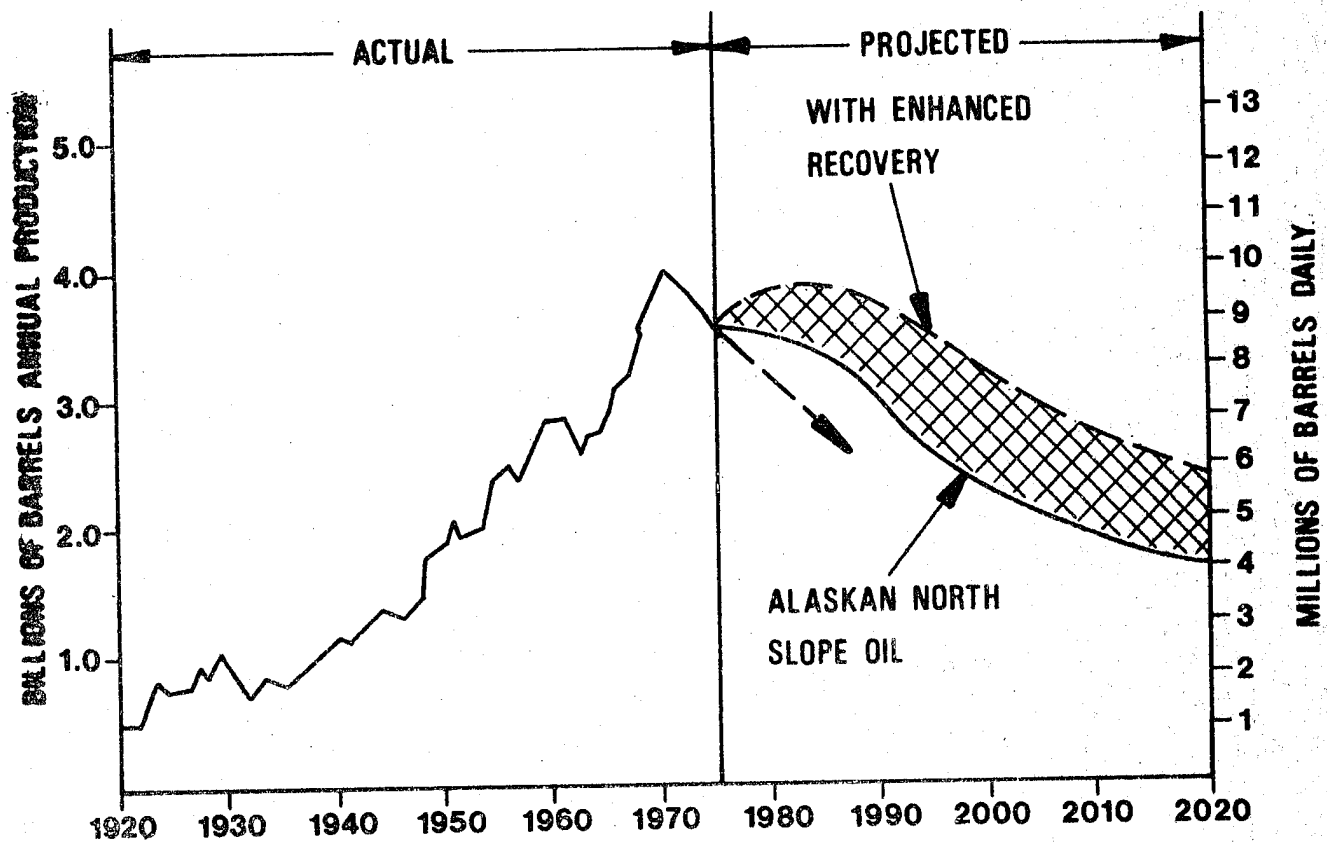
FIGURE 3   U.S. GROSS ENERGY END USES, 1973
(TOTAL GROSS ENERGY USE 74.7 QUADRILLION BTU)

COOLING, ELECTROLYTIC PROCESSES, & OTHER

REFRIGERATION ——

AIR CONDITIONING

FEED STOCKS

WATER HEATING

2% 4%

3%

4%

4%

LIGHTING 5%

TRANSPORTATION 25%

ELECTRIC
DRIVE 8%

SPACE HEATING 18%

DIRECT HEAT
11%

PROCESS STEAM 16%
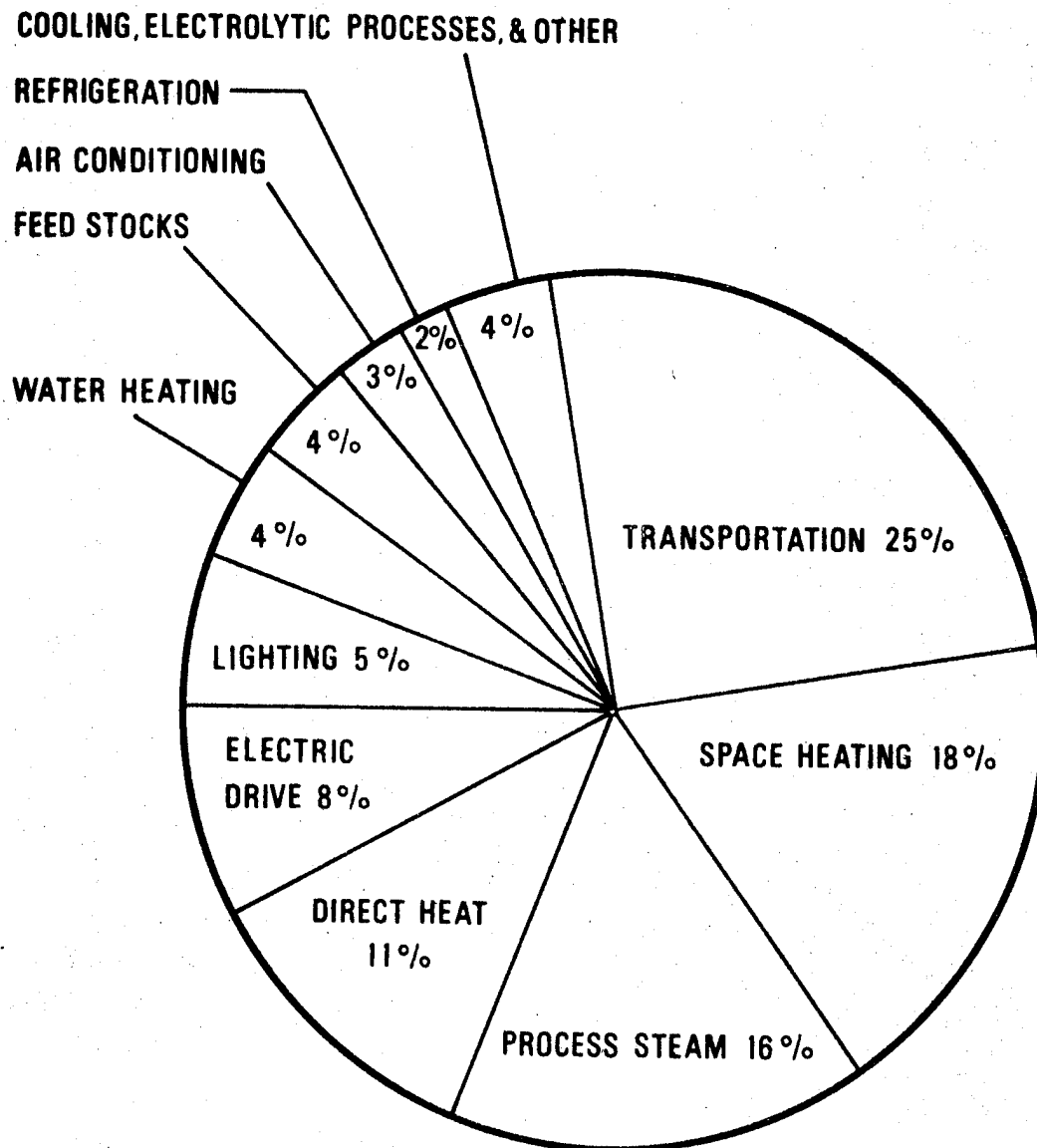
SOURCE: ENERGY PERSPECTIVES, U.S. DEPT. OF THE INTERIOR, FEB., 1975, pg. 33.

FIGURE 4 PROJECTED FUEL CONSUMPTION: AUTOMOBILES
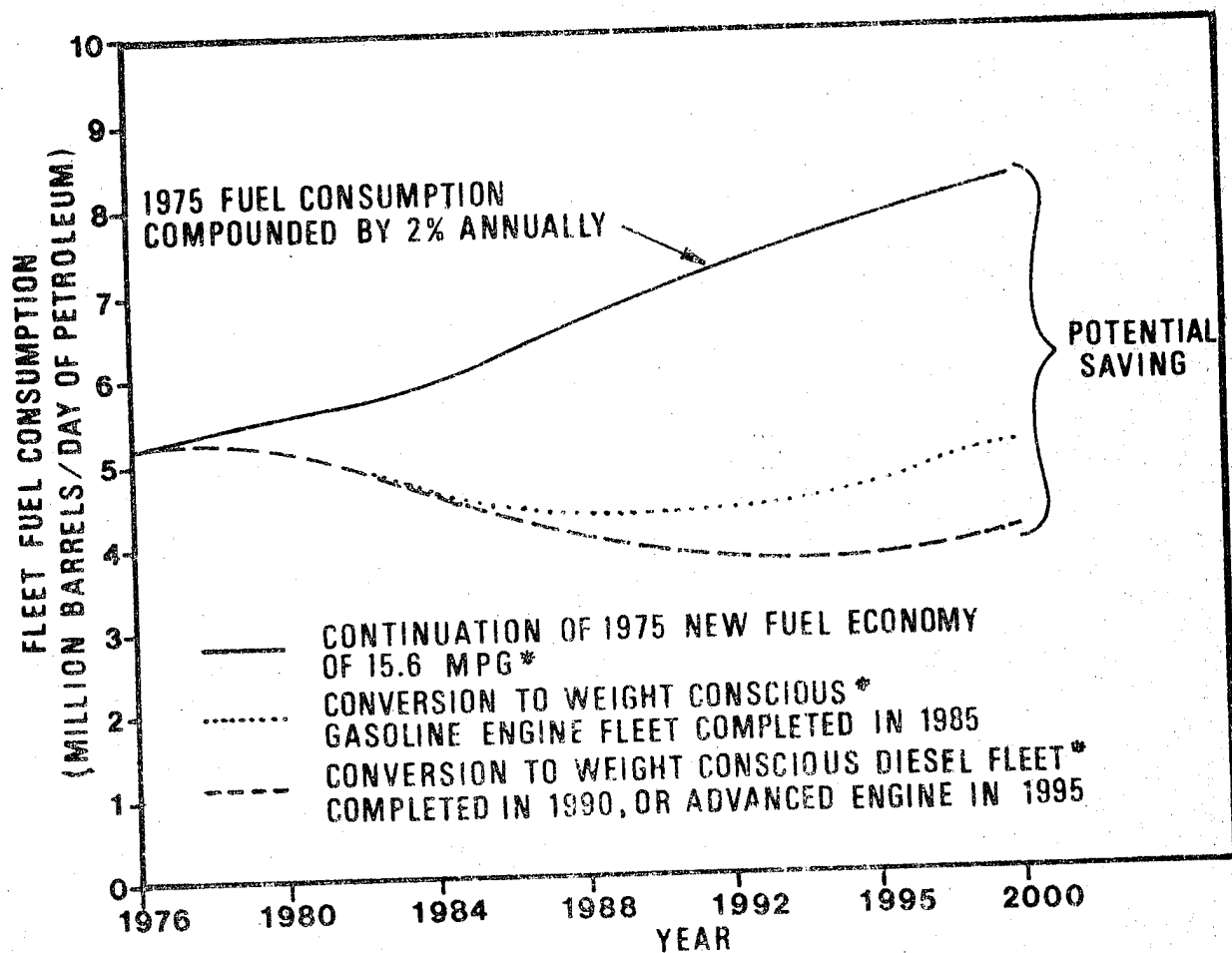
*AT CURRENT SAFETY AND EMISSIONS STANDARDS

REFERENCE: 5

TABLE 3: VEHICLE WEIGHTS PROJECTIONS

PASSENGERS	CURRENT	WEIGHT, LB. WEIGHT CONSCIOUS	INNOVATIVE
4	2500	2100	1900
5	3300	2575*	2275*
6	4300	3175*	2725*

* Basic vehicle without options. Some scenarios added 200 lb. for the five-passengers car, 500 lb. for the six-passenger car.

Reference: 5

9

To achieve the above two goals alternate materials and structural designs must be considered in future automobiles. Materials which show promise include low carbon steel, high strength low alloy steels (HSLA), aluminum alloys, magnesium alloys, reinforced thermoplastics and reinforced thermoset plastics.

The application of any material other than those currently used will require an evaluation of a number of factors which include:

1. Material availability
2. Total energy requirements
3. Disposability
4. Areas of application
5. Crashworthiness and safety

2.0 CANDIDATE MATERIALS

Current automobile structure is designed and fabricated primarily from low carbon steel (AISI 1008-1015). Engines, transmission housing, hubs and brake components are manufactured from cast iron although aluminum alloys have been used successfully for some of these components in limited production vehicles. Trim, upholstery and other non structural parts use zinc alloys and plastics materials.

A large number of relatively new materials have been suggested by materials suppliers for automotive construction. Some of these are available in current vehicles and are being evaluated for more extensive application.

Candidate materials for future automotive structures have been listed in five groups as follows:

1. Ferrous metals
2. Non-Ferrous alloys
3. Reinforced thermoplastics
4. Reinforced thermosets
5. Elastomers

Each of these groups of materials will be evaluated in the following sections to determine the most promising candidate materials for automotive structure.

2.1 Ferrous Metals

Iron based alloys considered for future automotive structure are listed in Table 4 with selected room temperature properties. Low carbon steel (AISI 1008-1015) has been included since it has good strength and stiffness, low cost and considerable experience in automotive construction.

TABLE 4: MATERIALS DATA (70°F.) FERROUS METALS

Material	Ultimate Tensile (KSI x 10^3)	0.2% Yield (KSI x 10^3)	Elastic Modulus (KSI x 10^3)	Endurance Limit (KSI x 10^3)	$\frac{\text{Modulus}}{\text{Density}}$ (in^{-1} x 10^6)	$\frac{\text{0.2\% Yield}}{\text{Density}}$ (in^{-1} x 10^3)	Ref.
1008-1015	45	25	30		105	87	7
945X,SAE	60	45	30		105	157	7
950X,SAE	65	50	30	31	105	175	7
960X,SAE	75	60	30	34	105	210	7
970X,SAE	85	70	30	37	105	245	7
980X,SAE	95	80	30	40	105	280	7

11

Automotive structure is currently fabricated from low carbon steel flat stock. Various grades have been developed through the years which can be press formed into complex shapes. These shapes are in turn joined by resistance spot welding and arc welding. Mechanical fasteners and adhesive bonding are used to a lesser extent during assembly. Highly automated procedures have been developed, extending from the rolling mills through the final paint ovens. Low carbon steel flat stock can be purchased for less than $0.20 per pound and the cost of a final assembly is approximately five times the total material cost.

While low carbon steel has high specific stiffness and excellent ductility, it has a low specific strength and poor corrosion resistance. Specific strength and specific stiffness are defined as the material strength or stiffness divided by the materials density.

High strength low alloy steels (HSLA) have been developed in recent years to be more amenable to automotive manufacturing processes. Metallurgical improvements have resulted in better press formability and improved welding characteristics for these higher strength steels.

The specific stiffness of HSLA steels is the same as for low carbon steel, however the specific strength can be as much as 3.5 times greater. While the greater strength may permit a weight reduction in automotive structure, better corrosion protection is required for the thinner gages of HSLA steels. Their corrosion rate is essentially the same as for low carbon steel, and for a similar corrosion environment a larger percent of load carrying capability is lost. HSLA steels cost more, 1.2 times, than low carbon steel but the greater strength may result in a 30 to 40% weight reduction.

HSLA steels are currently being evaluated as heavy members such as bumpers, brackets, anti-intrusion beams and frames. Further development is required before these materials can be used as thinner gage outer body panels.

Similar to all materials, the strength and stiffness of steels decrease at elevated temperatures and increase at lower than room temperatures. The elevated temperature short time tensile strengths and long time creep rupture strengths of low carbon steel are shown in Figure 5. Short time elevated temperature strengths of representative HSLA steels are also shown. At 400°F there is a 10 to 20% lower strength than at room temperature.

At lower temperatures the strength of steels increase and the low temperature applications are limited by loss in toughness. The toughness of a material is generally measured by a standard impact test and is used in a comparative sense. Toughness of the HSLA steels has been reported[to be excellent at -50°F (20 foot pound, Charpy V).

12

FIGURE 5 ELEVATED TEMPERATURE PROPERTIES OF STEELS.

CARBON STEEL
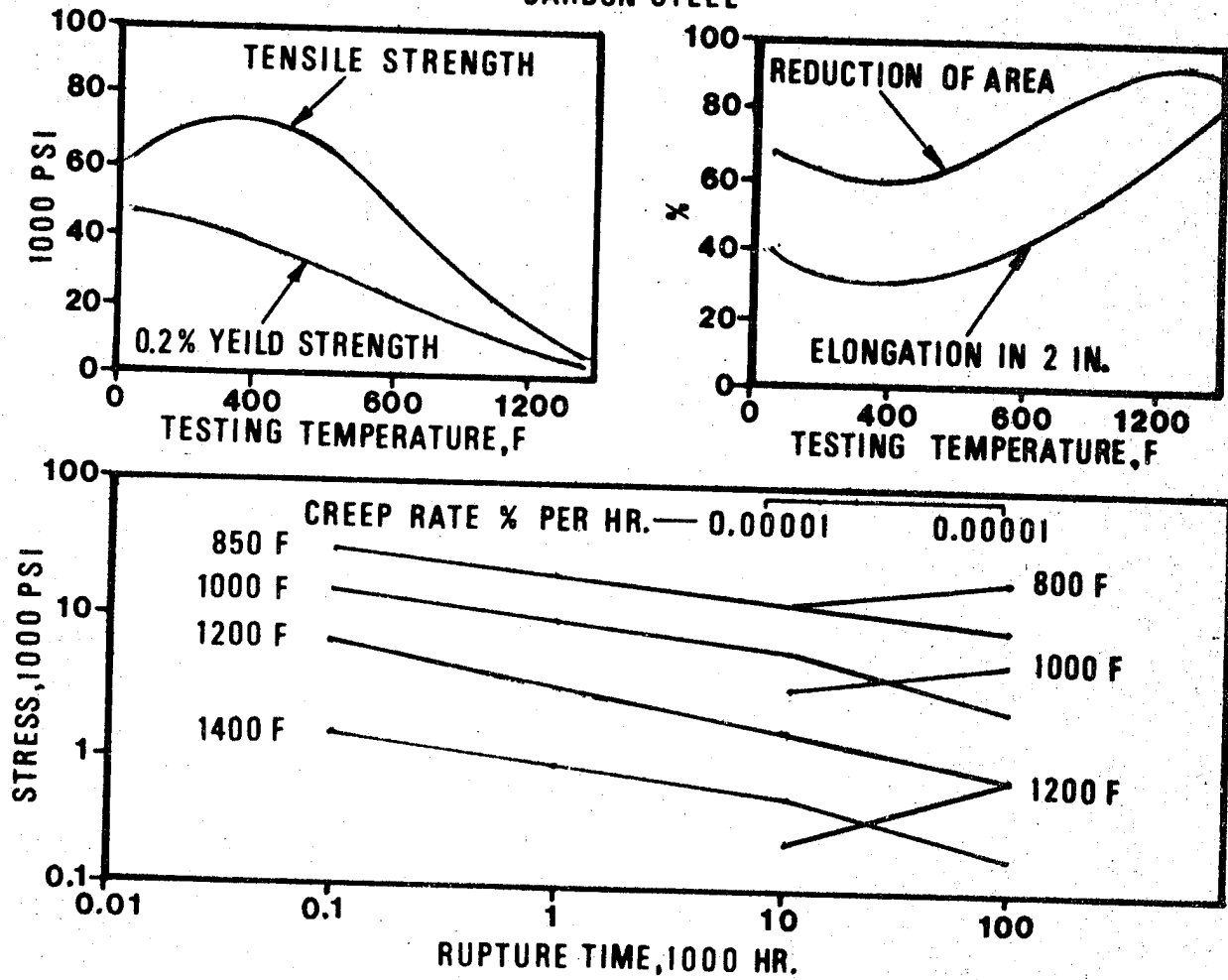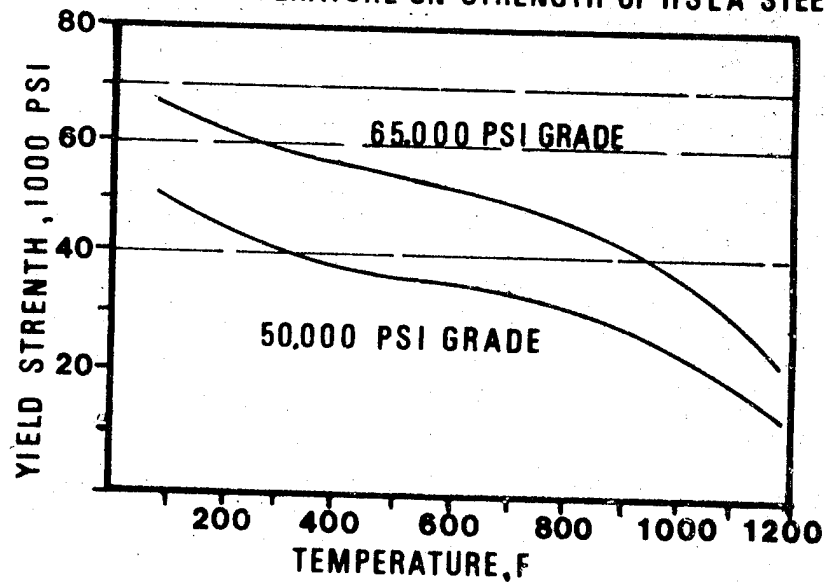
REFERENCE 7 AND 10

Cast irons, ductile irons and compacted graphite cast iron will probably continue to be used in future automobiles for engines, hubs and brake components. Cast irons are produced in cupolas and electric furnaces. Scrap iron, scrap steel and newly refined pig iron are melted and cast in the same plant facility. The cast irons provide a method of recycling ferrous base materials.

While the strength and ductility of cast irons are not particularly good they have been used successfully in engines for many years. As brake friction surfaces cast irons are outstanding. The greatest disadvantage of cast iron is its high density. In such applications as engines the mass of material is not required for strength, but from a casting stand point, the weights cannot be reduced substantially.

Stainless steels such as Type 201 and 430 require substantial quantities of alloying elements such as nickel, chromium and manganese. These steels are considerably more expensive than the low carbon steels and HSLA steels. The outstanding corrosion resistance at room and elevated temperatures of the stainless steels may result in specific applications in exhaust systems in future automobiles.

2.2 Non-Ferrous Alloys

Aluminum and magnesium alloys have received increased interest in recent years for automotive structure. Aluminum alloys have been used to a greater extent in Europe than in the United States. The specific stiffness of these alloys are equal to steel while the specific strength is equal to or greater than even the HSLA steels. Selected properties of candidate alloys are listed in Table 5.

Suppliers of aluminum alloys have developed four new sheet alloys, 2036, 5182, 6009 and 6010 to compete in the automotive market. These four alloys possess improved formability although still not equal to the steels. Resistance spot welding and arc welding can be used for joining but in aluminum these processes are not as acceptable as they are in steels. Mechanical fastening and adhesive bonding provide better joint properties, but they are also more time consuming and more costly than welding.

Aluminum alloys 6061, 7016 and 7046 may be used in heavier sections such as small forgings, extrusions, bumpers, anti-intrusion beams and brackets. A-356 or similar casting alloys may be used in engines, transmission housings and brake components.

Elevated and low temperature properties of the listed aluminum alloys are not readily available. Using the properties of 6061 in the T4 and T6 conditions as a guide, Table 6, the other alloys

TABLE 5: MATERIAL DATA (70°F.) NON-FERROUS METALS

Material	Ultimate Tensile (KSI x 10³)	0.2% Yield (KSI x 10³)	Elastic Modulus (KSI x 10³)	Endurance Limit (KSI x 10³)	$\frac{Modulus}{Density}$ (in⁻¹ x 10⁶)	$\frac{0.2\% \ Yield}{Density}$ (in⁻¹ x 10³)	Ref.
2036-T4	49	28	10.3	18	104	282	9
5182-0	40	19	10.3	20	104	191	9
6009-T4	34	19	10.3		104	191	9
6010-T4	43	27	10.3		104	272	9
6061-T6	45	40	10	14	101	404	9
7016-T5	52	46	10.2		103	464	9
7046-T63	68	55	10.3		104	555	9
A356-T6	33		10.5	8.5	106		10
AZ31B-H24	39	28	6.5	20	100	430	10
AZ63A-T6	40	19	6.5	11	100	292	10
AZ91A-F	33	23	6.5	14	100	353	10
HK31B-T6	32	16	6.5	10	100	246	10

15

TABLE 6: ELEVATED TEMPERATURE PROPERTIES, 6061 ALUMINUM ALLOY

Testing Temp, F.	Tensile Strength, psi	Yield Strength, psi	Elongation, %
	T4 Temper		
75	35,000	21,000	25
300	30,000	21,000	25
400	19,000	15,000	28
500	7,500	5,000	60
600	4,500	2,500	85
700	3,000	2,000	95
	T6 Temper		
75	45,000	40,000	17
300	34,000	31,000	20
400	19,000	15,000	28
500	7,500	5,000	60
600	4,500	2,500	85
700	3,000	2,000	95

Reference: 10

would be expected to lose 10% to 20% of their strength at 300°F and 50% at 400°F. At below room temperature the strengths of these alloys increase with a gradual loss in ductility. They do not suffer the severe loss in toughness that many steels do.

Magnesium alloys suffer from an even poorer formability and weldability than the aluminum alloys. Die castings of alloys such as AZ63A and AZ91A appear to be the most probable mode of magnesium application.

The elevated temperature strengths of AZ63A and HK31A have been listed in Table 7. These data reveal a moderate loss in strength, similar to the aluminum alloys.

2.3 Reinforced Thermoplastics

Reinforced thermoplastics considered for future automotive applications are listed in Table 8. The reinforcements listed are talc, glass fiber and carbon (graphite) fibers. Other reinforcements are available including calcium carbonate, asbestos and mica. The quantity of reinforcement in any plastic can vary appreciably to fit the needs of the final product. Maximum quantities are generally 30 to 40 weight percent and these quantities are used in the listed properties, Table 9.

Thermoplastics, unreinforced and reinforced, are now used in automobiles in such applications as interior trim, upholstery, fender liners, fender extensions, grill opening panels, fan ducts and heater ducting. These parts are made by injection molding and thermoforming. They are in general non-load carrying parts. Assembly is accomplished usually with mechanical fasteners, either metallic or non metallic. Some welding is used for such applications as ducts and batteries. Shapes of greater complexity can be made in a single operation with thermoplastics than can be achieved with metals.

Reinforced thermoplastics, Table 9, have excellent room temperature specific strengths compared to metals, however the specific stiffnesses are considerably lower than for the metals.

The strength properties of plastics are reduced at elevated temperatures and the maximum service temperatures of most thermoplastics are in the 250°F. to 500°F. range. Reinforced grades have higher service temperatures than do the non-reinforced grades. A standard test (ASTM 648) made of most plastics is the heat distortion test at 66 psi or 264 psi. The temperature is determined at which a 0.010" deflection occurs in flexure under either of the above loading conditions. The deflection temperatures of the listed thermoplastics are shown in Table 10.

TABLE 7:   ELEVATED TEMPERATURE PROPERTIES, MAGNESIUM ALLOYS

Testing temperature, F	Tensile strength, psi	Yield strength, psi	Elongation, %
As Cast			
75	28,600	13,700	4.5
150	30,500	....	3.0
200	30,100	....	4.5
250	27,700	....	7.5
300	24,100	....	20.5
400	15,300	....	50.0
500	10,300	....	38.0
Heat Treated			
75	38,800	13,600	10.0
150	36,700	....	9.0
200	34,300	....	7.0
250	30,000	....	9.0
300	22,400	....	33.2
400	14,600	....	38.0
500	10,900	....	26.0
Heat Treated and Aged			
95	38,700	17,700	5.5
200	36,000	17,300	11.0
250	32,400	16,500	11.0
300	24,500	15,000	15.0
400	17,500	12,000	17.0
500	12,000	8,800	15.0
600	8,200	5,600	20.0

Reference: 10

18

TABLE 7: ELEVATED TEMPERATURE PROPERTIES, MAGNESIUM ALLOYS, (Cont.)

Testing temperature, F	Tensile strength, psi	Yield strength, psi	Elongation, %
Sand Cast HK31A-T6 (a)			
75	31,000	16,000	6
400	24,000	14,000	17
500	23,000	13,000	19
600	20,000	12,000	22
700	13,000	8,000	26
Rolled HK31A-H24 (b)			
70 (c)	37,000	29,000	8
300 (c)	26,000	23,000	20
400 (c)	24,000	21,000	21
500	20,000	17,000	19
600	13,000	7,000	70
650	8,000	4,000	100

(a) Properties determined on separately cast test bars.

(b) Properties determined on bars sectioned from 0.040 -in. sheet.

(c) At the temperatures indicated, compressive yield strength, 23,000 psi.

(d) At the temperature indicated, compressive yield strength, 22,000 psi.

Reference: 10

19

TABLE 8: REINFORCED THERMOPLASTICS

Polypropylene   (PP)
Polypropylene - 40% talc (PP-40T)
Polypropylene - 40% glass (PP-40G)
Polypropylene - 40% carbon (PP-40C)
Polypropylene - 40% glass laminate (PP-40GL)

Nylon   (N)
Nylon - 40% glass (N-40G)
Nylon - 40% carbon (N-40C)

Polycarbonate   (PC)
Polycarbonate - 40% glass (PC-40G)

Polyester   (PES)
Polyester - 30% glass (PES-30G)
Polyester - 30% carbon (PES-30C)

Polystyrene   (PS)
Polystyrene - 30% glass (PS-30G)

ABS   (ABS)

Polyethylene   (PE)
Polyethylene - 40% glass (PE-40G)

TABLE 9: MATERIAL DATA (70°F.) REINFORCED THERMOPLASTICS

Material	Ultimate Tensile (PSI x 10³)	Flexural Strength (PSI x 10³)	Elastic Modulus (PSI x 10⁶)	Endurance Limit (PSI x 10³)	$\frac{\text{Modulus}}{\text{Density}}$ (in⁻¹ x 10⁶)	$\frac{\text{0.2\% Yield}}{\text{Density}}$ (in⁻¹ x 10³)	Ref.
PP	5	6.5	0.2		6	198	20
PP-40T	5		0.6		13.7		21
PP-40G	10.5	12.5	1.1	3	25	282	18
PF-40GL	10.7	22	0.8		18.5	609	22
N	11.8	15	0.4		9	362	17
N-40G	31	42	1.5	6	30	792	17
N-40C	40	60	3.4		70	1234	17
PC	9	13	0.4	0.8	18	298	20
PC-40G	23	27	1.6	6	29	490	20
PES	8	12.8	0.34		7	269	20
PES-30G	19.5	28	1.35		24	507	17
PES-30C	20	29	2		37	543	17
PS	7.5	12.5	0.5		13	331	20
PS-40G	15	17.5	1.65	6	33	350	18
PE	4.4		0.13				20
PE-40G	11.5	14	1.1		23	301	18
ABS	5	8	0.25		6	136	20

TABLE 10:   HEAT DISTORTION TEMPERATURES (°F.) THERMOPLASTICS

Material	66 PSI	264 PSI
PP	220	
PP-40G	330	300
PP-40T		270
PP-40GL		310
N	347	167
N-40G	425	420
N-40C		500
PC	280	270
PC-40G	310	295
PES	302	122
PES-30G	420	410
PES-30C		430
PS		190
PS-30G	270	245
ABS		180
ABS-40G	235	225

Reference: 79

In Table 11 are listed the tensile and tensile modulus of glass reinforced polypropylene, (PP-40G) at elevated temperatures. This data shows a greater than 50% loss in strength at 140° F. Similar data for Nylon 6/6 with 30% carbon fibers shows a loss of 40% of the room temperature flexural strength (51,000 psi) at 200° F. (30,000 psi).[17]

Stress relaxation is another method of indicating the creep resistance of a material. It also demonstrates the loss of torque in bolted joints. In Table 12 the stress relaxation of several of the glass reinforced thermoplastics are listed. This data is for room temperature and would be expected to be greater as the test temperature increases.

2.4 Reinforced Thermosets

Thermoset plastics are cross linked polymers formed by a reaction between two or more chemicals into a non-fusible substance. Typical thermosets commercially available are unsaturated polyester, epoxy and phenolic. They can be used as a matrix binder for various reinforcements such as glass fibers, Kevlar [TM], carbon (graphite) fibers and talc. A wide range of properties can be obtained by varying the weight percent of reinforcement. In the case of fibrous reinforcements the length and degree of orientation are also effective in varying the resulting properties.

Reinforced thermoset plastics have the following advantages over steel; lower density, higher specific strengths, the ability to be molded into extremely complex parts, and far superior corrosion resistance. Disadvantages compared to conventional steels include lower production rates, low ductility (toughness) and a lack of use experience in the automotive field in load carrying structure.

Reinforced thermoset plastics using the polyester resins are available in compound form. Components are molded by placing the wet compound in a heated mold and curing for one to three minutes. The molded components are assembled by adhesive bonding, mechanical fasteners, or a combination of these.

Epoxy matrix materials have moderately superior properties to those with a polyester matrix. Epoxies however require longer cure times which may limit their usefulness in a high production industry. The cost of epoxy pre-pregs or molding compounds are high. Those reinforced with unidirectional carbon fibers are over a hundred dollars per pound. It is expected that increased use would reduce the prices considerably.

23

TABLE 11: TENSILE STRENGTH AND TENSILE MODULUS (PP-40G) AT ELEVATED TEMPERATURES.

Temperature	Tensile Strength psi	Tensile Modulus
73	10,500	1.1
120	5,500	0.58
140	4,500	0.47

TABLE 12: STRESS RELAXATION OF THERMOPLASTICS (73°F. - 15 HOURS)

	Applied Stress	% Decrease
PC-40G	15,000 psi	14.7
N-40G	15,000	25
PC-40G	10,000	12
N-40G	10,000	20
PS-40G	10,000	15

Reference: 18

Reinforced thermoset plastics are expected to be applied to a greater extent in future automotive structure. The large weight reductions which are needed to improve gasoline consumption in large size vehicles may require extensive use of these materials.

Thermoset resins are not fusible such as metals and thermoplastics and so are not so readily recycled. Research has been underway in a number of laboratories to develop methods of recovering the material in one or more basic feedstocks. The inability to recycle these materials may limit their usefulness. It has been proposed that vehicles made of such materials may last certain owners for their lifetime. Engines and other worn out compoments could be replaced in a lifetime, non-degradable vehicle.

Selected properties of reinforced polyester and epoxy have been listed in Table 13. These values are only representative of the large number of materials available having a wide range of properties. The specific stiffness and specific strengths of the oriented materials are far superior to the metals when the properties are measured along the direction of the fibers. In most automotive applications the applied loads and resulting stresses are not unidirectional. The biaxial stress state developed requires multioriented composite laminates. The multioriented laminate composite will not show as high a level of superiority over metals.

Carbon fiber reinforced epoxy has excellent fatigue strength, usually above 70% of its flexural strength. Glass fiber reinforced epoxy and polyester do not have as good fatigue properties and can be as low as 10% of the flexural strength. Data has not been found on carbon fiber reinforced polyester composites although testing is reportedly in progress.

The tensile and flexural strengths of the reinforced thermosets decrease at elevated temperatures and increase at lower than room temperature. This increase or decrease can vary considerably depending upon the matrix plastic. Data on glass reinforced epoxy shows as little as a 10% loss in strength at 300°F.[14] to as much as 75% loss.[11] The increase at -65°F. may be 10%.

Similar temperature effects on carbon fiber reinforced epoxy can be obtained. Very good retention can be obtained[11] where there is no loss in modulus and only 5% loss in flexural strength at 350°F, even after 10,000 hours of aging at the test temperature.

Data on the reinforced polyesters is not as easily obtained for high temperature applications. Unconfirmed information indicates good elevated temperature property retention.

TABLE 13: MATERIAL DATA (70°F.) REINFORCED THERMOSETS

Material	Ultimate Tensile (PSI $\times 10^3$)	Flexural Strength (PSI $\times 10^3$)	Elastic Modulus (PSI $\times 10^6$)	Endurance Limit (PSI $\times 10^3$)	$\dfrac{\text{Modulus}}{\text{Density}}$ (in$^{-1} \times 10^6$)	$\dfrac{0.2\%\ \text{Yield}}{\text{Density}}$ (in$^{-1} \times 10^3$)	Ref.
PES-20G	6	15				217	15
PES-30G	12	25	1.5	3.8	22	368	15
PES-65G	30	50	2	6.1	31	786	16
PES-65G (D)	86	158	5.8		91	2486	16
PES-70C (D)		220	19.0		349	4039	80
PES-45K	60	30	3.5		74	638	13
E-62G-(D)	125	170	5.9		89	2575	11
E-60C-(D)	210	240	18	168	318	4240	11
E-60K-(D)	200	90	11	130	220	1800	13

2.5 Elastomers

Elastomers consist of synthetic rubbers, thermosets and thermoplastics. An elastomer is defined as a material which exhibits 100 percent or more elongation and which will return to its initial shape after the load is removed.

There has been interest in recent years to use such materials for energy absorbing front and rear systems for automobiles to meet Federal regulations at a minimum cost and weight penalty. Similarly front and rear fascia panels are gaining popularity in providing a styled vehicle which is less prone to permanent damage.

These materials can be pressure cast using a variety of techniques from injection molding to liquid reaction casting. Since the processing developments in these materials indicate that large area panels can be molded with low force requirements, additional applications such as fenders, quarter panels are being considered. These materials are low strength and they are not being considered as structural materials but rather as damage resistant outer panel material.

Numerous types of elastomers are available with a number of grades for each type. Recently there has been more interest in blends of various elastomers which result in hundreds of grades of elastomers. The major types or families are listed in Table 14. The density, tensile strength, % elongation and 1974 cost per pound are listed. Almost all of these materials can be found in automobiles primarily as seals, gaskets, mounts, hoses, etc.

Of those listed in Table 14 seven have been selected as most probable candidate materials for energy absorbing and damage resistant structural components. These seven are as follows:

> Ethylene Propylene EPDM
> Polyester Urethane AV
> Polyester Urethane EV
> Thermoplastic
>   Rubbers   TPR
>   Polyester
>   Polystyrene – butadiene – polystyrene
>   Polystyrene – Isoprene – polystyrene
>   Urethane

Blends of these materials, or with those in Table 14, can be obtained for a variety of mechanical and chemical properties.

These elastomers can be obtained as a solid or foam and with or without reinforcements. While some of the materials can be cast, the primary production methods would be injection molding of hot plasticated material or injection molding of a premixed two or more component liquid into a mold where polymerization occurs.

TABLE 14: ELASTOMERS

	Density lb/in^3	Strength psi	Elongation %	Cost #/lb
Natural isoprene (NR)	0.0338	4000	500	0.44
Synthetic isoprene (IR)	0.0338	2500	300	0.42
Polybutadiene (BR)	0.034	2500	450	0.30
Styrenebutadiene (SBR)	0.034	2000	450	0.30
Isobutylene isoprene (IIR)	0.0334	2000	300	0.43
Chloroprene (CR)	0.0446	3000	650	0.43
Nitrile (NBR)	0.0363	3000	400	0.55
Polysulfrite (PTR)	0.0486	1000	200	0.93
Ethylene propylene (EPDM)	0.031	2500	500	0.34
Chlorinated polyethylene (CM)	0.042	4000	100	0.35
Chlorosulfonated polyethylene (CSM)	0.04	2000	250	0.47
Propylene Oxide (PO)	0.037	2000	500	0.79
Epichlorohydrin (ECO)	0.046	2500	100	0.80
Polyacrylate (ACM)	0.04	1700	450	1.15
Silicone (MQ)	0.0344	1500	100	1.00
Fluorinated hydrocarbon (FPM)	0.051	3000	100	10.00
Polyurethane (AV,EV)	0.038	8000	250	1.17
Thermoplastic rubbers (TPR)	(0.034-0.044)	6400	350	0.50

Costs cited are lowest in group.

Reference: 23

28

2.6 Raw Materials Supply

An accurate assessment of future materials supply is difficult to make due to the many contradictory articles and documentaries. It appears that some of the materials are in short supply at least in the United States while other materials are not.

A forecast of time to depletion for several metallic materials based on one forecast [24] is shown in Table 15. The effects of an exponential growth rate indicates a short time to depletion. The same forecaster estimates the effect of zero growth in the United States, but with a world wide growth to the same consumption rate as the United States. This effect is shown in Table 16.

A second forecaster [25] indicates that iron ore is so plentiful that centuries will pass before there is a shortage. Bauxite shortages do exist but if technology could overcome the refining of aluminum clays there again would be no shortage of aluminum. Similar predictions are made for manganese and magnesium.

There does appear to be some agreement however that materials conservation would be beneficial and could be obtained in the automobile industry. This could be accomplished by redesign, materials selection and creating incentives for recycling.

2.6.1 Ferrous Metals

Two 1972 American made vehicles were disassembled and the various components weighed to determine the quantity of each material used.[26, 27] These breakdowns are shown in Table 17 and Table 18. The total ferrous based metals in these two separate studies were found to be 78.4% and 78.8%. Of this total 61% was uncoated or coated low carbon steel flat stock.

Typical compositions of low carbon steel and HSLA steels are shown in Table 19. The primary constituents are iron and manganese. These steels are melted, refined and alloyed in one of three processes:

    1. Open hearth furnace
    2. Basic Oxygen furnace
    3. Electric furnace

Typically, the open hearth and basic oxygen processes use hot metal (pig iron) and scrap to achieve the iron charge. The typical charge for a blast furnace to make one ton of pig iron is shown in Table 20. The typical materials consumption to produce low carbon steel and HSLA steels are shown in Tables 21, 22 and 23 for the open hearth, basic oxygen and electric furnaces.

The domestic capacity for raw steel is 160 million tons and is projected to be 185 million tons by 1980. Of the 160 million tons

TABLE 15:   FORECAST OF TIME TO DEPLETION OF SELECTED METALS
            (WORLD RESERVES)

Metal	Projected Growth Rate, %	Reserves 10^6 Tons	ERI Years
Iron	1.3	1×10^6	109
Aluminum (Bauxite)	5.1	1170	35
Copper	3.4	308	24
Zinc	2.5	123	18
Molybdenum	4.0	5.4	36
Silver	1.5	0.2	14
Chromium	2.0	775	112
Titanium	2.7	147	51
Uranium	10.6	4.9	44

E.R.I. - Exponential Reserve Index

TABLE 16:   TIME TO DEPLETION: WORLD CONSUMPTION
            EQUAL TO UNITED STATES

	World Consumption Yearly (Tons)	World Consumption at U.S. Rate (tons)	Static Index (Years)
Iron	42×10^8	2.1×10^9	47
Aluminum (Bauxite)	1.2×10^7	8.8×10^7	13
Copper	8.6×10^4	5.0×10^5	6
Zinc	5.3×10^6	2.1×10^7	37
Molybdenum	7.0×10	4.9×10^5	1

Reference: 24

30

TABLE 17: MATERIALS BREAKDOWN FOR A TYPICAL 1972 AMERICAN AUTOMOBILE

Material	No. of Parts	% of Total	Weight, lb (kg)	% of Total
Miscellaneous*	114	3.46	149.78 (67.94)	3.6
Aluminum	65	1.97	108.41 (49.17)	2.6
Cast Iron	84	2.55	711.92 (322.92)	17.1
Rubber	116	3.52	119.54 (54.22)	2.9
Composite†	56	1.70	124.78 (56.60)	3.0
Plastics	198	6.00	189.54 (85.97)	4.6
Zinc	41	1.24	33.61 (15.25)	0.8
Copper and Brass	30	0.91	56.29 (25.53)	1.4
Asbestos	4	0.12	0.66 (0.30)	0
Cardboard	9	0.27	8.37 (3.80)	0.2
Fabric	14	0.42	2.21 (1.00)	0
Glass	27	0.82	99.90 (45.31)	2.4
Steel	2,540	77.02	2,554.68 (1,158.78)	61.4
GRAND TOTAL	3,298	100.00	4,159.69 (1,996.80)	100.0

*Examples include speaker, spark plugs, lights, brake pads, air cleaner element.

†Examples include seat cushions, grill, fan shroud, heater duct, inner door trim panels.

Steel Types Specified by Automakers

Material	No. of Parts	% of Total	Weight, lb (kg)	% of Total
Hot-rolled	277	8.40	1,048.04 (475.38)	25.2
Cold-rolled grade 1	51	1.55	341.37 (154.84)	8.2
Cold-rolled grade 2	379	11.49	617.14 (279.93)	14.8
Galvanized	54	1.64	105.21 (47.72)	2.5
Aluminized	4	0.12	27.34 (12.40)	0.6
Terne	5	0.15	35.73 (16.21)	0.9
Stainless	68	2.06	19.08 (8.65)	0.5
Alloy	1,702	51.61	360.77 (163.64)	8.7
SUB-TOTAL	2,540	77.02	2,554.68 (1,158.78)	61.4

Reference: 26

TABLE 18:   MATERIALS BREAKDOWN FOR 1972 AMERICAN AUTOMOBILE

	Actuals Measured	Estimated From Measured Composites	Total Weight
Steel and Iron	1,972.4	1,369.8	3,342.2 lbs.
Stainless Steel	19.2	3.7	22.9 lbs.
Aluminum	15.5	74.5	90.0 lbs.
Rubber	18.4	160.6	179.0 lbs.
Plastics	92.8	147.5	240.3 lbs.
Copper and Brass	---	28.7	28.7 lbs.
Fluids	96.9	3.8	100.7 lbs.
Zinc Alloys	29.0	4.9	33.9 lbs.
Wiring	16.3	---	16.3 lbs.
Glass	109.9	7.3	117.2 lbs.
Rugs	34.9	---	34.9 lbs.
Galvanized Steel	31.3	19.9	51.2 lbs.
Chrome Plated Steel	97.6	---	97.6 lbs.
Paint	18.5 (est.)	---	18.5 lbs.
Undercoating	24.0 (est.)	---	24.0 lbs.
Others (Battery & Paper Board)	63.2	---	63.2 lbs.
TOTALS	2,639.9	1,820.7	4,460.6 lbs.

Reference: 27

32

TABLE 19:   COMPOSITIONS OF TYPICAL SHEET STEELS (wt %)

Steel Code	C	Mn	Si	Al	Ti	V	Cb	Zr
Low Carbon	.06	.39	.01	.005	.002	.005	.005	.005
Producer 'A'	.10	.34	.03	.070	.17	.005	.005	.005
Producer 'B'	.13	1.25	.60	.080	.002	.12	.005	.005
Producer 'C'	.10	1.20	.02	.065	.002	.005	.10	.005
Producer 'D'	.12	1.24	.22	.020	.002	.036	.037	.072
Producer 'E'	.12	.52	.03	.035	.31	.015	.005	.005

Reference: 7

TABLE 20:   MATERIALS CONSUMED TO MAKE ONE TON OF PIG IRON

Material	Amount Required
Iron Ore	0.408 ton
Pellets	0.759
Sinter	0.459
Coke	0.597
Mill Scale	0.05
Limestone	0.232
Scrap Steel	0.027
Refractories	5.0 pounds
Fuel Oil	3.864 gal.
Natural Gas	0.325×10^3 cu. ft.
Coke Oven Gas	0.121 cu. ft.
Oxygen	0.207 cu. ft.
Tar and Pitch	1.023 gal.

TABLE 21:   MATERIALS CONSUMED TO MAKE ONE TON OF STEEL
            BY THE OPEN HEARTH PROCESS

Pig Iron (Hot Metal)	0.620 ton
Scrap Metal	0.505
Limestone	0.044
Lime	0.013
Fluorspar	0.003
Ferromanganese (78% Mn)	0.011
Ferrosilicon (75% Si)	0.001
Aluminum	0.0005
Oxygen	1.22×10^3 cu. ft.
Refractories	40 lb.
Fuel Oil	9.0 gal.
Tar and Pitch	3.66 gal.
Natural Gas	1.128×10^3 cu. ft.
Coke Oven Gas	0.345×10^3 cu. ft.

Reference: 49

34

TABLE 22: MATERIALS CONSUMED TO MAKE ONE TON OF STEEL
BY THE BASIC OXYGEN PROCESS

Pig Iron (Hot Metal)	0.778 ton
Scrap Metal	0.314
Ferromanganese (78% Mn)	0.011
Aluminum	0.0005
Lime	0.075
Limestone	0.005
Fluorspar	0.008
Pellets	0.003
Scale	0.008
Refractories	13 lbs.
Oxygen	1.92×10^3 cu. ft.
Natural Gas	0.2×10^3 cu. ft.
Nitrogen	0.4×10^3 cu. ft.

TABLE 23: MATERIALS CONSUMED TO MAKE ONE TON OF STEEL
USING ELECTRIC FURNACE MELTING

Steel Scrap	1.10 ton
Lime	0.03
Limestone	0.01
Fluorspar	0.005
Ferromanganese (78% Mn)	0.011
Ferrosilicon (75% Si)	0.001
Aluminum	0.0005
Electrodes (c)	12.0 lbs.
Refractories	26.0 lbs.
Natural Gas	0.1×10^3 cu. ft.
Oxygen	0.25×10^3 cu. ft.

Reference: 49

26.4% is made by open hearth process, 55.2% by the basic oxygen process and 18.4% by the electric furnace. Finished steel capacity is currently 112 million ton of which 47.7 million ton is sheet and strip.

Using the above percentages of steel produced by the three steel producing processes and the data from Tables 20 through 23 the average consumption of each material can be determined to produce one ton of raw steel, Table 24. The quantity of iron ore and pellets can be added together to determine the total iron ore which is obtained from the earth as primary materials for each ton of raw steel. Current U.S. raw steel capacity is 160 million tons per year which would require 111 million tons of ore per year. Currently the U.S. imports 30% of its ore requiring a yearly domestic production of 86 million ton. Proven domestic reserves of domestic ore is 9000 million ton. At the present rate of consumption the domestic ore will last 105 years. Unproven estimated domestic reserves total 92 billion ton.

The data on iron ore is listed in Table 25 with other materials from Table 24 which have been found to be in short supply. The two materials which appear to be in short supply are manganese and fluorspar. The potential domestic reserve of manganese listed in Table 25 is that which is found on the Pacific Ocean floor. Politically, the availability of this material is unknown.

2.6.2 Non-Ferrous Metals

The composition of the aluminum and magnesium alloys selected as future candidate materials are listed in Tables 26 and 27.

World production of primary aluminum exceeded 12 million tons in 1974 and of this 42% or 5 million was produced in the United States. This production rate is essentially the total capacity of American production.

Bauxite is the principal ore for aluminum and consists of a mixture of two hydroxides with an average aluminum content of 40%. Currently the United States imports essentially 90% of its bauxite from Jamaica and Surinam. The United States reserves of bauxite are 11.9×10^6 tons and the estimated world reserves are 10×10^9 tons. Potential resources are estimated to be 10×10^9 tons.[25] At the present rate of consumption for the world, bauxite will be available for 100 years. At a growth rate of 5.1%[24] the bauxite is projected to be consumed in 35 years.

Other minerals have been used to produce aluminum on a limited scale. These processes are not currently active due to cost. With the advent of total bauxite consumption or political problems with foreign governments these alternate minerals could be used in the

TABLE 24:   MATERIALS CONSUMED TO MAKE ONE TON OF RAW STEEL

Composite Average

Material	Amount
Iron Ore	0.2418 ton
Pellets	0.4522 ton
Scrap	0.5251 ton
Sinter	0.2723 ton
Ferrosilicon	0.0010 ton
Ferromanganese	0.0110 ton
Mill Scale	0.0341 ton
Aluminum	0.0005 ton
Fluorspar	0.0160 ton
Limestone	0.1535 ton
Lime	0.0503 ton
Coke	0.3538 ton
Fuel Oil	4.67 gal.
Tar and Pitch	1.57 gal.
Natural Gas	0.62×10^3 cu. ft.
Coke Oven Gas	0.16×10^3 cu. ft.
Oxygen	1.5×10^3 cu. ft.
Refractories	25.5 lbs.
Nitrogen	0.12 cu. ft.
Electrodes (C)	2.2 lbs.

TABLE 25:   YEARLY REQUIREMENTS AND DOMESTIC RESERVES OF MATERIALS

Used to Make Raw Steel

	Yearly Requirement (Tons x 10^6)	Known Domestic Reserves (Tons x 10^6)	Potential Domestic Reserve (Tons x 10^6)
Iron Ore	111	9000	92,000
Ferromanganese (Mn)	1.76	0	0.4
Aluminum (Bauxite)	0.08	12	300
Fluorspar	2.56	25	45
Coke	56.6	1.581×10^6	1.643×10^6
Fuel Oil	17.8×10^6 bbls.	38×10^3 bbls.	38×10^3 bbls.
Natural Gas	99.2×10^3 cu. ft.	240×10^{12} cu. ft.	240×10^{12} cu.ft.

Other materials from Table 24 not included.   Materials are not
in critical supply.

TABLE 26: CHEMICAL COMPOSITION OF SELECTED ALUMINUM ALLOYS

Weight Percent

Alloy	Si	Fe	Cu	Mn	Mg	Cr.	Zn	Aluminum
2036	0.5	0.5	2.6	0.25	0.45	0.1	0.25	Remainder
5182	0.2	0.35	0.15	0.35	4.5	0.1	0.25	Remainder
6061	0.6	0.7	0.3	0.15	1.0	0.15	0.25	Remainder
6009	0.8	0.5 Max.	0.4	0.5	0.6	0.1 Max.	0.25 Max.	Remainder
6010	1.0	0.5 Max.	0.4	0.5	0.8	0.1 Max.	0.25 Max.	Remainder
7016	0.1	0.1	0.6-1.4	0.03	0.8-1.4	0.04-0.35	4-5.0	Remainder
7046	0.2	0.4	0.25	0.05-0.3	1.0-1.6	0.06-0.2	6.6-7.6	Remainder
A390	17.0	1.0	4.5		0.55			Remainder
A356	7.0				0.50			Remainder

All other elements 0.05% Max. each and total 0.15% Max.

39

TABLE 27: NOMINAL CHEMICAL COMPOSITION OF SELECTED
MAGNESIUM ALLOYS

Alloy	Al	Zn	Mn	Th	Zr
AZ63A	6.0	3.0	0.2		
AZ31B					
AZ91A	9.0	0.7	0.2		
HK31A				3.25	0.7

United States. The potential resources of aluminum clays in the United States are estimated to be considerably greater than those for iron.[25]

Other than the alloying elements and fuels the only material consumed in any quantity in the production of aluminum is caustic soda. Caustic soda in turn is made from sodium chloride by electrolysis. The supply of industrial sodium chloride is considered limitless.

Of the alloying elements used in aluminum, copper, manganese, and zinc are considered to be in critical supply, Table 15, 16 and 25. Manganese supplies are expected to increase with the ocean floor recovery previously considered in Section 2.6.1.

Magnesium used with aluminum as an alloying element and as the base material in the magnesium alloys is considered to be in limitless supply. Refining capabilities in the United States is 132,000 tons and is being increased yearly to an estimated production of 200,000 tons by 1980.[29] Approximately 45% of the magnesium consumption is as an alloying element for aluminum. Magnesium producers do not foresee any large use of magnesium alloys as structural items due to the high cost. Any such application in future automobiles would place a severe strain on domestic capacity. Approximately 31,000 tons of magnesium are exported each year. There is no predicted increase through 1980.

The supply of thorium and ziconium are sufficient for the magnesium alloys. These elements are obtained as by products in the recovery of titanium. Increased nuclear activity could develop shortage in these materials momentarily.

2.6.3 Glass Fiber Reinforcements

The major raw material for fiber glass is silica sand. Silicon is the most abundant metal on the earth's crust and there are abundant supplies of sand throughout the world. No shortage of silica sand for glass-making purposes will arise in the foreseeable future.[30] Increasing sand costs are expected, due to the increasing costs of transportation and energy. While there are a number of differing glass compositions, the type most used in fiber glass reinforcements is listed in Table 28. The primary raw materials necessary for the production of fiber glass are listed in Table 29.

The supply of quality sand, limestone, dolomite, borax, boric acid and alumina are excellent and reviews [33] indicate that these materials are in abundant supply with no shortage foreseen in the United States. Fiberglass for plastics reinforcement is purposely kept low in sodium and potassium to improve resistance to moisture. This is perhaps fortunate since potassium materials such as potash and feldspar are in short

TABLE 28: COMPOSITION OF E GLASS [2]

	% by Weight
$Si\ O_2$	52-56
Al_2O_3	12-16
$Ca\ O$	16-25
$Mg\ O$	0-6
$B_2\ O_3$	8-13
$Na_2O,\ K_2O$	0.3
$Ti\ O_2$	0-0.4
$Fe_2\ O_3$	0.05-0.4
F_2	0-0.5

TABLE 29: GLASSMAKING MATERIALS [3]

	Composition
Sand	$Si\ O_2$
Soda Ash	$Na_2\ CO_3$
Salt Cake	$Na_2\ SO_4$
Sodium Nitrate	$Na\ NO_3$
Potash	$K_2\ CO_3\ .1.5\ H_2O$
Limestone	$Ca\ CO_3$
Dolomite	$CA\ CO_3\ .Mg\ CO_3$
Boric Acid	$B_2\ O_3.\ H_2O$
Borax	$Na_2\ B_4\ O_7\ .10\ H_2O$
Feldspar	$K_2\ (Na_2)\ O\ .Al_2\ O_3\ .\ 6\ Si\ O_2$

supply in the United States. These materials are used in fertilizers and 65% of that material is imported from Australia.

Associated equipment and materials in the processing of fiberglass require platinum, rhodium and tin. These three metals have been reported in adequate supply.[30] The yearly demand for tin in glassmaking is not reported. The major uses of tin are in copper and lead alloys as in tin plate. While most of the tin is imported the yearly consumption in glassmaking is low and no significant problems are reported.

Based on 1973 statistics [33] the U.S. glass ceramics industries consumed 11% (72,400 troy ounces) of the total platinum sales and 23% (16,560 troy ounces) of the rhodium sales. This included newly mined materials and secondary (recycled) metals. The total production of domestic platinum group metals in the U.S. in 1973 was 19,980 troy ounces. The major producers of these metals are U.S.S.R. and South Africa which together produce 4,810,000 troy ounces out of a total world production of 5,173,000 troy ounces. These materials would be in critical supply if importing sources were not available. The annual consumption of platinum group metals per pound of glass fiber used for plastics reinforcement is not available.

2.6.4 Petroleum, Natural Gas and Plastics Resins

The domestic supply and demand for petroleum and natural gas liquids has been listed by the Department of Transportation,[62] Table 30. Percentage yield of petroleum products from U.S. refineries for the years 1956 through 1975 have remained relatively constant. The largest single refinery product has been gasoline as seen in Figure 6. Plastics, chemicals, pharmaceuticals and minor specialty products for metals production use 12.63% of the total refinery yield.

Petroleum and natural gas liquids are the primary sources (70%) of raw material for the plastics industry today.[54] This represents 4 to 7% of the total United States consumption of oil. The remainder of the plastics raw material (30%) is obtained from natural gas and coal.

Organic chemical feedstocks for plastics production can be sub-classified into three chemical sub groupings: methane derivatives (20% of total), aromatic chemicals (25%) and aliphatic chemicals (55%).

Methane derivatives are now completely obtained from natural gas. The main chemicals included in this group are methanol and ammonia. At present there are 90 ammonia plants and 12 methanol plants in the United States which use 600 billion cubic feet of natural gas per year. These existing plants cannot be converted to other raw materials such as synthesis gas from coal and new plants would have to be constructed if the supply of natural gas is insufficient.

43

TABLE 30: DOMESTIC SUPPLY AND DEMAND FOR PETROLEUM[1].
1974 and 1975

	1974		1975 (estimated)	
	Million bbl	Trillion Btu	Million bbl	Trillion Btu
Supply, crude oil:				
Production (including lease condensate)	3,199.3	18.556.0	3,056.1	17,725.4
Exports	-1.1	-6.4	-2.1	-12.2
Imports	1,269.2	7,361.4	1,461.1	8,474.4
Stock change: withdrawals (+), addition, (-)	-22.5	-130.5	+11.0	+68.8
Losses, transfers for use as fuel, and unaccounted for	-16.2	-94.0	-8.5	-19.3
Total	4.428.7	25,686.5	4,517.6	26,202.1
Exports	-79.4	-460.8	-75.0	-435.0
Imports	952.4	5,690.8	715.0	4,272.0
Stock change, including natural gas liquids	-42.8	-231.6	-34.0	-170.0
Transfers in, natural gas liquids	343.7	1,233.9	316.2	1,121.1
Losses, gains, and unaccounted for	-31.2	-13.5	48.6	352.0
Total	6,069.5	33,414.4	5,954.0	32,701.0
Demand by major consuming sectors:				
Houshold and commercial	882.2	4,896.1	847.0	4,687.6
Industrial	628.4	3,686.7	600.2	3,520.9
Transportation	3,267.9	17,563.7	3,297.2	17,699.4
Electricity generation, utilities	559.9	3,480.2	533.0	3,312.3
Other, not specified	18.6	112.2	11.3	67.9
Raw materials:				
Petrochemical feedstock offtake	386.1	1,640.3	373.3	1,575.0
Other nonfuel use	302.2	1,898.4	292.0	1,837.9
Miscellaneous and unaccounted for	24.0	133.8	---	---
Total domestic product demand	6,069.5	33,414.4	5,954.0	32,701.0

Reference: 62

44

FIGURE 6   PERCENTAGE YIELDS OF PETROLEUM PRODUCTS
AT U.S. REFINERIES, 1975

GASOLINE 46.67%

KEROSENE
1.22%

JET FUEL
NAPH. TYPE
1.44%

JET FUEL
KERO. TYPE
5.58%

OTHERS 12.63%

DISTILLATE FUEL OIL
21.32%

RESIDUAL
FUEL OIL
9.92%

LUBRICANTS 1.24%
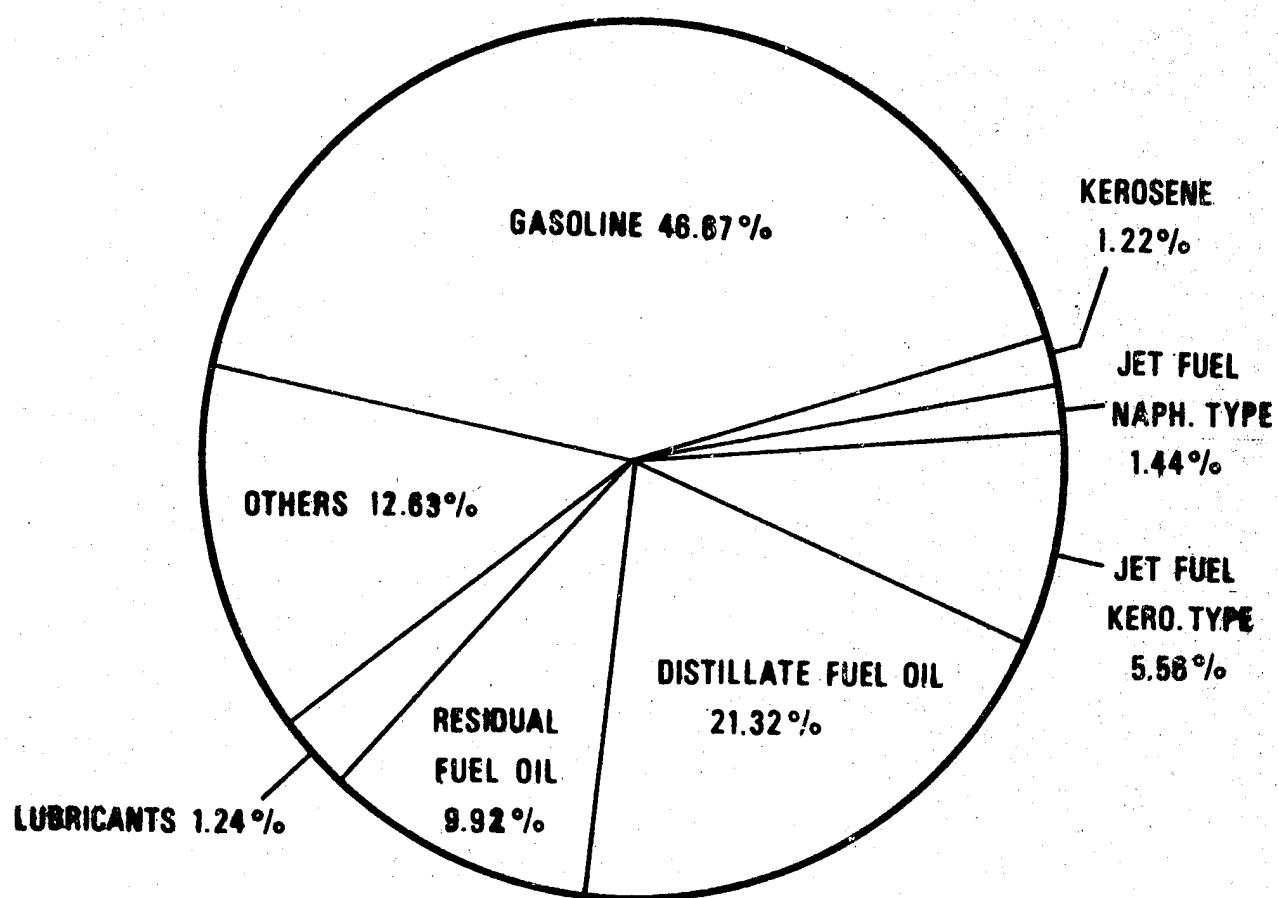
The majority of aromatic chemicals - benzene, toluene and xylenes - are based on petroleum. Currently about 7% comes from coal as a by product of the steel industries coking processes and is dependent upon the yearly steel industry requirements. It is estimated that coal could be a major supplier of aromatics, with increased research, by the year 2000.[54]

Aliphatic chemicals, such as ethylene, propylene and paraffins, are obtained entirely from petroleum or liquid petroleum gases recovered from natural gases. Again, the Society of the Plastics Industry [54] suggests that coal sources may be developed by the year 2000 to produce the necessary aliphatic chemicals.

Petroleum and natural gas reserves and productive capacity of the United States have been recently reviewed by the Federal Energy Administration.[55] The F.E.A. surveyed oil and gas producers and compared these results with estimates by the American Petroleum Institute and the American Gas Association. The F.E.A. estimates of proven reserves of oil were 38.0×10^9 bbls of crude compared to the API estimate of 34.2×10^9 bbls. Reserves of natural gas are estimated by F.E.A. to be 240.2 trillion cubic feet as compared to the AGA estimate of 233.2 trillion cubic feet. The term reserve means to be recoverable at present economic costs.

The U. S. productive capacity as of December 31, 1974 was estimated by F.E.A. to be 8.7×10^6 bbls of oil per day and 63.4×10^9 cubic feet of natural gas per day. As of October 18, 1976 the oil productive capacity was estimated to have declined to 8.0×10^6 bbls per day by the New York Times.[56] The rate of importing necessary to satisfy current requirements was estimated to be 42% or nearly 6×10^6 bbls per day.

Crude oil yearly production and projected productive capacity in the United States is shown in Figure 7 as presented by the F.E.A. This indicates an essential leveling off of productive capacity through 1985. Projections beyond 1985 are shown in Figure 2.

The U. S. natural gas supply projections are indicated in Figure 8. Again based on this projection the supply of natural gas is leveling and will decline after 1985.

The world proven oil reserves are estimated to be 660×10^9 bbls, and the average daily production, based on 1975 figures, for the world is 47×10^6 bbls of oil per day or 17×10^9 bbls/year. At the 1975 production rate the current known reserves would provide essentially 40 years of oil.

Oil production does not remove all of the available oil from the earth. Low cost production, primary recovery, averages approximately 25% yield.[59] Many U. S. oil reservoirs have exhausted their primary production and are in the secondary or tertiary (enhanced) stage of production. Current crude production by type of recovery

46

FIGURE 7 CRUDE OIL PRODUCTION AND PROJECTED PRODUCTIVE CAPACITY IN THE UNITED STATES
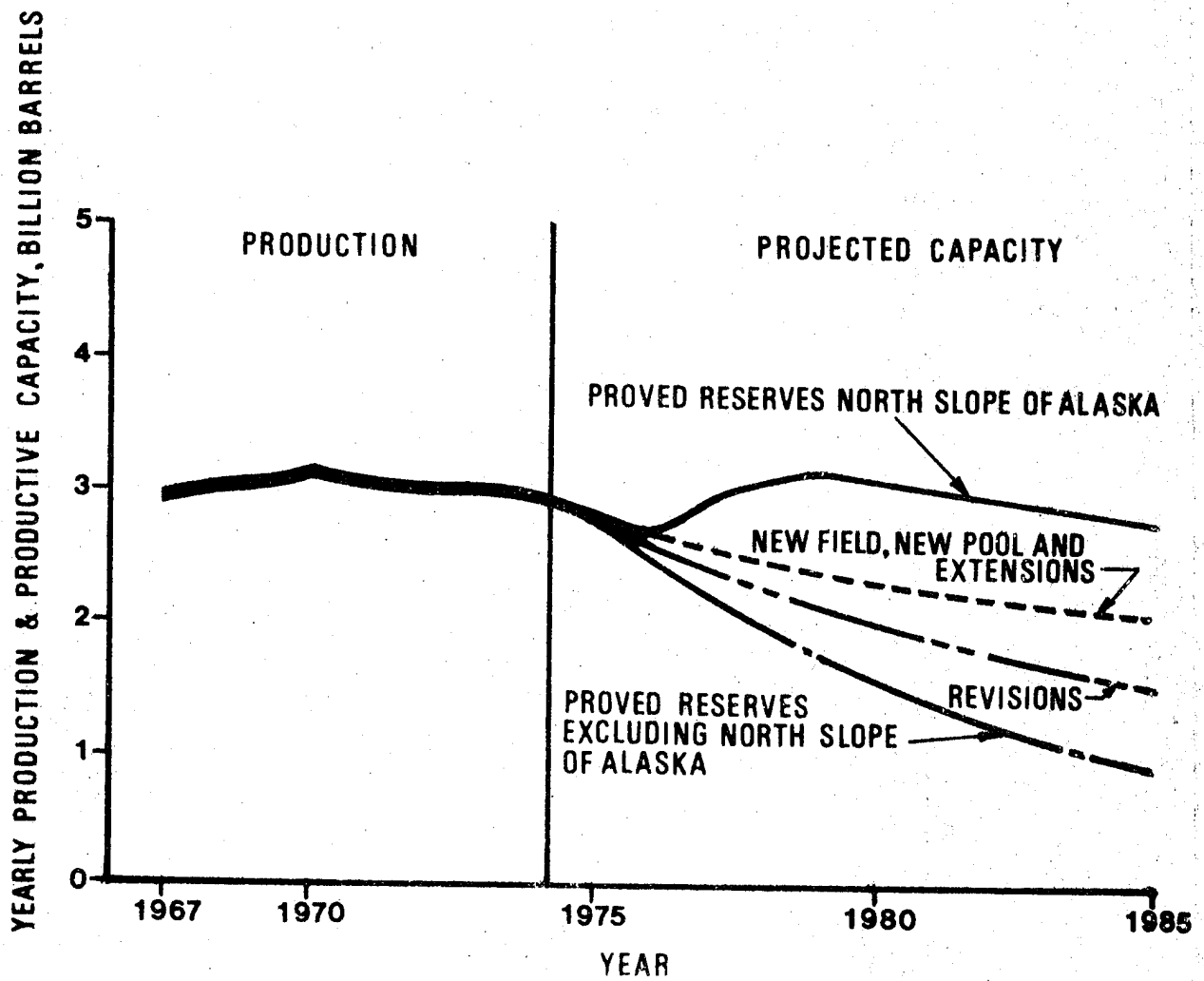
REFERENCE: 55

FIGURE 8 U. S. NATURAL GAS SUPPLY
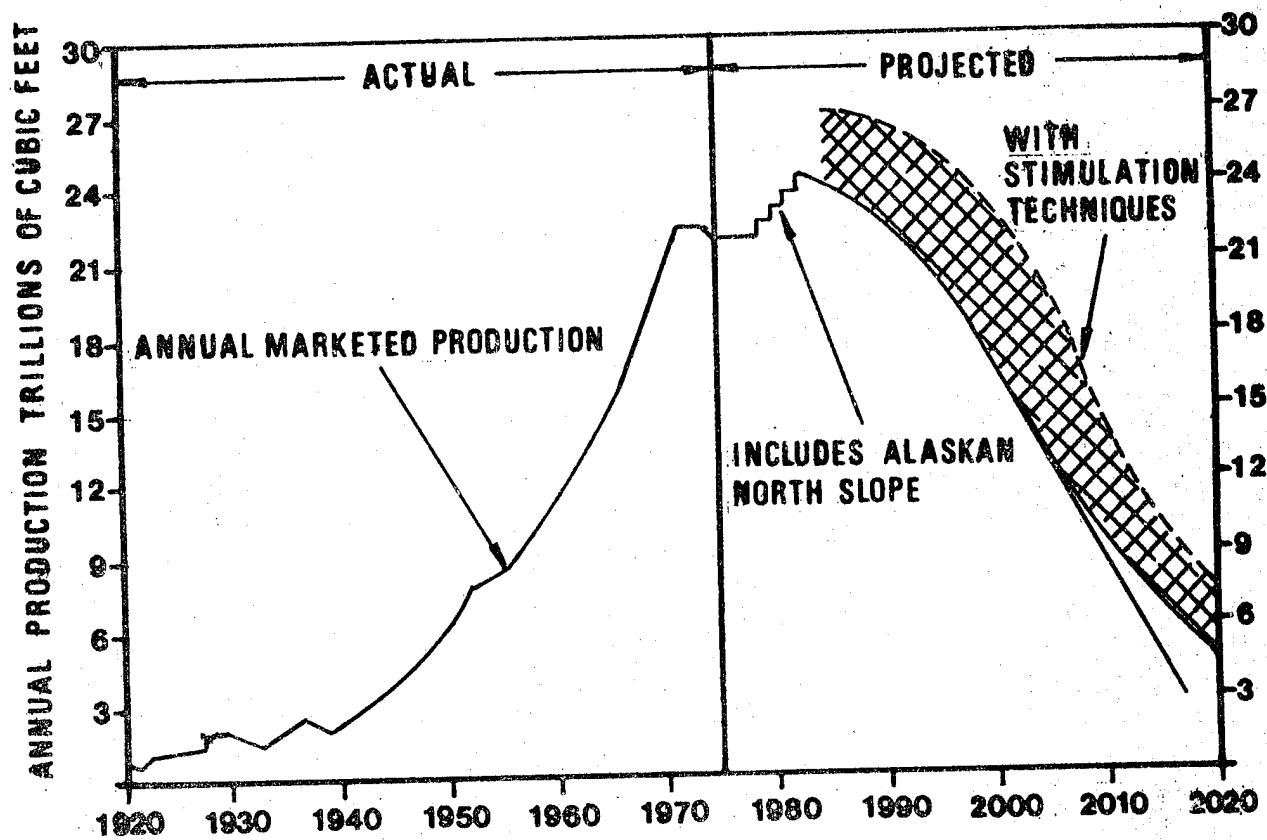
SOURCE: A NATIONAL PLAN FOR ENERGY RESEARCH, DEVELOPMENT AND DEMONSTRATION ERDA-48(1975)

REFERENCE: 55

is depicted in Figure 9. Enhanced recovery techniques now being used will provide an average of 38% recovery of the original oil in place. Additional "exotic" enhanced recovery technology has been proposed to obtain as much as 54% of the original oil in place. It is estimated that 60 billion barrels (20 years production) of additional oil could be recovered if these techniques were used.

Another source of oil which requires development and a proper economic environment is oil shales. A recent report [60] indicated that modified in situ recovery techniques may be economical. Based on 50,000 barrel per day production the total production cost was estimated to be 70 to 80% of current stated imported oil prices. However there has not been a large enough demonstration completed to determine facility life and total costs.

Estimated oil reserves of oil shales are 1.8 trillion barrels. Of this, 129 billion barrels are considered as the most economical. If a 60% recovery is feasible the total oil reserves would be 77 billion barrels. At the current yearly production rate of about 3.5 billion barrels, the oil shales could provide over 20 years of oil supply. Unfortunately a number of environmental problems must be solved. A lack of process water and subsequent disruption of large land areas must be considered and satisfactorily alleviated before the oil shales can be exploited.

2.7 Mill Products Capacity

Domestic mill product capacity is determined by a complex combination of demand, cost and planning. Many shortages historically reported have been due to improper planning over short and long periods. As the demand and willingness to pay the price have increased, mill capacity has quickly provided sufficient materials for industry.

In 1973 and 1974, shortages occurred in many materials throughout the world. This problem has been referred to frequently in the literature. Dr. Eads, executive director, National Commission of Supplies and Shortages, at the Fourth Hennikee Conference on National Materials Policy in discussing conclusions from a Commission Study said,[36] "The 1973-74 shortages had nothing to do with a basic scarcity of either domestic or overseas resources. They resulted from three events:

1. A slowdown in the rate of expansion of industrial capacity beginning in the late 1960's.
2. A sharp surge in demand that began in 1972. This upturn arrived virtually simultaneously in all major industrialized countries.
3. A "shortage mentality" that converted the tight condition created by 1 and 2 into a situation approaching near panic. The primary result was double ordering by purchasing agents. This artificially supported industrial production well

FIGURE 9 DISPLAY OF CURRENT CRUDE PRODUCTION
BY TYPE OF RECOVERY TECHNIQUE
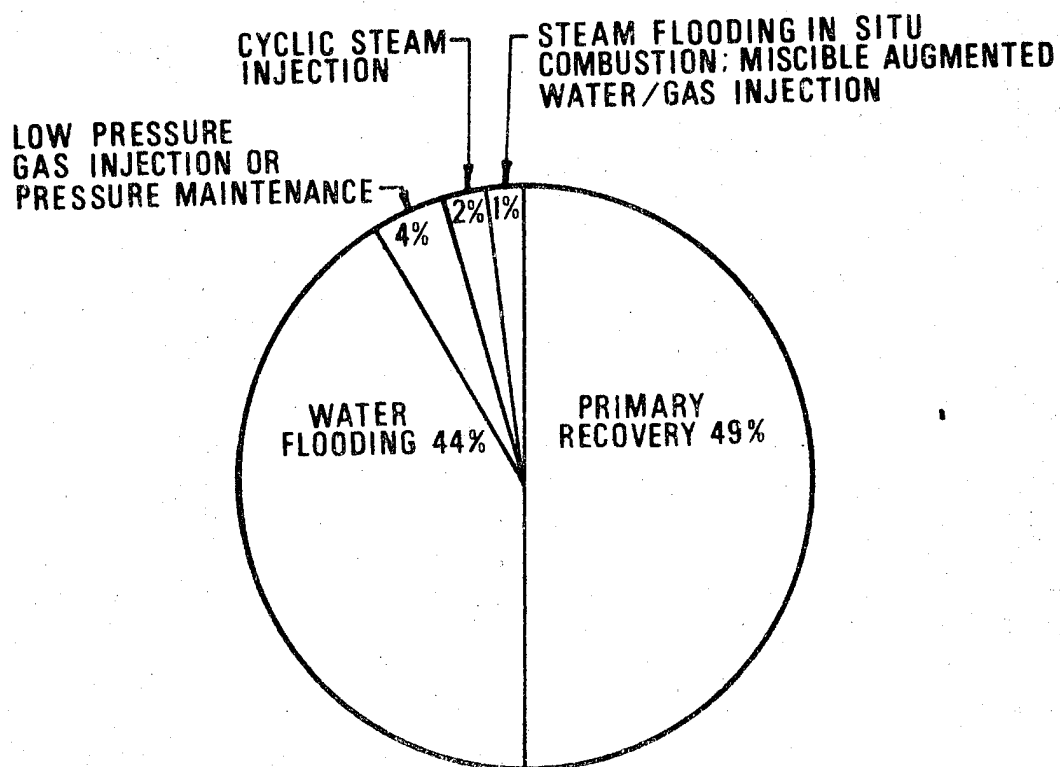
REFERENCE: 59

beyond the time when the economy had turned
downward. When it evaporated, industrial
production plunged sharply, accounting for
much of the severity of the 1974-75 recession."

2.7.1 Ferrous Metals

In a special report on the steel industry,[37] H. Chandler
reported the steel companies are expanding and modernizing at
a rate of $12 billion over the period of 1973 to 1980. This
capitalization is directed toward prevention of shortages through
the early 1980's. A possible shortage of flat rolled products
for automotive uses could occur if steel demand for capital goods
and for oil country goods increases as expected.[38]

Expansion has been slowed and even stopped in several steel
companies due to the increased cost of meeting environmental
regulations. The proportion of total expansion costs required
for pollution has been summed up by the American Iron and Steel
Institute[37] as follows: "The steel industry must spend at a
rate of $5 billion yearly in 1975 dollars to meet its expansion
goal of 185 million tons of raw steel by 1983. Of this sum,
about $1.5 billion would be for expanded facilities; $2 billion
for maintenance of existing capacity; $1 billion to meet pollution
control requirements, and $500 million for non-steel investment".

Flat rolled steel for automotive uses could be in short supply
for short periods of time whenever pressures of peaking business
cycles in other industries would create a greater demand for the
product. Similarly, an increase in flat steel products for in-
creased automotive production would create shortages. Reviewing
the many articles on supply and demand, business will only respond
to expansion when there is a continuous demand pressure for a pro-
duct in short supply.

2.7.2 Non Ferrous Alloys

The aluminum industry has a notoriously bad history of ups
and downs in sales of all of its products.[39] Aluminum shortages
or excessive inventories frequently occur due to "shortage men-
tality" referred to in section 2.7.

A substantial increase in aluminum alloy applications in
automobiles could be accomodated by the aluminum industry. Such
an increase might have a leveling effect. Comments made by Cornell
Maier, President of Kaiser Aluminum[40] indicate concerns over ex-
pansion.

"So it seems fairly apparent that the supply/demand situation
is going to be a little snug for a while. Unfortunately, there's
not much we can do to avoid that in the short-term. Due to siting
power, environmental, and financing considerations, primary plants

now seem to take so long to build that even if we started tomorrow, we could not materially ease the situation over the next 3 to 4 years. No one is starting much new capacity tomorrow -- although we and other producers are adding incremental capacity to existing plants...

The reasons we face a tightening aluminum supply situation are:

(a) the industry's rate of return has been too low to justify the enormous and rapidly rising costs of building smelters located on new sites. The per ton cost of adding new primary capacity has almost doubled in the past 5 years;

(b) while aluminum prices have increased since 1973, the cost of operating existing smelters has risen almost as quickly, leaving very little additional earnings that can be invested in new capacity;

(c) a very high percentage of capital spending by producers has gone to meet increasingly string-ment environmental control regulations..."

As indicated above a primary aluminum facility requires three to four years to bring on stream. A rolling facility to produce sheet requires a similar lead time of three years.[41] The user of sheet wants assurances of supply before committing a design to a new material.

Based upon the review of literature the supply-demand conditions for aluminum for future automobiles is similar to that which has existed in the past for steel. Mill capacity will be available if planning is provided and the customer is willing to pay the price. This price may be excessive due to the competition for energy. As the price of oil and natural gas increases there will be a greater demand for hydroelectric and coal energy sources.

2.7.3 Reinforced Plastics

The plastics industry has been for a number of years predicting solid growth. Except for a period in 1973-74 the supply has been ahead of demand. The supply of the major monomers, ethylene, pro-pylene, styrene and vinyl chloride are projected to be greater than demand as shown in Table 31.[42] This projection is based on 85 to 90% capacity with annual growth rates as follows:

Thermoplastic polyester	25%
Polypropylene	21%
ABS	19%
Polycarbonate	17%
Polyethylenes	16%

52

TABLE 31: SUPPLY AND DEMAND OF MAJOR MONOMERS
(MILLIONS OF METRIC TONS)

		Ethylene	Propylene	Styrene	Vinyl Chloride
1976	Supply	12.7	7.5	3.6	3.4
	Demand	10.5	5.0	2.7	2.5
1980	Supply	18.0	10.0	4.5	4.4
	Demand	15.0	7.7	3.8	3.6

Acetal	14%
Polystyrene	12%
PVC	12%
Nylon	10%

Building blocks for thermosets have been reported[43] to also be in good supply except for methanol. Of the thermoset resins polyesters have been growing most rapidly (15% annually). A continued growth rate in consumption (10%) is expected. Currently the supply is 30 to 40% in excess of demand. Epoxy capacity is equal to demand currently and will be so until 1978. A 10% growth rate of supply and demand is projected through 1981.

The overall capacity of resin conversion exceeds the projected demands of the thermoplastics through 1981.[44, 45, 46, 47, 48] Thermoplastics materials from converters of polymerizers are melted in a pelletizer extruder. At this pelletizer, additions are added to improve strength, color, etc. Pelletizers are not capital intensive as are rolling mills for metals. The pellets are sold then to molders who plasticate the mold by extrusion, injection molding, etc. into a final product.

Thermosets are supplied as liquids or soluble solids with reinforcements, fillers and other additives to the molder. Again low capital, modular, mixers and compounding equipment is used to prepare a molding compound for molding the part.

Plastics materials have the advantage over metals in that the high capital costs are not needed in the intermediate stage of production. Large investments are not required between the polymerization and final molded part, as needed between the melting furnace for metal and a final formed part.

2.8 Energy Requirements

The energy requirements to produce primary products such as ingots, slabs and castings of high priority materials have been determined by Battelle Columbus Laboratories for the Bureau of Mines.[49, 50] This information has been tabulated in Table 32. These values were calculated, including the energy for mining, transportation, fuels and materials consumed in preparation of ore, fluxing agents and fuel for final refining. A typical flow chart and compilation are shown in Figure 10 and Table 33 for aluminum ingot production from bauxite.[49] These energy figures include that expended for pollution control.

The value listed for steel slabs in Table 32 must be increased to include conversion to cold rolled and hot rolled sheet and transporting to a fabricating plant. Energy for rolling is not too significant being approximately 50 Btu per pound.

TABLE 32: ENERGY REQUIREMENTS FOR THE PRODUCTION OF
MILL PRODUCTS OF CANDIDATE MATERIALS

Material	Btu/lb	Major Source
Steel Slabs	12,140	Coal
Aluminum Ingot	122,000	Electric
Refined Copper	56,000	Oil, Gas, Electric
Zinc	32,500	Coal, Gas
Ferro Chromium	64,500	Electric, Coal
Ferro Manganese	23,000	Electric, Coal
Ferro Silicon	38,500	Electric, Coal
Magnesium	179,000	Electric, Gas
Kaolin	1,400	Gas
Talc	450	Electric, Gas

Reference: 49,50

FIGURE 10 PRODUCTION OF ALUMINUM FROM BAUXITE
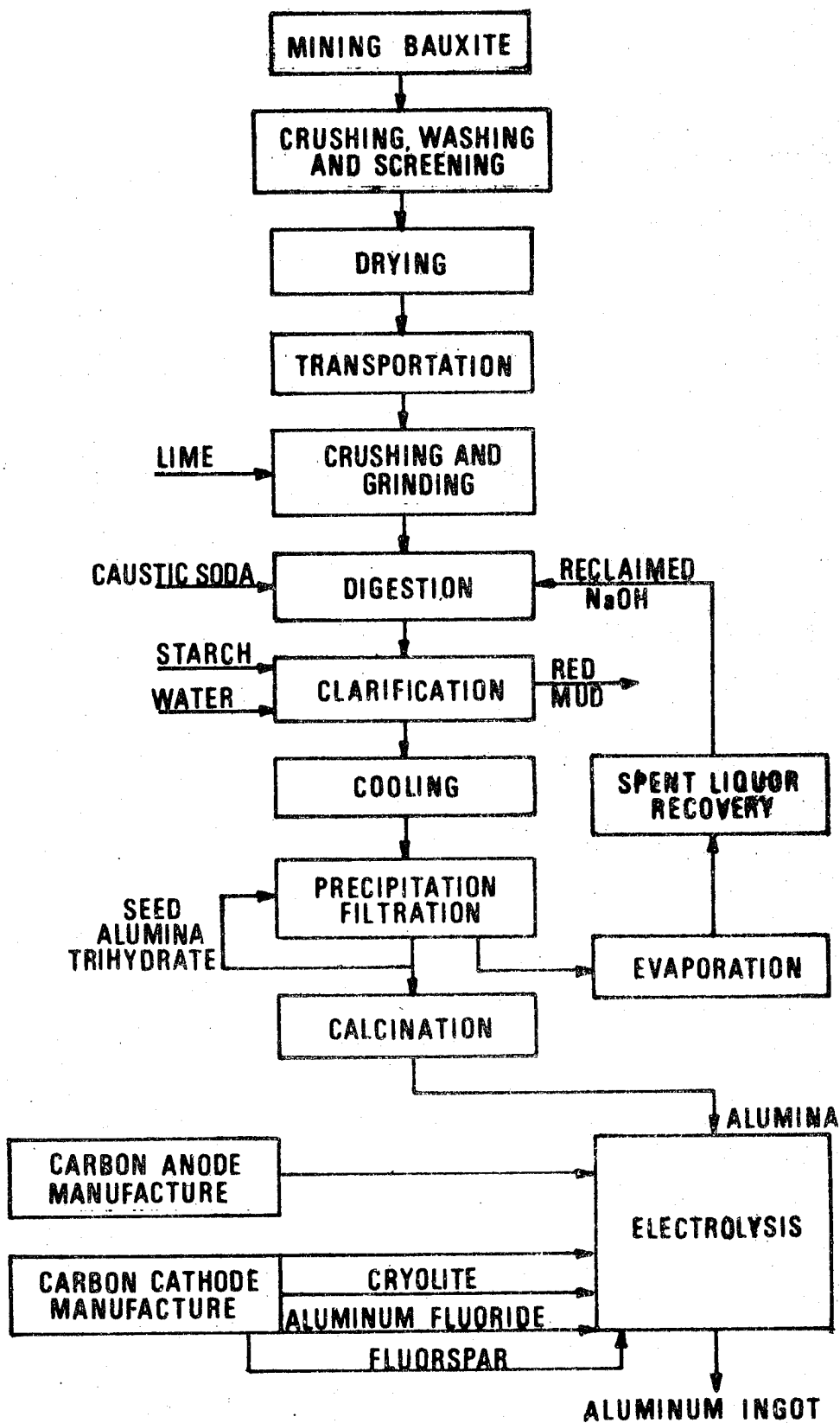
TABLE 33: ENERGY REQUIREMENTS FOR THE PRODUCTION OF ALUMINUM

	Unit	Units Per Net Ton of Aluminum	10^6 Btu Per Unit	10^6 Btu Per Net Ton of Aluminum
Mining				
Drilling	kwh	1.0	0.0105	0.01
Drill bits, drilling machines	lb	Negligible		
Explosives	lb	0.80	0.030	0.02
			Subtotal	0.03
Shovel loading				
Electrical energy	kwh	10.25	0.0105	0.11
Materials, repair & maintenance	Btu	0.03×10^6		0.03
			Subtotal	0.14
Truck transportation				
Diesel fuel oil	gal	0.70	0.139	0.10
Truck materials, tires & repair	Btu	0.02×10^6		0.02
			Subtotal	0.12
Crushing, washing, & screening				
Crushing & screening electrical energy	kwh	12.5	0.0105	0.13
Pumping electrical energy	kwh	6.4	0.0105	0.07
Machinery wear and service energy	Btu	0.02×10^6		0.02
			Subtotal	0.22
Drying	Btu	1.90×10^6		1.90
Transportation	net ton-mile	9,500.0	0.00025	2.38
Bayer processing (20)				
Crushing & grinding electrical energy	kwh	31.43	0.0105	0.33
Lime	net ton	0.10	8.5	0.85
			Subtotal	1.18
Digestion				
Steam	lb	12,143.0	0.0014	17.00
Caustic soda	net ton	0.15	30.00	4.50
			Subtotal	21.50

57

TABLE 33: ENERGY REQUIREMENTS FOR THE PRODUCTION OF ALUMINUM (Continued)

	Unit	Units Per Net Ton of Aluminum	10^6 Btu Per Unit	10^6 Btu Per Net Ton of Aluminum
Clarification				
Electrical energy	kwh	30.48	0.0105	0.32
Starch	---	---	---	0.00
Cooling				
Electrical energy	kwh	5.71	0.0105	0.06
Precipitation-filtration				
Electrical energy	kwh	66.67	0.0105	0.70
Evaporation				
Steam	lb	6,829.0	0.0014	9.56
Spent liquor recovery				
Electrical energy	kwh	69.52	0.0105	0.73
Net steam usage	lb	593.0	0.0014	0.83
			Subtotal	1.56
(19)				
Calcination				
Natural gas	ft^3	7.720.0	0.001	7.72
(13, 14, 19)				
Carbon anode manufacture				
Raw petroleum coke	net ton	0.425	30.0	12.75
Coke transportation (500 miles by rail)	net ton-mile	212.5	0.00067	0.14
Calcining				
Hydrocarbon fuels	Btu	---	---	1.0
Electrical energy	kwh	20.0	0.0105	0.21
Crushing and grinding				
Electrical energy	kwh	5.0	0.0105	0.05
Pitch binder	gal	28.44	0.16	4.55
Pitch transportation (400 miles by rail)	net ton-mile	52.4	0.00067	0.04
Natural gas for baking	ft^3	2,094.0	0.001	2.09
			Subtotal	20.83
(13, 14, 19)				
Carbon cathode manufacture				
Anthracite	net ton	0.02	25.94	0.52
Anthracite transportation (500 miles by rail)	net ton-mile	10.0	0.00067	0.07
Electrical energy for calcining	kwh	40.0	0.0105	0.42

TABLE 33: ENERGY REQUIREMENTS FOR THE PRODUCTION
OF ALUMINUM (Continued)

	Unit	Units Per Net Ton of Aluminum	10^6 Btu Per Unit	10^6 Btu Per Net Ton of Aluminum
Crushing and grinding				
Electrical energy	kwh	0.2	0.0105	0.00
Pitch binder	gal	0.74	0.16	0.12
Pitch transportation (500 miles by rail)	net ton-mile	0.17	0.00067	0.00
Electrical energy for baking	kwh	8.0	0.0105	0.08
			Subtotal	1.21
(19) Reduction				
Makeup cryolite ($Na_3 AlF_6$)	net ton	0.035	155.0	5.44
Cryolite transportation (300 miles by rail)	net ton mile	10.5	0.00067	0.01
Makeup aluminum floride	net ton	0.02	51.4	1.02
Aluminum floride transportation (300 miles by rail)	net	6.0	0.00067	0.00
Fluorspar (CaF_2)	net ton	0.003	1.59	0.00
Electrical energy (including ancillary)	kwh	16,000.0	0.0105	168.00
			Subtotal	174.47
TOTAL				243.90 (21)

Reference: 49

Material losses due to trimming and conditioning during rolling may be 25%.[53] At this loss rate the energy per pound of finished steel increased to 16,186 Btu. Hot rolling energy requirements have been calculated from data[53] on typical soaking furnaces and rolling mills to be essentially 1000 Btu per pound. Other energy consuming operations include slab and coil transport in the plant, steam descaling and slitting. While the exact energy consumption has not been determined it does appear that reported[35] values of 23,000 to 25,000 Btu per pound of finished sheet are reasonably correct.

The effect of alloying elements of Table 26 on the energy consumption of aluminum was considered by taking the percentage of each element times its energy of production. There was a slight change of up to 3% for all alloys except A390 and 5182. Alloy 5182 increased less than 1% and alloy A390 decreased by 5% to a value of 116,440 Btu per pound.

While data is not yet available on the newer sheet alloys in regard to metal lost during rolling and the energy consumed for the actual rolling, the energy cost of manufacturing steel sheet can be used for estimating aluminum energy costs. The heating and rolling of ingots to sheet thickness should require essentially the same quantity of energy as for steel. Based on this assumption a value of 10,000 Btu is considered reasonable. The production energy of the sheet alloys without scrap recycling is set as 132,000 Btu per pound.

Listed in Table 34 are the production energies for selected chemical feedstocks.[51] These materials are used in the compounding of the selected thermoset matrices. Reinforcement and filler production energies are also listed.

Using this data the energy required to produce a pound of epoxy, polyester and phenolic resin were determined as shown in Figures 11, 12 and 13. The data for the resins, the fillers and the fibrous reinforcements were then combined as shown in Table 35 to obtain the production energies of selected reinforced thermosets This information is then summarized in Table 36. The materials energy consumption has been listed on a per pound and a per cubic inch basis. It is interesting to note the large effect of glass and carbon fibers on the resulting production energies.

Energy requirements to produce thermoplastic resins for subsequent molding are summarized in Table 37. These values have been combined with the values for the fiber and filler requirements from Table 34 and the resultant production energies are summarized in Table 38.

TABLE 34:   PRODUCTION ENERGIES FOR SELECTED FEEDSTOCKS

Substance	Production Energy Btu/lb.
Acetone	35051
Acrylonitrile	31978
Ammonia	18147
Benzene	22604
Bisphenol - A	49527
Chlorine	16754
Ethylene Oxide	49976
Formaldehyde	22122
Hydrogen	216792
Maleic Anhydride	32882
Nitric Acid	8204
Phenol	40947
Propylene	28918
Sodium Chloride	1919
Sodium Hydroxide	17548
Styrene	42318
Glass Fiber	28000
Carbon Fiber	81136
Fillers	6000

Reference: 51

FIGURE 11: DETERMINATION OF PRODUCTION ENERGY OF EPOXY RESIN

The Epoxy modified system generally used for filament winding consists of an epoxy resin and a diamine. (For this example, we shall consider phenylene diamine (4).)

The most common epoxy resins are obtained by reacting epichloro-hydrin with bisphenol - A in varying ratios.
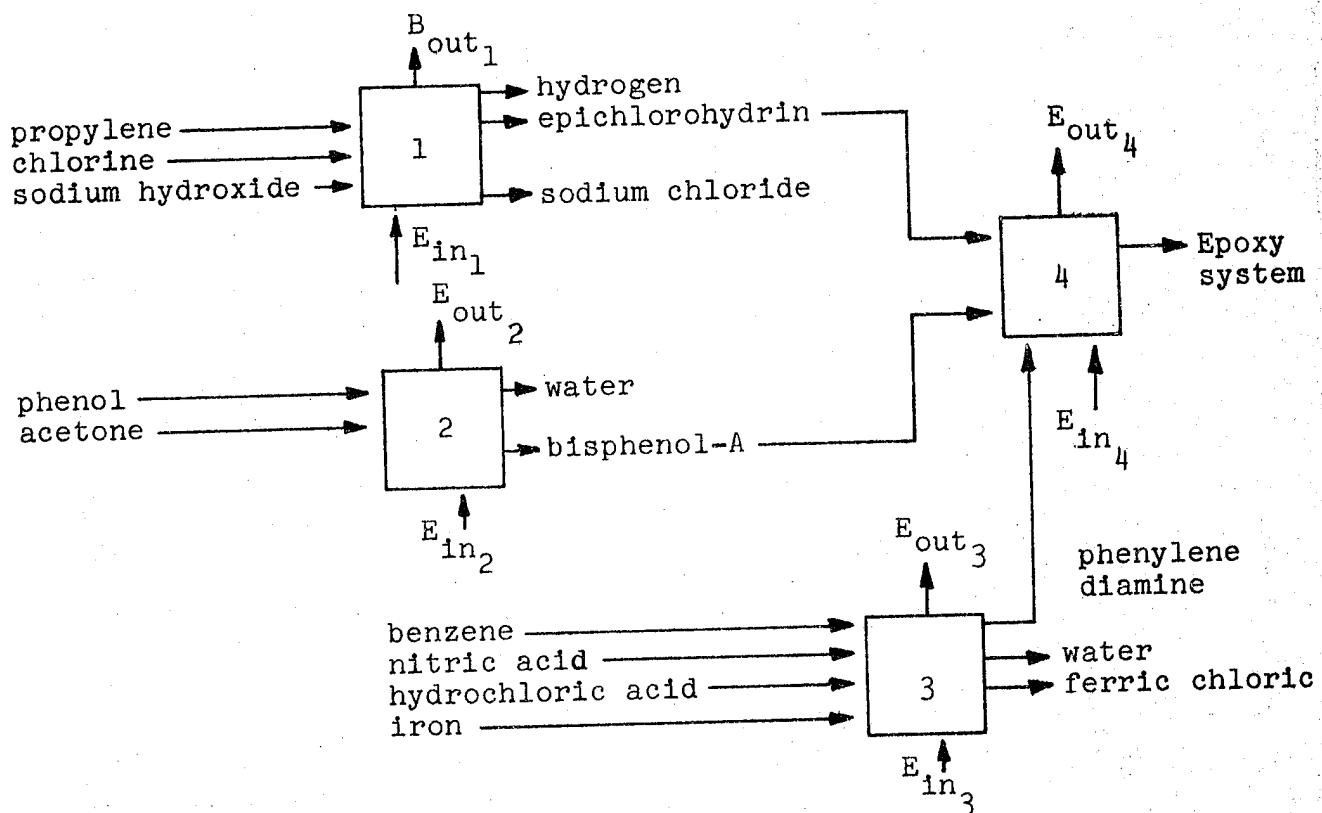
Consider Box 1:

The overall chemical equation for the reaction is:

$$CH_2 = CHCH_3 + Cl_2 + NaOH \longrightarrow CH_2\underset{O}{\diagdown\diagup}CHCH_2 \, Cl + NaCl + H_2$$

M.W.   42   70   40   92   58   2
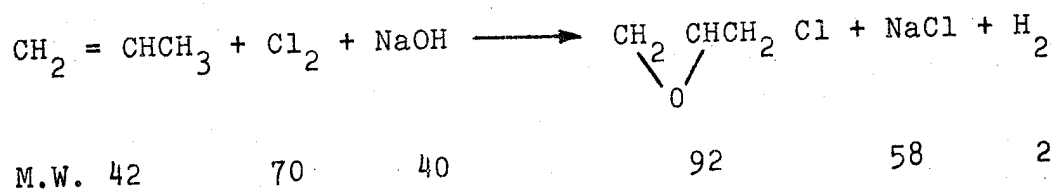
FIGURE 11: DETERMINATION OF PRODUCTION ENERGY OF EPOXY RESIN
(Continued)

COMPOUND	F_1	E_1 (BTU/lb.)	$F_1 E_1$
Propylene	.456	28918	13187
Chlorine	.761	16754	12750
Sodium hydroxide	.435	17548	7633
Hydrogen	.022	216792	4769
Sodium chloride	.630	1919	1209

$\therefore$ Production Energy for epichlorohydrin

$$= 27592 + (E_{in_1} - E_{out_1}) \text{ BTU/lb.}$$

Consider Box 2:

Chemical Equation:

$$2\ HO-\bigcirc \quad + CH_3\overset{O}{C}CH_3 \longrightarrow HO-\bigcirc-\underset{CH_3}{\overset{CH_3}{C}}-\bigcirc-OH + H_2O$$
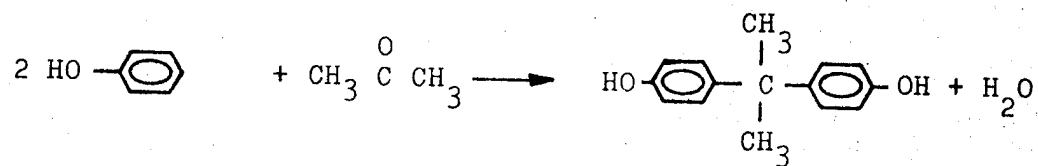
M.W.	188	58	228	18

COMPOUND	F_1	E_1 (BTU/lb.)	$F_1 E_1$
Phenol	.825	40947	33781
Acetone	.254	35051	8903
Water	–	0	

$\therefore$ Production Energy of Bisphenol – A

$$= 42684 + (E_{in_2} - E_{out_2}) \text{ BTU/lb.}$$

(In Hill and Teasley's Paper, they report Production Energy of Bisphenol – A as being 49527 BTU/lb.)

FIGURE 11:   DETERMINATION OF PRODUCTION ENERGY OF EPOXY RESIN
              (Continued)

Consider Box 3:

Overall chemical equation:

$$\text{C}_6\text{H}_6 + 2\text{HNO}_3 + 12\text{ HCl} = 4\text{ Fe} \longrightarrow \text{NH}_2\text{—C}_6\text{H}_4\text{—NH}_2 + 4\text{FeCl}_3 + 6\text{H}_2\text{O}$$

M.W. 78   126   438   224   108   650   108
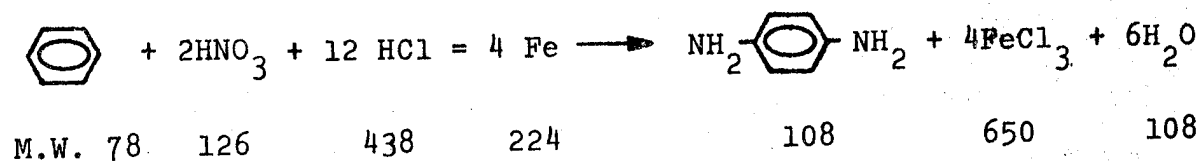
COMPOUND	F_1	E_1 (BTU/lb.)	$F_1 \times E_1$
Benzene	.722	22604	16320
Nitric Acid	1.167	8304	9691
Hydrochloric Acid	4.056	22235**	90185
Iron	2.074	10000*	20740
Ferric Chloride	6.019	14426***	86830
Water	–	0	

  * Ref. 1

** Obtained from $\text{H}_2 + \text{Cl}_2 \longrightarrow 2\text{HCl}$

*** Obtained from $2\text{Fe} + 3\text{Cl}_2 \longrightarrow 2\text{FeCl}_3$

∴ Production Energy of phenylene diamine

$$= 50106 + (E_{in} = E_{out})\ \text{BTU/lb.}$$

64

FIGURE 11: DETERMINATION OF PRODUCTION ENERGY OF EPOXY RESIN (Continued)

Consider Box 4:

Possible reaction:

$$n \ (6 \ CH_2 \ CH \ CH_2Cl) + n \ (4 \ HO \bigcirc \overset{\overset{CH_3}{|}}{\underset{\underset{CH_3}{|}}{C}} \bigcirc OH) + n \ (NH_2 \bigcirc NH_2)$$
$$\overset{\diagdown}{\underset{O}{\diagup}}$$

$$\longrightarrow \quad polymer$$
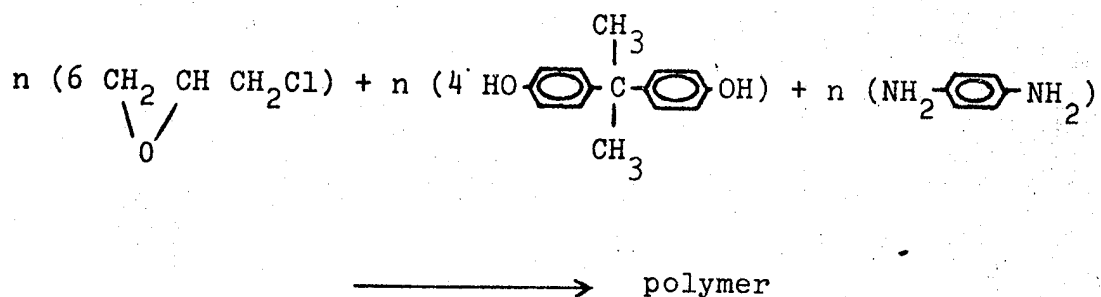
| N.W. | 555 | 912 | 108 $\longrightarrow$ 1575 |

COMPOUND	F_i	E_i, (BTU/lb.)	$F_i \ E_i$
Epichlorohydrin	.353	27592	9740
Bixphenol – A	.580	49527	28726
Phenylene diamine	.069	50106	3457

∴ Production Energy of a hardened epoxy resin

$$= 41923 + C \ \ BTU/lb. \overset{\sim}{=} 41923 \ BTU/lb.$$

C = a term which accounts for $\sum\limits_{i=1}^{4} (E_{in_i} - E_{out_i})$

65

FIGURE 12: DETERMINATION OF PRODUCTION ENERGY OF POLYESTER RESIN

Polyester Resin:
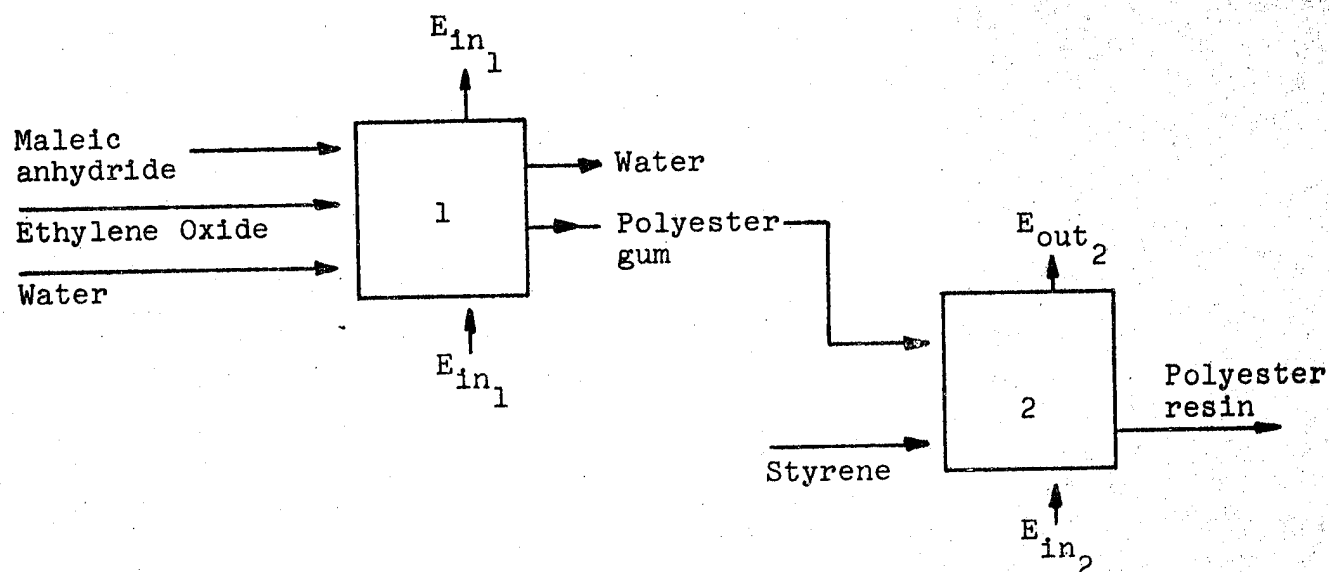
Consider Box 1:

Chemical reaction:
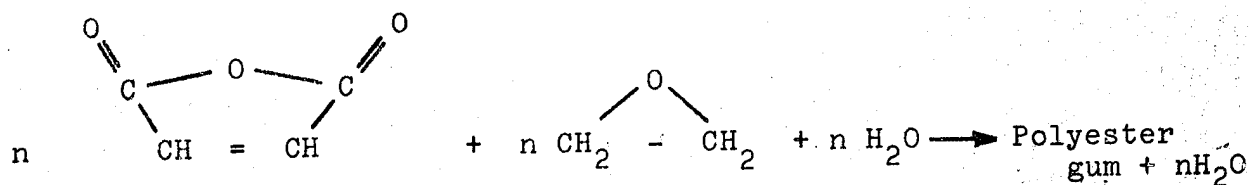
M.W.	98	+	44	+	18 $\longrightarrow$ 142

COMPONENT	F_i	E_i, (BTU/lb.)	$F_i E_i$
Maleic Anhydride	0.690	32882	22689
Ethylene Oxide	0.310	49976	15493

$\therefore$ Production Energy of polyester gum = 38182 BTU/lb.

FIGURE 12:   DETERMINATION OF PRODUCTION ENERGY OF POLYESTER RESIN
             (Continued)

Consider Box 2:

Polyester gum + Styrene ⟶ Polyester resin

COMPONENT	F_1	E_i, BTU/lb.	$F_1 E_1$
Styrene	0.30	42318	12695
Polyester	0.70	38182	26727

∴ Production Energy of polyester resin = 39432 +

$$\sum_{i=1}^{2} (E_{in_i} - E_{out_i}) \approx 39432 \text{ BTU/lb.}$$

(Production Energy of polyester resins have been reported to
be 39000 BTU/lb. in a recent OCF bulletin (Ref. 3)).

67

FIGURE 13:   DETERMINATION OF PRODUCTION ENERGY OF PHENOLIC RESIN

Chemical reaction:

$$2n \; \bigcirc\!\!-OH + 3n^2 \; HCHO \longrightarrow phenolic \; resin + 2n \; H_2O.$$
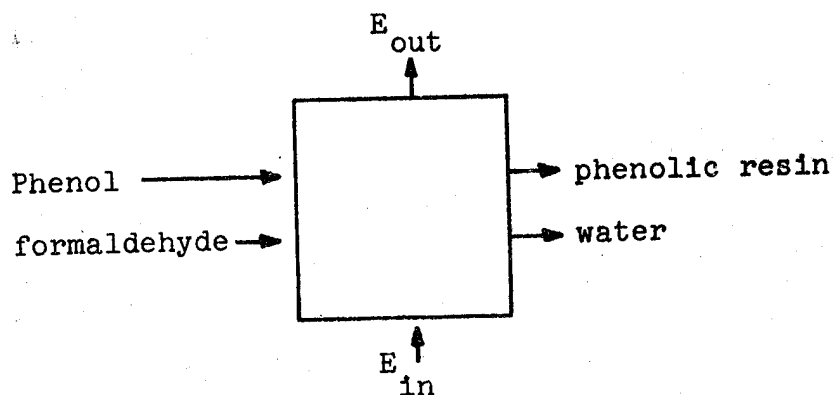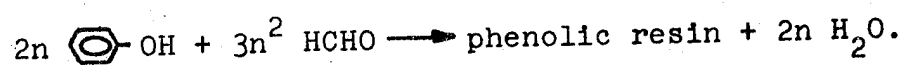
M.W.   188 $\longrightarrow$ 164   54

COMPOUND	F_1	E_1, (BTU/lb.)	$F_1 E_1$
Phenol	1.146	40947	46925
Formaldehyde	.183	22122	4047
Water	–	0	

$\therefore$ Production Energy of phenolic resins

= 50972 + $(E_{in} - E_{out})$ BTU/lb.

$\cong$ 50972 BTU/lb.

TABLE 35:   PRODUCTION ENERGY CALCULATIONS FOR FRP SYSTEMS

COMPONENT	PERCENTAGE BY WEIGHT	PRODUCTION ENERGY, BTU/LB.	PERCENT TIMES PRODUCTION ENERGY
A) BMC			
Polyester Resins	25	39432	9858
Filler	63	6000	3780
Glass	12	28000	3360
Energy to Mix & Mold			1500

∴ Production Energy = 18498 BTU/lb.

COMPONENT	PERCENTAGE BY WEIGHT	PRODUCTION ENERGY, BTU/LB.	PERCENT TIMES PRODUCTION ENERGY
B) SMC			
Polyester Resins	30	39432	11830
Filler	45	6000	2700
Glass	25	28000	7000
Energy to Mix & Mold			1500

∴ Production Energy – 23030 BTU/lb.

COMPONENT	PERCENTAGE BY WEIGHT	PRODUCTION ENERGY, BTU/LB.	PERCENT TIMES PRODUCTION ENERGY
C) H-SMC			
Polyester	35	39432	13801
Glass	65	28000	18200
Energy to Mix & Mold			1500

∴ Production Energy = 33501 BTU/lb.

COMPONENT	PERCENTAGE BY WEIGHT	PRODUCTION ENERGY, BTU/LB.	PERCENT TIMES PRODUCTION ENERGY
D) D-SMC			
Polyester	30	39432	11830
Glass	70	28000	19600
Energy to Mix & Mold			1000

∴ Production Energy – 32430 BTU/lb.

COMPONENT	PERCENTAGE BY WEIGHT	PRODUCTION ENERGY, BTU/LB.	PERCENT TIMES PRODUCTION ENERGY
E) H-SMC			
Polyester	56	39432	22082
Carbon	44	81136	35700
Energy to Mix & Mold			1500

∴ Production Energy = 59282 BTU/lb.

TABLE 35:   PRODUCTION ENERGY CALCULATIONS FOR FRP SYSTEMS
            (Continued)

COMPONENT	PERCENTAGE BY WEIGHT	PRODUCTION ENERGY, BTU/LB.	PERCENT TIMES PRODUCTION ENERGY
F) D-SMC			
Polyester	56	39432	22082
Carbon	44	81136	35700
Energy to Mold & Mix			1000

∴ Production Energy = 58782 BTU/lb.

G) D-SMC			
Epoxy	56	41923	23477
Carbon	44	81136	35700
Energy to Mold & Mix			1000

∴ Production Energy = 60177 BTU/lb.

H) D-SMC			
Phenolic	56	50972	28544
Carbon	44	81136	35700
Energy to Mix & Mold			1000

∴ Production Energy = 65244 BTU/lb.

Production Energy values of FRP systems have bee summarized
in Table III.

70

TABLE 36: PRODUCTION ENERGIES OF SELECTED
REINFORCED THERMOSETS

Substance	Production Energy, Btu/lb.	Density lbs./cu. in.	Specific Production Energy, Btu/cu. in.
EMC-Glass-Polyester	18498	.0509	942
SMC-Glass-Polyester	23030	.0664	1529
H-SMC-Glass-Polyester	33501	.0632	2117
D-SMC-Glass-Polyester	32430	.0661	2144
H-SMC-Carbon-Polyester	59282	.0516	3059
D-SMC-Carbon-Polyester	58782	.0516	3033
D-SMC-Carbon-Epoxy	60177	.0516	3105
D-SMC-Carbon-Phenolic	65244	.0516	3367

TABLE 37: ENERGY REQUIREMENTS FOR THERMOPLASTICS

Plastic	Btu/lb*	Reference
Nylon 66	92,500	66,68
Nylon 6 (Caprolactam)	92,683	66,68
Polyphonylene Oxide (PPO)	107,692 [1,3]	66,68
Acetal	105,000 [1,3]	66,68
Polyester (Thermoplastic)	68,085 [1,3]	66,68
Polystyrene	43,243 [1,3]	66,68
Urethane (Foam)	38,000 [4]	69
Acrylonitrale Butadiene Styrene (ABS)	48,649 [1,3]	66,68
Polyethylene		
Low Density	24,574 [2]	67
	30,303 [1,3]	66,68
High Density	15,393 [2]	67
	36,764 [1,3]	66,68
Polypropylene	40,751	51
Polycarbonate	67,442	66,68
Urethane Elastomer	27,273	69

*Fuel and Feedstock

72

TABLE 38:   PRODUCTION ENERGIES FOR CANDIDATE
REINFORCED THERMOPLASTICS

Material	Btu/Pound
Polypropylene (PP)	40,751
Polypropylene 40% Glass (PP-40G)	35,650
Polypropylene 40% Talc (PP-40G)	24,522
Polypropylene 40% Glass Laminate (PP-40GL)	35,650
Nylon (N)	92,683
Nylon 40% Glass (N-40G)	66,810
Nylon 40% Carbon (N-40C)	88,064
Polycarbonate (PC)	67,442
Polycarbonate 40% Glass (PC-40G)	51,665
Polyester (PES)	68,085
Polyester 30% Glass (PES-30G)	56,060
Polyester 30% Carbon (PES-30C)	72,000
Polystyrene (PS)	42,243
Polystyrene 30% Glass (PS-30G)	37,970
ABS	48,649
ABS - 40G	40,389

2.9 Recyclability

The recycling of steel materials has been an accomplished fact for many years. Recycling includes all materials within a steel plant which contain a large quantity of iron. Flue dusts, mill scale and grindings are included. Scrap from fabricating industries such as automobile stamping plants and discarded vehicles are recycled in steel mills. Recycled steel is produced in the open hearth, basic oxygen and electric furnaces. The electric furnace uses 100% scrap.

In discussions with a major steel producer[63] a number of potential problems were considered. Alloying elements in steel to be recycled which are not oxidized build up in steels. Such elements are copper, nickel and tin. These elements should be removed from scrap mechanically. They reduce hot toughness during rolling. Chromium and molybdenum are partially oxidized and result in low ductility in autobody steel. If these five elements are in the scrap they must be diluted by using more pig iron (hot metal).

Zinc present in scrap volatilizes and is collected in wet scrubbers. This material is difficult to dispose of since the zinc will dissolve in water and possibly polluting local water systems.

Sulfur contamination can occur if the scrap charge contains lubricants, oils, asphaltic coatings and rubber materials.

Shredded old steel scrap is generally cleaner than bundled old scrap but shredded material often produces a bridging effect over a molten pool in the basic oxygen furnace. This bridge is a skin of material which has fused together. The molten pool of metal sits in the furnace under this skin without bonding it.

Similarly, aluminum alloys are recyclable if the materials are first cleaned and segregated to prevent alloying impurities.[64,65] Aluminum beverage cans have been recycled successfully in recent years because they are all of essentially the same composition and are readily recognized and separated.

Unsegregated aluminum scrap is melted and an analysis made of the resulting ingot. This material can then be added to known compositions or diluted. Scrap is frequently used in castings rather than sheet since castings have a greater tolerance for alloying element contamination.

Magnesium alloys can also be, and are, recycled. The restraints of cleanliness pertain to the magnesium alloys also.

Thermoplastics materials can be recycled when their composition is known and they can be added to virgin material of the same type. Again like aluminum and magnesium alloys a clean scrap material can be readily recycled. Reinforcements may be degraded by reducing their length when plasticated in an extruder. Thermoset plastics are not readily recycled. Some industries are using ground thermoset materials as fillers for new components. The benefits gained by using this ground filler compared to low cost mineral fillers is unknown.

2.10 Candidate Materials Summary

There are a number of factors which will force a reduction in the average or composite weight of American made vehicles. These include material and energy conservation and the increased costs due to shortages of both. Sources of energy appear to be the most vital link since if the energy supply was sufficient, lower grade raw materials could be processed to provide the necessary metals, plastic resins and composite reinforcements.

Depending upon the statistics used for automobile performance, the effect of a one pound weight reduction can be calculated. These values are normally in the range of 1×10^{-5} to 2×10^{-5} gallons per pound for one mile. If a lifetime of 100,000 miles is assumed then the gasoline saved is 1 to 2 gallons over the lifetime of the vehicle for each pound reduction in weight. The energy value of a gallon of gasoline, considering the energy used to produce it, is approximately 150,000 Btu.

The aluminum alloys, if used in place of steel, could reduce the weight of the vehicle approximately one pound for each pound of aluminum alloy used. Similarly 1.2 pounds of reinforced plastic may replace 2 pounds of steel. Without considering the energy of manufacturing and the energy saved by the recycling of aluminum and plastics it is obvious that a net savings in energy would result by using aluminum or plastics in place of steel.

All of the ferrous and non-ferrous materials listed in Tables 4 and 5 must be considered as candidate materials for future automobiles. Certain of these materials may not be used and variations, new alloys, within these areas may be developed replacing those listed. New alloy developments would be expected to improve properties but have minimal effect on supply or production energy requirements.

The reinforced thermoplastic materials, Table 9, should also be considered as future automotive materials. Their use may be relegated to lesser load carrying structure and other applications where creep is of less importance. Newer thermoplastics are being developed, e.g., polyimide, polyphenyl sulfide and poly-phenylene, which possess better resistance to high temperatures. These materials

are at present very expensive, $14.00 per pound, and in the early stages of development as major structural parts. If further development reduces their costs they would become candidate materials.

Reinforced thermoset plastics, Table 13, are competitive with metallic materials for automotive structure. Hybrid materials consisting of mixes of fiber reinforcement within a resin matrix offers a means of reducing costs of the materials. The most effective application of these fibers requires manufacturing processes which will preserve or obtain a desired fiber orientation. These processes have not been developed except for small discrete parts and manufacturing costs will restrain the application of these materials.

The final selection of candidate materials depends on other factors to be discussed in following sections of this report. While the steels, aluminum alloys and reinforced thermoplastics can be recycled, the mechanism of segregating these materials, and the related costs, from automobile hulks are an important factor and will be discussed further in section 3.

Evaluation of the effects of using the candidate materials on the vehicle safety and crash energy management must also be completed prior to final material selection and applications. This evaluation will be discussed in sections 6 and 7.

If a mix of materials is to be used then a number of factors including: thermal expansion, galvanic corrosion and methods of manufacturing and assembly must also be evaluated. This will be discussed in section 4.

An overall energy savings obtainable using the candidate materials in future vehicles will depend upon the final weight and the amount of each material used. While it would appear feasible to reduce energy consumption by replacing steels entirely with either aluminum alloys or reinforced plastics, other factors must be considered such as first cost, and the source of energy. The steel industry uses coal primarily and would appear to have an advantage over the other materials in this respect.

3.0 DISPOSABILITY OF DISCARDED VEHICLES

When the automobile has served the owner and is to be dis-
carded, it may be traded in on a new purchase or abandoned. If
it is accepted as a trade-in then the existing economic system
provides for its disposal as spare parts or by recycling. When
the vehicle is abandoned, the local government usually must pro-
vide a method of collecting and transporting these vehicles to
a disposal area. Various means of taxing and creating incentive
have been proposed[72,75] to assure that all discarded vehicles
enter into the disposal system.

There has been an apparent measure of success as the number
of abandoned vehicles has been reduced considerably within the
past two years. This improvement has been attributed to higher
scrap prices and an economic incentive rather than a regulatory
pressure.[73] Any further vehicle design which would enhance the
economic incentive rather than an expensive tax and administration
cost would be most desirable.

3.1 Recycling of Automotive Materials

Discarded vehicles are presently either pressed into bundles
or shredded. Tires, starter motors, alternators, batteries, radia-
tors, fuel tanks and bumpers are removed prior to bundling or shred-
ding. Tires and fuel tanks are removed to prevent explosions during
melting and to reduce sulfur and lead contamination of the melt and
atmosphere. The other items are salvaged and repaired for resale.

As stated in section 2.9 the ability to recycle any material,
metal or plastic, depends on the cleanliness and degree of segre-
gation. Copper, nickel and chromium on bumpers that are not re-
pairable and other trim items remain in the bundle or shreddings
and enter into the melting furnaces. Copper, lead and tin remain
with electrical wiring, soldering joints, lights and small motors.
Lead, tin and zinc remain with steel body parts as coatings and
body solders. Molybdemum and other alloying elements contained
in bearings, bushings and drive shafts also remain.

The retention of these contaminating elements is greater in
press bundles than in the shredded material. During the shredding
process, magnetic, air and flotation separation produces a cleaner,
better segregated material. Bundled automotive scrap is approxi-
mately $20.00 per ton less in value than shredded scrap. Steel-
makers prefer the shredded material from a cleanliness stand point
but the press bundled material melts more readily. Shredded material
charged into a furnace often forms a bridge over the molten pool
which must be broken during remelting.

With present techniques, automobile hulks can not be recycled
directly into a material suitable for fabricating a new vehicle.

The impurity level must be reduced by dilution with virgin pig iron (hot metal). Due to the thermochemical balance of the basic oxygen furnace a maximum scrap charge is 30 percent of the total heat. Material remelted in the electric furnace is used for lower quality products such as reinforcing bar (rebar) and other construction applications.

Research and development[74] activity has been completed to remelt automotive hulks and refine the steel sufficiently without virgin metal dilution for automotive applications. The results of this work indicate that present technology is insufficient.

A similar situation exists in the aluminum and plastics industries. Unsegregated aluminum is currently recycled primarily in castings[73] which have lower requirements in finish and toughness than wrought products. Beverage cans have been reportedly recycled into new cans. In this case the composition of the metal is known and segregation is readily achieved due to the recognizable shapes. When unrecognizable and unknown composition scrap is accumulated it is often melted and cast into pigs. Analysis of the pigs is completed, and the ability to use the material is then determined. Aluminum alloys in an automobile would be contaminated by the same substances which contaminate steels.

Recycled thermoplastic scrap must be free of all metals. Clean segregated plastic scrap from automobiles could be used with virgin material for low quality automotive parts such as splash shields and ducting. Since there is some degradation due to oxidation and fiber reinforcement break-up, the resulting properties of 100% recycle are lower than those for virgin materials.

To obtain the full value of recycled scrap materials from automotive hulks a method of segregating and identifying each of the materials is necessary. This would in part be obtained by making components which are readily removed and identified from the more shortage critical and energy critical materials. Another approach might consist of making vehicles of essentially one material, such as all plastic, all aluminum or all steel instead of mixing the three in one structure.

3.2 Energy Conservation

Energy conservation obtained through the recycling of steel contained in automobile hulks is now accounted for in the overall industry. Hulks which are recycled in basic oxygen furnaces with virgin pig iron is the primary source of steel for fabrication. The energy requirements for the production of steel using the basic oxygen furnace should then be considered as the value of energy cost to make a vehicle.

Energy conservation possible with aluminum alloys 6009 and 6010 can be substantial if the alloys are used by themselves or together

78

in a hang-on component such as a hood and deck lid.[76] In this case the materials recycled would require only 5 percent of the energy to produce new sheet stock as the sheet originally produced from ore. Vehicle reprocessers could remove the hood by torch cutting and remove hood and deck lights, insulation, locks, hinges and latches if made from another metal. The necessity of removing these smaller items can be appreciated by noting that one percent of a possible aluminum hood weight of 30 pounds is only 0.3 pounds. Steel latches, hinges or tapping blocks weighing 0.3 pounds total if not removed would contaminate the alloy over specification.

Recycling of segregated thermoplastic scrap at a rate of 30 percent of the charge into a plasticator has the potential of reducing the energy requirements by the same amount. Again as in the case of aluminum, to achieve this the plastic component must be removable from the vehicle without contaminating materials nor metallic objects which would destroy the plasticating and molding equipment.

Thermoset polyester and epoxy cannot be recycled in large quantities with existing equipment and currently there can be no reduction in production energy assigned to these materials by recycling into a new product.

3.3 Materials Conservation

Materials conservations obtainable through recycling should be of the same magnitude as that expressed in energy conservation. Steel materials in automobiles are approaching 100 percent recycle. Even though this material is not necessarily used in the production of new automobiles, it does reduce the depletion of basic raw materials in the overall economy.

Similar conservations can be obtained with aluminum and thermoplastic materials provided an economic system of segregation is developed.

Since reinforced thermoset plastics can not be considered recyclable at present there is no material conservation due to recycling. If the experiences encountered in small pleasure boats were applied to automobiles then reinforced thermosets may be considered effective in conserving materials. Pleasure boats made from reinforced polyesters are frequently refitted with engines and other equipment having a finite life. Similarly, reinforced thermoset automotive structure may outlive several engines.

3.4 Ecological Impact

The application of aluminum alloys and HSLA steels in future automobiles is not expected to significantly change the current methods of disposal.[73] As the amount of aluminum increases there would be a subsequent increase in manual labor requirements to

separate these metals. This in turn is dependent upon the aluminum scrap market. Storage would be required until a sufficient quantity of material is inventoried for a car load shipment. Larger scrap dealers may well compact the aluminum scrap by melting and casting into ingot form. Aluminum scrap remaining in the steel scrap will be oxidized and slagged in the steel melting furnaces and should not alter present practices.

Increasing application of plastics could create problems. Much of this material is currently used in landfill and if continued would increase the costs of disposal. Again there could develop an inventory or temporary storage problem until sufficient material is accumulated for transport. Incineration, if now used to dispose of plastics in some facilities, could not continue with larger applications of plastics without additional capital costs to prevent air pollution. The increased use of plastics has been examined in the light of vehicle disposal[73] for the Environmental Protection Agency. This study indicated that no major problems would occur which could not be overcome.

Recycling of thermoplastic materials in automobiles could be more attractive by specifying the same materials for trim and non-load carry applications. For example, all "intermediate" car lines of a vehicle producer could use polypropylene based plastics while the same parts for compact car lines were made from ABS. Manual labor costs would undoubtedly increase to identify the vehicle, schedule and store the materials. Shredder operators would not necessarily have to remove, by hand, each of the parts prior to shredding.

3.5 Non-Recycling Disposal

Disposal of non-recyclable materials is accomplished currently by landfill primarily. This type disposal is used for the organic based materials which include plastics.

Plastics materials are a source of heat energy. The heats of combustion of several materials are compared in Table 39. Reinforcements and fillers such as glass fibers and inert minerals would reduce the heat of combustion on a per pound basis of the material actually used. These materials are potential sources of heat energy.

Several cities have conducted studies on the beneficial use of municipal waste.[78] The heating value of such waste is around 5000 Btu/lb and is considered a valuable resource as a fuel for electric generation. Tests in the city of St. Louis with Union Electric Company indicated that such waste could be used at a rate of 12.5 tons per hour with coal. The rated load of the boiler was 125 MW. Experiences with these tests have been favorable from a cost and pollution evaluation. Such a program of utilization of municipal wastes could be readily applied to shredded unrecyclable

TABLE 39:   HEATS OF COMBUSTION

Material	Btu/Pound
Wood	8,835
Polyester	9,300
Nylon - 6	12,989
Bituminous Coal	15,179
Urethane	16,000
Polystyrene	17,870
No. 1 Fuel Oil	19,800
Polyethylene	20,050

Reference: 77

plastic scrap from automobiles. Based on the values for municipal waste, a ten percent reduction in coal use would be expected.

3.6 Summary of Disposability

The incorporation of HSLA steels will not alter the current methods of disposing of vehicles nor will their use produce new problems. Since HSLA materials will be used to reduce weight the quantity of steel per vehicle will decrease. This effect could develop a higher demand and price for scrapped vehicles which in turn would develop an incentive to collect and recycle.

Corrosion of HSLA steels will be more ciritcal than current low carbon steels due to thinner gages and higher stresses. A greater use of metallic coatings, such as zinc, might be expected to control this corrosion. The use of zinc instead of organic paint systems would be detrimental to the recycling as described in section 2.9.

Recycling of wrought aluminum alloys is feasible although there is no experience in recycling entire aluminum vehicles nor those extensively made of aluminum alloys. Using the value for rolling sheet, section 2.8, from virgin material and the energy costs of remelting scrap, section 3.2, a new production energy can be estimated. If all of the aluminum sheet is obtained from ore the production energy would be 132,000 Btu/pound. If 100% of the aluminum sheet is obtained from scrap the production energy is 5%[81] of 122,000 Btu per pound of ingot plus 10,000 Btu for conversion to sheet or 16,000 Btu per pound.

It would seem difficult to ever produce aluminum sheet directly from scrap for two reasons. Approximately 35% of the sheet shipped is returned as trimmings and fabrication scrap. The second reason is based on the current steel recycling. A minimum contamination will probably occur in recycled automotive hulks or components requiring some dilution. Based on these two factors the total scrap charge into a melting furnace has been arbitrarily picked to be 50%. Using 50% of virgin material and 50% of scrap the production energy for aluminum sheet has been reduced to 74,050 Btu per pound. This energy savings is dependent upon using alloy mixes of 6009 and 6010 in automotive sheet structure to reduce or eliminate the need for scrap segregation.

The energy conservation possible with reinforced thermoplastics can be calculated in the same way assuming all of the trim and load carrying items are made from one material in a vehicle for easy segregation. The energy requirements for recycling of thermoplastic[82] scrap in injection molding is approximately 3000 Btu per pound which includes granulating. Using a maximum of 30% recycle, which has been frequently suggested, the energy requirements per pound of product can be determined. To the values of the reinforced grades in Table 38 has been added the molding energy and this has

82

been used on a 70/30 ratio with recycled materials to determine new values for production energy based on recycling.

The thermosets are not considered recyclable yet the value of energy which can be obtained upon using these materials must be considered. The heats of combustion from Table 39 have been used to calculate this fuel energy by using the appropriate percentage of resin in all of the materials from Table 36.

The production energies of the steels, aluminum alloys, thermoplastics and thermosets with recycling and fuel value considered have been summarized in Table 40.

TABLE 40: PRODUCTION ENERGIES OF CANDIDATE
MATERIALS WITH RECYCLING

	Btu/Pound
Steels	24,000
Aluminum Alloys	74,050
PP	31,500
PP - 40G	27,950
PP - 40T	20,150
N	67,850
N - 40G	49,750
N - 40C	64,650
PC	50,200
PC - 40G	39,150
PES	50,650
PES - 30G	42,250
PES - 30C	53,400
PS	32,550
ABS	37,050
ABS - 40G	31,250
PES - 20G[a]	15,700
PES - 30G[a]	20,240
PES - 65G[a]	30,700
PES - 65G(D)[a]	29,640
PES - 70C(D)[a]	56,492

a - Thermoset Polyester Matrix

4.0 AREAS OF APPLICATION

Early automobiles were fabricated from wood, with ferrous materials used for engines, suspensions and drive trains. The development of the all steel body and resistance spot welding led to lower price, mass produced vehicles. Demonstration vehicles have been fabricated through the years from aluminum alloys, stainless steels and plastics materials. While these demonstrations have shown that vehicles could be designed and fabricated from materials other than low carbon steel, each material has specific weaknesses or attributes which either limit or promote their use in future automotive structure.

4.1 Properties

Reviewing the data from Tables 4, 5, 9 and 13; all of the candidate materials are superior to low carbon steel (1008-1015) on the basis of specific strength. This data has been listed in Table 41 as a percent of the low carbon steel weight for equal strength. Production energies for the materials taken from Table 40 have then been used to determine the energy requirements for these quantities of each material. The materials have been listed also, with their ranking in Btu's for equal tensile strength. Disregarding the magnesium alloys and Kevlar ^{TM} reinforced plastics, low carbon steel ranks 30th out of the 32 materials on the energy per unit strength basis with only 5182-0 and 6009-T4 ranking lower. The four highest ranking materials had unidirectional fiber orientation and loading in the fiber direction.

To compare the materials on a stiffness basis it is preferable to use the flexural stiffness parameter Et^3 rather than E by itself. In Table 42 the candidate materials have been listed with the percent of low carbon steel weight for equal stiffness. The production energy is also listed for equal stiffness, and again ranked on this basis. All materials show a potential weight reduction compared to carbon steel using the Et^3 parameter. The majority of the reinforced plastics require lower production energy than steel while the aluminum alloys require approximately 1.5 times the Btu's based on this comparison.

The endurance limits (fatigue strength) of steels are generally between 40 and 50 percent of the ultimate strength. Aluminum alloys also possess good fatigue properties, but care must be taken in fabrication and design to eliminate stress risers. Welded joints in aluminum alloys have lower endurance limits, as a percentage of the material strength, than do steels.

Glass reinforced plastics are generally poor in their resistance to cyclic loading. As seen in Table 9 and 13, the data is meager, but the endurance limits are low compared to their ultimate strengths. Carbon fiber reinforced thermosets are, on the other hand, extremely good in fatigue and the endurance limits are 75 to 80 percent of the ultimate strength.

TABLE 41: MATERIALS COMPARISON – PERCENT OF LOW CARBON
STEEL WEIGHT FOR EQUAL TENSILE STRENGTH AND
PRODUCTION ENERGY REQUIREMENTS FOR EQUAL
STRENGTH.

Material	Weight for Equal Strength; % of Low Carbon Steel	Production Energy for Equal Strength Btu	Energy Ranking
E60C-(D)	2.1	1263	4
PES-70C-(D)	2.15	1214	3
E62G-(D)	3.4	1141	2
PES-65G-(D)	3.5	1037	1
E60K-(D)	4.8		
N-40C	7.1	4590	7
N-40G	11	5472	8
PES-65G	11	3377	5
PES-45K	13.6		
PP-40GL	14.3	3997	6
7046-T63	15.7	11626	19
PES-30C	16	8544	14
PES-30G	17.2	7267	11
PC-40G	17.8	6969	10
7016-T5	18.8	13921	22
AZ31B-H24	20.2		
6061-T6	21.5	15921	24
PES-30G	23.6	9971	18
N	24	16284	25
AZ91A-F	24.6		
PS	26.3	8560	15
PC	29.2	14658	23
AZ63A-T6	29.8		
2036-T4	30.9	22881	27
PP-40G	30.9	8636	16
SAE-980X	31.1	7464	12
6010-T4	32	23696	28
PES	32.2	16359	26
HK 31B-T6	35.4		
SAE-970X	35.5	8520	13
PES-20G	40.1	6296	9
SAE-960X	41.4	9926	17
PP	43.9	13829	21
5182-0	45.5	33693	31
6009-T4	45.5	33693	32
SAE-945X	55.4	13296	20
ABS	64	23712	29
1008-1015	100	24000	30

86

TABLE 42: MATERIALS COMPARISON - PERCENT OF LOW CARBON STEEL WEIGHT FOR EQUAL STIFFNESS (Et^3) AND PRODUCTION ENERGY FOR EQUAL STIFFNESS

Material	Weight for Equal Stiffness % of Low Carbon Steel	Production Energy for Equal Et^3, Btu	Energy Ranking
PES-70C-(D)	22	12,428	4
E-60C-(D)	24	14,442	8
E-60K-(D)	24		
PES-45K-(D)	34		
N-40C	35	22,627	12
PES-65G-(D)	39	11,559	2
E-62G-(D)	40	13,316	6
PP-40G	42	11,739	3
PS-40G	46		
PES-30C ⓐ	47	25,098	17
PP-40T	47	9,470	1
N-40G	50	24,875	16
PE-40G	50		
Aluminum Alloys	51	37,765	19
PP-60GL	51	14,254	7
PC-40G	51		
PS	52	16,926	9
PES-30G ⓐ	55	23,237	13
PES-65G	56	17,192	10
PP	61	19,215	11
ABS	63	23,341	14
PC	64	32,128	18
PES-30G	65	13,156	5
N	66	44,781	20
PE	75		
Steels	100	24,000	15

ⓐ   Thermoplastic Polyester

The compression strengths of metals are essentially the same as their tensile yield strengths. This should not be confused with failure of a structural column by buckling which may be lower than the true compression strength. As might be expected the compression strengths of reinforced plastics depend upon fiber orientation in a manner similar to the flexural and tensile strengths. Glass fiber and carbon fiber reinforced plastics may have compression strengths equal to their tensile strengths while Kevlar^{TM} reinforced grades have comparatively low compression strengths.

The impact strength (toughness) of a material is determined by striking a small specimen with a mass at low velocity. The specimen may be prepared with stress risers such as machined notches or holes. Loading may be in direct tension or in bending. Various types of testing equipment are available such as drop testers or pendulum testers which permit direct reading of the energy absorbed by the specimen during its failure. This property of materials is difficult to use in design or analysis and is more of a material quality test although minimum impact properties are specified based on experience.

While the yield strength, ultimate strength and modulus of elasticity increase as the testing temperature decreases, the ductility or strain to failure decreases and the energy absorbed in failure decreases. This results in a decrease in the impact strength and the curve of energy absorbed may be gradual or abrupt with decreasing temperatures. Certain steels have large losses in energy absorption within a short temperature range which is then known as the ductile-brittle transition zone or nil-ductility temperature. A similar abrupt loss in toughness may be found in other materials including plastics.

The HSLA steels have good toughness down to -50° F. Aluminum alloys do not exhibit the nil-ductility zone. Lower quality grades of unreinforced thermoplastics do exhibit poor toughness at 32° F and below. Glass fiber reinforcements improve this property and resin blends based on elastomerics are beneficial. The requirement of service should be specified to the resin supplier.

Creep resistance, stress relaxation and limiting service temperature are interrelated in structural applications. The creep resistance decreases and stress relaxation increases with higher service temperatures. Aluminum alloys are relatively resistant to long time static stress up to 350° F. Steels are useful up to 900 to 1000° F. Note that the useful temperatures are near one third of the melting points which is true of most metals. Plastics materials are more susceptible to creep, as might be expected, when considering their low melting or degradation temperatures. This lower resistance to long time static loads must be carefully evaluated in the application of plastics materials. Unfortunately much of this data is yet to be developed. Prior to final selection of a plastic material, the service temperatures

and limiting creep stress should be evaluated by testing.

Uncoated, unprotected low carbon steel is notoriously poor in its resistance to salt water corrosion. A ten year life is predicted for well prepared and painted unalloyed steel. A break in the protective film usually leads to catastrophic failure. Zinc or zinc rich primer coatings on steel are superior to painted surfaces in that a disruption of the coating does not necessarily lead to rapid corrosion. The zinc present in the coating is galvanically sacrificial and protects the uncoated steel areas. The use of zinc however increases the weight of a structural component without increasing its load carrying ability.

Aluminum alloys are nore resistant to salt water than are the steels. Within the family of aluminum alloys the 5000 series and 6000 series are superior. For this reason sheet alloys 5182, 6009 and 6010 are preferred.

Plastics materials are in general resistance to salt water corrosion. Numerous examples of continuous, long time exposure of pleasure craft and recreational facilities have confirmed this characteristic.

Other than environmental water, the main solvents used in automobiles consist of anti-freeze (ethylene glycols), gasoline, engine and transmission fluids, battery acids, windshield washing solutions, brake oils and grease lubricants. Of all these materials the battery acid is the most deteriorating and primarily to steel and aluminum. Plastics are frequently used to contain these solvents during distribution and sale and are quite satisfactory. Solvents exterior to the automobile, especially in severe industrial atmospheres, can be detrimental to the materials considered. It is impossible to foresee all such conditions; however, if the atmospheric contaminants attack the normal painted surfaces then one can expect some attack on the candidate materials. Strong cleaning solvents should not be used on plastic materials since stress crazing may occur. Polycarbonates for example will crack when cleaned with acetone.

4.2 Manufacturing Procedures

The manufacturing procedures for steel and aluminum automotive structure are expected to be essentially the same. The equipment used will in general be the same although the resistance spot welding and arc welding process for aluminum will require some new equipment in the automotive industry. Thermoplastic molding may or may not require equipment capitalization depending almost entirely on part design. Thermoset plastics can be molded on existing equipment although some modifications may be required. For each of the material groups the manufacturing processes used, and processes in development for automotive fabrication will be briefly discussed.

4.2.1 Ferrous Metals

Automobiles are currently fabricated from steel by the following major processes.

1. Stamping, Trimming and Punching
2. Casting
3. Forging
4. Machining
5. Resistance Spot Welding
6. Arc Welding
7. Mechanical Fastening
8. Adhesive Bonding and Sealing

The major portion of the steel used is in the form of cold rolled and hot rolled flat steel. Cast irons and cast steels are used in engines, transmissions and brakes. Forgings are used in engines, transmissions and suspension systems. The greatest amount of machining is performed in manufacturing engines, transmissions, brakes and suspension. Resistance spot welding is used to join the thinner gage sheet metal components. Arc welding is used for frames, sills and areas where resistance spot welding cannot be used because of inaccessability. Mechanical fasteners are used in engines, transmissions, brakes, suspension systems and to attach those components which may require subsequent removal such as doors, hoods, deck lids and front fenders. Weld nuts or tapping blocks may be incorporated in the sheet structure to facilitate mechanical fastening. Adhesive bonding and sealing are used for weatherproofing, noise suppression, and as a substitute for welding to preserve a superior finish.

Flat steel sheet stock is received from the steel mill as coils or stacked sheets. Proper size blanks must be sheared from the incoming stock. This may be accomplished in - line with the stamping presses as the first operation or separately where several size blanks are sheared and separated for later transport to a stamping line. The majority of the blanks are rectangular and are sheared from the incoming steel in a manner to reduce waste. When irregular shaped blanks are required they may be nested to conserve material, and the initial blanking scrap is collected and bundled from the shear for remelting at the steel mill.

The sheared blank of proper size is manually or machine placed in the lead off stamping press. This first form stamping is then removed automatically from the press and positioned manually into a second press which may trim, punch holes or perform a second shaping action. The stamping is then removed and either goes to a third, fourth and fifth press for further shaping or is placed on a conveyor to be assembled with other parts.

The lead off press is generally the largest in tonnage and bed size. Its stroke rate determines the rate of producing parts. The presses following the lead off are smaller in size and faster in

stroke rate. Lead off presses have stroke rates generally in the 10 to 20 strokes per minute. Loading and unloading of the presses takes approximately the same time as the press stroke and 300 to 600 stampings per hour are common. Smaller parts requiring short press strokes may be made at a higher rate up to two times that of a large stamping press line.

Presses for sheet metal stamping are generally mechanically operated. An electric motor is used to bring a flywheel to operating speed, maintain that speed, and recoup the speed after slow down during a press cycle. When the press run cycle is actuated, a clutch is engaged transmitting the flywheel energy to a crank system which lowers and raises the ram. During this cycle the flywheel slows down as energy is consumed in forming the sheet metal.

The force required to form sheet metal can be determined by multiplying the cross sectional area (perimeter x thickness) by the ultimate strength of the material. As an example, an outer hood panel, 50 inch x 50 inch, made from 0.040 inch thick low carbon steel would require a 180 ton ram force. The energy consumed in forming this panel is estimated by multiplying the final tonnage by one half of the draw depth. In the case of the above hood panel the energy required would be 180 inch ton (38.6 Btu).

The inner panel for the hood size considered above would require approximately three times the tonnage, 540, and energy, 115.8 Btu, due to its greater complexity and metal flow requirements.

Additional press operations for restriking, trimming and punching holes, require an estimated 25 percent of the first form operations or 9.7 and 28.9 Btu for the outer and inner panel respectively. The total press energy required is then 193 Btu.

Material requirements to produce the above example hood is 1.35 times the final product weight. The sheet stock trimmed consists of an approximate 4" hold down flange on the periphery of both panels and 25% of the inner panel to reduce final part weight. The initial weight of the two blanks is 82.2 pounds requiring 2,054,880 Btu to produce. The trimmed material is 28.77 pound, equivalent to 719,250 Btu. Since this quantity of material is required to produce the hoods it cannot be subtracted from the total energy cost due to materials.

After the two hood panels are removed from the press lines they are assembled by resistance spot welding or adhesive bonding. Each spot weld in 0.040" to 0.040" steel requires 0.4 Btu, assuming a 50% thermal efficiency. Sixteen spot welds would be required for a total 6.4 Btu requirement. Replacing the 16 resistance spot welds with an epoxy structural adhesive would require 482 Btu for the 0.01152 pounds of adhesive used, including curing.

The estimated total energy requirements to fabricate the above example hood from steel sheet is as follows:

Material	2,054,880
Press Operations	193
Joining-bonding	482
	2,055,555

The greatest portion of the energy is consumed in producing the initial sheet. Based on 10 men performing the tasks necessary to fabricate the hood at a rate of 300 per hour and each man consuming 12 Btu in foodstuff per day, the energy required for each assembly would be 0.05 Btu.

4.2.2 Non-Ferrous Metals

Manufacturing processes for aluminum alloy sheet components are essentially the same as for the steel components. Aluminum alloys have a lower elongation to failure than carbon steels and a greater ratio of thickness strain to in-plane strain during plastic deformation which accounts for lower formability. Part re-designs or additional press operations are required for the aluminum alloys as compared to low carbon steel. Since the yield and ultimate strengths of the automotive aluminum sheet alloys are similar to the low carbon steel there is little difference in press tonnage and energy required in stamping.

In joining aluminum alloys by resistance spotwelding a higher electric current is required due to the lower electrical resistance of the aluminum and the higher heat loss because of its higher thermal conductivity compared to low carbon steel. Efficiency does suffer somewhat in comparison to resistance spotwelding steel, but since welding energy requirements are so small compared to the material energy consumption this is not too important.

The higher welding current requirements for aluminum does require the acquisition of heavier duty welding equipment. For an aluminum alloy of 0.040 inch thickness 30,700 amperes are required while for the same thickness steel 9,000 amperes are required. These higher currents require heavier transformers, cables and welding tools. Heating, I^2R, is greater for the same size welding electrodes and additional water cooling system may be required depending upon the rate of welding. Electrode deterioration due to higher temperatures and subsequent alloying with the aluminum work pieces may result from inadequate cooling. Electrode life in aluminum welding is approximately 20% that for low carbon steel welding.

Aluminum alloys form a tight, high electrical resistant oxide film in air. If this film is present during welding, high tempera-

tures are developed at the electrode - sheet interface. When this film breaks down the aluminum may be melted uncontrollably resulting in blowing out of the entire weld area. If the film does not break down then undersize welds are produced. To assure good weld quality the aluminum must be deoxidized prior to welding. This is most frequently accomplished by acid bath etching although mechanical abrading processes are being developed.

Adhesive bonding of aluminum components does eliminate or reduce the necessity of resistance spot welding. However, the cleaning process prior to bonding is necessary to provide long time durability in the joint.

Resistance spot welds in the aluminum alloys such as 2036-T4 and 6010-T4 in 0.040 thickness have a minimum average static shear strength of 415 pounds. In a low carbon steel of the same thickness the minimum weld strength is 1000 pounds. It is readily apparent that the number of welds joining two aluminum components would have to be 2.5 times as many as in low carbon steel to have the same load carrying capability. The fatigue strength of an aluminum alloy spot weld in shear is 22% of the static shear strength while for carbon steel resistance spot welds this fatigue strength is 30% of the static strength.

Aluminum alloys come in three basic conditions which provide a wide range of mechanical properties. The softest stable condition is annealed and is designated by the letter "O" placed after the alloy number such as 5182-O. Some alloys respond to cold working to provide higher strength than in the "O" condition. The cold rolled strength ranges are designated by the letter "H" and a number such as 5052-H32. Other alloys are strengthened by precipitation hardening, a form of heat treating. The alloy is heated to a high temperature, say 900° F, to dissolve all alloying constituents. The material is then rapidly cooled to room temperature and after a number of hours at room temperature, natural aging takes place to result in an intermediate strength level denoted as T4. Higher precipitation hardening strength levels can be obtained during artificial aging for 8 to 16 hours at temperatures in the area of 400° F. Such higher strength levels may be denoted for example, T6.

If an aluminum alloy in the cold rolled (H) condition or aged (T-4 or T-6) condition is heated in paint ovens, during adhesive bonding or during welding a temporary or permanent softening will result. This is one of the basic reasons why an aluminum alloy has low weld strength compared to steel even through the parent metal strengths may be the same.

Arc welding of thin gage aluminum alloys is generally not recommended due to the low speeds and also due to the low strength, brittle weld deposits. It is only used where resistance spot welding or bonding cannot be used because of inaccessibility. Not only are the weld deposits themselves of low strength, but the heat

93

effected zone, near the weld is over aged to the "O" condition, the weakest condition of the alloy. In those cases where arc welding is necessary the structure and joint must be closely analyzed to be certain that the welded joint is satisfactorially applied.

Resistance spot welding and bonding is recommended for thin gage aluminum alloys, under 0.050" thick. The combination of these two processes, called weld bonding, provides the highest strength and best resistance to cyclic fatigue loading. While the process is more expensive than either one alone, it does provide the optimum joint strength.

Mechanical fasteners such as rivets are excellent for aluminum but quite expensive due to the need for matching holes in panels to be joined and the placement of rivets in each of these holes. This process is far to slow and expensive for automotive assembly.

Comparing aluminum to steel in the manufacturing of automotive components such as the hood described previously the major, by far, energy consumption is in the material. The other energy consuming processes are essentially the same as for steel. The example steel hood weighed 53.4 pounds and an aluminum hood would weigh an estimated 27 pounds. Initial aluminum material weight would be estimated 1.35 x 27 or 36.45 pounds. Using the production energy of 74,050 Btu/pound from Table 40 then the production energy to produce the aluminum hood is 2,700,000 Btu compared to 2,055,000 for the steel hood.

4.2.3 Thermoplastics

Thermoplastics are molded into automotive components by a number of methods. The method used will depend upon part design, material to be used, process cost and production rate. Molding processes are based on the ability to heat the materials to softening or melting temperatures and then resolidifying and cooling in cold or moderately heated molds.

Thermoplastic materials can be obtained from the mills in the form of compounded or uncompounded pellets. Standard grades of compounded pellets may contain reinforcements, extenders, colorants and other additives. If the molder wants specific properties he can do his own compounding by mixing the ingredients in a compounding extruder to produce his own pellets.

The compounded material in the form of pellets, 1/8 inch diameter and up to 1/2 inch long, is consolidated in an extruder. The extruder, through the mechanical action of a screw in a heated barrel, plasticates the pellets into a homogeneous hot extrudate. Hot plasticated thermoplastic can then be forced through a shaped nozzle and cooled to form sheet, bars and irregular cross section profile shapes. Instead of producing the above mill shapes the hot extrudate can be stored in discrete quantities or shots. The shots

94

are then discharged periodically by a pumping action of the extruder screw. This shot is forced under high pressure into a mold, moderately heated, clamped to the end of the extruder. After a short time the mold is unclamped and the injection molded part is ejected from the mold.

High injection pressures, up to 50,000 psi, are required to force the hot plastic through the nozzle, runners and thin mold passages. The pressure is maintained until the mold is well filled to prevent uneven shrinking at thick and thin portions of the part. Because these high pressures are required the size of such moldings is limited. Very complex shapes can be molded in one piece which can reduce cost and provide greater structural integrity without joints.

Extruded sheet exiting from the extruder can be maintained at a moderate temperature, cut continuously into blanks, reheated to a higher temperature in continuous ovens and molded in mechanical presses in a manner similar to sheet metal parts. Large parts such as fender liners can be made with the thickness relatively uniform. Ribs, bosses and thickness changes are not feasible due to the high press forces required even though the material is soft.

Extruded sheet can also be cooled to room temperature and reheated in infra-red ovens prior to vacuum thermo-forming over a male or female shape. This process is used also for relatively uniform thickness parts. Uniform thickness trim parts where production levels are low can be made by this process. Parts with grain embossment cannot be readily made by vacuum thermoforming.

Laminated-fiber reinforced sheet such as the continuous glass fiber mat polypropylene, PP-40GL, (Azdel ^{TM}) can be compression molded in mechanical or hydraulic presses. The cold sheet is cut into predetermined blank sizes smaller than the molding plan area. Infra-red ovens are used to heat the material above the liquid temperature of the polypropylene. The glass mat retains the soft plastic sufficiently to permit transfer to a cold mold. During press closure the glass and polypropylene flow to fill the mold and are subsequently rapidly cooled to solidify the part. With good part and mold design, adequate long glass fiber flow into ribs and bosses can be obtained.

A relatively new method of manufacturing thermoplastics into large useful products is by structural foam molding. During the extrusion process a foaming agent is incorporated into the hot plastic. This foaming agent may also be present in the original pellets. This material is injected at high or low pressures into a moderately heated or cold mold. A pore free solid skin forms at the mold surface. The core or interior material retains the gaseous products of the blowing agent. As solidification and cooling proceeds a foam core sandwich material is completed. Due to its natural

sandwich structure good stiffness is obtained at low weight. Large panels such as sports or recreational vehicle roofs and seats are molded in this fashion.

One other pertinent method of molding thermoplastics is termed blow molding. In this process the hot plastic exiting from an extruder is formed into a parison or bubble. Internal gas pressure inside the bubble expands the bubble until the material contacts a mold wall and solidifies. Seamless gasoline tanks, ducting, radiator overflow bottles and windshield washer solution bottles can be made in this fashion.

Of the above processes only in the case of the compression molding of glass mat polypropylene, PP-40GL, is recycling not immediately available to recover trim and scrapped parts. These materials are ground or cut into small pellet size particles and re-extruded. In the case of PP-40GL the fiber length is reduced to 1/8 to 1/4 inch long. This material is no longer suitable to refabricate long fiber laminate but is available for injection molding.

Thermoplastic parts can be joined to other materials with mechanical fasteners and to like materials by welding processes. Since these materials are non-conductive, heat for melting at joints can be generated by friction or ultrasonic vibration of the molecular structure. Relatively good joint strengths can be obtained in unreinforced materials by these melting processes.

It is difficult to foresee the use of thermoplastics for hoods and other large exterior panels due to the inability to match the surface finish with other panels made of metal or thermoset plastics. PP-40GL (Azdel ^{TM}) might be a candidate material for such an application; however, improvements or reduced surface requirements, in quality would be necessary. Structural foam hoods and deck lids have also been made with low pressure systems. Again the surface finish is far inferior when compared to steel hoods and thermoset moldings.

The estimated weight of a thermoplastic hood would be ten percent greater than the aluminum hood mentioned previously. A 30.25 pound hood of 40% glass reinforced polypropylene (PP-40G or PP-40GL) would require 845,500 Btu to produce. This is 34% of the energy required for the example aluminum hood and 41% of the example steel hood.

4.2.4 Thermoset Plastics

Reinforced thermoset plastics, particularly the glass reinforced polyester molding compounds PES-20G and PES-30G, are compounded by local compounders or the molder himself. These compounds normally contain 30% polyester resin with 20 to 30% glass fiber of

2" length. Extenders such as clay or calcium carbonate make up the large proportion of the other ingredients. Colorants and other additives are included as desired for moisture resistance, flame resistance, chemical resistance, mold release and viscosity control.

Mixing may be accomplished in batches to produce a "dough" or bulk molding compound (BMC). After mixing, the material is stored for several days in a temperature controlled room to maturate the material to obtain proper viscosity. The mix can be cut into wads of proper weight or extruded, cold, into a constant cross section rope which is then cut to proper charge weight. The BMC is then charged into an open compression mold which has been preheated to temperatures of 275 to 300° F. The press ram is lowered to close the mold and maintain a pressure of 1000 psi for a period of one to two minutes. During this mold closure the compound cures by polymerization.

Sheet molding compounds (SMC) contain 30% glass by weight. These materials are prepared by placing the polyester and extender mix on a polyethylene film which is carried in turn by a conveyor. A doctor blade controls the thickness, and weight, of the mixed material. Chopped glass fibers are then uniformly dispersed over the mix and a second polyethylene film is continually placed over the glass fiber. This sandwich is then kneaded by rolls to mix the fiber and resin thoroughly. The soft sheet of mix is taken up on rolls to a desired quantity. After maturation the SMC is cut into proper size (and weight) charge blanks and placed into heated molds for curing as in the BMC process.

A small quantity of thermoplastic resin is added to SMC during compounding to improve the surface finish of the molded product. Such moldings have been used extensively in most land transportation vehicles.

The complete molding cycle for BMC or SMC ranges from 1 to 2-1/2 minutes depending on part thickness. The production rate is 24 to 50 parts per hour which is approximately 1/10 the rate of metal stamping production. Economical application of the molding compounds is feasible through integration and reduction of the number of steel parts into one plastic molding. An excellent example of this approach is seen in the grille opening panels used on most American vehicles. One reduced weight SMC molding can replace 10 to 16 metal parts with a cost savings.

For comparison to the steel, aluminum and PP-40GL hood production energies, an SMC hood is considered with an estimated weight equal to 30.25 pounds. Using the data from Table 40 for PES-30G or 20,240 Btu per pound, this hood would require a total of 612,260 Btu. This is the lowest value of energy consumed in making the hoods of all three materials. The values from Table 40 included the molding energy which is primarily to replace heat lost from the molds.

97

Glass reinforced polyester can be joined to other materials and itself by mechanical fasteners and structural adhesive bonding. Bosses with driven studs can be provided for mounting and assembly such that the mechanical fasteners are hidden. A number of adhesives are available having joint strengths varying from 500 psi to 2000 psi in shear. The adhesive is selected on the basis of strength and compatability with the production rate.

4.2.5 Elastomers

Elastomers can be molded into automotive components by casting, injection molding, extrusion and reaction injection molding (RIM, LIM). The thermoplastic rubbers (TPR) and ethylene propylene (EPDM) are extruded into profiles and are injection molded into complex shapes. Polyester urethane (AV) and polyether urethanes (EV) can be cast or reaction injection molded. These two urethanes are thermoset materials which are introduced into the mold as two component mixtures. Polymerization is completed in the mold.

The casting process is slow and expensive but is suitable for rotational molding and gravity casting of low production or prototype components. Reaction rates between the two components is reduced to permit proper handling.

When the reaction rate is increased for the thermoset urethanes the materials must be mixed at high speeds and injected into the mold in seconds. Machine mixers and injectors are required to accomodate the high reaction speed. The mixed liquid fills the mold rapidly and at low pressures permitting large area components to be molded without associated high clamping forces.

Little material is wasted in the RIM process and the production energy is essentially 27,273 Btu per pound, Table 37. Due to the low modulus of elastomers, a hood for example, would require at least a stiffer material as an inner panel to prevent distortion. This becomes a poor application of the material and should not be compared.

4.2.6 Foamed Plastics

Structural foams were discussed in section 4.2.3 where a sandwich construction is formed as the material cools in the mold. Non-skinning foams and in particular low density rigid polyurethane foams have been studied for energy attenuation during collisions.[83,84] This material is used to fill closed structure within the automobile to improve crushing characteristics during high speed collisions.

Rigid polyurethane foams are prepared by mixing two reacting chemicals in a mixing gun as it is being dispensed. The mixed liquid reacts rapidly inside the closed structure and by the foaming action completes the fill. A moderate pressure is exerted by the foam which will distort thin walled structural elements. A

restraining system is required to prevent this undesirable distortion.

While rigid polyurethane foams of the densities used (2 pounds per cubic foot) are not structural materials their use in conventional automotive structure or in structure designed for the foam does improve the crushing characteristics and energy absorption of the structure.

4.3 Repairability

Repairing of damaged automotive structure can be separated into two areas: that which affects appearance but not performance, and that damage which does effect performance and degrades structural durability and crashworthiness.

The repair of components for appearance sake in current automobiles consists primarily of partial straightening, finishing using organic adhesives and final painting. If the results of the straightening work is questionable due to severe crippling and creasing then an entire component is replaced. In the case of steel, the majority of repair shops are capable of completing the repair including arc welding requirements. In those areas where resistance spot welding is used in the original fabrication, most repair shops would have to resort to riveting and bonding for reassembly.

Aluminum alloys and thermoset plastics components having minor damage would be repaired using the same basic procedures for steel. In the case of aluminum, extra care would be necessary in cleaning the metal surface prior to adhesive patching to prevent exfoliation after exposure to moisture. Riveting and bolting of components would be no problem but resistance spot welding and arc welding of thin gage parts would be extremely difficult for the majority of repair shops. Precautions in welding aluminum described in Section 4.2.2 would be difficult to provide in most facilities due to power requirements and the need for good welding practices.

Thermoplastic materials, although expected to be more resistant to gentle bumps, is difficult to repair if permanent minor damage occurs. The lack of patching adhesives, finishing and painting techniques makes repair impractical without considerable development.

Major damage is that which will reduce performance, durability or crashworthiness, varying in degree, and may be difficult to assess. While damage to a frame or sill component might be sufficiently repaired to operate a vehicle, this damage may act as a weak point or trigger during collision. This was demonstrated in the study of rigid polyurethane foam [84] where minor damage to the foam filled components reduced the ability to absorb crash energy. In unfilled

metallic structure localized permanent deformation can not generally be straightened adequately to prevent low force failure in a second collision.

Since the repair of critical structural items is left to the judgement of the vehicle owner and repair shop, and the preparation and enforcement of regulations would be difficult or impossible, other means of anticipating severe damage should be studied.

One approach would be to make parts of the structure modular for easy replacement and permit better assessment of damage. Any example of this concept is to have a low speed, 20 mph, crush structure at the front end of the vehicle. The structure behind this module would not be damaged and repair of the vehicle would consist primarily of the front end module. This concept has been considered in the RSV program [85] currently under Department of Transportation sponsorship.

While this discussion has been negative toward the repair of structural damage there will be instances where this can be accomplished. Provided with proper dimensions and gaging tools, steel structure may be repaired using known techniques of hammer forming, riveting and arc welding. The repair of aluminum alloy and thermoset structure must be considered feasible yet techniques are not currently developed nor is the experience available which would indicate the repairs are adequate. This feasibility of repair must be demonstrated on actual components and tested. If test results are positive then the procedures can be evaluated for use in low technology repair shops.

4.4 Crash Energy Attenuation

Considering frontal collisions the impact energy can be absorbed by plastic deformation of metals, tearing of metals, plastic deformation of thermoplastics and ultimate failure of thermosets. The efficiency, foot-lbs energy absorbed divided by the weight of material deformed, is dependent upon the number of folds per inch in metal or thermoplastics, and the number of ultimate failures per inch in thermosets. Beams will generally bend or fail locally in one area. Columnar panels can be made to fail at many points depending on thickness and radius of curvature. As the radius of curvature increases the number of folds and efficiency decreases, and as the thickness of the panel decreases the efficiency again decreases. Cylinders are very efficient energy absorbers and this inefficiency increases as the thickness of the cylinder walls increases and the diameter decreases. Flat sided, thin wall rectangular tubes are, as expected, less efficient.

Large, thin wall, flat sided rectangular columns filled with rigid polyurethane foam, density 2 pounds per cubic foot, are more efficient than similar unfilled columns. [84] Steel tubes 6" x 8" x 30" long made from 0.022 to 0.024" thick walls were tested with and

without rigid polyurethane foam. These tubes were impacted with a 228 pound weight at 30 mph. The foam filled tube crushed 15 inches while the unfilled tube crushed 30 inches. The foot pounds kinetic energy absorbed per pound of the unfilled tube was less than 1112. For the foam filled tube, 1662 foot pounds were absorbed for each pound of specimen crushed. The foam filled tube was over 1.5 times as efficient on a weight basis in absorbing the crush energy.

A similar test was performed using a foam filled aluminum alloy (5182-0) tube with a wall thickness of 0.032". The tube had an energy absorbing efficiency of 2416 foot pounds per pound of crushed structure.

Two inch diameter tubes made from 0.039" steel, 0.053" aluminum alloy 2036-T4, and 0.096" glass reinforced polyester were crushed at 20 mph.[86] Cylinders were also tested with 8 pound per cubic foot foam filling. The presence of the foam in these test specimens actually reduced the energy absorbing efficiency slightly. Both the filled and unfilled specimens had an energy absorbing efficiency of 7841 foot pounds per pound of steel, 12037 foot pounds per pound of aluminum and 13,317 foot pounds per pound of glass reinforced polyester.

The kinetic energy absorption, ft-lb, per Btu of energy required to produce a 2 inch tubular specimens was calculated using the values from Table 40. These values are 0.327 for steel, 0.163 for aluminum alloys and 0.658 for the glass reinforced polyester. The foam filled steel, unfilled steel and foam filled aluminum alloy, 5182-0, 6" x 8" x 30" test results were also examined for their foot-pound per Btu efficiencies. The energy, Btu, for production of the urethane foam was taken from Table 37. Based on these calculations the foam filled steel tube was best at 0.060 ft-lb/Btu. The unfilled steel tube had an efficiency of 0.046 and the foam filled aluminum alloy 5182-0 was the least efficient with a value of 0.040 ft-lb/Btu.

4.5 Disposability

The problems associated with disposability, including recycling, was discussed in section 3.0. It is difficult to conceive that automobiles in the next 15 to 20 years would be made of one single material. The pressure of reducing weight and energy consumption will require the use of aluminum alloys and plastics. All aluminum and all plastic vehicles may be manufactured but at a low annual production. Vehicles which are predominantly plastic show promise but even in this instance durability and crashworthiness may require steel roll cages and reinforcements in doors, as an example, where high bending resistance and toughness are required. Regardless of the material, every effort should be made to permit the easiest, most economical method of separating the materials to improve materials and energy conservation.

4.6 Areas of Application

Low carbon steels have been used for automotive structure for years with wide industry experience. The incorporation of HSLA steels especially in the hot rolled gages, greater than 0.060" thick, can be made readily with little change in the manufacturing processes. Since the HSLA steels have higher strength but the same modulus of elasticity as low carbon steel redesign of structural elements may be required to utilize the higher strength and obtain a weight reduction. Hot rolled HSLA steels could be applied in frames, sills, roll cages, bumper beams and back up structure fire walls, floor pans and door intrusion beams. When cold rolled gages, less than 0.060" thick, are developed, these steels could be used in door structure to improve crashworthiness with reduced weight. The use of thinner HSLA steels in either the hot rolled or cold rolled gages will require improved corrosion protection to assure long structural life.

Aluminum alloys can be used for the entire automotive structure, but may never be achieved due to availability of material and high first cost. Steels, low carbon and HSLA, range in price from $0.16 to $0.22 per pound while the aluminum alloys are currently near $0.70 per pound. Since the aluminum alloy required by weight is estimated to be 50 percent of the steel the vehicle cost of raw material would be approximately twice that of steel. The additional cleaning operations for assembly, lower welding speeds, more frequent replacement of electrodes, increased maintenance of forming dies and increased finishing costs will increase the manufacturing costs over low carbon steel by a factor of 1.5 to 2.0. The aluminum alloy structure would cost an estimated 3 times that for low carbon steel not including new capitalization costs.

The inability to weld aluminum alloys to steel and the development of galvanic couples at these dissimilar joints limits the application of aluminum in a mixed material vehicle. The obvious areas of applications of aluminum in such vehicles is in hang on components such as hoods, deck lids, front fenders, bumper beams, doors and access cover panels in baggage compartments.

Cast aluminum alloys can be used in most applications where cast iron is used currently in the power system and braking system.

Forged aluminum alloys can be used in areas of the suspension where forged steel parts are currently used. Bearing and wear surfaces will require additional bushing materials due to the lower surface hardness of aluminum alloys.

The use of aluminum in mixed material vehicles as hang on components also facilitates the ability to recycle these materials.

102

Alloys 6009 and 6010 are recommended for these sheet metal applications due to their similar chemical compositions which reduces segregation during manufacturing and vehicle disposition.

Thermoplastics, due to their low creep resistance and lower temperature of application are also recommended for hang on components and trim. Such applications consist of front and rear exterior trim, fenders, hoods and deck lids. Ducting for heaters and air conditioners and non structural dust covers are also potential applications. Fender liners, support structure for front and rear fascia panels and for seats are other applications of these materials. Again, the ability to segregate materials from discarded vehicles in hang on components is an important factor in their application.

Thermoset plastics consisting of glass reinforced polyesters could be used for the entire body structure. The low toughness in bending of these materials would almost necessarily require steel or aluminum roll cages to support the passenger compartment at the "A" and "B" posts, around the doors and over the roof. Considerabe redesign of vehicles is necessary to develop large panel or molding size to keep manufacturing costs at a minimum and reduce the number of joints. Since the molding pressure of sheet molding compounds is high, the panel size must be coordinated with press capabilities.

Glass polyester molding compounds are currently made in hydraulic presses. Recent developments within the automotive industry has resulted in the ability to use mechanical presses for SMC molding. This reduces the potential need for large capitalization costs to make thermoset plastic automotive structure.

SMC moldings can be attached to themselves or other material by adhesive bonding or mechanical fasteners. There are no galvanic couples developed at dissimilar material interfaces. This permits the use of such materials throughout the vehicle. Hoods, deck lids, fenders, quarter panels, bumper beams, frames, roofs, floors and seats can utilize these materials.

Carbon (graphite) fiber reinforced polyester can be combined with the glass reinforced material to locally strengthen and stiffen portions of the structure. Production molding techniques rely on large flow of the molding compound. This feature complicates the use of oriented carbon fiber reinforced materials in that control of orientation is difficult due to large flow. The part design, mold design and charge placement must be well coordinated.

Carbon fiber reinforced polyester can be used by itself to mold separate reinforcing members. In this case better control can be achieved in the molding since the part design will require less or minimal flow of the oriented fiber mold change. Due to the high cost of carbon fiber its use would be limited to the more critical portions of the structure such as frame, sills and

"A" and "B" posts. Other interesting applications being developed in the automotive industry are drive shafts, leaf springs and torsion bars.

Rigid, low density polyurethane foams can be used with any of the above materials to provide crash energy attenuation. One excellent feature of such crush structure is that the crush force density is reduced, eliminating hard spots and distribution of the impact force over a larger area of structure. Application of foams would be primarily in sills and cross members throughout the body structure.

Elastomers can be used primarily in areas of low level energy attenuation such as front and rear bumper facia, front and rear trim and front fenders. The ability of these materials to recover to their original shapes after high elongation promotes their application in areas of minor damage.

5.0 DAMAGEABILITY

The exterior surface finish of American automobiles has been developed to a high level for customer appeal on the show room floor. This appearance quality is based primarily on large panels formed from low carbon steel.

The quality of low carbon steel has been developed over many years to provide a scratch and dent resistant surface which is readily painted. Metallurgical investigations have been conducted to prevent strain lines due to discontinuous yielding and to prevent "orange peeling" during the deformation of large surface grains.

Material handling procedures, inspection and quality control have been developed to produce a good appearing automobile. Design and fabrication methods have been altered to improve surface finish and reduce costs. As an example, structural adhesive bonding is being used to reduce or eliminate resistance spot welding in hoods and deck lids.

The improvements in low carbon steel to meet the demand for greater formability for styling flexibility has reduced the resistance to denting and minor damage. [87] Increased cost of automobile repair and collosion insurance has increased the desirability of damage resistant automobiles. The effects of the candidate materials on the resistance to minor damage and non injury producing accidents may have a significant effect on their selection for future automobiles.

5.1 Minor Damage

The resistance to denting by flying objects, swinging doors, parking lot mishaps and shopping carts is difficult to completely assess due to the many various sized objects, striking velocities and directions of impact involved.

An evaluation of steel for dent resistance [87] indicated an agreement with $d = \sigma_y t^2$, where σ_y is the yield strength and t is the thickness. Tests were performed on a number of autobody steel samples of varying strength and thickness. Impactor weights of 1/2 to 5 pounds were used at velocities of 2 to 10 feet per second. Energy requirements to produce dents of 0.005 and 0.050 depths were determined from the data plots. For a 0.005 inch indentation the energy required varied from 0.79 to 3.55 inch pounds and for the 0.050 inch deep dent the energy varied from 11.7 to 51.3 inch pounds depending on thickness and strength. This study concluded that sheet thickness was twice as important as yield strength in dent resistance. Based on this relationship for thin sheets a 50 percent weight reduction would require a steel with 4 times the yield strength or approximately 140,000 psi for equal dent resistance to current construction. A 25 percent weight reduction (thickness reduction) would require a sheet steel with a 70,000 psi yield strength to obtain equal dent resistance.

105

The denting of aluminum alloys has also been studied [88,89,90] in considerable depth. Flat panels, curved panels and actual formed body panels were tested in aluminum alloys 5182-0 and 2036-T4. Carbon steel panels were similarly tested to compare results. Based on these tests using a 1" diameter ball impacting the panels at velocities up to 88 feet per sec, the 2036-T4 alloy had essentially the same dent resistance as low carbon steel. Alloy 5182-0 had a lower resistance to denting. These tests showed that for the same thickness and strength level the aluminum alloys performed as well as steel regardless of panel curvature. Panel curvature however, did contribute to dent depth, the more convex curved the panel the greater the dent depth. The above tests on actual automotive shapes indicated the very low energy levels are required to dent the panels. The ball impactor weighed 0.52 pounds, and at 30 mph impact the kinetic energy of the impactor is 189 inch pounds, and produces dents in the order of metal thickness.

Recent developments in new aluminum alloys has resulted in 6010 and 6009. These alloys would be obtained by the fabricator in the T-4 condition. During exposure to the paint oven temperatures sufficient aging occurs to increase the strength to the T-6 condition. At this strength level the scratch and dent resistance of alloy 6010-T6 is reported by the Aluminum Corporation of America to be equal to the same thickness of low carbon autobody steel.

Other tests [91] performed on flat panels of steel, aluminum alloys, glass reinforced polyester and glass reinforced polypropylene have indicated only minor differences in denting resistance of all these materials. Conclusions reached were that all of the thin outer panel materials are readily damaged by low energy impacting objects. Only those materials which do not possess a yield point and do possess high elastic elongation, such as elastomerics, are truly dent resistant.

Based upon the review of the above test data and observations in metal stamping plants it would appear that elastomeric outer panels would be more resistant to minor impact damage than metal panels. This concept has been proposed previously in the general literature by General Motors Corporation spokesmen as the "friendly fender" concept. An elastomeric glove, forming the entire skin structure forward of the fire wall has been proposed and prototyped in the Minicars RSV program for the Department of Transportation.

5.2 Non-Injury Damage

The concept of preventing damage to automotive structure and body panels in non-injury producing accidents has been stimulated by higher repair costs and higher insurance premium costs. A number of new ideas for front and rear bumper structure have been proposed and in many instances prototyped and tested. Federal

Motor Vehicle Safety Standard 215 requires front bumper systems to have a capability of resisting a 5 mph impact without vehicle damage. The rear end requirements are somewhat less, 2.5 mph. A greater capability than the above FMVSS 215 requirements has always been considered desirable.

To put the requirements of a non-damageable (recoverable) front or rear bumper system in proper perspective, the kinetic energy of moving vehicles at 5, 10, 15 and 20 miles per hour have been listed in Table 43. A first test condition assumes the vehicles listed are striking a flat barrier. The acceleration - distance crush curve desired is shown in Figure 14. This curve is taken in part from that suggested for a 2700 pound vehicle [86] in previous studies represented by the dashed line. The solid line smooths out the initial crushing and eases the calculations for this evaluation.

Using the solid line of the acceleration - distance crush curve and assuming for the moment no loss in vehicular mass during the crush, then the required crush force - distance curve can be calculated for the energy absorption required as listed in Table 43. Crush distances of 3, 6, 9 and 12.5 inches are arbitrarily selected as examples for each vehicle weight. The average crush force is calculated based on kinetic energy equals force times distance. The maximum crush force is twice the average.

The recoverable long stroke or crush distance can be accomodated by hydraulic cylinders, shock absorbers, or elastomeric shapes. Hydraulic cylinders and shock absorbers suffer from directionality and weight problems. When more than one of these are used in a system a heavy beam generally is required.

An experiment conducted by General Motors and the New York Taxi fleet utilized an elastomeric bumper system shown in Figure 15. This concept could be used to accept larger loads and stroke distances especially if rear end engine vehicles are considered. Elastomeric buckling columns have been examined by other investigators. [86,92] Prediction of crushing forces of elastomeric columns has been studied by Tundermann, Larson and Anderson.[92] In the cited study, the basic Euler equation defining the critical load at which buckling is initiated was used as described in Figure 16. Load-deflection curves for rectangular elastomeric columns were expected to look like that shown in Figure 17. Results of static tests indicated agreement within 8% of the critical buckling load and 6% of the critical deflection equations listed in Figure 16.

Combining four rectangular elastomeric columns into a square hollow column effectively increased the crushing force by a factor of 1.5 due to the corners. A further increase, 1.6 times, in static values were obtained when testing at 5 mph for EPDM type elastomeric. EPDM (ethylene-propylene-diene terpolymer) can be obtained in various hardness, strength and modulus levels. This

107

TABLE 43:   PARAMETERS OF NON-DAMAGEABLE FRONT & REAR ENDS

Vehicular Weight (Pounds)	Impact Velocity (ft/sec)	Kinetic Energy (in.-lbs.)	Crush Distance (inches)	Maximum Acceleration (9)	Ave. Force (Pounds)
2500	7.33	25,185	3	5.5	8,395
	14.67	100,879	6	11.5	16,813
	22.0	226,875	9	17	25,208
	29.33	403,242	12.5	23.5	32,259
3000	7.33	30,223	3	5.5	10,074
	14.67	121,055	6	11.5	20,176
	22.0	272,250	9	17	30,250
	29.33	483,890	12.5	23.5	38,711
3500	7.33	35,260	3	5.5	11,753
	14.67	141,231	6	11.5	23,538
	22.0	317,625	9	17	35,292
	29.33	564,538	12.5	23.5	45,163

FIGURE 14 ACCELERATION-CRUSH DISTANCE

CRUSH DISTANCE INCHES
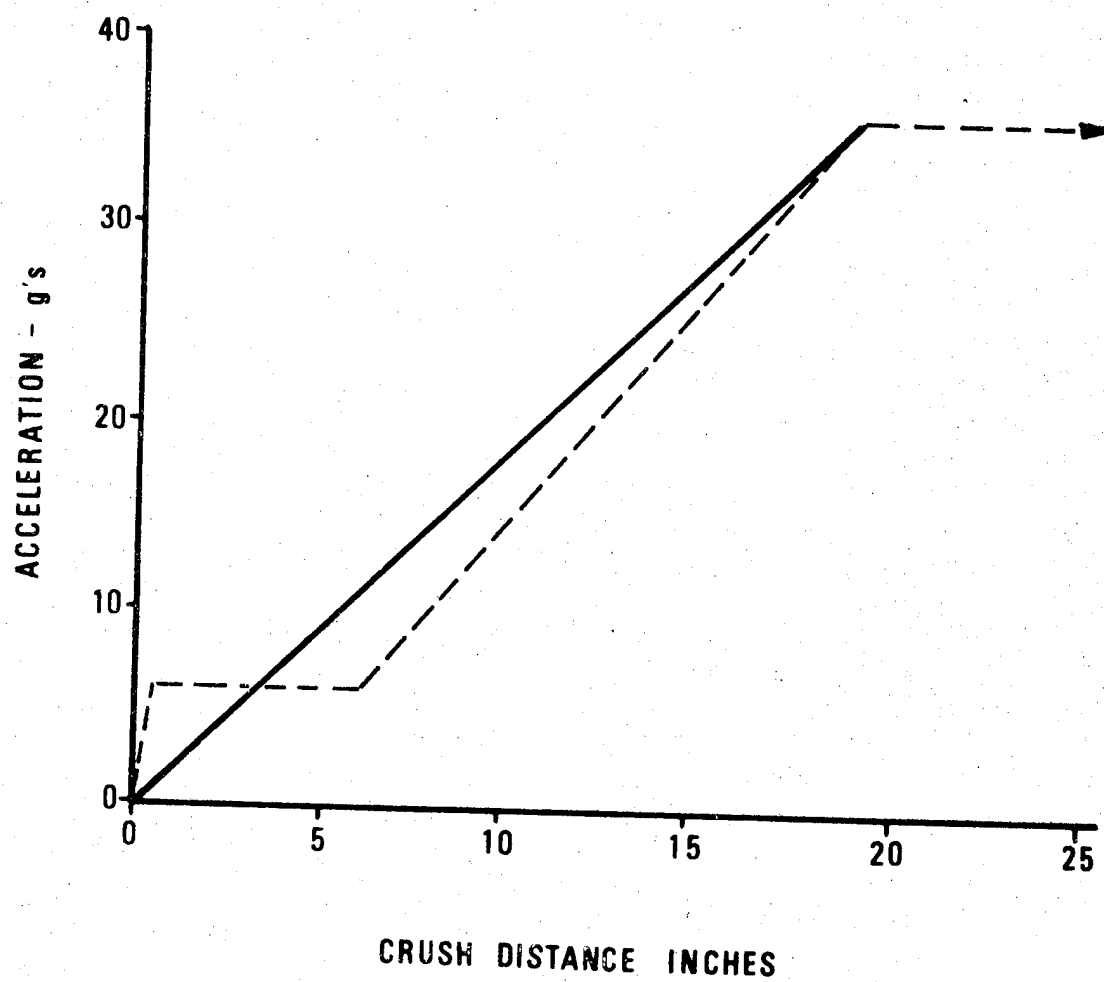
FIGURE 15   GENERAL MOTORS TAXI BUMPER
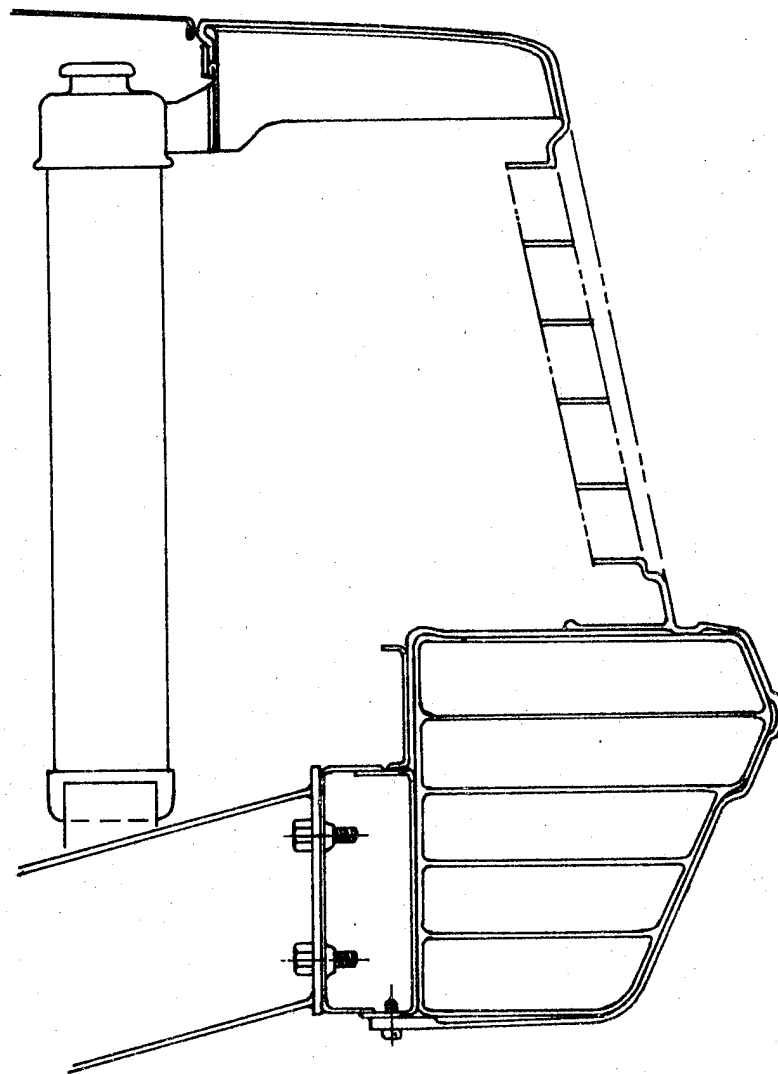
FIGURE 16

EULER EQUATION

1. Critical Load

$$P_{cr} = \frac{C\pi^2 EI}{L^2} = \frac{C\pi^2 EA}{(L/r)^2}$$

2. Critical Deflection

$$D_{cr} = \frac{C\pi^2 t^2}{12 L} \qquad \text{for rectangular cross sections}$$

P_{cr} = Critical Buckling Load (lbs.)

D_{cr} = Critical Deflection (in)

C   = Euler's end restraint coefficient (with fixed ends restrained from lateral movement, C = 4.0)

E   = Compressive Mod of Elas (lbs/in^2)

A   = Cross sectional area (in^2)

I   = Bending movement of inertia about t (in^4)

     ($I = Ar^2$)

L   = Length of column

r   = Least radius of gyration of cross section (in)

t   = Thickness of rectangular cross sectional area (in)

111

FIGURE 17 ELASTOMETRIC COLUMN BUCKLING
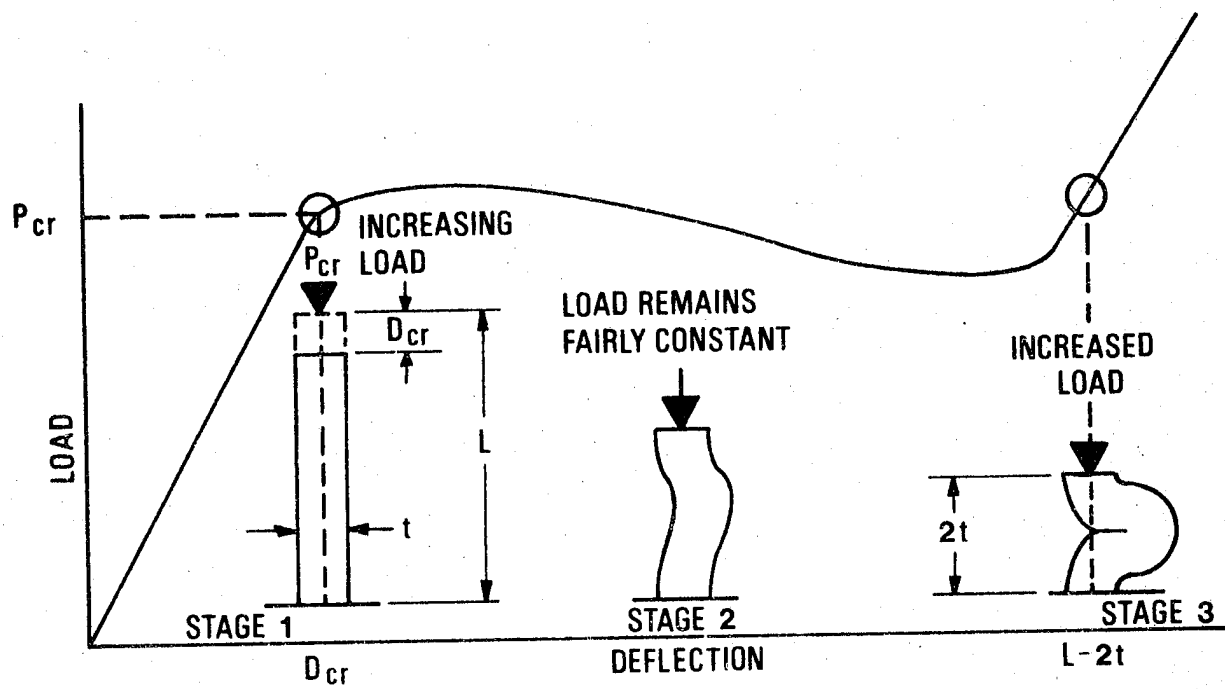
REFERENCE: 92

material is also the least affected by temperature variations from 20°F to 140°F.

Using the suggested elastomeric square, hollow columns 6.5" long, 4.5" square and 0.75" wall thickness, the number of such units needed to provide the force and stroke distances required in Table 43 have been listed in Table 44. Such an absorber has an average crush force of 1875 pounds over an effective crush length of 3 inches. Each of these absorbers weigh 2.28 pounds. Since the effective crush length is only 3 inches it is assumed that 2 in series are required for 6 inch stroke and 3 in series for a 9 inch stroke.

The elastomeric weights listed in Table 44 do not include any supporting or mounting structure, no jacking provisions and no facing skin.

For comparison, values of energy absorption for steel cylinders [93] are compared for the conditions in Table 43 to compare the weight of this frontal or rear structure with that of Table 44. From the above reference a 4 inch diameter low carbon steel cylinder (at 30 mph) has an average crush force of 6000 pounds which will absorb 36000 inch pounds over a 6 inch stroke. The weight of such a cylinder is 0.115#/inch. Based on observations of specimens tested in 30 mph drop towers a cylinder 4 inch diameter could be made 16 inches long for a total weight of 1.84 pounds and be able to crush a total of 12.5 inches at average force of 6000 pounds. Six such cylinders would absorb the energy of the 2500 pound vehicle impacting at 29.33 ft/sec (20 mph). The total structure weight would be 11.04 pounds compared to the 159.14 pounds of elastomeric required to do the same job. However the elastomeric structure would be recoverable while the steel tubes would not. The total material cost would be seventy times greater for the elastomeric than for the steel.

Various trade offs could be proposed where the elastomeric would be used for the 5 or 10 mph portion of the structure and the steel cylinders for the remaining structure up to 20 mph. This type of replaceable package attached to the front or rear of a vehicle could protect aft structure under low speed collisions and be replaced if a collision up to 20 mph did occur. An elastomeric fascia could be provided over the entire 20 mph module to hide the underlying structure.

Similarly, glass reinforced polyester cylinders filled or unfilled with rigid polyurethane foam could also be used. Based on data taken from studies on plastic automotive structure, [86] a 6000 pound average crush force over the 12.5 inch distance (16" deep structure) could be obtained for a total weight of 6 x 0.04414#/in x 16 in or 4.24 pounds, 7 pounds less than the steel cylinder structure. Again a fascia panel would cover the glass polyester structure.

113

TABLE 44:   WEIGHT OF ELASTOMERIC MATERIAL FOR ENERGY ABSORPTION

Vehicular Weight (Pounds)	Impact Velocity (ft/sec)	Required Absorbers	Weight (Pounds)
2500	7.33	4.5	10.3
	14.67	18	41.0
	22.0	41.5	94.6
	29.33	69.8	159.14
3000	7.33	5.4	12.31
	14.67	21.6	49.2
	22.0	48.4	110.4
	29.38	84.6	193.0
3500	7.33	6.2	14.1
	14.67	24.8	56.6
	22.0	55.9	127.4
	29.33	97.7	222.8

5.3 Elastomeric Foam Energy Absorbers

Recent developments in foam technology is resulting in families of foams having various densities and associated stress strain characteristics. Block of 10.2 pcf EM1052 polyurethane foam, obtained from Davidson Rubber Company, were tested statically (2 inches per minute), and dynamically (5, 12 and 18 mph), Figure 18. These tests were made to insure that the material would be the same at higher speed impact as well as at 5 mph for which it was originally intended.

Stress strain data supplied with the material for -20°F, 70°F and 125°F at an impact speed of 5 mph is shown in Figure 19. Specific energy vs strain at the three temperatures are plotted in Figure 20.

Data from Figure 20 is listed in Table 45. Using this data and the following equations the foam requirements for various weight vehicles can be determined.

$$K. E. = 1/2 \ mv^2$$

$$F = ma$$

$$F = sA$$

$$K. E. = At \ S.E.$$

The impacting vehicle energy will be absorbed by the elastomeric non damageable portion of the front or rear system. The maximum force developed in the elastomeric must be accommodated by the supporting vehicle structure without permanent failure. This force can be selected from the acceleration - crush distance curve, Figure 14. For example a 20 g acceleration developed by the elastomeric would for a 2300 pound vehicle produce a 46,000 pound force. From Table 45 at a selected strain of 0.65 the strength of the foam is 220 psi and the foam area is 209.1 square inches.

The specific energy at that strain is 69 and knowing the kinetic energy for an impacting speed (20 mph) the thickness of foam is determined. Multiplying the strain, 0.65, times the thickness, 25.6 inches, results in a stroke of 16.6 inches. Calculations have been made for a 2300 and a 4000 pound vehicle at a 15 and 20 mph impact. This data is listed in Tables 46 and 47. The stroke distances are reasonable, especially for the 15 mph impact condition. For the 15 mph condition the weight of foam required for the two size vehicles are 17.6 and 30.6 pounds. This is again a reasonable weight compared to the existing bumper systems.

The maximum force that can be developed in the foam absorber is dependent upon the frame, in a framed vehicle, or the front sill structure in a unibody structure. For an integrated crashworthy

115

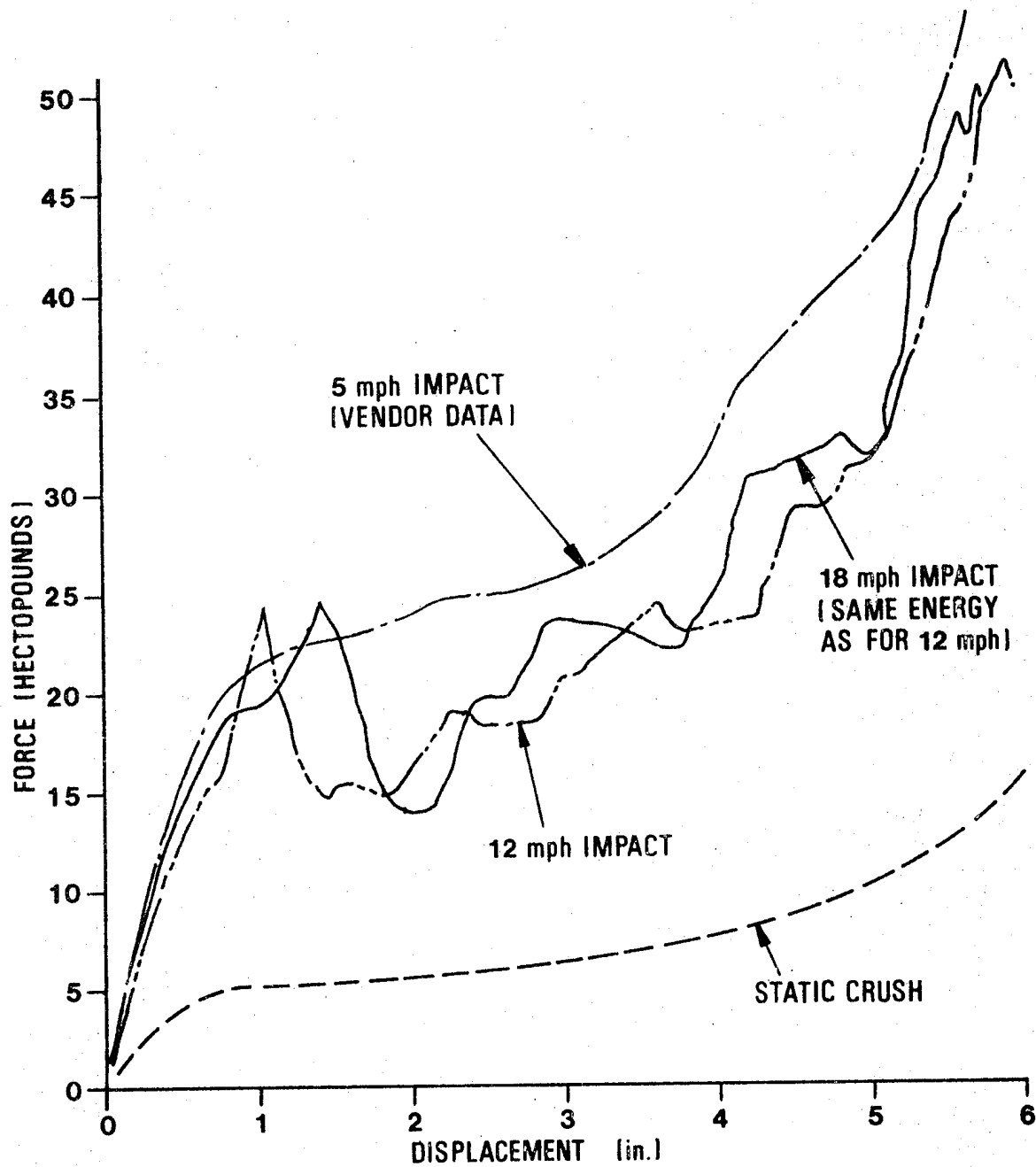FIGURE 18 FORCE-DISPLACEMENT: 10 pcf POLYURETHANE FOAM

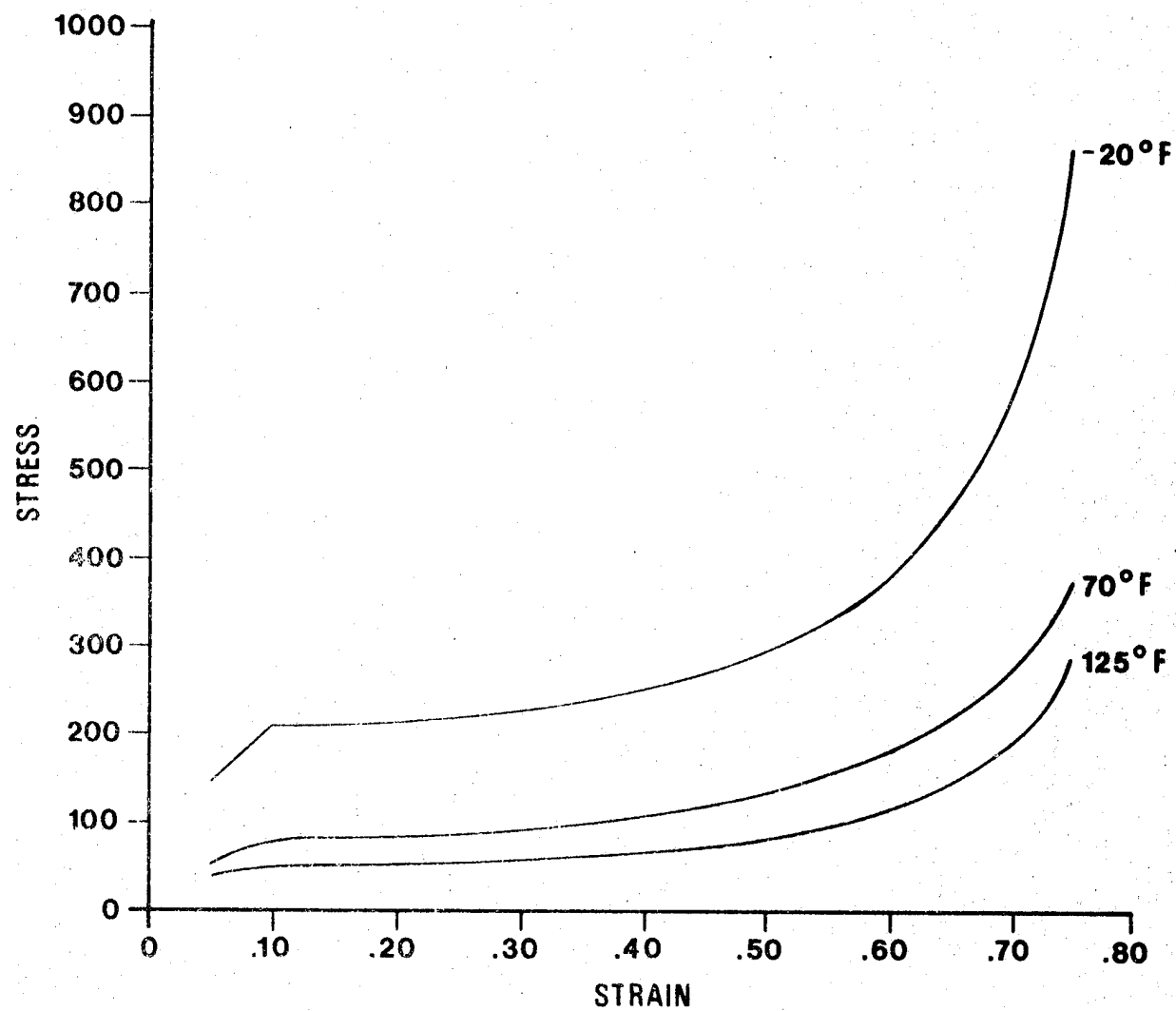FIGURE 19   STRESS-STRAIN EM 1052
URETHANE FOAM (10 pcf)

117

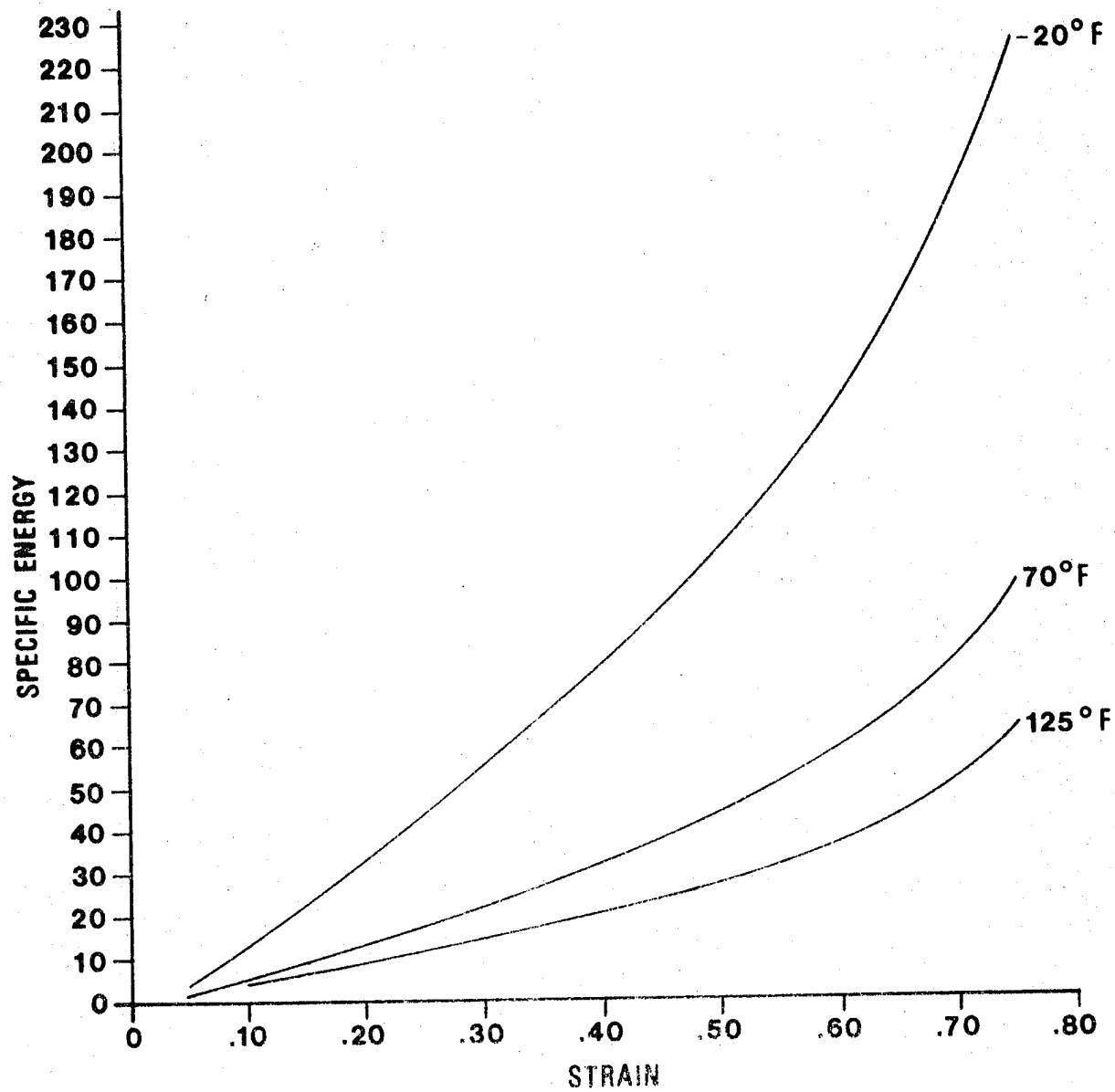FIGURE 20   SPECIFIC ENERGY-STRAIN   EM 1052
URETHANE FOAM (10 pcf)

TABLE 45: STRESS-STRAIN-ENERGY 10 PCF URETHANE FOAM

STRAIN	STRESS -20	STRESS 70	STRESS 125	SPECIFIC ENERGY -20	SPECIFIC ENERGY 70	SPECIFIC ENERGY 125
0.05	146	53	38	4	1	****
0.10	208	77	49	12	4	3
0.15	208	83	51	23	9	6
0.20	214	85	52	33	13	8
0.25	217	90	54	44	17	11
0.30	229	90	55	55	22	14
0.35	235	97	58	67	26	16
0.40	252	106	63	79	31	19
0.45	270	123	71	92	37	23
0.50	297	140	86	106	44	27
0.55	330	154	101	122	51	31
0.60	386	179	114	140	59	37
0.65	478	220	144	161	69	43
0.70	597	276	189	188	82	51
0.75	864	377	287	225	98	63

EM 1052

119

TABLE 46: NON DAMAGEABLE FOAM REQUIREMENTS

10.1 PCF Urethane Foam, 15 mph Impacts, 0.65 Strain

Vehicle Weight lbs.	Acceleration g's	Force lbs.	Foam Area in^2	Foam Thickness in	Stroke in
2300	15	34,500	156.8	19.2	12.5
	20	46,000	209.1	14.4	9.4
	25	57,500	261.4	11.5	7.5
	30	69,000	313.6	9.6	6.2
4000	15	60,000	272.7	19.2	12.5
	20	80,000	363.6	14.4	9.4
	25	100,000	454.5	11.5	7.5
	30	120,000	545.5	9.6	6.2

17.6 lbs. foam required for the 2300 lb. vehicle

30.6 lbs. foam required for the 4000 lb. vehicle

TABLE 47: NON DAMAGEABLE FOAM REQUIREMENTS

10.1 PCF Urethane Foam, 20 mph Impacts, 0.65 Strain

Vehicle Weight lbs.	Acceleration g's	Force lbs.	Foam Area in^2	Foam Thickness in	Stroke in
2300	15	34,500	156.8	34.1	22.2
	20	46,000	209.1	25.6	16.6
	25	57,500	261.4	20.5	13.3
	30	69,000	313.6	17.0	11.1
4000	15	60,000	272.7	34.1	22.2
	20	80,000	363.6	25.6	16.6
	25	100,000	454.5	20.5	13.3
	30	120,000	545.5	17.0	11.1

31.1 lbs. foam needed for 2300 lb. vehicle

54.5 lbs. foam needed for 4000 lb. vehicle

121

structure the peak load, or triggering load, for the aft structure must be equal to or greater than the maximum force developed in the foam.

A concept of how the foam might be used in a frame vehicle for the front is shown in Figure 21. In Figure 22, 23 and 24, an absorber has been fit into the front end of a 1977 model Impala. The foam absorber has been selected to develop a 17 g (68000 pound) maximum force. At a 0.65 strain the cross sectional area of the foam is 309.1 in^2 and the depth is 16.9 inches. The stroke for a 15 mph impact would be 11 inches. For a 10 pcf foam the weight of this energy absorber would be 30.23 pounds.

The foam absorber would have to be covered with a tear resistant, non porous skin or fascia panel. This fascia would be approximately 0.100 inch thick and is estimated to weigh 16 pounds. A RIM polyurethane or EPDM elastomeric material could be used. The fascia would extend from the lower side of the reinforcing bar up to the hood line.

The foam would be adhesively bonded into an aluminum channel which is in turn mounted to the front end of the frame. The aluminum channel weight is estimated to be 9.25 pounds.

To provide sufficient stroke distance the front of the load and fenders would be trimmed and the metal cosmetic panel would be removed with its brackets.

The cosmetic panel, fender extensions, bumper, bumper support members and two energy absorbers weighs approximately 80 pounds on the 1977 Chevrolet Impala. The estimated foam, fascia and support bar weight is 56 pounds, resulting in a 24 pound weight reduction and improved non-damageability.

One major disadvantage of the elastomeric foam front energy management system is that new jacking provisions must be provided to replace the normal bumper jack.

Further evaluation of the foam concept will be made in section 7 of this report.

5.4 Energy Absorbing Bumper Beams

To provide the ratios of the energy absorbed by each part of the Energy Management Bumper System (EMBS) in a frontal barrier impact, equations are developed giving percentages to the total energy absorbed by the bumper face bar and each of the two energy absorbers, while the energy absorbed by the vehicle frame is held at a constant ratio. These equations are then used to compare five different materials (HSLA Steel 950, HSLA Steel 980, Aluminum Alloy, X7046-T63, 30% random glass polyester, 65% random glass polyester), at different vehicle masses and velocities. An approximate thickness

FIGURE 21 FOAM ENERGY ABSORBER CONCEPT

SUPPORT BEAM

FOAM

FASCIA
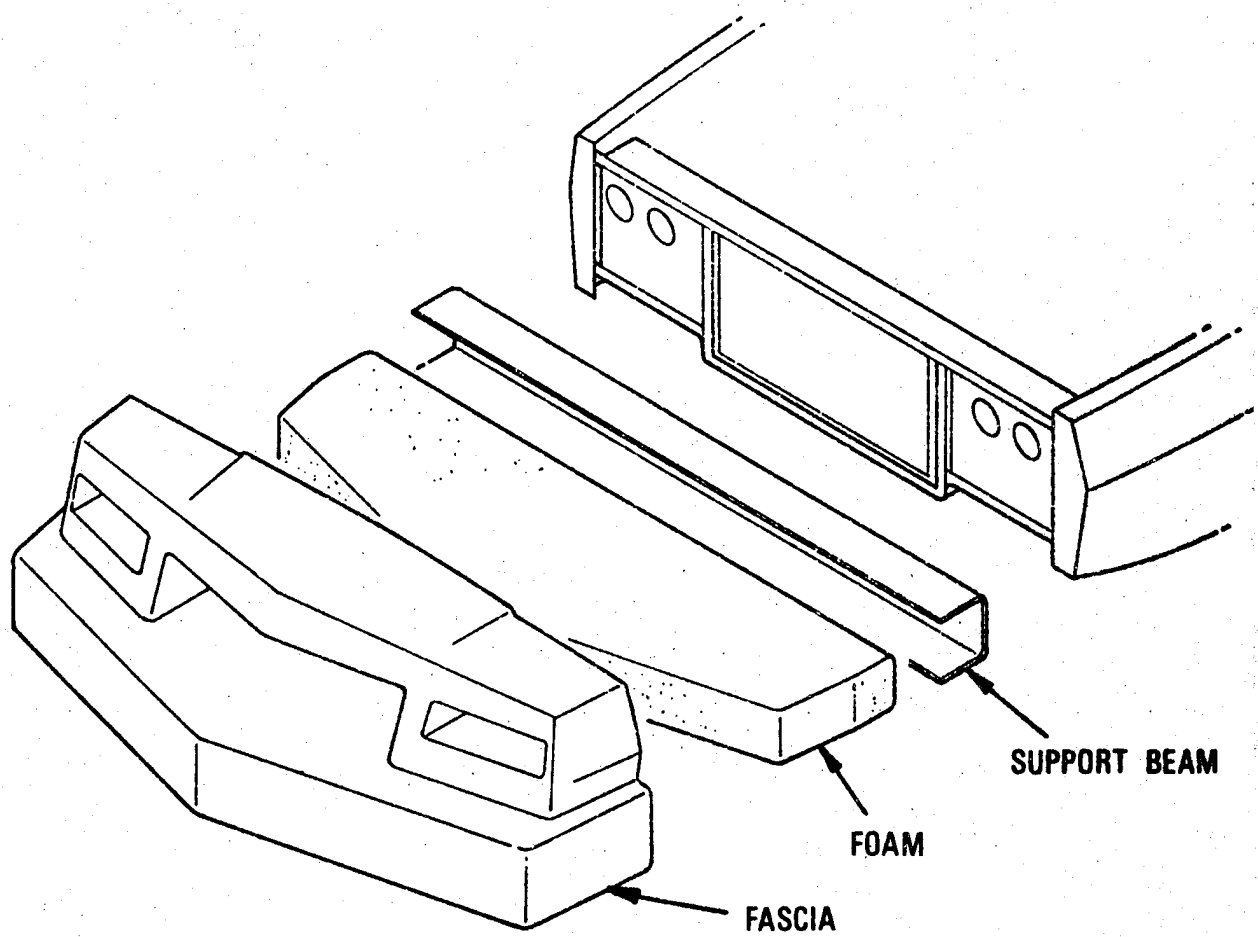
FIGURE 22 FOAM ENERGY ABSORBER, IMPALA FRONT END,
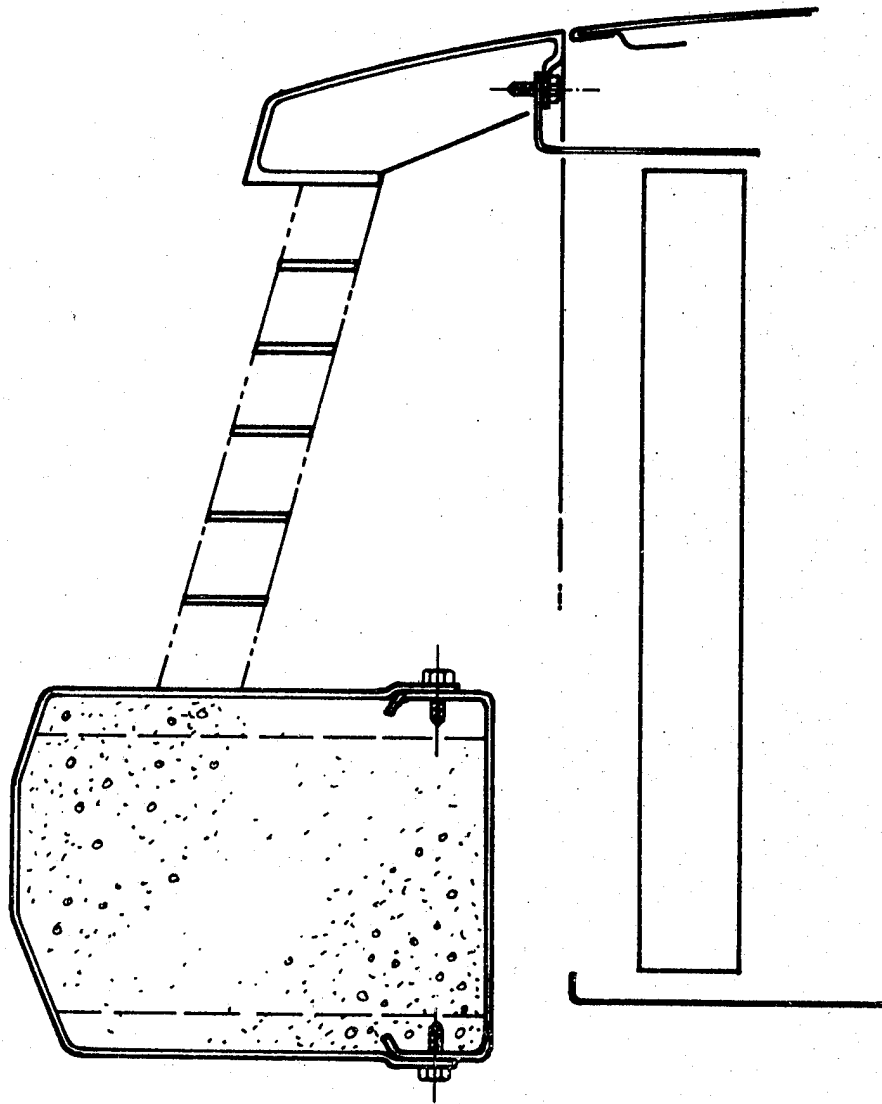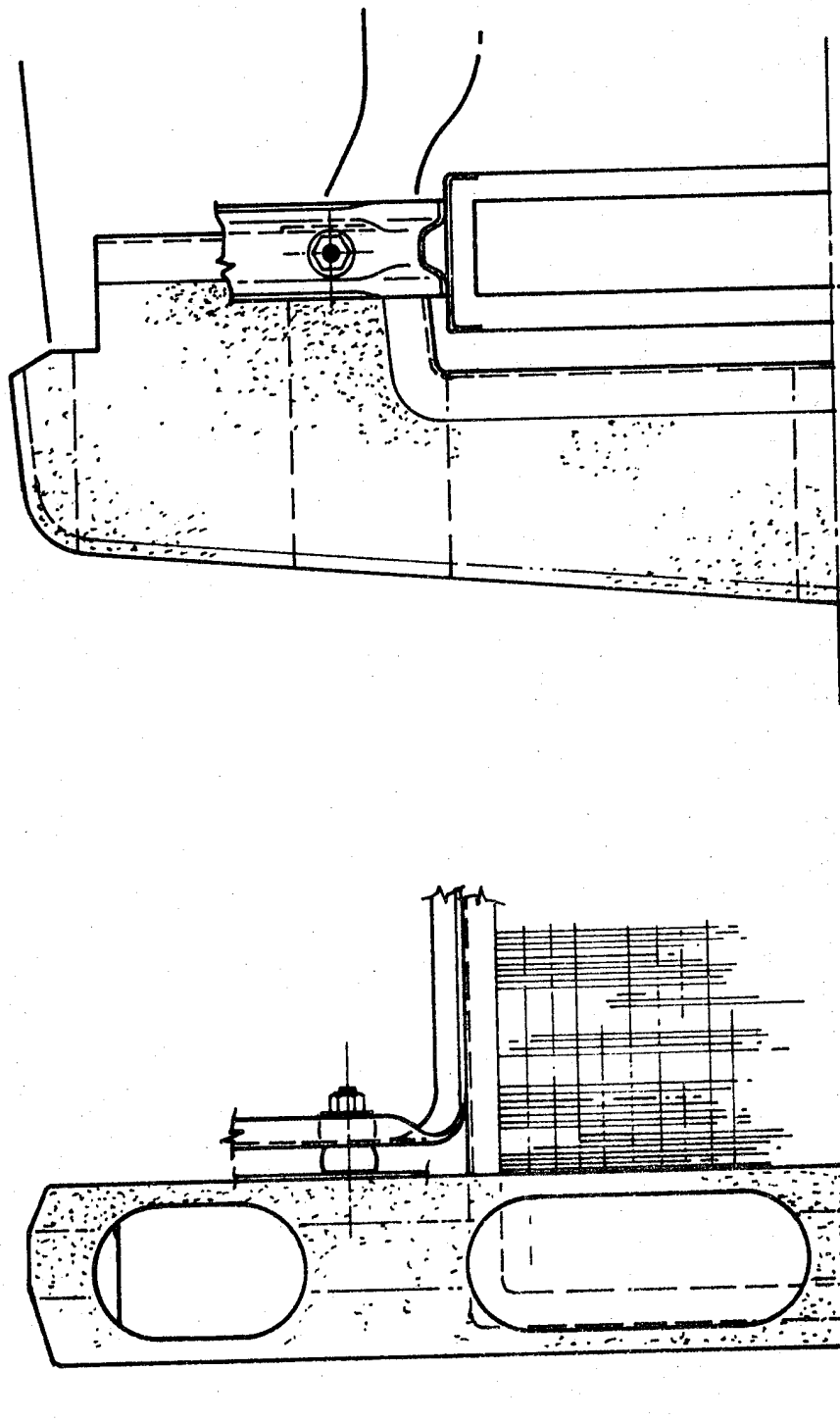SECTION THROUGH FRAME MOUNTING

FIGURE 24 FOAM ENERGY ABSORBER, IMPALA FRONT END, TOP AND FRONT VIEWS

and weight for the face bar can be calculated and the final comparison of the materials made.

The energy absorbed by the bumper face bar is equal to the area under the load-deflection curve. For no permanent damage to occur the bumper will only be stressed to its yield point. This implies that the load-deflection curve is linear and the corresponding absorbed energy is 1/2 x P x d.

It is assumed that the plan view of the bumper will be an arc or a shallow V-shape. The load can then be considered as a point load centered between the two energy absorbers.

The following nomenclature is used:

d_m — deflection of the bumper (at the yield point)

E — flexural modulus

E_b — energy absorbed by the bumper

E_s — energy absorbed by each shock absorber

E_t — total energy of the impact

I — moment of inertia of the bumper cross-section

L — distance between energy absorbers

m — mass of the vehicle

P_m — load on the bumper (at the yield point)

r_b — ratio of the energy absorbed by the bumper to the total energy

r_c — ratio of the energy absorbed by the car frame to the total energy

r_s — ratio of the energy absorbed by each energy absorber to the total energy

R — reaction force of an energy absorber

v — velocity of the vehicle

y_a — distance from the neutral axis of the bumper to the outer fibers

y_s — stroke of the energy absorber

σ_y — yield stress

Previous studies have shown that for a barrier impact eighty per cent of the energy is absorbed by the EMBS while the remaining energy is absorbed by the frame of the car. That is,

$$r_c = 0.20 \quad \text{and} \quad r_b + 2\,r_s = 0.80$$

The face bar will be considered as a simply supported beam with a concentrated load applied at the center.
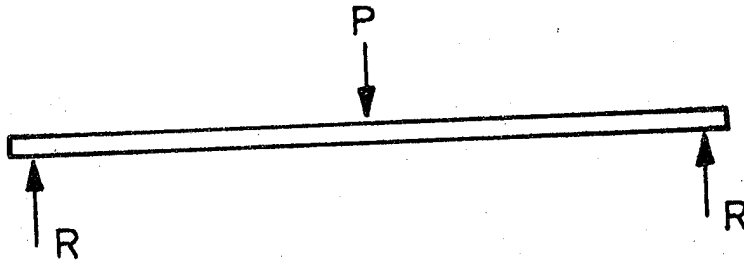
R is the reaction of each energy absorber

The maximum moment and deflection of the beam occur at the midpoint.

$$M_{max} = (1/4)\ Pm\ L \qquad \text{(a)}$$

$$\sigma_y = \frac{M\ y_a}{I} \qquad \text{(b)}$$

substitute (a) into (b) and solve for Pm

$$Pm = \frac{4\ \sigma_y\ I}{L\ y_a} \qquad \text{(1)}$$

The deflection is $dm = \dfrac{Pm\ L^3}{48\ EI}$ \qquad (2)

The energy absorbed by the bumper is

$$E_b = (1/2)\ x\ Pm\ x\ dm \qquad \text{(c)}$$

128

substitute (1) and (2) into (c) and solve for E_b

$$E_b = \frac{\sigma_y{}^2 \; L \; I}{6 \; E \; y_a{}^2} \qquad (3)$$

The total energy of the impact is $E_t = .5 \; m \; v^2$

$$r_b = \frac{\sigma_y \; E_b}{E_t}$$

$$= \frac{\dfrac{\sigma_y{}^2 \; L \; I}{6 \; E \; y_a{}^2}}{.5 \; m \; v^2}$$

$$r_b = \frac{\sigma_y{}^2 \; L \; I}{3 \; E \; y_a{}^2 \; m \; v^2} \qquad (4)$$

The energy absorbed by each energy absorber is one half of the difference between the total energy absorbed by the EMBS and the energy absorbed by the bumper.

$$E_S = (1/2) \left[.8 \, (.5 \; m \; v^2) - \frac{\sigma_y{}^2 \; L \; I}{6 \; E \; y_a{}^2} \right] \qquad (5)$$

The energy absorbers are considered to be linear decelerator shock absorbers. They will be approximated by a constant force versus deflection curve.

$$E_S = R \; y_S \qquad (6)$$

Equate (5) and (6):

$$1/2 \left[.4 \; m \; v^2 - \frac{\sigma_y{}^2 \; L \; I}{6 \; E \; y_a{}^2} \right] = R \; y_S$$

129

Solve for R

$$R = \frac{.2\,m\,v^2}{y_s} - \frac{\sigma_y^2}{12\,E}\frac{L\,I}{y_a^2\,y_s} \qquad (7)$$

The force developed by each energy absorber is R. The total force Pm = 2R.

$$Pm = \frac{.4m\,v^2}{y_s} - \frac{\sigma_y^2}{6\,E}\frac{L\,I}{y_a^2\,y_s} \qquad (8)$$

Equate (8) and (1) and solve for I

$$\frac{4\,\sigma_y\,I}{L\,y_a} = \frac{.4m\,v^2}{y_s} - \frac{\sigma_y^2}{6\,E}\frac{L\,I}{y_a^2\,y_s}$$

$$\left(\frac{4\,\sigma_y}{L\,y_a} + \frac{\sigma_y^2}{6\,E}\frac{L}{y_a^2\,y_s} \right) I = \frac{.4m\,v^2}{y_s}$$

$$I = \frac{2.4\,m\,v^2\,E\,y_a^2\,L}{(L^2 + 24\,E\,y_a\,y_s)} \qquad (9)$$

Substitute (9) into (4)

$$r_b = \frac{\sigma_y^2}{3\,E\,y_a^2\,m\,v^2}\,L\left(\frac{2.4\,m\,v^2\,E\,y_a^2\,L}{(L^2 + 24\,E\,y_a\,y_s)} \right)$$

$$r_b = \frac{.8 \; L^2}{L^2 + 24 \; E \; y_a \; y_s} \tag{10}$$

$$r_s = 1/2 \; (1 - r_b - r_c)$$

$$r_s = 1/2 \left(1 - \frac{.8 \; L^2}{L^2 + 24 \; E \; y_a \; y_s} - .2 \right)$$

$$r_s = \frac{9.6 \; E \; y_a \; y_s}{L^2 + 24 \; E \; y_a \; y_s} \tag{11}$$

$$\text{Let} \quad = \frac{24 \; E \; y_a \; y_s}{L^2} \tag{12}$$

$$r_c = 0.20 \tag{13}$$

$$r_b = \frac{0.8}{1 + \gamma} \tag{14}$$

$$r_s = \frac{0.4}{1 + \gamma} \tag{15}$$

$$I = \frac{2.4 \; m \; v^2 \; E \; y_a^{\;2}}{2 \; L \; (1 + \gamma)} \tag{16}$$

131

The criteria that is used in evaluating the different materials is the force in the shock absorber needed to withstand the impact, the thickness of the material, (which is approximately linearly proportional to the moment of inertia), the weight of the bumper, and the deflection of the bumper.

The properties of the material that will be used are:

TABLE 48: BUMPER MATERIALS

	E		
HSLA Steel - 950	30×10^6 psi	50 ksi	493 lb/ft^3
HSLA Steel - 980	30×10^6 psi	80 ksi	493 lb/ft^3
X7046-T63 AL	10×10^6 psi	55 ksi	176 lb/ft^3
30% Glass Polyester	2×10^6 psi	30 ksi	110 lb/ft^3
65% Glass Polyester	2×10^6 psi	50 ksi	110 lb/ft^3

The following values are also used in the calculations:

TABLE 49: BUMPER PARAMETERS

	Small Car	Large Car
y_a	2.3 in.	2.6 in.
y_s	3.0 in.	3.0 in.
L	40.0 in.	45.0 in.
m	2500 lb.	3600 lb.
I	54 t in^3	84 t in^3

For evaluation of the bumper bar, the cross-section will be approximated by Figures 25 and 26. The moments of inertia were calculated and linearized in t, the thickness of the material.

Table 50 gives the energy ratios for each of the five different materials. It can be seen that as the flexural modulus decreases the percentages of energy absorbed by the bumper increases.

TABLE 50: ENERGY RATIOS-BUMPERS

SMALL CAR

		r_c	r_b	r_s
HSLA-950-St.	62.10	0.2000	0.0127	0.3937
HSLA-980-St.	38.81	0.2000	0.0201	0.3900
X70-46-T63-Al	18.82	0.2000	0.0404	0.3798
SMC	6.90	0.2000	0.1013	0.3494
HMC	4.14	0.2000	0.1556	0.3222

LARGE CAR

		r_c	r_b	r_s
HSLA-950-St.	55.47	0.2000	0.0112	0.3929
HSLA-980-St.	34.67	0.2000	0.0224	0.3888
X70-46-T63-Al	16.81	0.2000	0.0449	0.3775
SMC	6.16	0.2000	0.1117	0.3442
HMC	3.70	0.2000	0.1703	0.3149

The deflections of the bumpers are:

$$dm = 58.0 \frac{\sigma}{E} \quad , \quad \text{small car}$$

$$dm = 64.9 \frac{\sigma}{E} \quad , \quad \text{large car}$$

133

FIGURE 25 SMALL CAR BUMPER CROSS-SECTION
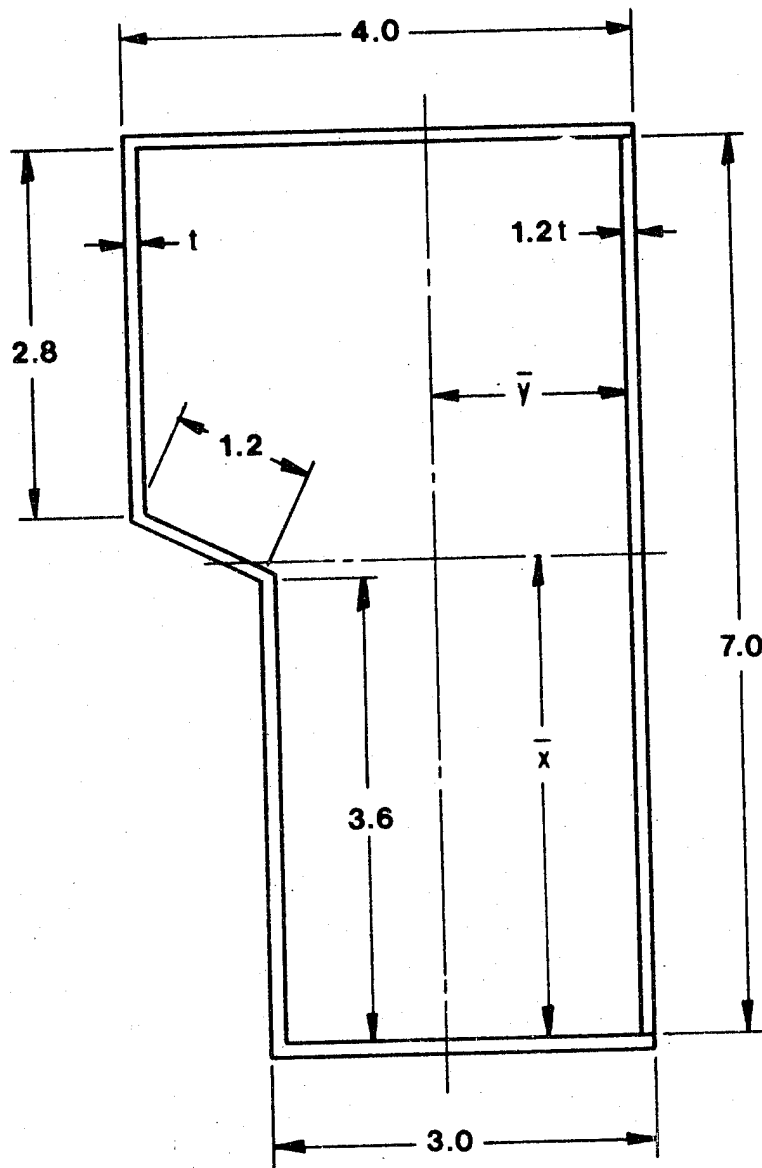
FIGURE 26 LARGE CAR BUMPER CROSS-SECTION
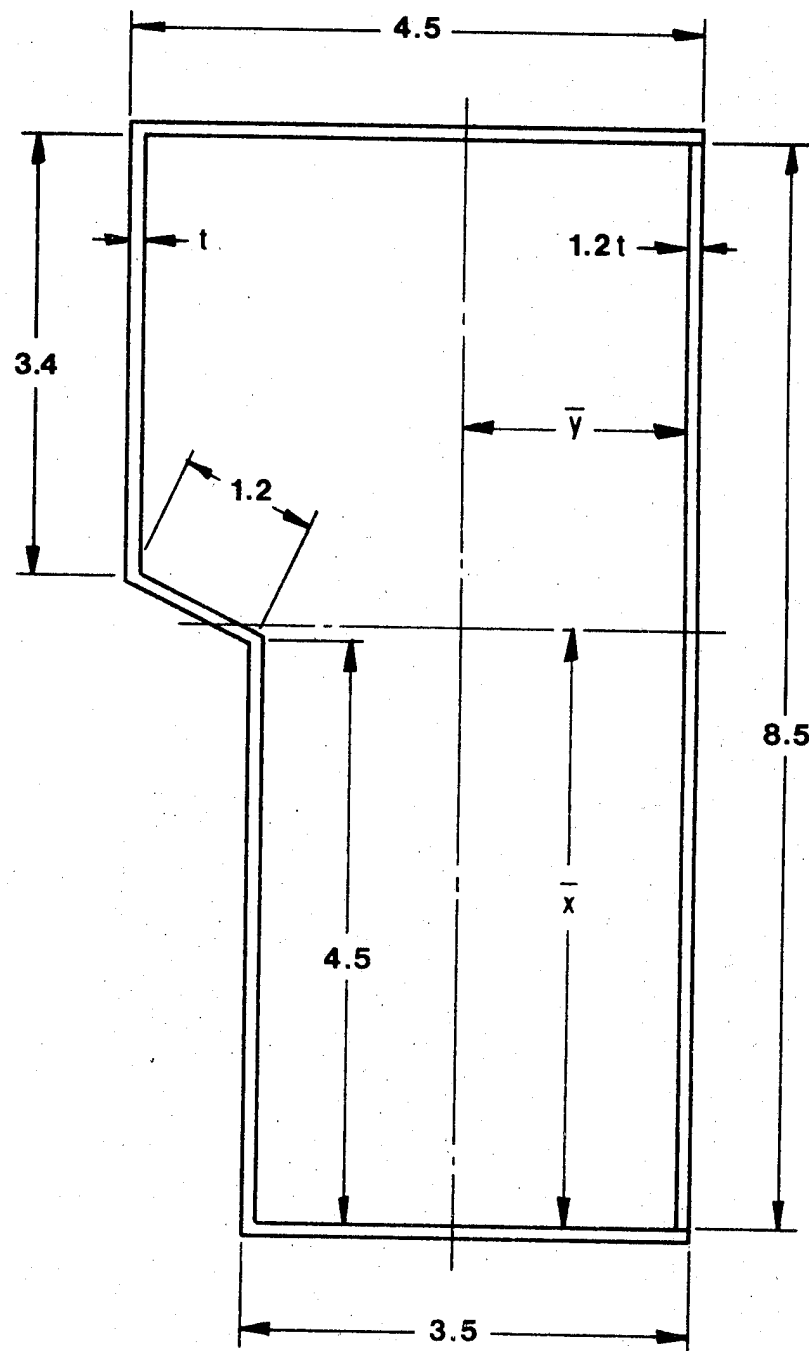
The results obtained with the five selected materials at two velocities, 5 and 10 mph, are tabulated in Table 51 through 55.

5.5 Damageability Summary

Non damageability can be achieved by using materials capable of having very large elastic deformations and subsequent recovery of their original shape. Such materials are exemplified by the elastomers. Lesser levels can be achieved by using materials having low flexural moduli, with reasonably high yield strengths, for example reinforced or non-reinforced thermoplastics and thermosets. Metals such as aluminum and steel having higher elastic modulii than reinforced or non-reinforced plastics absorb less energy elastically and result in yielded, damaged, surfaces. However, the degree of denting and dinging of metals is directly related to its tensile yield strength.

Elastic foams developed in recent years possess sufficient elastic energy absorption capabilities to change the basic concepts of energy absorption at impact speeds in the range of 15 to 20 mph. Such materials in conjunction with elastomeric higher density fascia skins offer a new area for design and styling with low damage probability.

136

TABLE 51: HSLA-950-STEEL BUMPERS

	5 MPH	10 MPH
Moment of Inertia I (in^4)	3.027	12.110
Shock Absorber Force R (lb)	3291	13.163
Bumper Deflection dm (in)	0.097	0.097
Thickness t (in)	0.056	0.236
Weight W (lb)	23.9	100.7

SMALL CAR

	5 MPH	10 MPH
Moment of Inertia I (in^4)	5.533	22.130
Shock Absorber Force R (lb)	4730	18.919
Bumper Deflection dm (in)	0.108	0.108
Thickness t (in)	0.066	0.287
Weight W (lb)	38.5	167.7

LARGE CAR

TABLE 52:   HSLA 980-STEEL BUMPERS

	5 MPH	10 MPH
Moment of Inertia I (in^4)	1.874	7.497
Shock Absorber Force R (lb)	3.260	13.039
Bumper Deflection dm (in)	0.155	0.155
Thickness t (in)	0.035	0.140
Weight W (lb)	14.8	59.7

SMALL CAR

	5 MPH	10 MPH
Moment of Inertia I (in^4)	3.422	13.689
Shock Absorber Force R (lb)	4680	18.720
Bumper Deflection dm (in)	0.173	0.173
Thickness t (in)	0.041	0.167
Weight W (lb)	23.8	97.6

LARGE CAR

TABLE 53: X-7046-T63 ALUMINUM BUMPERS

			5 MPH	10 MPH
Moment of Inertia	I	(in^4)	2.655	10.621
Shock Absorber Force	R	(lb)	3175	12.700
Bumper Deflection	dm	(in)	0.319	0.319
Thickness	t	(in)	0.049	0.205
Weight	W	(lb)	7.5	31.2

SMALL CAR

			5 MPH	10 MPH
Moment of Inertia	I	(in^4)	4.833	19.333
Shock Absorber Force	R	(lb)	4545	18178
Bumper Deflection	dm	(in)	0.357	0.357
Thickness	t	(in)	0.058	0.244
Weight	W	(lb)	12.0	50.9

LARGE CAR

TABLE 54: SMC BUMPERS

	5 MPH	10 MPH
Moment of Inertia I (in^4)	4.478	17.912
Shock Absorber Force R (lb)	2920	11.682
Bumper Deflection dm (in)	0.870	0.870
Thickness t (in)	0.083	0.366
Weight W (lb)	7.9	34.7

SMALL CAR

	5 MPH	10 MPH
Moment of Inertia I (in^4)	8.082	32.327
Shock Absorber Force R (lb)	4142	16.570
Bumper Deflection dm (in)	0.973	0.973
Thickness t (in)	0.096	0.457
Weight W (lb)	12.5	59.6

LARGE CAR

TABLE 55: HMC BUMPERS

			5 MPH	10 MPH
Moment of Inertia	I	(in^4)	2.478	9.911
Shock Absorber Force	R	(lb)	2693	10.773
Bumper Deflection	dm	(in)	1.449	1.449
Thickness	t	(in)	0.046	0.192
Weight	W	(lb)	4.4	18.3

SMALL CAR

			5 MPH	10 MPH
Moment of Inertia	I	(in^4)	4.432	17.729
Shock Absorber Force	R	(lb)	3790	15.162
Bumper Deflection	dm	(in)	1.624	1.624
Thickness	t	(in)	0.222	0.222
Weight	W	(lb)	6.9	28.9

LARGE CAR

141

6.0 DESIGN CONCEPTS - FRAMED VEHICLE

The application of an alternate material in an automotive structural design may require changes of a micro or macro nature depending upon the function of the component. Automobiles are styled for sale and the styles are presently based on the ability to produce them using low carbon steel and some interior and exterior plastic cosmetic parts. As the fuel efficiency regulations become more restrictive the styling must be less appearance conscious and more functional to efficiently use all of the weight.

Since each of the candidate materials has its own set of properties and manufacturing procedures, structural concepts different from those now applied may be required. If these different concepts are not required due to material manufacturing limitations then they may be required, or desired, to more efficiently use the materials.

For the evaluation of a framed, six passenger family vehicle the 1977 Impala was selected by NHTSA. This vehicle represents the General Motors B Body structure which is available in several other vehicle lines under other names. The 1977 Impala represents the first major commercial attempt to down size vehicles (3709 pounds curb weight) without radically changing the passenger compartment volume (6 passenger).

6.1 Vehicle Structure Characterization

The 1977 Impala structure can be described by reviewing the following major components.

1. Frame
2. Passenger Compartment
3. Hood and Deck Lid
4. Front Fender Structure
5. Radiator Support
6. Front and Rear Bumper Systems
7. Doors

Each of the above areas or major structural components will be reviewed separately to determine its function and requirements.

6.1.1 Frame

Frames for the Impala are made of hot rolled low carbon steel. A representative sketch of the "B" frame is shown in Figure 27. The passenger compartment and engine are attached to the frame through elastomeric mountings. Generally speaking the noise and vibration harshness are lower for a framed vehicle when compared to a non-framed vehicle of similar size.

The hot rolled steel for frames is supplied as strip, coiled sheet or flat blanks. Appropriate size blanks are sheared and holes punched prior to single action forming. Trimming after press forming

FIGURE 27 GENERAL MOTORS "B" FRAME

REAR OUTER

REAR INNER

CENTER SIDE OUTER

FRONT OUTER

SUSPENSION SUPPORT

FRONT INNER

TRANSMISSION SUPPORT

UPPER AND LOWER CROSSMEMBERS
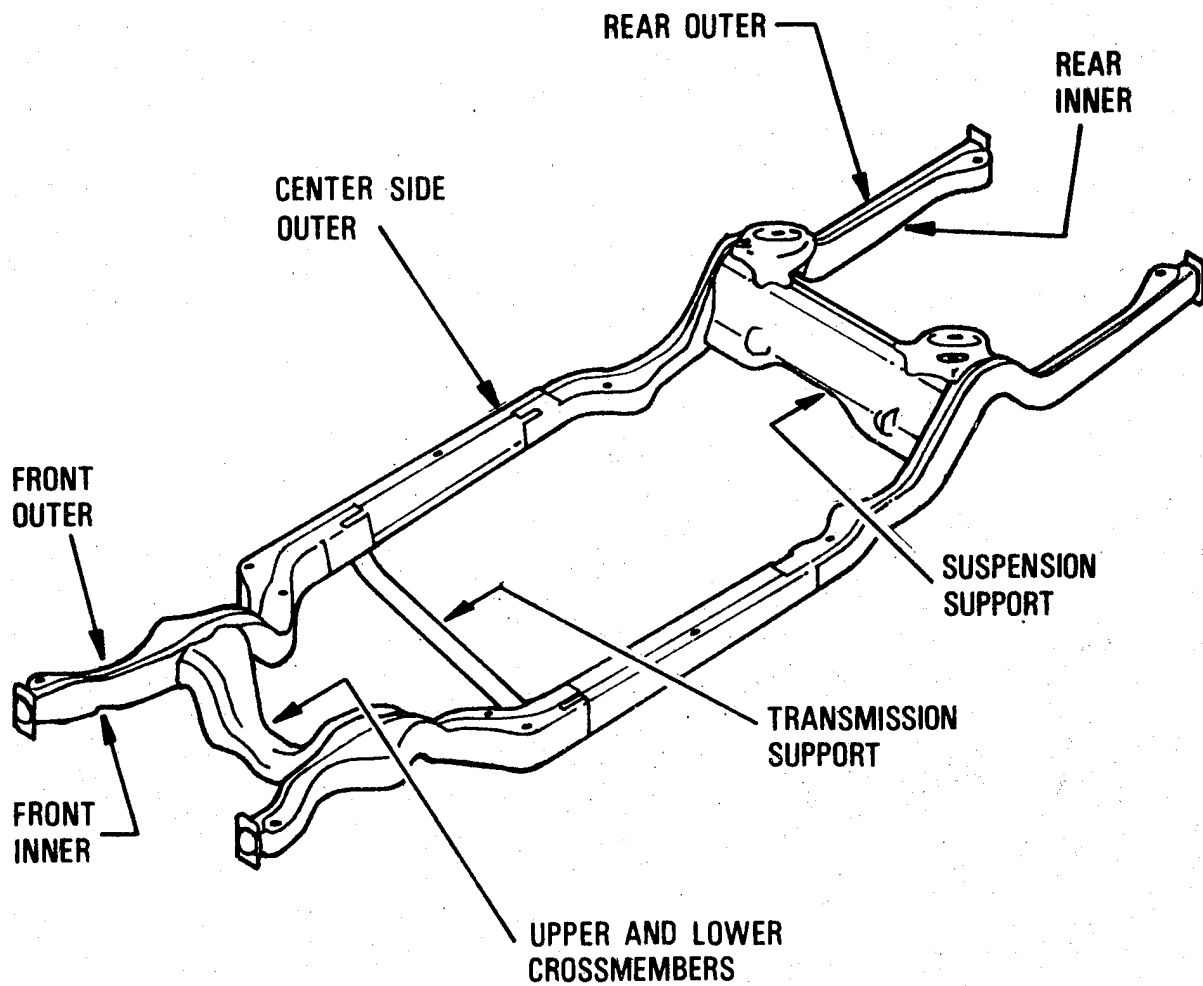
is kept at a minimum. These parts are then assembled to each other in a progressive assembly line. Joining is primarily by arc welding and may be automatic or manual. After assembly, the frame is painted inside and out to provide adequate corrosion protection and resistance to the impact of road debris.

The costs of frames are minimized by carefully controlling material and labor costs. Blanks are nested to utilize a very high percent of the incoming material. Even though much of the welding may be performed manually, tooling and assembly aids are used to obtain high productivity.

A study was completed to design a 1977 GM "B" frame that is lighter in weight and as stiff in bending as the existing frame using aluminum alloys and high strength low alloy steels. The design criteria used were (a) the general shape of the frame was to remain the same, (b) the flexural and torsional rigidities were to be maintained, and (c) the maximum increase in height and/or width of the corss-section was to be 0.75 inches.

Cross-sectional views at ten different points on the frame (Figure 28) were obtained from General Motors drawings 369877 "Frame Chart-Front" and 373101 "Frame Chart-Rear". These sections (Figures 29 to 38) were used as the basis for the investigation of weight savings.

A computer program ("RCSECTIONS") developed by the Budd Company Technical Center was used to calculate the moments of inertia of the different cross-sections. For HSLA steel the moment of inertia for the new frame had to be equal to the moment of inertia for the existing frame since Young's modulus is approximately the same for all steels. For aluminum, however, since Young's modulus is one third that of steel, the moment of inertia had to be increased by a factor of three.

It is known that an increase in height, width and thickness of a cross-section would increase its section properties. An analysis of section BM-BM (Figure 29) was performed by increasing the height and width by small amounts while the thickness was decreased to maintain a constant moment of inertia. For a constant moment of inertia the minimum cross-sectional area corresponded to the maximum possible increase in height and width, and all further analysis considered the maximum allowed increase in the height and width, 0.75 inches. The correct moment of inertia was then obtained by thickness variations only. The moments of inertia (in^4) of the existing frame are listed in Table 56.

The weight summaries for the three frames are shown in Table 57. The existing frame weighs approximately 293 lbs. and varies in thickness from 0.098" to 0.138". The HSLA-45 frame weighs 226 lbs. and varies in thickness from .063" to .088". The aluminum frame weighs 258 lbs. and varies in thickness from .209" to .313".

FIGURE 28 LOCATION OF SECTIONS "B" FRAME
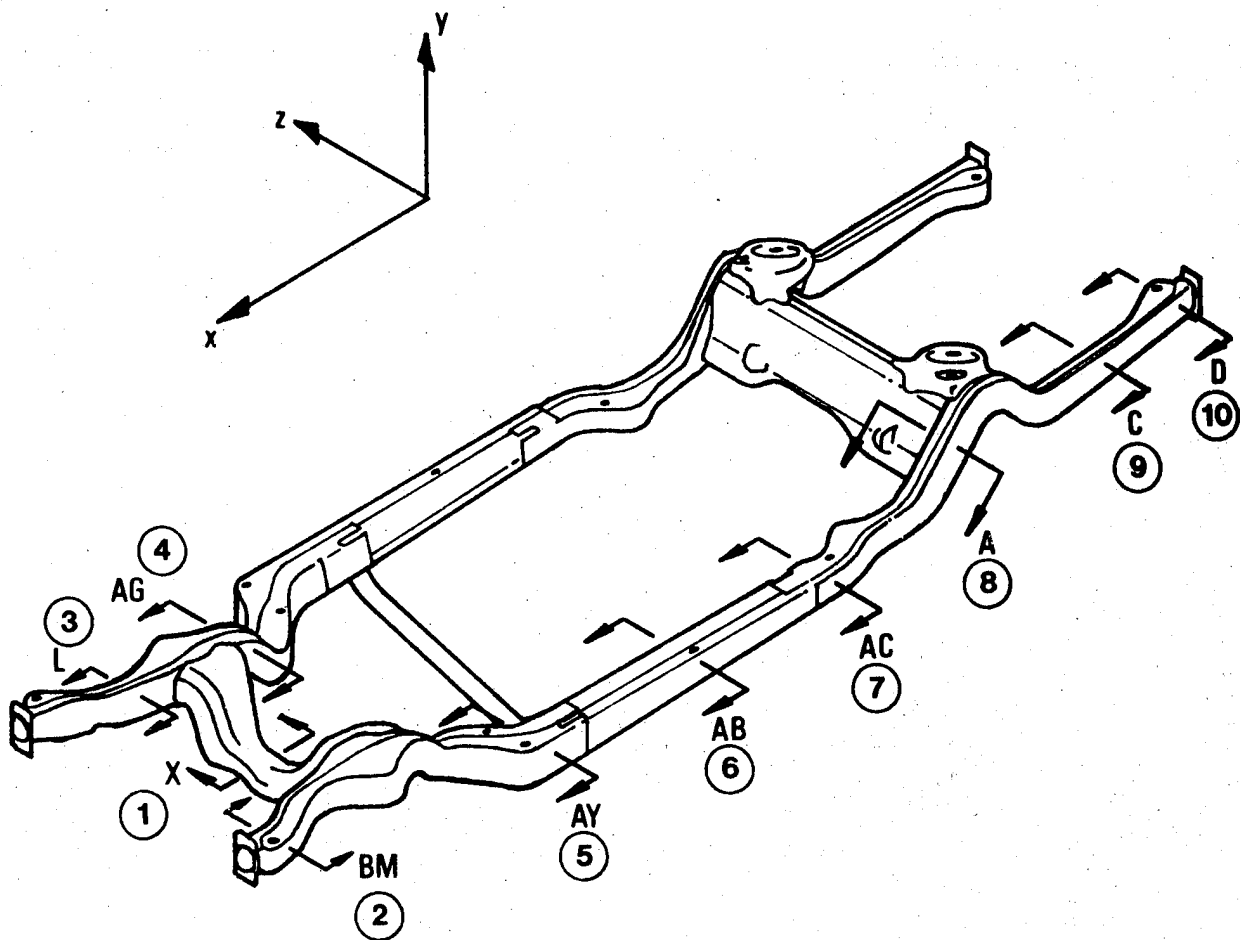
FIGURE 29 SECTION X-X
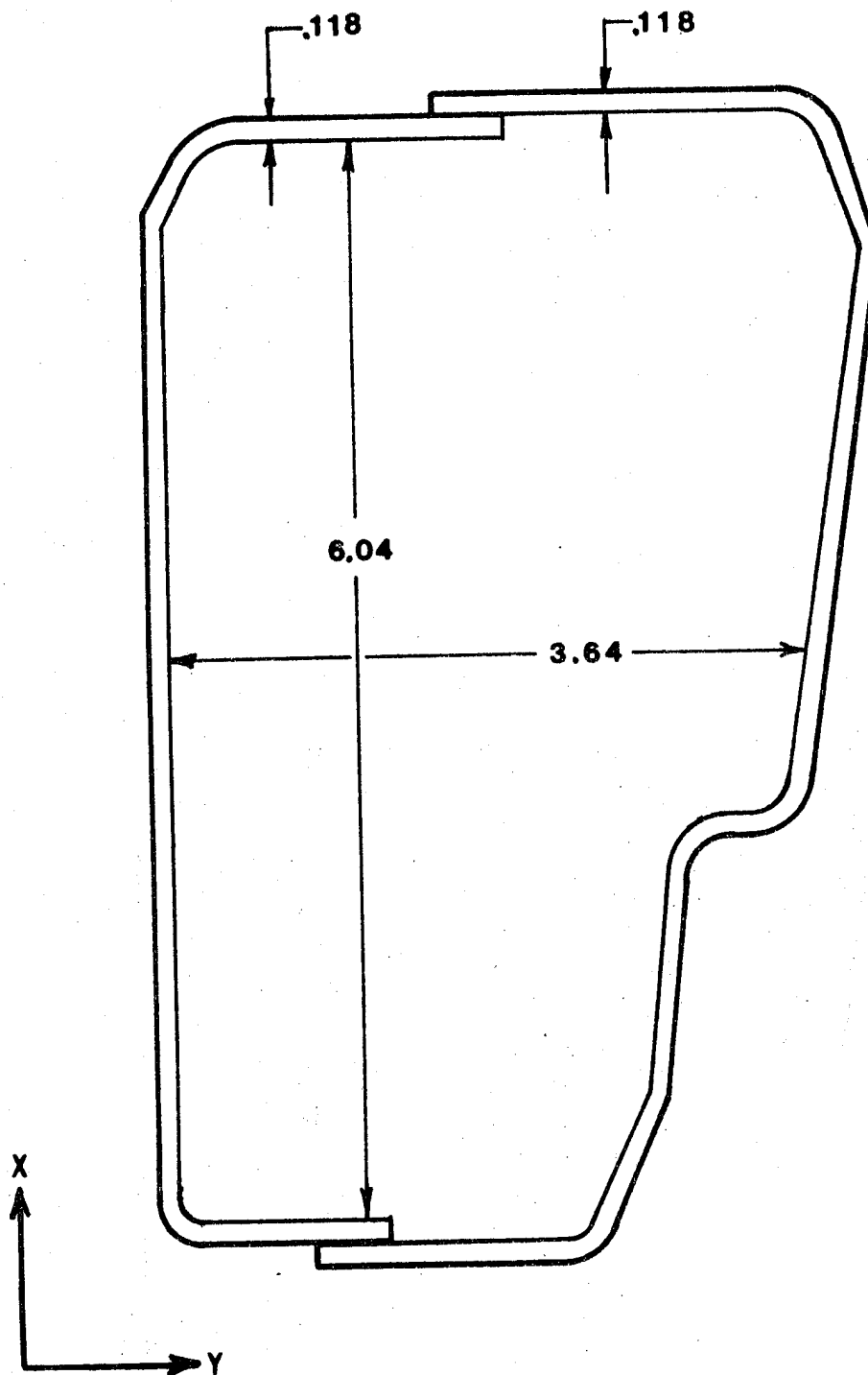
FIGURE 30 SECTION BM-BM

147
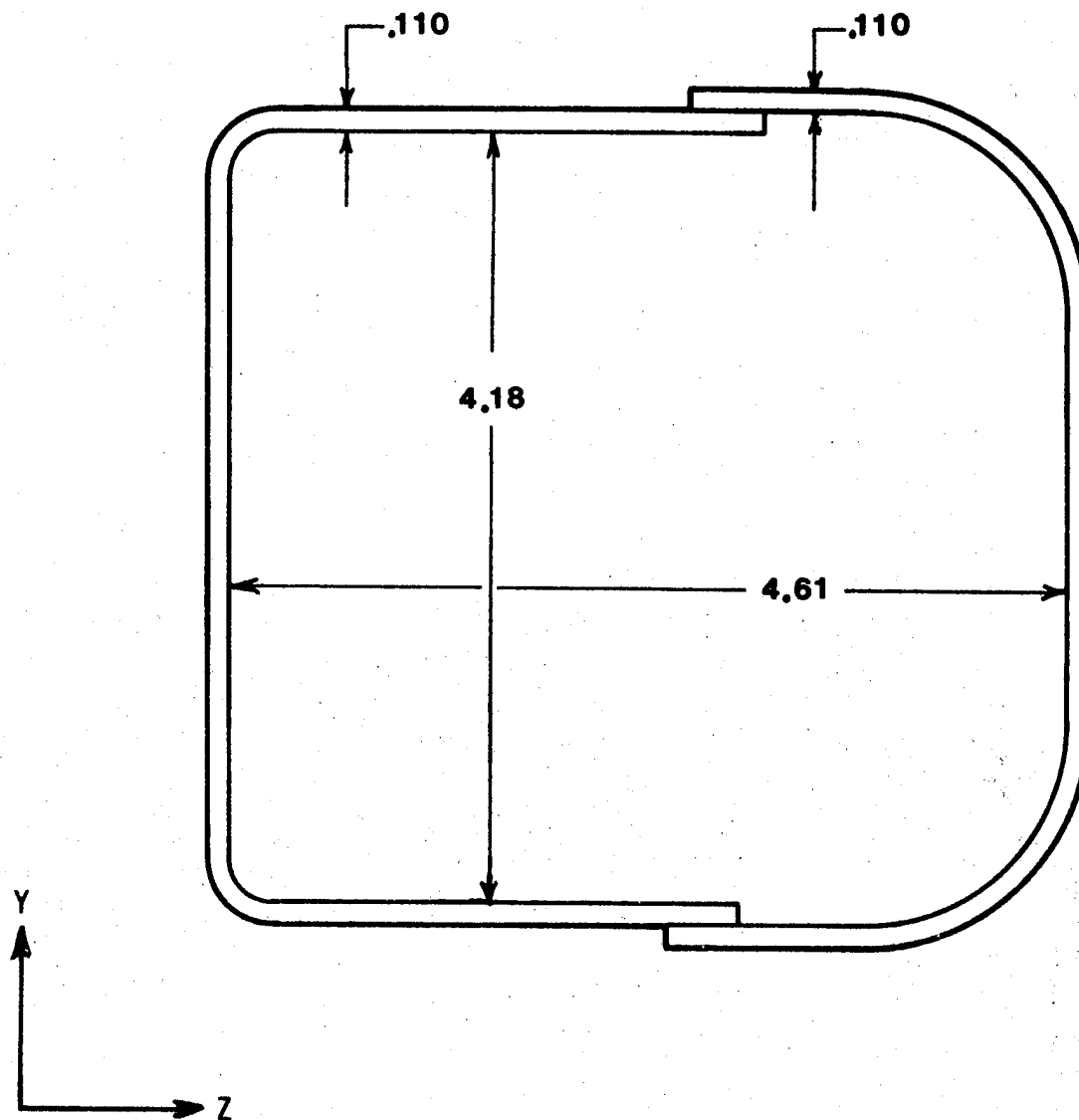
FIGURE 31   SECTION L-L
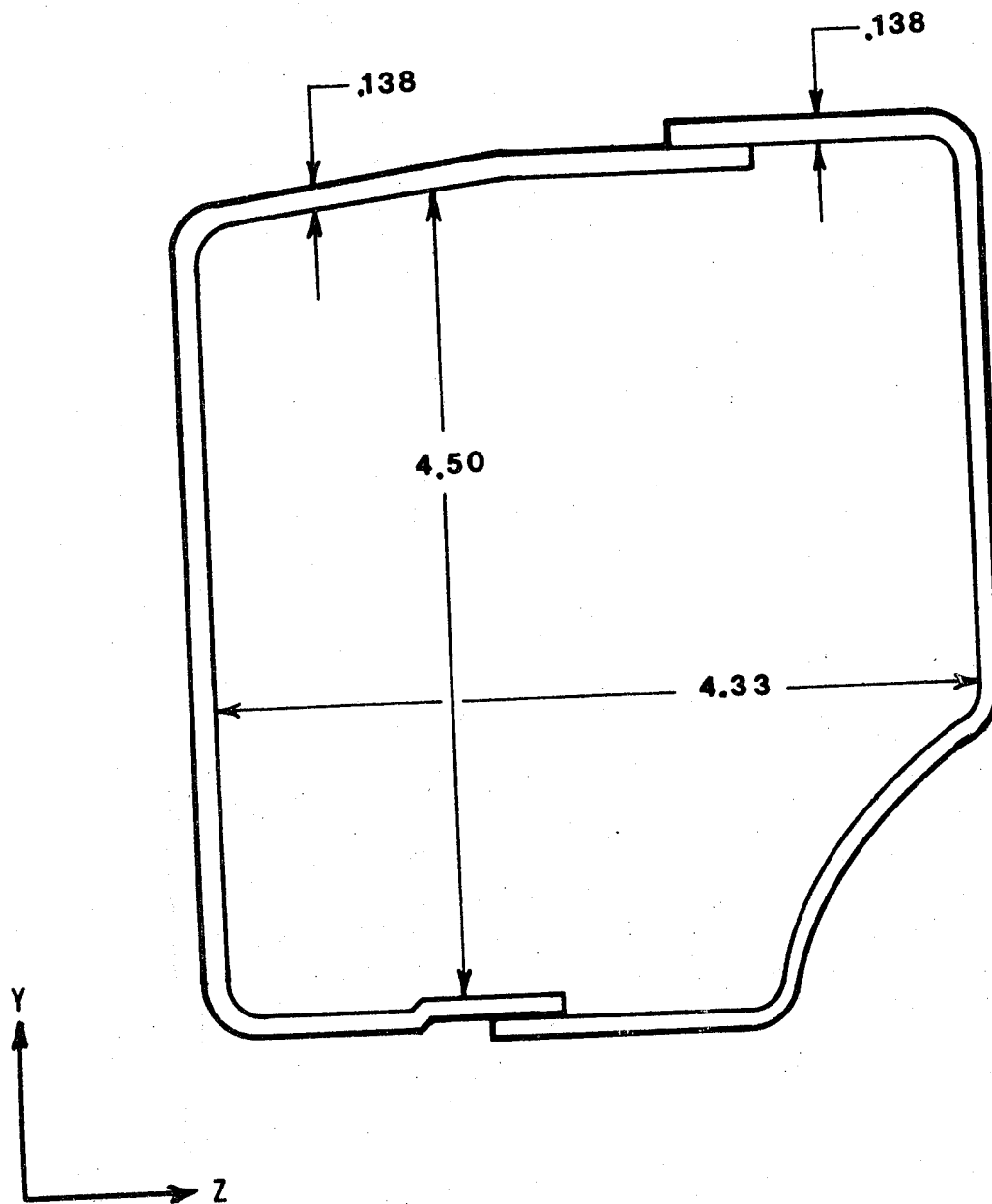
FIGURE 32 SECTION AG-AG
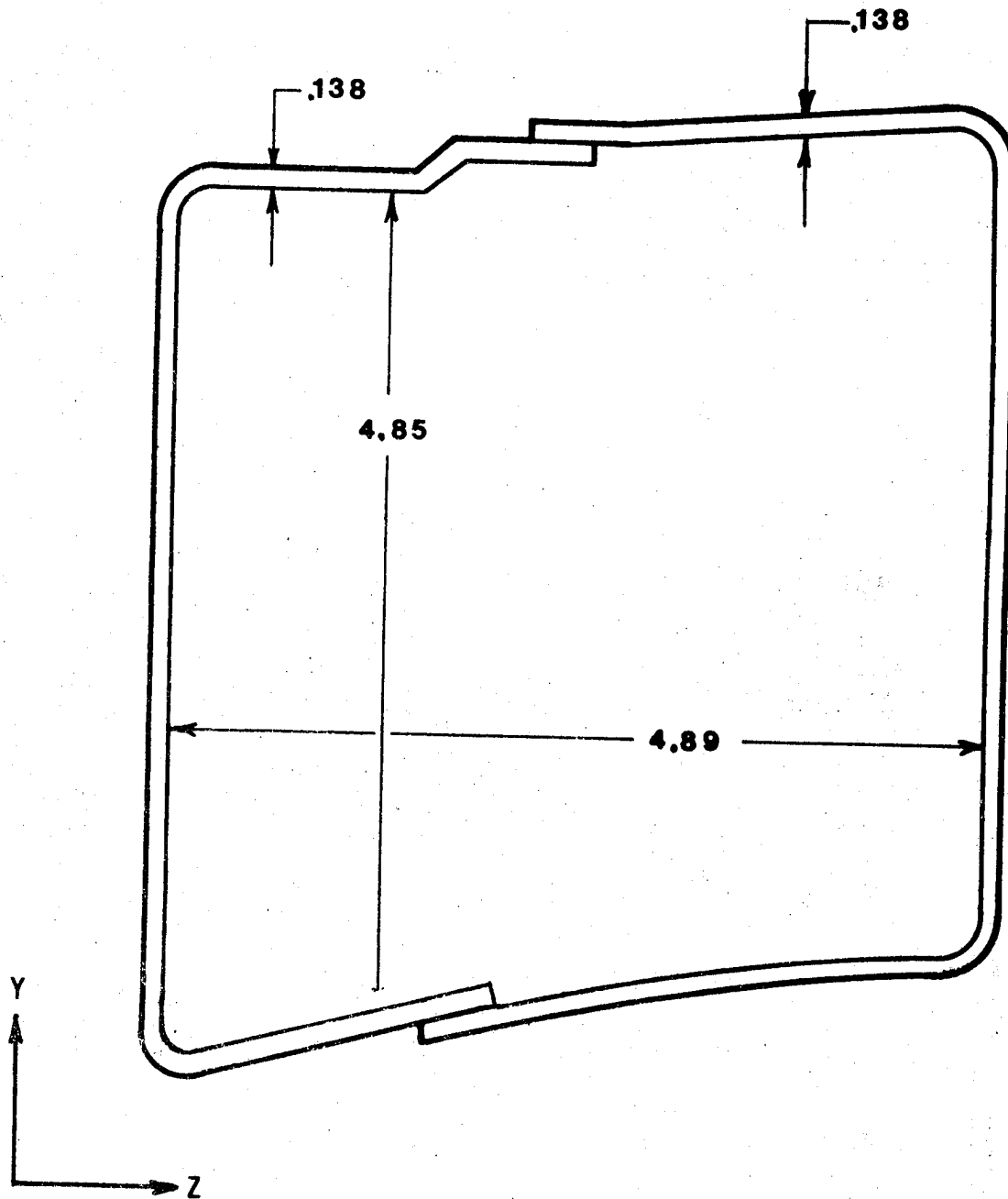
FIGURE 33 SECTION AY-AY
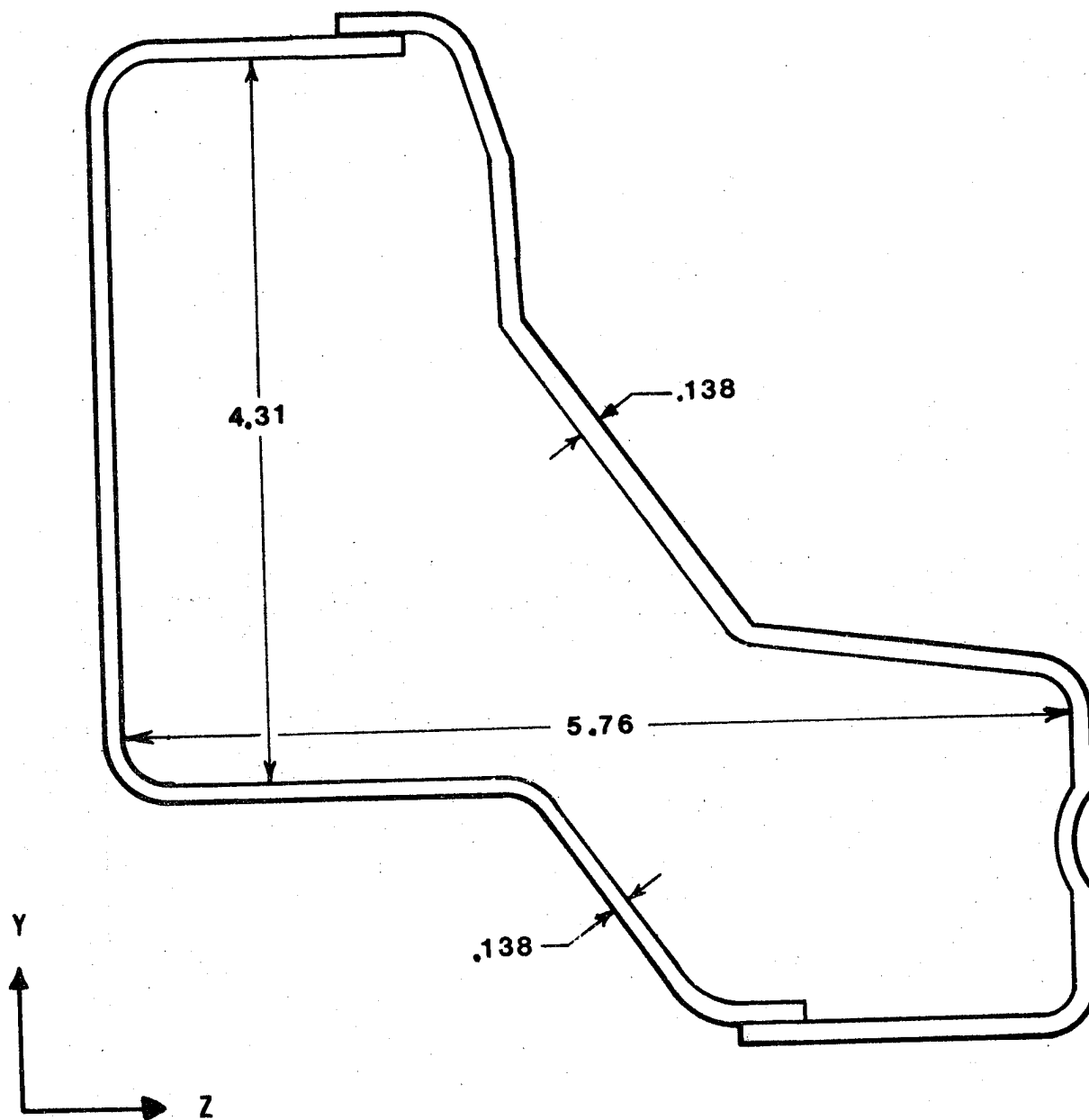
FIGURE 34 SECTION AB-AB

151
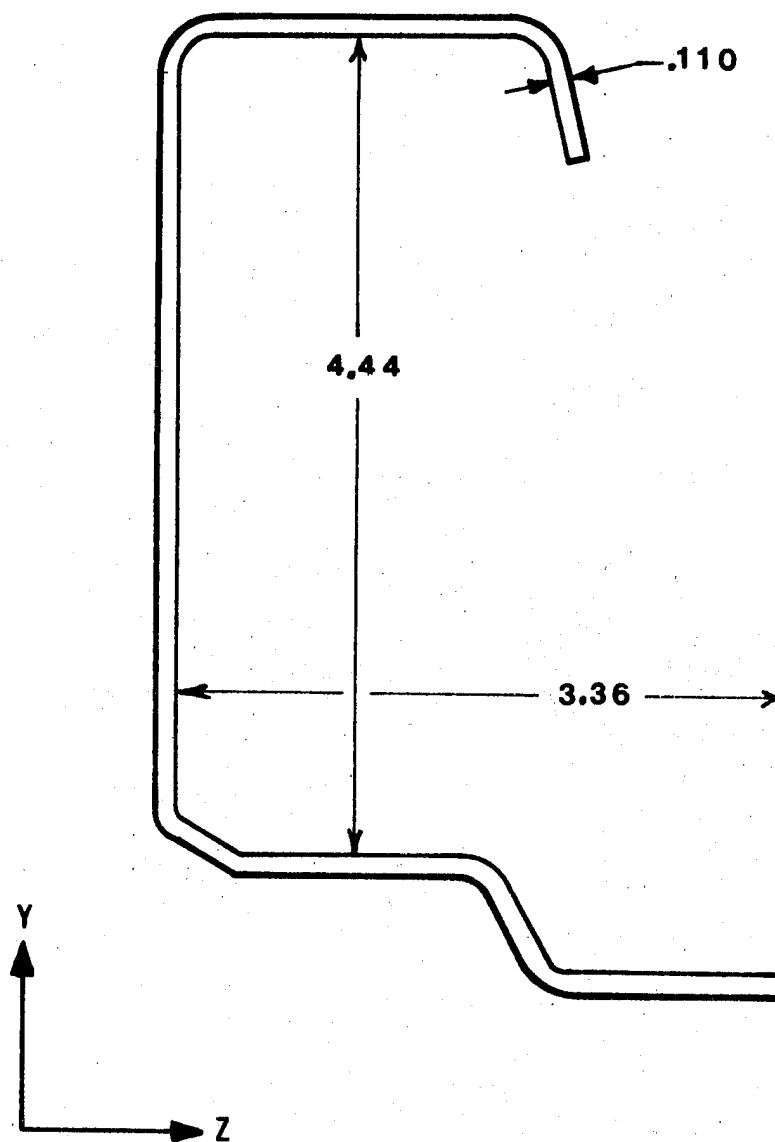
FIGURE 35 SECTION AC-AC
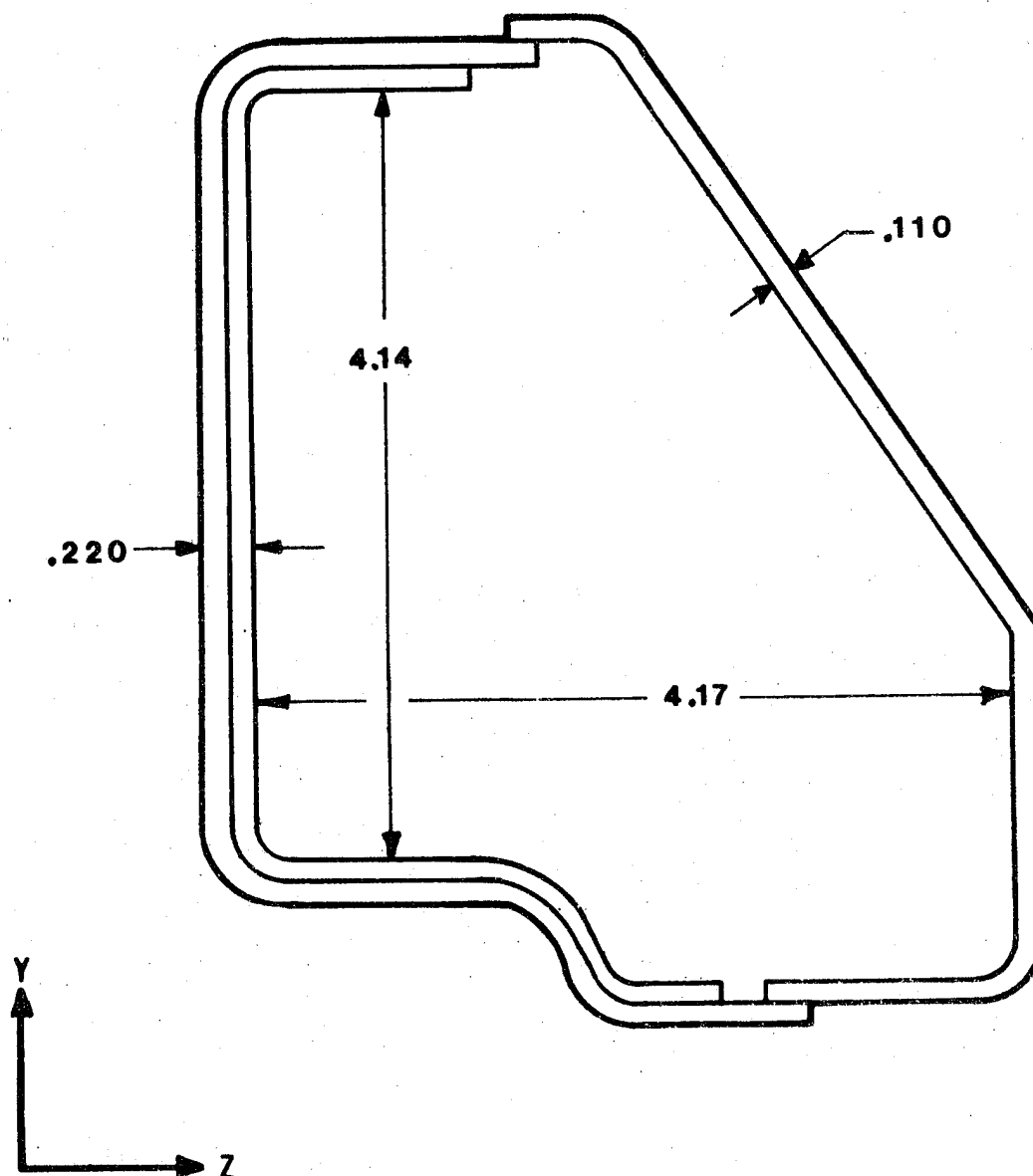
FIGURE 36 SECTION A-A.
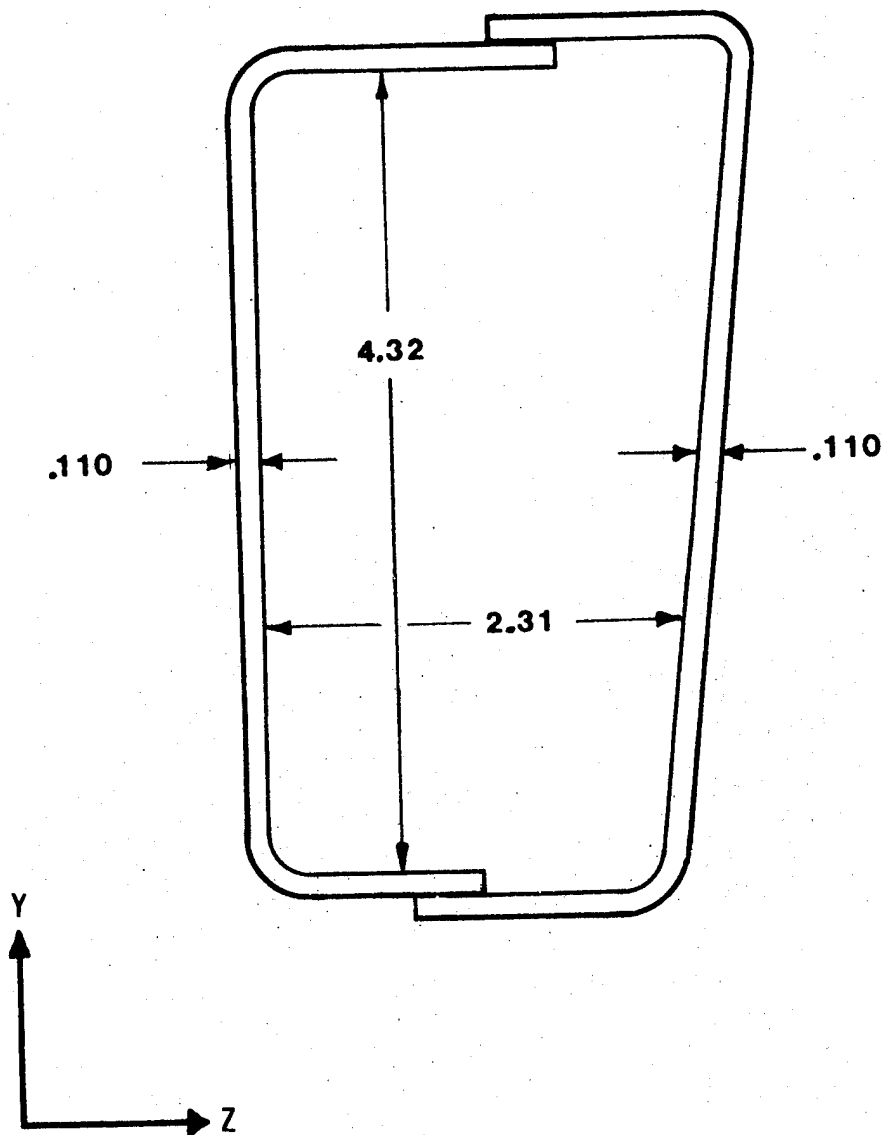
FIGURE 37 SECTION C-C

154
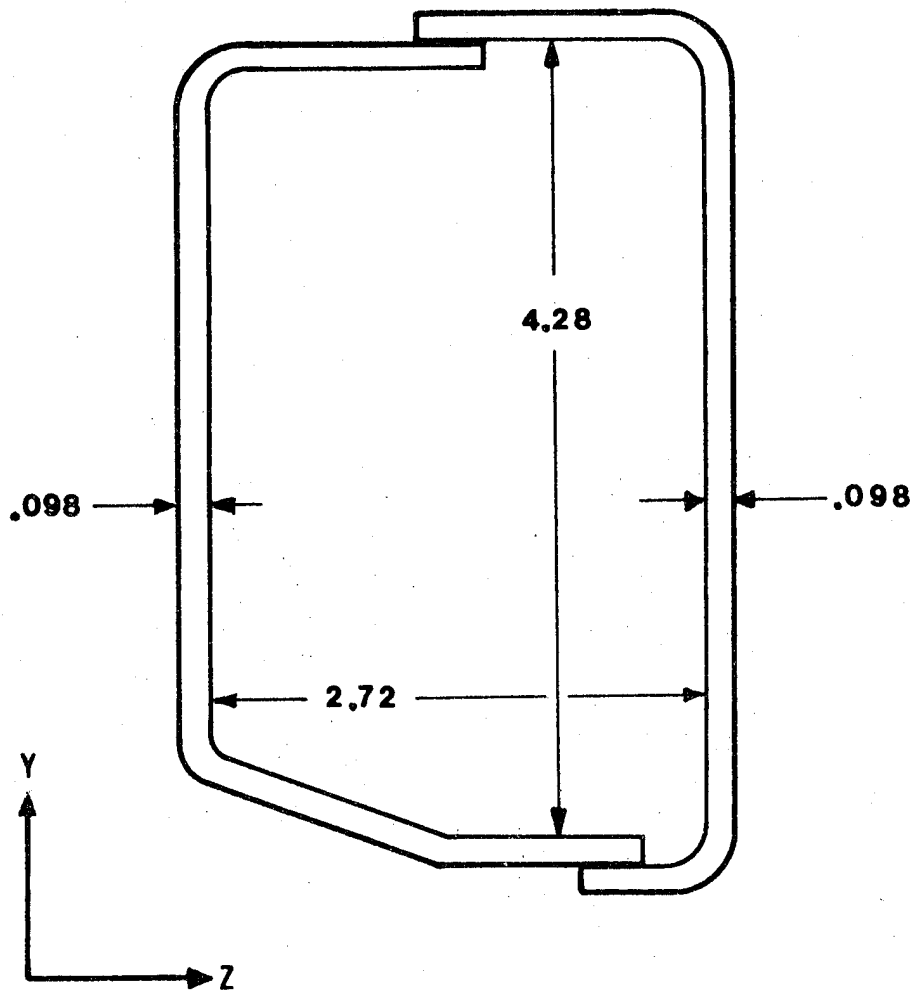
FIGURE 38 SECTION D-D
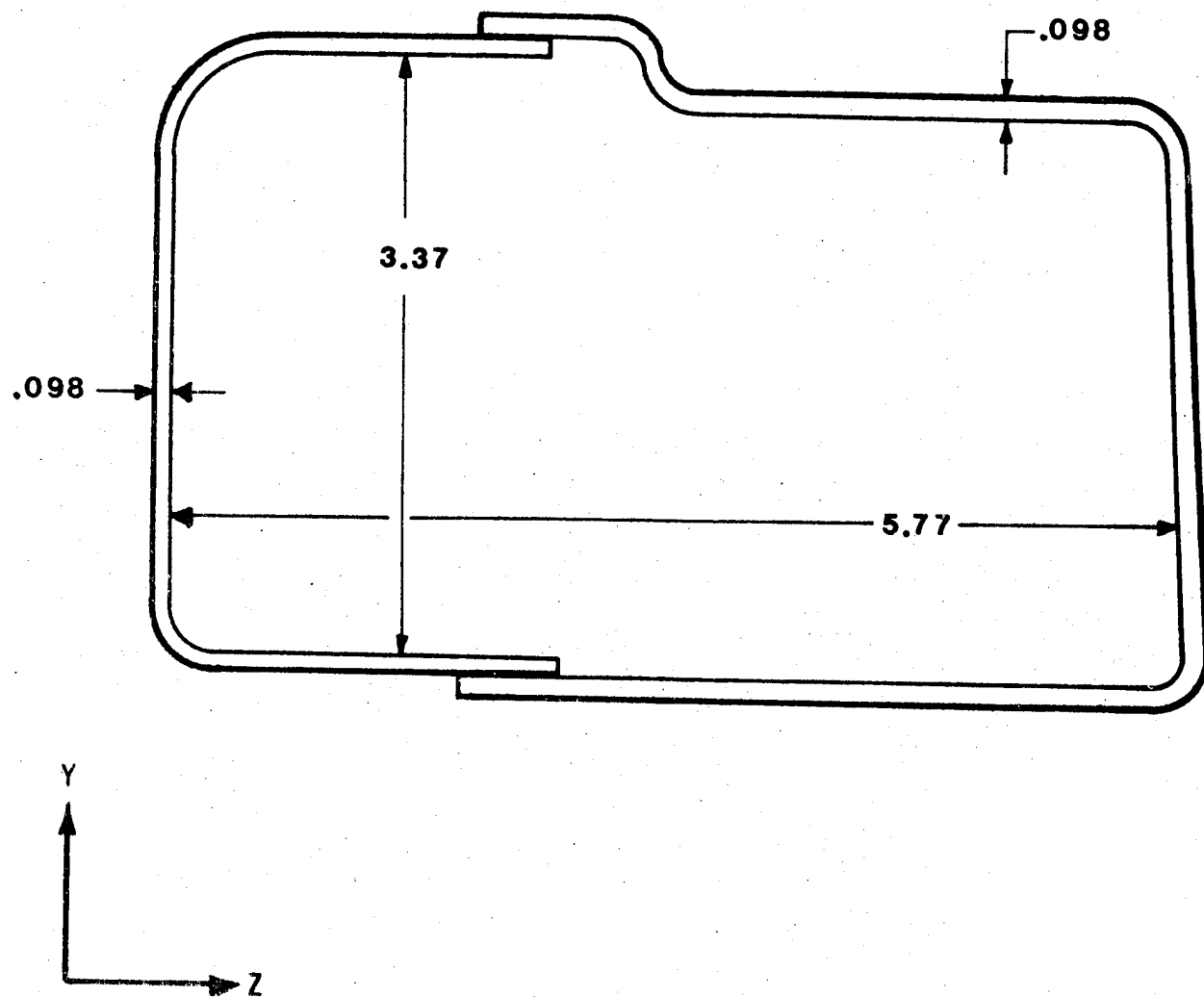
TABLE 56: MOMENTS OF INERTIA, EXISTING FRAME

Section	I_y	I_z
X-X	13.38	6.02
BM-BM	6.28	6.05
L-L	6.03	7.33
AG-AG	9.34	10.43
AY-AY	9.69	9.34
AB-AB	1.23	4.74
AC-AC	6.54	9.41
A-A	1.73	4.53
C-C	2.22	4.43
D-D	8.65	4.20

TABLE 57: CALCULATED FRAME WEIGHTS

	Existing		HSLA-45 (3/4" deepening)		Aluminum (3/4" deepening)	
	Wt.	Thk."	Wt.	Thk."	Wt.	Thk."
Front Side Inner	45.64#	(.118)	35.56#	(.079)	40.96"	(.265)
Front Side Outer	40.40#	(.110)	31.48#	(.074)	36.26#	(.247)
Center Side Outer	40.35#	(.110)	30.34#	(.069)	33.68#	(.331)
Rear Side Inner	41.04#	(.098)	30.94#	(.063)	35.70#	(.209)
Rear Side Outer	40.50#	(.098)	30.53#	(.063)	35.22#	(.209)
Front X-M Upper	14.11#	(.138)	10.51#	(.088)	12.71#	(.313)
Front X-M Lower	13.61#	(.126)	10.14#	(.081)	13.26#	(.286)
Rear Susp. Sup't X-M	19.87#	(.110)	15.16#	(.072)	17.33#	(.238)
Misc. Items & Brackets	37.13#		31.17#		34.15#	
TOTAL	292.64#		225.82#		258.27#	
			Δ W = 66 83#		Δ W = 34.37#	
			22.8% Weight Savings		11.7% Weight Savings	

157

A significant weight savings can be realized in the existing 1977 GM "B" frame by increasing the height and width of the cross-section by .075 inches. Approximately 23% or 67 pounds can be saved by using HSLA-945 steel and 12% or 34 pounds can be saved by using an aluminum alloy. From a stiffness stand point a similar weight reduction, 23%, could be obtained by using hot rolled carbon steel.

The stress in the outer fibers would increase with the increased depth of the section. This increase would be approximately 20%. Without a detailed stress analysis and assuming the yield strength, 35,000 psi, of the hot rolled steel now used is adequate, then the HSLA steel SAE 945X would be sufficiently strong. For the aluminum alloy the outer fiber stresses would be considerably lower due to the increased wall thickness.

Considering fiber reinforced plastics, the section properties can be increased by thickening the frames locally thus realizing a greater efficiency. As an example, the existing center side rail, section AB of Figure 34, has a moment of inertia of 4.74 in^4, and for steel the EI value is 134.1 x 10^6. Graphite reinforced epoxy, 0° orientation, has an elastic modulus of 19 x 10^6 and the required I is 7.06 to be equivalent to the steel. This increased moment of inertia to resist longitudinal frame bending can be obtained by changing the section as shown in Figure 39.

The weight of the existing steel side rails are 20.17 pounds each and the calculated weight of a graphite reinforced plastic side rail is 6.38 pounds each. The possible resulting vehicle weight reduction would be 27 pounds.

Using a modulus of elasticity value of 5 x 10^6 for glass reinforced plastic and a 12 x 10^6 psi value for Kevlar^{TM} reinforced composite it is found the glass side rail is 25% heavier than the steel and the Kevlar^{TM} side rail weighs only 7.26 pounds.

The rear and forward portions of the existing steel frame are closed. A duplicate closed section of a fiber reinforced section is shown in Figure 40. The two halves are to be joined together in a manner to prevent wiping away of the structural adhesive.

Estimated weights of a graphite reinforced composite and a Kevlar^{TM} reinforced composite frame are listed in Table 58. These weights are based on unidirectional (0°) orientation of the fibers parallel to the length of the side rails and the two cross members. In actual service twisting, or torsion will be found at the cross member to side rail joints due to uneven wheel loading, jacking and engine loading on the cross member. Accounting for these loads will increase the frame weight. A detailed finite element analysis would be required.

The current steel frame configuration was developed to fit into the smallest package and obtain optimum structural efficiency.

158

FIGURE 39 MODIFIED SECTION AB-AB FOR GRAPHITE EPOXY
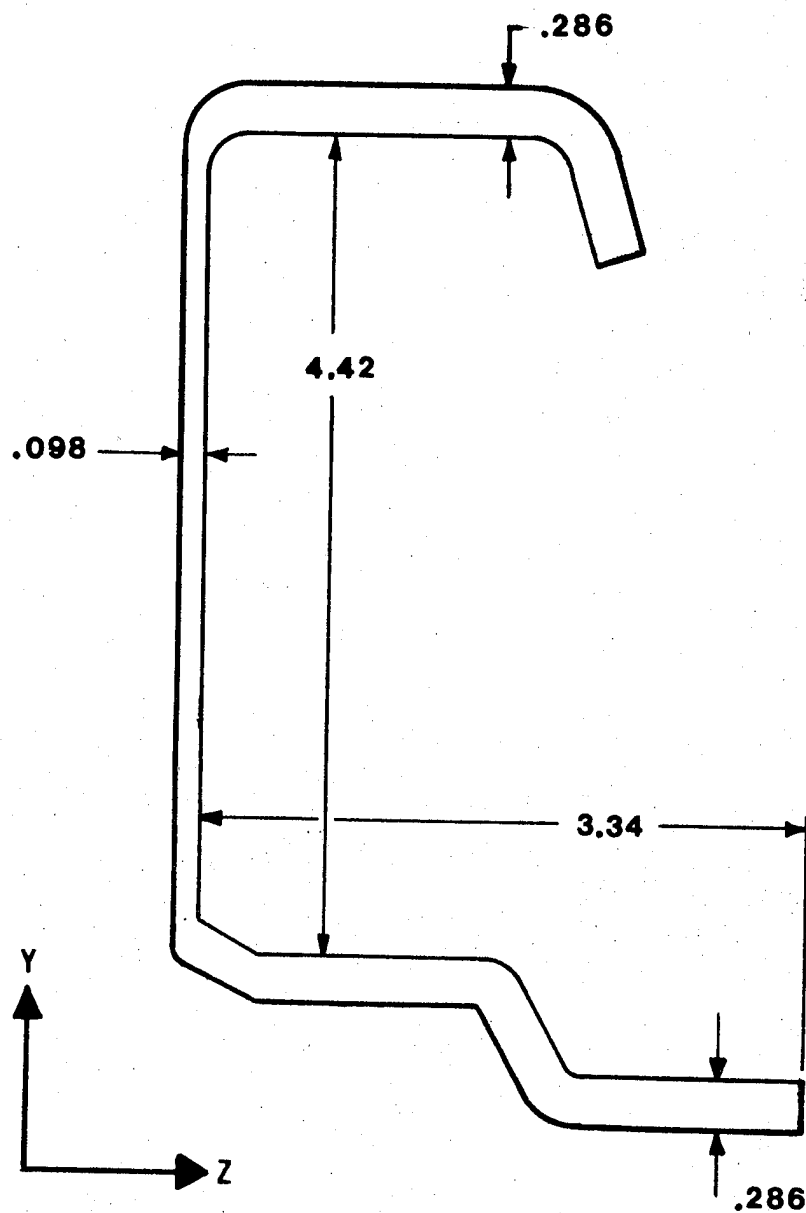
FIGURE 40 MODIFIED SECTION A-A FOR GRAPHITE EPOXY

160
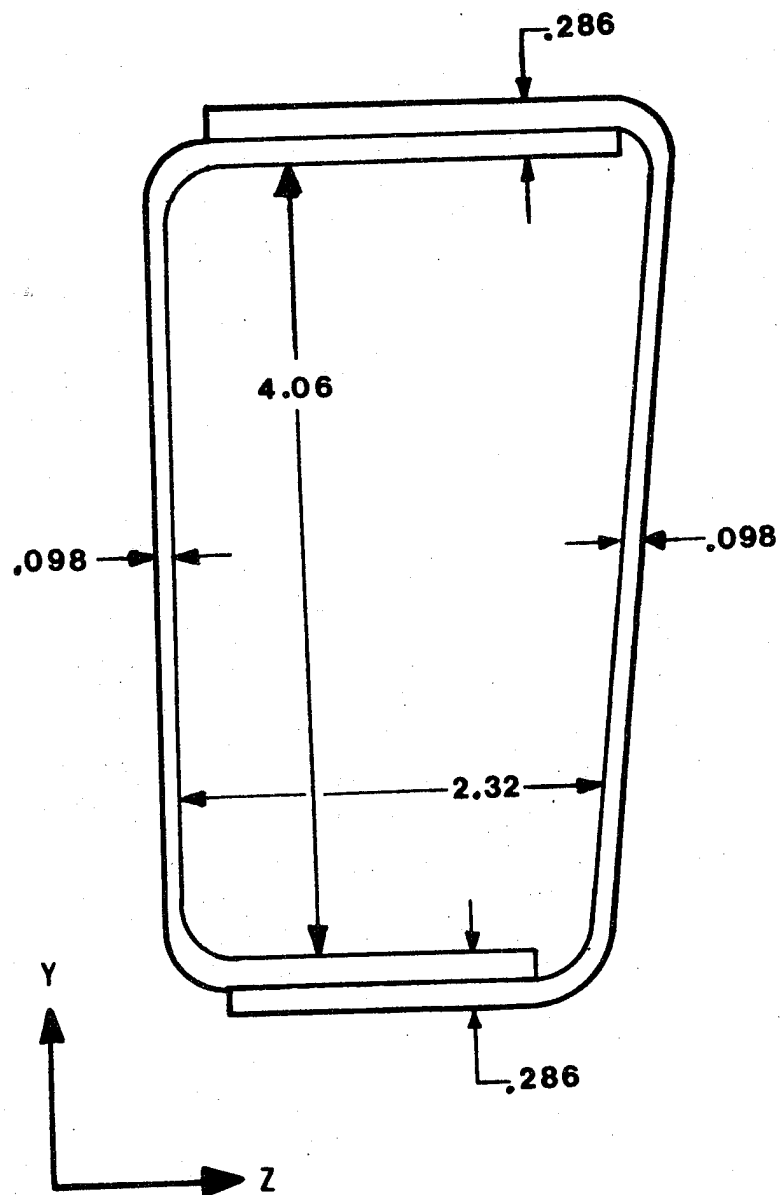
TABLE 58: CALCULATED COMPOSITE FRAME WEIGHTS

	Existing	Graphite Composite	Kevlar[TM] Composite
Front Side Inner	45.64		
		27.3	30.9
Front Side Outer	40.40		
Center Side Outer	40.34	12.8	14.5
Rear Side Inner	41.04		
		27.	30.6
Rear Side Outer	40.50		
Front X-M Upper	14.11		
		8.8	10.
Front X-M Lower	13.61		
Rear Susp. Sup't X-M	19.87	6.3	7.1
Misc. Items & Brackets	37.13	37.13	37.13
	292.64	119.33	130.23

Fabricating this complex configuration from an oriented fiber rein-
forced plastic requires that it be made in essentially the same num-
ber of pieces as made from steel. The front and rear outers could
be combined with the side rail in one continuous piece. The front
and rear inners could be combined with the respective cross members.

Molding of oriented fiber reinforced plastics requires a well
planned charge which will not distort during pressurizing and curing.
If the orientation is lost then the fiber efficiency decreases. It
is not certain that the frame configuration as now used for steel
could ever be effectively molded from oriented fiber composites. A
straighter design could be more readily molded and would perform
more efficiently in front or rear collisions as will be discussed
in Section 7.

The existing low carbon steel frame could be modified, Figure
41, in a manner similar to that shown for the fiber reinforced com-
posite. The manufacturing procedures would change slightly, requir-
ing deeper formed sections and additional welding. The arc welded
lap joint would have to be essentially continuous with additional,
spaced plug welds to insure there is no local buckling. This con-
struction would result in an estimated 11% weight reduction.

While the above methods of utilizing other materials for frames
have shown possible weight reductions by maintaining the same longi-
tudinal bending stiffness level, there has been no consideration of
crashworthiness. This subject will be discussed later in Section 7.0.

6.1.2 Passenger Compartment

Currently the 1977 Impala passenger compartment structure is
made from sheet steel. This low carbon steel may be hot rolled or
cold rolled and annealed, depending upon the thickness and whether
the part is visible. Galvanized steel or Zincrometal ® coated steel
may be used in certain parts to improve corrosion resistance. Cold
rolled and annealed steel is used for the exterior or visible sur-
faces to obtain the high quality appearance. There are several
grades of the cold rolled and annealed steels which are selected
primarily by the fabricator to reduce the cost of manufacturing.
As an example, rimmed steels have a superior surface finish, and
killed steels provide better drawing formability. Killed steels are
generally more expensive, 5%, than rimmed but may be required for
certain parts.

All of the above steels have the same elastic modulus and simi-
lar strength properties. The primary differences in mechanical pro-
perties are found in their ductility or plastic deformation charac-
teristics during forming.

Coated steels have superior corrosion resistance to uncoated
steels, however the coatings add weight without increasing the
strength. Coatings also increase the cost in the areas of purchased

162
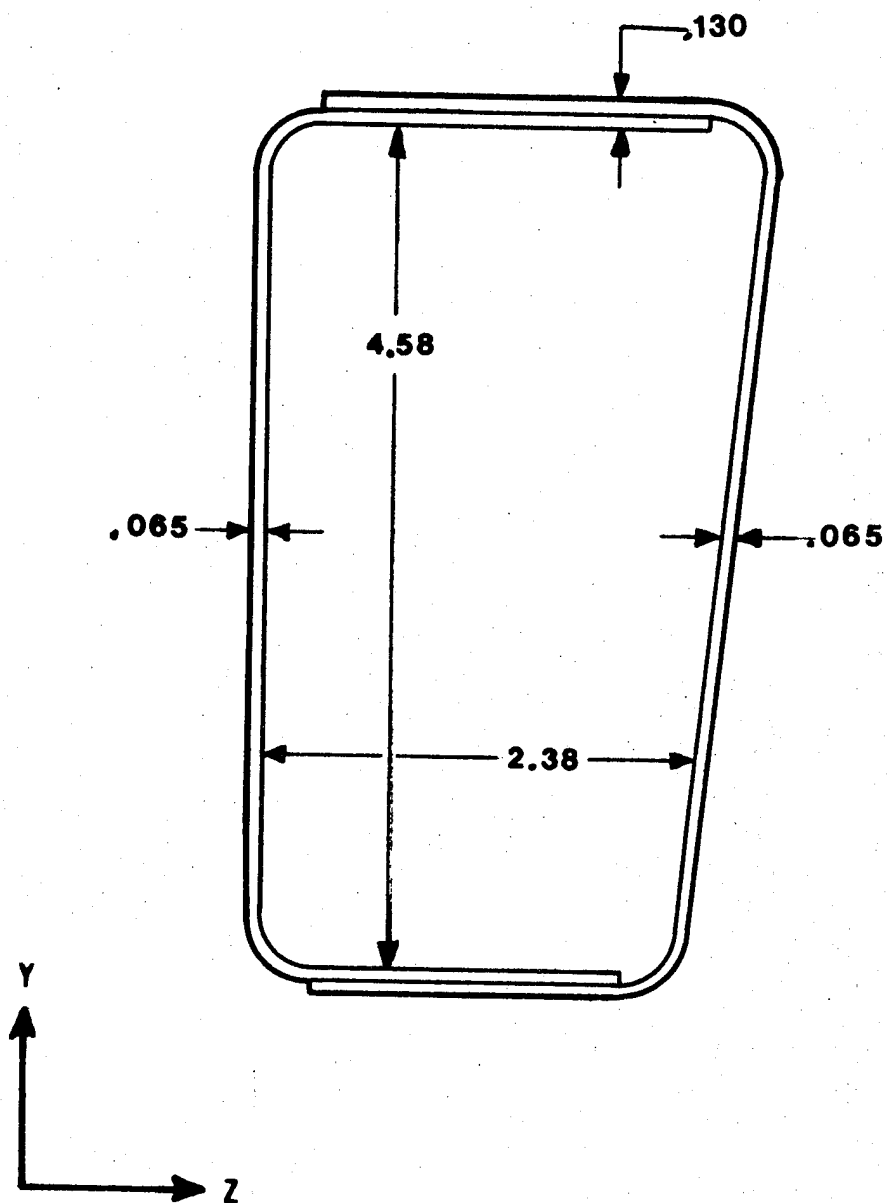
material, poorer formability, increased handling costs and increased welding costs. As an example, zinc coated steels reduce the resistance spot welding electrode life by requiring a higher power input, which results in more heating, and by alloying of the zinc with the copper electrodes. This alloying in turn softens the electrodes and increases their electrical resistivity. As the electrodes soften they lose their shape, and the weld nugget strength is lower than the designed value. Electrode life is reduced from an average 8000 welds for uncoated to 1500 for zinc coated steel.

The trimmed metal stampings are placed in fixtures which locate and hold the various parts in their proper position. Portable resistance spot welding equipment may then be used to join the pieces. In some instances a number of parts, such as those in a floor may be placed in a large fixutre and a large number of welds are completed with several welding tools permanently located in the multi-welder fixture.

Small parts may be joined in a sub-assembly at off line assembly points. These sub assemblies, such as a "B" post, are then brought to the final assembly line for incorporation into the passenger compartment assembly.

The majority of the joining is by resistance spot welding. Arc welding is used in closing the structure where it is no longer possible to position resistance spot welding electrodes on both sides of the work pieces. Sealants or low strength adhesives may be used in the resistance spot welded joints or added to all of the joints after assembly is completed. Solders or adhesives are added to certain joints such as that at the rear quarter panel to the roof for cosmetic purposes.

A sketch of one half of the 1977 Impala passenger compartment is shown in Figure 42. The weight of the passenger compartment including paint, mastic sealers and rust preventatives is estimated to be 461 pounds. The formed panels are so designed to develop a frame work connected by panels. This compartment is sealed and insulated against heat, noise and the environment. The passenger compartment, rigid in itself, is mounted to the frame. The side sills interface with the frame between the "A" post and rear fender well as shown in Figure 43. The body mounts (14 in all) are as depicted in Figure 44.

Several concepts of the passenger compartment can be suggested as listed below:

1. All steel, low carbon and HSLA steel
2. Steel skeleton frame with aluminum alloy panels
3. Steel skeleton frame with reinforced plastic panels
4. Aluminum skeleton frame with reinforced plastic panel;
5. All aluminum alloy
6. All fiber reinforced plastic

FIGURE 42   1977 IMPALA PASSENGER COMPARTMENT
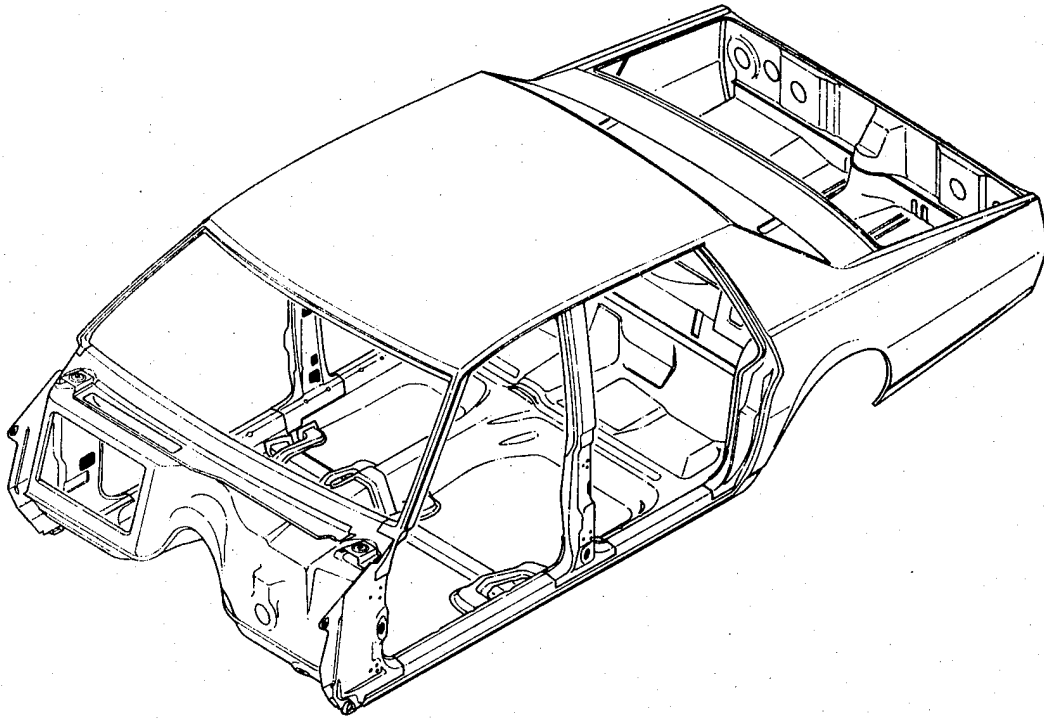
FIGURE 43 SIDE SILL-FRAME

FIGURE 44 BODY MOUNT

BODY

RUBBER
BUSHING

1.25

FRAME

2.50 DIA.
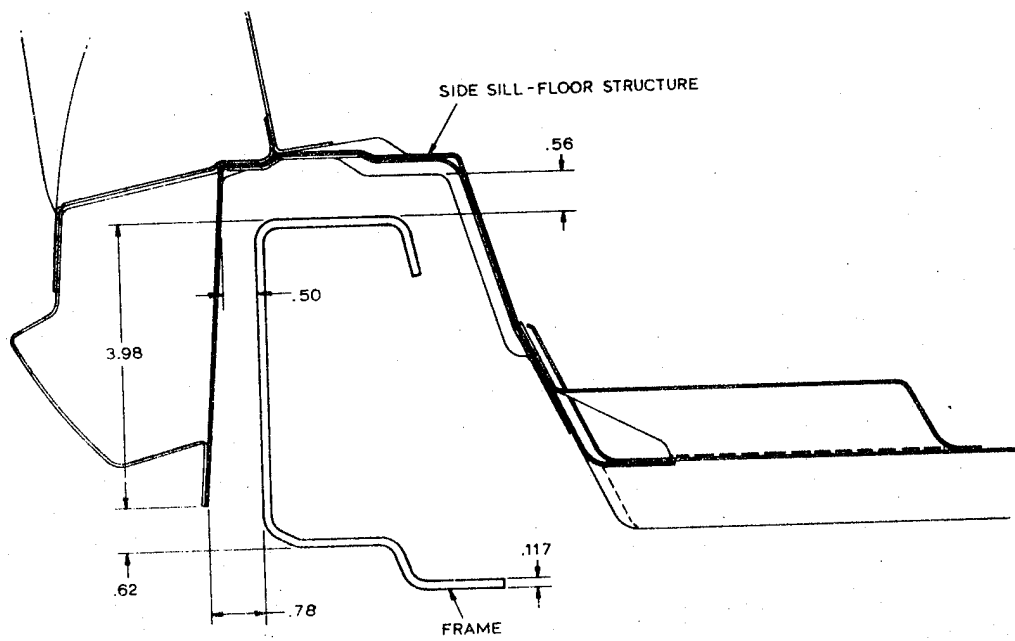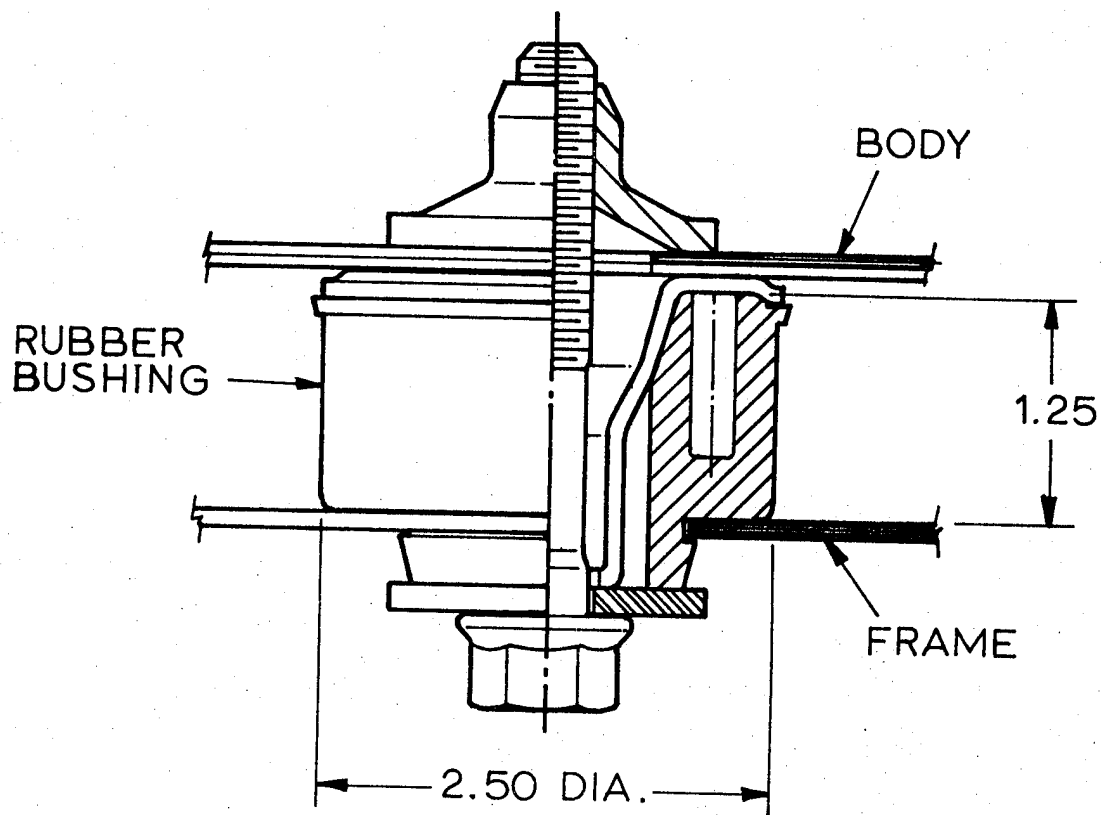
High strength low alloy steels can be fairly easily incorporated with low carbon steel or as a direct replacement. These materials have the same elastic modulus, coefficient of expansion and fabrication procedures such as forming and welding. The advantage of HSLA steels over low carbon steels is questionable. From a stiffness stand point there is no advantage, although if there is a strength limitation in the use of low carbon steel then HSLA steels can be used to minimize the weight.

Since the current Impala passenger compartment is fabricated from a number of steel stampings, the use of isolated aluminum stampings has not been actively pursued. Further interest has been generated recently with the use of a transition metal which permits joining of the two dissimilar metals. The transition metal consists of a strip of aluminum alloy diffusion bonded to a low carbon steel strip. While the conditions of making the transition metal are not fully known, the process provides a method of welding aluminum to steel without the development of brittle alloy phases at the molten interface and accommodates the wide differences in melting points of the two metals.

A frame skeleton concept for the passenger compartment is shown in Figure 45. The "A" and "B" posts, the cowl reinforcement and the roof reinforcements would remain essentially the same in steel. Three floor cross members are retained at the firewall-toe board, at the "B" post and at the rear seat. Using this steel frame, aluminum alloy or reinforced plastic panels could be attached to complete the passenger compartment.

With this skeleton concept the trunk compartment could be considered a hang on item similar to the front fender and hood. This trunk compartment would be supported by the frame and attached to the rear of the passenger compartment.

Aluminum alloys have a coefficient of thermal expansion of 13×10^{-6} inches per inch per degree Fahrenheit, while the coefficient for low carbon steel is 8.5×10^{-6}. Glass reinforced polyesters (SMC) have coefficients of expansion similar to aluminum, 10 to 14×10^{-6}. The difference in expansion of the aluminum and SMC from steel is 4.5×10^{-6}. For the Impala roof panel (56" wide, 62" long) the expansion difference from 70° to 200° F is 0.036 inches front to rear. The maximum thermal stress developed at this temperature increase would be 5800 psi.

A transition strip could be added in various ways for the joints of the roof panel to the reinforcements. Two such approaches are shown in Figure 46 and Figure 47 for the front, rear and side joints of an aluminum outer roof panel and steel inner reinforcemtns.

168

FIGURE 45 FRAME-PASSENGER COMPARTMENT CONCEPT
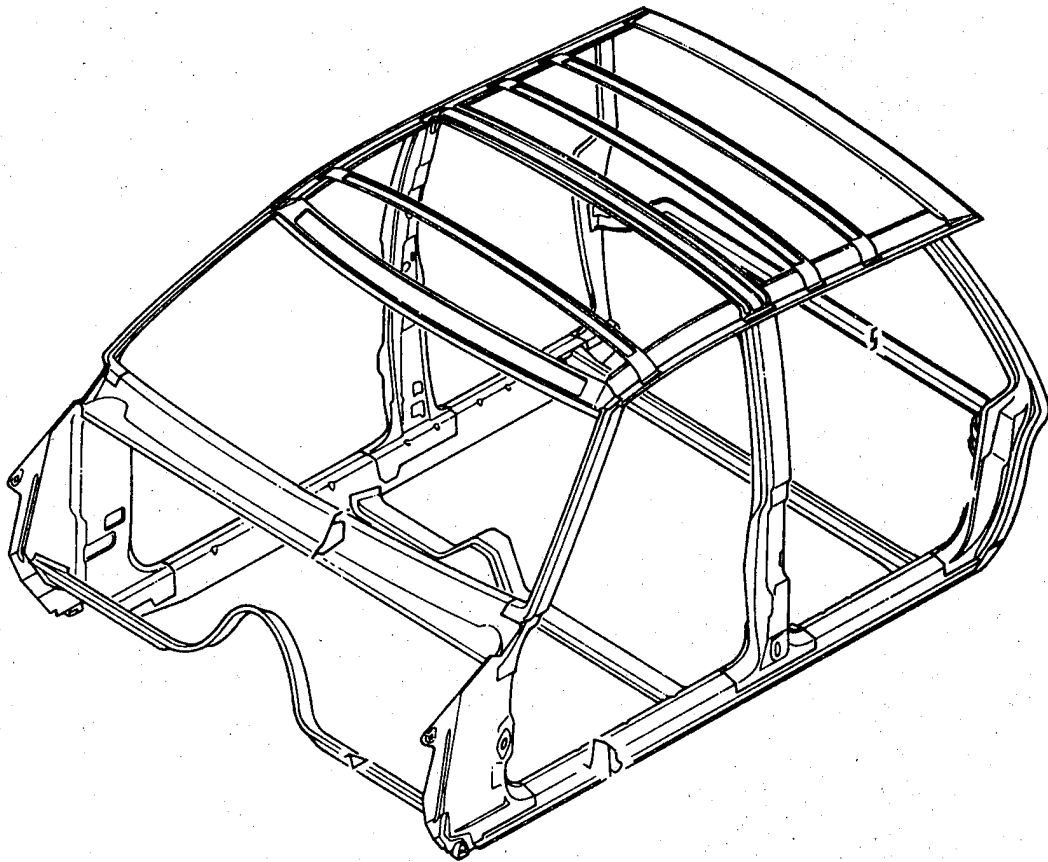
FIGURE 46 ROOF TO REINFORCEMENT JOINT, WINDSHIELD AND REAR WINDOW

EXISTING STEEL TYP. DIM'S.
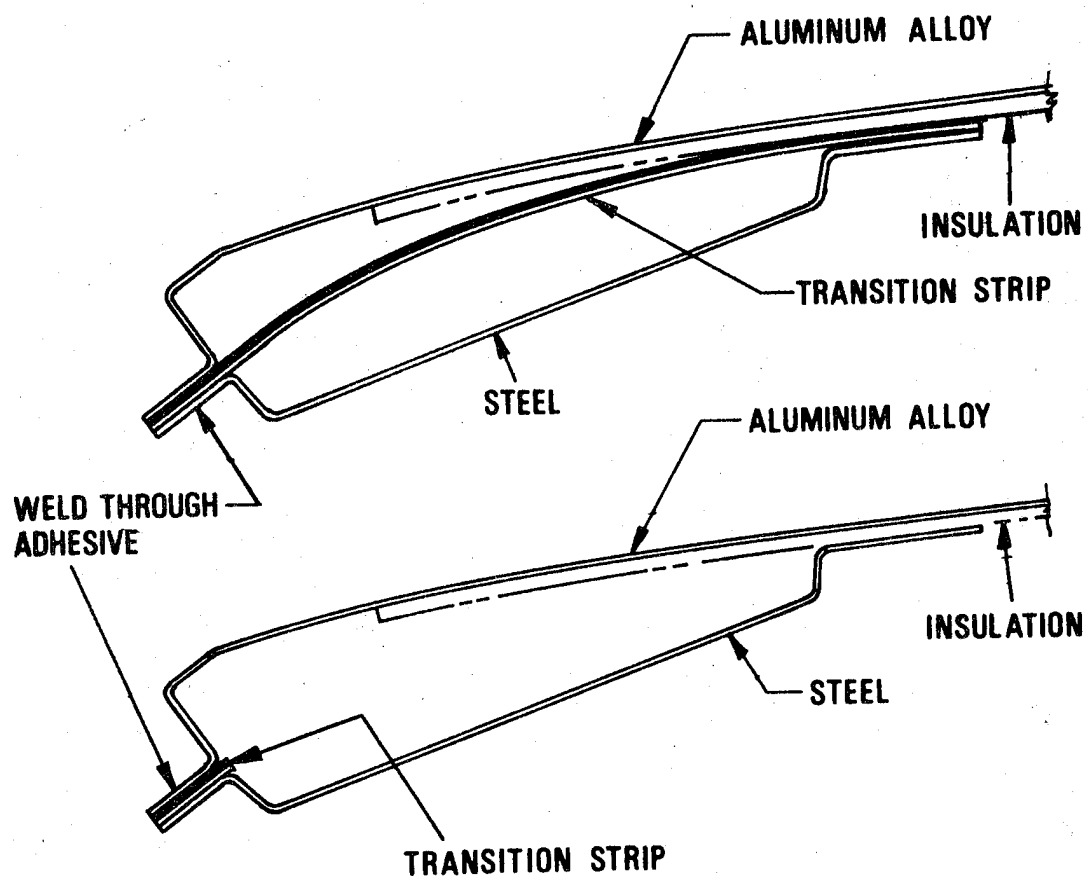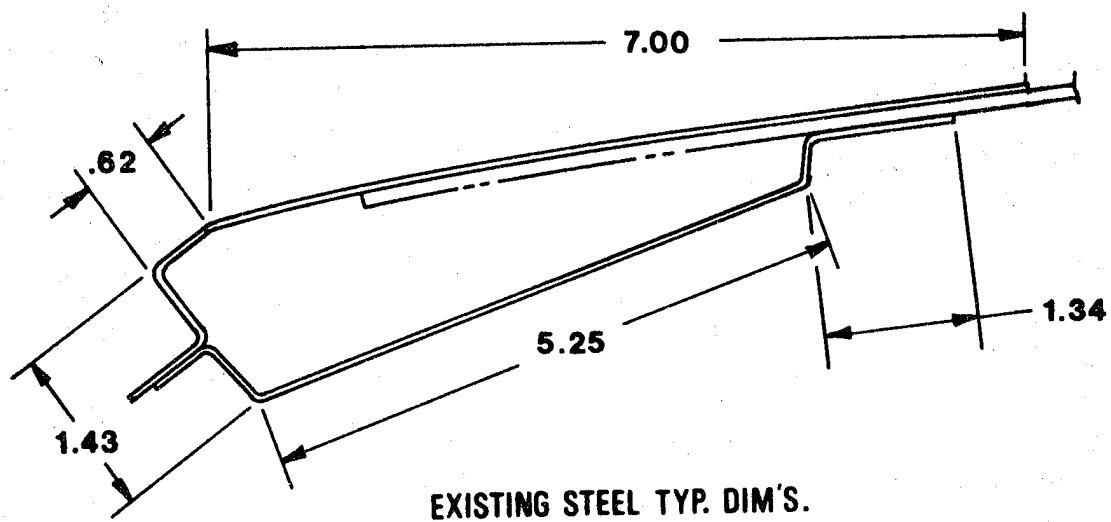
FIGURE 47 ROOF TO REINFORCEMENT JOINT, LEFT AND RIGHT SIDES

INSULATION

1.56

.43

1.40

.81

EXISTING STEEL
TYP. DIM'S.

INSULATION

ALUMINUM ALLOY
TRANSITION STRIP

ADHESIVE BETWEEN
AL.OUTER AND
TRANSITION STRIP

STEEL

WELD THROUGH
ADHESIVE

STEEL

171
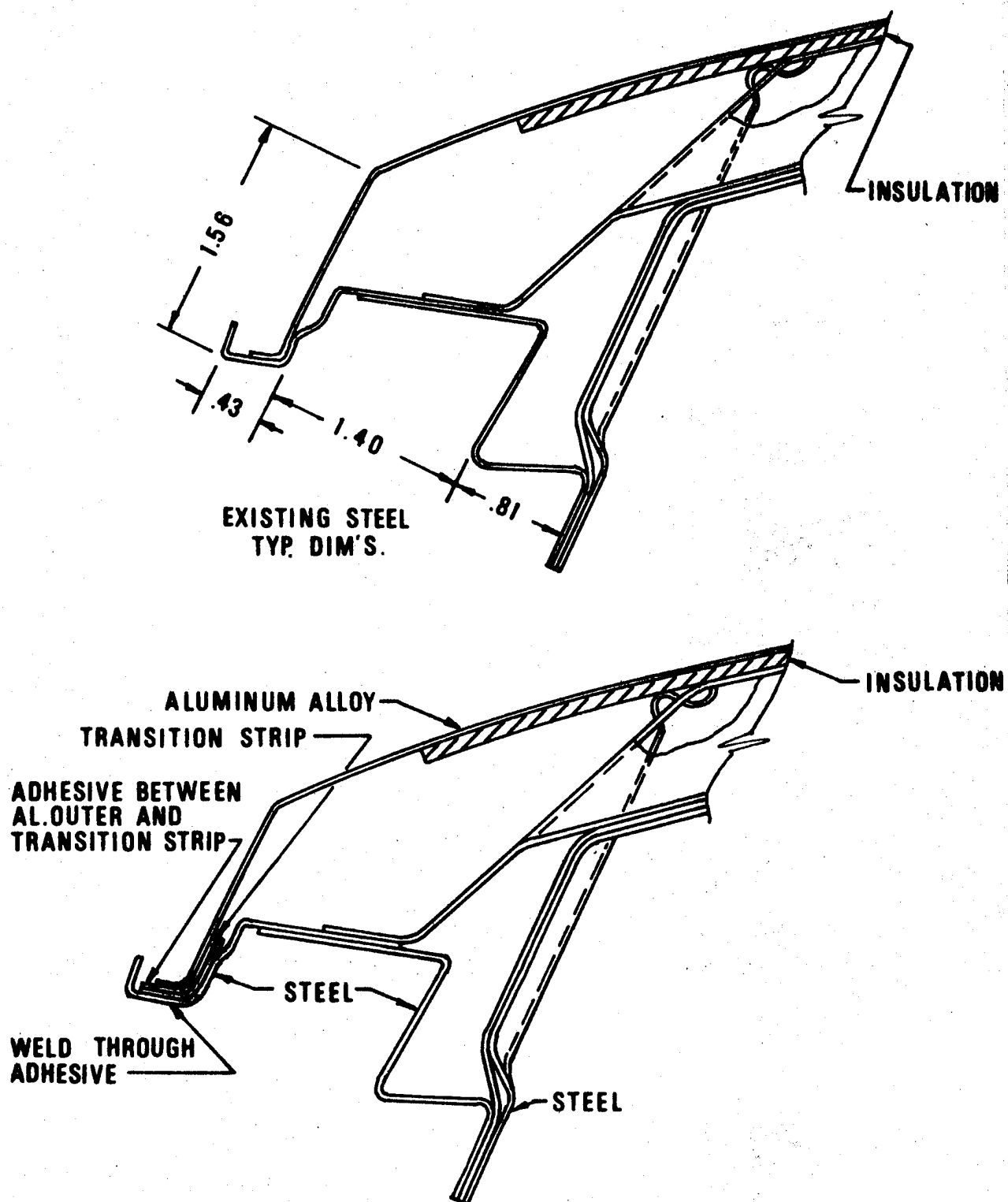
The steel outer skin roof panel weighs 35 pounds and is 0.030 inches thick. The transition strip would add between 3.6 pounds to 5 pounds of the roof. Using an 0.030 aluminum alloy skin panel would then reduce the weight by 23 pounds or a net reduction of 19.4 pounds. To maintain the same stiffness as the steel in the outer aluminum skin, the thickness could be increased to 0.042 inches thick. The net weight reduction is then reduced to 14.4 pounds.

For a reinforced plastic roof panel on a steel or aluminum sheet metal frame work the methods of joining are primarily adhesive bonding with mechanical fasteners. The fasteners can be either rivets or one of many of the screw or such type mechanical fasteners. In an adhesive joint it is always best to take up the loads in shear. This may not always be possible, and mechanical fasteners can be used to prevent catastrophic failure of the joint in peel or cleavage.

Two possible joints between an outer roof skin panel of glass reinforced polyester (SMC) and a metal frame work are shown in Figure 48. The SMC in this case could be any one of the large number of materials containing 25 to 65% glass as a random chopped fiber, continuous oriented fiber or combination of these. For equal stiffness the glass polyester at an elastic modulus of 2×10^6 must be 2.5 times as thick as the steel or 0.075 inches. While this thickness may be on the low side of producibility it is used to calculate the roof skin weight of 20.75 pounds.

An alternate concept would consist of an all aluminum alloy roof consisting of the outer skin and reinforcements made as an entity and then joined to the passenger compartment at the steel "A" and "B" posts.

The "B" post to roof joint appears the easiest to provide without change except for the incorporation of the transition metal. At the "A" post there are three thickness pile ups requiring double transitions strips which complicate the assembly procedure and require space provisions for the added thicknesses.

To maintain the same bending stiffness for the all aluminum roof as for the current steel roof the aluminum cross members have to be 2.9 times thicker, 2.9 times wider, or an approximately $\sqrt{2.9}$ times deeper section. The deeper section will reduce the head room slightly, 0.3 inches. Those reinforcements 2.9 times thicker and 2.9 times wider do not offer any weight reduction advantage.

A roof structure completely of glass reinforced polyester (SMC) is best made of a minimum number of moldings. A concept using only two moldings is shown in Figure 49. Concepts of joints above the door and at the "B" post are shown in Figure 50. The outer skin would be made from a low profile, good finish grade of glass polyester sheet molding compound of 25 to 40% chopped random glass.

172

FIGURE 48 ROOF TO REINFORCEMENT JOINT

REINFORCED PLASTIC

7.00

.62

5.25

1.34

1.43

INSULATION

REINFORCED PLASTIC

1.56

SEAL

INSULATION

.43

1.40

STEEL OR ALUMINUM

.81
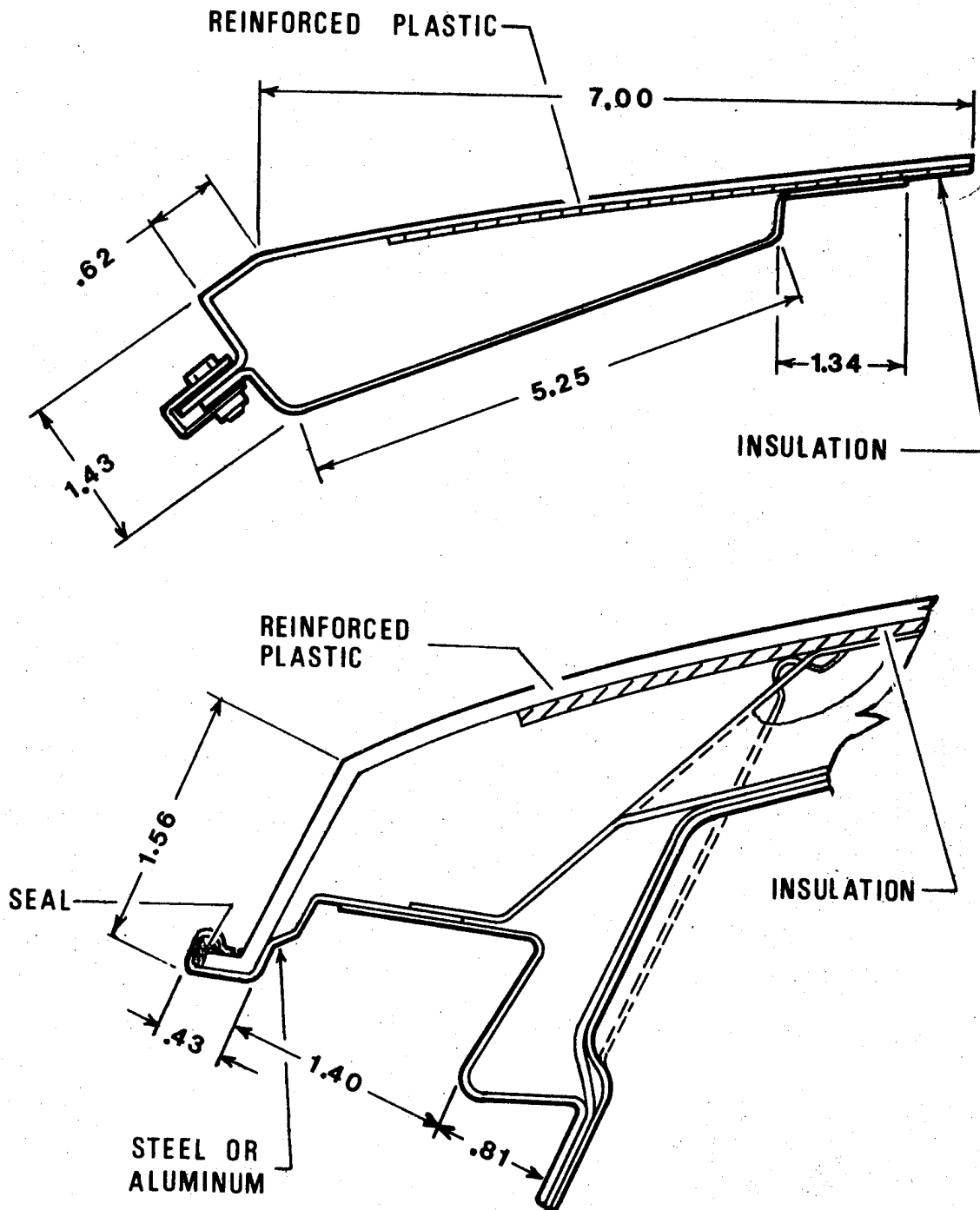
FIGURE 49 GLASS POLYESTER ROOF STRUCTURE CONCEPT
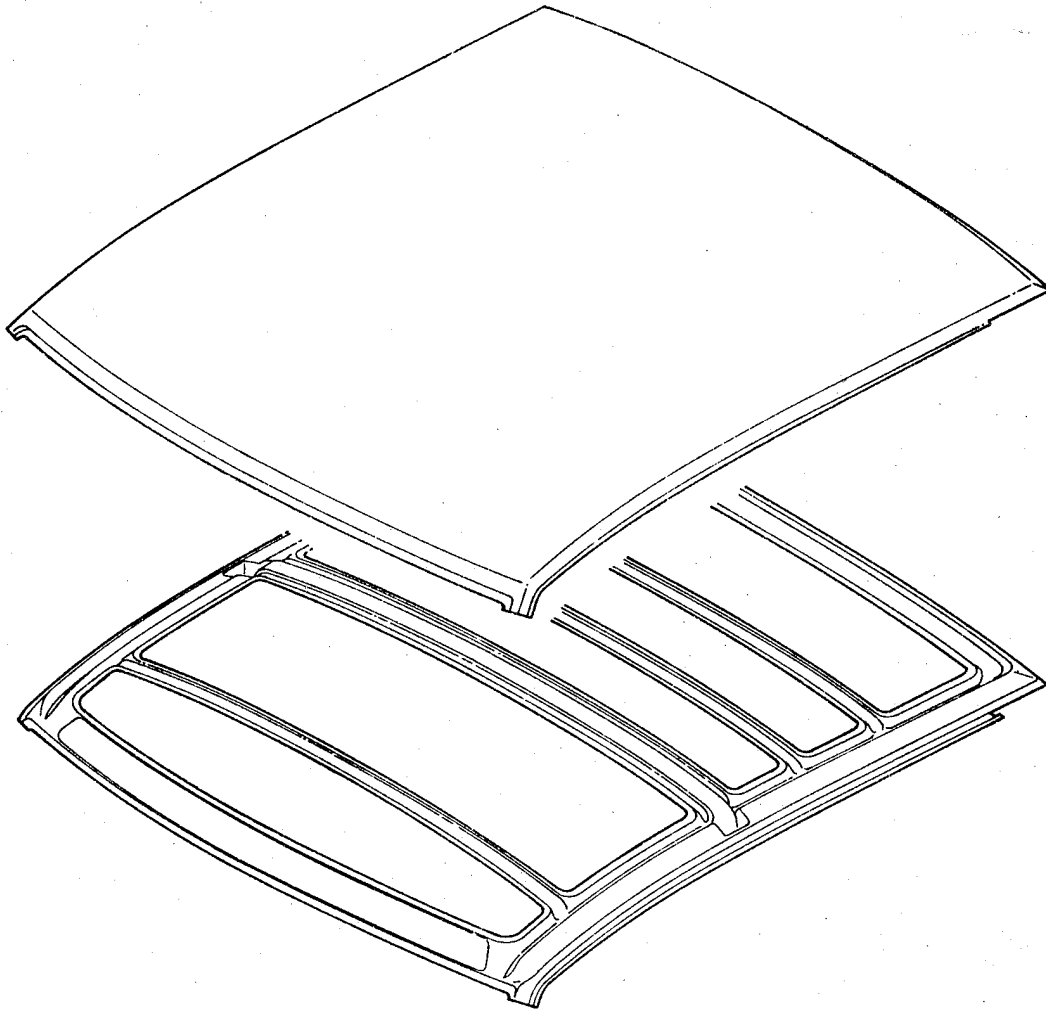
FIGURE 50 GLASS POLYESTER ROOF STRUCTURE JOINTS
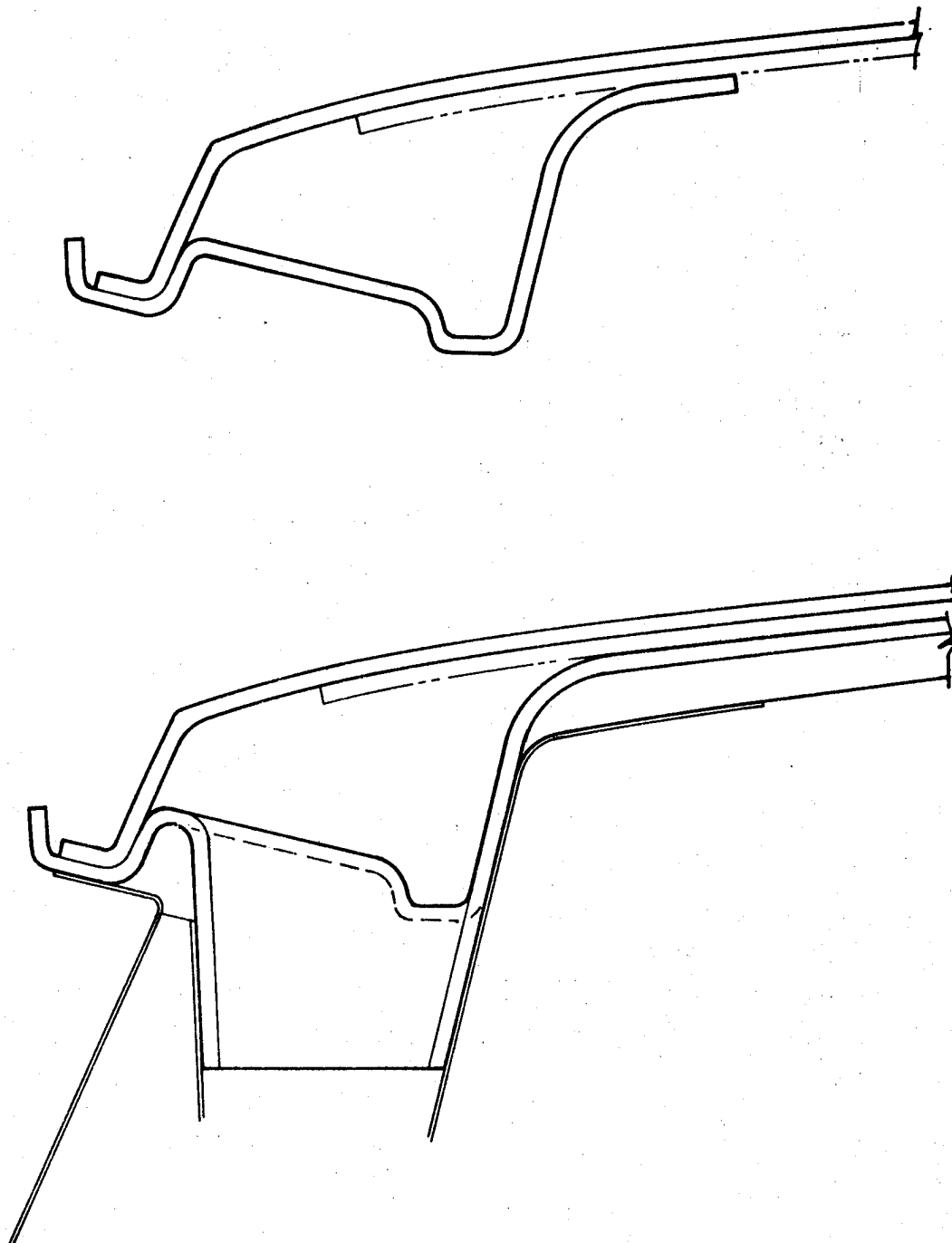
The inner support structure would be made from an oriented glass molding compound. The higher elastic modulus available from the oriented fiber grades is desired to resist the bending loads. At an elastic modulus of 5×10^6 the support structure material must be six times the thickness of the steel in the support structure or 1.37 times heavier. The resulting roof is estimated to be only four pounds lighter than the steel roof, if it must stay within the clearance and styling lines of the current vehicle.

Estimated weights of several roof concepts are listed in Table 59. These concepts are based on remaining within the existing clearance lines. The all aluminum roof (Item 2) and all glass polyester roof (Item 5) could perform as well as the steel at a weight reduction only at the expense of increasing the outside styling lines or decreasing the internal head room. This section deepening for the all aluminum roof would be approximately 0.3 inches as mentioned previously and the oriented glass polyester would have to be deepened approximately 0.5 inches greater than the steel section. In the use of the deepened all aluminum roof the total roof weight is estimated to be 23 pounds and the deepened all glass reinforced roof is estimated to be 47 pounds.

The case for steel can be reworked based on deepening of the roof support structure. With deeper sections the steel thickness can be reduced to maintain the same stiffness.

The skeleton frame could be fabricated from an aluminum alloy also. Aluminum alloy or reinforced plastic roof panels, fire walls and floor panels could be attached as with the steel skeleton frame. The aluminum frame will not have the same stiffness as the steel frame due to its lower elastic modulus. Whether this has to be taken into account with thicker material or selective reinforcing depends upon the combined stiffness of the steel chassis frame and the aluminum frame and attached panels. This will be discussed in Section 6.3 static analysis.

From a manufacturing stand point the parts can be made from aluminum alloys although the part design may have to be changed locally to permit the press stamping of acceptable parts. The forming limit curve, Figure 51 , indicates the poorer formability found in aluminum alloys when compared to low carbon steel. The end result in a stamping or its shape is to make it look less sharp. Where tight bend radii are possible in steel, they cannot be made in aluminum alloys without more press operations (restriking) and possibly solution treating to restore ductility. Thus styling would be bulkier with larger gaps between components. In general, tools and parts designed for aluminum can be used to stamp steel components but the reverse is seldom true.

The aluminum alloy part designs would also be modified to reduce stresses particularly in areas where joining is performed. For example, where the "A" and "B" posts join the roof or sills the joint strength and part configuration is based on steel.

176

TABLE 59: ROOF CONCEPTS AND ESTIMATED WEIGHT

	Component Wts.	Assembly Wts.
1. Current Steel Roof		60.5
Two Side Beams	15	
Cross Supports	10.5	
Outer Skin (0.030)	35.0	
2. Aluminum Roof		38.1
Two Side Beams	15	
Cross Supports	10.5	
Outer Skin (0.030)	12	
Transition Metal	0.6	
3. Aluminum Skin on Steel Supports		41.1
Two Side Beams	15	
Cross Supports	10.5	
Transition Metal	3.6	
Outer Skin (0.030)	12	
4. Glass Polyester Skin on Steel Supports		46.75
Two Side Beams	15	
Cross Supports	10.5	
Outer Skin	20.75	
Adhesive	0.5	
5. Glass Polyester Roof		56.58
Outer Panel	20.75	
Inner Panel	34.83	
Adhesive	1.00	
6. All Aluminum Roof Deepened		22.95
Two Side Beams	6.04	
Cross Supports	4.31	
Outer Skin	12.0	
Transition Metal	0.6	
7. Glass Polyester Roof Deepened		47.25
Outer Panel	20.75	
Inner Panel	25.5	
Adhesive	1.0	

FIGURE 51 FORMING LIMIT CURVES

178
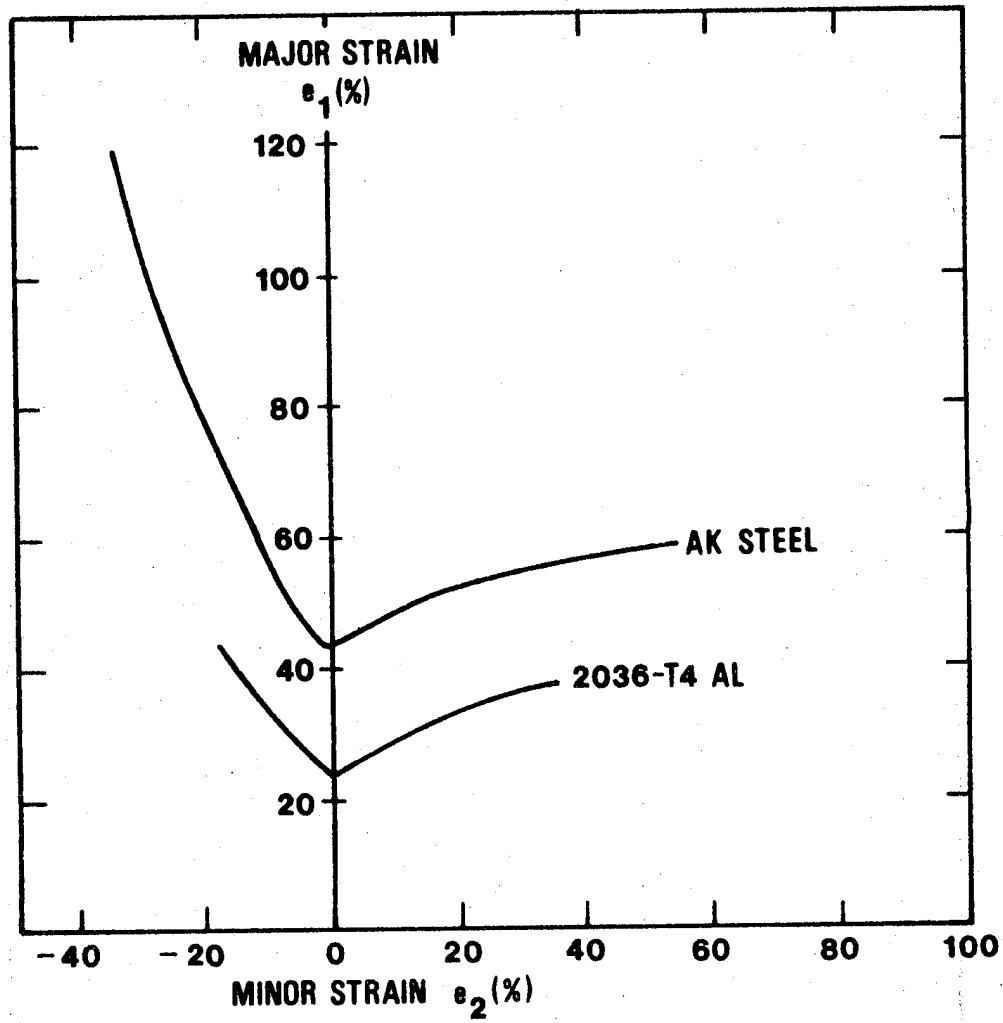
Stiffening by doublers or material thickening added to larger joint areas with an increased number of spot welds will be required. The exact size and number of welds would require an in depth stress analysis and possibly a simulated test. Static or fatigue failure may occur.

An all reinforced plastic passenger compartment can be made to establish a similar to steel structure, by combining parts into fewer moldings. In the case of reinforced plastics, local areas can be increased in thickness in the single part without having to bond in a doubler or reinforcement. This does permit the strengthening or stiffening of a section locally. Added to this the ability to place oriented fiber to resist high loads in one direction offers further flexibility.

Longitudinal sills in the floor and roof are combined by an inner and outer molding on each side of the vehicle as shown in Figure 52. Typical sections are shown in Figures 53, 54, 55, 56, 57, 58 and 59. The roof panel is the same as shown in Figure 49 and the deck reinforcement and floor are shown in Figures 60 and 61. The floor as one piece is a large molding requiring a large press, well over 5000 tons. Dividing the floor into three pieces which when fit together by rivet-bonding provides transverse reinforcing beams and seat mounting locations, as well as reducing the press requirements. The bonded joints in proximity with the stiffer beams and also in multidirections reduces the tendency toward peeling failure. The fire wall and cowl are shown in Figure 62.

The rear portion of the passenger compartment containing the rear quarter panels, luggage compartment floor, rear light panel and rear window frame is shown in Figure 63. While there is parts consolidation the structure looks like the steel parts in a effort to retain packaging volume. A typical section through the quarter panel and deck lid is shown in Figure 64.

6.1.3 Hood and Deck Lid

The hood and deck lid for the Impala are essentially covers which protect the engine and luggage compartment from the environment. They also provide beneficial aerodynamic effects and improve the styling aesthetics of the vehicle. The hood, being so visible to the driver, passenger and pedestrian is required to have a class "A" appearance and not flutter at high speeds. Both deck lids and hoods must be stiff and resist bending, open or closed, and must feel firm when pressed locally.

Hoods and deck lids consist of two sheet metal stampings, (inner and outer) reinforcements for the hinges and a latching mechanism. The current steel Impala hood stampings are shown in Figure 65 and the deck lid stampings are shown in Figure 66. The inner panel is formed such that when mated with the outer panel a number of reinforcing hat sections are formed, providing stiffness to the assembled component. Joining is accomplished by resistance

FIGURE 52 REINFORCED PLASTIC SIDE STRUCTURE

OUTER

INNER
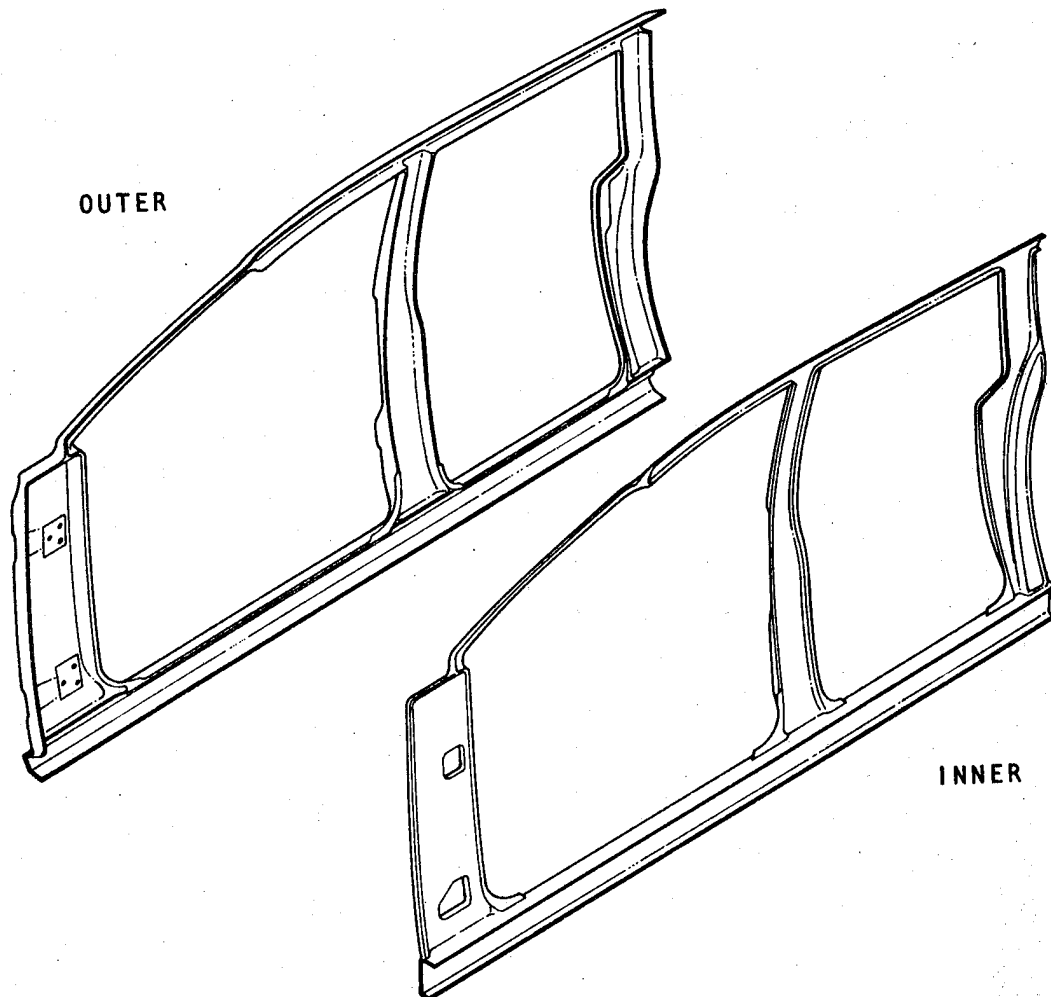
FIGURE 53 SECTION: A POST, REINFORCED PLASTIC

HINGE TAPPING BLOCK

SIDE, OUTER

SIDE, INNER
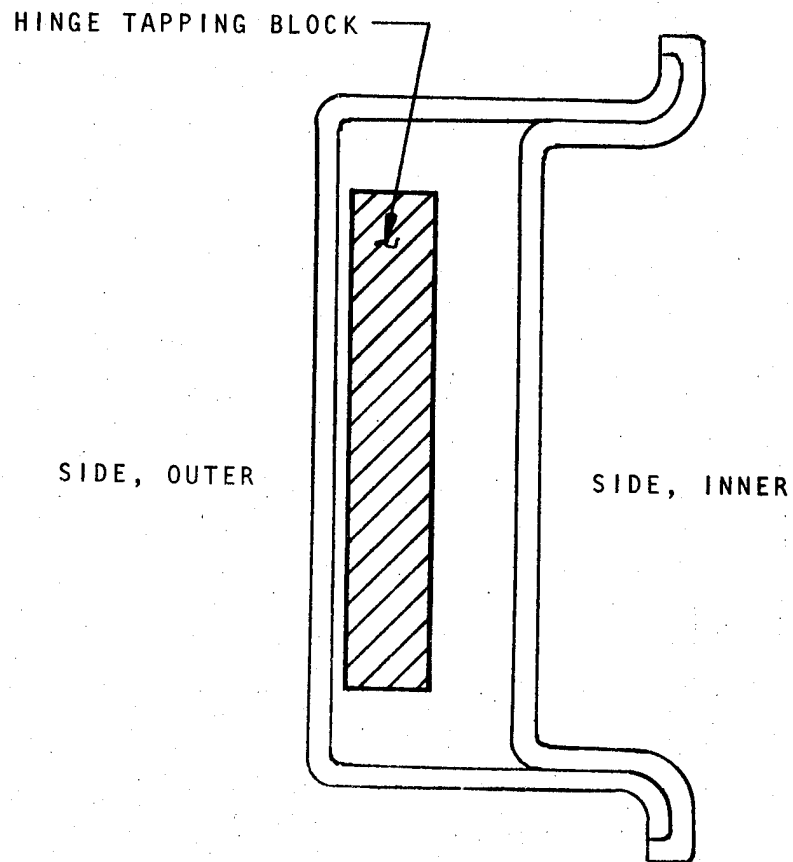
FIGURE 54 SECTION: B POST UPPER, REINFORCED PLASTIC

SIDE, OUTER   SIDE, INNER
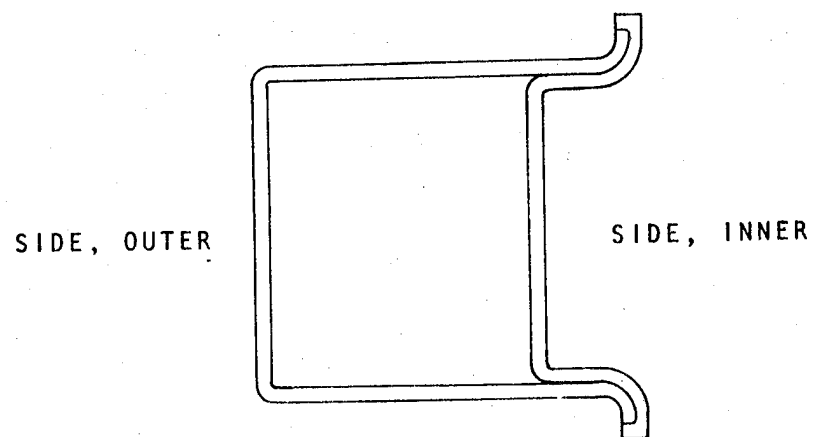
FIGURE 55 SECTION. B POST LOWER, REINFORCED PLASTIC

SIDE, OUTER

SIDE, INNER

LATCH TAPPING BLOCK

183
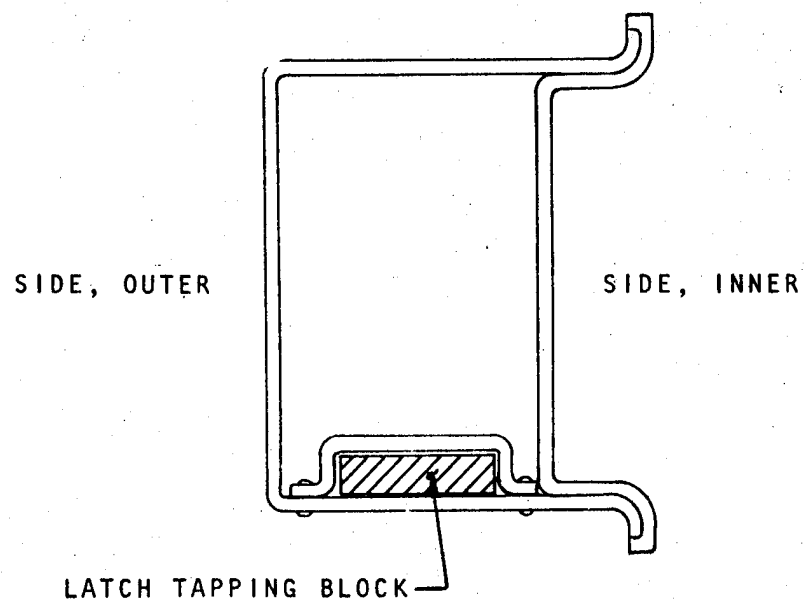
FIGURE 56 SECTION: QUARTER PANEL, REINFORCED PLASTIC

SIDE, INNER

SIDE, OUTER

REAR QUARTER PANEL

184
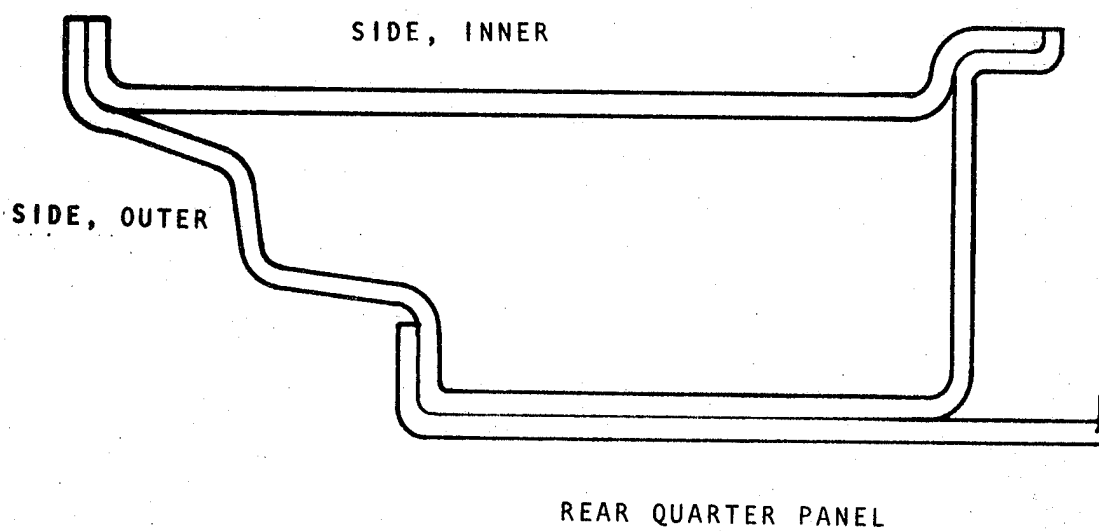
FIGURE 57 SECTION: SIDE TO ROOF, REINFORCED PLASTIC

ROOF

INNER

OUTER
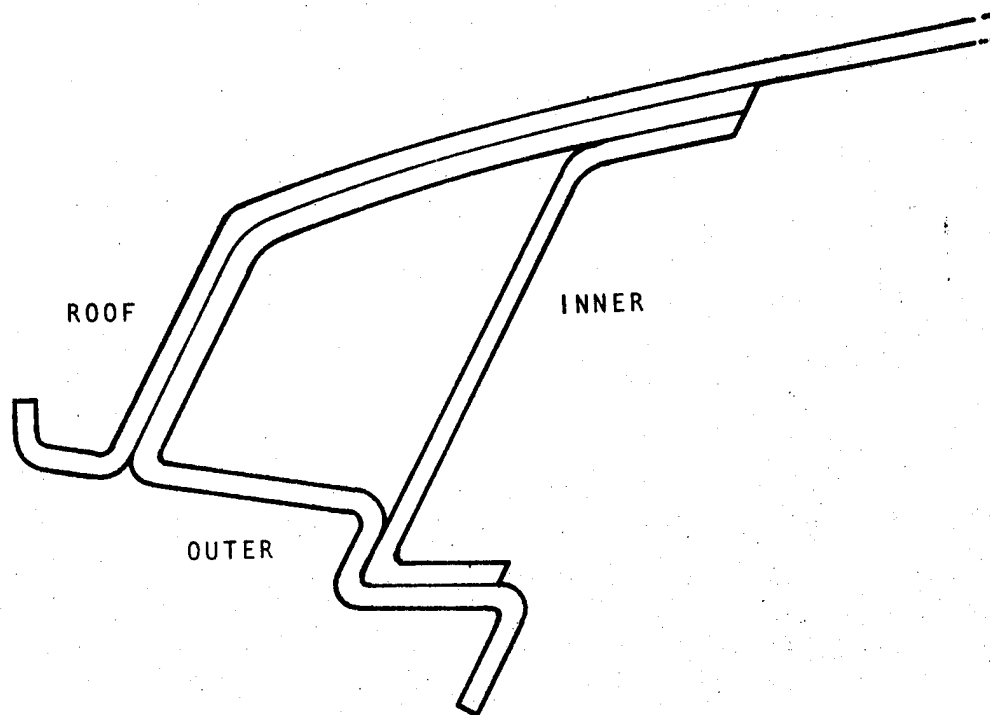
FIGURE 58 SECTION: SIDE TO FLOOR, REINFORCED PLASTIC

OUTER

INNER

FLOOR

FRAME
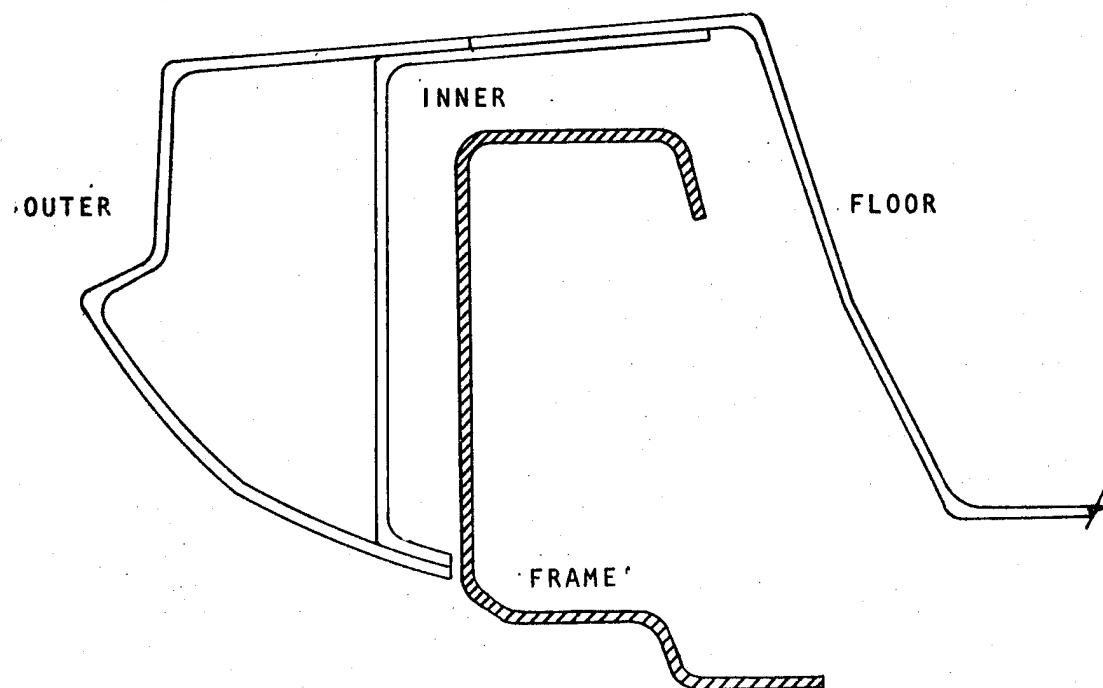
FIGURE 59 SECTION: ROOF TO REAR WINDOW REINFORCEMENT
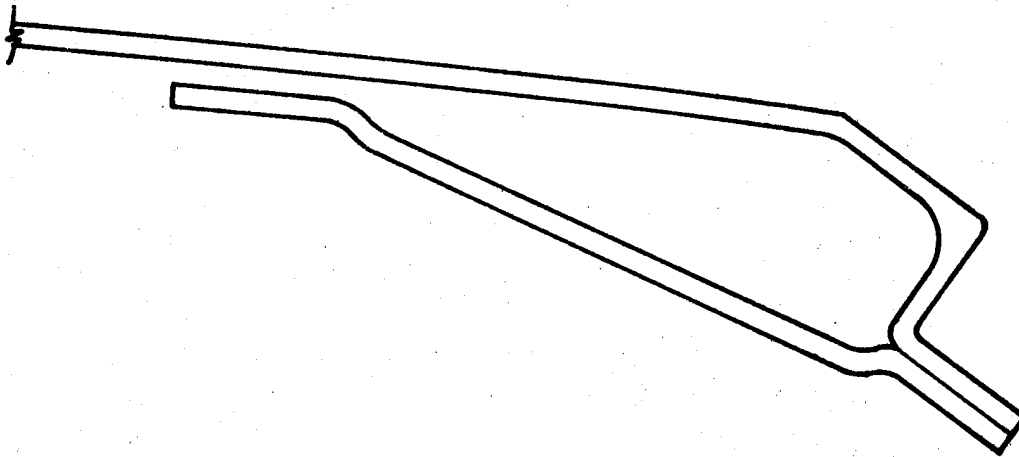
FIGURE 60 DECK REINFORCEMENT, REINFORCED PLASTIC
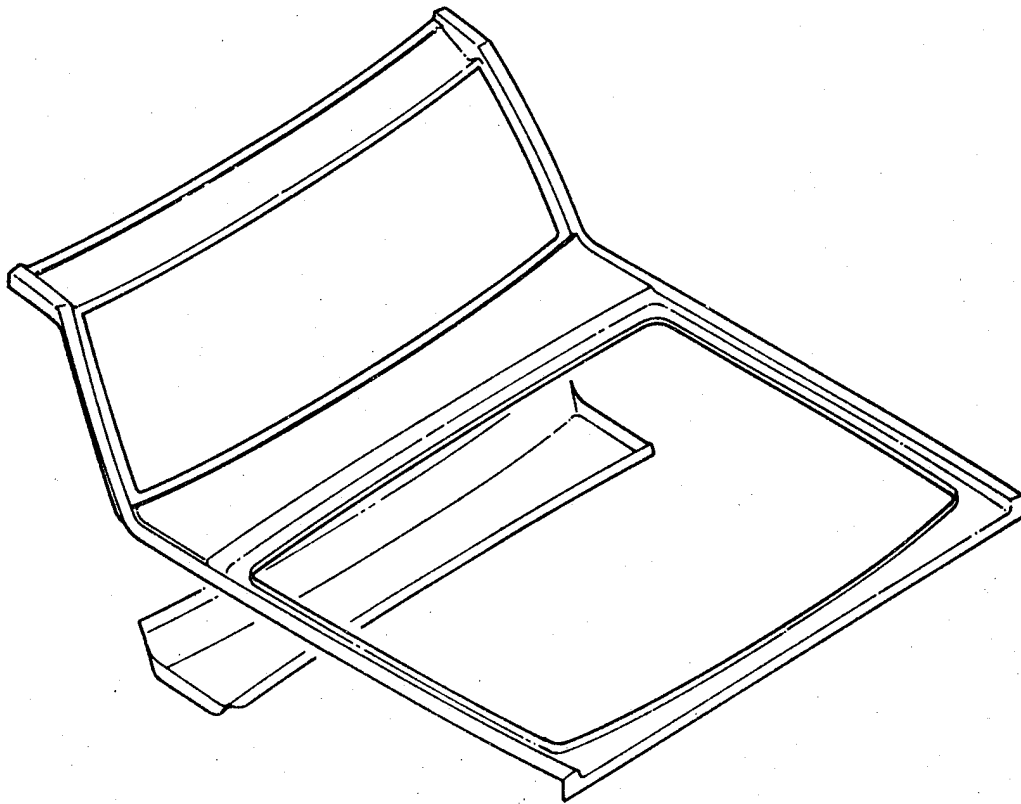
FIGURE 61 FLOOR, REINFORCED PLASTIC

FIGURE 62 FIREWALL AND COWL, REINFORCED PLASTIC

190
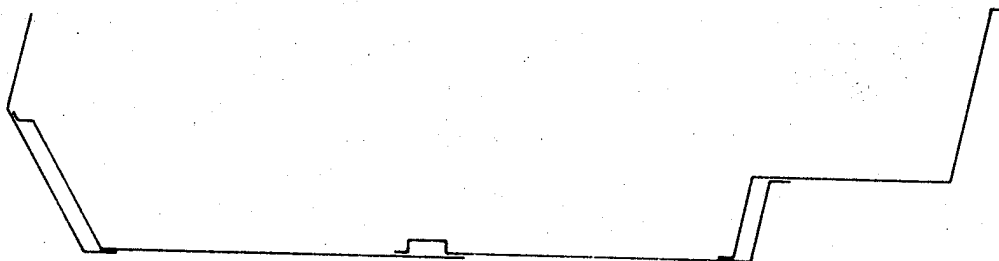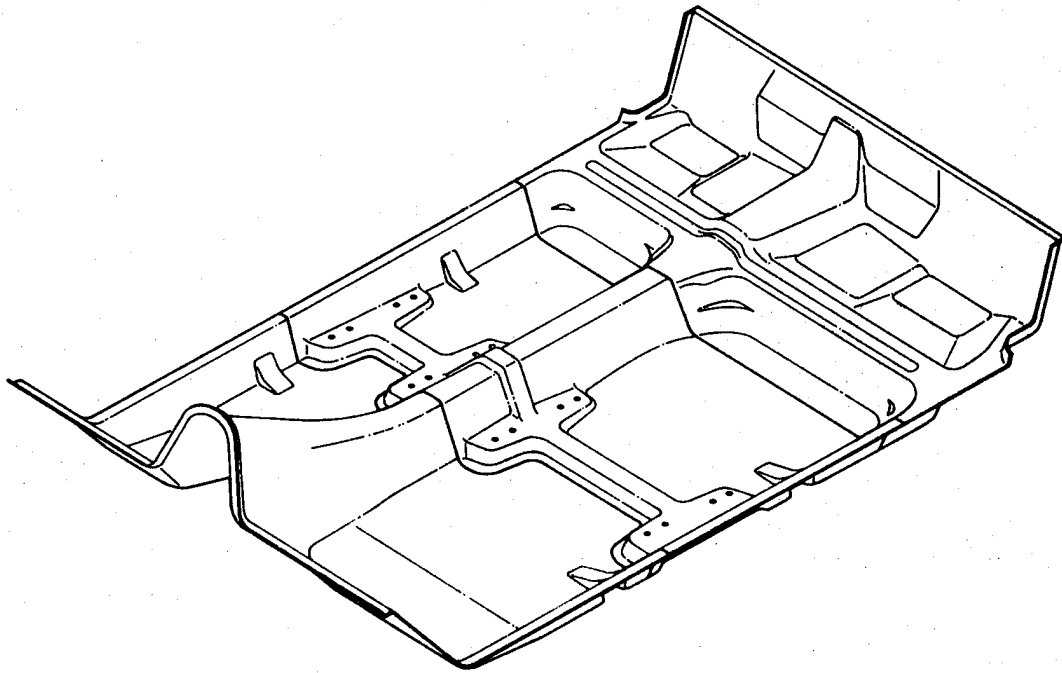
FIGURE 62 FIREWALL AND COWL, REINFORCED PLASTIC
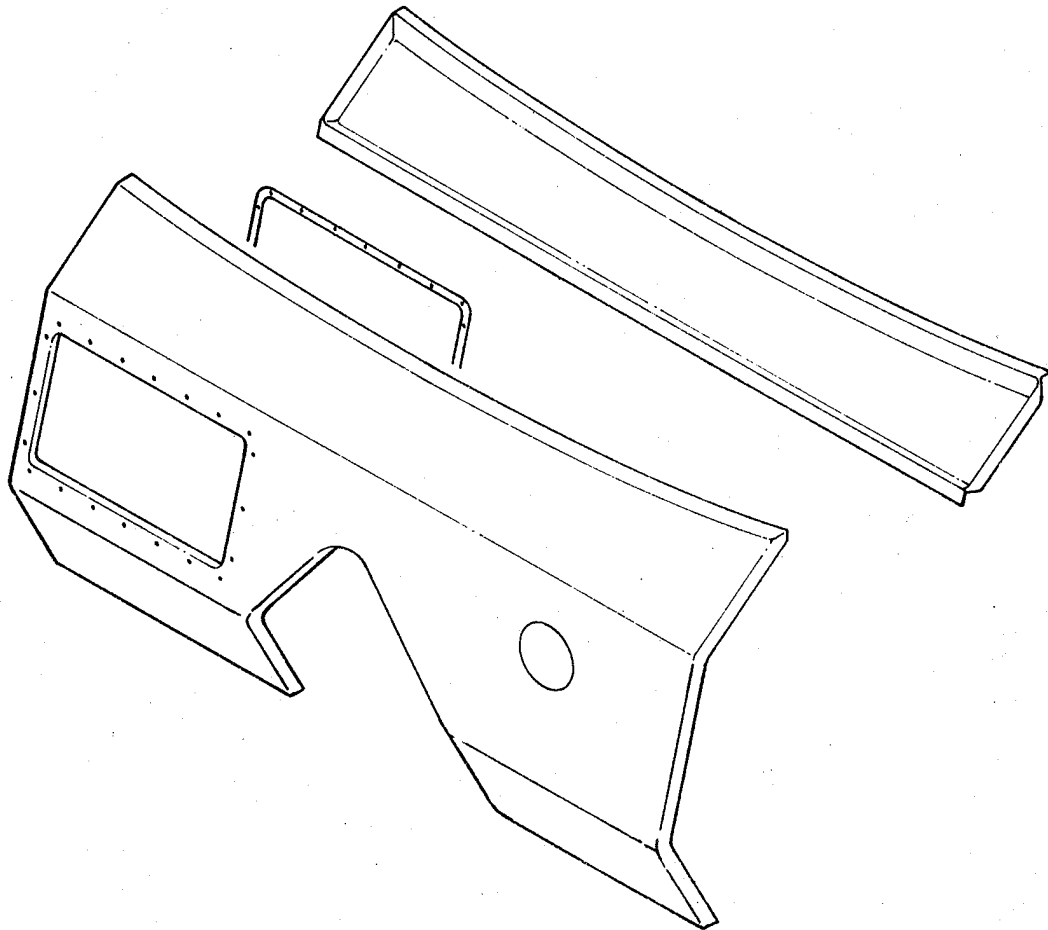
FIGURE 63 LUGGAGE COMPARTMENT, REINFORCED PLASTIC
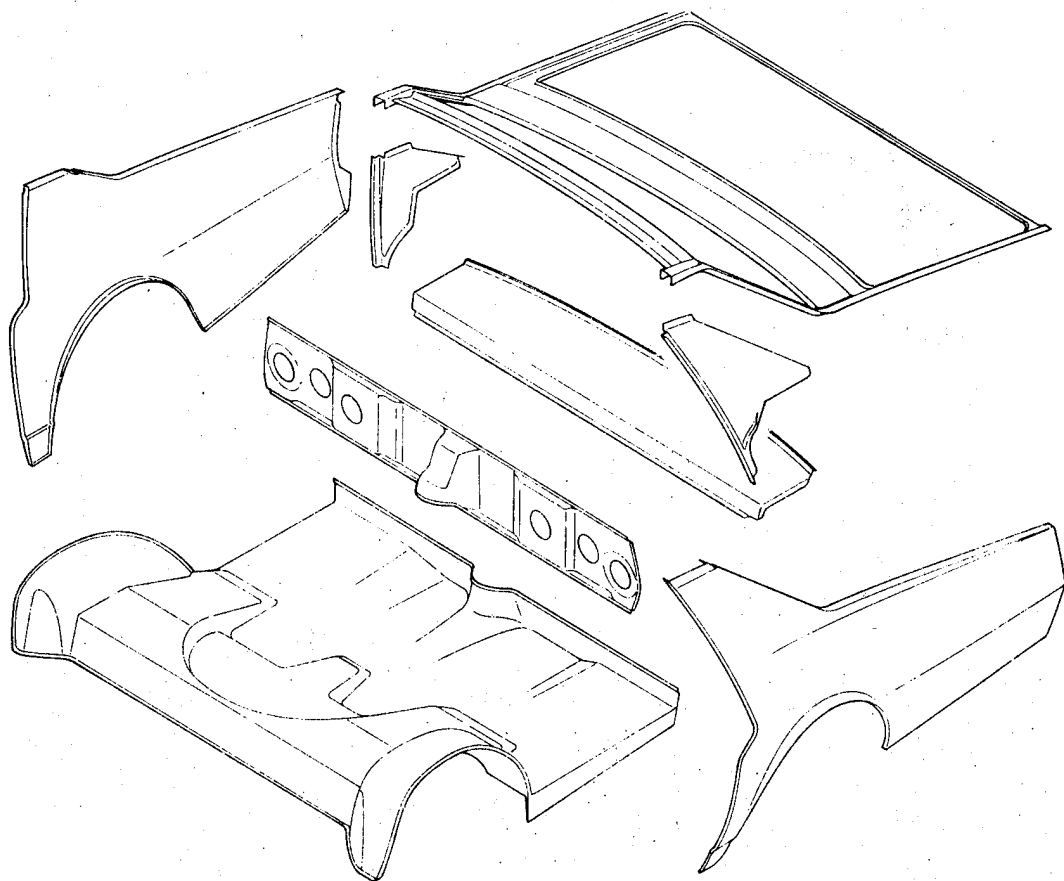
FIGURE 64 SECTION: QUARTER PANEL-DECK LID, REINFORCED PLASTIC

DECK LID

QUARTER PANEL

DECK REINFORCEMENT
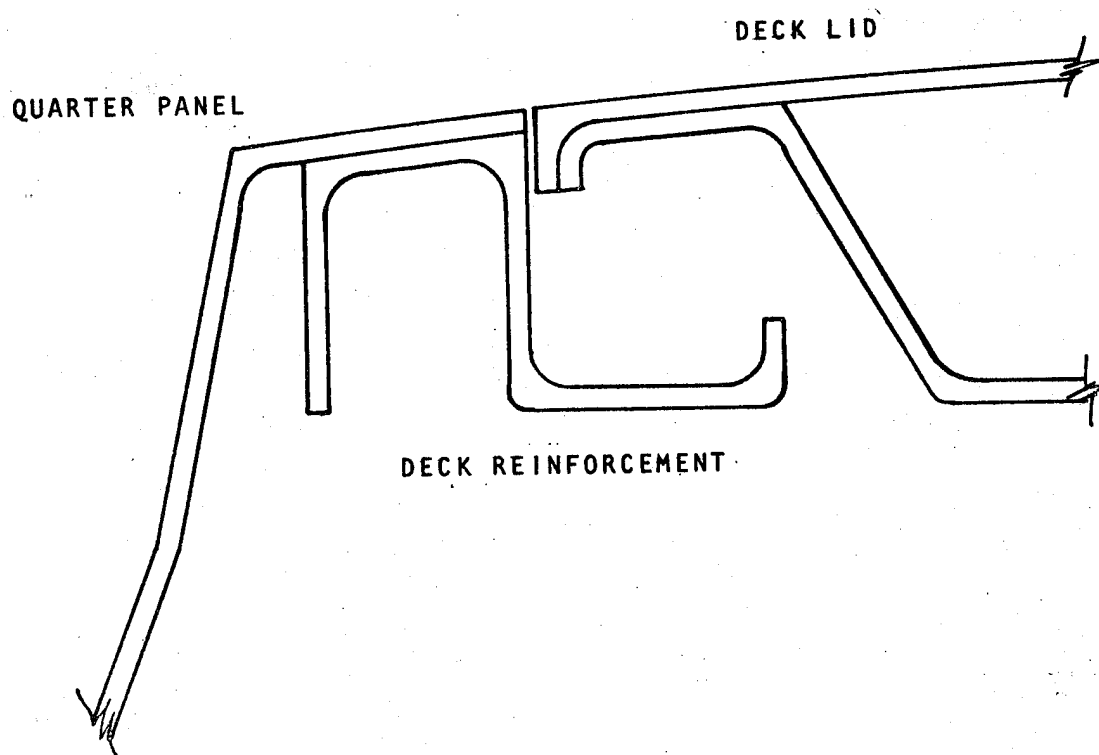
FIGURE 65 INNER AND OUTER HOOD PANELS
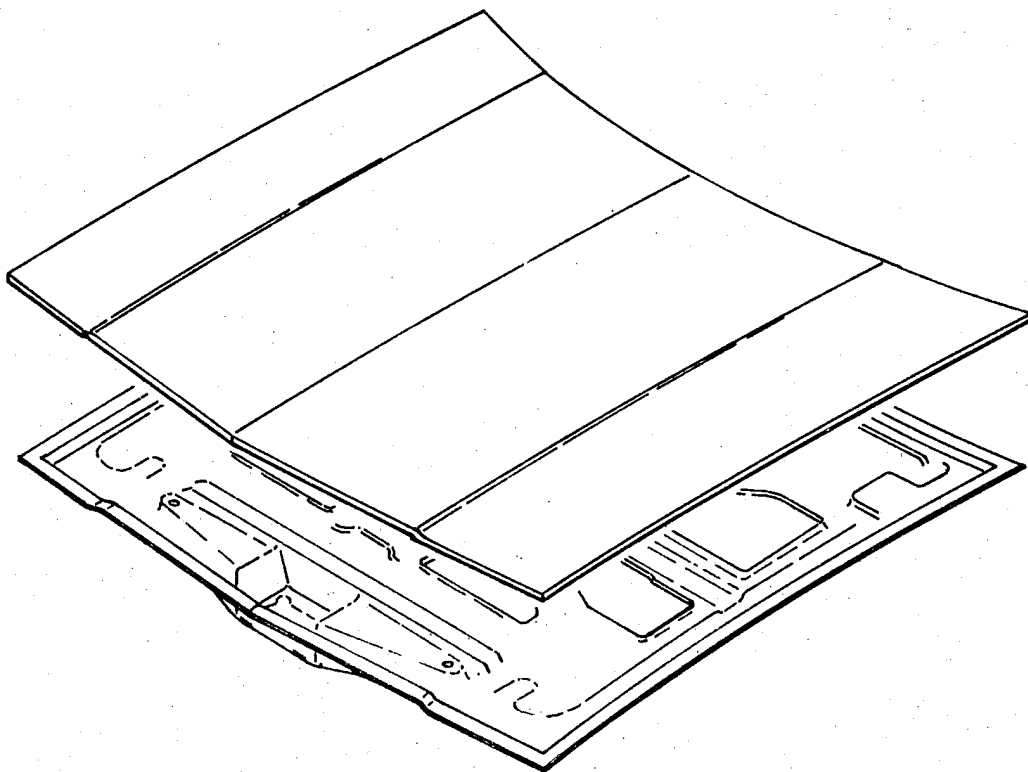
FIGURE 66 INNER AND OUTER DECK LID PANELS
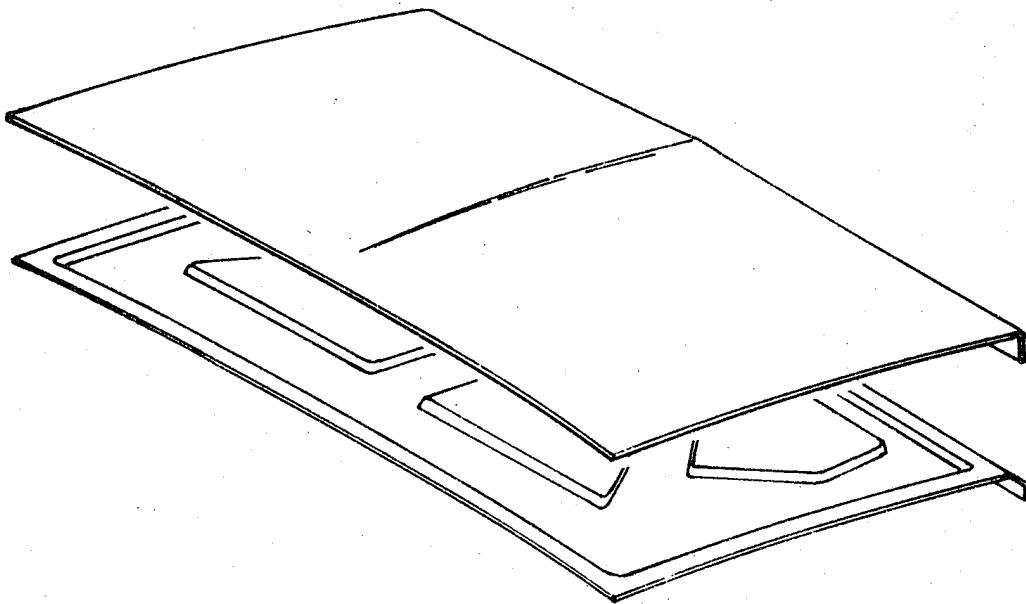
spot welding of the downstanding perimeter flanges and with a mastic adhesive at local areas where the inner panel touches the outer panel. The deck lid panels are hem flanged and resistance spot welded, with mastic adhesive in local spots throughout the component.

The hood weighs 52.5 pounds and the deck lid weighs 42 pounds, in steel. Both items have been, in all automobiles, targets of weight reduction and alternate materials application.

The hood and deck lid requirements consist of the following items:

1. Appearance
2. Bending stiffness
3. Twisting stiffness
4. Flutter
5. Local firmness

Appearance is an important factor especially for the hood due to its high visibility. Carbon steel outer panels have been preferred for this reason. Aluminum and plastic outer panels can be made to the same appearance quality but at a reported high finishing cost penalty.
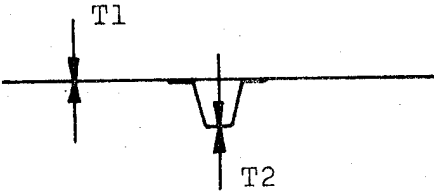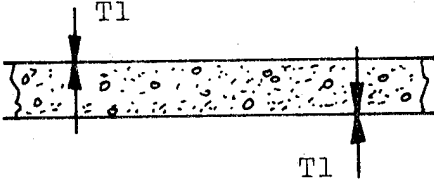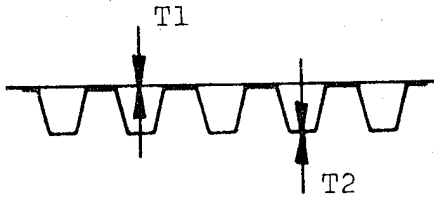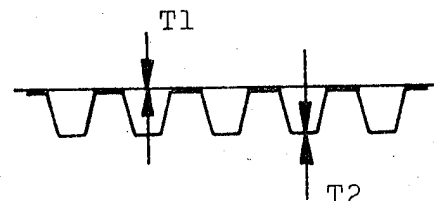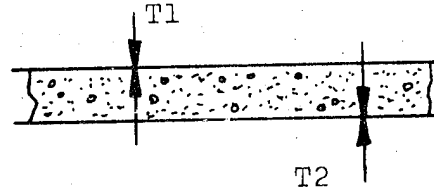
Bending and twisting stiffness and flutter is dependent upon the IE product. The hood depth is controlled by internal interference and external styling or line of sight. Based on maintaining the same section thickness (1.5 inches) weights of several configurations have been calculated as shown in Table 60 to provide the same bending deflection as in the existing steel hood.

The steel-foam configuration (#2) is not practical due to the inability to produce the thin gage steel in wide enough coil widths and inability to form the shaped panels without local buckling or tearing.

The aluminum configuration (#3) is based on using three times as many hat sections as the existing steel hood. This has another beneficial effect besides meeting the steel hood bending stiffness. Increasing the number of stiffening hat sections reduces the unsupported area of the outer skin, permitting the use of the same thickness metal in the outer panel.

It is difficult to pattern and then form the inner panel of aluminum if the hat sections become too close. An alternate pattern would have to be selected. One pattern could be developed from parallel, side to side hat sections as shown in Figure 67. Another could be formed using nested circular dimples also shown in Figure 67. The circular dimple panel can be nested to provide or simulate the desired stiffening pattern. The side to side parallel hats may not provide the diagonal stiffness equal to the current

TABLE 60: POSSIBLE IMPALA HOOD STRUCTURE FOR EQUAL STIFFNESS

MATERIAL	CONFIGURATION	THICKNESS (INCHES)	WEIGHT (POUNDS)
1. Steel (Existing)		$t_1 = 0.035$ $t_2 = 0.021$	52.5
2. Steel – Foam		$t_1 = 0.009$	25.6
3. Aluminum		$t_1 = 0.035$ $t_2 = 0.021$	21.2
4. Glass Polyester SMC		$t_1 = .100$ $t_2 = .100$	49.4
5. Graphite (0/90) Foam		$t_1 = 0.0135$	12.7

Outer Panel Area = 3520 square inches.

Inner Panel Area = 2816 square inches existing steel only.

Hinge & Latch Reinforcements: 1.5 pounds

Foam: 2 pcf = 6 pounds/hood

FIGURE 67   ALTERNATE HOOD INNER PANELS FOR ALUMINUM
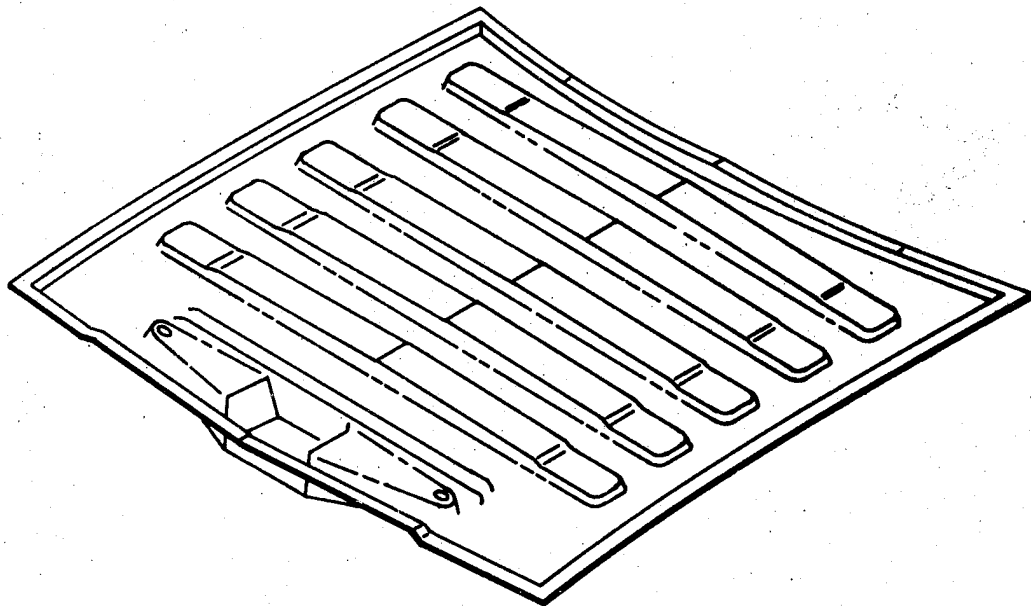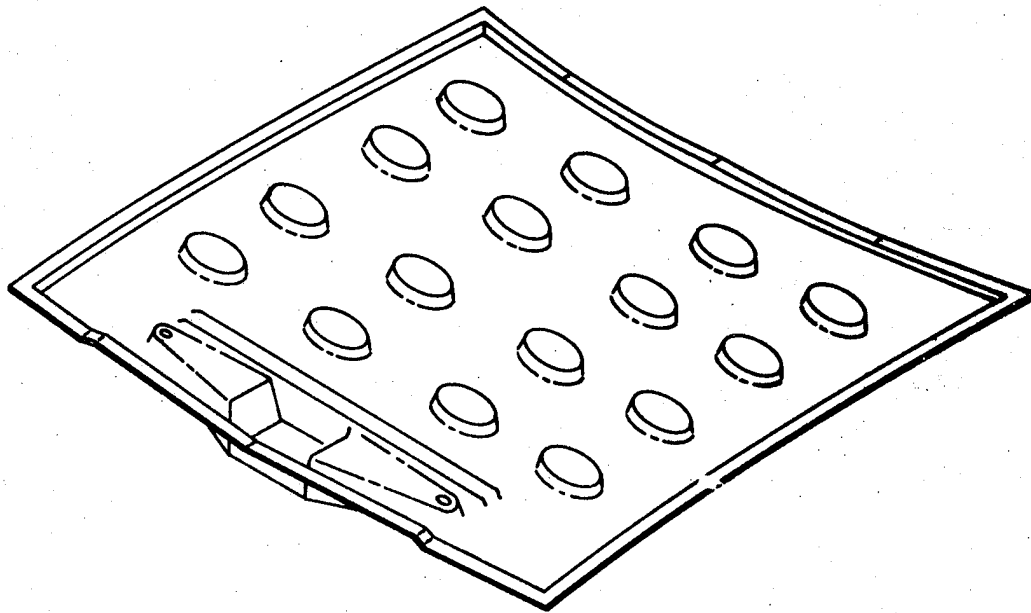
steel hood. Examination of the current Impala hoods indicates that either of the modified inner panels would not interfere with any of the under hood equipment.

The two inner hood panels shown above require a close examination of the shapes to permit stamping. The increased use of ribs and dimples restricts the flow of metal by drawing, and stretching is required to form the panels. Aluminum metal is more difficult to draw or stretch and care must be taken. Previous experience has shown that the die and punch should be shaped to obtain a configuration as shown in Figure 68 to prevent failures in the aluminum.

For the glass-polyester hood the number of hats would have to be increased 12 times. As in the case of the aluminum panel the pattern could be of several forms but probably like the circular dimples shown in Figure 67. There is no real difficulty in molding such a pattern.

The graphite reinforced polyester skins with a foam core produce the lightest weight hoods. It is not known whether this hood could provide an acceptable surface finish, equivalent to that now required. Attachment of the hinges and latch might require additional bonded on tapping plates to distribute the loads more adequately.

Calculations of the deflections of the current steel hood and actual measurements on a hood in place indicates the bending deflection is very small, 0.065 inches for a 150 pound load. If this deflection is increased by a factor of say five to 0.325, it is doubtful the customer would know. Using this philosophy the aluminum alloy hood weight might be reduced to 17.5 pounds and the glass polyester hood might be reduced to 38.1 pounds. The SMC outer panel would probably have to remain at 0.100 inches thick to preserve an acceptable appearance. The inner panel could be reduced in thickness or cut outs made to reduce weight. Oriented, longer length, glass fiber could also be utilized with the short random surface glass polyesters to obtain both finish and stiffness.

Deck lid concepts are essentially the same as for the hood and proportionately similar weight reductions can be made, Table 61.

Cost penalties associated with the fabrication of aluminum alloy or glass-polyester hood and deck lids have limited their applications. Sheets of the soft aluminum alloy are easily scratched or dented during press and assembly operations. Special handling and added repair and finishing operations are needed to meet show room requirements. With glass reinforced polyesters; ribs and bond lines develop appearance defects which can be eliminated by extra material use or finishing. Direct material costs of aluminum and glass polyester are greater than that for low carbon steel.
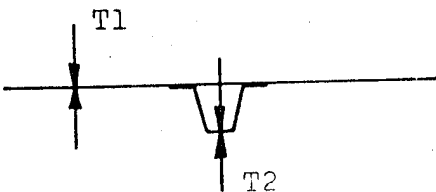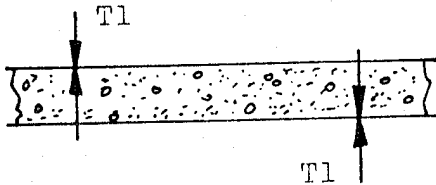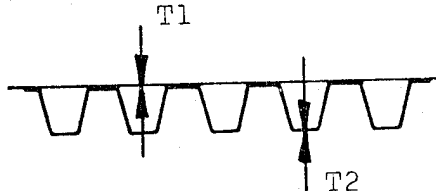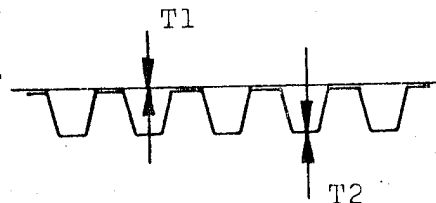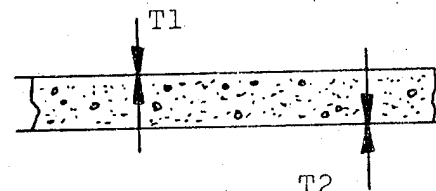
FIGURE 68   FORMING LIMITATIONS, ALUMINUM ALLOYS
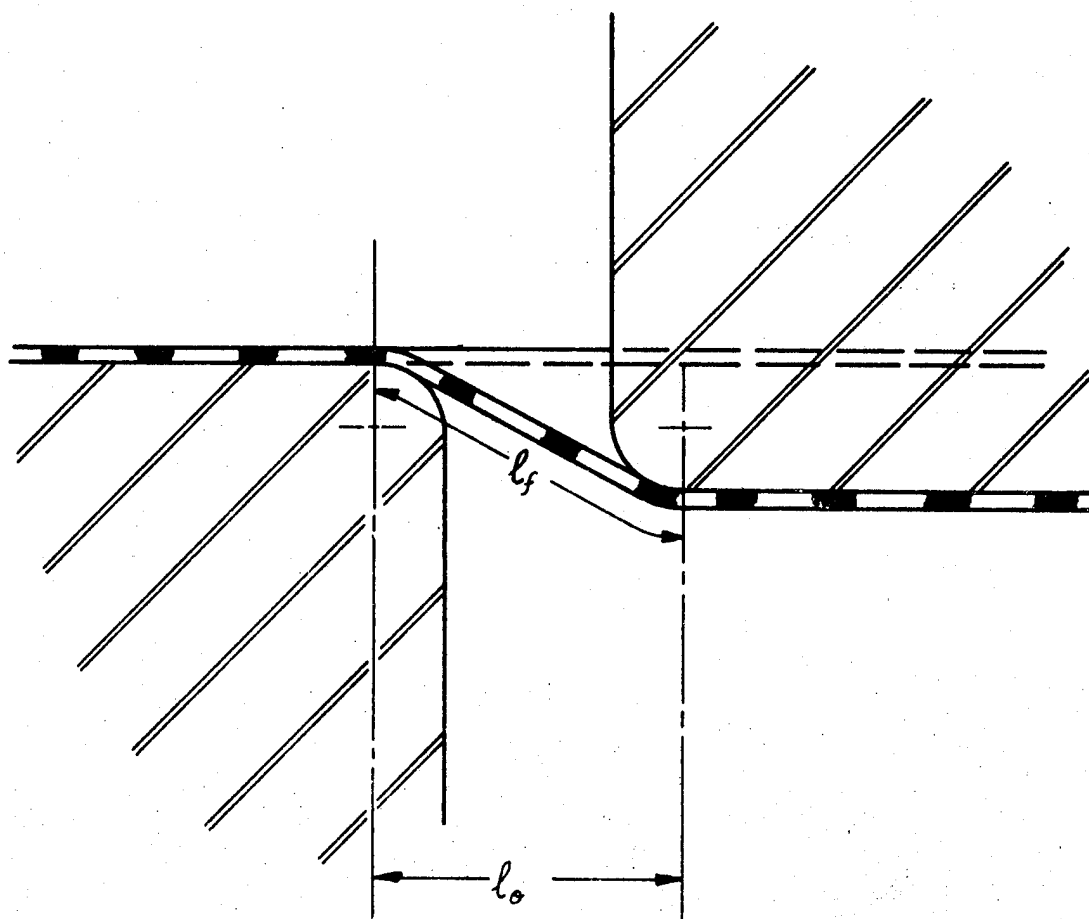
$$\frac{\ell_f - \ell_o}{\ell_o} = < 0.20$$

TABLE 61: POSSIBLE IMPALA DECK LID STRUCTURE
FOR EQUAL STIFFNESS

MATERIAL	CONFIGURATION	THICKNESS (INCHES)	WEIGHT (POUNDS)
1. Steel (Existing)		$t_1 = 0.035$ $t_2 = 0.021$	42
2. Steel - Foam		$t_1 = 0.009$	20.5
3. Aluminum		$t_1 = 0.035$ $t_2 = 0.021$	17
4. Glass Polyester SMC		$t_1 = .100$ $t_2 = .100$	39.5
5. Graphite (0/90) Foam		$t_1 = 0.0135$	10.2

200

The hood utilizes a joint between the inner and outer panels known as a downstanding flange, Figure 69. The deck lid joint is a hemmed flange. In the use of aluminum alloys it is necessary to have a sufficiently large radius in downstanding flanges and a rope type hem flange is required to prevent cracking during the bending operations.

6.1.4 Front Fender Structure

The existing steel front fender structure is shown in Figure 70. It is bolted to the "A" post and the fire wall in the rear and the frame and radiator support in the front. The front frame mounting is made through a standard body mount, Figure 44. The fender system covers the engine compartment and protects the engine and passenger compartment from debris thrown up by the wheels. It also ties in the frame, radiator support and passenger compartment to form a support for the radiator, lights and hood. Being a hang on item that is removable for repair or replacement it is a prime candidate for material studies.

It is suggested that the present fender structure could be changed as shown in Figure 71. The rectangular tube provides the necessary structural rigidity and adds crashworthiness as will be discussed in Section 7.0. Various combinations of materials can be utilized including a metal rectangular tube and metal or plastic outer fender panel. The rectangular tube can be easily shaped to permit fabrication and assembly. It is necessary to insure that it does not interefere with hood closure or wheel jounce.

From a weight reduction stand point the structure could be fabricated from aluminum alloy, preferably one composition, 6010-T4 or if necessary including 6009-T4. For weight reduction and non damageability the outer skin panel could be molded from an elastomer such as EPDM or polyurethane and the fender liner made of polypropylene.

6.1.5 Radiator Support

The radiator support, shown in Figure 72 with the fender structure ties in the front end of the vehicle. Its primary purpose is to provide a mounting for the radiator and carry the lights, horn, latch lock and fan shroud.
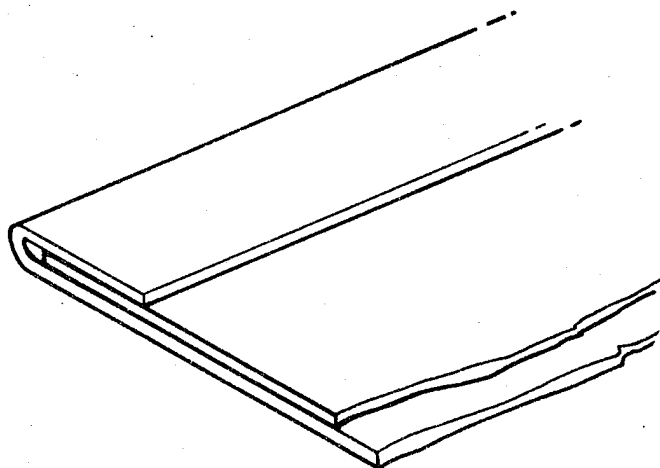
Again, in the industry, numerous attempts are being made to use alternate materials for this component since it is a hang on item. The radiator support must be able to withstand racking which will occur during jacking or when one front wheel is subjected to road force out of synchronization with the opposite wheel.
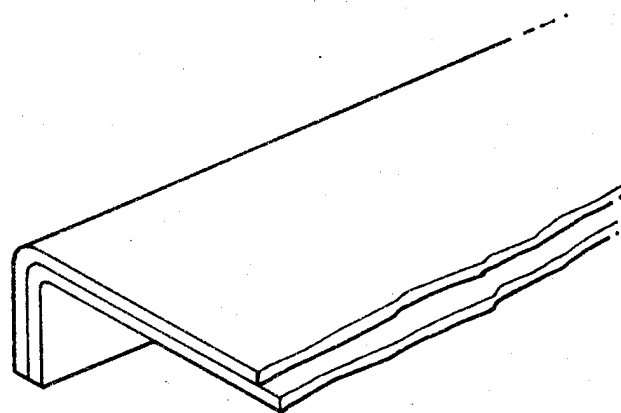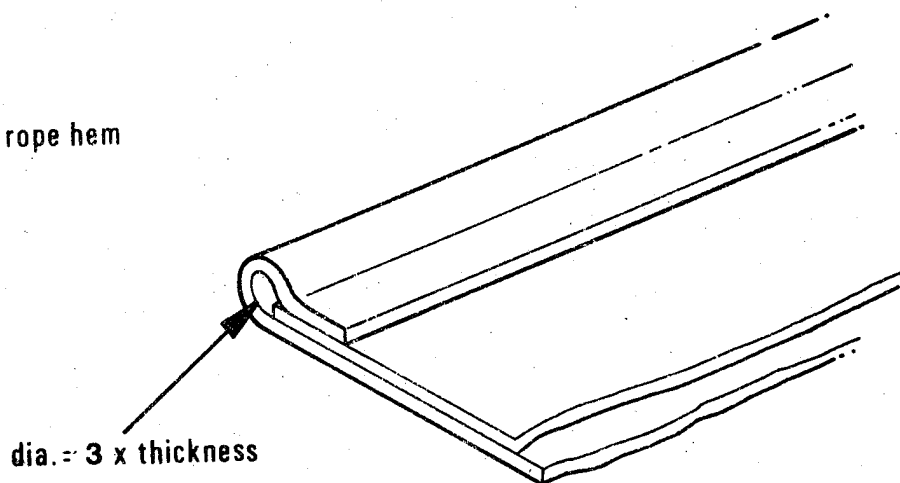
a. hem

b. downstanding

c. rope hem

dia. = 3 x thickness
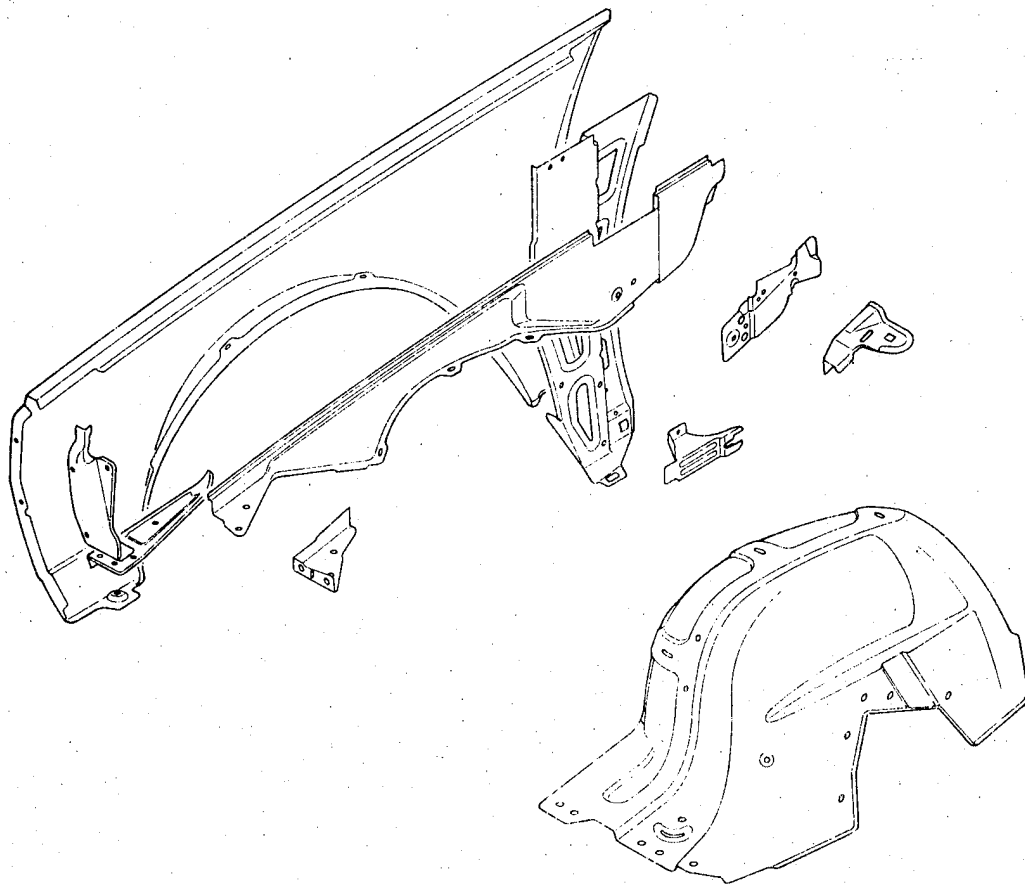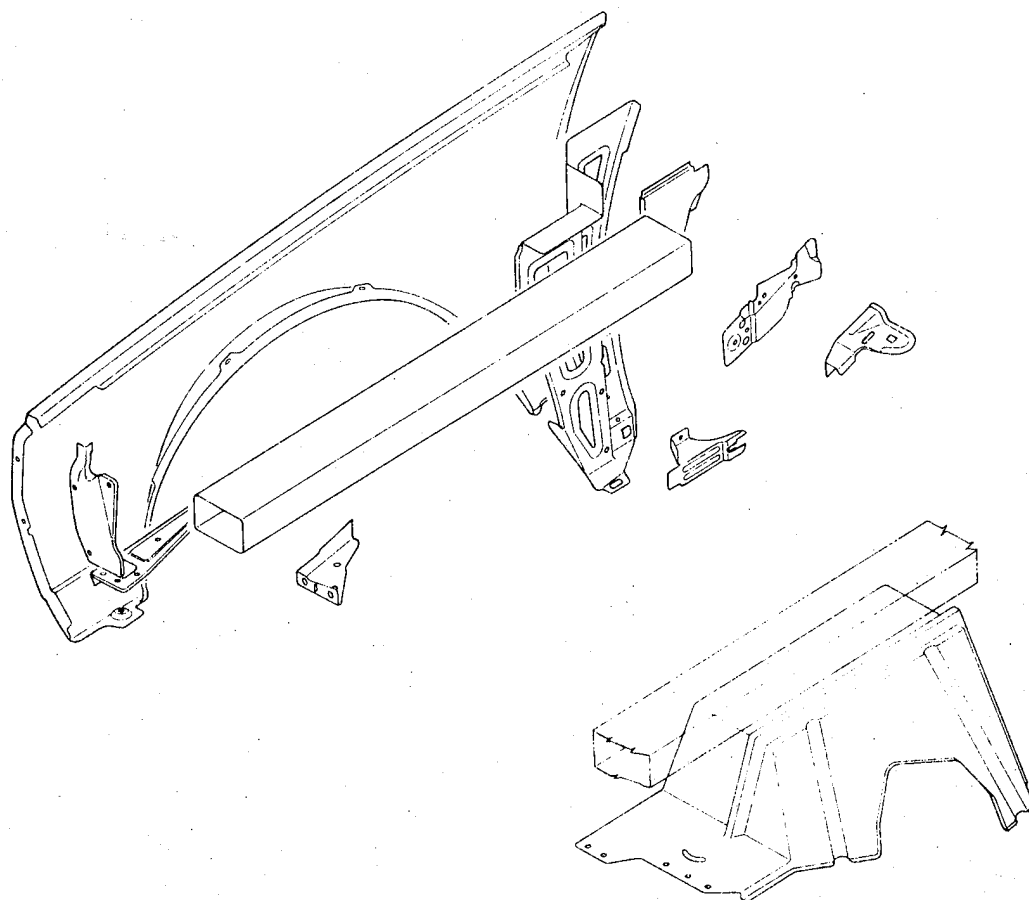
FIGURE 70   FRONT FENDER IMPALA
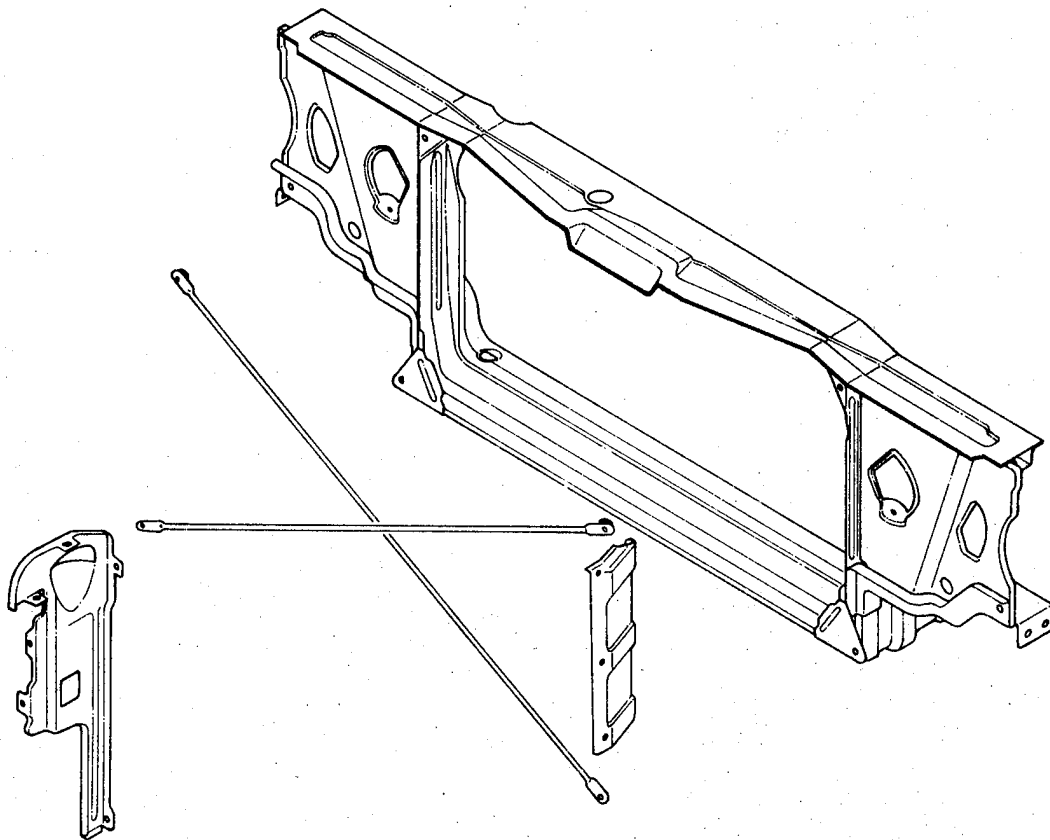
FIGURE 71   MODIFIED FRONT FENDER STRUCTURE

FIGURE 72   RADIATOR SUPPORT, 1977 IMPALA

The steel radiator support is made of 10 separate parts and might be replaced with one or two reinforced plastic moldings. Such a plastic support might look like that shown in Figure 73. In this case two moldings are used; one primary molding and a second molding used to provide a box beam at the top of the radiator support. Either or both moldings could utilize oriented glass fiber for increased stiffness or strength.

6.1.6 Front and Rear Bumper Systems

The front and rear bumper systems are essentially the same, as shown in Figures 74, 75 and 76. The back up bars are made from aluminum, and steel is used for the exterior bumper face bars. Hydraulic low speed energy absorbers are used to meet the requirements of FMVSS 215 and attach the bumper beams to the rear most or forward most points of the chassis frame. The bumper face could be made from aluminum alloy or glass reinforced polyesters as described in Section 5.0, with an expected weight reduction.

As flexible energy absorbing foams and fascia elastomers are developed it is expected that these type materials will gradually take over the bumper systems. The ability of such systems to absorb collision energy up to 15 mph and to rebound to their original shape without damage is considered a great benefit. Since there is an associated weight reduction over existing systems the potential of the flexible system is increased, Figure 21.

6.1.7 Doors

The general requirements of automobile doors include the following:

1. Sealable means of entering and exiting the passenger compartment.
2. Resistance to side intrusion during collision.
3. Resistance to collapse during frontal collision.
4. Provide mounting and containment of window and its mechanisms.
5. Provide suitable appearance and resistance to damage.

The Impala door consists of an inner panel formed from low carbon steel into the shape of a rectangular pan. A number of holes are punched into the panel for access to the window mechanism and locks and for mechanical fasteners. Reinforcements are welded to the front and rear side of the inner panel to support the hinges and latch. A formed S shape welded to the inner panels forms a frame for the window. An intrusion beam is welded to the inner panel and an outer panel is then clinch flanged and welded to the periphery of this inner panel. A front door is shown in Figure 77. The rear doors are similar in construction and structure.

FIGURE 73   REINFORCED PLASTIC RADIATOR SUPPORT
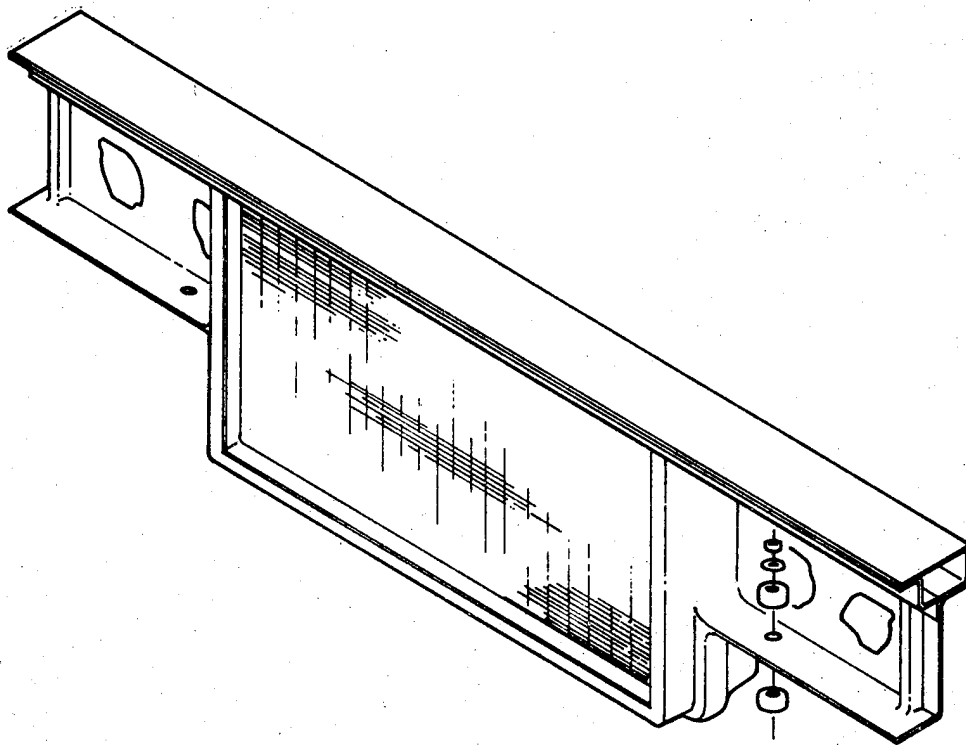
FIGURE 74 FRONT BUMPER
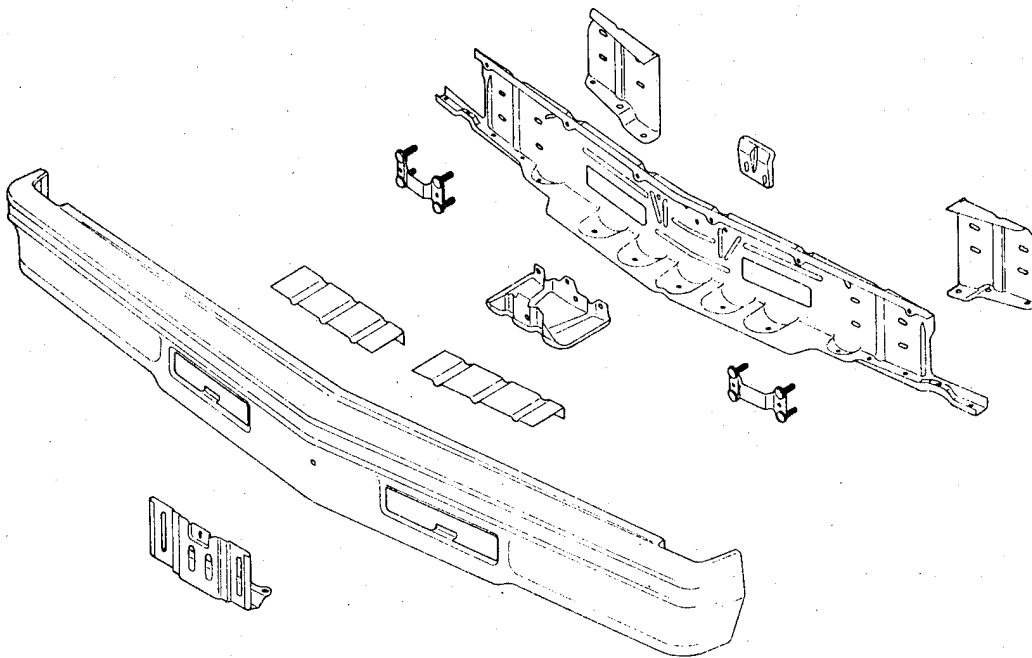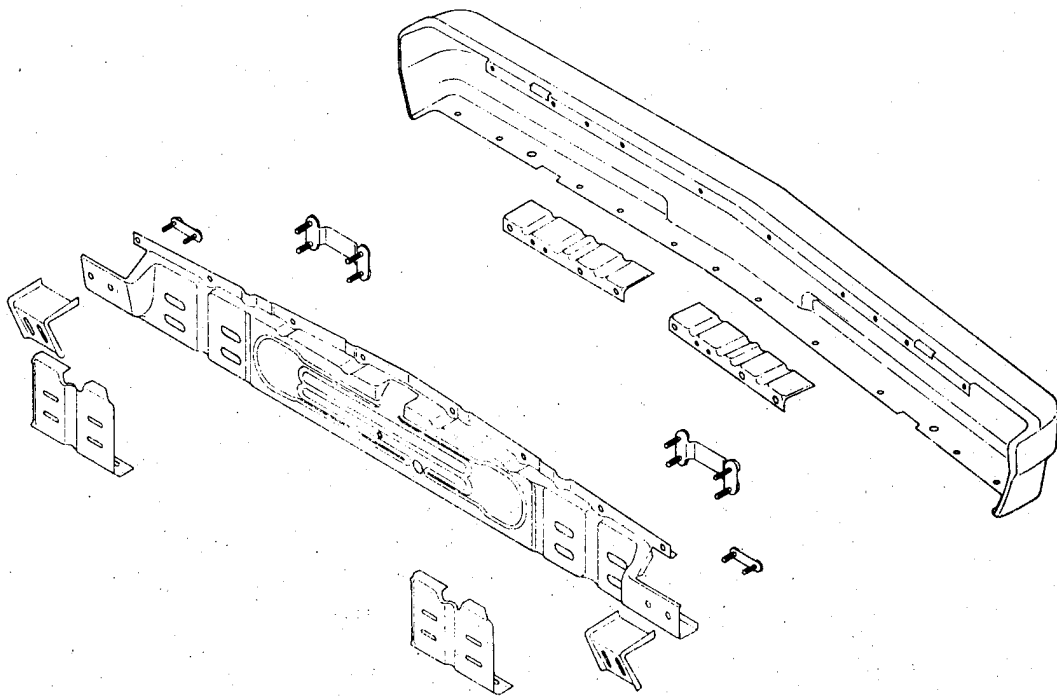
FIGURE 75 REAR BUMPER

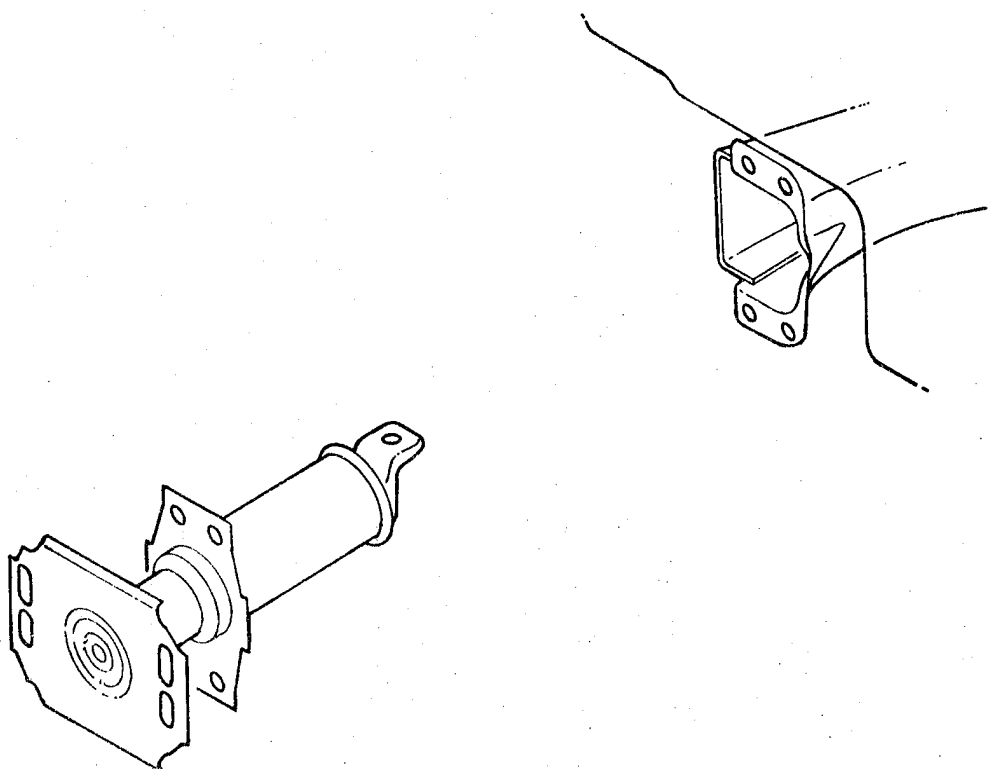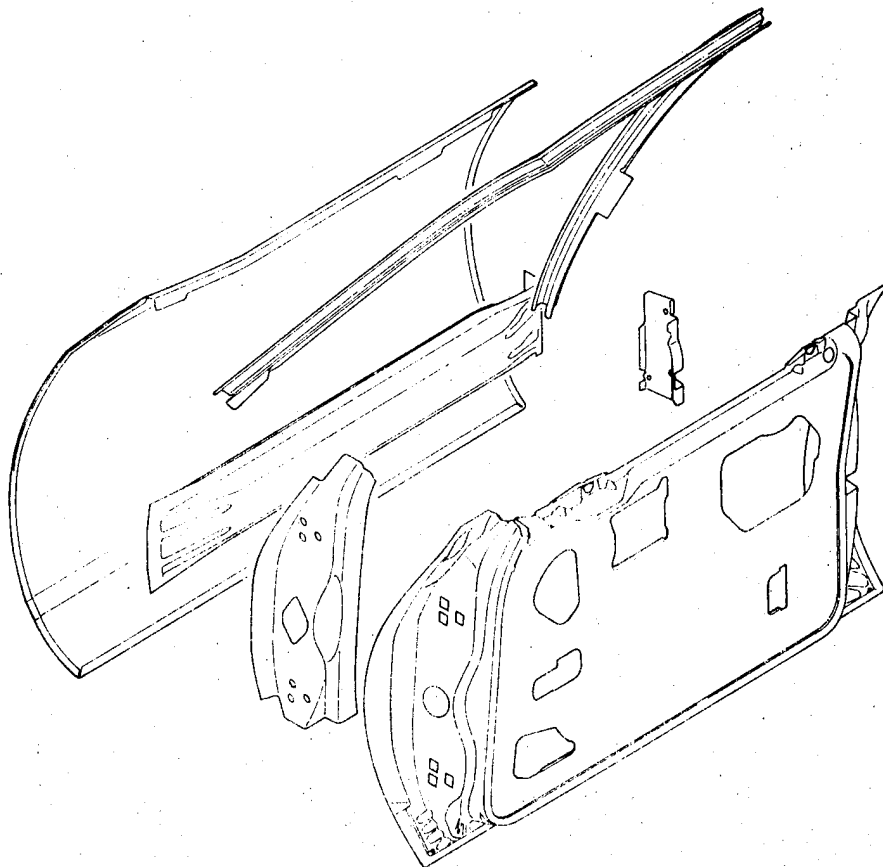FIGURE 76   LOW SPEED E A DEVICES

FIGURE 77 FRONT DOOR IMPALA

The current door structure is fabricated from low carbon steel sheet. The intrusion beam is made of a high strength steel having an 80,000 psi ultimate strength (approximately 60,000 psi yield) estimated from a hardness test result, RB86.

Resistance to side intrusion Figure 78 can be increased by one or more of the following:

1. Stiffening and strengthening of the intrusion beam.
2. Supporting the intrusion beam at intermediate points.
3. Increasing the fixity of the intrusion beam at the "A" and "B" posts.
4. Increasing the bending and, or torsional strength of the "A" and "B" posts.

While no actual test data is available on the 1977 Impala on side intrusion, the above suggestions are made based on test activity on Contract DOT-HS-7-01588, "Lightweight Subcompact Vehicle Side Structure Program".

The door and its intrusion beam should also provide some support to the "A" post during frontal collisions. In this case the beams contribution can be increased by providing a larger resistance to buckling and carrying loads from the "A" post back to the "B" post.

High strength low alloy steels could be used on all door components. The most benefit could be obtained however, by using them in the outer skin panel and in the intrusion beam. In the outer skin, the increased yield strength improves dent resistance, σ_{yt}^2. A 50,000 psi yield material, SAE 950, would permit a thickness reduction of 0.038 to 0.0295 inches. The strength, $\sigma_y t$, of the panel is increased which would, to a small degree, improve side intrusion. As an intrusion beam material a higher strength, yet tough, steel would either increase the beam yield strength or permit a reduction in weight.

Aluminum alloys would also be suitable for the inner and outer panels and the latch and lock reinforcements. It is necessary to note that in the case of the current steel and in an aluminum door that the hinges are attached to thick, 3/8 inch, tapping blocks held loosely between the inner panel and the reinforcements. Aluminum alloy 6010 would be recommended for the outer skin panel and 6009 for the inner panel. Alloy 6010 has a higher yield strength and a better dent and scratch resistance. The latch and lock reinforcements would be made from a plate or heavy sheet alloy such as 6061. Some difficulty would be expected in forming the hem flanges in the outer door skin panels and a rope hem as described in Figure 69 would have to be used to prevent cracking of a high percentage of outer skins. Aluminum thickness for the outer and inner panels, and reinforcements would be the same as for the current steel parts.

FIGURE 78   **FRONT TO SIDE CRASH CONFIGURATION**
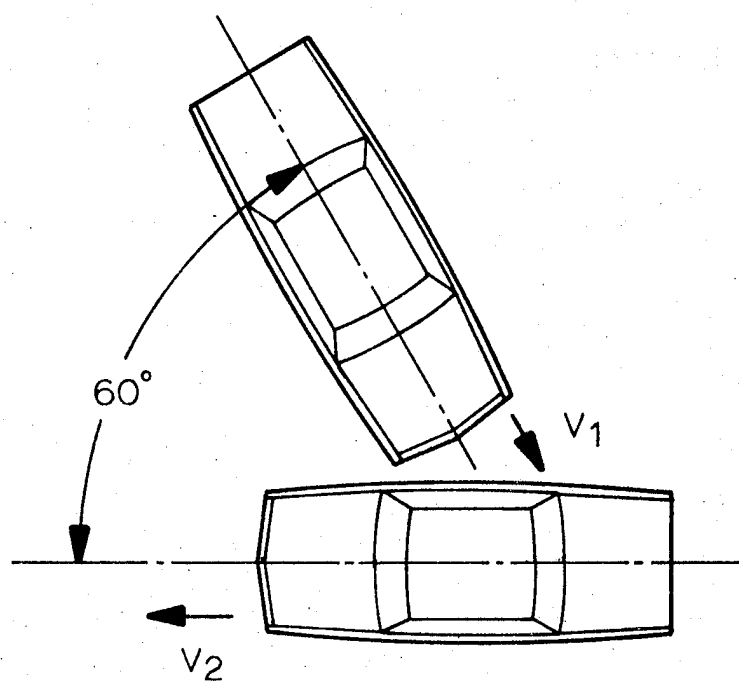
The window frame as now made from steel could not be made from aluminum sheet satisfactorily without a high scrap rate. An extrusion would be made from an alloy such as 6061 having the proper cross section and then cut, welded and mildly formed to the outer vehicle and post contours. This extrusion would then be resistance spot welded to the inner panel in a manner similar to the current steel doors. Adhesives may be incorporated in the joint for additional strength. An alternate procedure would use the current steel window frame and weld it to the aluminum inner panel through a strip of transition metal as described before.

A stamped aluminum intrusion beam or an extruded beam could be substituted for the high strength steel. Its benefit, either for weight reduction or for increased intrusion resistance, appears to be small or non existent. The reasoning is that if this beam is to rely on its beam stiffness then the weight of an equivalent beam would be greater than for steel. If the beam is to rely on its tensile strength, as a belt, then ultra high strength steels could be used to match the high strength 7000 series aluminum alloys on a specific strength comparison.

Reinforced plastics could also be utilized for the entire door structure. Glass reinforced polyester in the form of sheet molding compounds could be used to mold the inner and outer panels and their reinforcements. It would be advantageous to combine some of the parts such as the beam and end reinforcements into one molding. Such a concept is shown in Figure 79. In this case the hinges are attached to the single piece intrusion beam as shown in Figure 80. This beam would be made from continuous glass fiber polyester oriented parallel to the length of the beam with additional chopped fiber to provide a modest transverse strength. Using an E = 5,000,000 psi and an ultimate strength of 120,000 psi the beam could support a load of 18,200 pounds at mid span. Elastic deflection at that load would be 3.65 inches. Based on tests of similar beams the load-deflection curve in simple bending would be expected to look like that shown in Figure 81.

Further discussion of side intrusion during collisions will be discussed in Section 7.0.

6.2 Suspension and Steering

The front suspension acts independently at each wheel. Upper and lower control arms are attached to the frame and the steering arm. A coil spring and shock absorber are held between these two control arms, Figure 82. The front wheels move up and down, guided by the control arms, and vehicle turning is accomplished through the pivots on the steering arm.

FIGURE 79   REINFORCED PLASTIC INTRUSION BEAM
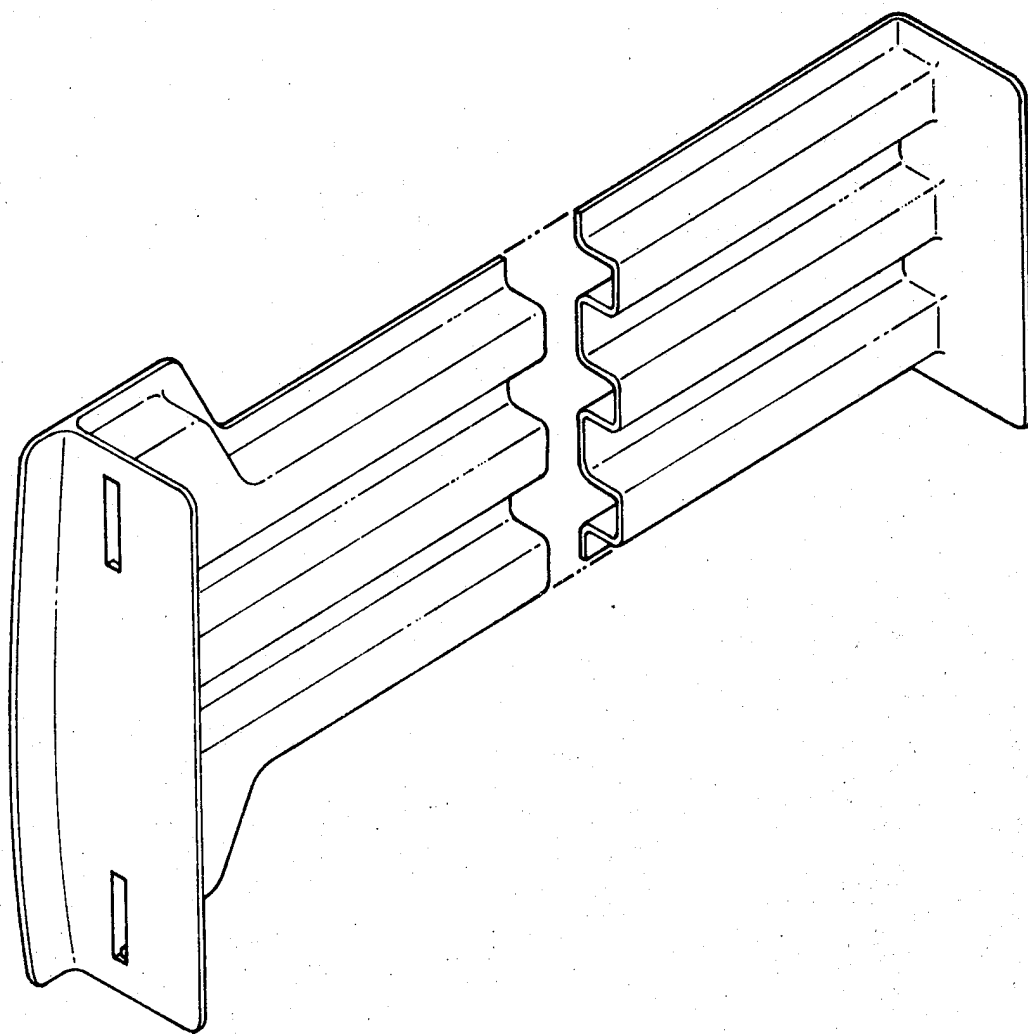
FIGURE 80   HINGE ATTACHMENT REINFORCED PLASTIC DOOR
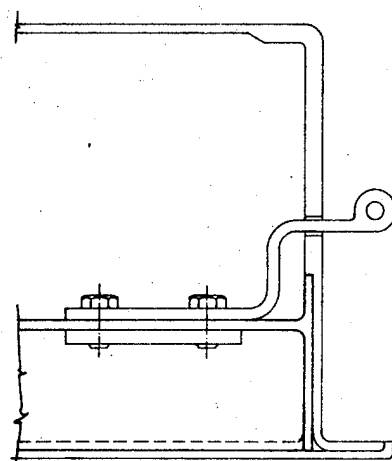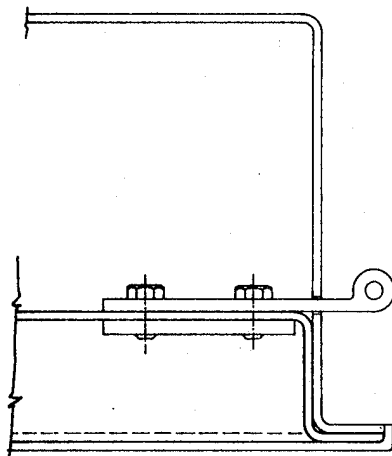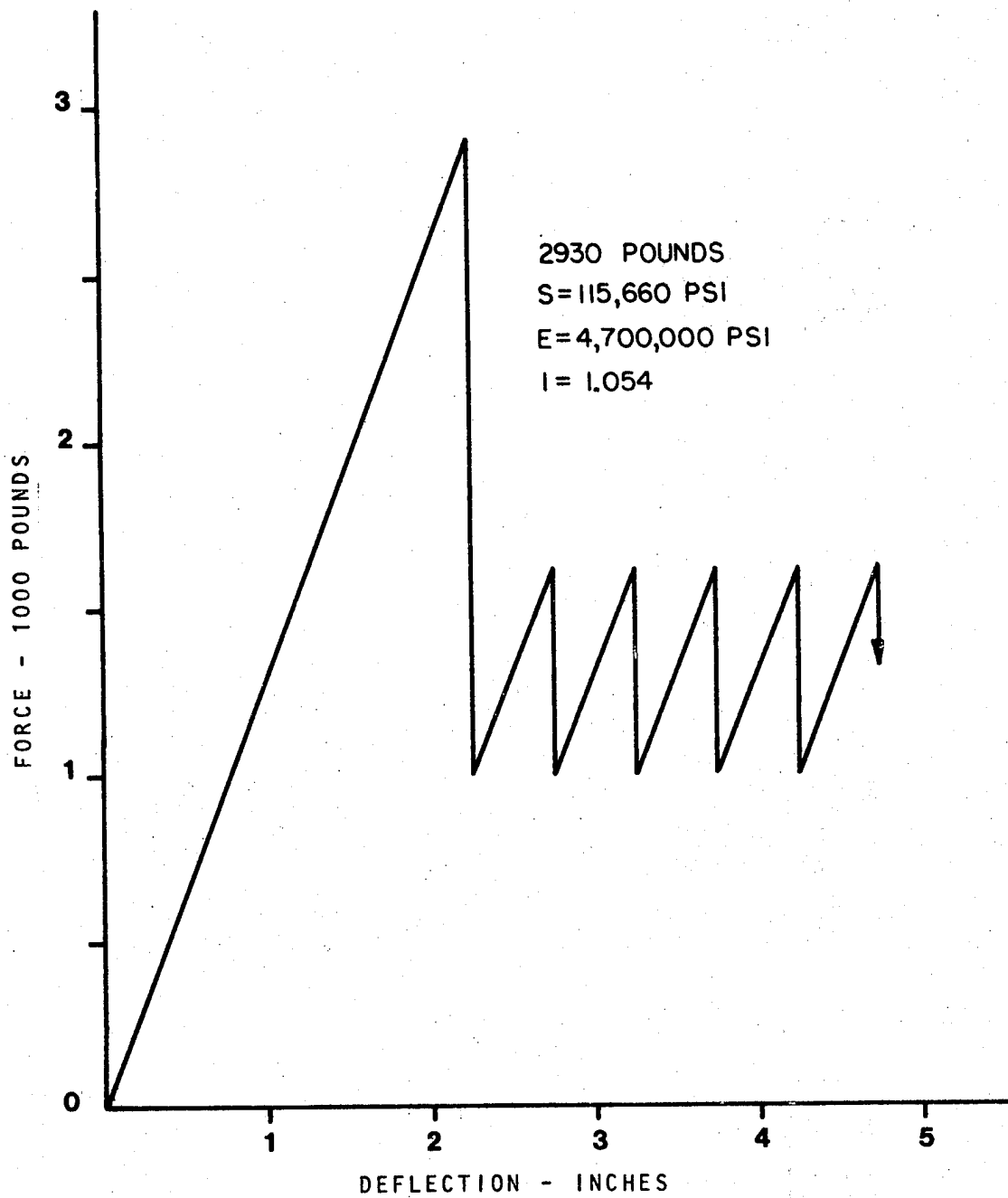
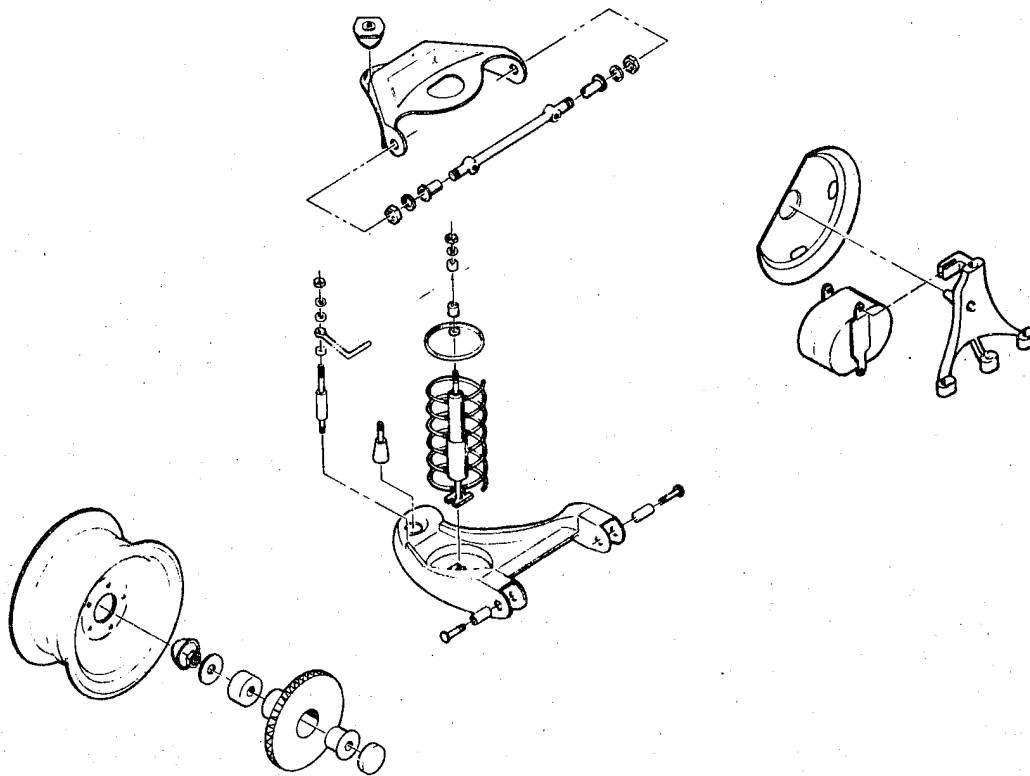FIGURE 81   LOAD DEFLECTION CURVE GLASS POLYESTER BEAM

2930 POUNDS
S=115,660 PSI
E=4,700,000 PSI
I= 1.054

FORCE - 1000 POUNDS

DEFLECTION - INCHES

217

FIGURE 82   FRONT SUSPENSION

A stabilizer bar, attached to the left hand and right hand lower control arms, is mounted to the frame, in front of the wheels.

Steering is accomplished by a five arm linkage system. A tie rod is attached to the left and right hand steering arms. These two tie rods are attached to a single relay rod. The relay rod is then driven by the pitman arm. An idler arm at the opposite end from the pitman arm stabilizes the relay rod.

The rear suspension, Figure 83, consist of two upper and two lower control arms attached to the rear axle and frame to maintain alignment and permit up and down movement of the rear wheels. Two coil springs and two shock absorbers are used to reduce and dampen road impacts.

The parts briefly described above are made from steel. The grade of steel is unknown although it is expected to be hot rolled low carbon steel sheet and bar. Selective hardening may be performed by induction hardening as required.

Without a detailed knowledge of the stresses in the suspension and steering assembly the feasibility of using alternate materials can be accomplished by an equivalency comparison. Using the parameters for stiffness (EI), tensile ($A\sigma$) and bending ($Z\sigma$) materials of different properties can be compared. For example the modulus of elasticity, E, of steel is 30×10^6 compared to 10×10^6 for aluminum alloys. The moment of inertia, I, of the aluminum round bar must then be three times that for steel. Determining the volume increase and ratio of densities a factor of 0.611 is obtained. The weight of an equivalent aluminum round bar for equal stiffness is 0.611 times that for a steel bar.

The tensile and bending allowable strengths used are the respective fatigue strengths. For hot rolled steel this value is 35,000 psi and for 7075-T6 aluminum alloy it is 23,000 psi. For equal tensile fatigue strength then, the cross sectional of the aluminum member must be 1.52 times greater and the weight factor becomes 0.538. Similarly, for bending the weight factor becomes 0.406.

Making such calculations for all of the suspension and steering system parts an estimated weight reduction for aluminum alloys applications are listed in Table 62 .

6.3 Static Analysis

The passenger compartment structure is quite complex and although it can be analysed by isolating components a finite element analysis of the entire structure is more desireable. The purpose of the analysis of the Impala body was to determine a baseline response to loading and a response to the same loading if the structure was made of another material.
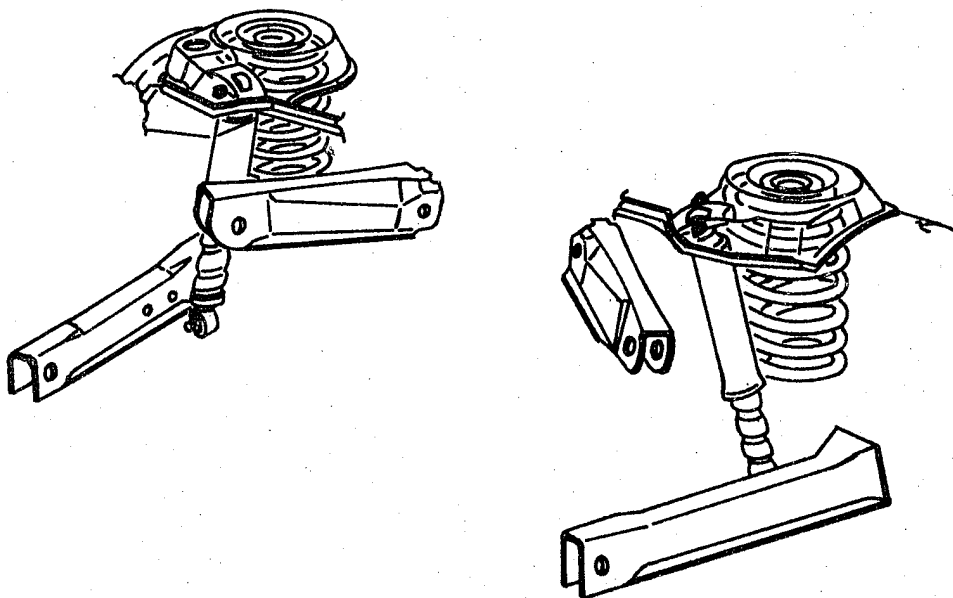
219

FIGURE 83   REAR SUSPENSION

TABLE 62:   ESTIMATED WEIGHT REDUCTION USING 7075-T6 ALUMINUM
            ALLOY IN SUSPENSION AND STEERING SYSTEMS.

PART DESIGNATION	APPROX. STEEL WEIGHT	APPROX. ALUMINUM WEIGHT	#/VEHICLE	ESTIMATED WEIGHT REDUCTION
Pitman Arm	2.78 lbs.	1.42 lbs.	1	1.36 lbs.
Idler Arm	1.46	.74	1	.72
Tie Rod Ass'y	2.00	1.22	2	1.56
Relay Rod	4.08	2.50	1	1.58
Front Stabilizer Bar	14.66	8.97	1	5.69
Front Lower Control Arm	9.17	4.67	2	9.00
Front Upper Control Arm	4.14	2.11	2	4.06
Rear Stabilizer Bar	----	----	1	5.69
Lower Control Arm	6.51	5.60	2	1.82
Upper Control Arm	7.82	5.53	2	4.58
		TOTAL WEIGHT REDUCTION	–	36.06

The Budd Company Structural Analysis Program which has been used in a number of vehicle studies was selected for the 1977 Impala analysis. This program is a small, relatively lower cost program. The model, Figures 84 and 85, consisted of 243 nodes, 103 section property beams, 349 dummy beams, 157 quadrilateral plates and 40 triangular plates. This is the modeling effort for one half the car assuming symmetry, depending upon the loading conditions.

The loading conditions are listed in Table 63 and schematically illustrated in Figure 86 through Figure 90. The loads on the car were distributed over the entire 243 nodes. They were calculated by using the component weights determined from a number of separate sources. The weights were applied as loads to the nearest node or were averaged out over a number of nodes. For example, if the steel roof structure weighs 30 pounds and is broken down into 20 nodes, then each node would receive 1.5 pounds. The loads for the aluminum bodied car were calculated in a similar manner with the difference in densities taken into consideration. Using the same example of the roof structure in aluminum, the weight would be 30 ÷ 2.83 = 10.6 pounds and each node would receive 0.53 pounds. Half weight of the all steel body vehicle is 1885.5 pounds and the aluminum body vehicle was 1547.5 pounds. The aluminum body was mounted on a steel frame and the aluminum sheet thickness was the same as for the steel.

The two nodes closest to the centerline of the front and rear wheels on the half-car model were taken as the reaction points in cases 1, 2, 4 and 5. In case 3, torsion, only the rear node was used as a reaction point.

Case 4, braking, presented a challenge in obtaining a true to life loading condition. In an actual braking situation the reaction points are where the tires meet the road which causes a tendency for the car to rotate forward. Since in the model reaction points can only be at nodes (and not at the tire-road interface) the tendency to rotate must be applied as a moment. There are different methods for applying moments: the application of a full moment at a node, breaking up the moment over several nodes, or applying equal and opposite loads at different nodes to obtain the needed moment. The latter case was selected because it was felt that the first two methods would create too large of a stress concentration at the chosen nodes. Also it is believed that the application of downward forces in the area of the front crossmember coupled with upward forces in the area of the rear crossmember creates a loading condition much closer to the actual case.

The section properties of the frame were listed in Table 56. Other sections used in the analysis are listed in Table 64.

FIGURE 84   IMPALA COMPUTER MODEL SIDE
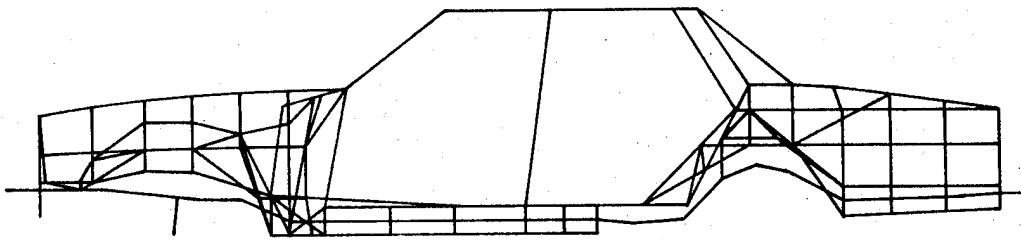
FIGURE 85   IMPALA COMPUTER MODEL ISOMETRIC
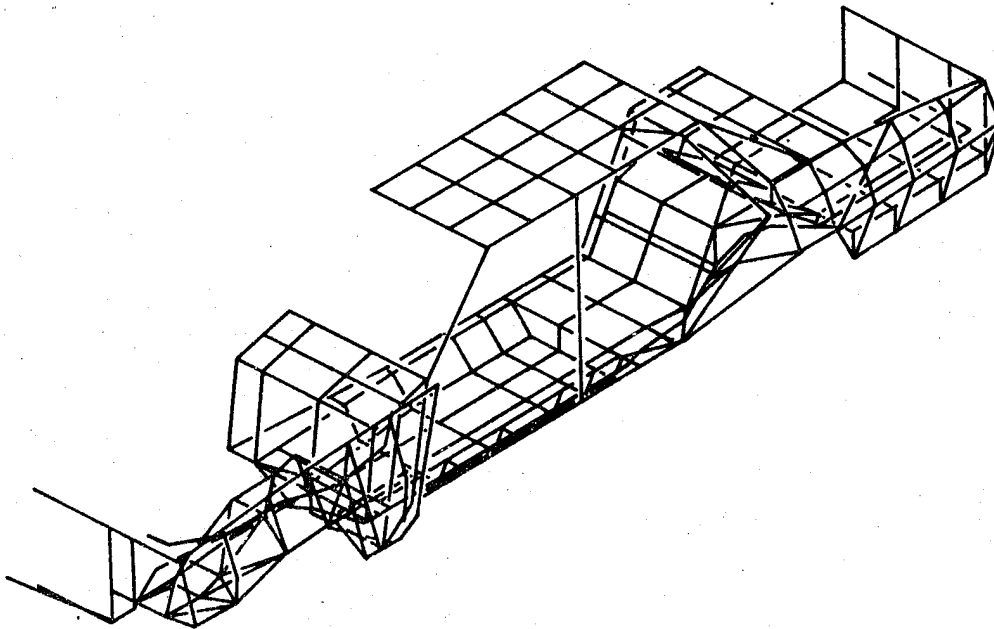
TABLE 63:   LOADING CONDITIONS IMPALA COMPUTER MODEL

Loading Condition	Vertical (1) (Additional Weight Factor)	g - Level	
		Lateral	Longitudinal
1. Static	0 + 1.0 (2)	0	0
2. Downward Inertia	2.5 + 1.0 (3)	0	0
3. Torsion	2.5 + 1.0	0	0
4. Braking	1.0 + 1.0	0	1.0
5. Cornering	1.0 + 1.0	0.7	0

(1) Weight of the car is distributed over the length.

(2) Over both front wheels.

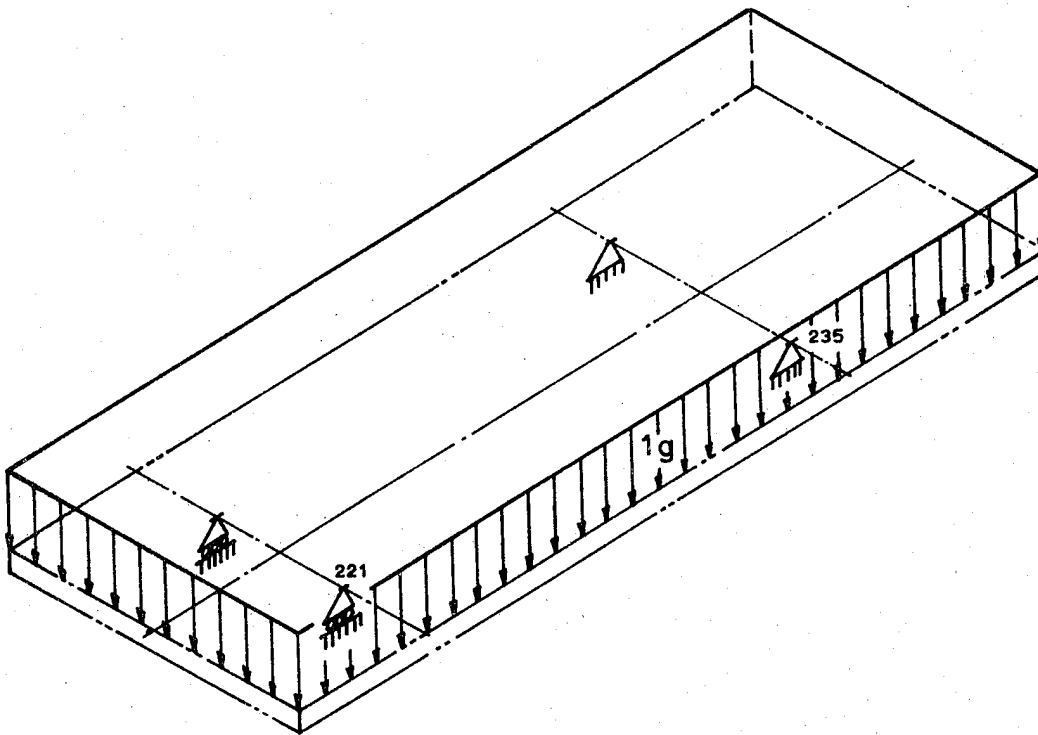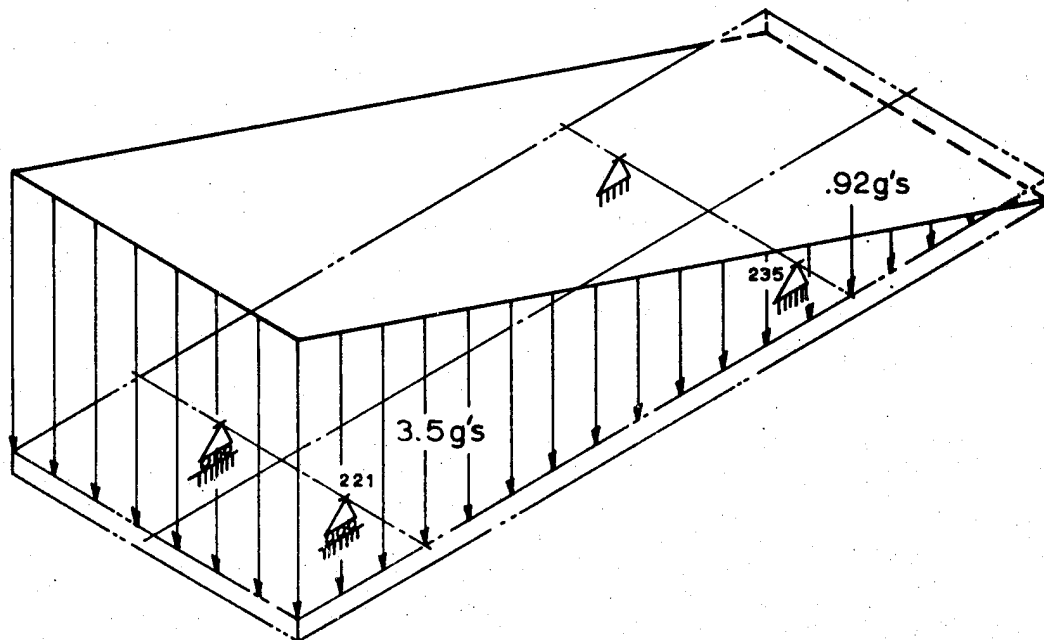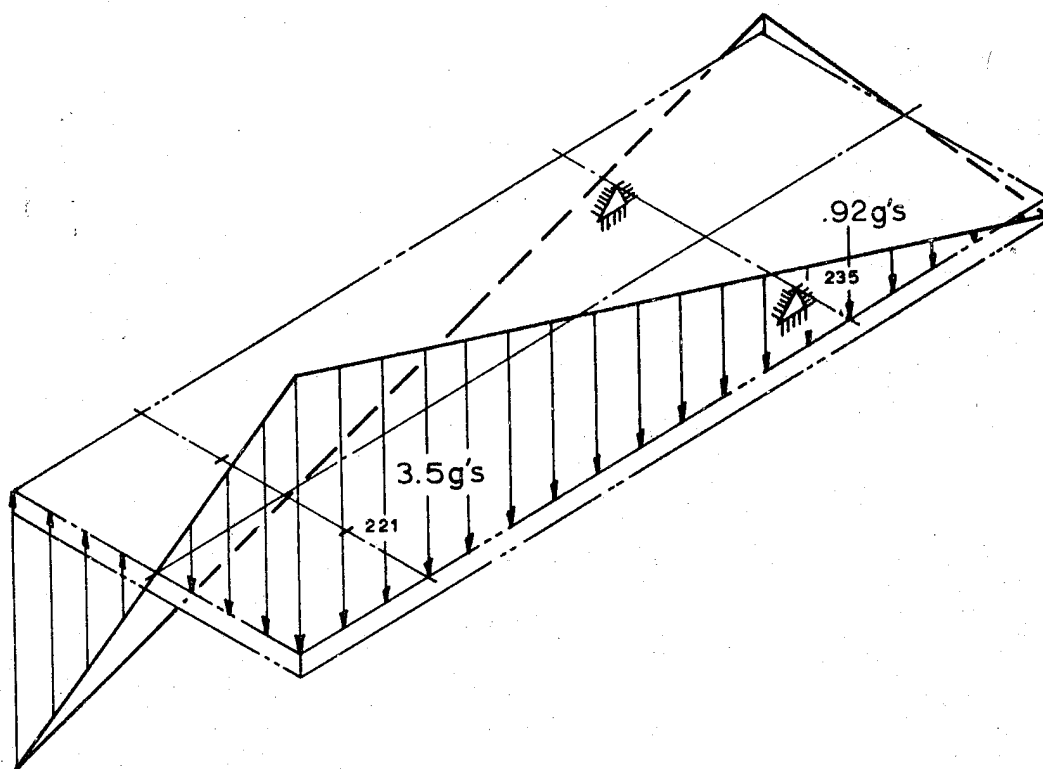(3) Over one front wheel.

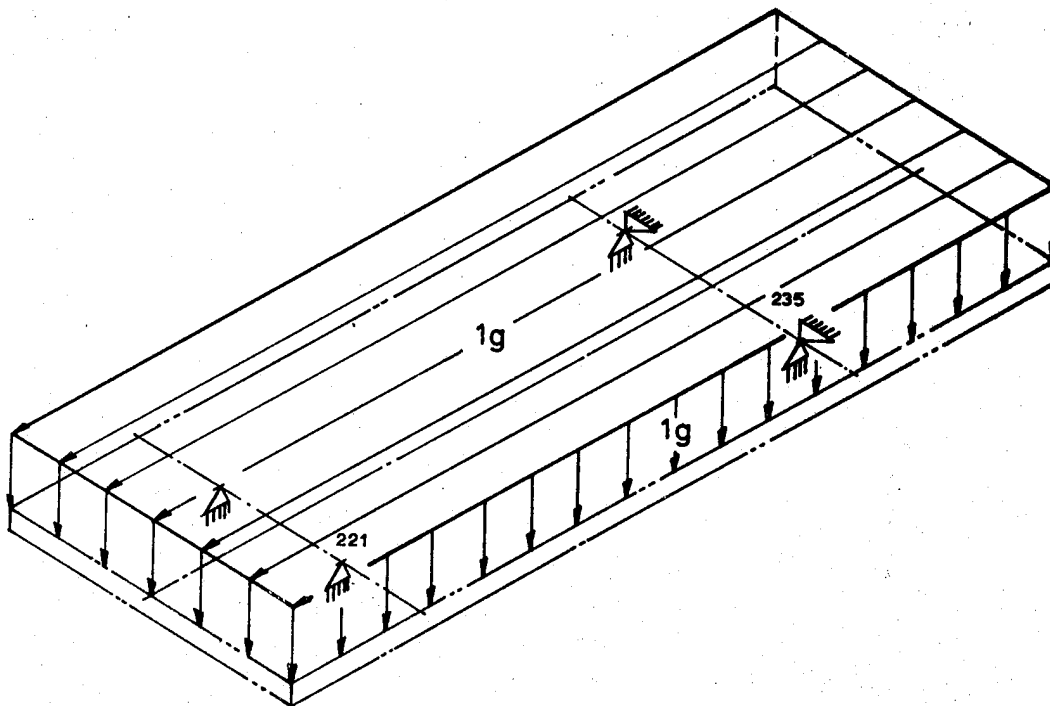**FIGURE 86   STATIC LOADING**

FIGURE 87   DOWNWARD INERTIA LOADING

227

FIGURE 88   TORSION LOADING

.92g's

235

3.5g's

221

FIGURE 89   BRAKING LOADS

FIGURE 90   CORNERING LOADS
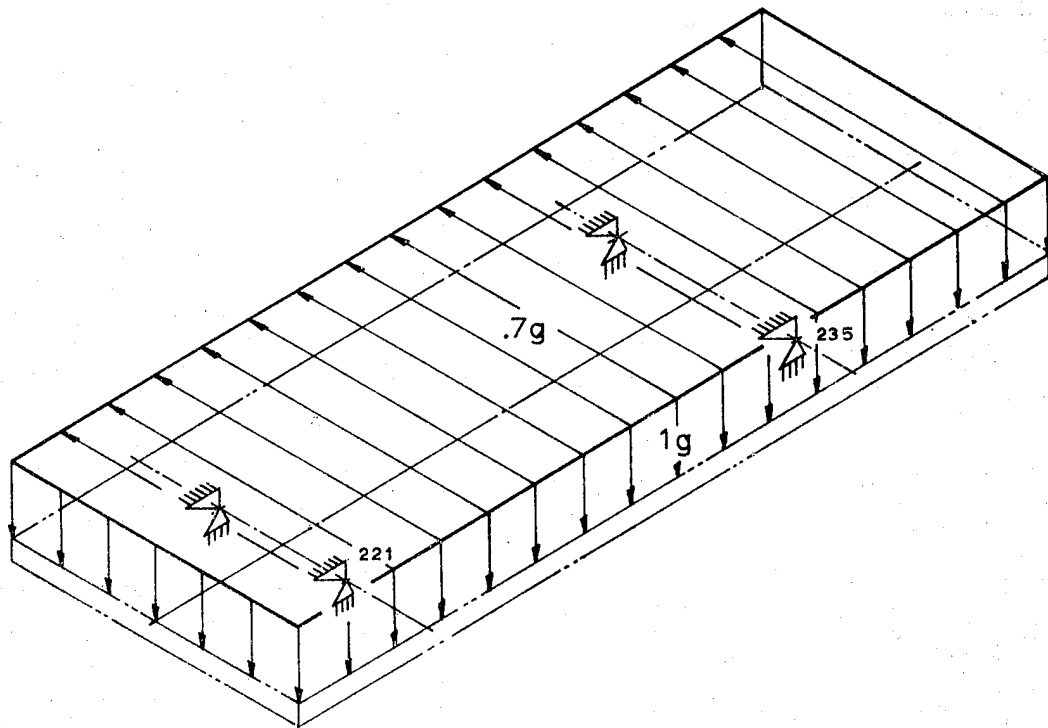
TABLE 64:   SELECTED SECTIONS AND PROPERTIES, IMPALA

LOCATION	I MIN.	I MAX.
Transmission Support	1.08	1.42
Radiator Support - 1	0.134	6.09
Radiator Support - 2	0.164	1.61
Radiator Support - 3	0.069	0.635
Radiator Support - 4	0.149	1.55
Radiator Support - 5	0.318	1.97
Radiator Support - 6	0.099	1.98
"A" Post - 1	0.113	0.177
"A" Post - 2	0.435	0.736
"A" Post - 3	0.054	0.213
Cowl	1.22	7.87
"A" Post - 4	0.13	0.379
Roof Front	0.126	2.23
"B" Post	0.884	4.052
Roof Side	0.624	1.65
Roof Center	0.004	0.369
Quarter Panel - 1	0.011	0.201
"C" Post - 1	0.535	8.014
Rear Shelf	0.011	0.132
Roof Rear	0.065	0.878
"C" Post - 2	0.043	0.203
Roof - Quarter Panel	0.019	0.042
Floor Pan - 1	0.107	0.613
Trunk Close Off	0.065	0.658
Trunk Cross Member	0.052	0.823
Side Sill	0.780	1.86
Firewall Floor	0.415	4.61
Floor Pan - 2	0.110	1.75

Results of the analysis are reported as stresses and deflections found in various locations within the Impala. The various cases and stresses and deflections for aluminum and steel are shown in Figures 91 through 105. The total car weight savings would be 676 pounds (18%) but this does not consider further weight reduction in the frame and suspension due to this weight decrease. Based on a two pounds per total vehicle for one pound of body the total weight reduction using aluminum would approach 1350 pounds, based on the finite element analysis.

An interesting result of the analysis is that the aluminum body is not as highly stressed as the steel body. For the same, or similar, amounts of deflection the stresses in a lower modulus material such as aluminum will be lower.

The finite element analysis as shown here for the Impala does not have sufficient detail to determine stresses at the joints. It is believed that most of the joints would have to be redesigned and analysed when using aluminum alloys. The lower resistance spot weld and arc weld strength of aluminum alloys compared to steel has been discussed previously.

6.4 Cost Comparisons

The cost of using alternate materials in a vehicle, compared to steel, is dependent upon a number of factors. For this comparison the factors shown in Figure 106 will be used, and specifically the variable costs; direct material, direct labor and variable burden.

It is believed that the automobile companys will continue to strive to produce the lowest cost vehicle possible. Luxury vehicle and multiple options will always be available. A cost analysis is generally completed prior to or in conjunction with the technical development of a material or component for an automobile.

In the discussions to follow several basic assumptions have been made. The first is that it is now technically feasible to manufacture vehicle components from all of the materials considered. Since there are distinct differences in material properties which may never be improved upon then the styling and appearance qualities of the vehicles will be lowered to accommodate the alternate materials in certain instances. The third assumption is that alternate materials will not be applied as substitutes but rather will be designed into new model years; therefore, duplicate tooling is not a production cost. The fourth assumption is that technical developments will be made to optimize and reduce the costs of manufacturing vehicles with the alternate materials. The current cost of producing automobiles from low carbon steel has the benefit of fifty years of production experience.

FIGURE 91   STEEL BODY, MAXIMUM STRESSES CASE 1

5600 psi ROOF

3000 psi ROOF

2700 psi QUARTER PANEL-ROOF

2600 psi FLOOR

2600 psi FRAME
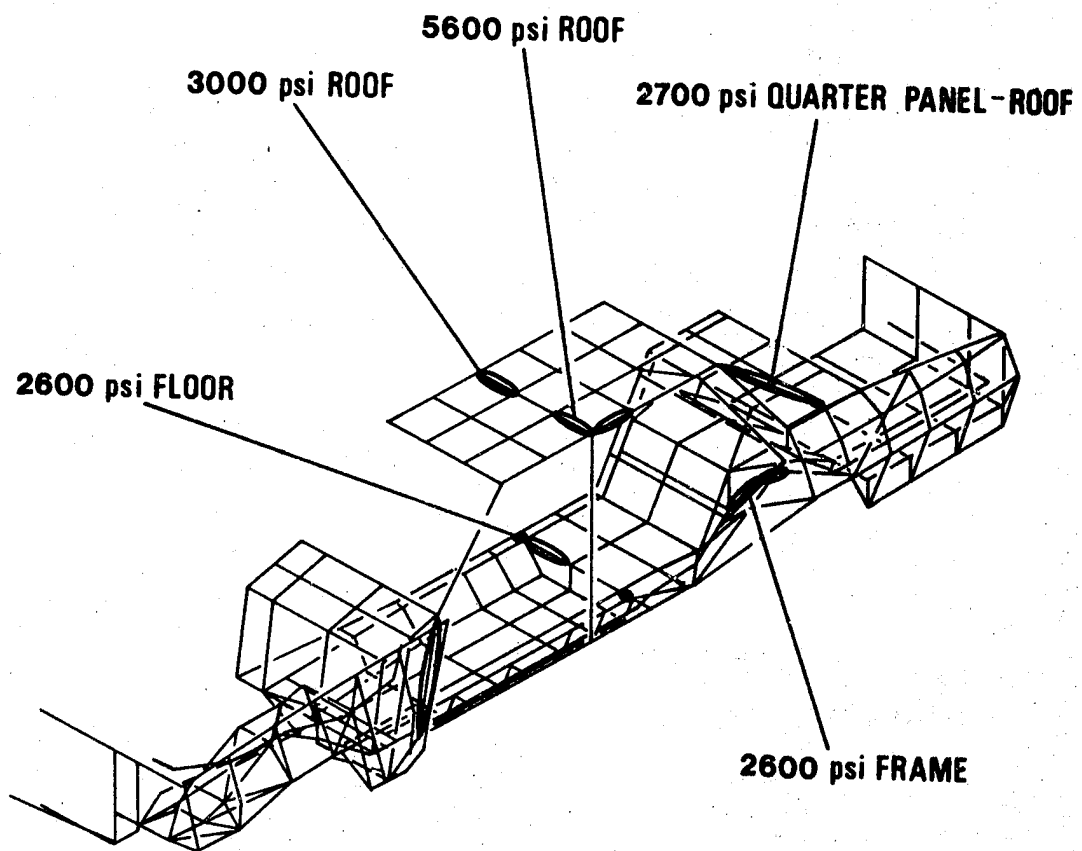
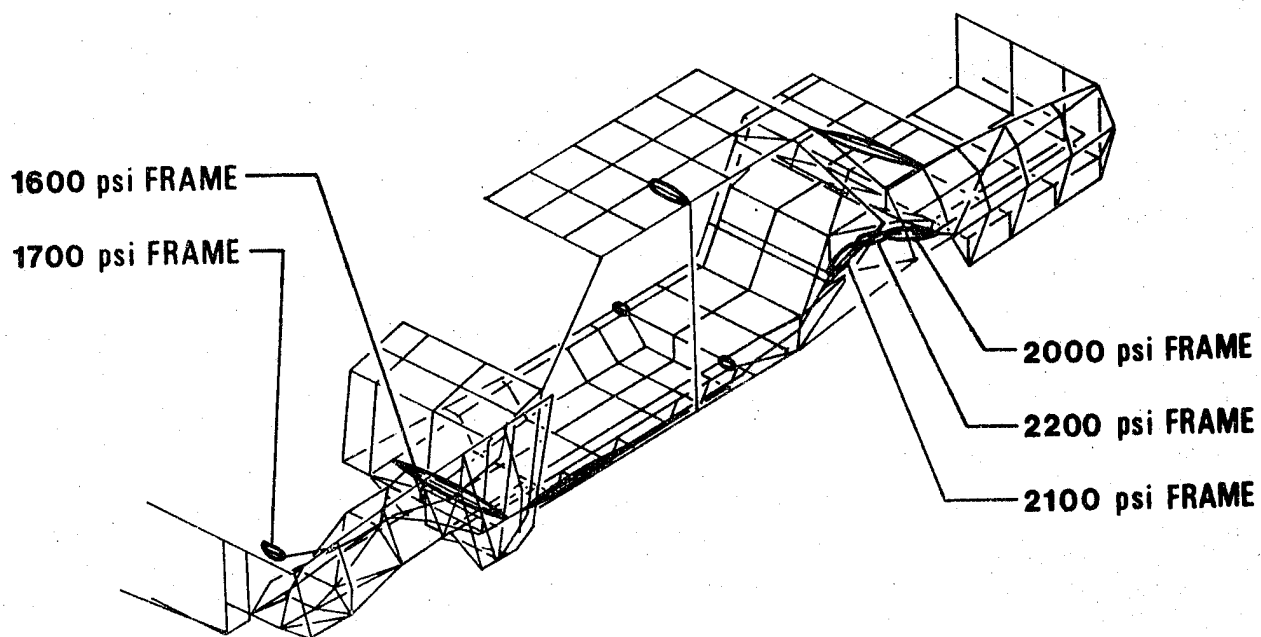CASE NO. 1 – 1 "g" STATIC

STEEL BODIED CAR – LOCATION OF 10 MOST HIGHLY STRESSED BEAMS

FIGURE 92   ALUMINUM BODY, MAXIMUM STRESSES CASE 1

1600 psi FRAME
1700 psi FRAME
2000 psi FRAME
2200 psi FRAME
2100 psi FRAME

CASE NO. 1 – 1 "g" STATIC

ALUMINUM BODIED CAR – LOCATION OF 10 MOST HIGHLY STRESSED BEAMS

FIGURE 93   CASE 1 DEFLECTIONS

STEEL DEFLECTION   .073   .059   .081   .063   .067

(ALUMINUM DEFLECTION)   (.052) (.043) (.054) (.047) (.045)
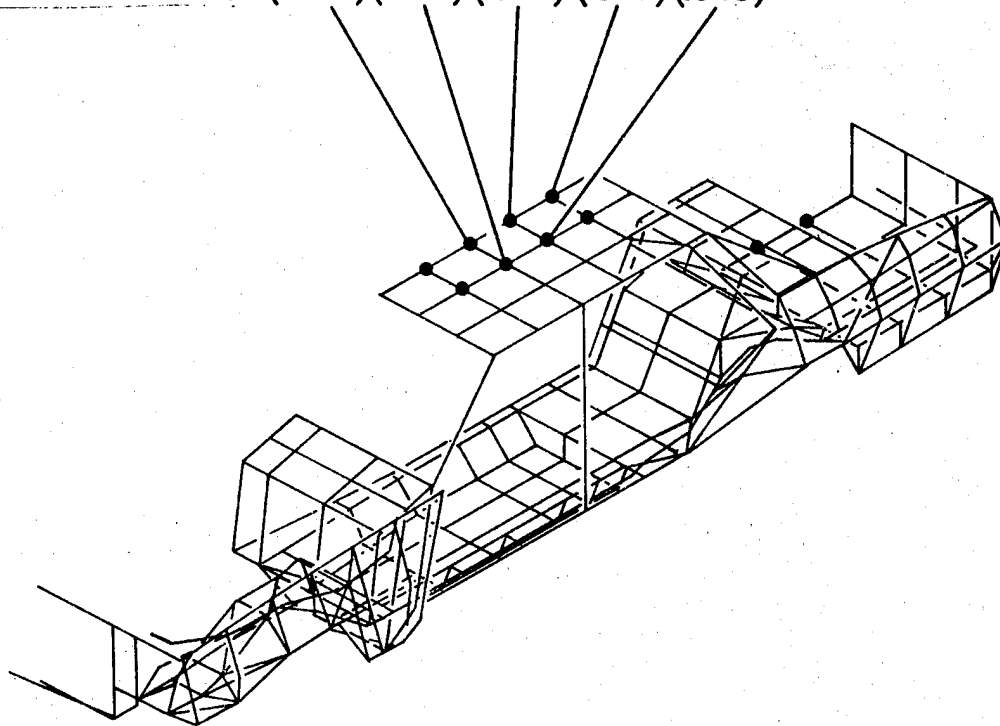
CASE NO. 1 – 1 "g" STATIC

LOCATION OF 10 MOST HIGHLY DEFLECTED NODES

FIGURE 94   STEEL BODY, MAXIMUM STRESSES CASE 2
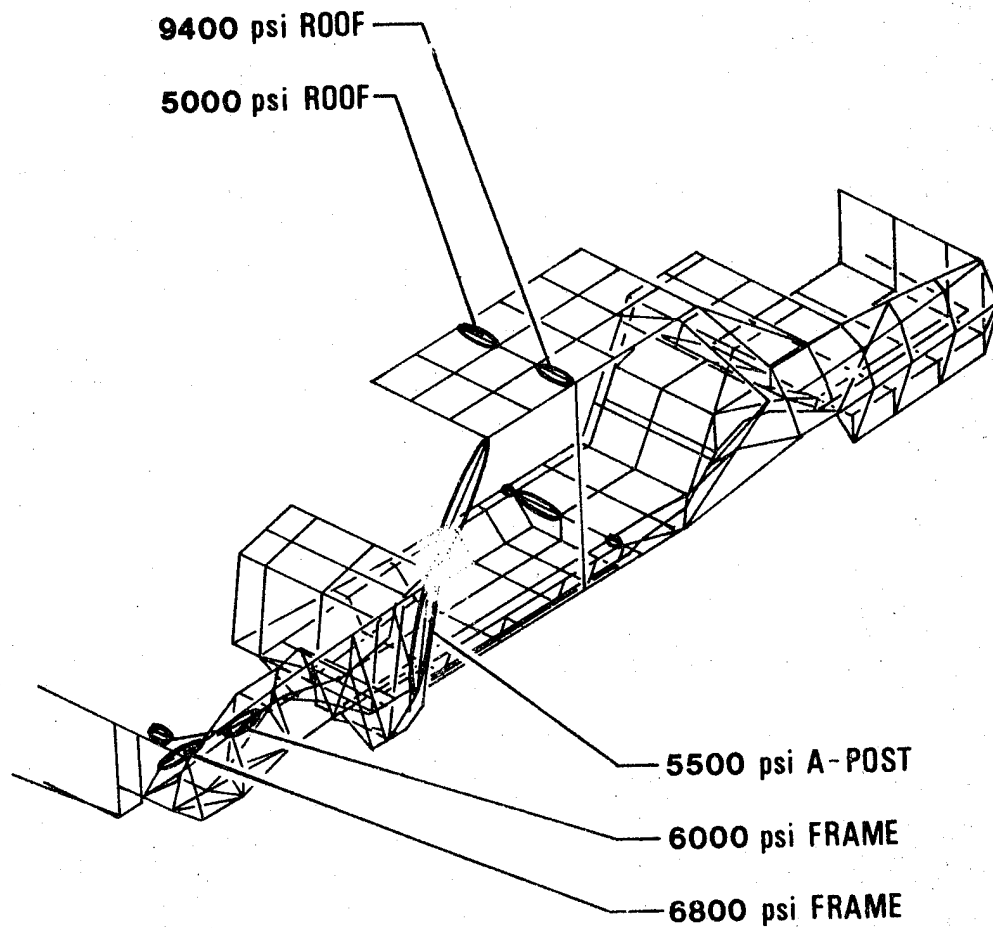
CASE NO. 2 – 3.5 "g" DOWNWARD INERTIA OVER FRONT WHEELS

STEEL BODIED CAR – LOCATION OF 10 MOST HIGHLY STRESSED BEAMS

FIGURE 95   ALUMINUM BODY, MAXIMUM STRESSES CASE 2

4500 psi FRAME

5700 psi FRAME

3600 psi FRAME

4800 psi FRAME

5300 psi FRAME
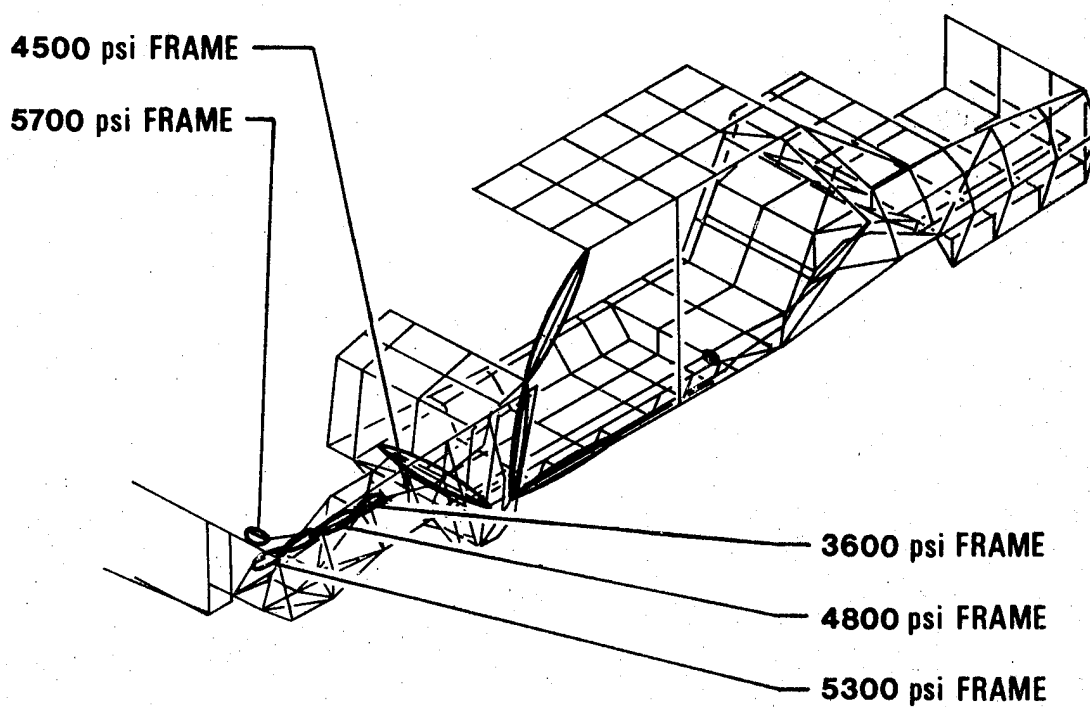
CASE NO. 2 – 3.5 "g" DOWNWARD INERTIA OVER FRONT WHEELS

ALUMINUM BODIED CAR – LOCATION OF 10 MOST HIGHLY STRESSED BEAMS

FIGURE 96   CASE 2 DEFLECTIONS

STEEL DEFLECTION   .128   .103   .134   .098   .110

(ALUMINUM DEFLECTION)   (.088)(.073)(.087)(.068)(.073)
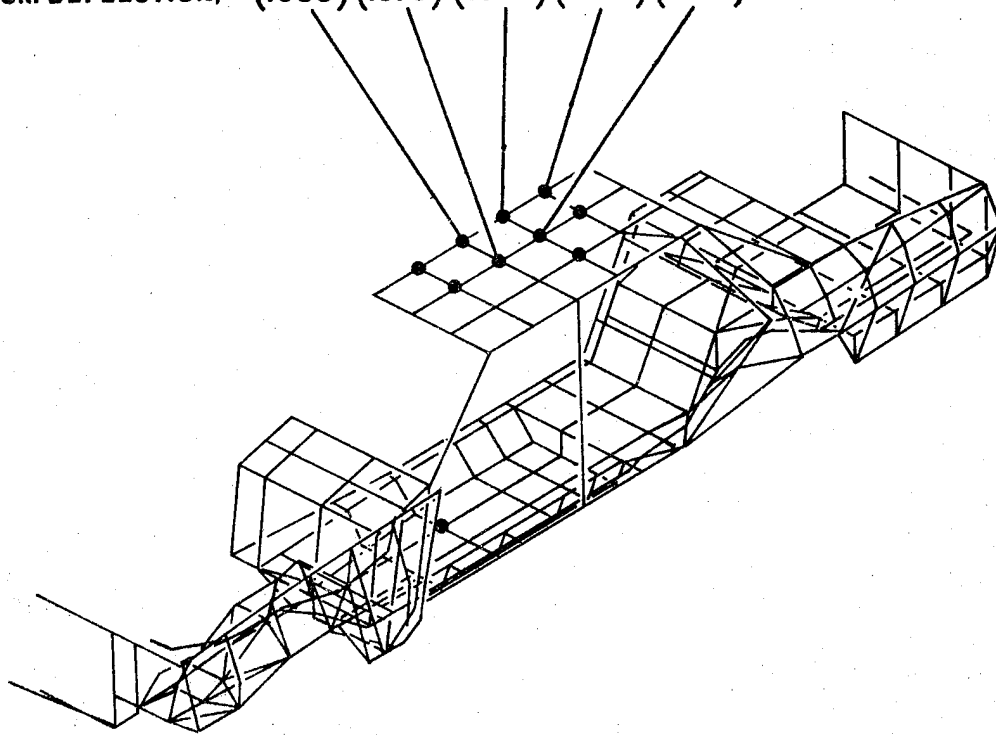
CASE NO. 2 – 3.5 "g" DOWNWARD INERTIA OVER FRONT WHEELS

LOCATION OF 10 MOST HIGHLY DEFLECTED NODES

FIGURE 97   STEEL BODY, MAXIMUM STRESSES CASE 3

14,000 psi ROOF

16,000 psi ROOF

37,000 psi ROOF
TO A-POST

37,000 ROOF TO QUARTER PANEL

22,000 psi C-POST
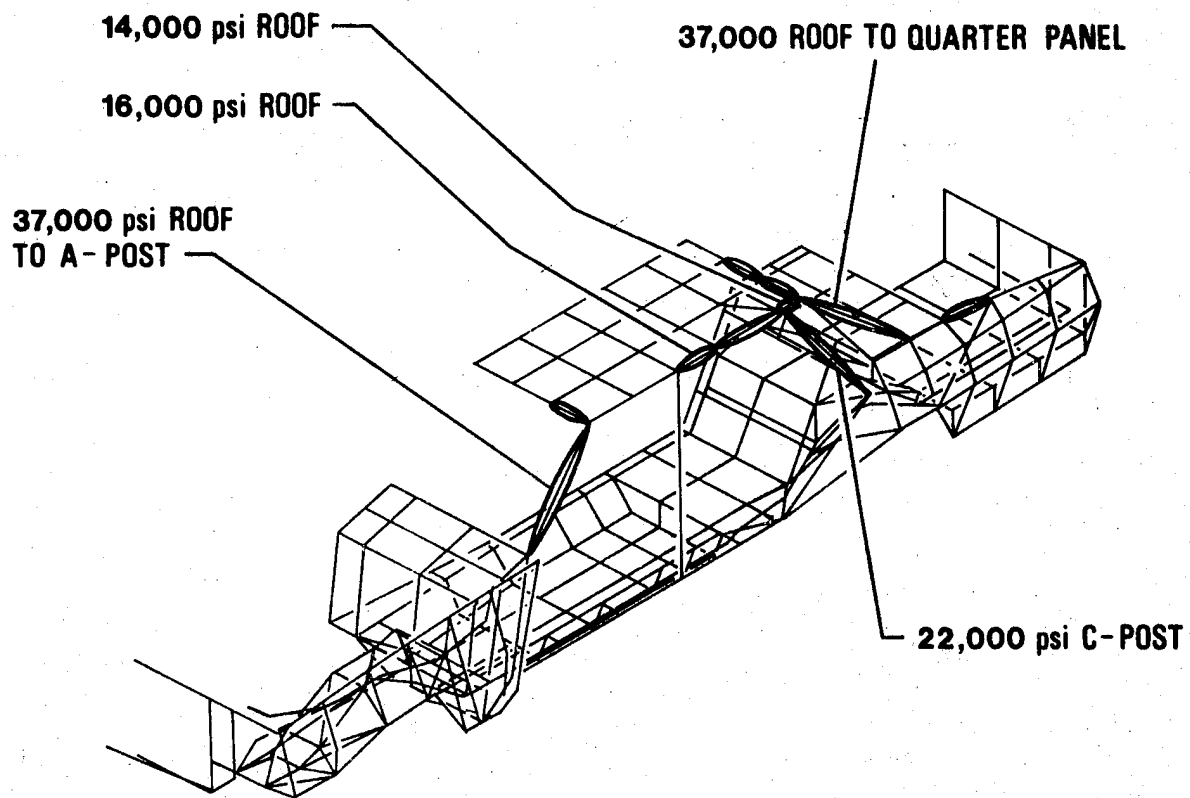
CASE NO. 3 -- TORSION, 3.5 x STATIC

STEEL BODIED CAR -- LOCATION OF 10 MOST HIGHLY STRESSED BEAMS

FIGURE 98   ALUMINUM BODY, MAXIMUM STRESSES CASE 3

9000 psi ROOF —

9000 psi ROOF —

20,000 ROOF TO QUARTER PANEL

23,000 psi ROOF
TO A-POST —

12,000 psi C-POST
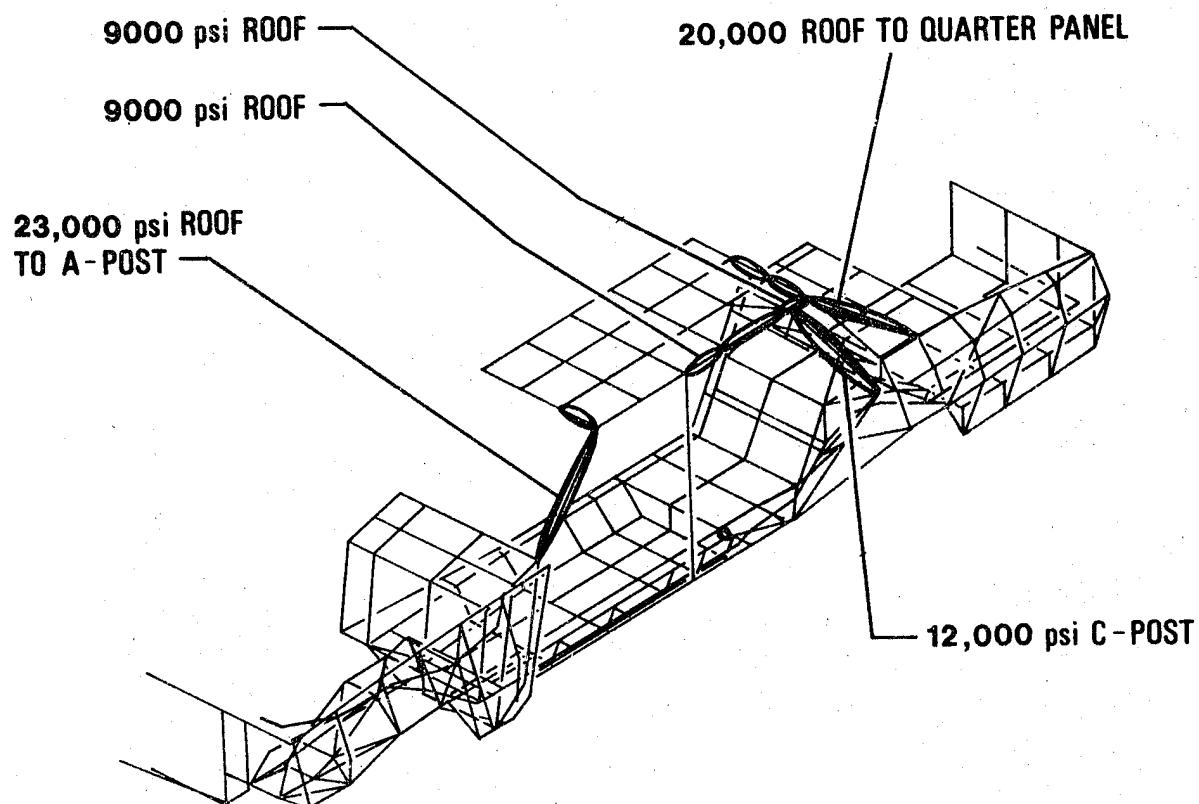
CASE NO. 3 — TORSION, 3.5 x STATIC

ALUMINUM BODIED CAR — LOCATION OF 10 MOST HIGHLY STRESSED BEAMS

FIGURE 99 CASE 3 DEFLECTIONS

STEEL DEFLECTION

(ALUMINUM DEFLECTION)

.243

(.383)

.253

(.397)

.268

(.414)

.240

(.373)

.252

(.389)
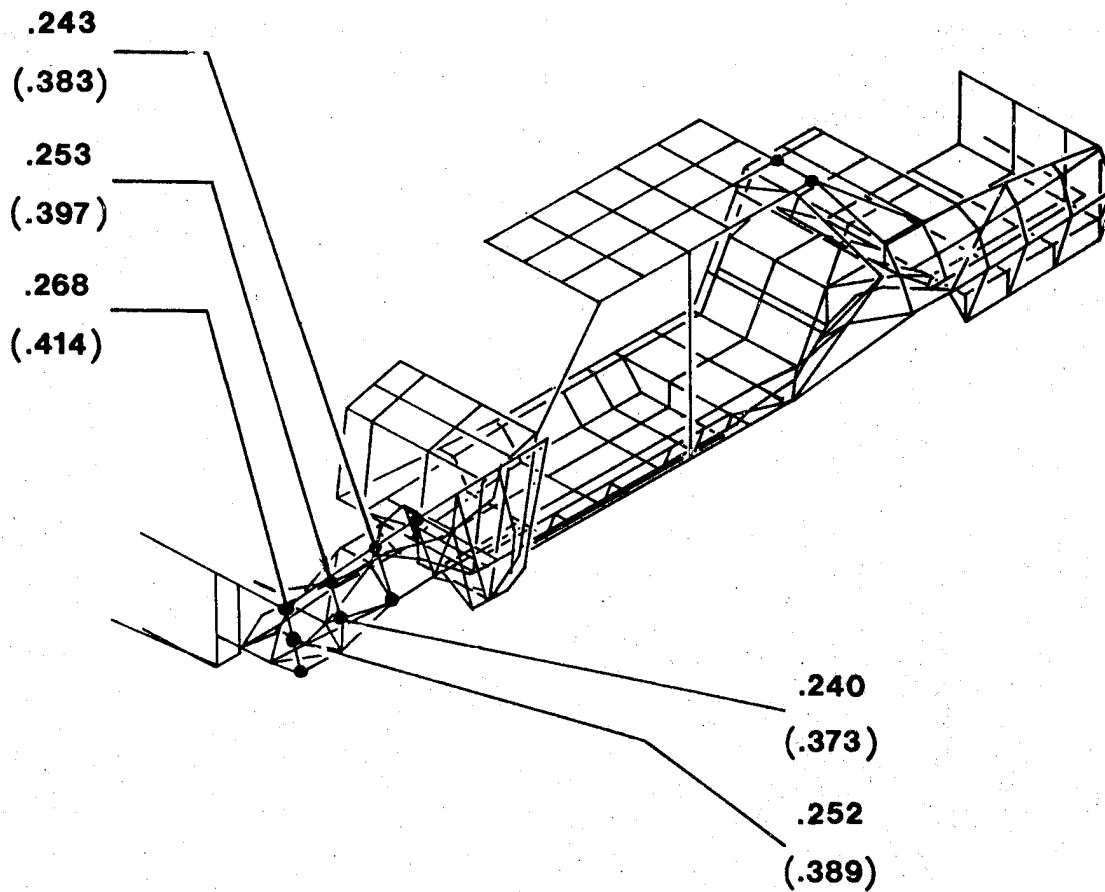
CASE NO. 3 — TORSION, 3.5 x STATIC

LOCATION OF 10 MOST HIGHLY DEFLECTED NODES

FIGURE 100   STEEL BODY, MAXIMUM STRESSES CASE 4

8500 psi CLOSE-OFF

3600 psi CLOSE-OFF

6300 psi CLOSE-OFF

5500 psi ROOF

3000 psi FRAME
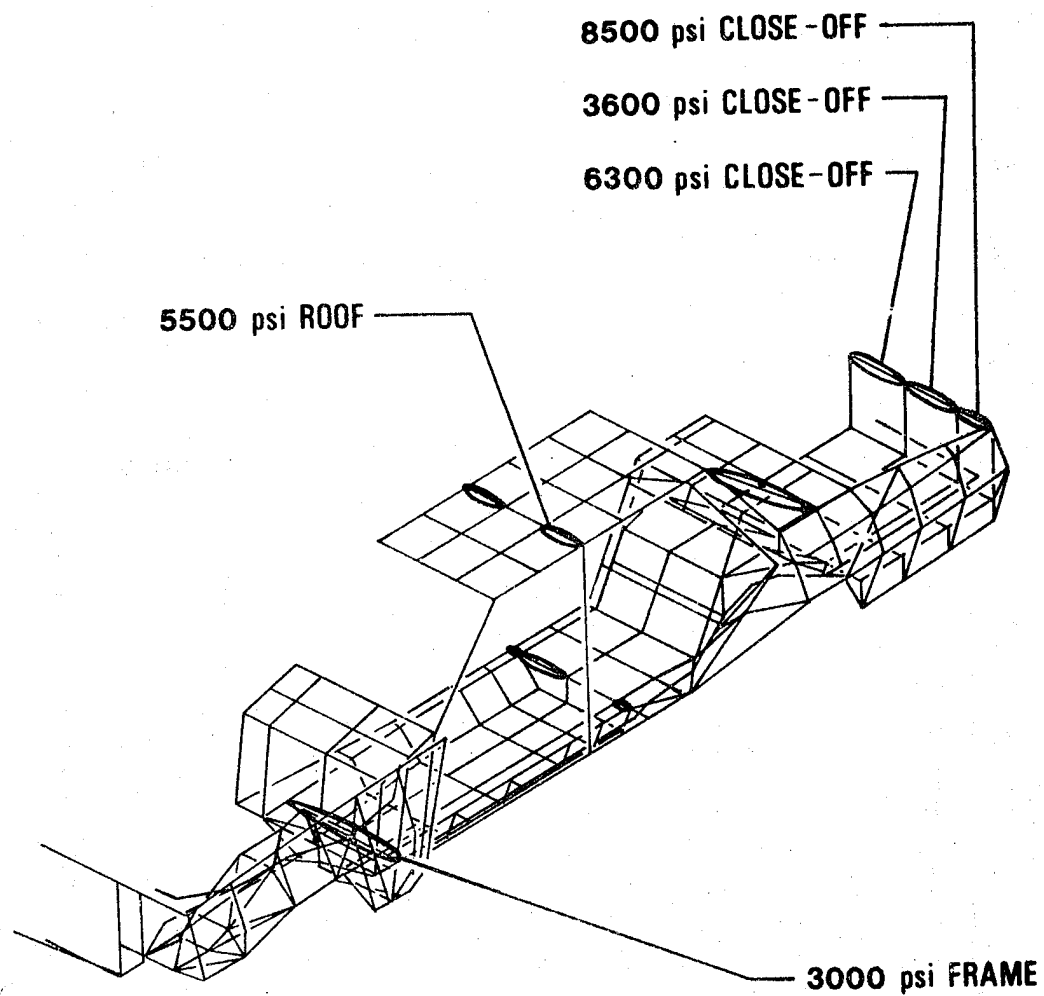
CASE NO. 4 – 1 "g" BRAKING

STEEL BODIED CAR – LOCATION OF 10 MOST HIGHLY STRESSED BEAMS

FIGURE 101   ALUMINUM BODY, MAXIMUM STRESSES CASE 4

2700 psi CLOSE-OFF

3000 psi FRAME

2400 psi FRAME

2500 psi FRAME

2200 psi FRAME
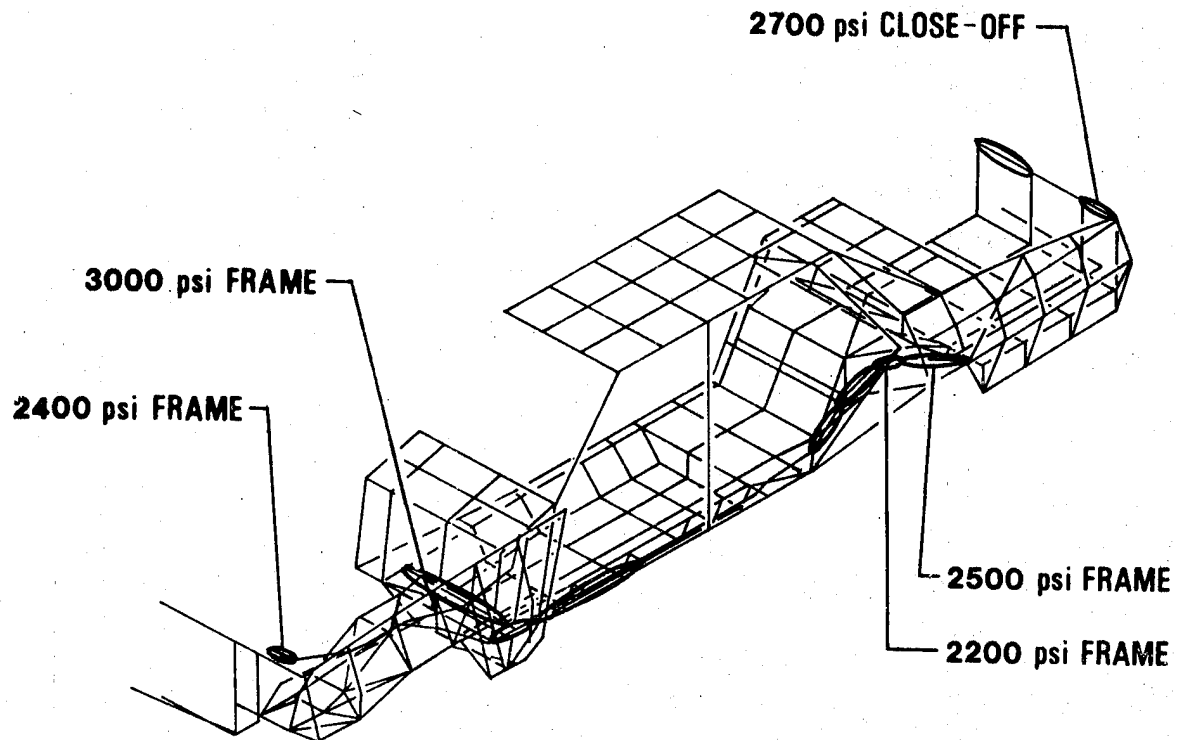
CASE NO. 4 — 1 "g" BRAKING

ALUMINUM BODIED CAR — LOCATION OF 10 MOST HIGHLY STRESSED BEAMS

FIGURE 102   CASE 4 DEFLECTIONS

STEEL DEFLECTION   .075   .082   .068   .078   .057

(ALUMINUM DEFLECTION)   (.053) (.056) (.046)   (.068) (.051)
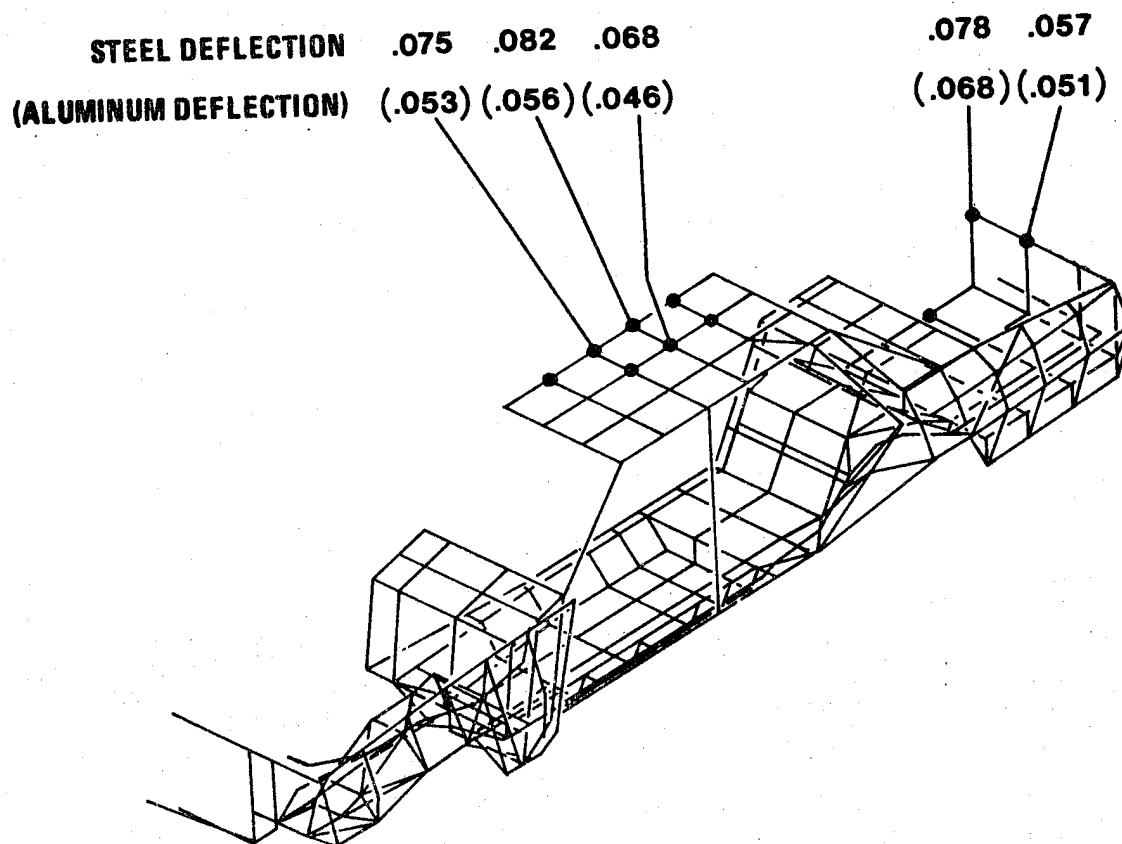
CASE NO. 4 – 1 "g" BRAKING

LOCATION OF 10 MOST HIGHLY DEFLECTED NODES

FIGURE 103   STEEL BODY, MAXIMUM STRESSES CASE 5

5100 psi ROOF

9600 psi ROOF

8400 psi ROOF

8300 psi C-POST

4300 psi ROOF TO A-POST
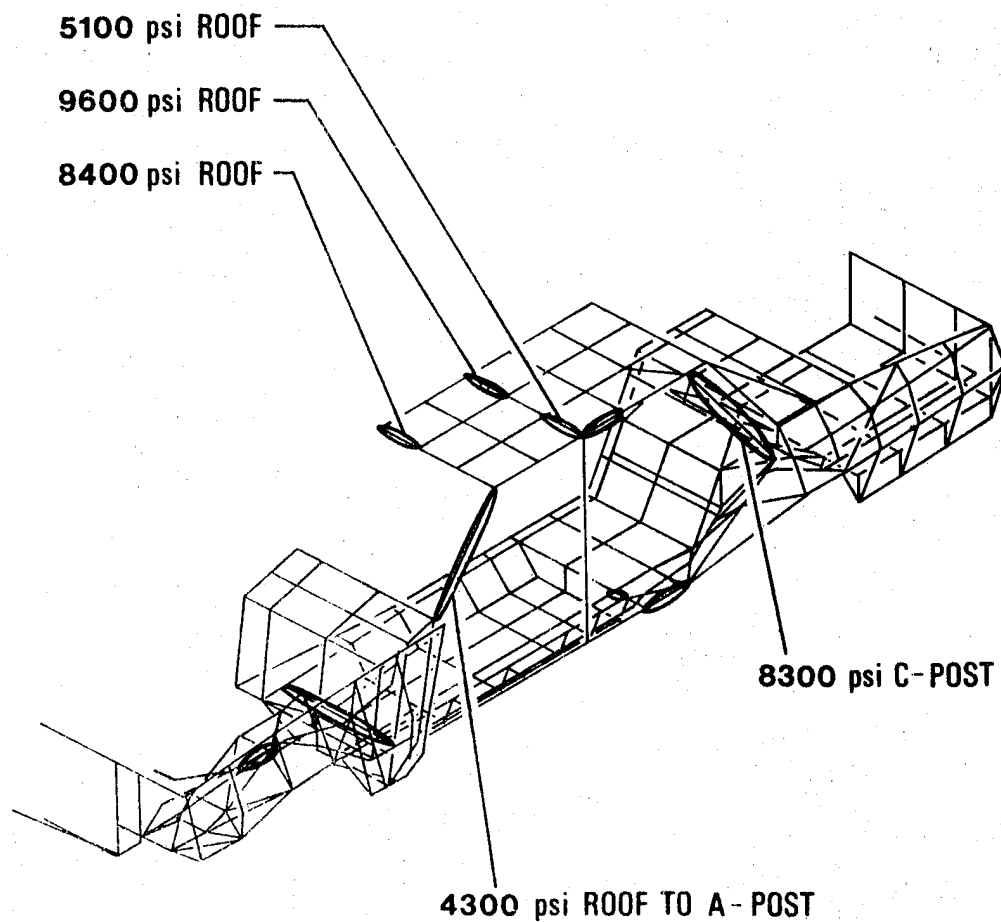
CASE NO. 5 — .7 "g" CORNERING

STEEL BODIED CAR — LOCATION OF 10 MOST HIGHLY STRESSED BEAMS

FIGURE 104   ALUMINUM BODY, MAXIMUM STRESSES CASE 5

7100 psi ROOF

6200 psi ROOF

3600 psi FRAME

5600 psi C-POST

4900 psi ROOF TO A-POST
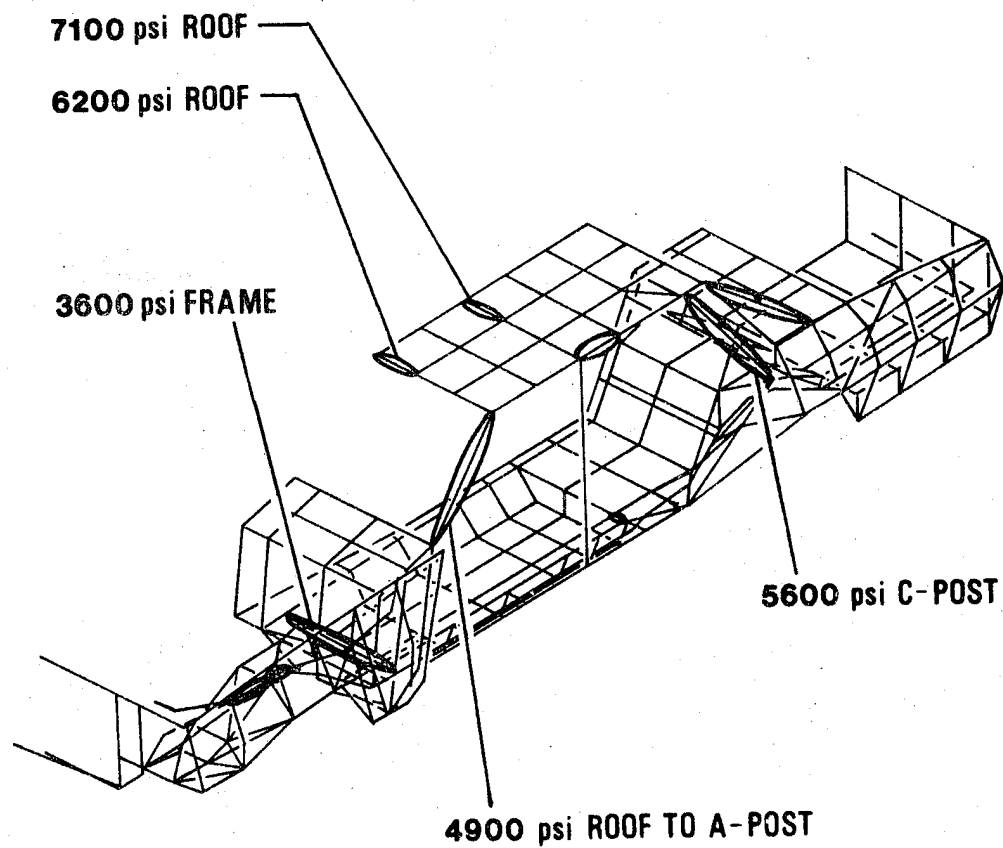
CASE NO. 5 – .7 "g" CORNERING

ALUMINUM BODIED CAR – LOCATION OF 10 MOST HIGHLY STRESSED BEAMS

FIGURE 105   CASE 5 DEFLECTIONS

STEEL DEFLECTION   .201 .223 .241 .259 .200

(ALUMINUM DEFLECTION) (.314) (.338)(.362)(.388)(.323)
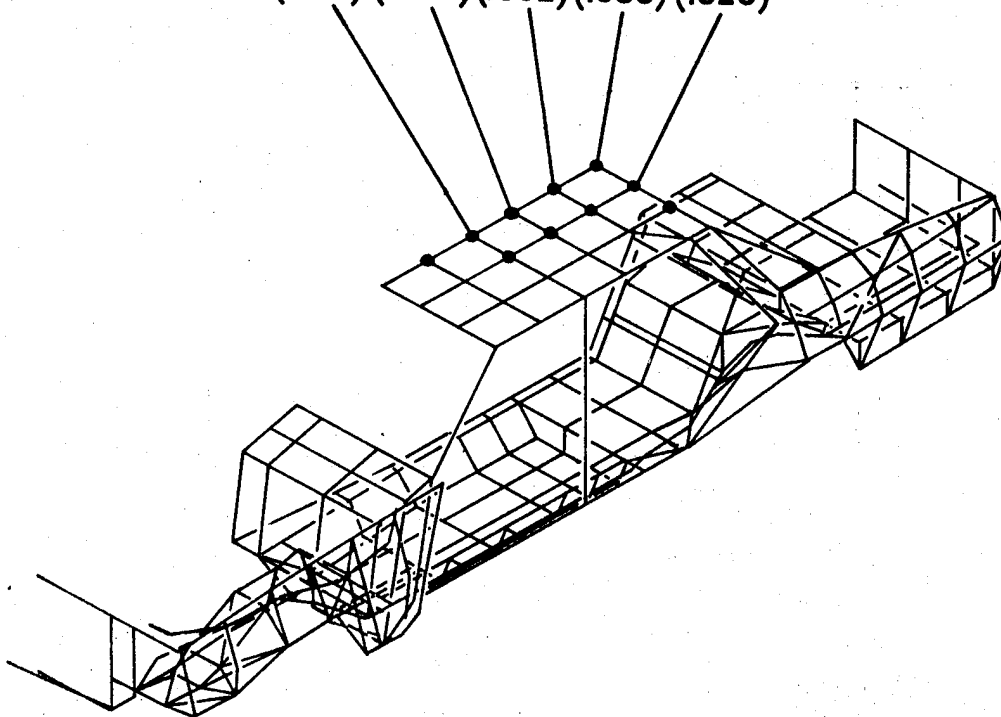
CASE NO. 5 — .7 "g" CORNERING

LOCATION OF 10 MOST HIGHLY DEFLECTED NODES

FIGURE 106   ELEMENTS OF VEHICLE COST

DIRECT MATERIAL

DIRECT LABOR ──────────────── VARIABLE COSTS

VARIABLE BURDEN

FIXED COSTS ──────────────── MANUFACTURING COSTS

TOOLING COSTS ────────────────

OTHER COSTS
AND PROFIT ────────────────

WHOLESALE
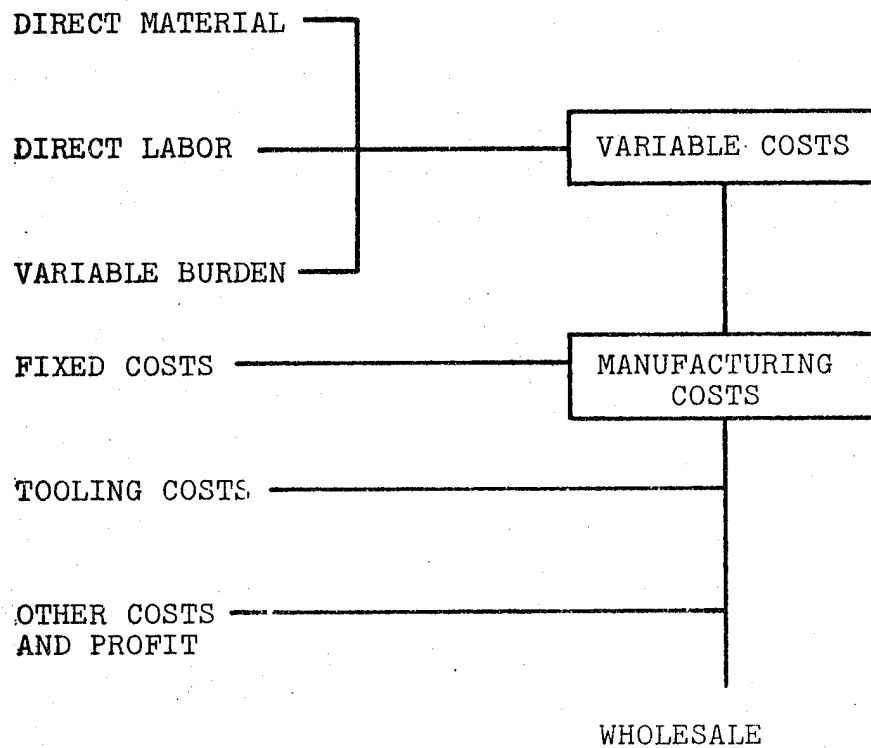
6.4.1 Direct Material Costs

A price list of materials to be used is shown in Table 65. These are average prices and do not reflect the differences in grade which may be selected. For example, rimmed or killed low carbon steel could be selected depending upon the requirements of formability. Killed is generally more expensive and is used only if required. In the case of graphite reinforced epoxy, two values are listed reflecting the optimism of the material suppliers projecting lower costs if large quantities of material a used.

HSLA steels and aluminum alloys would almost certainly be used in the same manner, stamped sheet metal, as low carbon steel. The weight of low carbon steel sheet in the 1977 Impala body structure is 805.5 pounds. The actual weight of sheet steel required from the mill is 35 percent greater or 1087 pounds due to trimmings and blank holder offal.

For each vehicle 281.5 pounds of good clean scrap (No. 1 Bundles) is produced. This material is collected from each press line by conveyors, bundled and shipped to a scrap dealer or a steel mill. The price of such prime scrap is $0.0375 per pound. Experience has shown that the cost of the collection and shipping is generally equal to the scrap price and no actual benefit is derived.

The direct material cost, low carbon steel, for the 805.5 pounds of finished metal stampings for the Impala is therefore estimated to be 1087 x $0.17 = $184.79.

Similar estimates can be made for HSLA steel and aluminum alloys. For HSLA the estimated finished part weight is 90% x 805.5 and for aluminum alloy 35% x 805.5. These direct material costs for the three sheet metals are shown in Table 66.

Similar cost breakdowns can be made for an individual component such as a hood although in each of these isolated cases the ratio of mill requirements to finished stamping weight will vary.

The direct material costs of reinforced plastics are estimated with different scrap or offal considerations. As an example, the offal or loss of material in molding glass polyester moldings is less than five percent. This loss is primarily due to that lost on each edge of the SMC sheet. Offal from oriented, continuous fiber prepregs or molding compounds will vary considerably. In a part like a door beam the molding compound could be cut from the larger sheet to fit well and with little flow to fill the mold. Such a part would have essentially no offal. A fender, on the other hand would have offal at the ratio of the wheel opening area to the full area. Overall, an estimated 15% loss in the oriented fiber material is expected although the experience factor is non existant.

TABLE 65: MATERIALS PRICE LIST, AVERAGE 1978

MATERIAL	COST, $/LB.	COST, $/CU.INCH.
Low Carbon Steel	0.17	0.048
HSLA Steels	0.21	0.059
Aluminum Alloys	0.90	0.090
Magnesium Alloys	2.00	0.134
Polypropylene, 30% talc pellets	0.35	0.0127
Polypropylene, 40% glass laminate	0.90	0.036
Polyester, 30% glass	0.50	0.035
Polyester, 65% glass	0.70	0.049
Epoxy, Graphite 65%	55.00	3.025
Epoxy, Graphite 65%	8.00*	0.44
Polyurethane, RIM	1.50	0.056

*Some projections of graphite prepreg prices have been set at $8.00 per pound if larger quantities are used.

TABLE 66: ESTIMATED SHEET METAL DIRECT MATERIAL COST

	LOW CARBON STEEL	HSLA STEEL	ALUMINUM
Finished Sheet Metal, Weight	805.5	725	282
Mill Requirements Weight	1087	979	381
Material Cost/$/Vehicle	184.79	205.59	342.90
Scrap Weight	281.5	254	99
Scrap Cost $/pound	0.0375	0.0375	0.06
Scrap Price $/pound	0.0375	0.0375	0.18
Scrap Benefit $/Vehicle	0	0	11.88
Direct Material Cost/$/Vehicle	184.79	205.59	331.02
% Increase	0	11	79

1978 Prices: TABLE 65

Cost of collecting aluminum alloy estimated to be 150%
that of carbon steel due to segregating requirements.

A comparison of direct material costs for reinforced plastic with low carbon steel is shown in Table 67. In this comparison the glass polyester estimated weight is 60% of the steel and the estimated graphite epoxy weight is 35% of the steel.

Again, as with aluminum, similar comparisons of direct material costs can be made on isolated items such as hoods and in each case the offal quantity would have to be adjusted.

Since the polyurethane materials appear so promising in damage resistant applications a comparison of material costs compared to steel is made on the basis of using it for a front fender. The Impala steel fender weighs 12 pounds and a polyurethane fender is estimated to be 3.5 pounds. The steel material cost is $2.86 and the polyurethane cost is $5.25.

There is no scrap benefit from the polyurethane and the offal quantity is expected to be essentially zero.

6.4.2 Direct Labor Costs

The direct labor costs in building the sheet metal body structure of an automobile consists primarily of press forming, assembly, finishing, inspection and handling.

To assist in obtaining an estimate of the total direct labor costs in producing the sheet metal components the results of Contract DOT-HS-5-01153 were used. In this study, "Development of a Motor Vehicle Materials Historical, High-Volume Industrial Processing Rates Cost Data Bank" by Pioneer Engineering and Manufacturing Company, weights and costs were tabulated. The sheet metal component weight of 741.6 pounds was completed for $371.55 or $0.50 per pound. Using this data the direct material cost was estimated to be $170.20. The difference, $201.55, was divided into direct labor of $79.50 and variable burden of $122.05. The labor rate plus fringes was estimated at $26.50 per hour. The three hours of labor sounds reasonable when the number of stamped parts, press rate, number of welds and finishing time are taken into consideration.

For the 1977 Impala estimate the labor has been inflated to $30.00 per hour and the burden rate to $137.14. The number of labor hours has been increased from 3 to 3-1/2 hours. Based on this estimate the 1977 Impala steel sheet metal fabrication costs are as follows:

Direct Material	$184.79
Direct Labor	105.00
Variable Burden	137.14
Manufacturing Costs	$426.93

While the accuracy of this estimate can be questioned it does put in perspective the magnitude of material, labor and burden costs.

TABLE 67: ESTIMATED REINFORCED PLASTIC DIRECT
           MATERIALS COST

	LOW CARBON STEEL	65% GLASS POLYESTER	65% GRAPHITE EPOXY
Finished Structure Weight	805.5	483.	282
Mill Requirements Weight	1087	508	324
Material Cost $/Vehicle	184.79	355.60	17,820.00 (1) 2,592.00 (2)
Scrap Weight	281.5	25	42
Scrap Price $/Pound	0.0375	0	0
Scrap Benefit $/Vehicle	0	0	0
Direct Material Cost, $/Vehicle	184.79	355.60	17,820.00 (1) 2,592.00 (2)
% Increase	0	92	9,643 (1) 1,403 (2)

1978 Prices: TABLE 65

(1) Price Used: $55.00/pound 1978

(2) Price Used: $ 8.00/pound 1990

253

When comparing HSLA steels with low carbon steel the direct labor costs are expected to be the same.

Aluminum alloys are expected to require more labor hours. The various problem areas which will contribute to an increased cost are listed below:

1. Cleaning of dies required periodically to remove aluminum particle build up.

2. Increased use of lubricants required to obtain better formability.

3. Higher rates of scrap due to poor formability are expected.

4. Degreasing and deoxidizing will be necessary prior to resistance spot welding or adhesive bonding.

5. An increase in the number of welds or amount of adhesive bonding to obtain adequate joint strength is anticipated.

6. More down time will be encountered in resistance spot welding due to shorter electrode life.

7. Higher costs of finishing and straightening before painting is anticipated.

While there is not a great deal of experience in using aluminum alloys in automobile fabrication to assist in the estimation, a doubling of the direct labor costs would not be surprising. The estimated direct labor cost would be $210.00 to fabricate an all aluminum alloy body structure.

Reinforced composites such as a glass polyester system require a cure time of sixty seconds for each 0.125 inch of thickness. The time to open and close the press, place the charge and remove the molded part requires at least 15 seconds. For parts such as a grill opening panel, door panel or fender; one mechanic could prepare the charge and place it in the mold and a second mechanic could clean off the flash and clean out holes in the molded part. At this rate the manpower requirements are 2-1/2 man minutes per part.

To obtain an equivalent press time for plastic molding as for steel stamping the number of parts cannot exceed 70 ÷ 2-1/2 or 28 parts.

Some automation might be considered in the above analysis. Some of the molded parts can be automatically removed from the mold and press such that one mechanic could clear two presses.

254

This could also require that the part could be trimmed in a press operation. That is, all flash removal and hole clean up can be done by a trim punch moving in one direction. It is also considered feasible that the charging of some parts can be automated such that one mechanic could feed two presses. However, the weight of many parts will be in the twenty pound or greater range and will be difficult to handle due to the width and length. These parts may require two press feeders and two mechanics for clean up. For this reason the number of parts, 28, of reinforced plastic to maintain the same press labor cost cannot be changed to any degree.

As the part design becomes more sophisticated, requiring oriented, continuous fibers; then the loading rate may decrease due to the greater care in charging the mold. This consideration increases in importance when using the higher cost fiber rein- forcements. A loss in efficiency in these materials results in a higher initial material cost.

After molding and trimming, the reinforced plastic parts would be assembled. This assembly would be primarily adhesive bonding with mechanical fastener assists. An assembly procedure would have to be developed depending upon the rate of automobiles to be made. Considering the 1977 Impala, approximately 500,000 are made per year or actually in 10 to 11 months. Using 500 production shifts per year, 1000 vehicles have to be made per shift (8 hours). At an 87% efficiency (7 hours) 143 vehicles have to be assembled per hour. One set of 28 molding presses at a 1-1/4 minute molding rate would produce 48 car sets of moldings per hour. Three press lines would be required.

Since most known adhesives require several minutes to build up a reasonable strength, the number of clamping fixtures required becomes impressive. If the cure time for handling is 30 minutes then at least 72 sets of clamping fixtures are needed to meet the production rate. Sub-assemblies such as the floor, roof and sides would be completed first of course, and these would then be combined at the final assembly point.

The surface of the molded part will generally have a zinc stearate rich surface. Zinc stearate is a mold release agent which must be removed by abrading and solvent wiping, or primed, to permit satisfactory adhesive bonding.

The total assembly time is estimated to be 112 minutes. This allows 60 seconds per part for each of the four operations: prim- ing, applying adhesive, fixturing, and removing of the fixture. There should be some allowance for finishing which is estimated to be 30 minutes per bonded vehicle. This finishing time is low compared to current practices, but new developments within the industry hold greater promise. The 30 minutes is based on satis- factory development of these processes.

The estimates of the direct labor costs are for the three basic materials as follows:

Low Carbon Steel	$105.00
Aluminum Alloy	210.00
Glass Reinforced Plastic	108.00

It must be remembered that these costs have been estimated on the assumption that manufacturing developments will be satisfactorily completed and without full production experience on the aluminum alloy and glass reinforced composites.

6.4.3 Variable Burden

Variable burden costs are those directly chargeable to the production process and are not covered by direct material or labor. Such charges may contain labor to replace resistance spot welding electrodes, the electrode costs, power requirements and other perishable tools and supplies such as sanding wheels. Direct supervision and clerical labor are also included in variable burden if these activities can be attributed to the production item or process.

Variable burden is determined largely by experience since the shop production conditions are difficult to simulate or predict. This group of costs would be expected to increase with the fabrication of aluminum alloys. Forming lubricants, cleaning solutions, deoxidizing chemicals, sanding discs and resistance spot welding electrodes will be used in greater quantities. Where the variable burden for the steel Impala body was estimated to be $137.14 previously, this cost for aluminum is estimated to be at least 50% greater or $205.71.

Composite materials would be expected to generally require lower variable burden costs since there are fewer operations, out of necessity to reduce direct labor costs. Adhesives would be a part of the direct material cost. Glass and the other fibers are generally quite abrasive requiring a large supply of hand knives or replacement shear blades for cutting the uncured material. The estimated burden costs for steel are considered to be 50% greater than those for composites. The estimated variable burden cost for the composites is calculated to be $91.42 per vehicle.

6.4.4 Capitalization

The equipment available in the automotive plants is directed toward stamping, welding and painting of low carbon steel. Mechanical presses can be used for aluminum alloys as well. The tooling dies have to be altered, but this is dependent upon, and can be changed during styling and design.

Resistance spot welding equipment used for low carbon steels is incapable of welding aluminum alloys. Higher current require-

ments necessitate new equipment purchase and installation. A
single portable welding unit costs $40,000 to $50,000 each. As
an example an Impala hood probably requires 4 to 5 welding guns
to meet the production rate. At a production of 500,000 per year
and based on 500 shifts, 1000 hoods must be assembled per shift.
Based on a 7 hour (420 minute) effciency day one hood must be
assembled every 2.4 minutes. This then requires a capitalization
of $250,000 for the welding guns.

Each of the aluminum parts must be cleaned to remove the
forming lubricants and subsequently deoxidized to remove the
oxide film present on the surface. Failure to remove this oxide
skin results in non uniform size and strength weld nuggets. A
cleaning line for an aluminum hood at the Impala production rate
requires an estimated $105,000 capitalization. The cost of
pickling solutions and solvents are included in the variable bur-
den.

Painting systems used for low carbon steel can be used in
painting aluminum. No additional capital is required in changing
from steel to aluminum alloy.

Depending upon how the existing press lines are arranged,
additional scrap and offal collection facilities may be required.
An inner hood panel of one alloy will of course develop offal of
a different composition from that second alloy used for the outer
hood panel. These can be mixed resulting in a large loss in value
of the scrap, or they can be collected separately and kept segre-
gated. Segregation will require two collection systems. The
permanence of the collection system and cost must be compared
to the scrap value retained or lost.

Composite molding will require new press acquisition.
Mechanical presses can be used for some hidden parts, but for
outer panels hydraulic presses are required to obtain an acceptable
surface finish. Hydraulic presses for compression molding are
single action and cost approximately $100 per ton of rated capacity.
For a composite Impala, based on 28 parts and 3 press lines, 84 new
presses would be required.

Press capacity depends upon the molding pressure which again
depends upon the material being molded. In general the pressure
is 1000 to 2000 psi and a hood panel could require between 1200
to 2500 ton. It is reasoned that each line should have one 5000
ton press, twelve 2500 ton presses and fifteen 1000 ton presses.
Capitalization costs for molding presses would be $15 million.
Other trimming presses would be required at an estimated 1/3 the
cost or $5 million. A certain number of standby presses might
also be required, to be used if a line press broke down.

As can be seen by the above described examples capitalization
and related interest charges will play an important part in the
selection of a material for automotive structure. These costs
are in addition to the normal costs used for low carbon steel.

6.5 Energy Summary

Using the production energy values from Table 40 and the estimated body structure weights from Tables 66 and 67, the energy requirements for each material can be calculated, Table 68. Using a value of 1.26 gallons of gasoline saved over 100,000 miles driven for each pound of vehicle weight then a lifetime savings can be calculated. The maximum volume of gasoline saved based on 1977 performance would be approximately 10%.

6.6 Summary - Concepts Framed Vehicle

The body on frame concept utilizes a strong, stiff, heavy frame which can be used as the primary load carrying componenet in normal service and during collisions. For such a concept it is doubtful that alternate materials will replace the hot rolled low carbon steel presently used. This conclusion is based on the low weight reduction possibilities, loss of collisions control and cost. For the large six passenger size vehicle an alternative approach would be to eliminate the frame entirely to reduce weight and materials cost.

Since the frame does provide an excellent support for the passenger compartment and the front structure, complete or partial replacement of the low carbon steel could be accomplished with any of the alternate materials. Further development studies are required to optimize designs and manufacturing procedures. Joining of components, overall design and analysis experience and manufacturing confidence are required.

Large weight reductions in the body structure can be achieved but only at a high finished vehicle cost increase. Energy consumption based on a lifetime of 100,000 miles would be reduced due to the savings in fuel consumption. However, the actual fuel use reductions are not that convincing.

TABLE 68: LIFETIME ENERGY SAVINGS FOR CANDIDATE
          STRUCTURAL MATERIALS

	STEEL	HSLA STEEL	ALUMINUM	GLASS - POLYESTER	GRAPHITE-EPOXY
Body Weight, lbs. (Estimated)	805.5	725	282	483	282
Mill Weights, lbs. (Estimated)	1087	979	381	508	324
Production Energy (BTU/Vehicle)	26×10^6	23.5×10^6	28.2×10^6	15×10^6	18.3×10^6
Weight Savings	0	80.5	523.5	322.5	523.5
Fuel Savings BTU/100,000 miles	0	15.2×10^6	98.9×10^6	61×10^6	98.9×10^6
Lifetime Savings BTU/Vehicle	0	17.7×10^6	96.7×10^6	72×10^6	106.6×10^6

1 gallon gasoline = 150,000 BTU

Glass-Polyester - 65 weight percent glass fiber

Graphite-Epoxy - 70 weight percent graphite fiber

259

7.0 CRASHWORTHINESS - FRAMED VEHICLES

Various aspects of crashworthiness of a framed vehicle will be considered in the following sections. Test data, calculations and approaches used for evaluating alternate materials will be described.

Test data on the 1977 Impala described or referred to in the following sections was completed at the Calspan Corporation and Dynamic Science testing facilities for the Department of Transportation under separate contracts having no immediate bearing on this study. These tests consisted of a static frontal crush and a 40 mph frontal barrier impact test at Calspan, and a rear end moving vehicle test for fuel containment at Dynamic Science.

7.1 Frontal Crashworthiness

Static crush data was obtained on a 1977 Impala by static compression. The vehicle was anchored to a test bed and then crushed with a segmented barrier consisting of five load cells, Figure 107 . The test data for each panel is shown in Figures 108 through 119, which are tracings of the original test curves. These curves were combined, Table 69, to provide force-deflection data for later analysis. These combined curves are shown in Figures 120 through 126.

For the front of the frame curve, Figure 120, a spike of 32,000 pounds was added to the measured data. It represents an approximation of the load-deformation capability of the low speed impact absorbers present on the Impala. These absorbers are velocity sensitive and hence their contribution were not measured during the static crush test. The load-deformation values used for these absorbers was suggested by Calspan Corporation and is based on previous experience with such devices. Also in Figure 120, a very steep rising "tail" was added after the 18.7 inches of measured data, to insure that crushing continues in the rear portion of the frame when the front portion becomes fully crushed.

Results from a dynamic barrier test on a 1977 Impala are shown in Figure 127. This test was performed at Calspan Corporation for the Department of Transportation on a separate contract as mentioned previously.

The tool used in the crash analysis was a five discrete mass model connected by massless elements which are characterized by force-deformation relationships, Figure 128 . The equations of motion are written for the five masses and are then solved using IBM's "Continuous Systems Modeling Program", CSMP, which is a digital-ar log simulation program. The program used was developed by John T ssoni of NHTSA and used previously.[86]

FIGURE 107 SEGMENTED BARRIER LOADING

PANEL 2

PANEL 1

PANEL 4
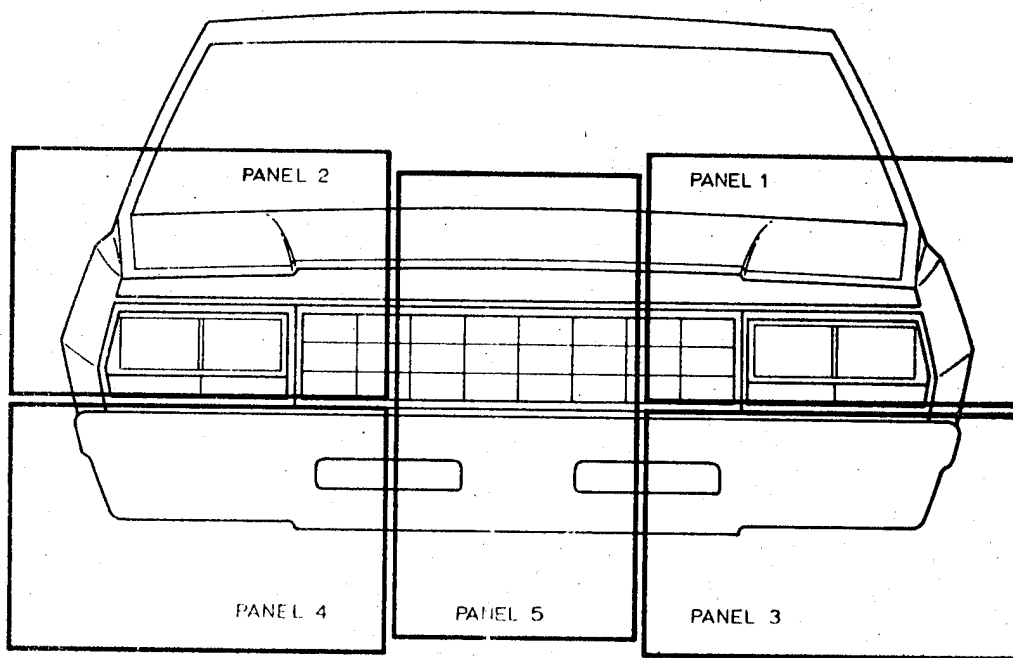
PANEL 5

PANEL 3

FIGURE 108 FRONT RAIL—CRUSH — PANEL 1

2000
POUNDS

5
INCHES
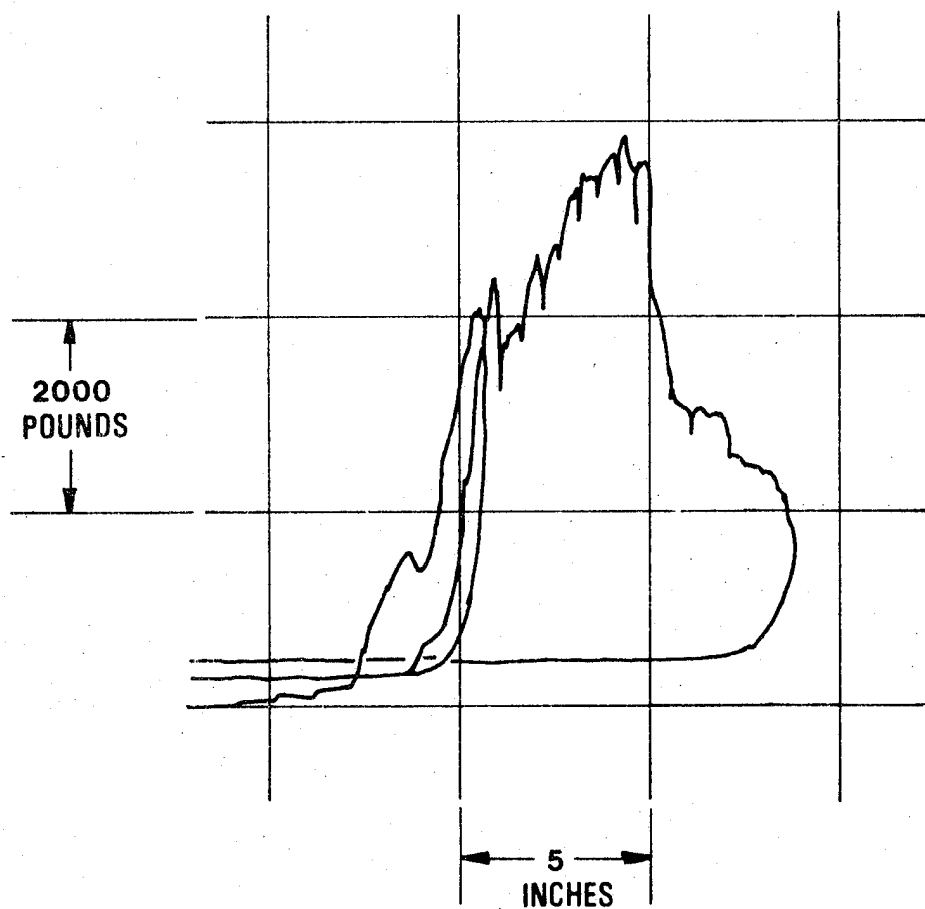
FIGURE 109   FRONT RAIL–CRUSH – PANEL 2

2000
POUNDS

5
INCHES

263
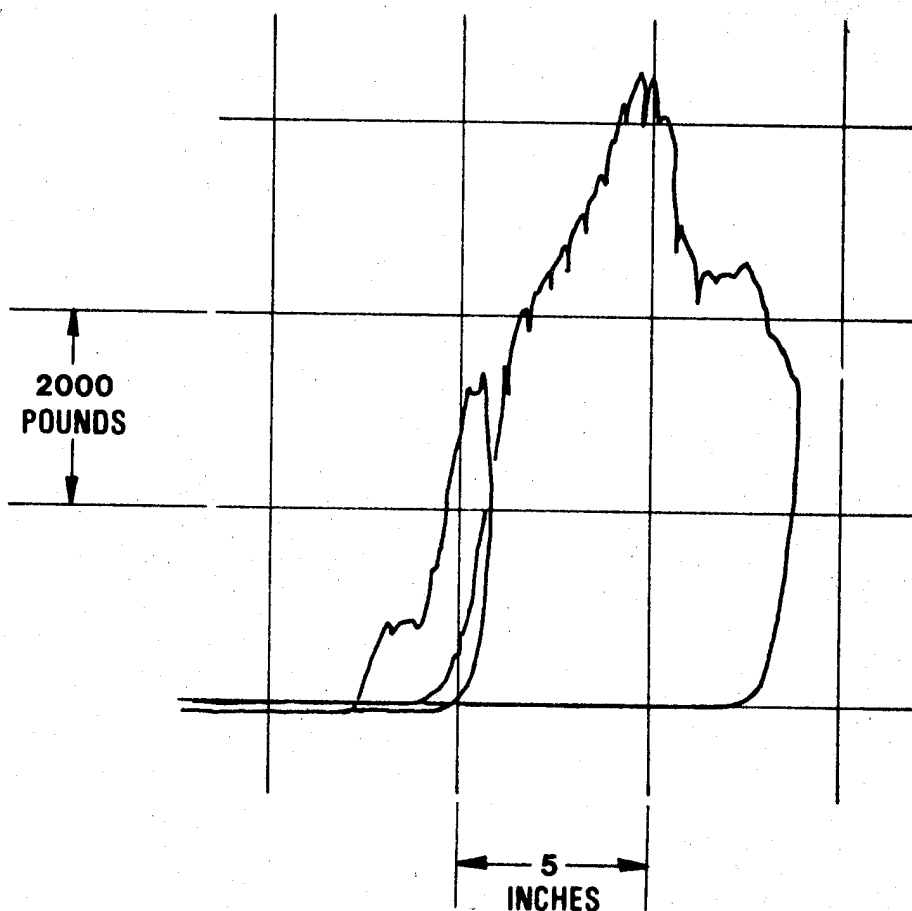
FIGURE 110   FRONT RAIL CRUSH – PANEL 3

4000
POUNDS

5
INCHES
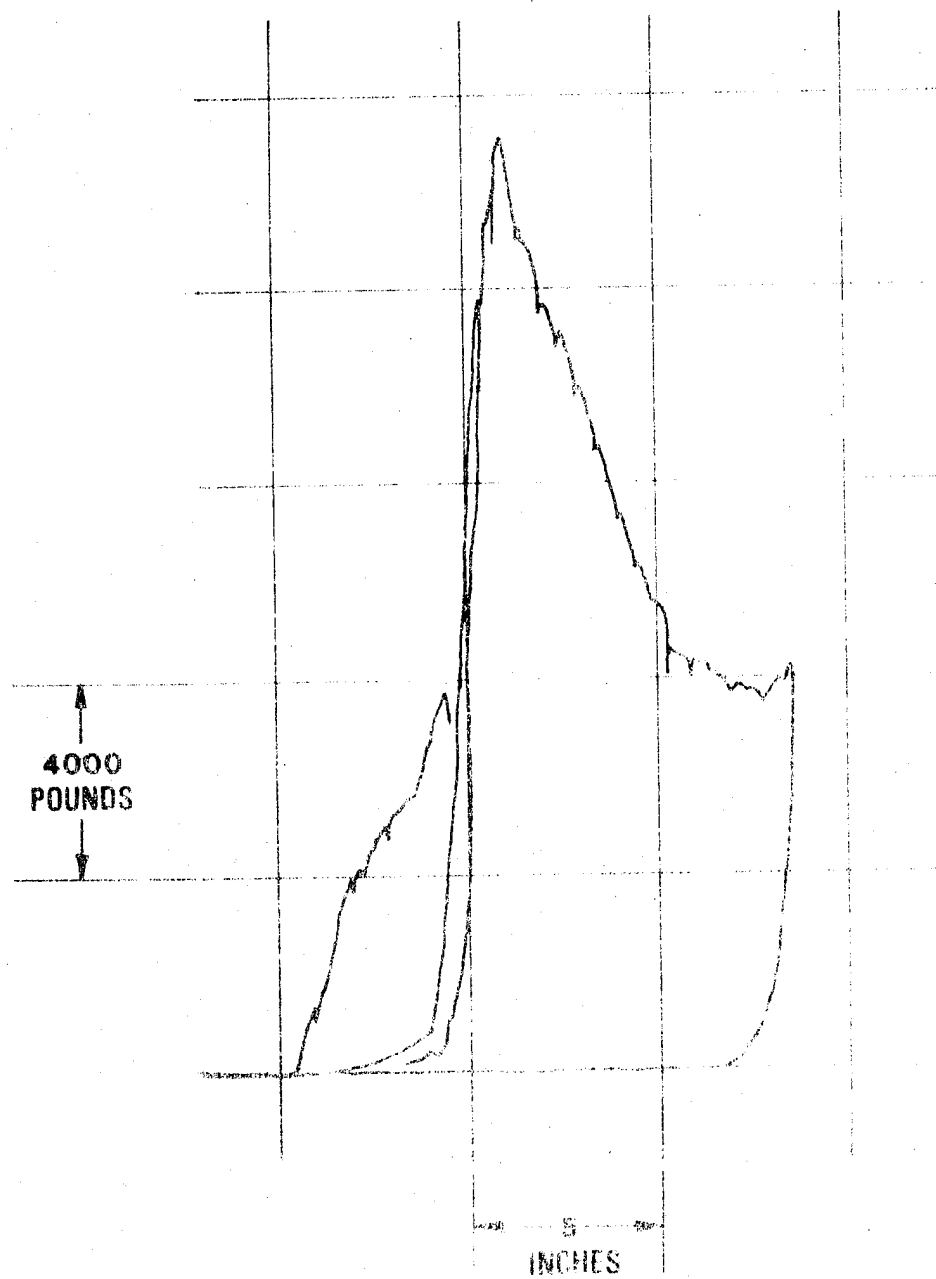
FIGURE 111   FRONT RAIL–CRUSH – PANEL 4
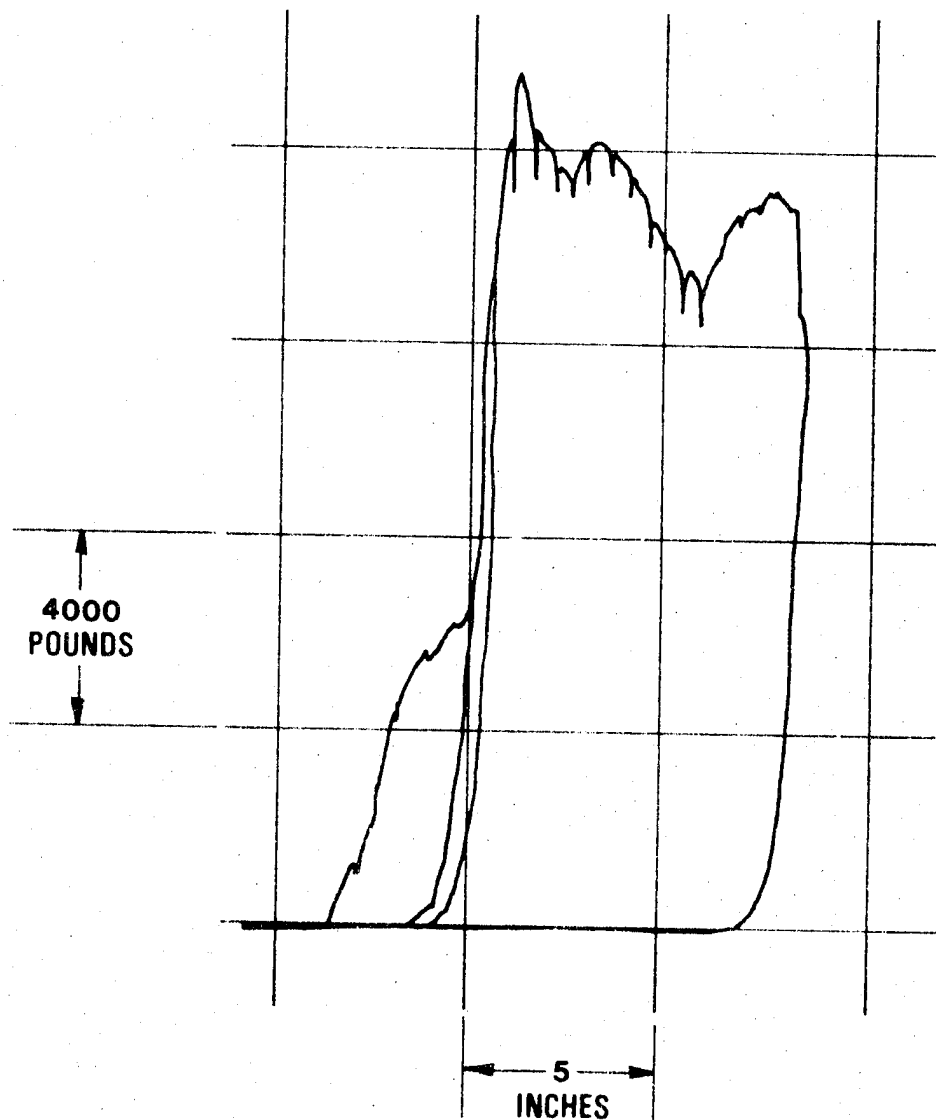
FIGURE 112   FRONT RAIL–CRUSH – PANEL 5

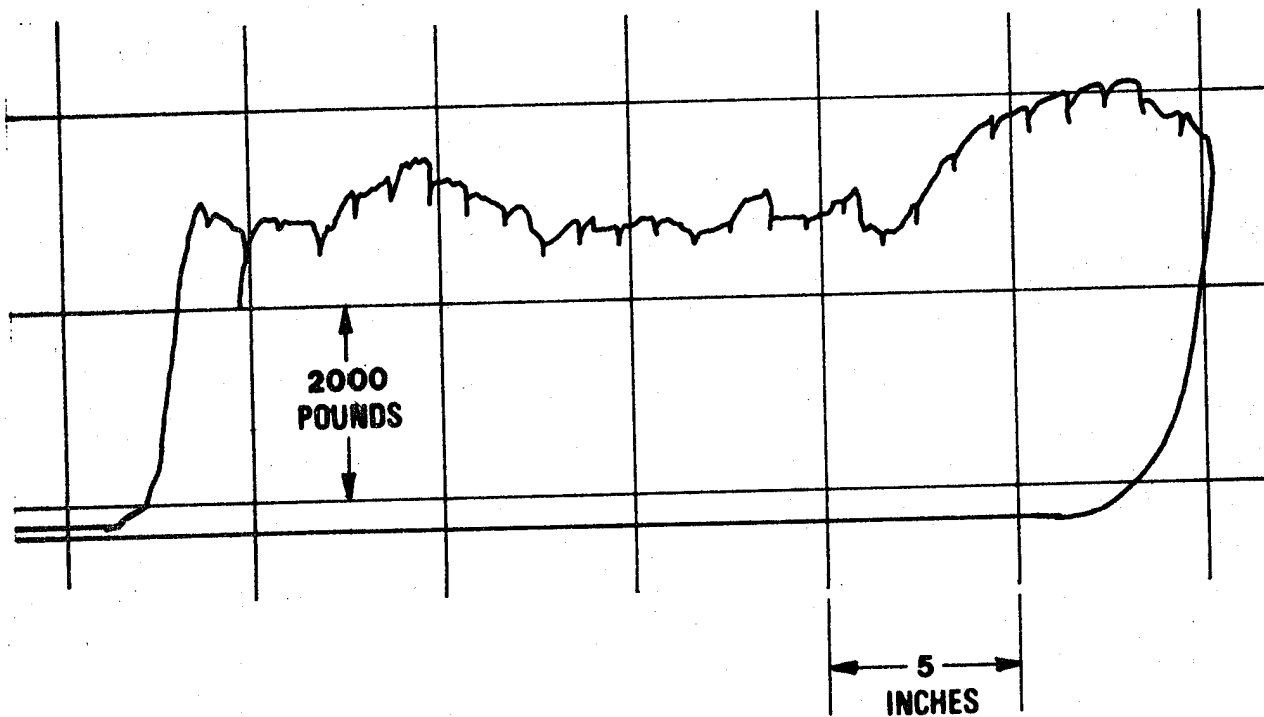4000
POUNDS

5
INCHES
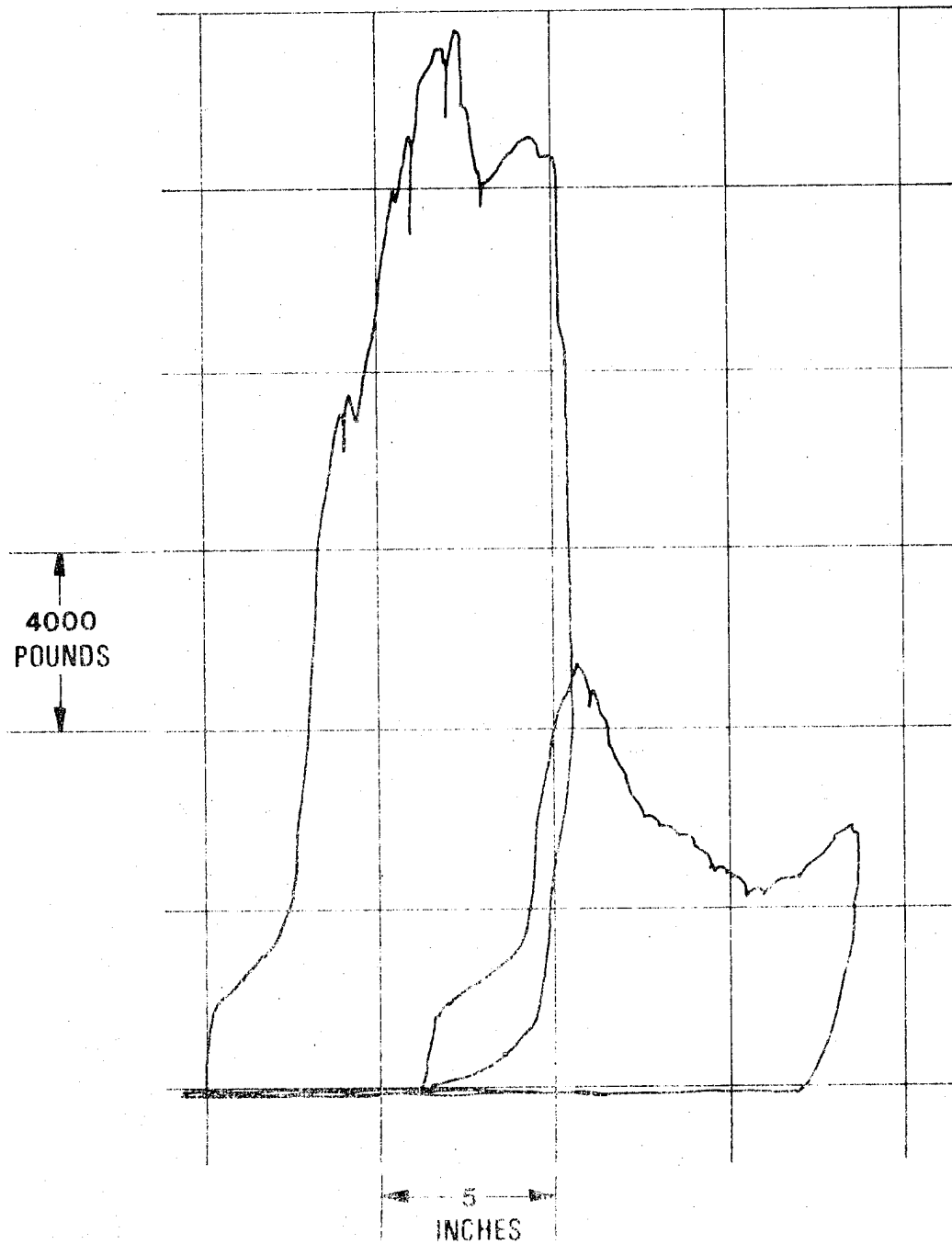
FIGURE 113   **REAR RAIL—CRUSH — PANEL 1**

2000
POUNDS

5
INCHES
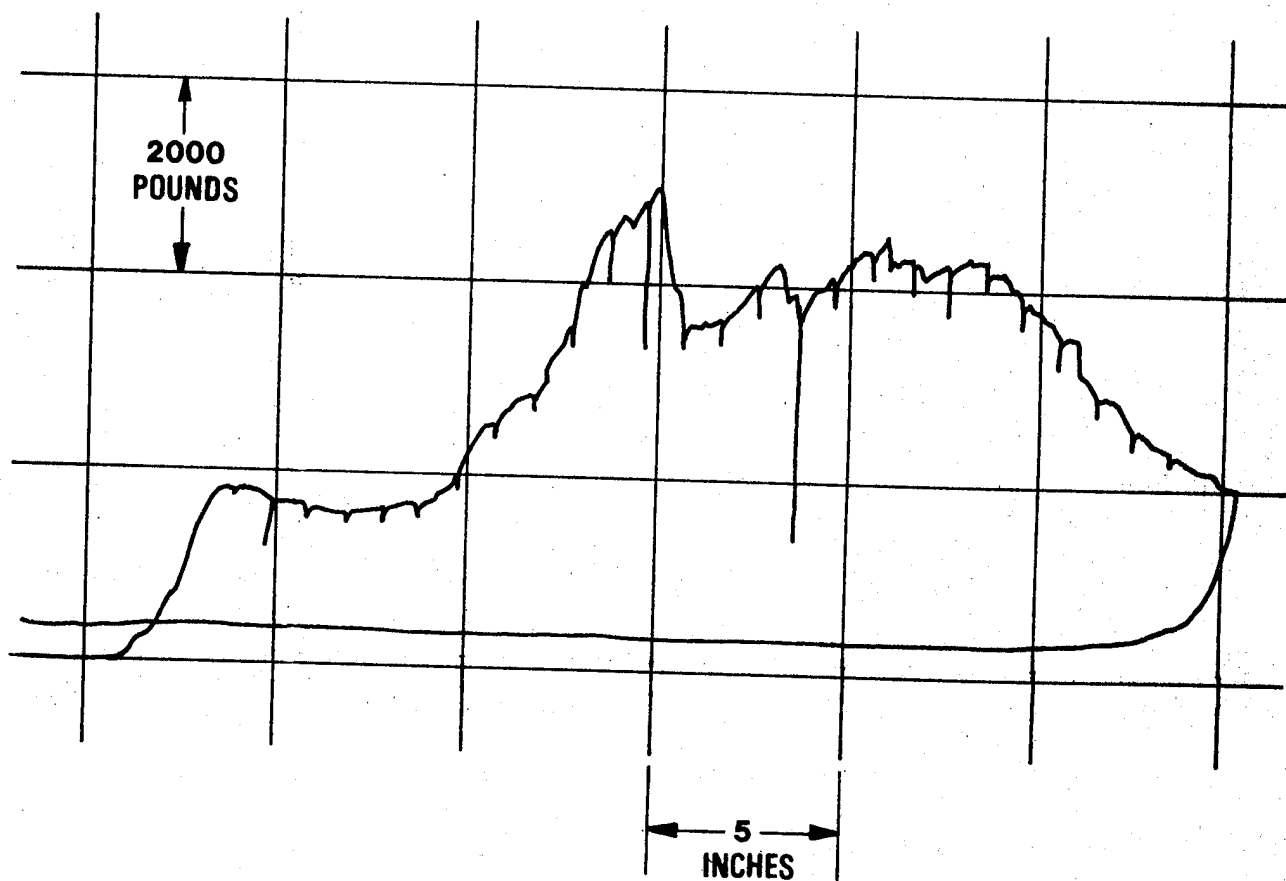
FIGURE 114   REAR RAIL—CRUSH — PANEL 2

2000
POUNDS

5
INCHES

FIGURE 115   REAR RAIL—CRUSH — PANEL 3

4000 POUNDS

5 INCHES
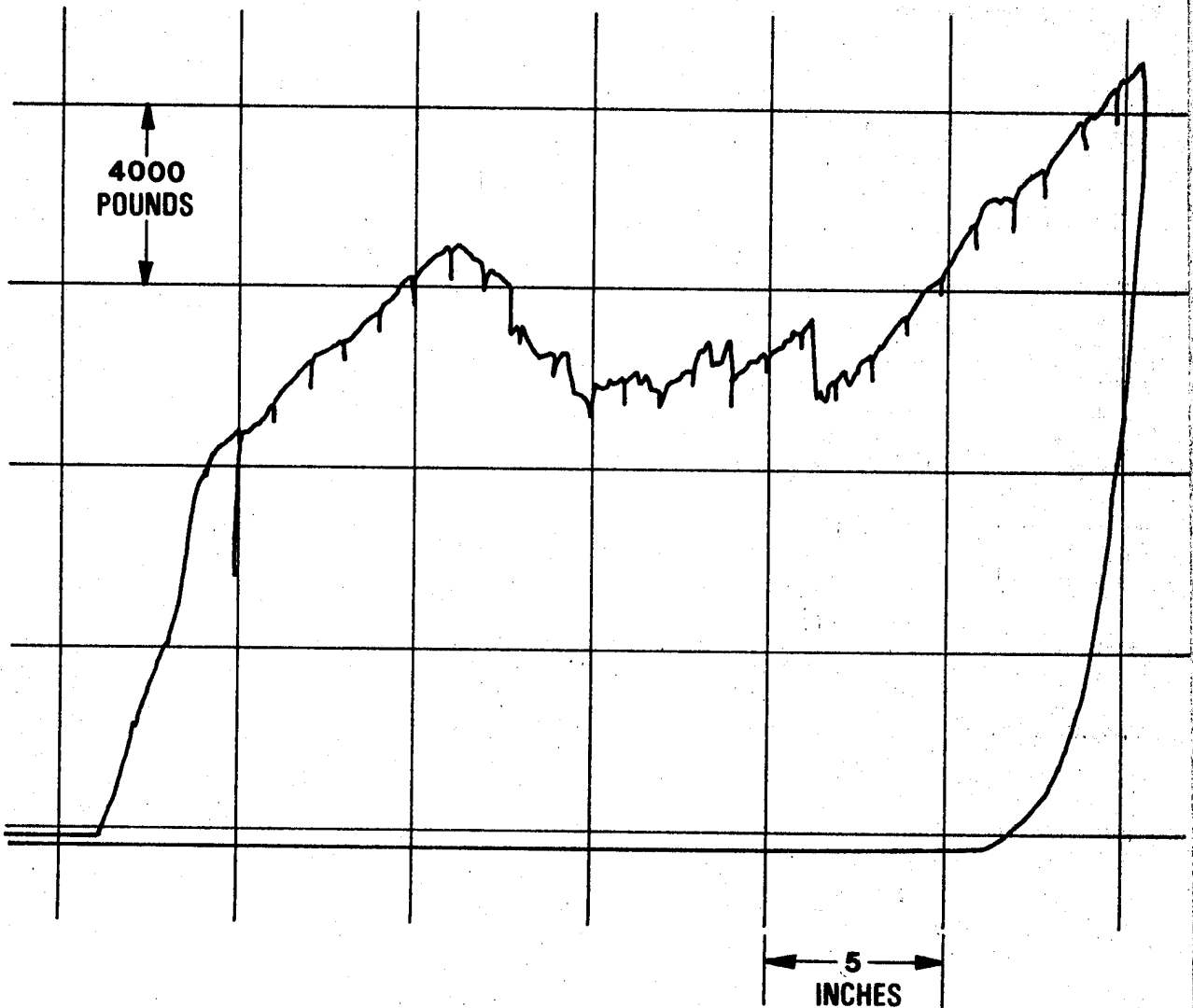
FIGURE 116   REAR RAIL–CRUSH – PANEL 4

4000
POUNDS

5
INCHES
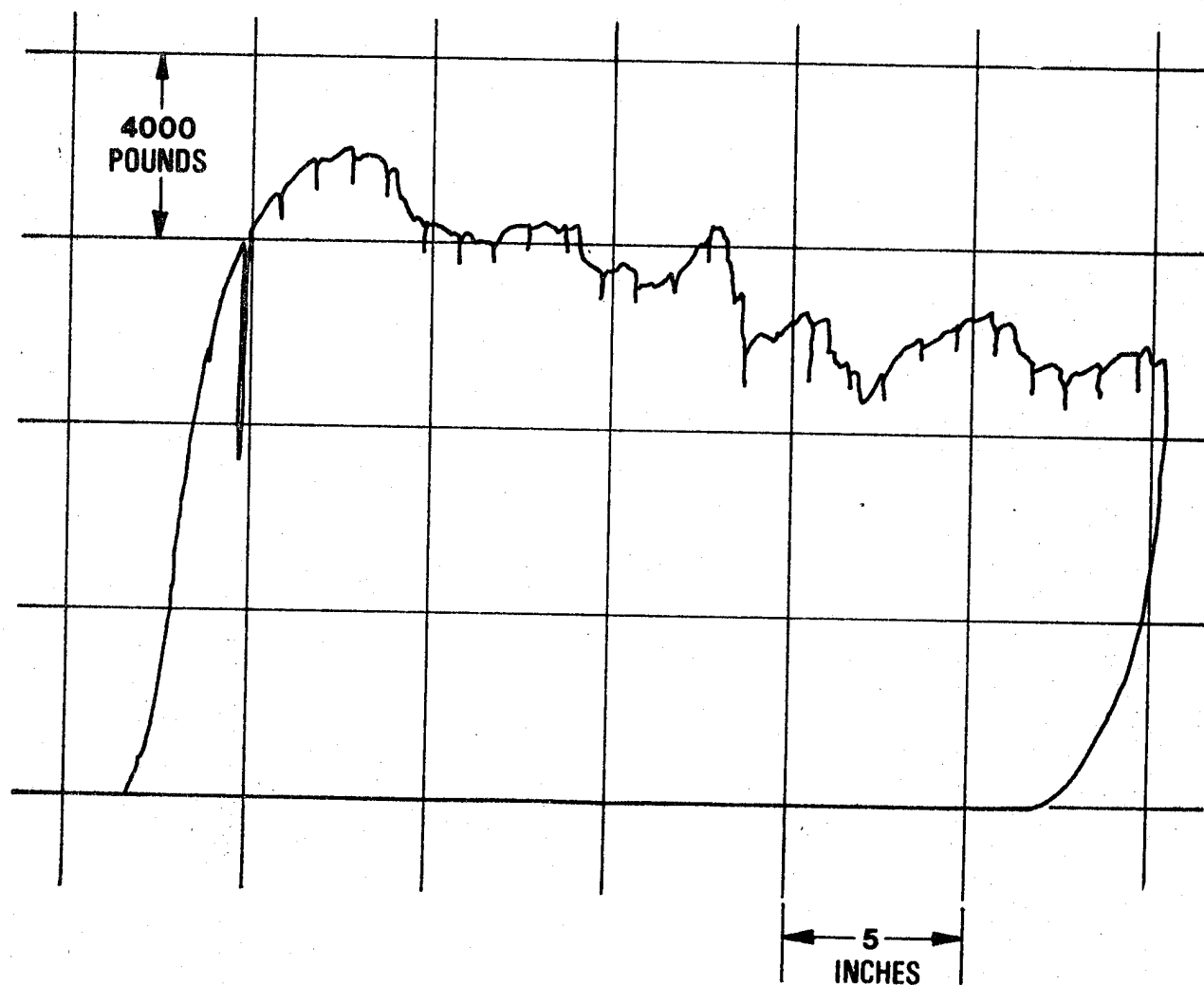
FIGURE 117   REAR RAIL–CRUSH – PANEL 5

FIGURE 117   REAR RAIL–CRUSH – PANEL 5

4000
POUNDS
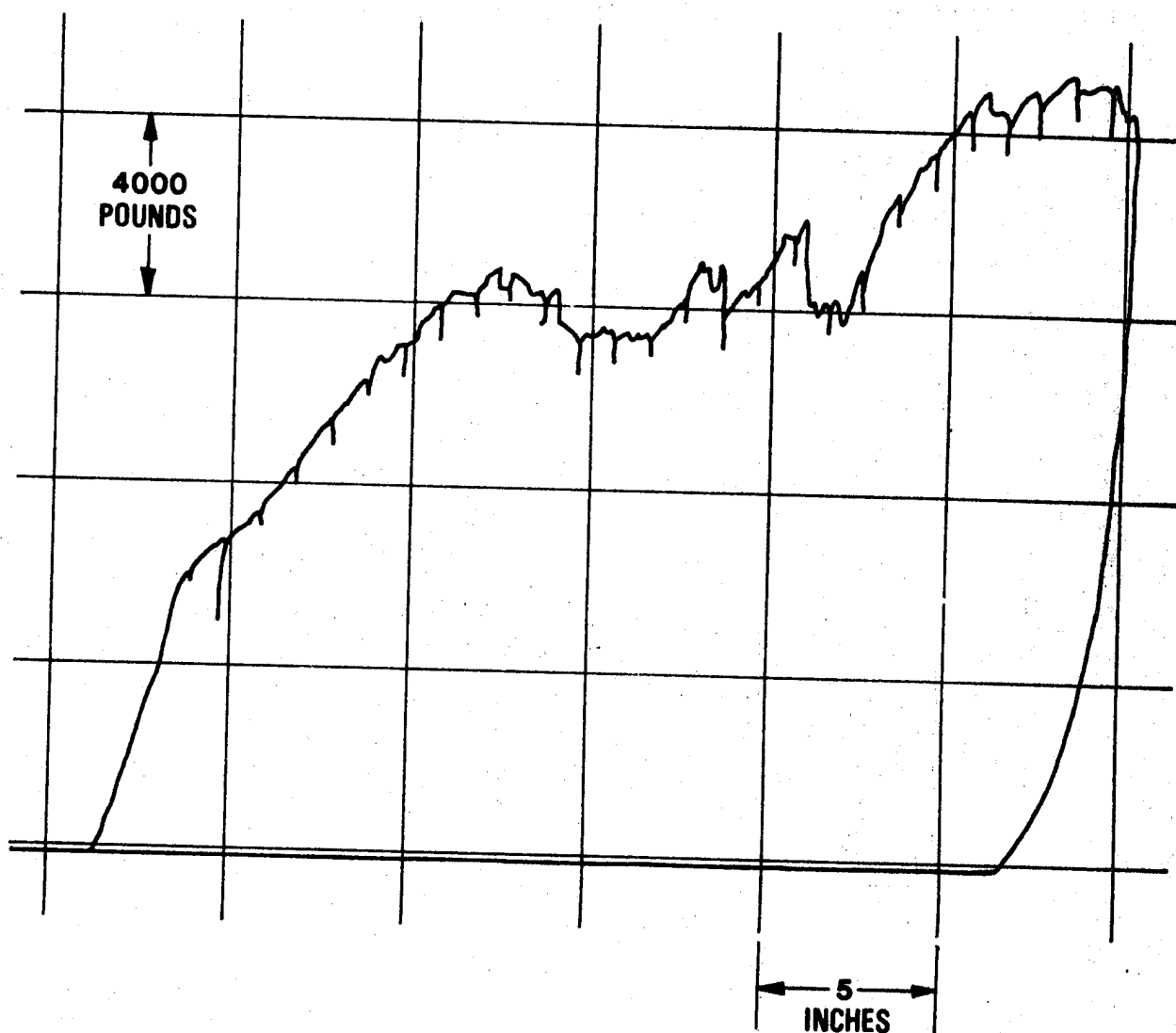
5
INCHES

271

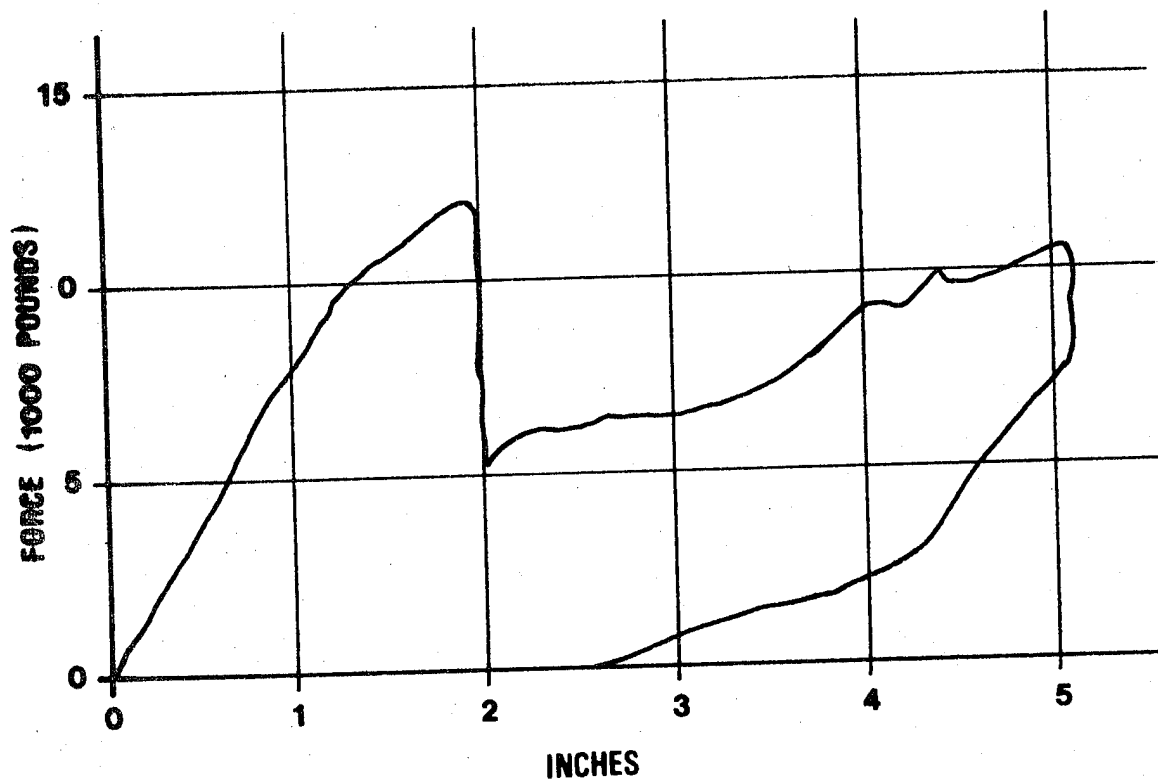FIGURE 118   DRIVELINE – CRUSH

FIGURE 119   ENGINE MOUNT – CRUSH

273
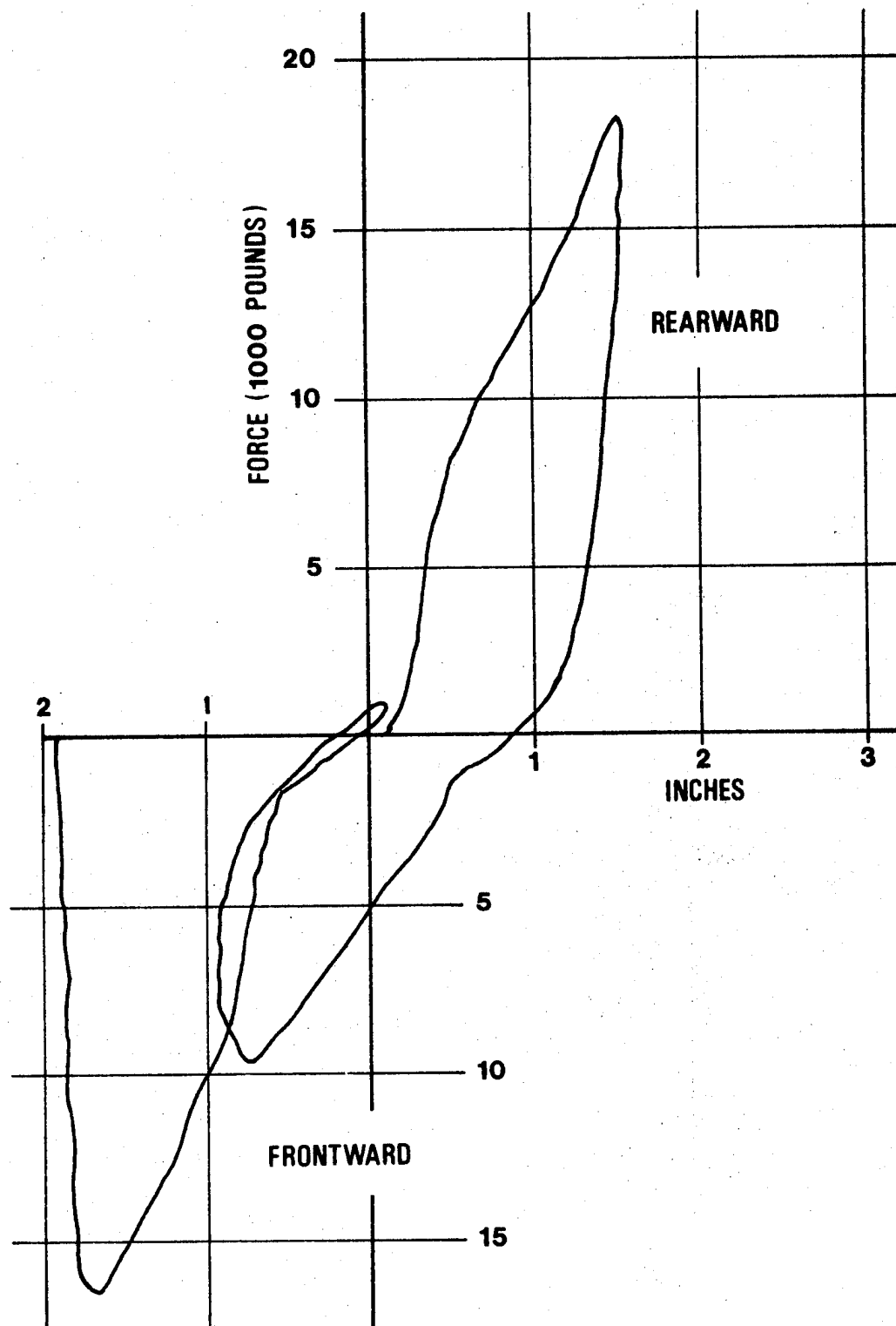
TABLE 69 :   COMPONENT FORCE/DEFORMATION CURVES

For crush load reacted at the engine mount area:

   Panels 3 + 4 + 5 ——→ S11, Forward portion of
                               the frame crush

   Panels 1 + 2 ——→ S14, Forward portion of
                          sheet metal crush

For crush load reacted at the sill and "A" post area:

   Panel 5 ——→ S18, Engine into firewall
                     crush

   Panels 1 + 2 ——→ S14, Rear portion of sheet
                          metal crush

   Panels 3 + 4 ——→ S12, Rear portion of the
                          frame crush

FIGURE 120   IMPALA FRONT OF FRAME — S11

275
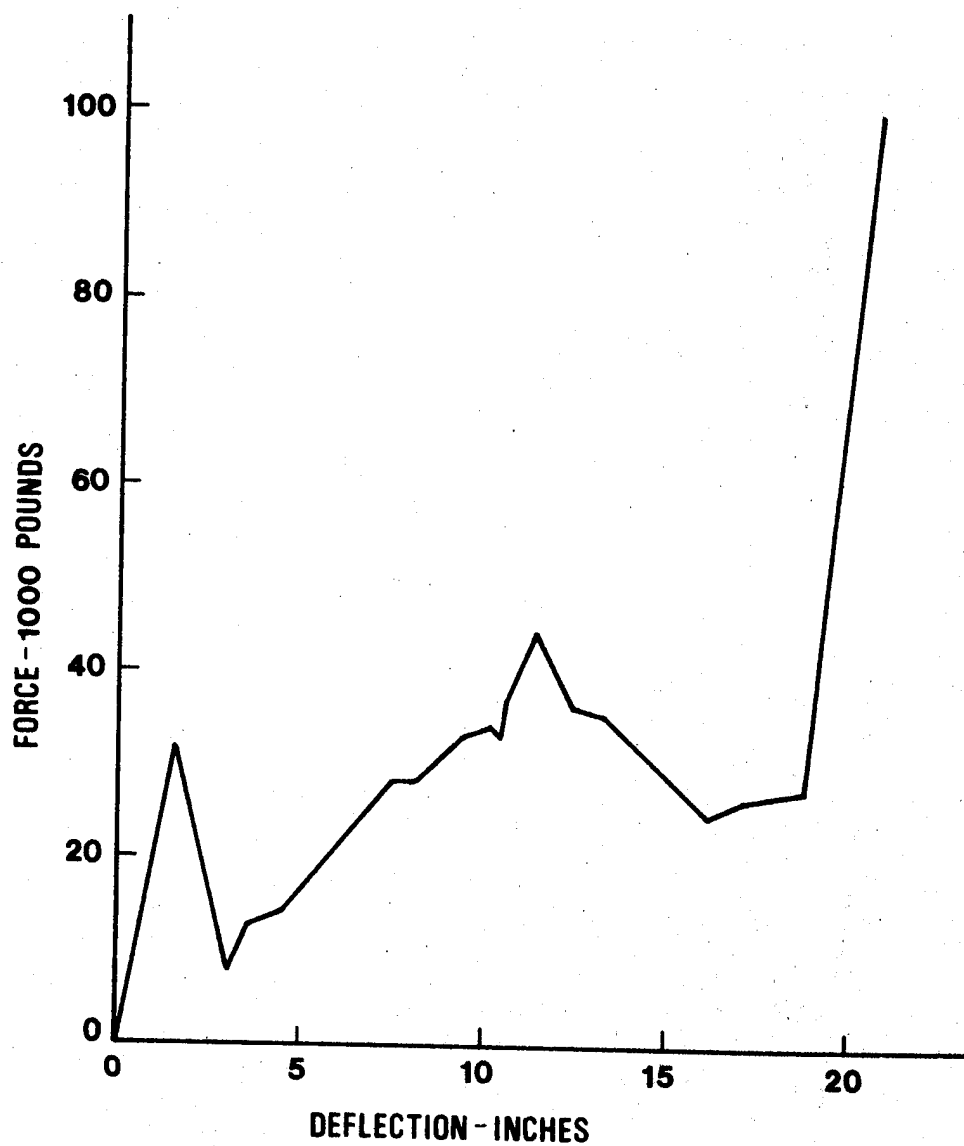
FIGURE 121   IMPALA SHEET METAL – S14

276
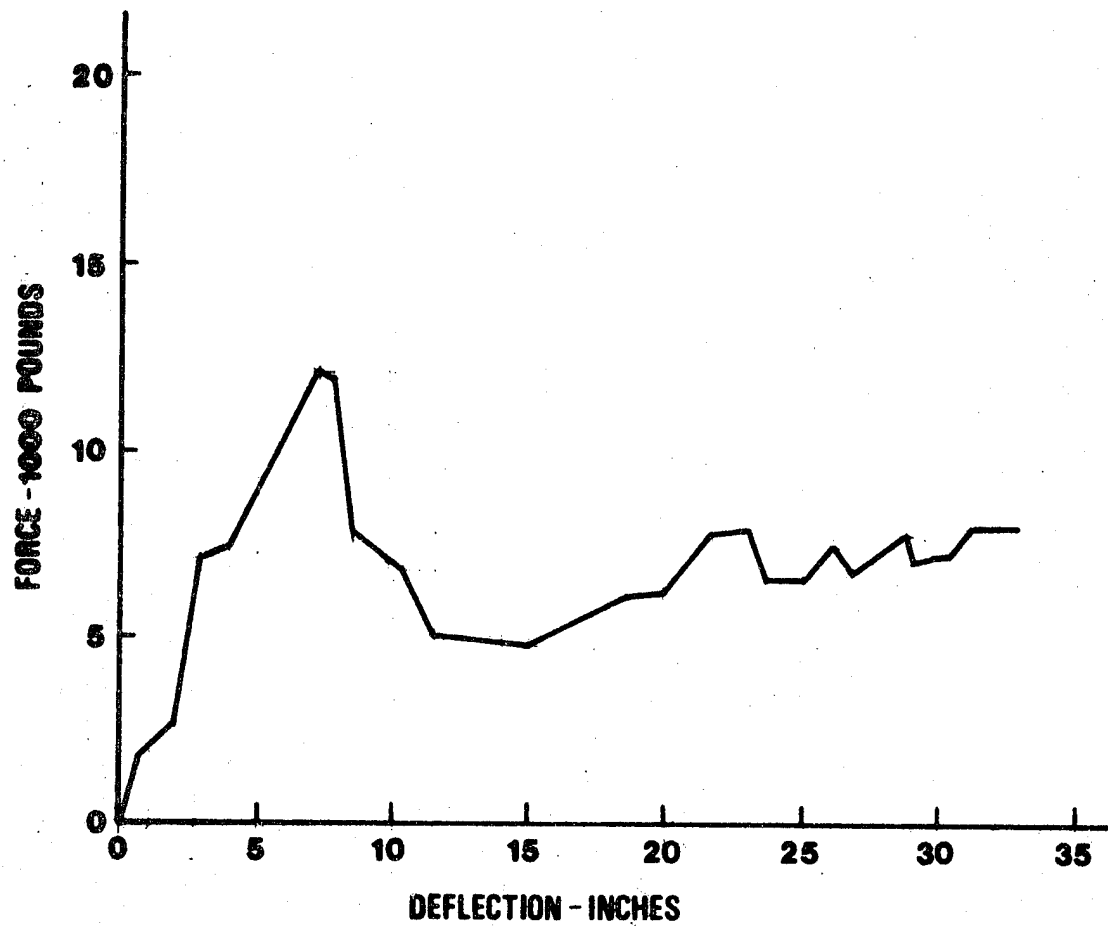
FIGURE 122   IMPALA REAR OF FRAME – S12
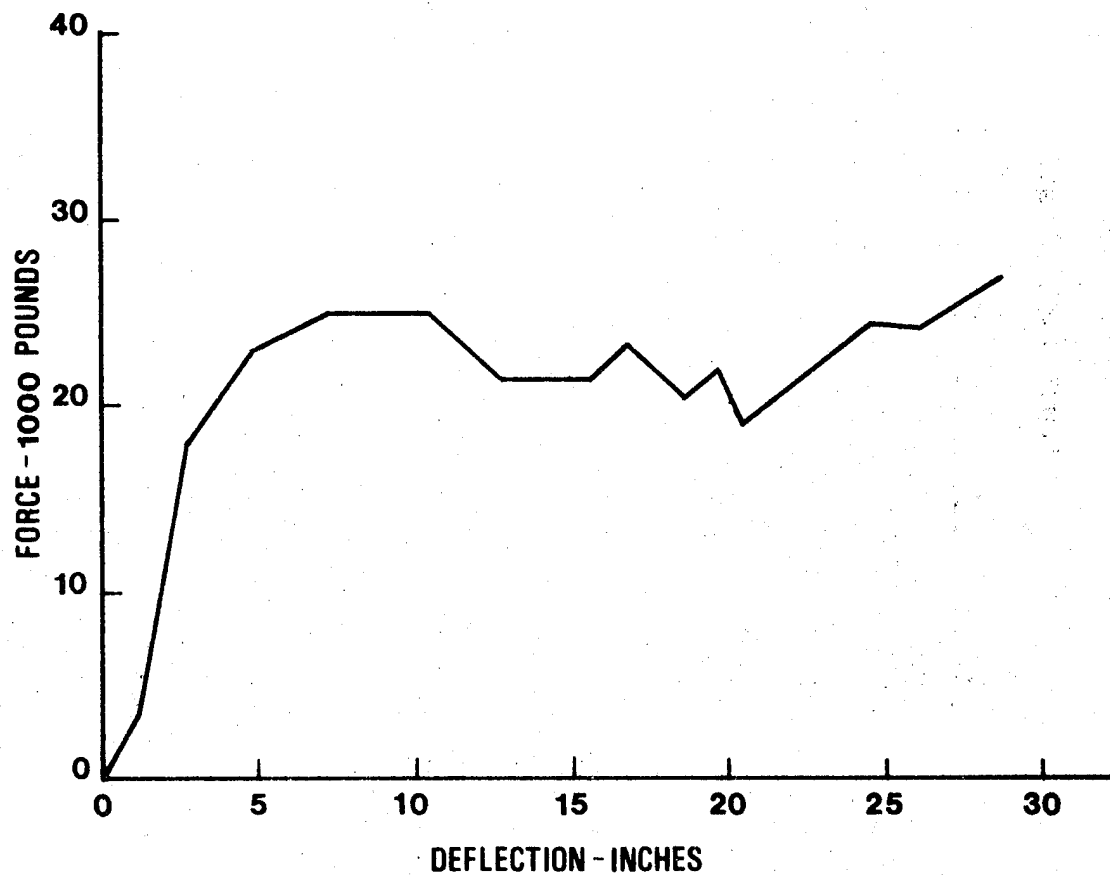
FIGURE 123   IMPALA FIREWALL — S18
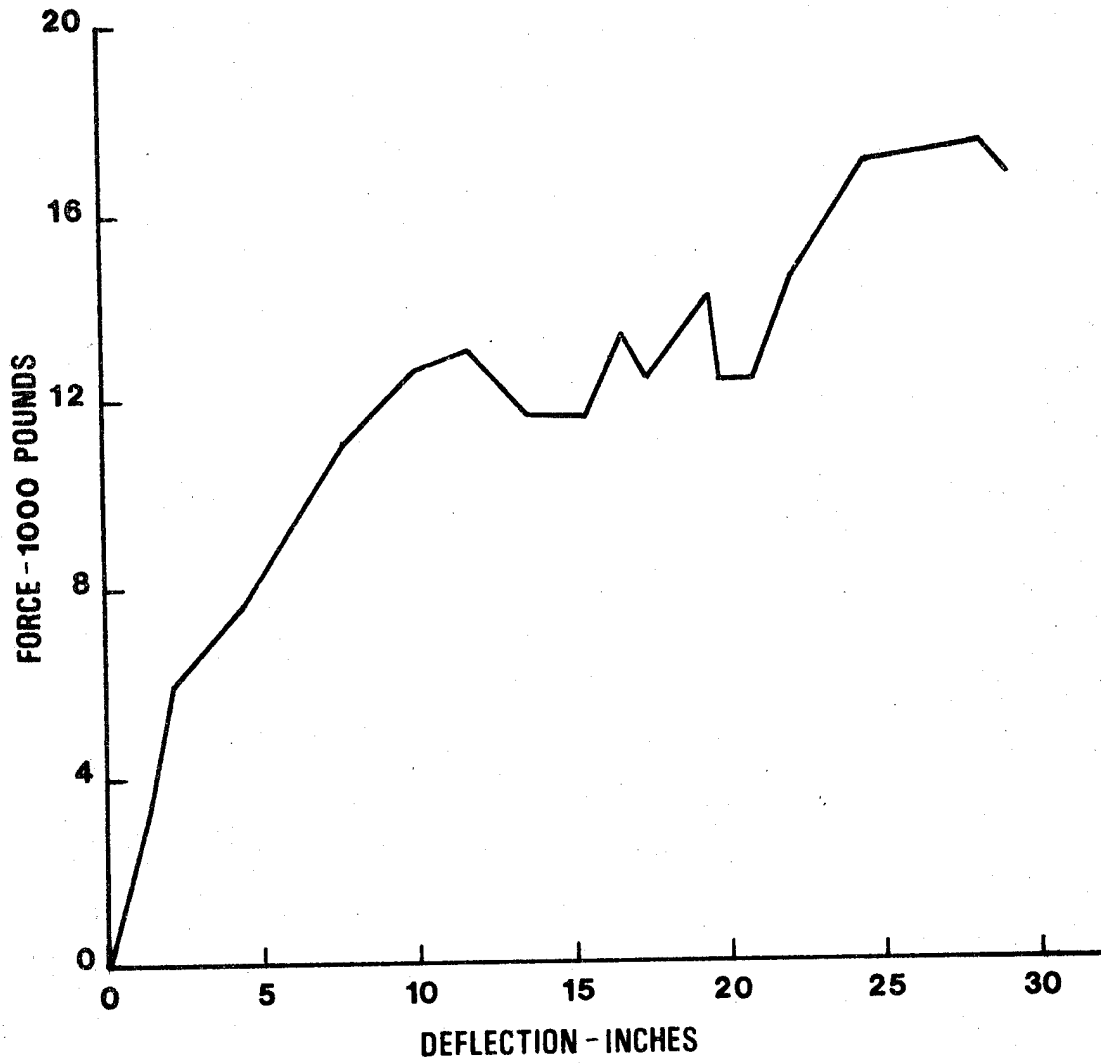
FIGURE 124   IMPALA DRIVELINE – S16
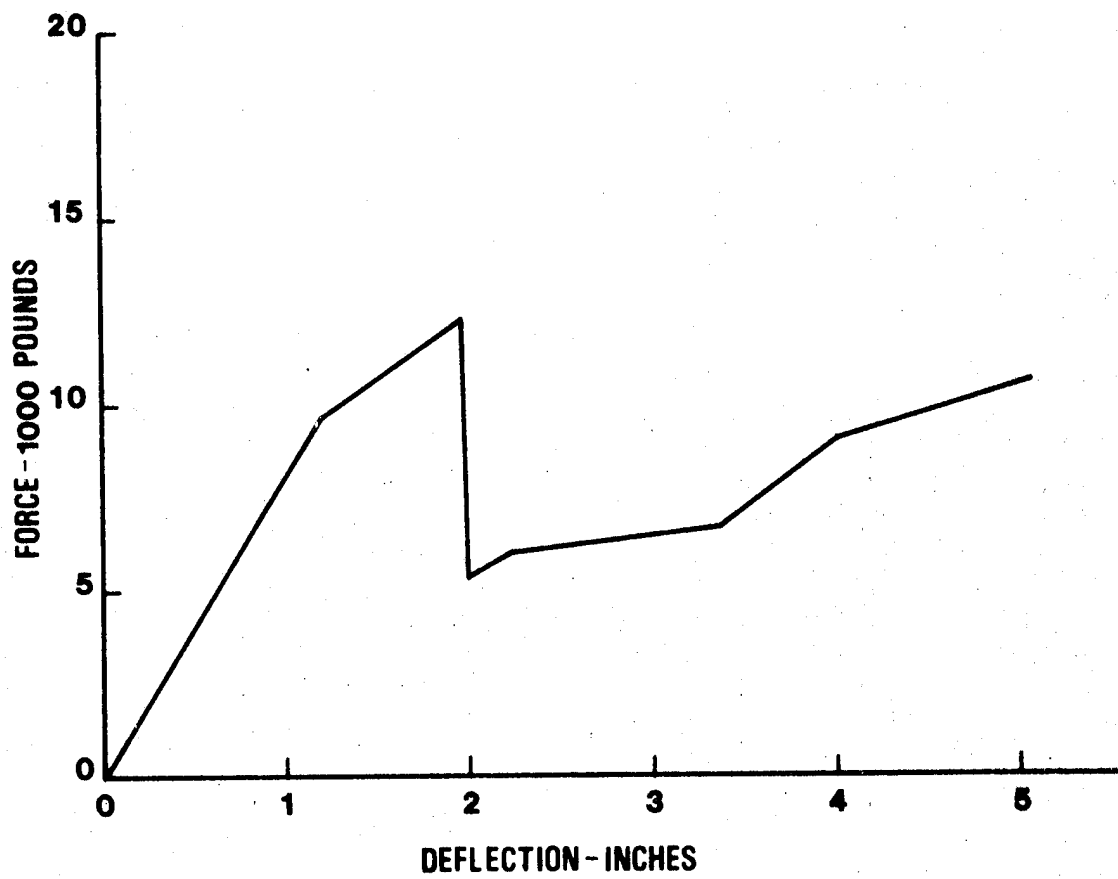
FIGURE 125   IMPALA ENGINE MOUNTS – S15
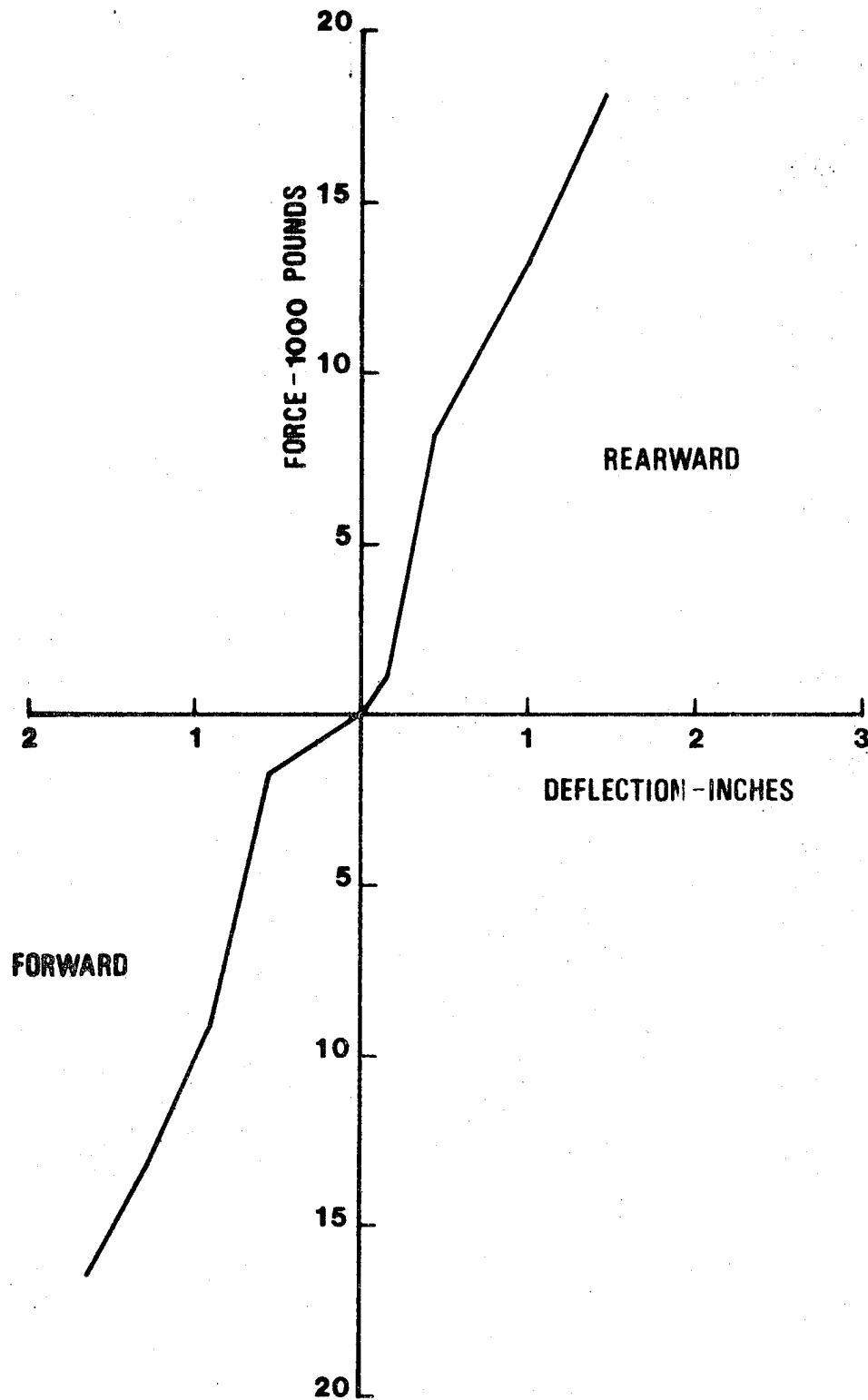
FIGURE 126   SIMULATED RADIATOR – S13

281
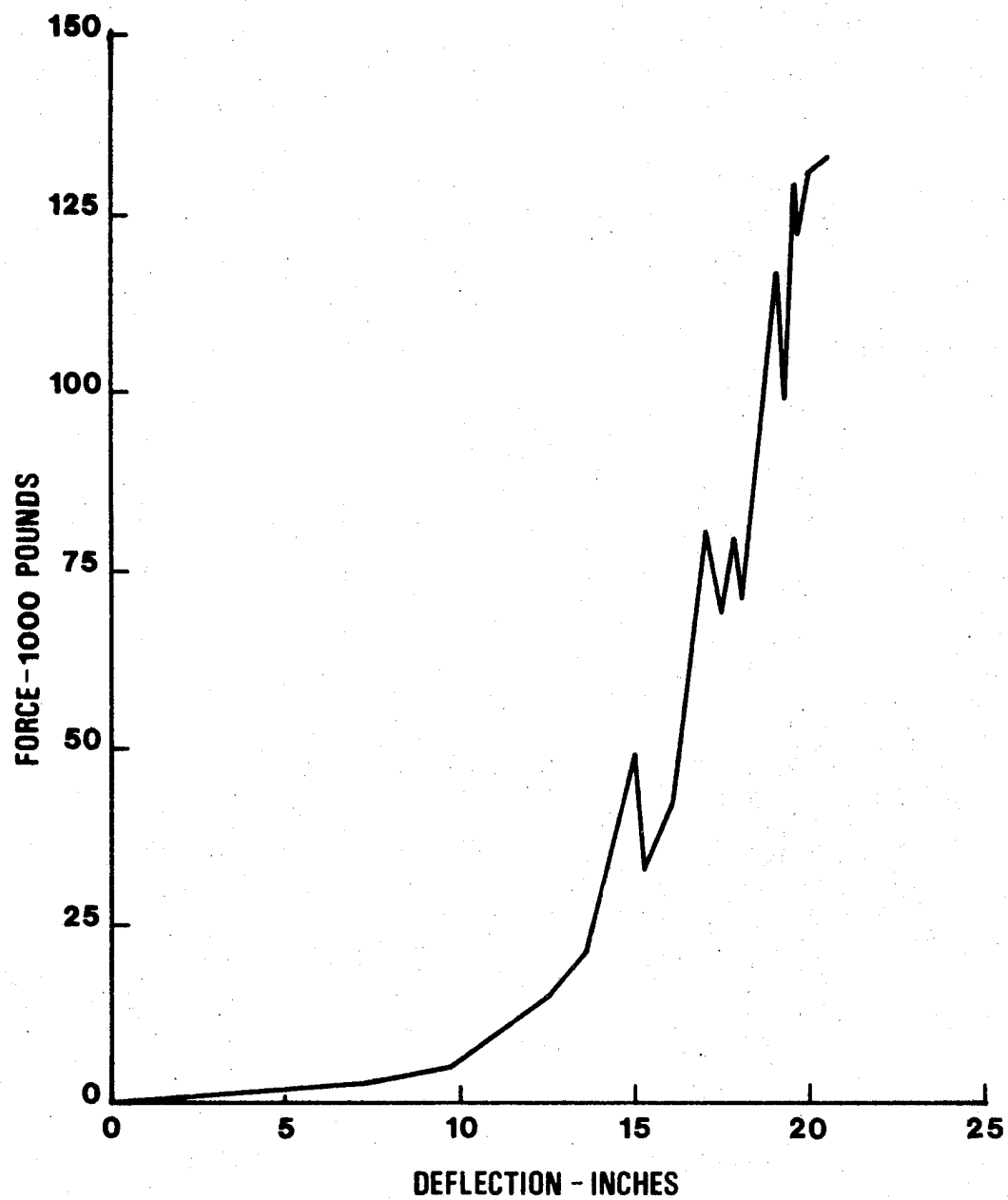
FIGURE 127   DYNAMIC BARRIER TEST RESULTS

FIGURE 128   FIVE MASS CRASH SIMULATION MODEL

BUMPER

SHEET METAL
— S 14 —

FIREWALL
— S 18 —

PASSENGER
COMP.

RADIATOR
— S 13 —

ENGINE
E 1

DRIVELINE
— S 16 —

B 1

S 17 — C 1

C 1

OCCUPANTS

ENGINE MTS.
S 15

FWD. FRAME
— S 11 —

AFT FRAME
— S 12 —

X-MEMBER & SUSPENSION
F 1

The computer program, as originally developed, incorporated a linear relationship between deformation rate and a dynamic magnification factor. For the present study, the program was modified to use the logarithmic strain rate factor shown in Figure 129. Numerous studies have shown that ductile steels exhibit greater force resistance as the strain rate increases.

Data [94] available on the tensile yield and tensile ultimate strength of low carbon steel, HSLA steels and aluminum alloys indicate a low or essentially non existent strain rate effect for aluminum and sizeable similar effects for low carbo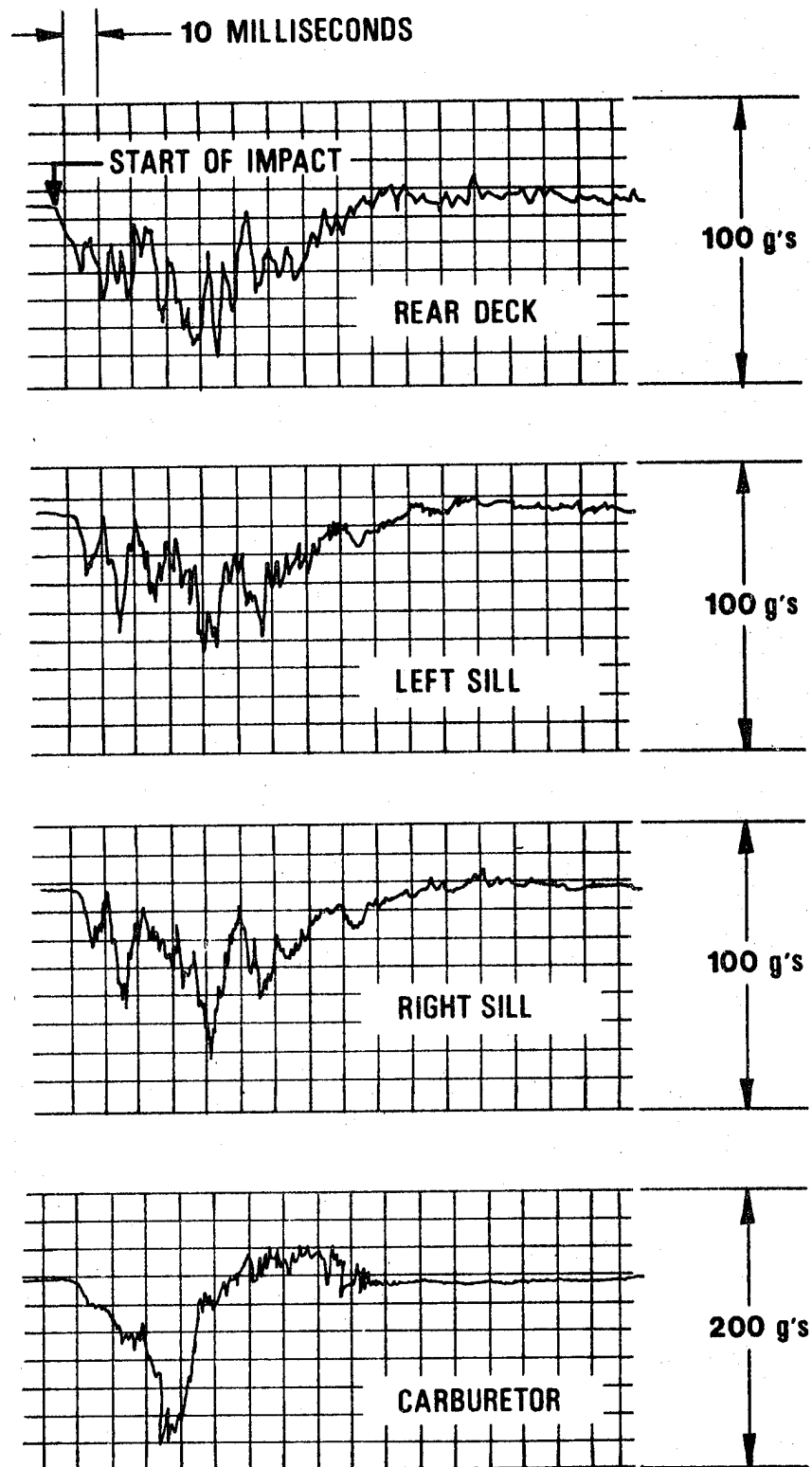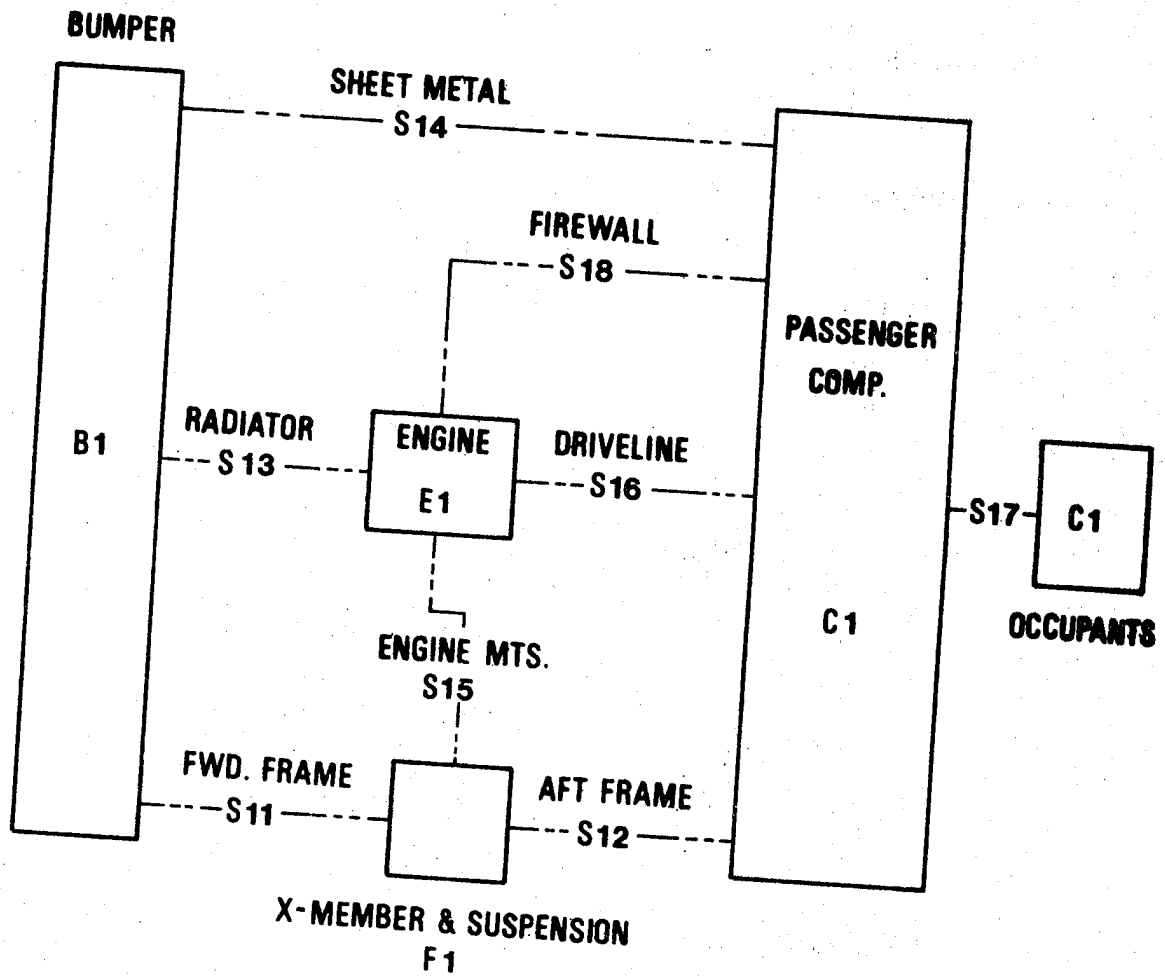n and HSLA steels. While the HSLA steel does not appear, at first glance, to have as high of a strain rate as low carbon steel, when determined as a ratio of total strength, the increase in yield strength of the two materials are very similar.

Dynamic compression test data from Budd Company records are shown in Table 70 for low carbon steel, aluminum alloy and HSLA steel tubes tested statically and at 40 fps impact in a drop tower. This data shows a higher ratio of dynamic to static average crush force for low carbon steel than for the other two materials. The difference between the dynamic and the static average crush forces have also been listed and again show that the strain rate effect is somewhat greater in the low carbon steel than in the HSLA steels. Crush tests conducted by Bethlehem Steel Corporation [93] indicated similar strain rate effects for the two steels.

In comparing the as received data to the results prepared for the computer program, it will be observed that all of the data for the computer starts at the 0-force/0-deflection intercept while not all of the as received data starts there. The computer program takes this into account through the input of the three clearances shown in Figure 130. The clearances A and C are easy to measure and input into the program. Clearance B consists of non force resistant crushable space between the barrier and engine. The bumper, both radiators and those items of the engine (i.e., water pump, crankshaft pulley, etc.) which are directly in line with the radiator and the engine block should be subtracted from the gross distance between the barrier and the engine block. While there is some degree of uncertainty associated with this dimension, it will be shown that the response of the passenger compartment is not drastically changed with large variations in this clearance.

The results of a study of the "B" clearance in the simulation model described previously, Figure 130, is presented in Figure 131. As can be seen, large variations in the "B" clearance do not significantly change the peak deceleration value while the maximum crush distance changes in a predictable manner. Figure 132 replots the curves for the three "B" values investigated as a function of time and compares them with the envelope of the deceleration curves from Figure 127 for the rear deck, and left

$$= \begin{cases} 1.0, & \text{FOR } \dot{X} = 0 \\ 1.2728 + .01971 \log_e \dot{X}, & \text{FOR } \dot{X} > 0 \\ \text{WHERE } \dot{X} = \text{CRUSH RATE (IN/SEC)} \end{cases}$$
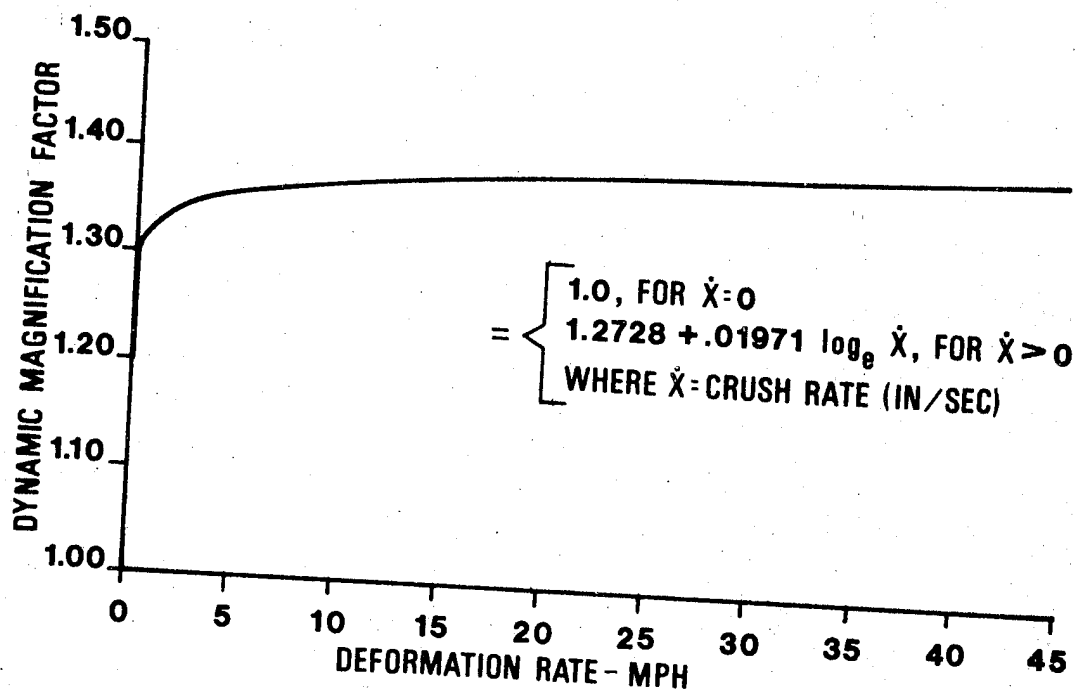
TABLE 70 : EFFECTS OF TESTING RATE ON CRUSH FORCE OF STEEL TUBES

	Low Carbon Steel	HSLA Steel	6061-T6 Al
Peak Load Static	21,000	30,000	21,000
Peak Load Dynamic	21,746	21,615	19,519
Ave. Crush Force Static	8,835	10,299	6,564
Ave. Crush Force Dynamic	12,245	13,091	7,680
$\dfrac{\text{Ave. C.F. Dynamic}}{\text{Ave. C.F. Static}}$	1.386	1.271	1.17
$\dfrac{\text{Ave. C.F. Dynamic}}{\text{Ave. C.F. Static}}$	3410	2792	1116

FIGURE 130   **CLEARANCE INPUTS FOR COMPUTER SIMULATION**
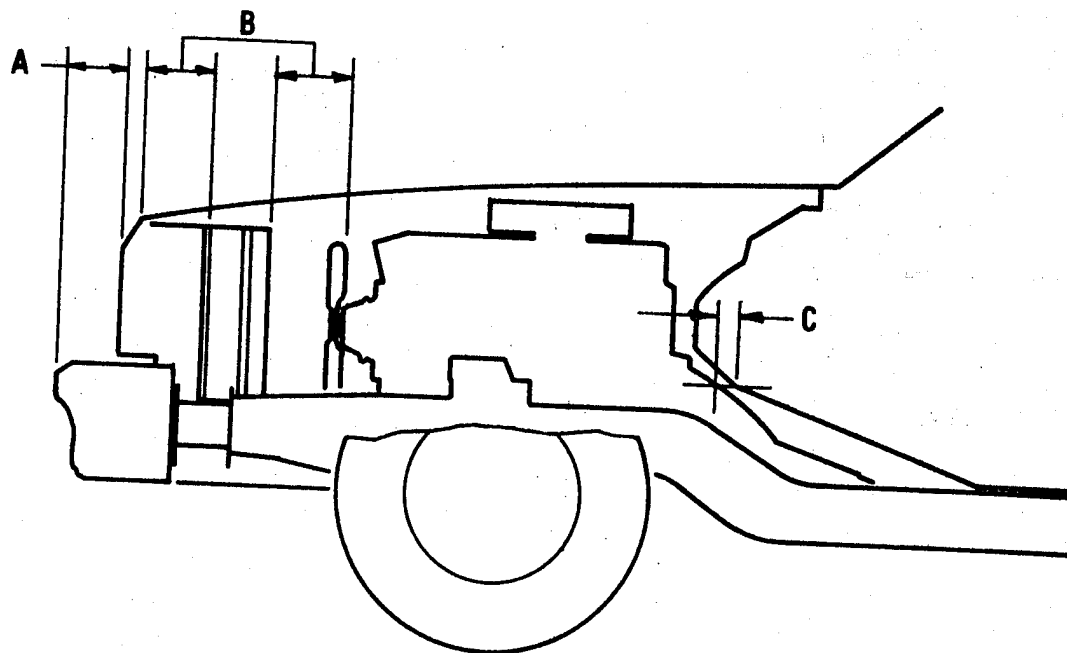
A: FRONT OF SHEET METAL TO BARRIER ; **6** INCHES .

B: BACK OF BUMPER TO ENGINE LESS THE TWO
RADIATORS ; **17** INCHES.

C: REAR OF ENGINE / TRANSMISSION TO FIREWALL ; **1** INCH.

IMPACT VELOCITY	39.73 MPH
BUMPER WEIGHT	60 POUNDS
ENGINE WEIGHT	708 POUNDS
CROSS MEMBER AND SUSPENSION WEIGHT	250 POUNDS
PASSENGER COMPART-MENT WEIGHT	2892 POUNDS

FIGURE 132   COMPARISON OF PREDICTED AND MEASURED
PASSENGER COMPARTMENT RESPONSE

and right sills. Figure 133   presents comparable computer re-
sults for the engine deceleration and compares it to the carbure-
tor data of Figure 127.

The correlation between measured and predicted deceleration
results was not very good. An excellent exchange of information
and suggestions was undertaken between John Tomassoni and Gary
Bell of NHTSA, Robert Galganski of the Calspan Corporation, and
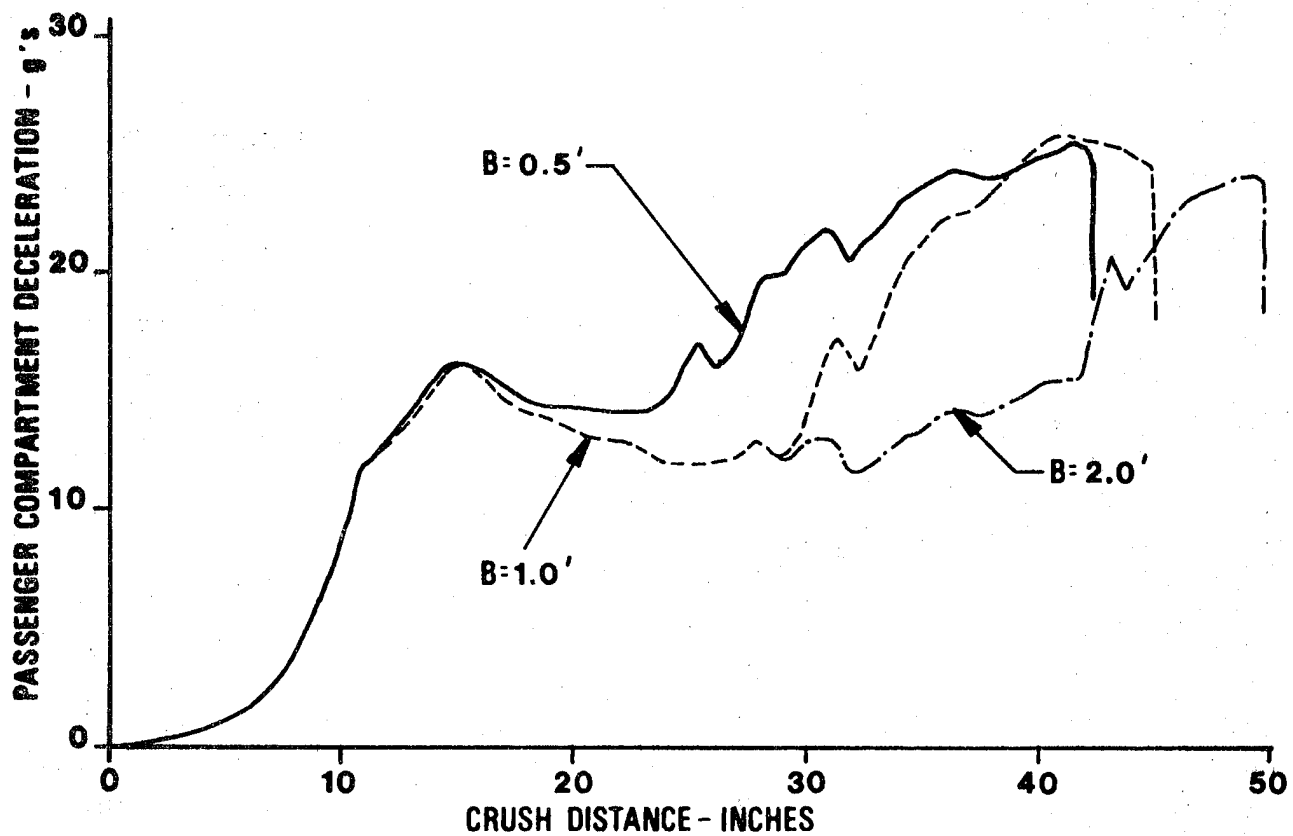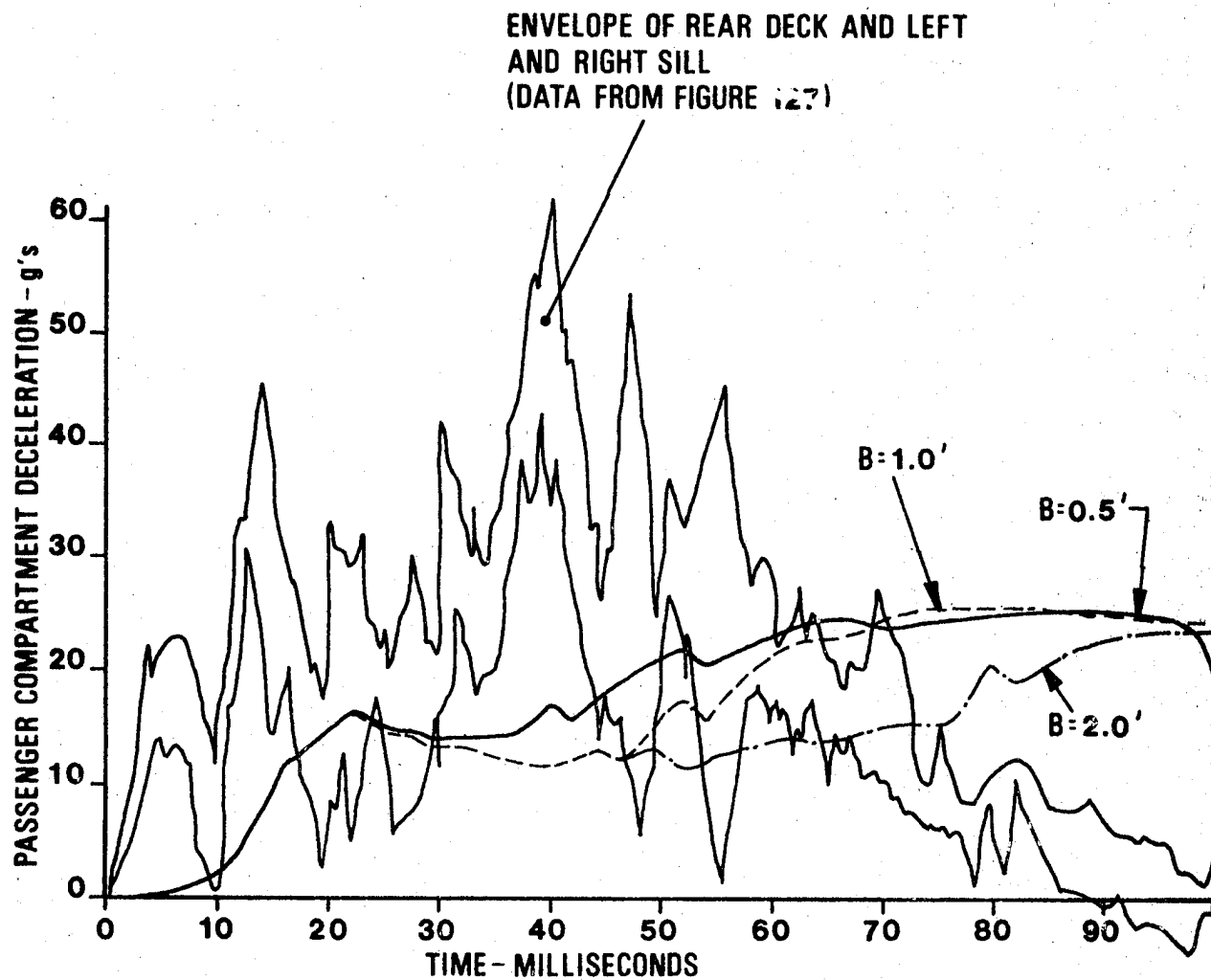The Budd Company in an attempt to improve the correlation. Un-
fortunately, the Impala was the first vehicle to be statically
crushed using a five panel segmented barrier instead of the pre-
vious method where four panels and two cars were used to obtain
all of the required force/deformation relationships. Because
of the test technique employed for the Impala, a greater dif-
ficulty in the subsequent interpretation of the data exists. The
difficulty has caused some of the poor correlation experienced.

As an example of the potential of the analytical approach, an
attempt was made to establish what the force/deformation response
would be for an ideal front end structure for the Impala. The
firewall, driveline, engine mounts, and radiator force/deformation
curves were kept as previously presented, while the sheet metal
and the front and rear portions of the frame were considered for
modification. Figure 134 presents the assumed force/deformation
shapes for the three components of structure investigated. For
the analysis, it is assumed that F_{11} equals F_{12} and that the de-
sired total crush would be 44 inches for a 50 mph frontal impact.
In addition, from the DOT-HS-4-00929 report "Feasibility Study
of Plastic Automotive Structure"[86] it is suggested that the sheet
metal should be capable of sustaining one-third of the total
energy absorbed by the sum of the sheet metal and the front and
rear portions of the frame.

$$\text{Energy }_{14} = 1/3 \left[\text{Energy }_{14} + \text{Energy }_{11} + \text{Energy }_{12} \right]$$

or

$$\text{Energy }_{14} = 1/2 \left[\text{Energy }_{11} + \text{Energy }_{12} \right]$$

$$2.409 \ F_{14} = 1/2 \left[1.642 \ F_{11} + 2.092 \ F_{12} \right] = 1.867 \ F_{11}$$

$$F_{14} = .775 \ F_{11} = .775 \ F_{12}$$

An iterative computer solution was required to obtain the
magnification factor for F_{11} and F_{12} which would yield the re-
quired total crush. A factor of 1.7 (using a linear strain rate
correction) was established. The correlation between the actual

290

FIGURE 133   COMPARISON OF PREDICTED AND MEASURED ENGINE RESPONSE
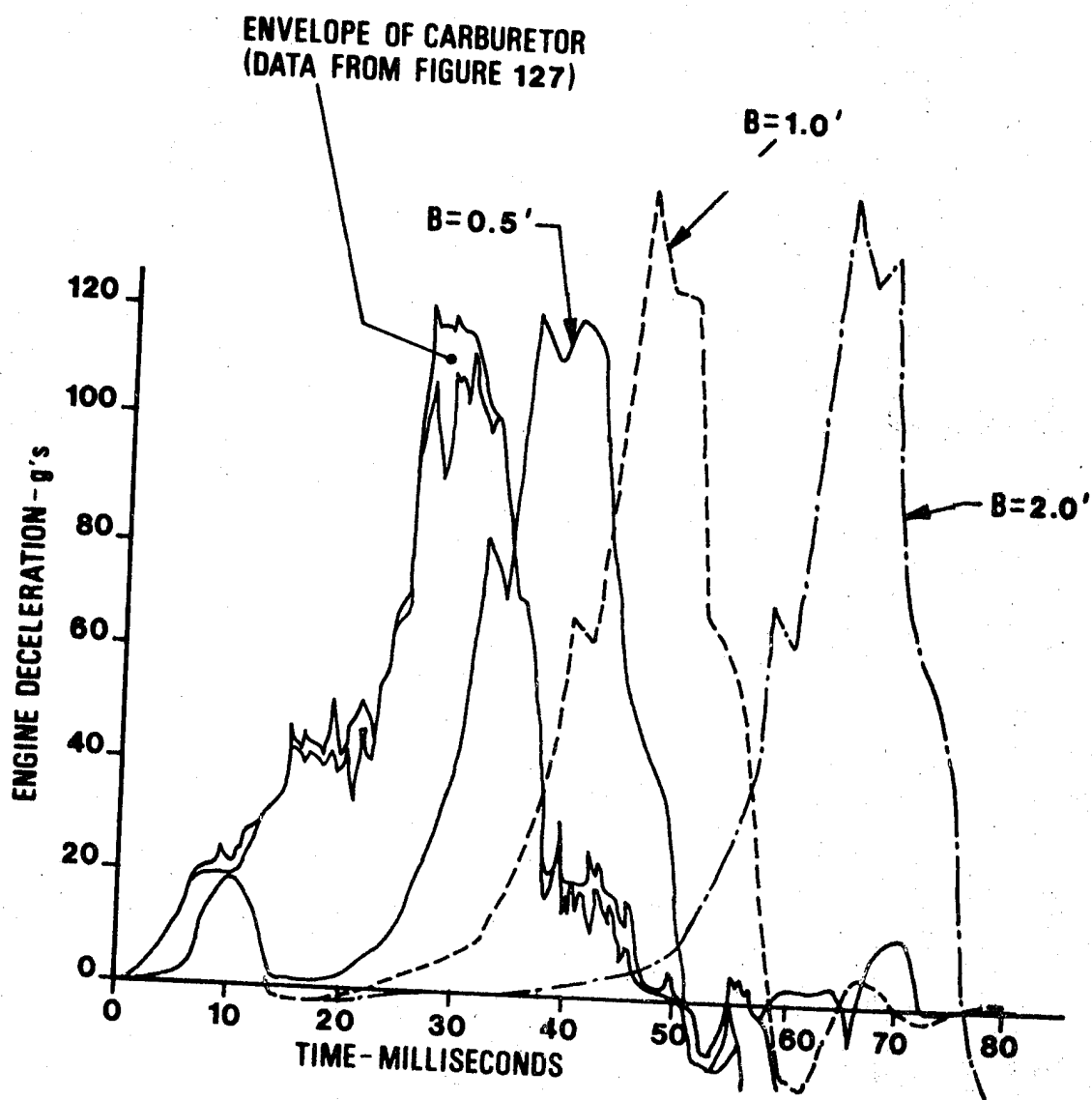
FIGURE 134   FORCE/DEFORMATION ASSUMPTIONS FOR IDEAL FRONT END STRUCTURE

SHEET METAL

F_{14}

$ENERGY_{14} = 2.409 \ F_{14}$

.667   2.742

FRONT OF FRAME

100,000

F_{11}

$ENERGY_{11} \approx 1.642 \ F_{11}$

.167   1.558   1.725

REAR OF FRAME

F_{12}

$ENERGY_{12} = 2.092 \ F_{12}$

.667   2.425

DEFLECTION - FEET

292
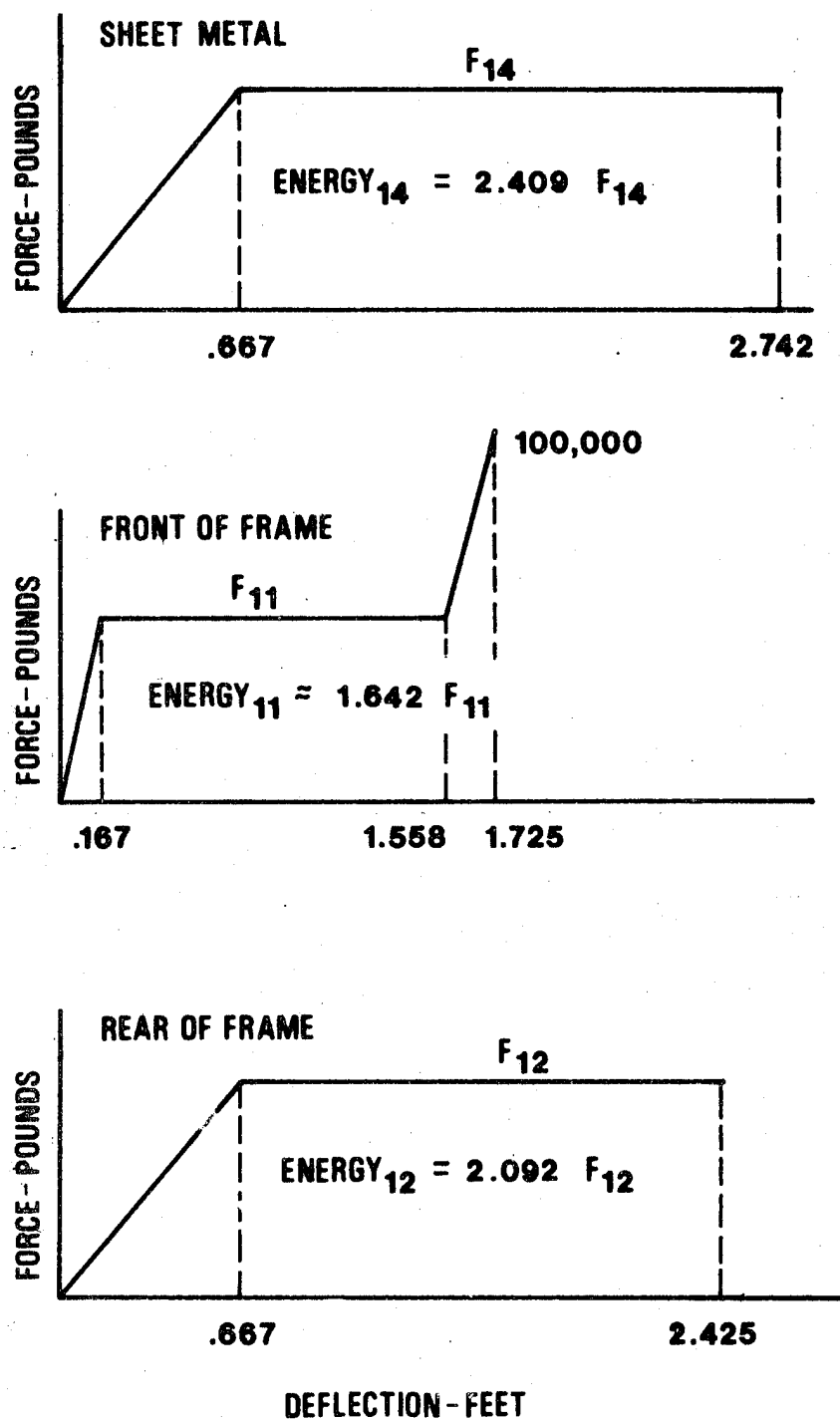
force/deformation Impala curves and the ideal situation is shown in Figures 135 through 137. The comparison for the front portion of the frame appears satisfactory while the comparisons for both the sheet metal and the portion of the frame aft of the suspension shows a significant deficiency, especially for the sheet metal. It therefore seems reasonable that these two components of the Impala structure would receive the most review during any redesign effort to improve the Impala's crashworthiness.

In an attempt to gain a better correlation between static and dynamic crush data the initial spike on the rear rails static crush data was further modified as shown in Figure 138.

The starting point of the force/deformation was shifted as shown because it was felt that the initial portion of the curve corresponds to elastic response of the whole front of the frame, and not representative of just the rear portion of the front frame.

In re-evaluating the radiator force/deformation curve, it was decided that the assumed curve should be used with a zero clearance. With these changes, the predicted compartment and engine responses are shown in Figures 139 and 140. By comparison to the curves shown previously, the assumption of the large initial spike for the rear portion of the front frame force/deformation improves the passenger compartment correlation while the use of no clearance for the radiator improves the engine correlation. Correlation to the basically unfiltered data (except for 1000 Hz) was used because some of the original filtered data was in error.

The ability to correlate with test data through the use of assumed variations in the measured force/deformation curves is not acceptable to the intent of the program. Therefore an attempt was made to acertain the validity of the assumed spike in Figure 138 and to determine if such a spike could be measured in a static crush. Investigations of inhouse data from impacting of a GM "A" frame in the area in question resulted in the typical data shown in Figure 141. Another test specimen was fabricated and statically crushed to compare the results. While the "A" frame is not exactly the same as that used in the Impala, it was thought that the geometry was close enough to evaluate the present concern. The test results were to be qualitative only because of the difference in materials used in the frame.

A static crush test of the torque box section of GM's "A" frame was performed. The test setup of the 3/8 scale model is shown in Figure 142 with the force/deformation output shown in Figure 143. The corresponding impact test result is shown in Figure 141 for a 13 mph impact speed where the data has been scaled up to full size. In scaling up the model data to full size, the deformation is multiplied by 8/3 while the force is ratioed by $(8/3)^2$. Figure 144 shows the velocity change during

FIGURE 135   CORRELATION BETWEEN MEASURED AND IDEAL IMPALA FRONT OF FRAME
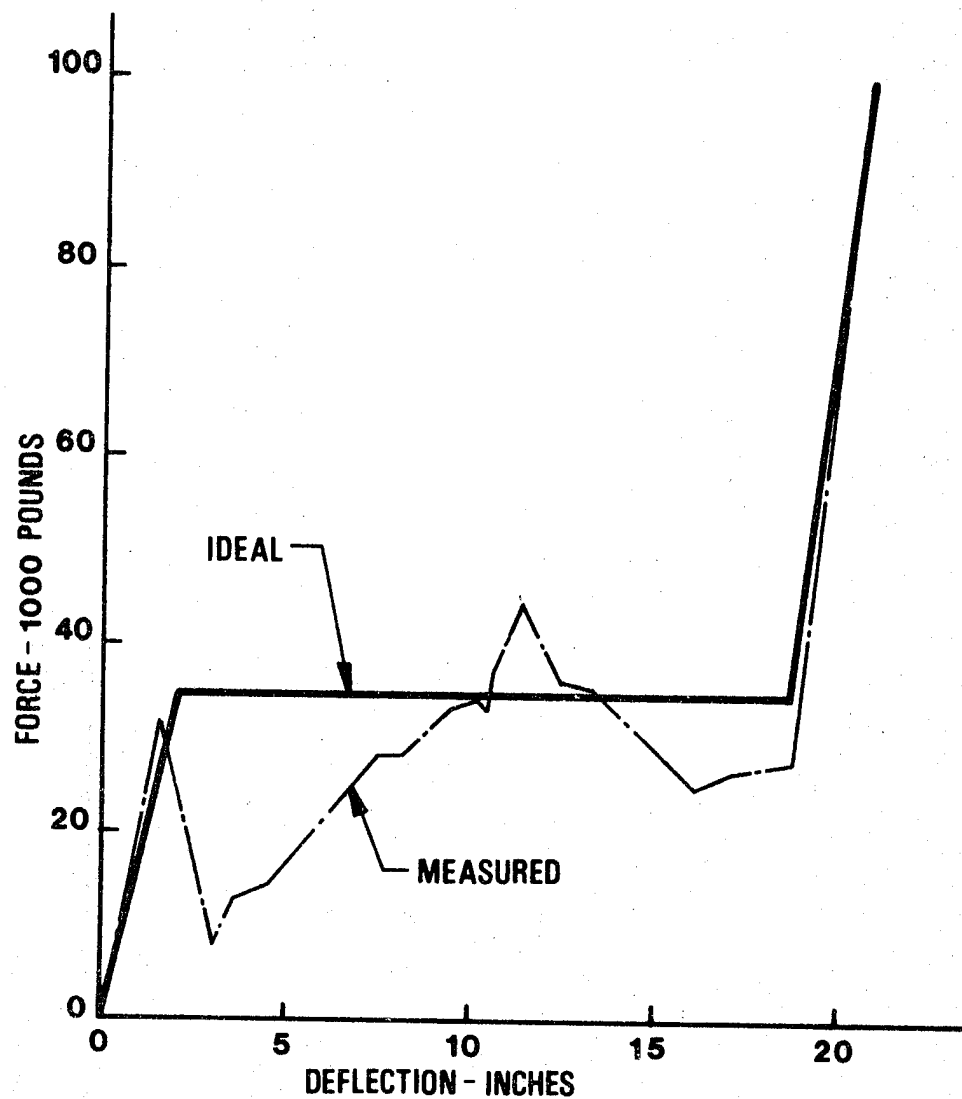
FIGURE 136   CORRELATION BETWEEN MEASURED AND IDEAL IMPALA REAR OF FRAME
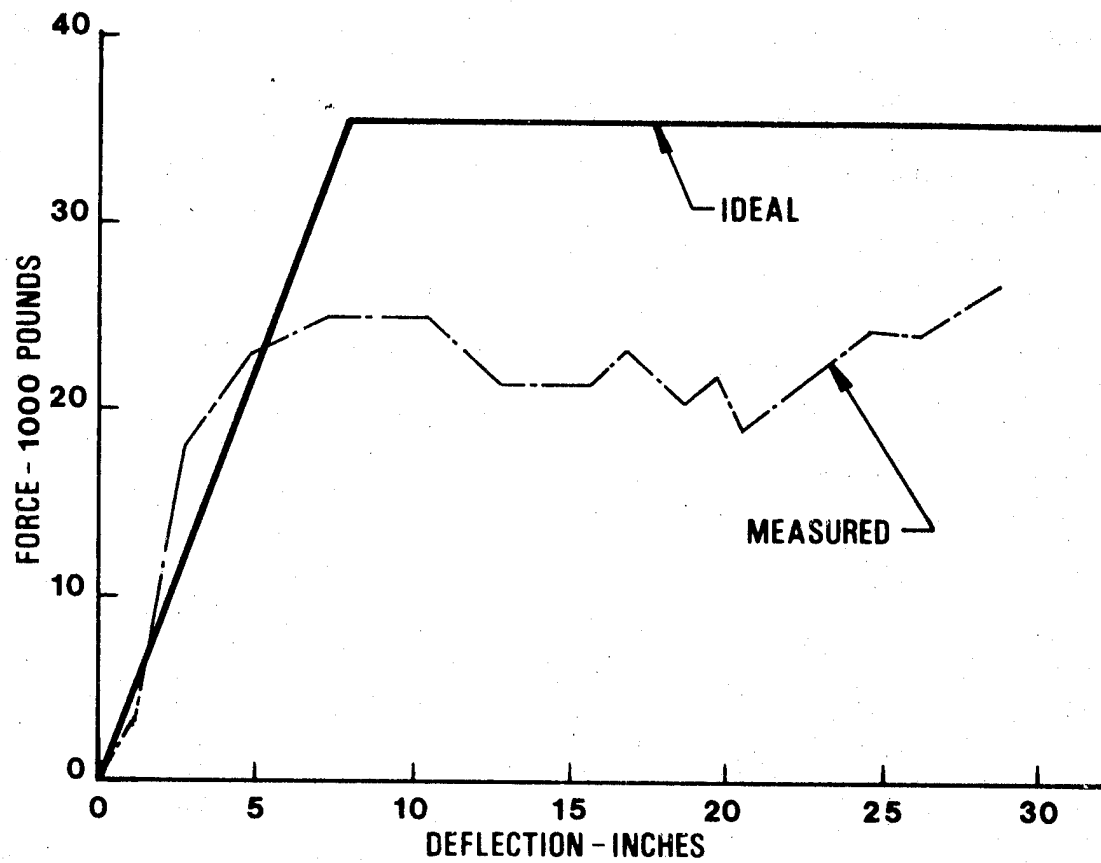
FIGURE 137   CORRELATION BETWEEN MEASURED AND IDEAL IMPALA SHEET METAL
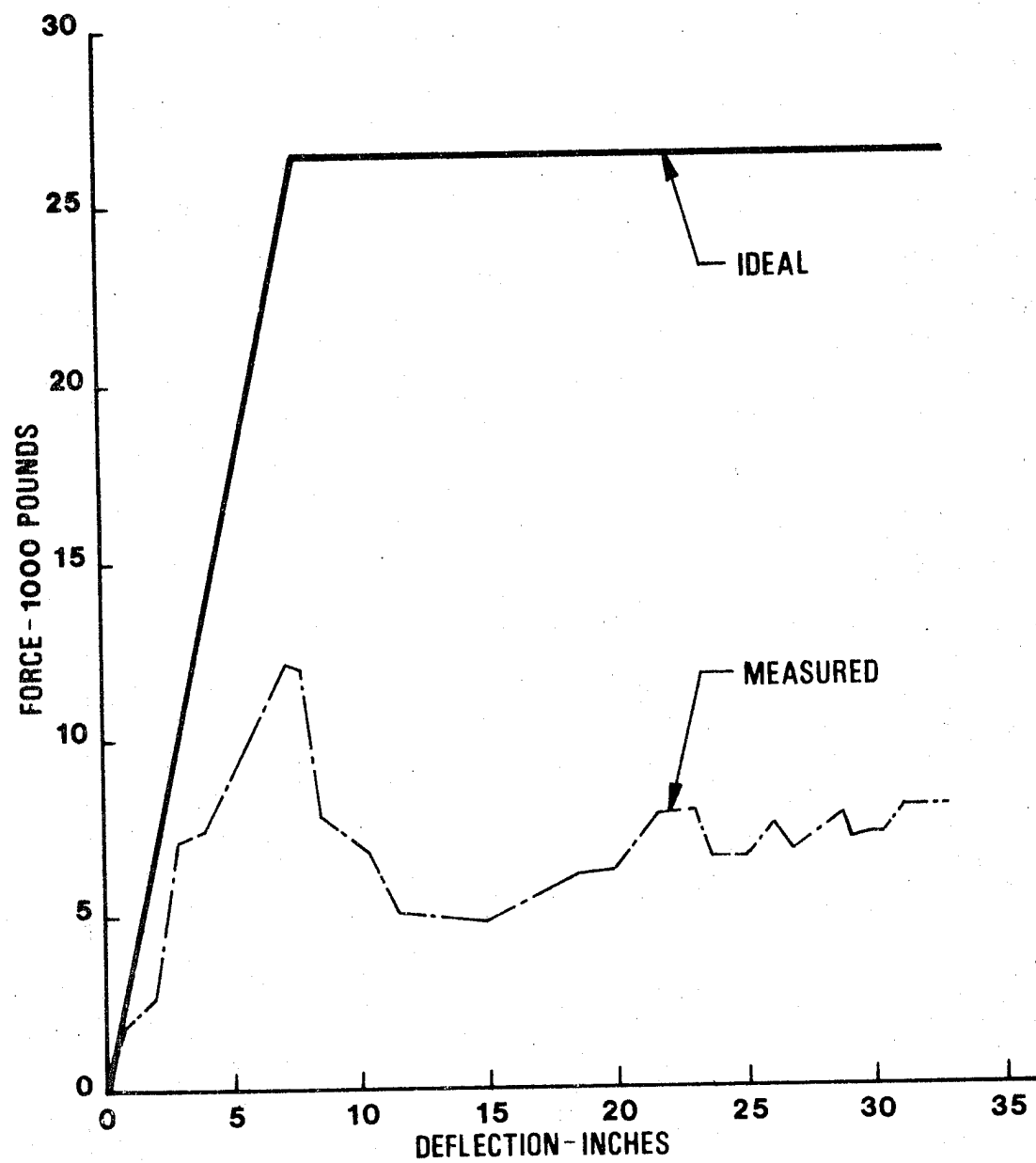
FIGURE 138   MODIFICATION OF IMPALA REAR OF RAILS STATIC CRUSH DATA
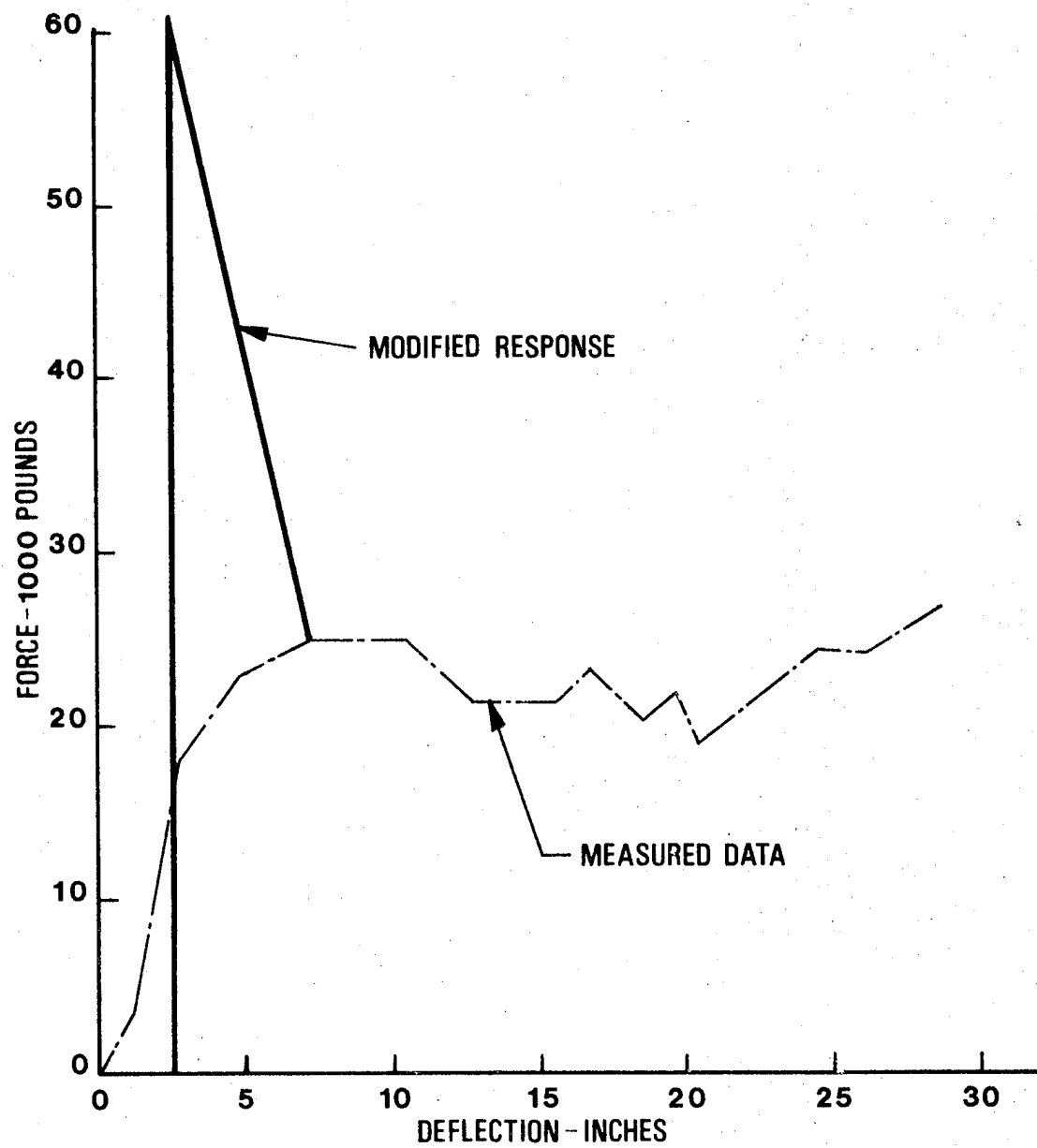
FIGURE 139   COMPARISON OF PREDICTED AND MEASURED
PASSENGER COMPARTMENT RESPONSE
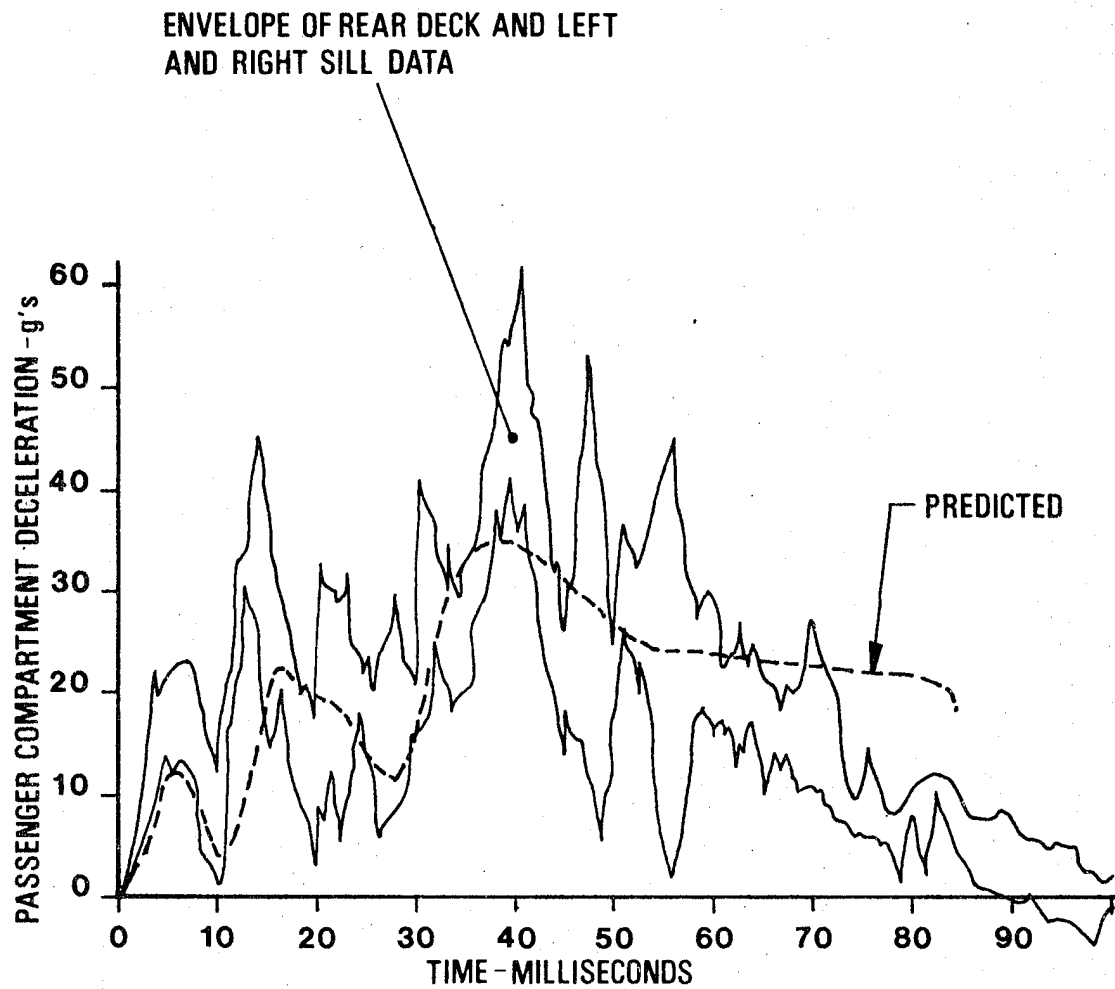
FIGURE 140   COMPARISON OF PREDICTED AND MEASURED ENGINE RESPONSE

FIGURE 141   IMPACT RESULTS FROM SCALE MODEL PROJECTED TO FULL SIZE
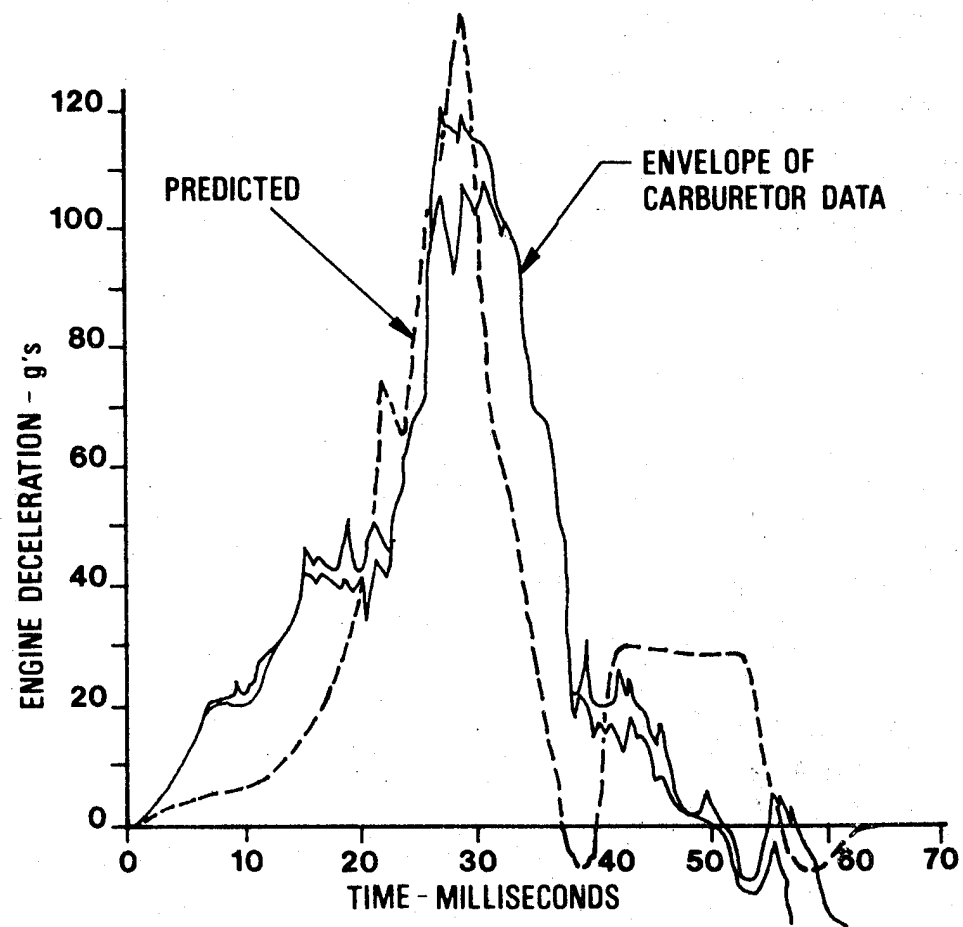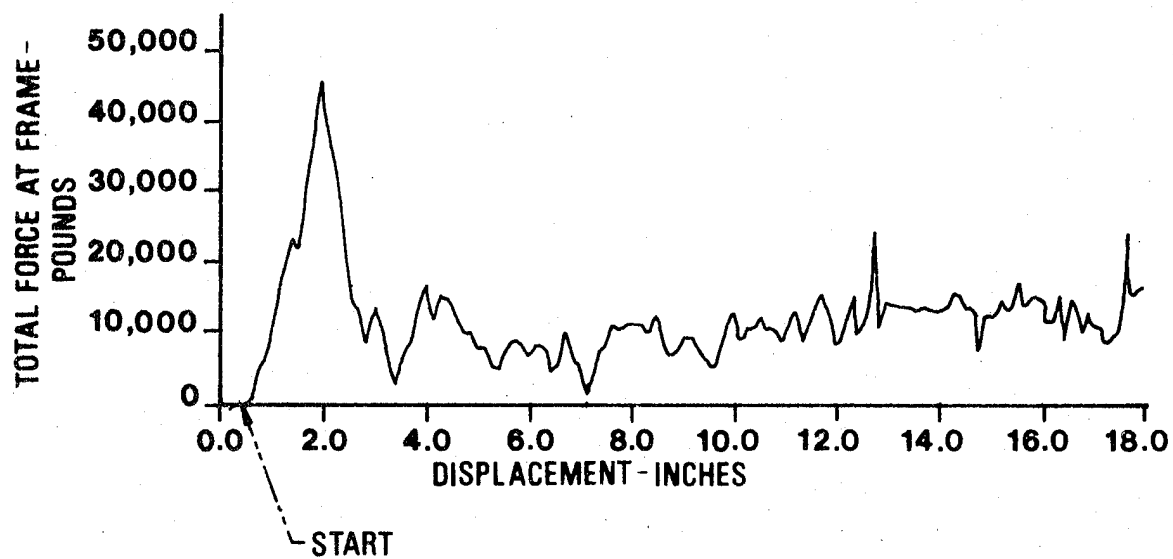
FIGURE 142   STATIC CRUSH TEST OF MODEL
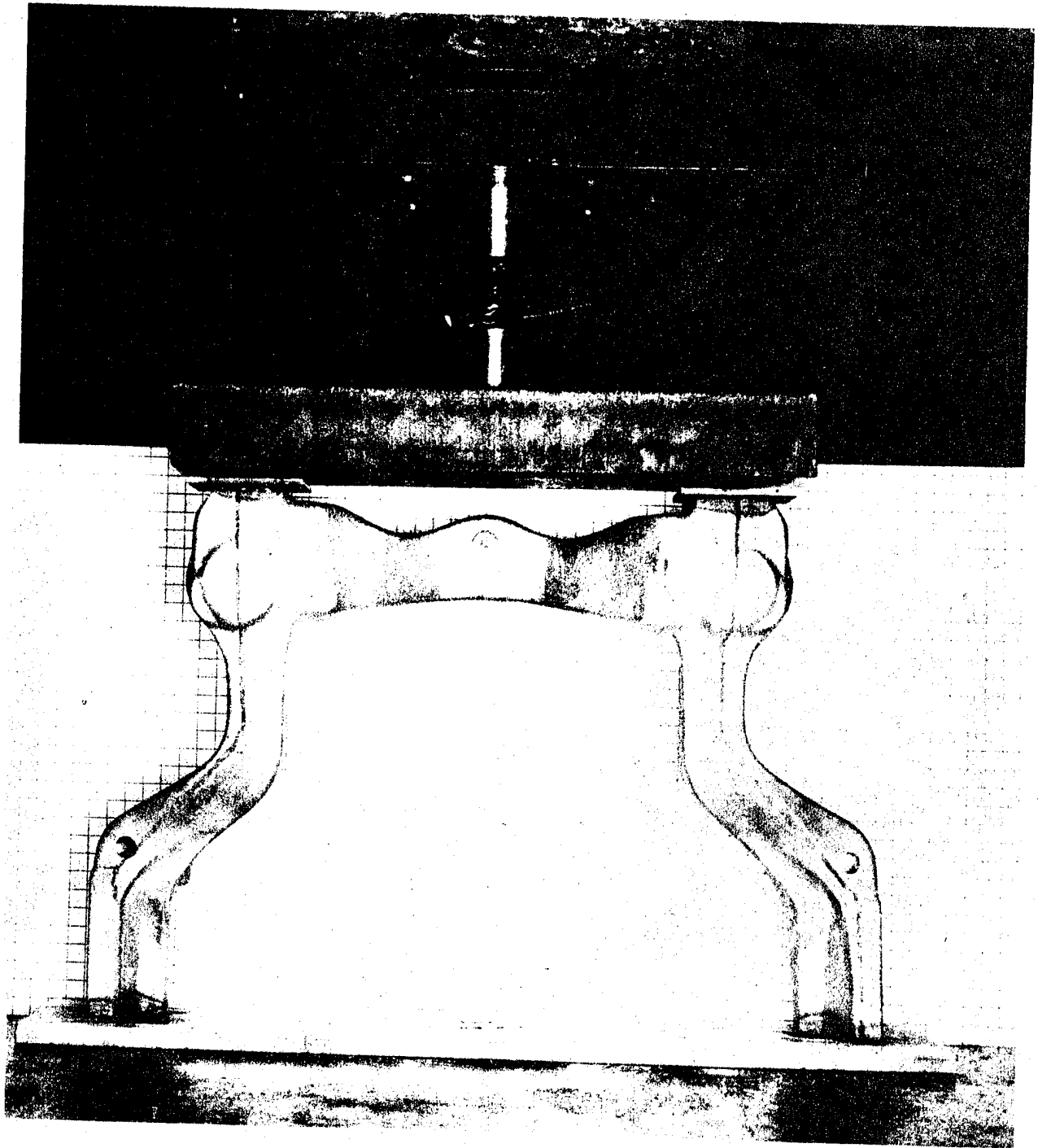
FIGURE 143   STATIC CRUSH RESULTS FOR SCALE MODEL
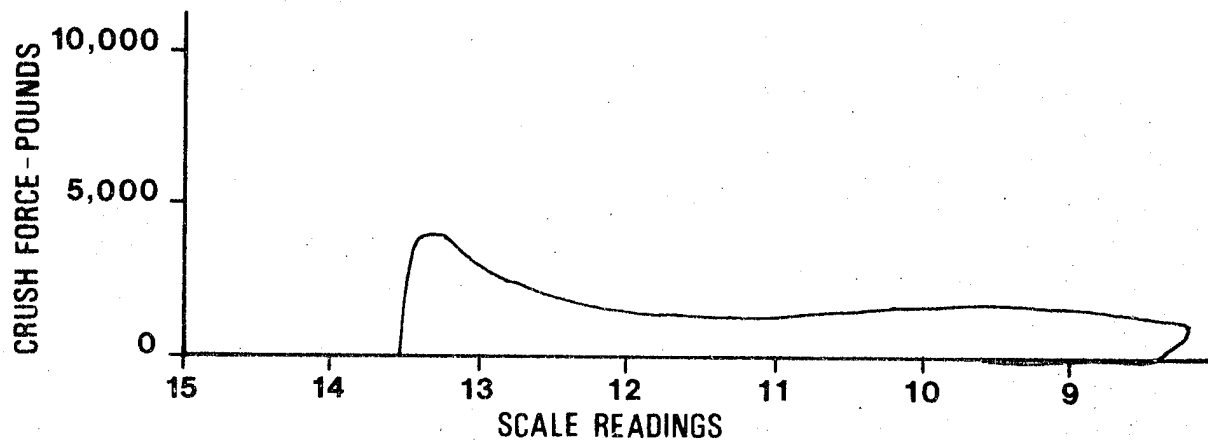
FIGURE 144   VELOCITY CHANGE DURING IMPACT TEST

303
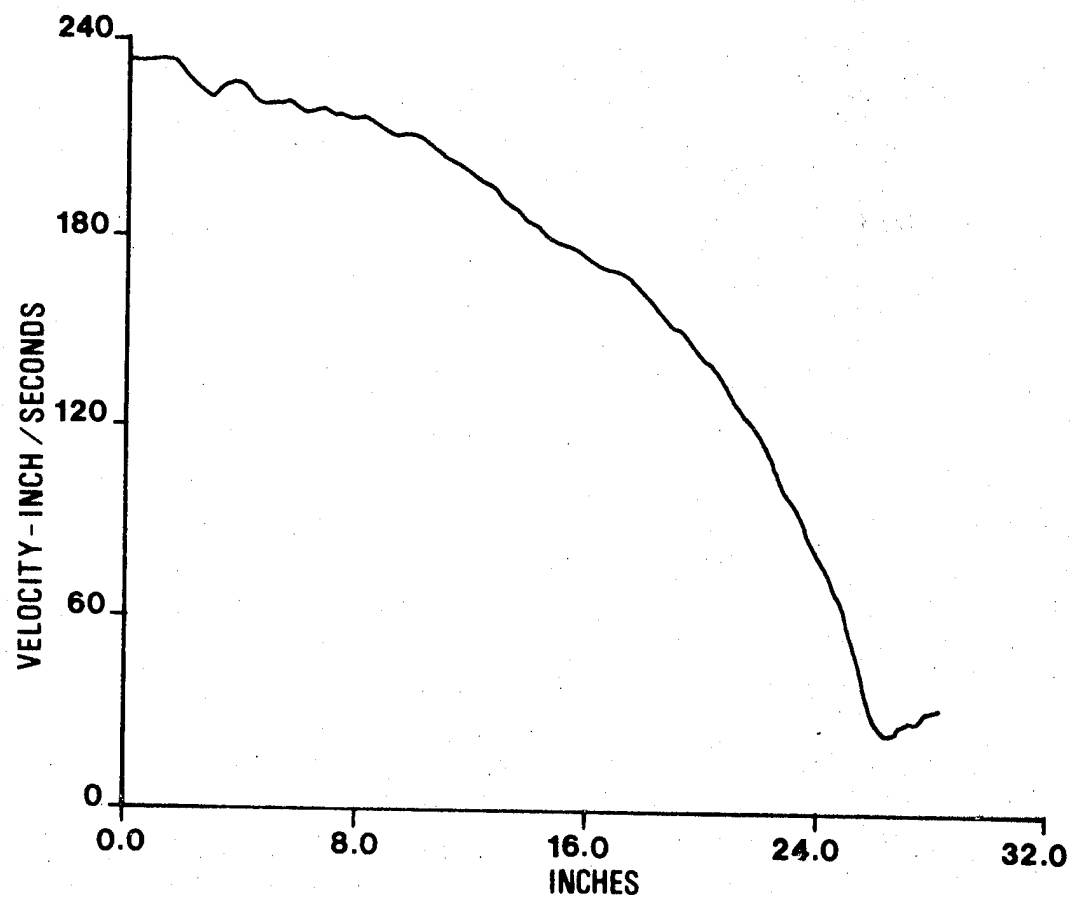
the impact test where the velocity remained relatively constant during the initial portion of deformation.

Figure 145 shows the force/deformation curve obtained by Calspan Corporation for the torque box section of the 1977 Impala frame. The initial portion of the data represents the elastic response of the previously crushed frontal portion of the frame as well as the elastic response of the torque box section. A rough estimate of 1 in. was determined from the movies to be the elastic recovery of the portion of the frame in front of the cross member. This estimate correlates with projecting the second straight line segment of the Calspan data back to zero force, which occurs at approximately 1 in. This point is then considered to be the starting point for correlating the Calspan data to the projected scale model data which is also shown in Figure 145.

Direct comparison of the scale model test results, when projected to full size, and the Impala test results is not really possible because two different frames are involved. The Impala uses GM's "B" frame while the scale model is of GM's "A" frame.

Figure 146 display's the geometric difference between the two frames involved. In terms of wall thicknesses, the scale model uses a scaled .120 in. thickness for both inside and outside halves while the Impala frame uses a .118 in. inside wall and a .110 in. outside wall. It is important to note that while the torque box portion of the frame is weaker for the "A" frame compared to the "B" frame, the scale model yields a higher peak force than the test result shown for the Impala frame. Also of interest is the fact that the peak occurs extremely early in the crush history of the scale model test. A possible explanation for this last difference is that the Calspan crush test is a load incremental one while the scale model was a continuously increasing load to the peak.

The purpose of the scale model static test was two-fold: First, a direct comparison was to be made with the scale model impact results to try and establish whether or not an initial peak exists dynamically which cannot be explained by applying a strain rate correction factor to the static data. Secondly, the relative response of the scale static crush compared to the Impala crush is important in evaluating whether the torque box force/deformation curve could be correctly portrayed from segmented barrier test data.

The strain rate correction factor, determined from data such as that of Reference 93 is based on absorbed energy for an arbitrary crush length (6 inches was used) for regular, smooth circular or square cross section elements. Applying this procedure to the present static and dynamic scale model tests shown in Figure 147 leads to the conclusion that the effective strain rate correction factor for the torque box segment is approximately one, and should be compared to Figure 127.

304

FIGURE 145   STATIC CRUSH RESULTS FOR 1977 IMPALA TORQUE BOX

"A" FRAME (SCALE)

"B" FRAME (IMPALA)
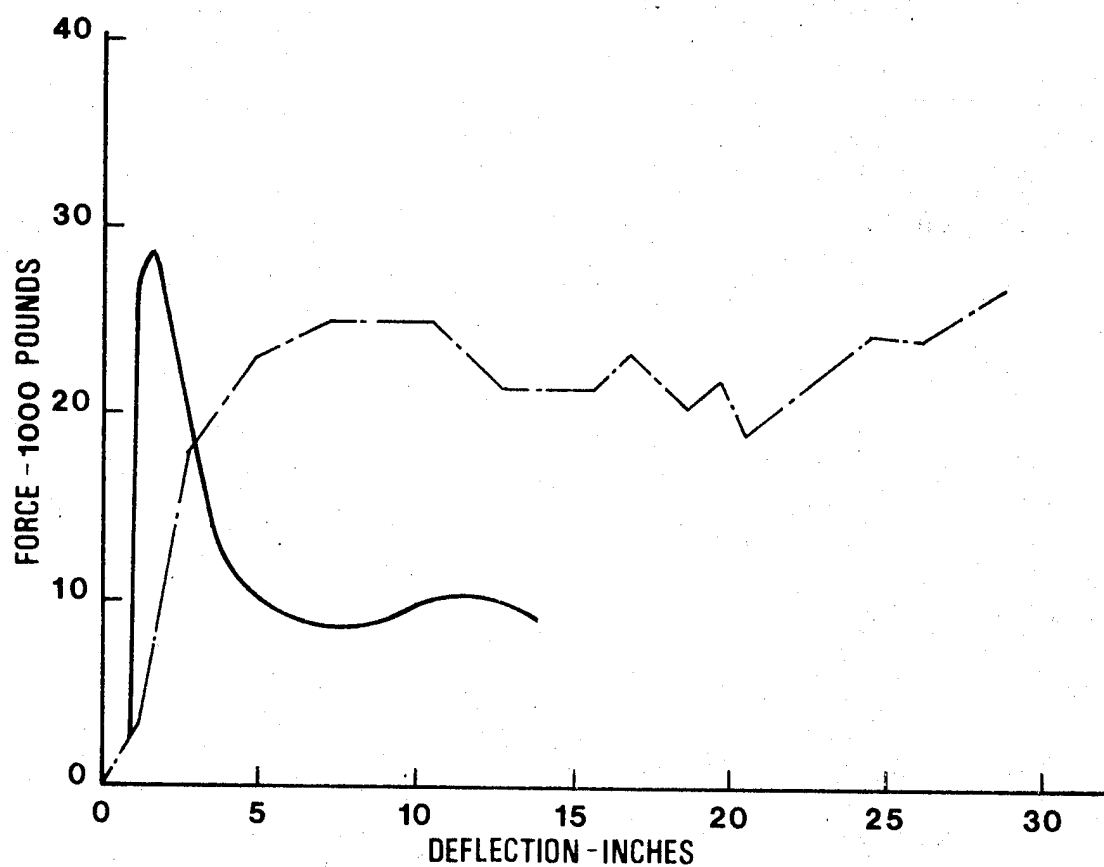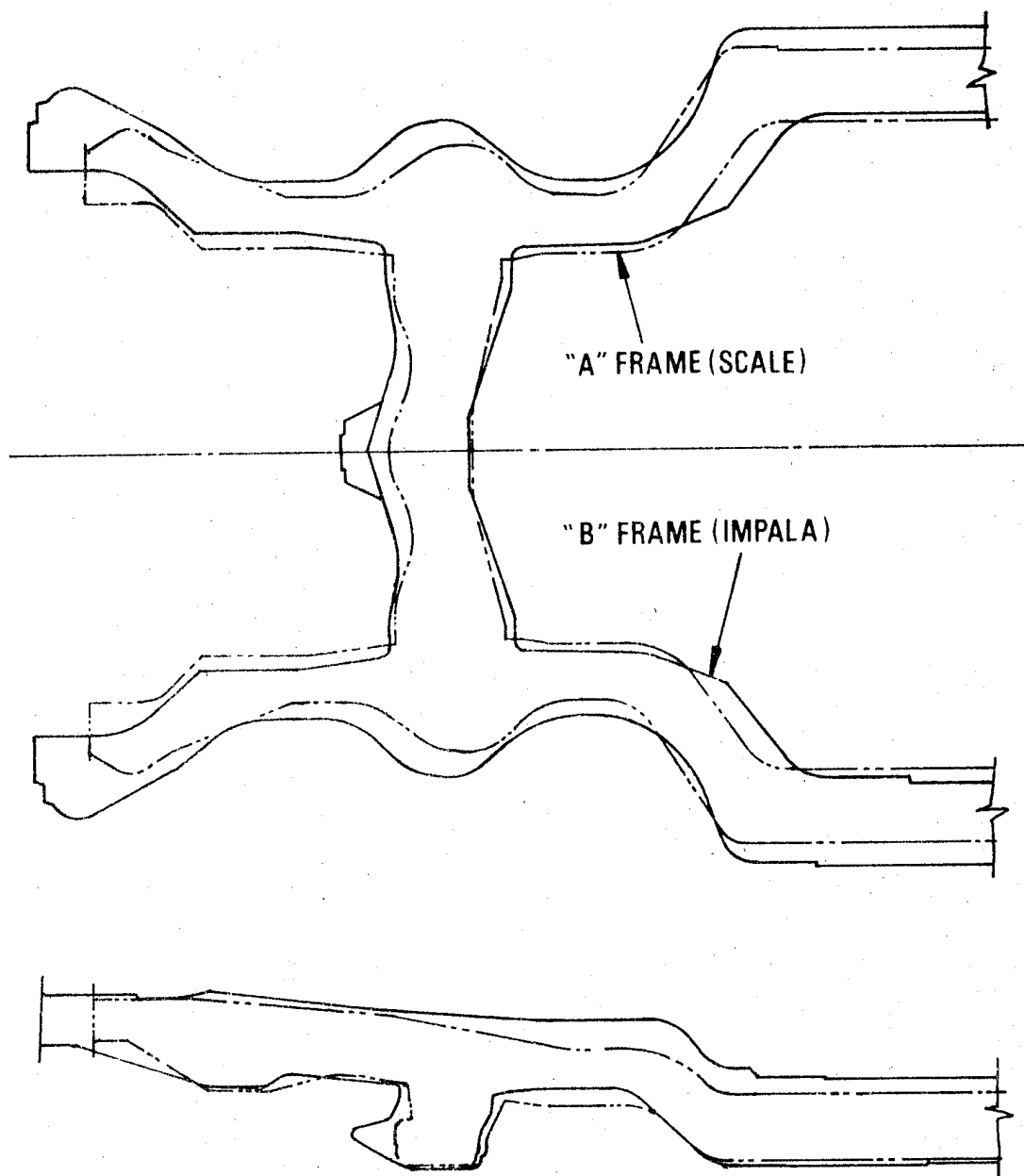
FIGURE 147   COMPARISON OF STATIC AND IMPACT CRUSH RESULTS FROM SCALE MODEL PROJECTED TO FULL SIZE

Other factors should be considered which may explain or cloud the issue further. Tensile testing of carbon steels and HSLA steels, Reference 94 and 97 , indicate a strain rate effect at all speeds of testing. However, the strain rate factor used is not an absolute increase in static yield or static ultimate strength but rather a ratio of the yield to dynamic yield and static ultimate to dynamic ultimate strengths. Thus the increase in strength in dynamic testing of two steels might be the same but for an initially higher strength steel, the factor is of course smaller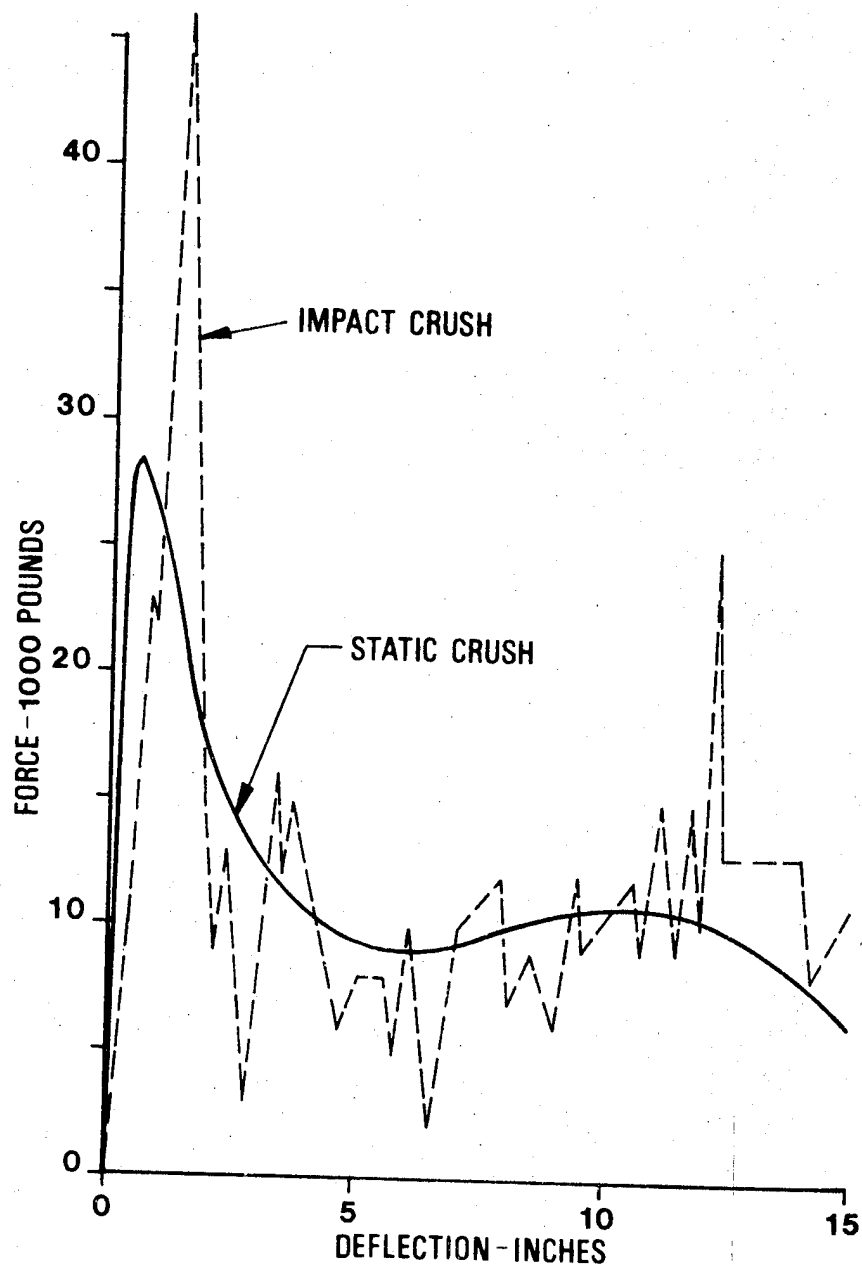. The crushing strength (also crippling strength) of a columnar element is dependent upon the yield strength of the steel used.

The yield strength will vary depending upon the grain size, chemistry and prior mechanical working. To determine what variation might be found in such steels in current production, test data from formability studies of frame steels conducted at the Budd Company Technical Center were reviewed. Material obtained from three suppliers of frame steel was tensile tested. All three heats of material had properties in excess of that required for the part. The test properties are shown in Table 71 for the as received material.

During the fabrication of frames, various deformations occur which work harden the materials. One such operation is to "edge bend" which allows a normally straight strip to be used to fit the contour of the frame before flanging. This "edge bending" work hardens the strip as shown in Table 72 . The specimens for these tests were taken at similar locations of the edge bent strips. The materials and suppliers of Table 72 are the same as those in Table 71 .

The two materials listed in Table 71 and Table 72 were not purchased for use in the GM "B" frame, but are listed only to show variations in properties which might occur in hot rolled frame steel. This variation in properties would result in a variation of crush test results or response to a collision.

Another factor which is thought to be responsible for variations in test results is that of structure similarity. This has not been proven nor conclusively demonstrated but the strain rate factor may not be the same for smooth circular cross section elements, smooth rectangular cross section elements and irregular shaped elements such as frames. Scale modeling would appear to be an acceptable procedure with a control of the material properties.

Further efforts to understand the Impala crush characteristics used the mass model program with General Motors' component force deformation curves. The General Motors' data was obtained from their document, Research Publication GMR-1943 entitled "Computer Simulation of Vehicle-to-Barrier Impact - A User's Guide" by K. Lin, J. Augustitus, and M. Kamal. While the example cited in the report does not actually indicate that the

TABLE 71 :   VARIATION OF TENSILE PROPERTIES OF FRAME STEELS

Supplier	0.2% Yield Strength	Ultimate Strength	Test Direction
1	30,900 30,900	47,700 47,200	L T
2	38,600 40,200	56,300 56,200	L T
3	35,500 35,900	51,100 50,300	L T

Average of three tests for each value.

L   Parallel to rolling direction

T   Transverse to rolling direction

TABLE 72:   EFFECT OF EDGE BENDING ON TENSILE PROPERTIES

Supplier	0.2% Yield Strength	Ultimate Strength	Test Direction
1	49,600 48,300	57,900 54,100	L T
2	57,400 57,800	65,200 69,700	L T
3	66,900 53,900	69,100 63,200	L T

force/deformation curves Figures 148 through 155 are for an Impala, it is believed that they represent the full size Impala, prior to being downsized in 1977. The force/deformation curves generated by Calspan's testing of the downsized 1977 Impala are also shown. Even though there is a size and weight difference between the two cars, it was decided to run the computer simulation using the General Motors data since reasonable agreement is observed between most of the two data basis. Significant differences exist for the sheet metal, Figure 148, and for the torque box frame area, Figure 150 where General Motors develops an initial force peak similar to Figure 143. It is this force peak which is the subject of the previously mentioned 3/8 scale model test. It is important to note that General Motors' testing consisted of individual component tests while the Calspan data was obtained from the static crush of a complete car using 5 piece segmented barrier.

The results of running the computer simulation model using General Motors' data for the front and rear portion of the frame and the sheet metal, while leaving the other component force/deformation curves unchanged, is shown in Figure 156 and 157. Using the General Motors data, the correlation is, however, still poor.

As a backup to the static test of the 3/8 scale model frame test, the development of a computer program to investigate large dynamic structural deformations was completed. For the Impala's torque box section of the frame, the computer prediction yields an effective static peak of 136,000 pounds. Deformation of the cross section was ignored because of empirical relationship is not presently known for the full size frame. Some studies performed by General Motors have indicated that for scale models, the peak load predicted by the computer could be reduced in the neighborhood of 25% with the inclusion of the frame deformation. Since the computer solution is a numerical one, the determination of this peak load is hard to establish, but it occurs almost instantaneously.

Figure 158 presents the computer prediction of the deformed shape 0.005 seconds after impact, which is after the peak load has occured. While both ends could have been considered to be fixed for this run, instead of fixed/simply supported, other studies have indicated that the peak load, because it occurs very early is relatively independent of the fixity condition of the impacted end. A simplified buckling approach was taken to evaluate if the computer simulation gave a reasonable solution. The results, Figure 159, yield an axial force of 153,000 lbs. which would be reduced with the application of the axial load component.

FIGURE 148   STATIC FORCE—DISPLACEMENT CURVE OF SHEET METAL

312
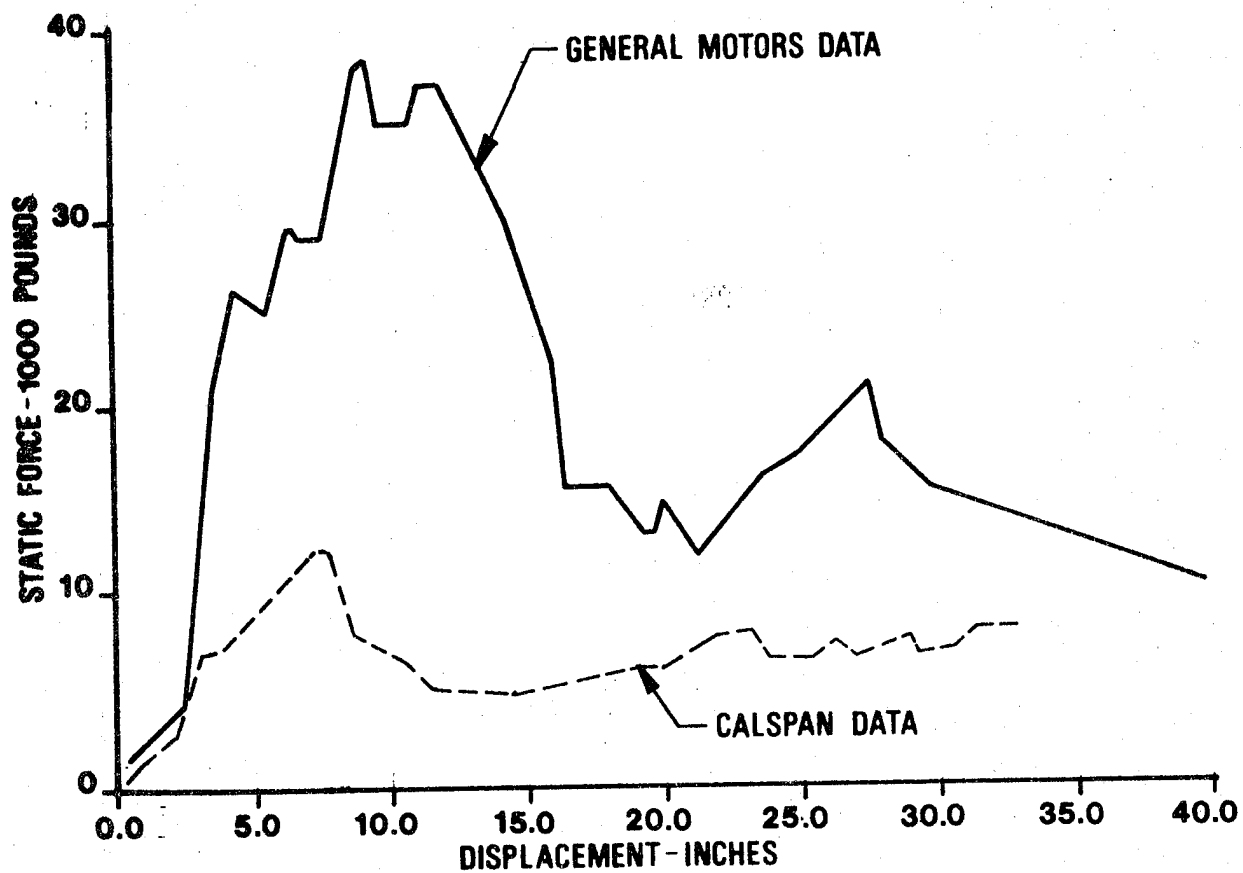
FIGURE 149   STATIC FORCE—DISPLACEMENT CURVE OF FRONT FRAME
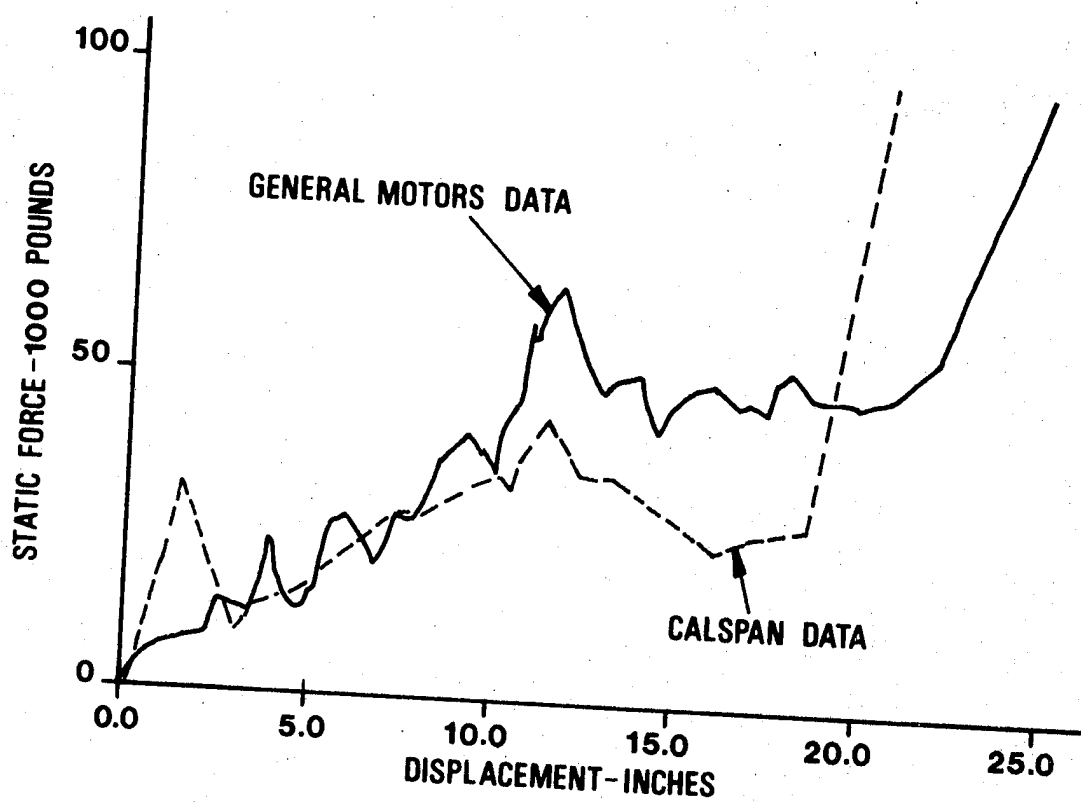
FIGURE 150   STATIC FORCE—DISPLACEMENT CURVE OF TORQUE BOX
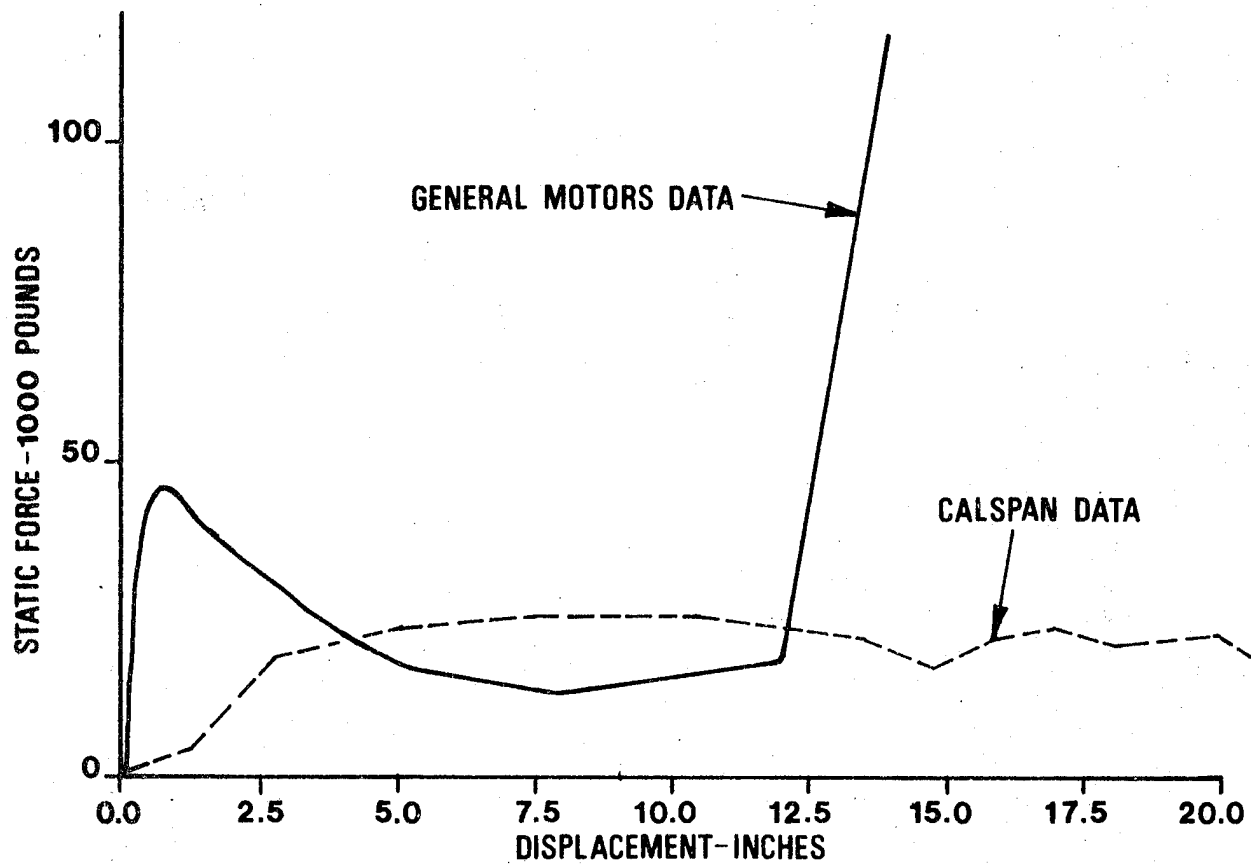
FIGURE 151   STATIC FORCE–DISPLACEMENT CURVE OF FIREWALL

315
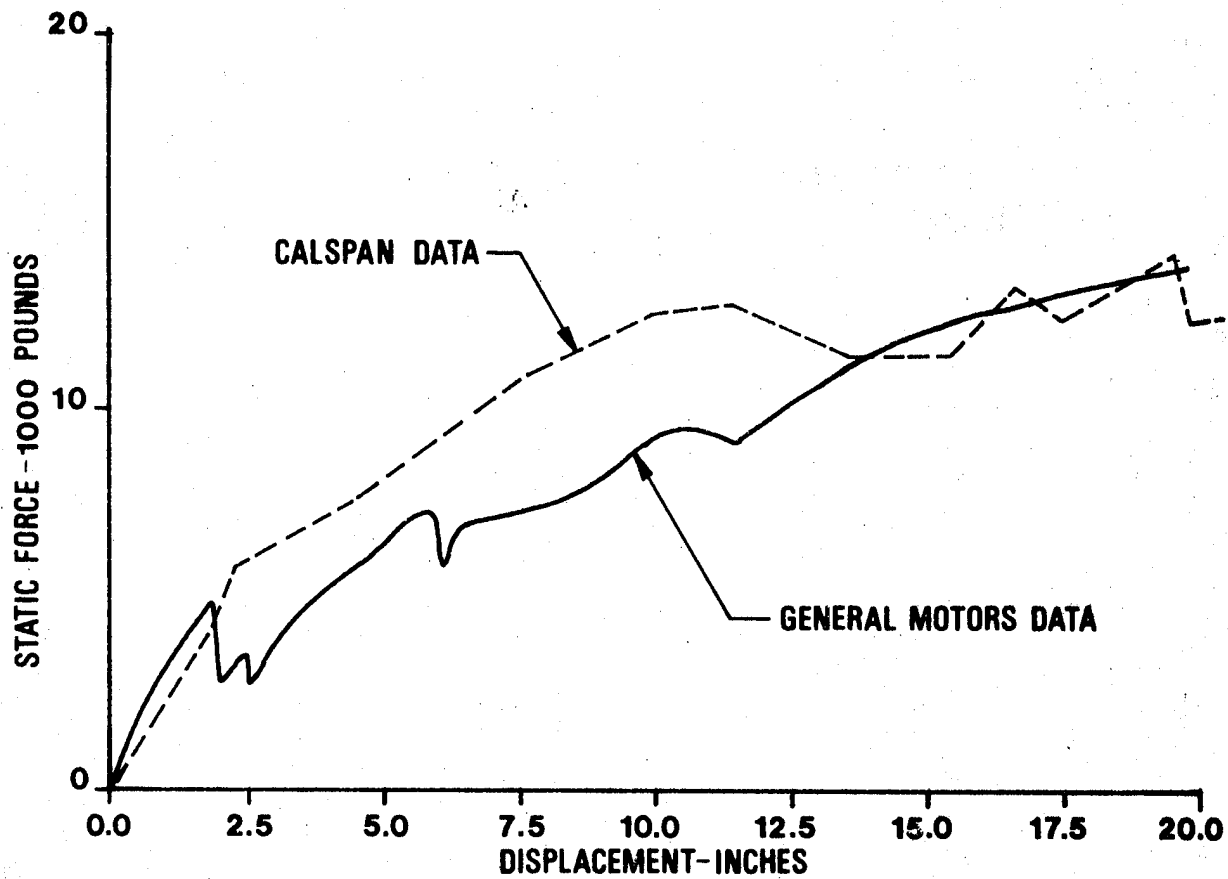
FIGURE 152   STATIC FORCE—DISPLACEMENT CURVE OF RADIATOR

CALSPAN DATA

316
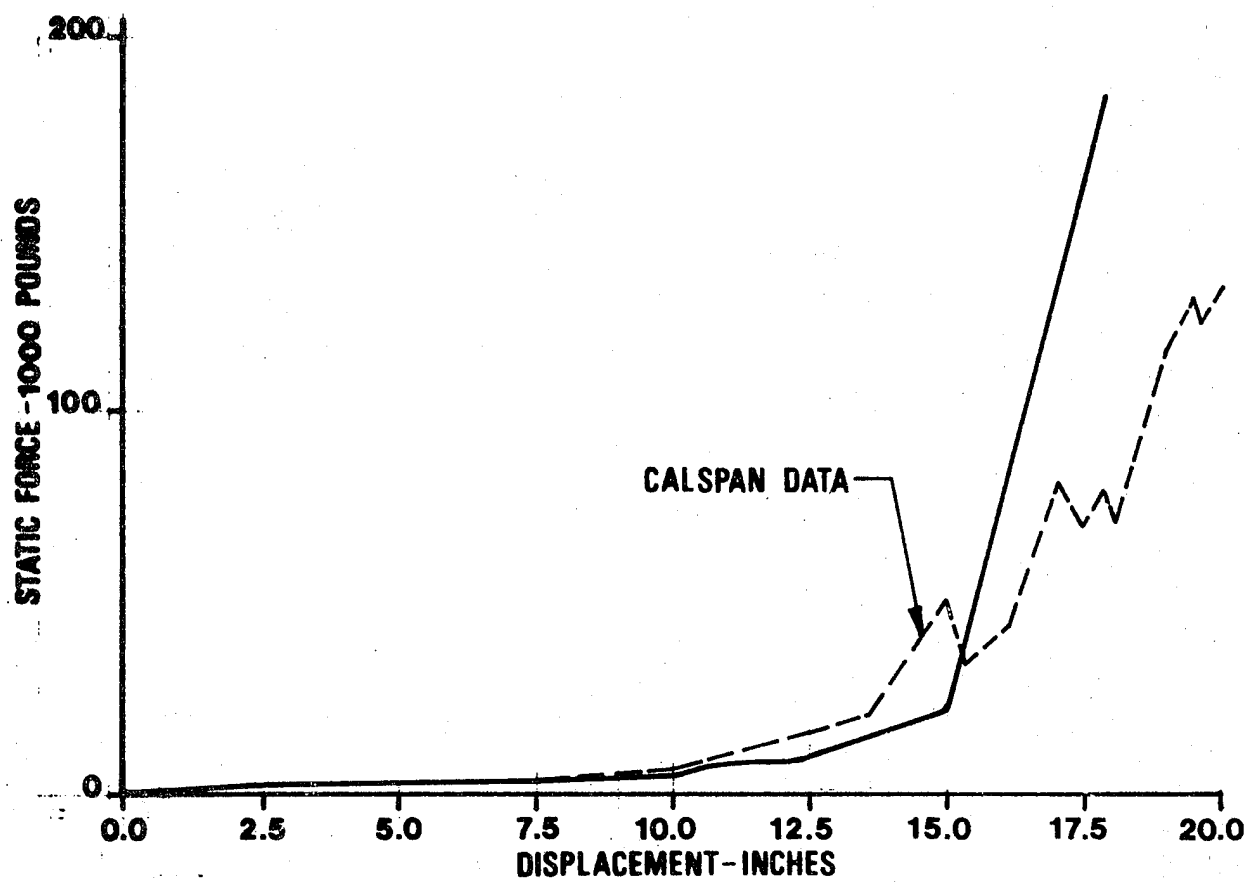
FIGURE 153   STATIC FORCE—DISPLACEMENT CURVE OF DRIVELINE
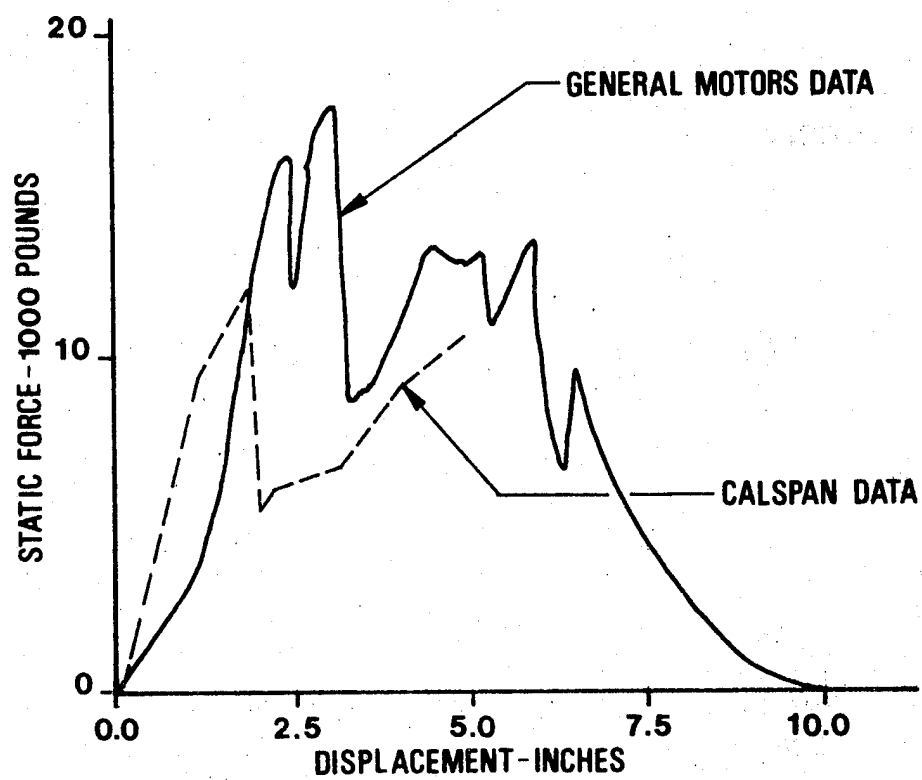
FIGURE 155   **STATIC FORCE—DISPLACEMENT CURVE OF ENGINE MOUNTS REARWARD**
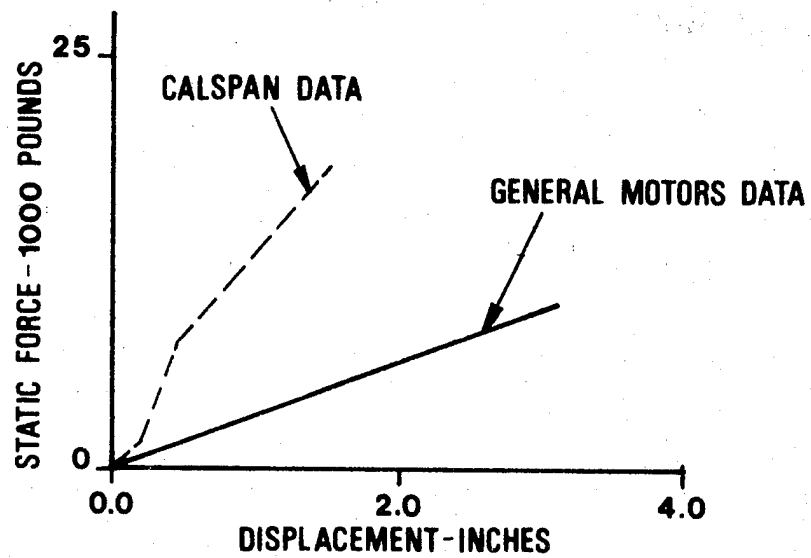
FIGURE 156   PREDICTION OF PASSENGER COMPARTMENT RESPONSE
USING GENERAL MOTORS DATA
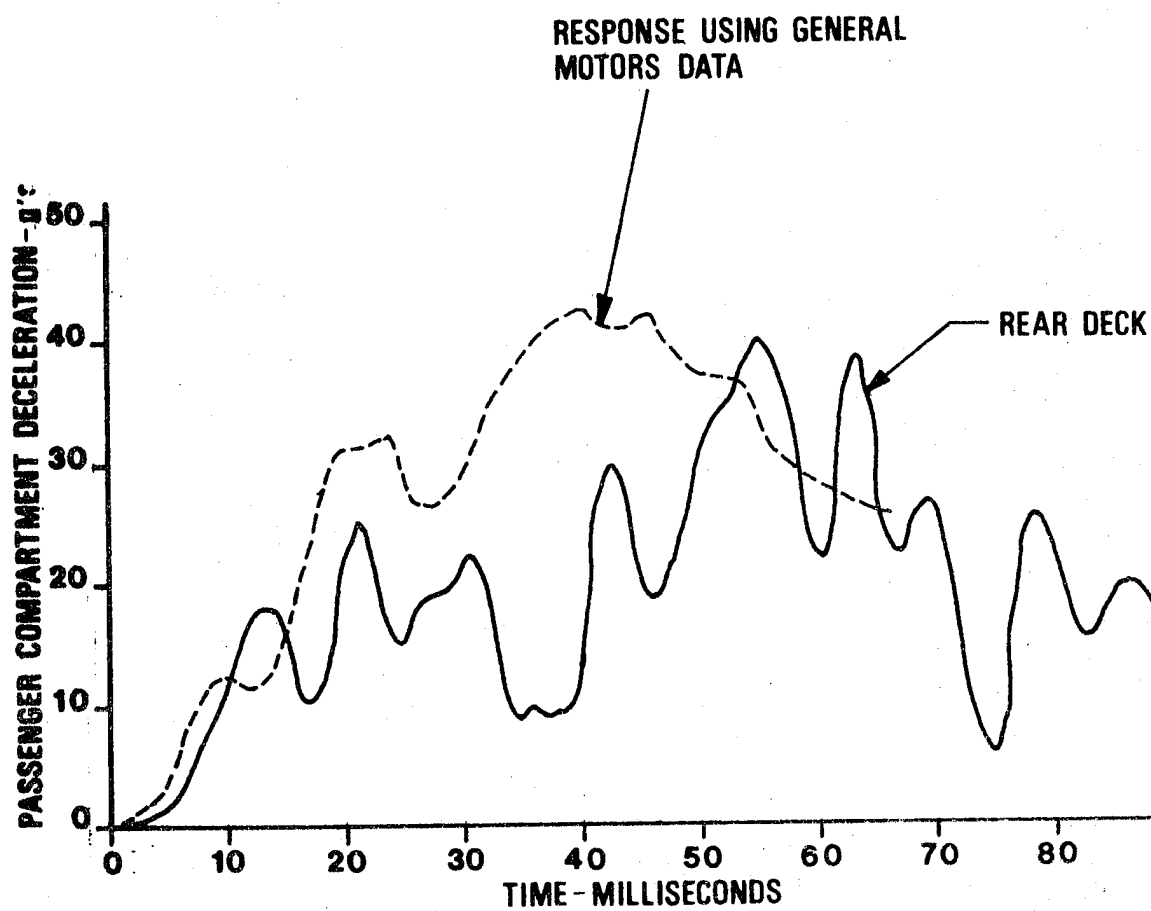
FIGURE 157   PREDICTION OF ENGINE RESPONSE USING GENERAL MOTORS DATA

321
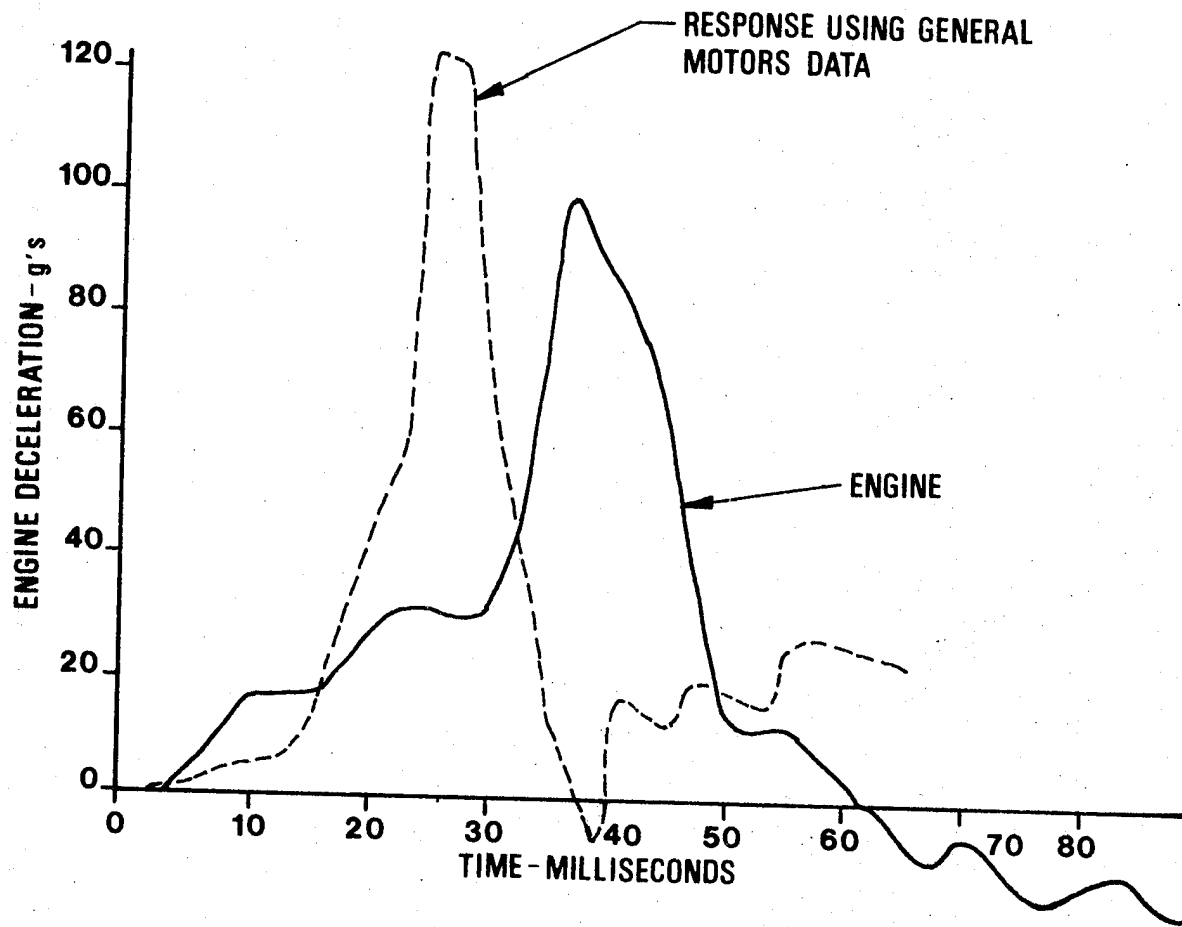
FIGURE 158   1977 IMPALA TORQUE BOX RESPONSE

322
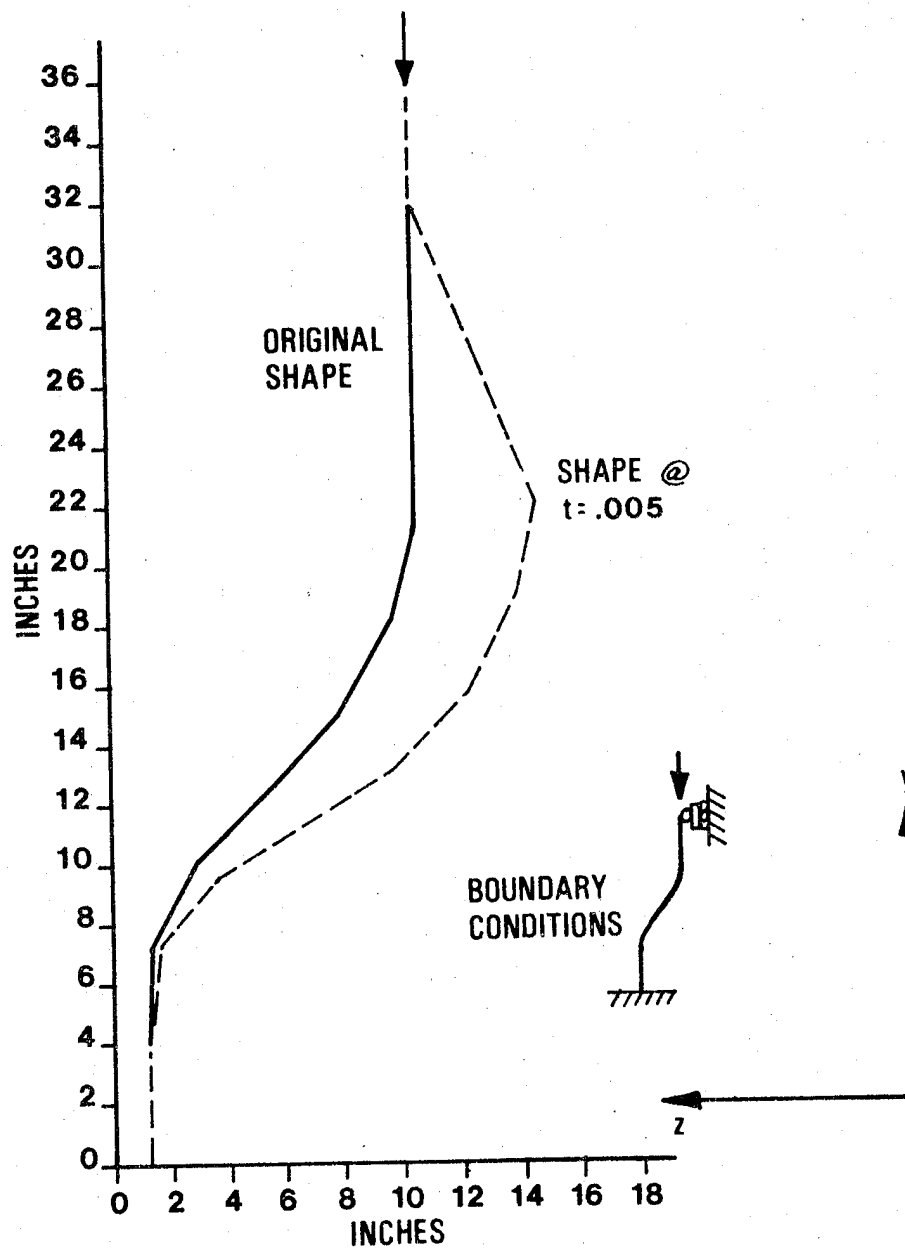
FIGURE 159   PEAK FORCE FOR AFT PORTION OF IMPALA FRAME

CONSIDER THE FOLLOWING SIMPLIFIED STRUCTURE:

CRITICAL SECTION
BY SYMMETRY
WHERE $M = \left(\dfrac{9.387}{2}\right) P$
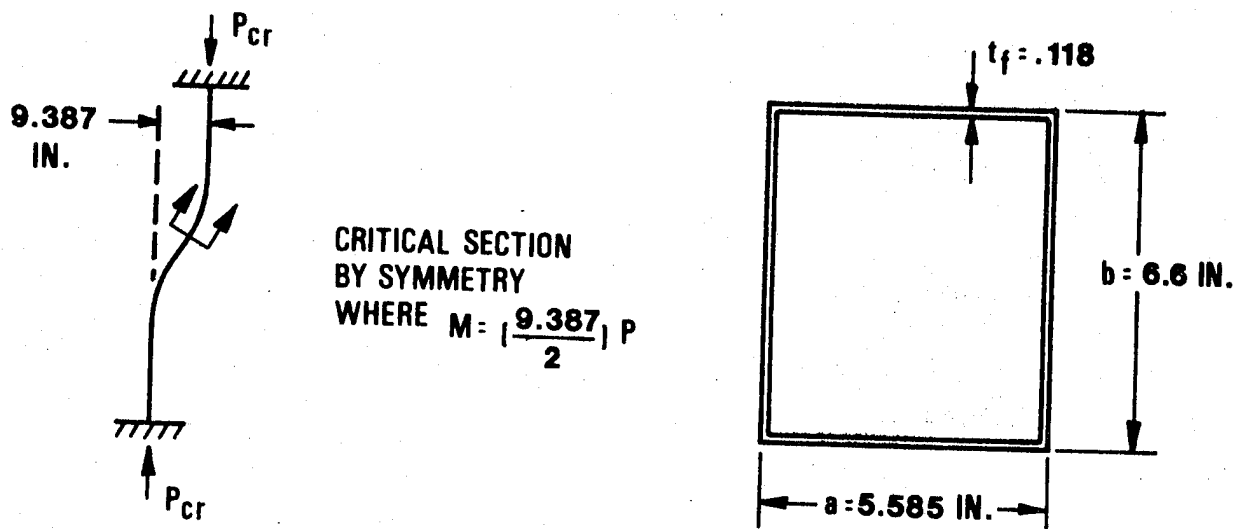
FROM THE REFERENCE:

$$M_{cr} = k \left(\frac{2 I \pi^2 D_f}{b a^2 t_f} \right)$$

WHERE

$$D_f = \frac{E t_f^3}{12(1 - 2^2)} = 4514$$

$M_{cr} = (9.387)(P_{cr})(1/2)$
$I = 19.57$

Reference: "The Local Buckling of Box Girders Under
Bending Stresses," by T. R. Graves Smith,
published in the International Journal of
Mechanical Sciences, 1969.

323

FIGURE 159   CONTINUED

k IS DETERMINED FROM THE FOLLOWING FIGURE
TAKEN FROM THE REFERENCE:
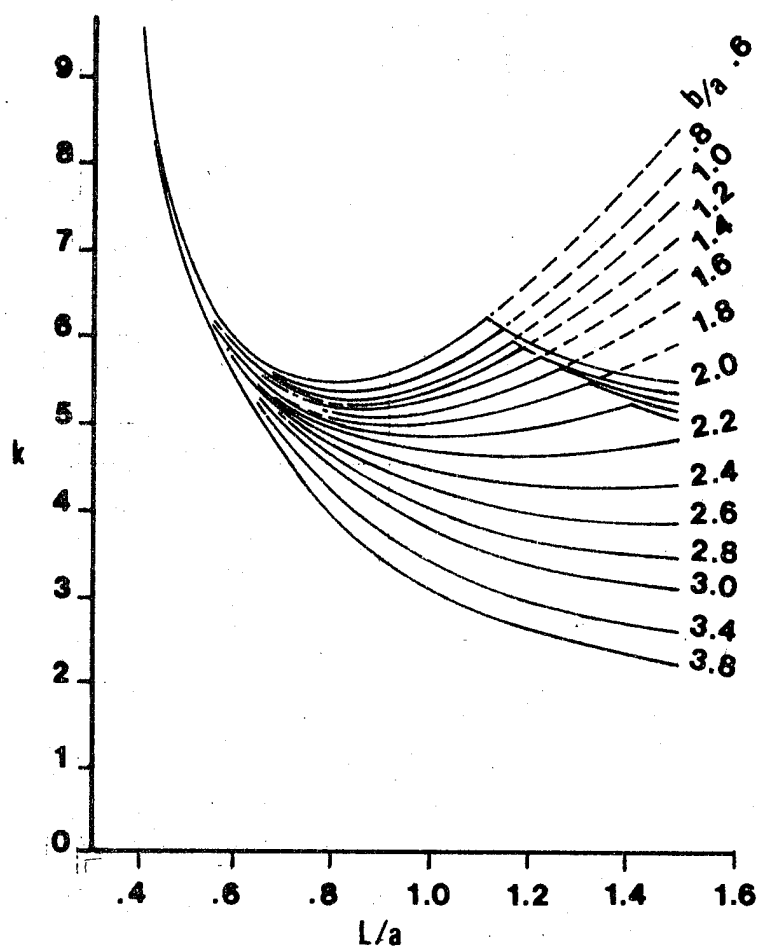
$b/a = 1.13$
ASSUME $L/a = 1$
$\Rightarrow k = 5.5$

$$(1/2)\,9.387\ P_{cr} = 5.5 \left[\frac{(2)(19.57)(\pi^2)(4514)}{(6.6)(5.85)^2\,(.118)} \right] = 359,837$$

$$P_{cr} = 76,667 \text{ POUNDS}$$

FOR BOTH SIDES OF THE FRAME
$P_{peak} = 153,000$ POUNDS vs $136,000$ POUNDS FROM COMPUTER

7.2 Fuel Containment

A 1977 Impala was tested by Dynamic Sciences, Inc. for the U. S. Department of Transportation, National Highway Traffic Safety Administration under Contract No. DOT-HS-6-01479. The test was conducted on May 3, 1977 to determine compliance with the FMVSS 301-75 Standards Enforcement Test. The summary of the test results as reported are quoted:

"3.0 SUMMARY OF TEST RESULTS

3.1 MOVING BARRIER GUIDANCE AND IMPACT

A steel follower shoe riding on the monorail guided the moving barrier into the test vehicle. The follower shoe is detached from the moving barrier just prior to barrier impact. The impact speed was 28.98 mph, based on breakwire speed traps located within 5 feet of the impact point. The required speed range at impact is 29.4 ± 0.5 mph.

3.2 FUEL SYSTEM NON-COMPLIANCE DETAILS

No fuel spillage occurred during or following barrier impact. However, as indicated in the Fuel System Integrity Post-impact Test Data Sheet presented following Section 3.4, some fuel spillage occurred during the rollover. The amounts of spilled fuel were well below the FMVSS 301-75 criteria and thus the vehicle appeared to comply with the requirements of FMVSS 301-75 as specified for the vehicle manufacture date.

3.4 GENERAL DAMAGE OBSERVATIONS

A post-test inspection of the vehicle revealed the following:

- The trunk opened and the spare tire came loose. The right rear fender well wall separated from the trunk floor. The resulting gap measured approximately 1-1/2 x 12 inches. The rear fenders pushed against the tires.

- The backlight shattered and the windshield cracked in both lower corners.

- The seat backs broke and the left side of the seat moved back approximately 3/4 inch.

- The right side of the bumper was pushed further in than the left side. The rear bumper put a slight dent in the fuel filler pipe.

- The doors were jammed by the rear fenders but they opened easily.

- Slight buckling occurred in the roof and severe buckling occurred in the body, as far forward as the "A" pillar.

- The frame buckled ahead of the rear axle.

- The vehicle came to a stop approximately 35 feet from the point of impact."

The side view of the rear of a 1977 Impala is shown in Figure 160. The location of the fuel tank can be seen to be 23 inches from the outermost point of the rear bumper. The filler tube at its lower edge is 9 inches from the tip of the bumper.

At 30 mph the kinetic energy to be absorbed is 121,000 foot pounds. That portion of the frame parallel to the gas tank should not shorten or crush. Similarly it would appear that any buckling or shortening of the frame forward of the gas tank should be prohibited to prevent the gas tank from crushing against the rear axle housing. The crush should occur within the 23 inches between the outer bumper point and the gas tank. This can be accomplished by reducing the axial crush strength of the frame rearward and increasing the strength forward. Since the frame did bend, or buckle, approximately where the rear inner and outers are welded to the side rail a strengthening in this area would appear to be appropriate.

A controlled crush of the rearward, last portion of the frame appears feasible. Assuming an 18 inch crush, the average crush force is 40,350 pounds for each frame rail if the energy is to be 100% absorbed by crushing with no elastic strain energy considered. The above values could be obtained quite readily with increased strength of the remainder of the frame. The one disadvantage may be found in reduced jacking or towing ability.

Similarly the non damageable foam bumper system, Figures 161 and 162, could be used in conjunction with a frame collapse but with reduced jacking and towing ability.

The use of plastic gas tanks in place of steel has been suggested. Nylon is by far the most resistant of all plastic materials to the permeability of gasoline. It is, however, expensive and has poor low temperature impact resistance. Some life experience is being gained in a bus application.

High density polyethylene gas tanks require a permeability barrier which can be obtained by sulfonation or fluorination. This material, with the barrier coating, is the prime candidate for gasoline tanks. Experience is being gained through use on military vehicles and some commerical trucks.

326

While some weight reduction is expected from plastic gas tanks the big advantage of these is in the ability to contour the tank to fit more advantageously into the vehicle packaging. Since this invariably increases the surface area to volume ratio of the tank the weight reduction potential will be limited.

7.3 Side Impact and Intrusion

The current Federal Motor Vehicle Safety Standard 214 covers the side door strength of passenger cars. The door strength is measured in a static crush test. A punch is forced into the vehicle a distance of 18 inches from an initial position shown in Figure 163. Crush resistances are determined and must meet minimum values as follows:

1. The initial crush resistance, 2250 pounds minimum, is the average force during the first six inches penetration.

2. The intermediate crush resistance, 3500 pounds minimum, is the average force during the first twelve inches of penetration.

3. The peak crush resistance is the largest force, 7000 pounds or twice the vehicle weight, recorded over the entire 18 inch crush distance.

These requirements can be met by various force deformation curves such as those shown in Figure 164.

Curve ① is the most representative of the current Impala intrusion beam when tested as a simply supported, mid-point loaded beam by itself.

Actual tests [101] on a Volkswagen Rabbit door structure, in a vehicle, results in a curve which looks more like curves ② or ③. In these tests the intrusion beam was not distorted at the mid section but rather at the ends. The "A" and "B" posts were also severely distorted and rotated. Test data on the Impala door structure is not available but comparing its structure with that of the Rabbit door similar results are expected. The maximum load would not be reached until the sheet metal link from the end of the beam to the respective posts has been straightened into a taut tension member.

To improve the load-deformation curve, increase resistance and decrease intrusion, at a minimum weight penalty or actual decrease in weight a tension net should be used. This could be done by redesigning the beam, or strap, ends and its attachment to the hinges and latch. The hinges would probably be better redesigned not unlike that shown previously in Figure 80. The hinges could be attached directly to the intrusion strap, Figure 165 which is increased in width to cover a greater area of the door.

327

FIGURE 160   NON DAMAGEABLE FOAM BUMPER CONCEPT

9"

23"
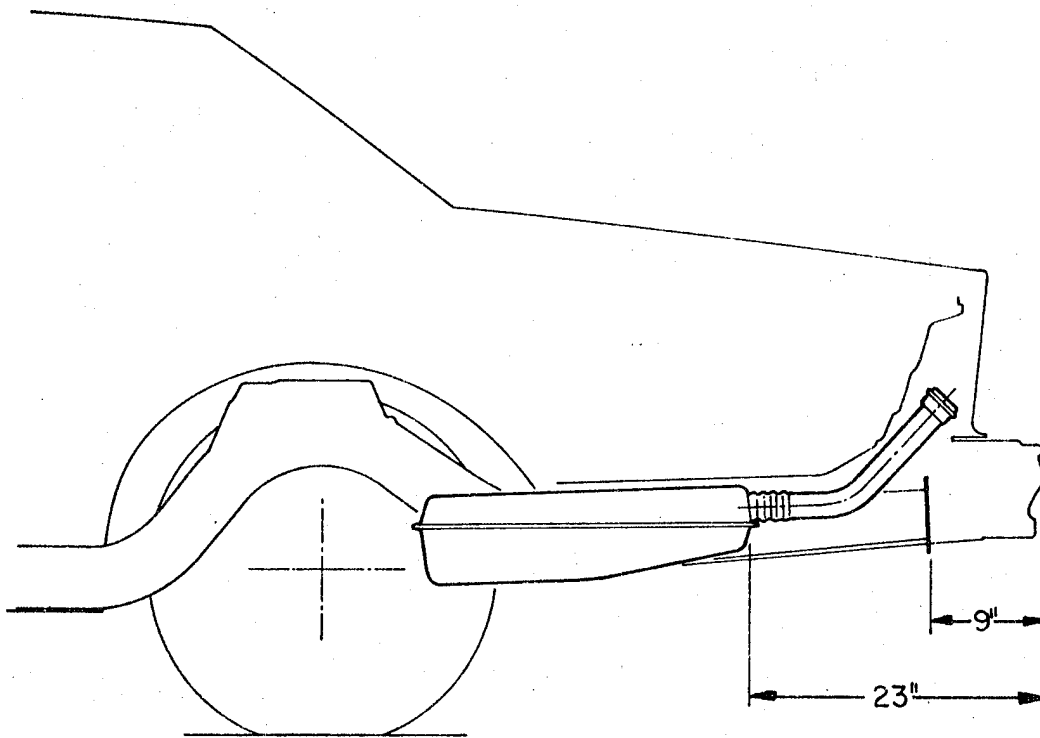
FIGURE 161   NON DAMAGEABLE FOAM BUMPER CONCEPT

329

FIGURE 162   IMPALA FUEL TANK, REAR END
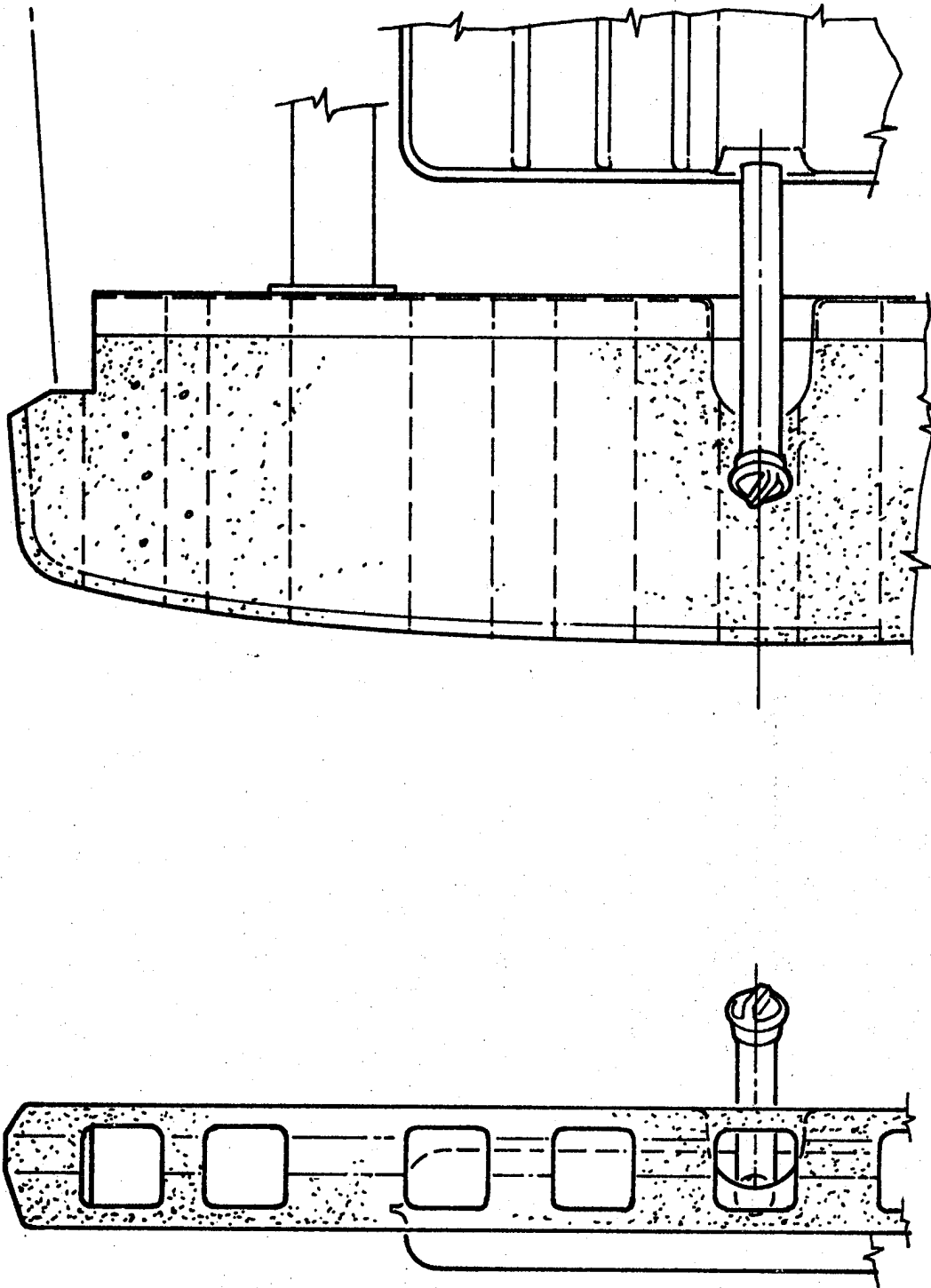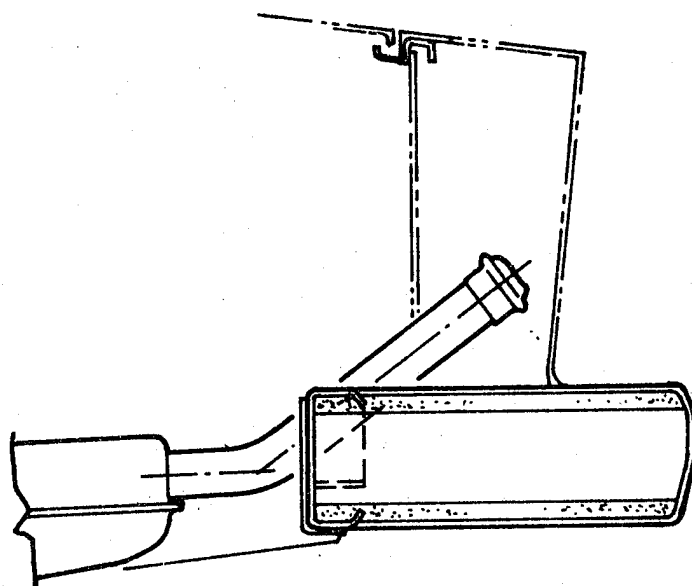
FIGURE 163   LOADING DEVICE LOCATION AND APPLICATION TO THE DOOR

DIRECTION OF LOAD
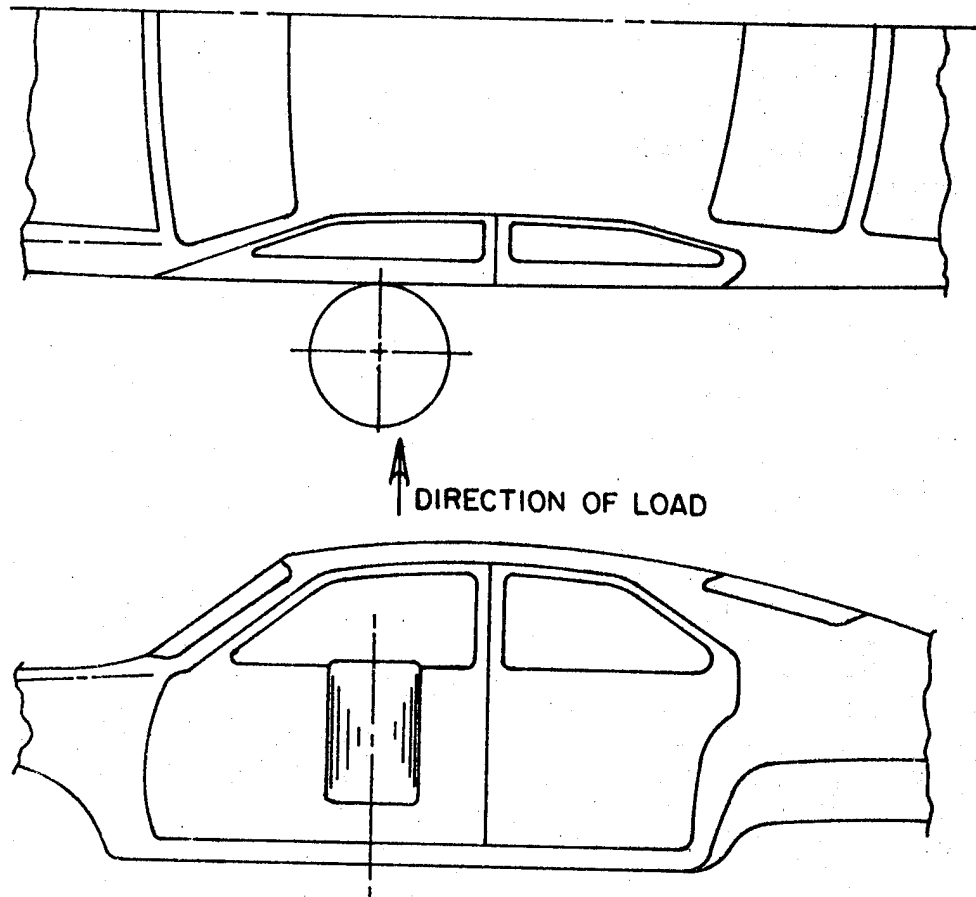
FIGURE 164   SCHEMATIC LOAD DEFORMATION CURVES
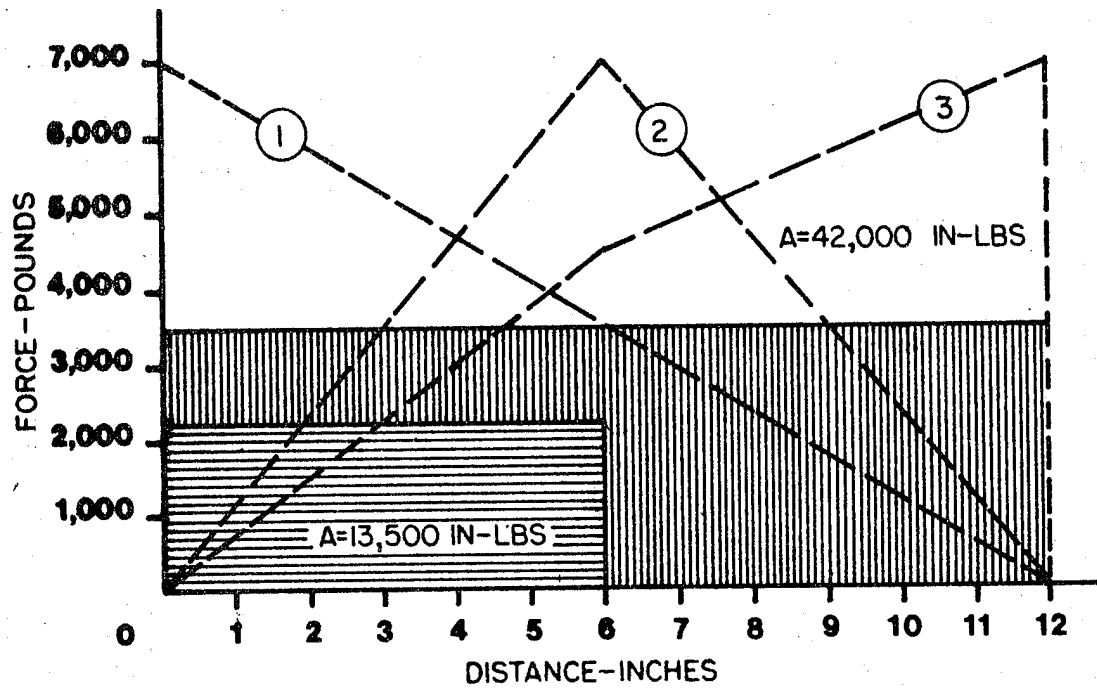
FIGURE 165   HINGE AND INTRUSION STRAP CONCEPT
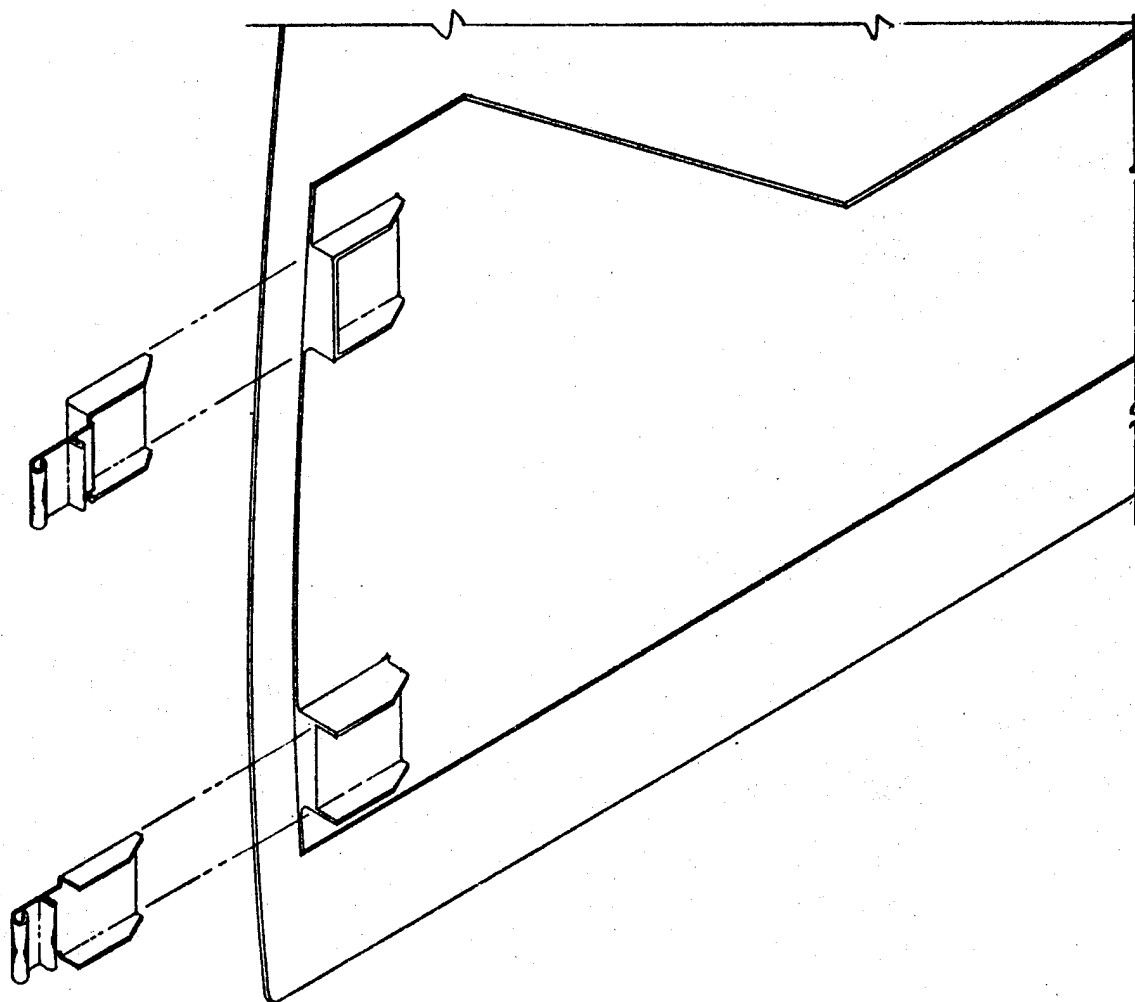
The hinge, or a link between the hinge and the intrusion strap, can contain a folded configuration which will unfold in intrusion only and at a controlled force-deformation.

Considering a higher level of crush resistance, 12,000 pounds at six inch intrusion, the load on a strap is 19,000 pounds. A strap of aluminum alloy, steel or oriented glass fiber composite, 12 inches wide, and of appropriate thickness to meet this tensile load could be used.

Attachment to the hinges may pose some problem in the glass polyester case. The adhesive bond strength per hinge would have to be at least 10,000 pounds. To prevent peeling of the stiffer metal hinge from the glass composite, ribs will be required to stiffen the intrusion strap at the bond location.

Additional improvement can be obtained by extending the strap down to the side sill where it can be engaged during intrusion. The added support of the side sill has been found [101] to be of considerable importance.

While the crush resistance of the side structure can be increased other penalties may occur such as additional padding in the vehicle interior. As the strength increases the acceleration at impact will probably also increase. The actual benefit to passenger survivability is unknown.

7.4 Energy Absorption Characteristics of Alternate Materials

The fender structure concept of Figure 71 was used as a basis for testing HSLA steels and aluminum alloys to determine their ability to absorb collision energy. It was shown in Figure 137 that the existing fender structure might be improved, based on various assumptions on crashworthiness, by increasing its crush resistance.

Each material of construction has properties which may reduce its applicability to resist high energy level collisions. For example, in a resistance spot welded structure, aluminum alloys might be suspect due to their low weld strength. Both aluminum alloys and HSLA steels have low elongation to fracture, compared to carbon steel and may not possess sufficient toughness to withstand the severe deformation. To further evaluate HSLA steel and aluminum alloy a short test program was conducted.

Most automotive structure is complex in that all panels are curved, beams are of varying section properties and prediction of crash energy absorption has been difficult. Numerous methods of testing and prediction have been suggested. Scale modeling appears to be an excellent procedure due to the cost and time savings as well as accuracy.

334

The utilization of columnar structure as shown in the concept of Figure 71 is compared in Figure 166 to the current production structure. This section of the fender structure is taken through the top of the wheel opening. The rectangular box shape is selected to minimize loss of wheel jounce and to comply with the manufacturing process.

An emperical equation developed [98] to predict the static crushing forces of flat sided sheet metal columns is as follows:

$$P_m = 1.8 \, t^{5/3} \, b^{1/3} \, \sigma_y^{2/3} \, E^{1/3}$$

where b is the length of a flat side. It has been found that rectangular cross section boxes, 3" x 5", are equivalent to square cross sections, 4" x 4". This equation provides an average resistance value which occurs during the folding deformation. Peak forces occurring at the beginning of the crush are predicted by crippling equations [99] such as the following:

$$P_{cr} = (0.56) \left[\left(\frac{12t^2}{A} \right) \left(\frac{E}{\sigma_y} \right)^{1/2} \right]^{.085}$$

Rectangular boxes were made to the dimensions shown in Figure 167 and with lengths of 12 to 36 inches. The materials used, and calculated crippling and static crush loads are listed in Table 73.

Examples of the actual crush curves, force-distance are shown in Figures 168, 169, 170 and 171. The calculated average crush force is also noted by the dashed line. The agreement is considered quite good.

Dynamic tests, with impact speeds of 30 miles per hour, indicate fair agreement with the static results. The aluminum alloys in the T4 condition show a 10% higher dynamic crush load and the T6 shows a lower dynamic crush load (-24%). HSLA steels exhibit an 10% increase in average crush load. While the number of specimens were not sufficient to draw many conclusions the results fit an unexpected pattern. The dynamic test results would expected to be higher for the T4 aluminum alloys and the steel due to their greater toughness. The T6 aluminum alloy will show a lower dynamic crush force due to its lower ductility and toughness.

The fender structure was crushed statically and dynamically. Static tests on the production fender, HSLA rectangular tube modified fender, and an all aluminum fender with aluminum rectangular tube are shown in Figure 172. The results of two dynamic tests of aluminum fenders with aluminum tubes are shown in Figure 173. Unfortunately the current production fender could not be tested in the drop tower due to its uncontrollable mode of collapse.

335

FIGURE 166   FENDER STRUCTURE – SECTION

EXISTING FENDER

MODIFIED FENDER
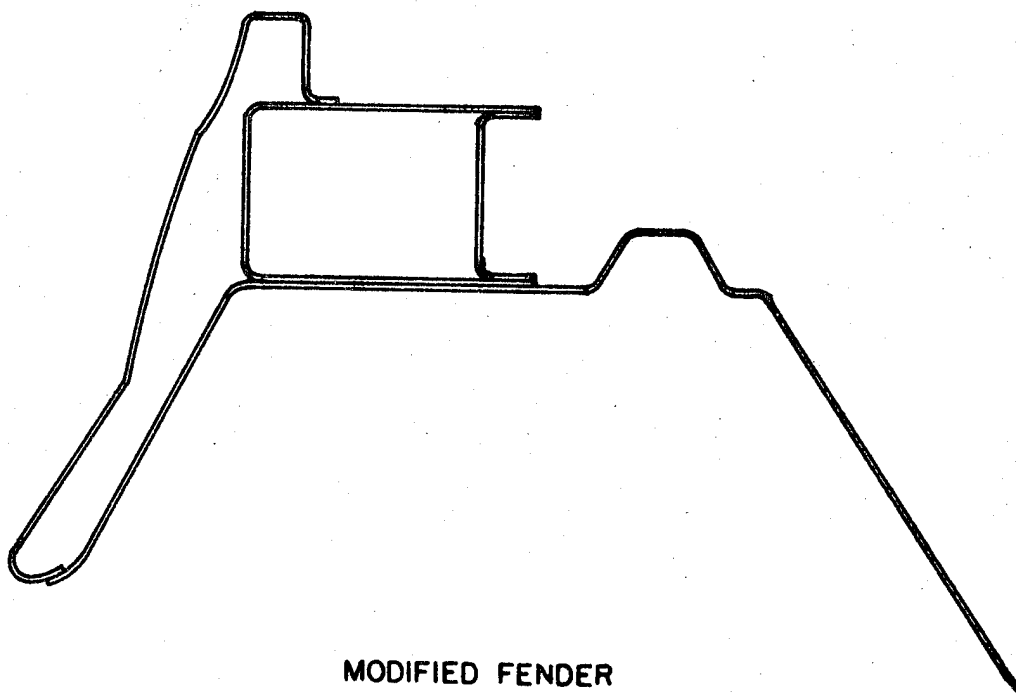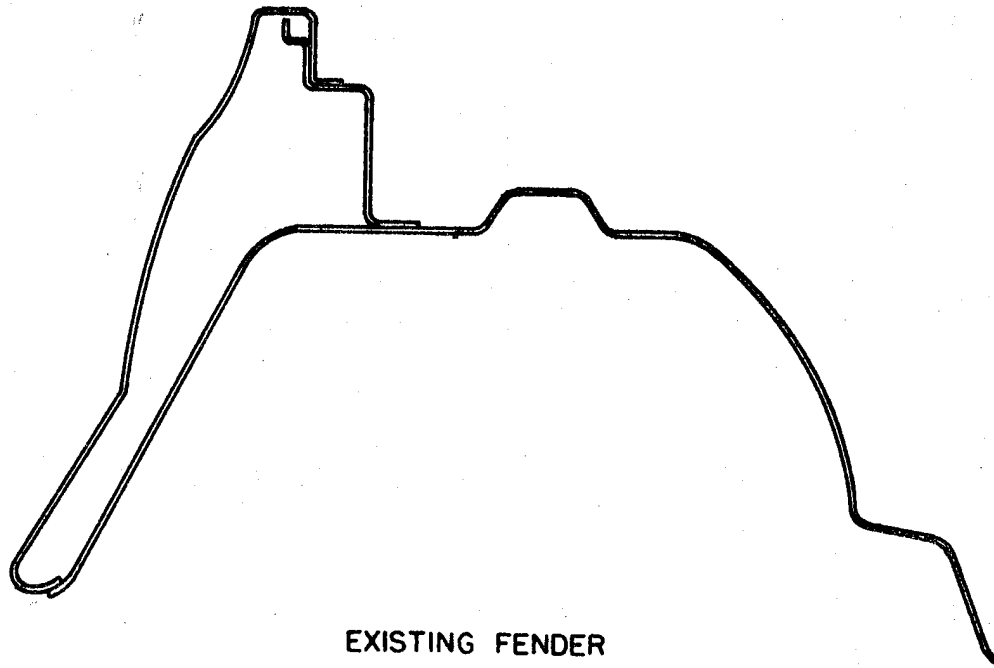
FIGURE 167   RECTANGULAR BOXES

.100 RADIUS

3.00

30°

.62

5.00
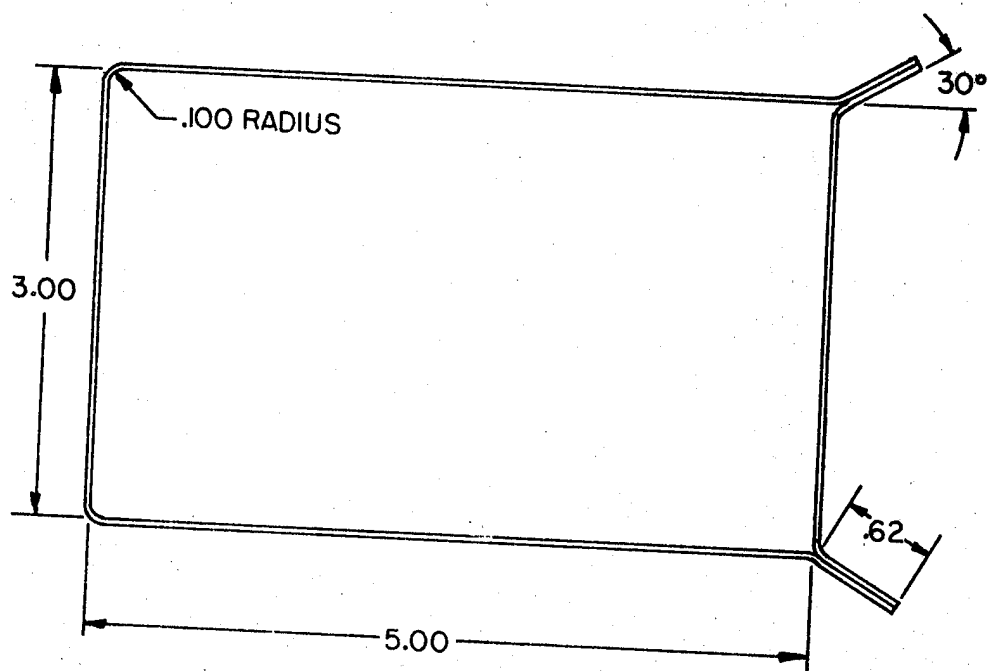
TABLE 73:   SPECIMEN CRIPPLING AND CRUSH LOADS

Material	t Thickness (in)	E Modulus of Elasticity (MSI)	F_y Yield Strength (KSI)	PCR Crippling Load (Pounds)	PM Crushing Load (Pounds)
6010-T4	.037	10	28.6	5550	2365
6010-T6	.037	10	49.3	7590	3555
6010-T4	.063	10	28.3	14760	5700
6010-T6	.063	10	49.3	20300	8510
Low Carbon	.055	30	37.6	21560	7930
HSLA 950	.030	30	47.3	8020	3370

FIGURE 168   STATIC CRUSH — LOW CARBON STEEL

339
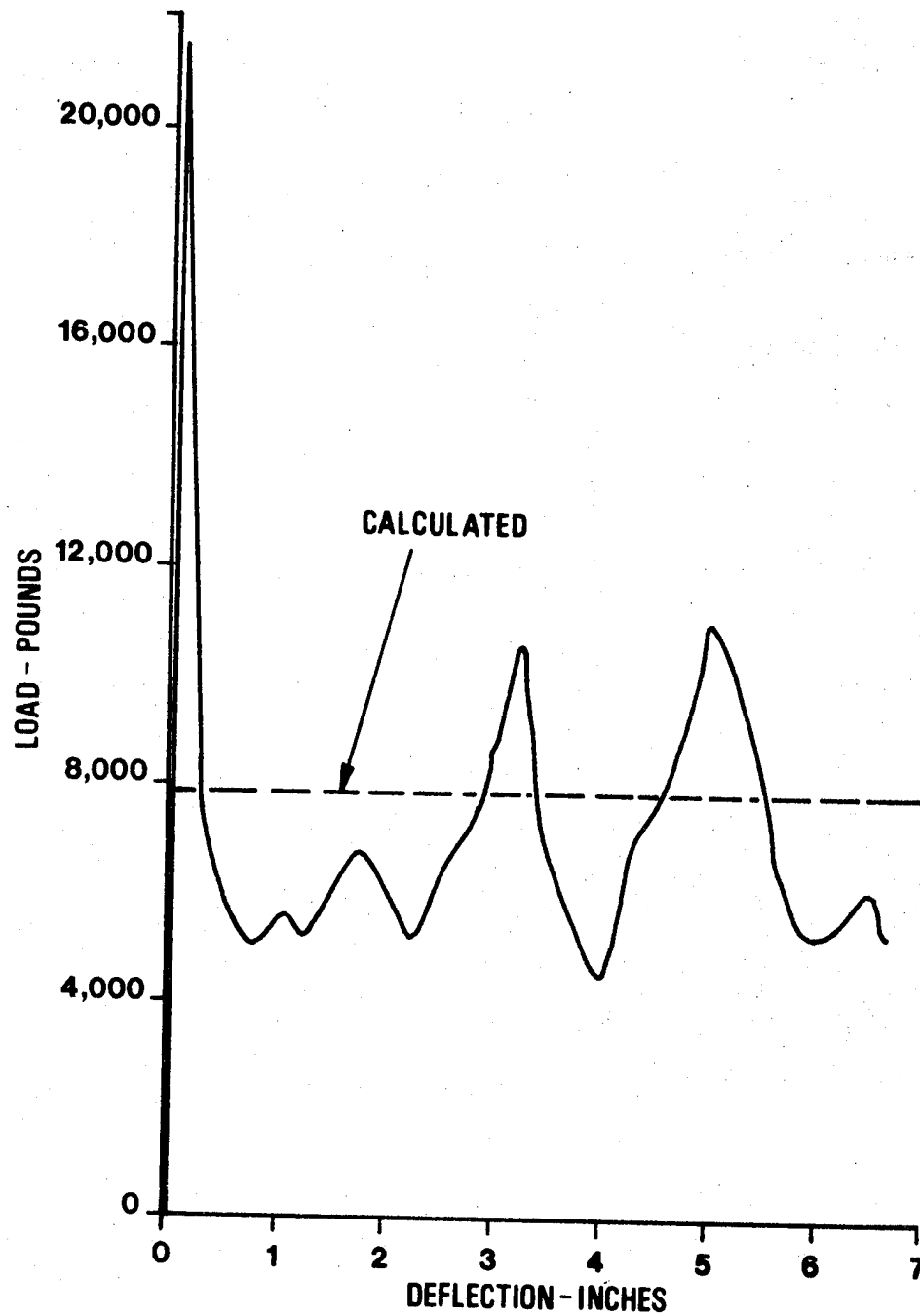
FIGURE 169   STATIC CRUSH – SAE 950
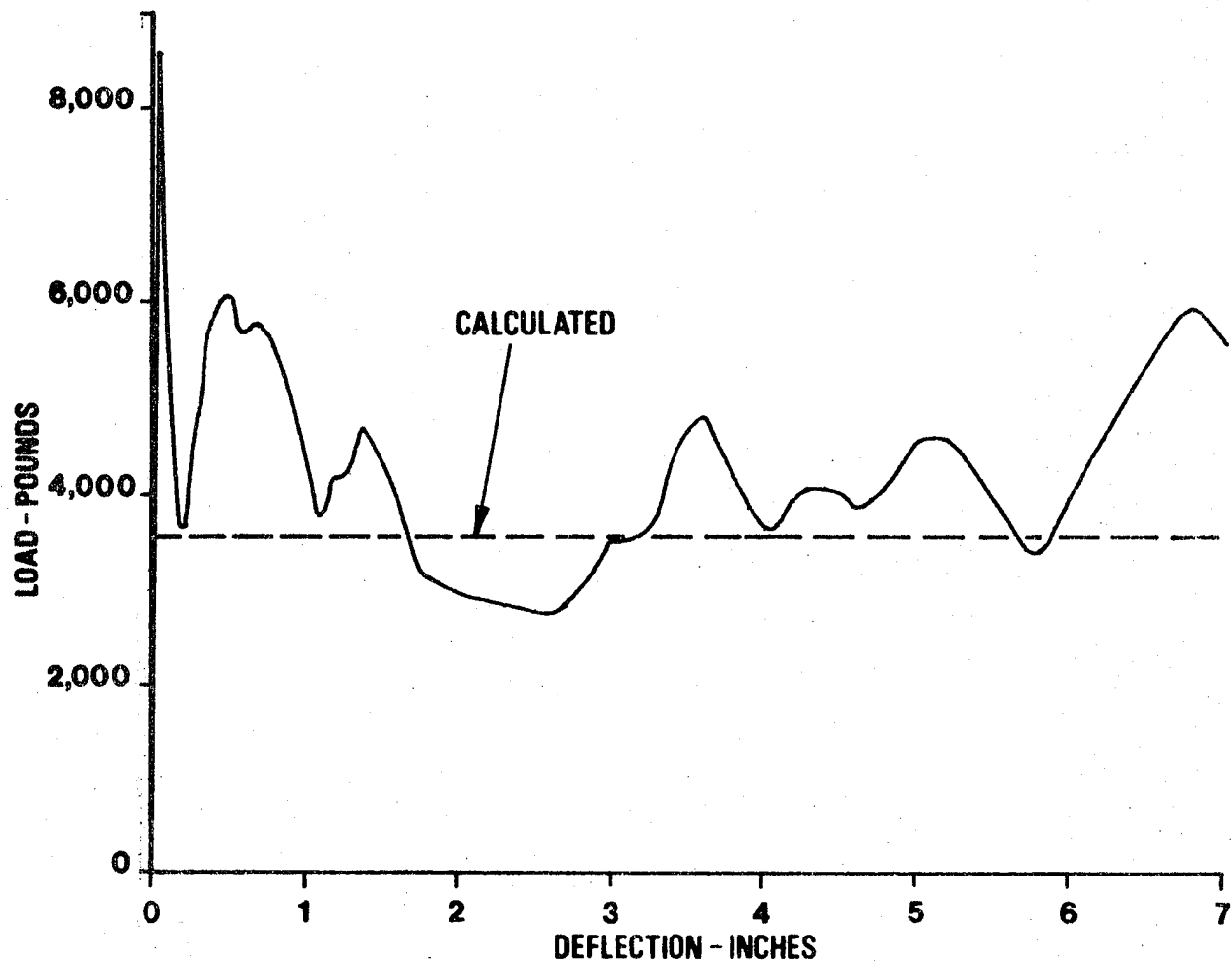
FIGURE 170   STATIC CRUSH – 6010-T6

341
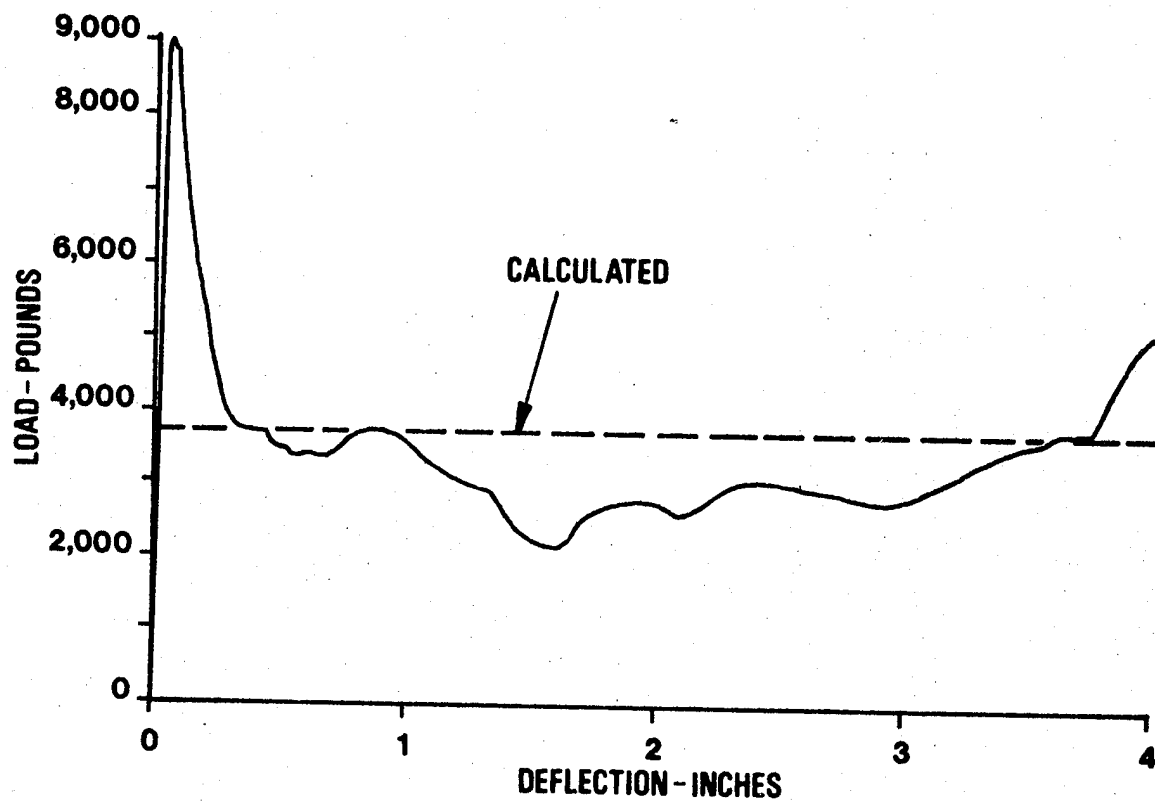
FIGURE 171   STATIC CRUSH – 6010-T4
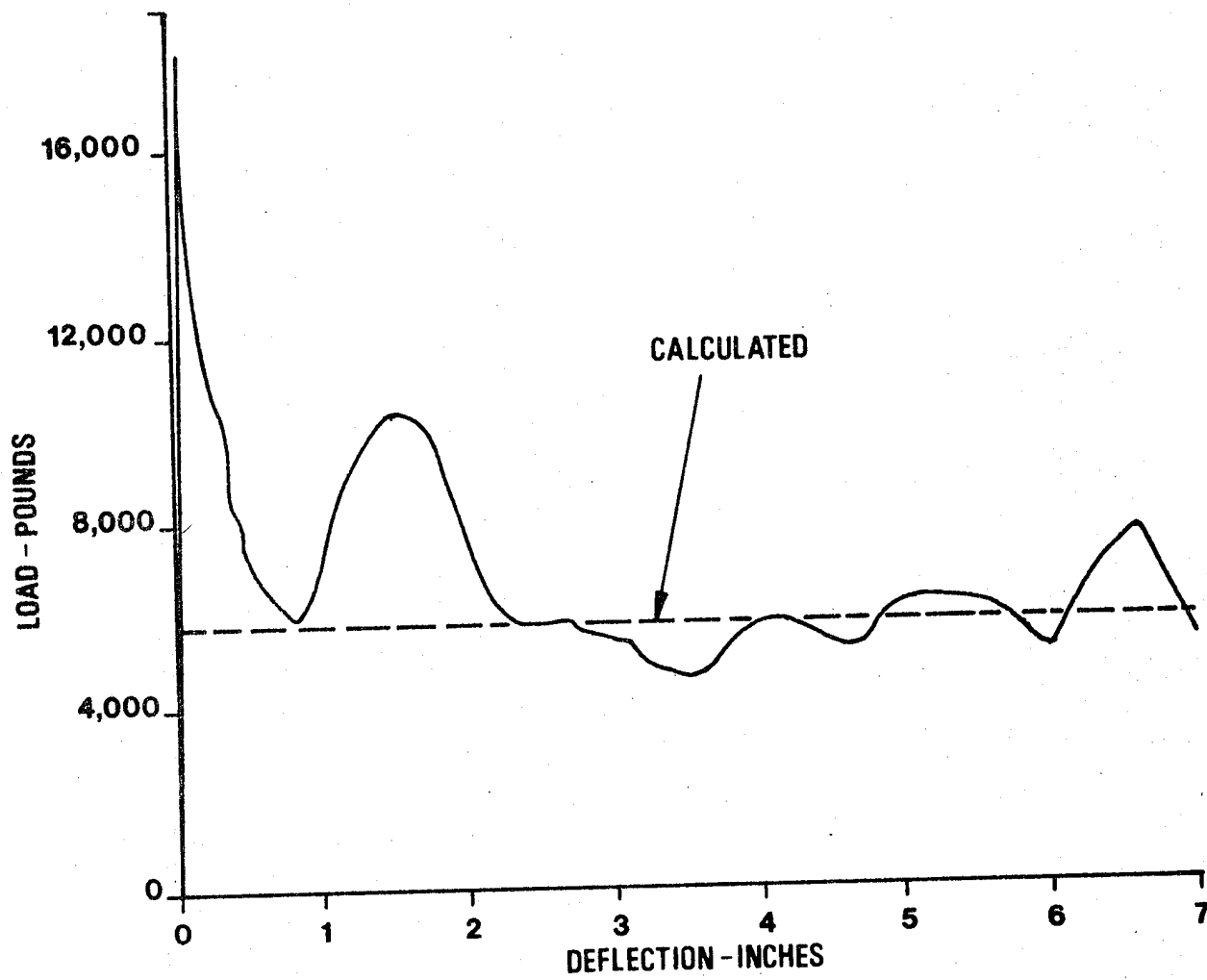
FIGURE 172   STATIC CRUSH TESTS – MODIFIED IMPALA FENDERS

343
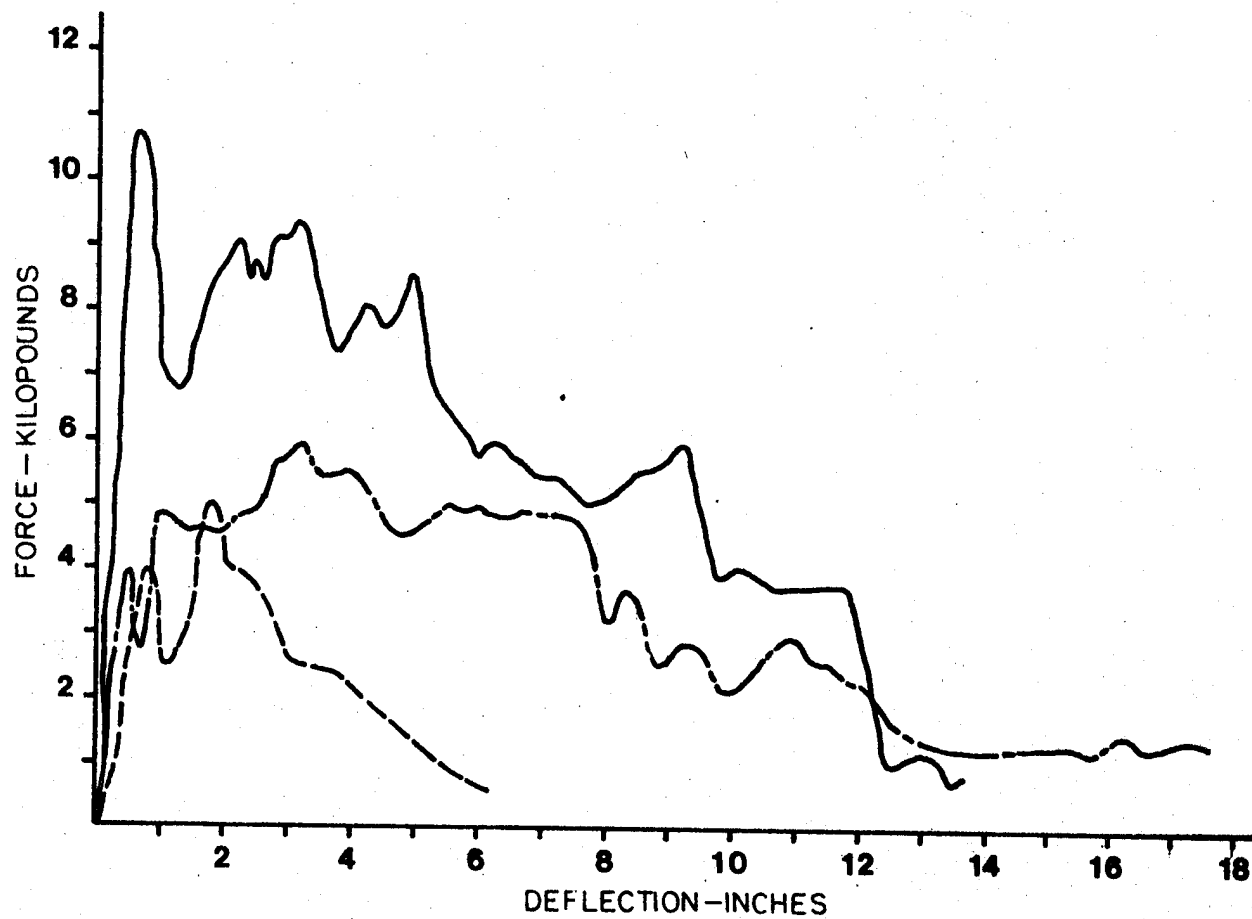
FIGURE 173   DYNAMIC CRUSH – MODIFIED ALUMINUM IMPALA FENDERS
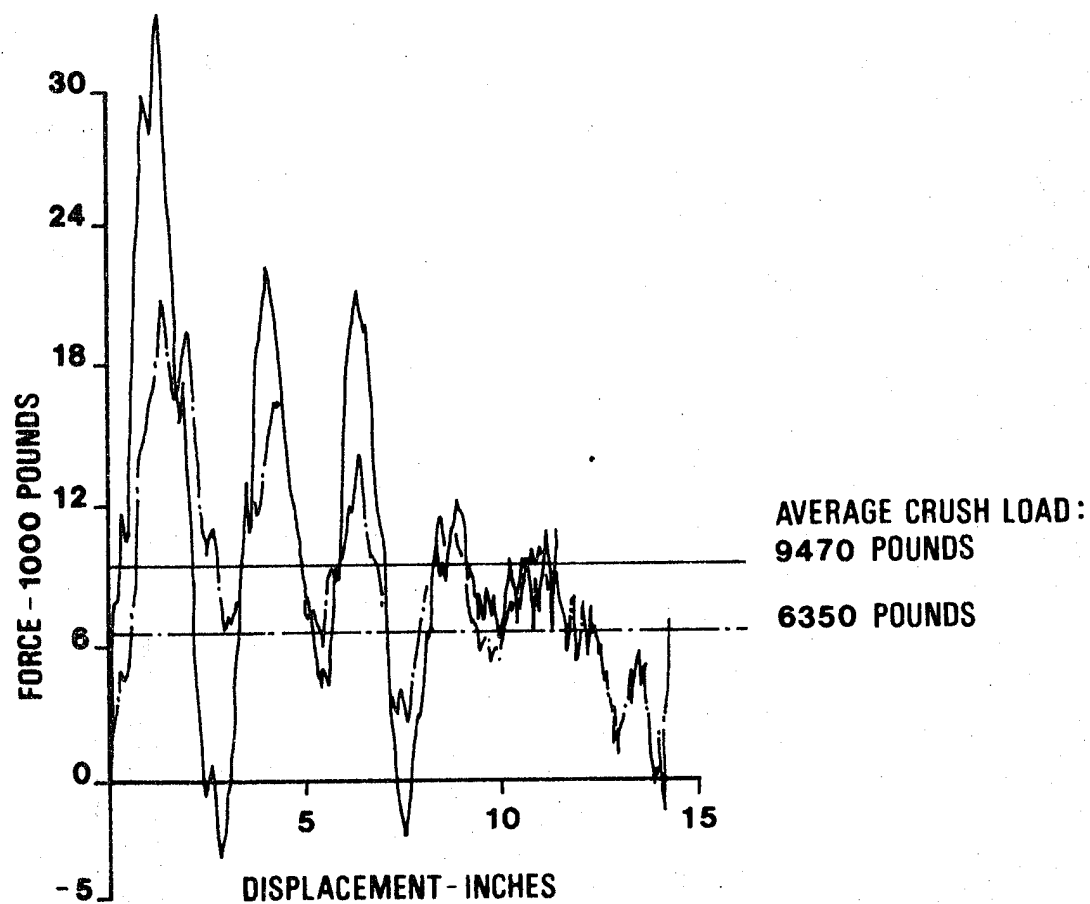
Glass reinforced composites have been utilized in experiments[86] or prototype vehicles [102] to obtain excellent energy absorption in frontal barrier tests. The use of a rigid polyurethane foam with glass reinforced polyesters is recommended. Circular crush elements can be triggered and the crush force controlled by the combination of thickness control, foam density and radius of curvature of the cylinder wall. Rectangular cross sections are not as efficient and are more difficult to control. Failures of flat walled elements are difficult to predict. Thickness variations or corrugations can be used to control the crush force and mode. A corrugated concept has been used successfully with two pound per cubic foot foam filling in an electric powered vehicle [102]. The design is discussed further in regard to concepts for a Volkswagen Rabbit structure, Section 8 and 9.

In summary, the use of alternate materials poses no major problem to crashworthiness. For each application consideration must be given to all design criteria and the crashworthiness then evaluated. Redesign may be required to efficiently use a material.

8.0 UNITIZED BODY STRUCTURE CONCEPT - VOLKSWAGEN RABBIT

The 1977 Volkswagen Rabbit structure consists of a large number of low carbon steel stampings, assembled by resistance spot welding and arc welding. Welding is used to provide efficient joint strengths at a high production rate and low cost per finished vehicle. Incorporation of alternate materials within this structure is limited to HSLA steels without assembly and design changes due to the welding procedures and joint strengths.

Transition strips, consisting of a diffusion bonded aluminum alloy and carbon steel bimetallic, can be used to introduce aluminum alloys into parts of the structure. The use of these strips would require redesign locally at all joint areas to provide space. The use of these transition strips is expected to gain in applications in the industry. There are added cost and manufacturing problems, however, which must be considered.

Strips of proper size have to be cut and supplied to the welders and assembly personnel. The number of welding operations will double since the strips would be welded to one piece, say an aluminum panel and then later this would be welded to the steel members. Chances of production errors increase where the strips are not welded in their proper location or occassionally left out entirely. This results in increased scrap rate or repair costs.

The 1977 Volkswagen Rabbit steel structure is shown in the half vehicle isometric, Figure 174 . The outer side panel is one stamping and together with a number of smaller pieces makes one complete side as shown in Figure 175 . Selected sections of the side structure are shown in Figure 176 . The floor structure is shown in exploded views in Figures 177 and 178 which show the front and rear halves separated. Typical sections through the assembled floor are shown in Figure 179 . The roof, fire wall and suspension support structure, fender and sill structure, radiator support and front close off panel and the rear close off panel are shown in Figures 180 through 184.

This entire Rabbit structure could be fabricated from HSLA steels or from aluminum alloys. However, each part would have to be reviewed in detail to determine if the part design needs modification to permit economical stamping. The most obvious changes occur in flanging radii. Other changes are necessary where the lower ductility, 20% elongation, or less, of HSLA steels and aluminum alloys cannot physically make the parts. Low carbon steel has typically 40% elongation or more. A formability diagram comparing stretching and drawing performance of 2036-T4 aluminum alloy with annealed killed steels is shown in Figure 51 . This data indicates why, in general, tools and parts designed for steel cannot be used for aluminum alloys while tools and parts designed for aluminum can be made from low carbon steel in the press shop.

346

FIGURE 174   RABBIT – BODY STRUCTURE

FIGURE 175   RABBIT – SIDE STRUCTURE
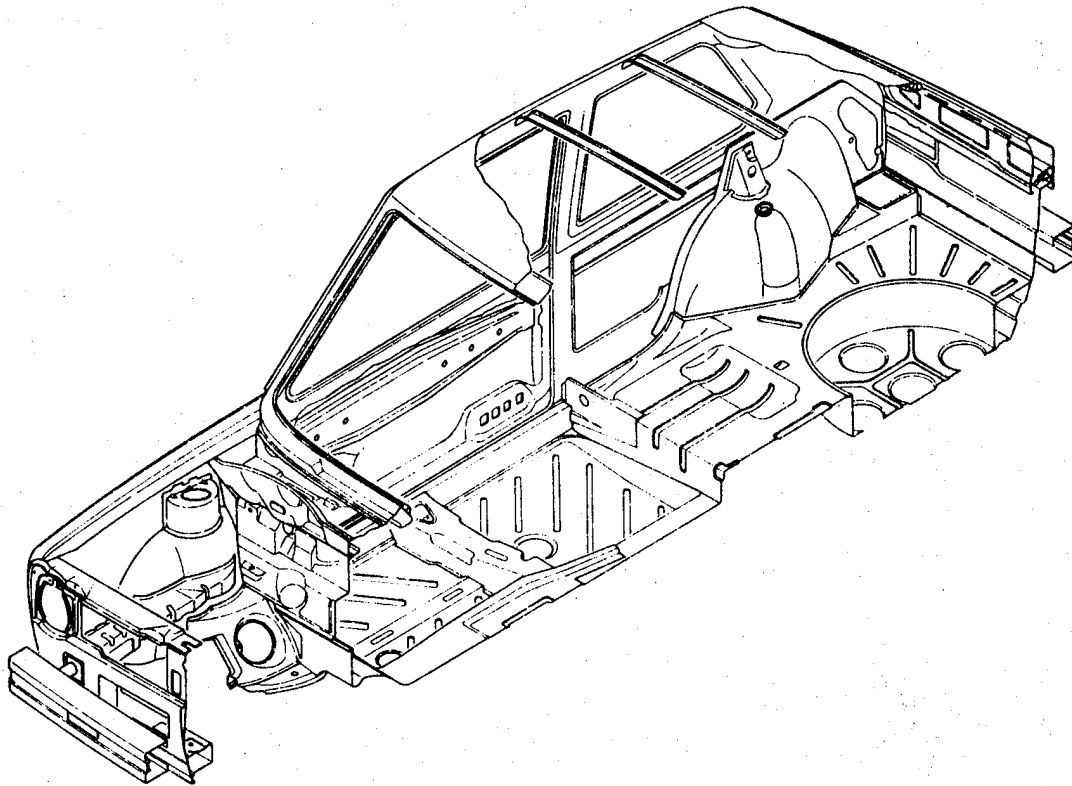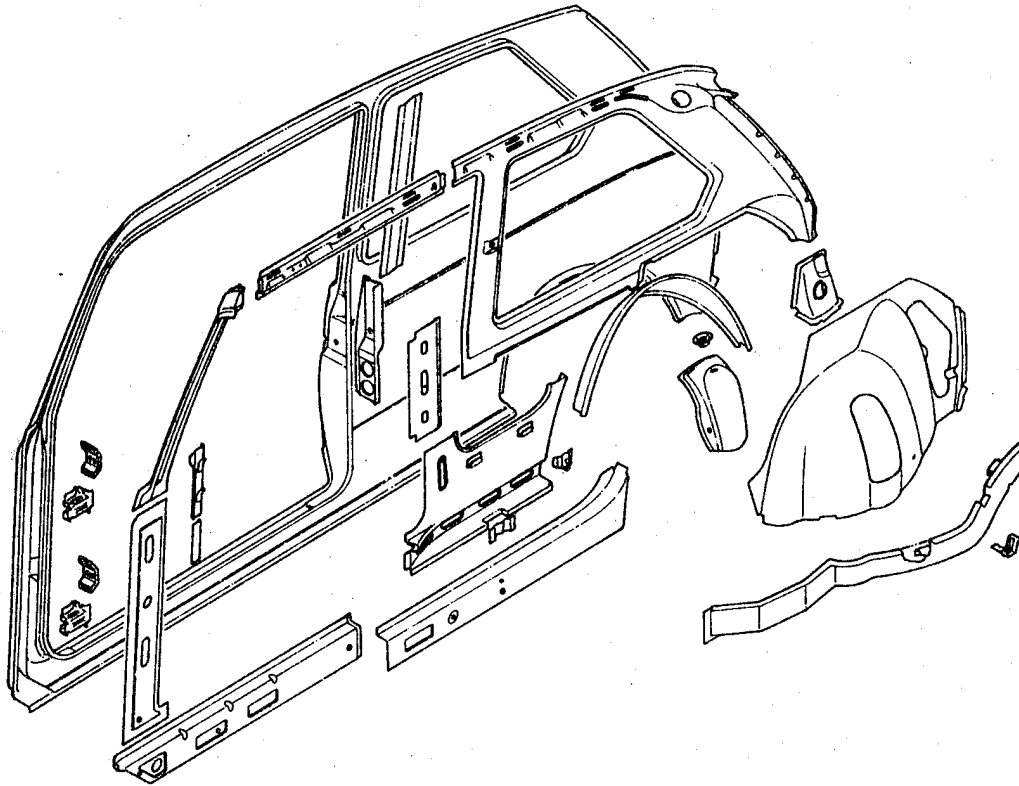
FIGURE 176   SECTIONS – SIDE STRUCTURE
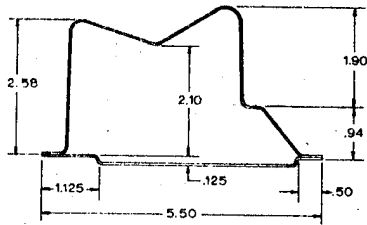
SECTION A-A
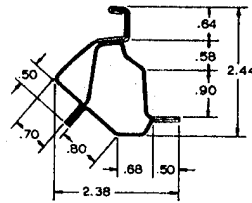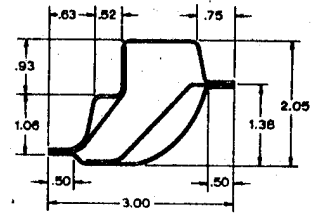
SECTION B-B
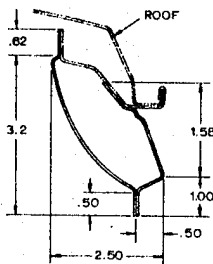
SECTION C-C
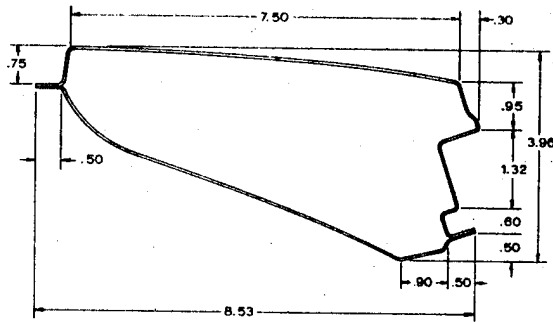
SECTION D-D
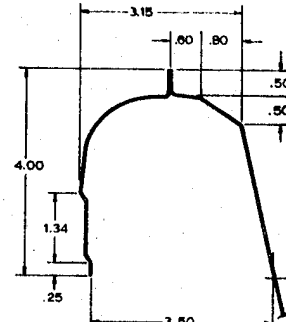
SECTION E-E
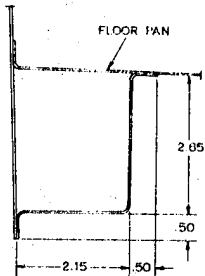
SECTION F-F
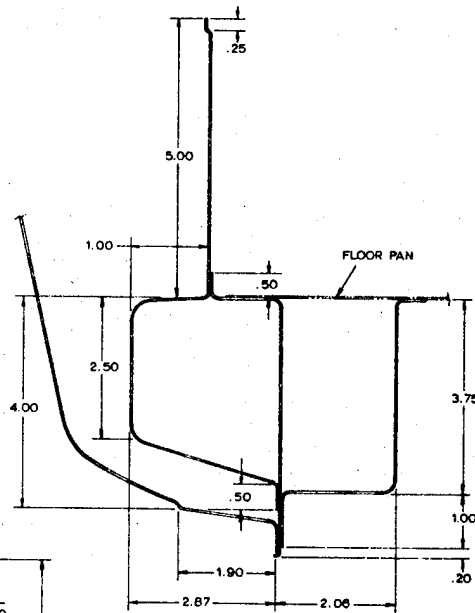
SECTION G-G
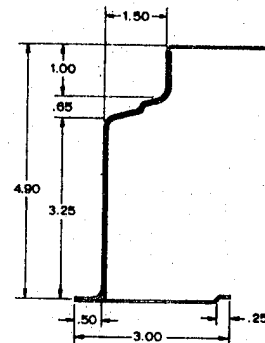
SECTION H-H

SECTION I-I

SECTION J-J

349
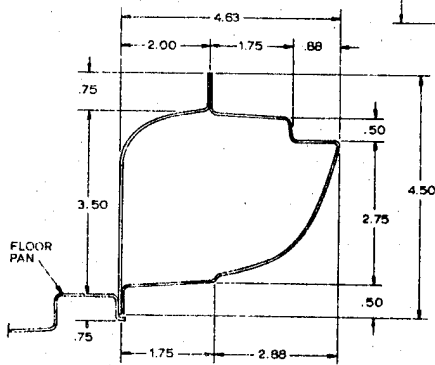
FIGURE 177   RABBIT – FLOOR – FRONT
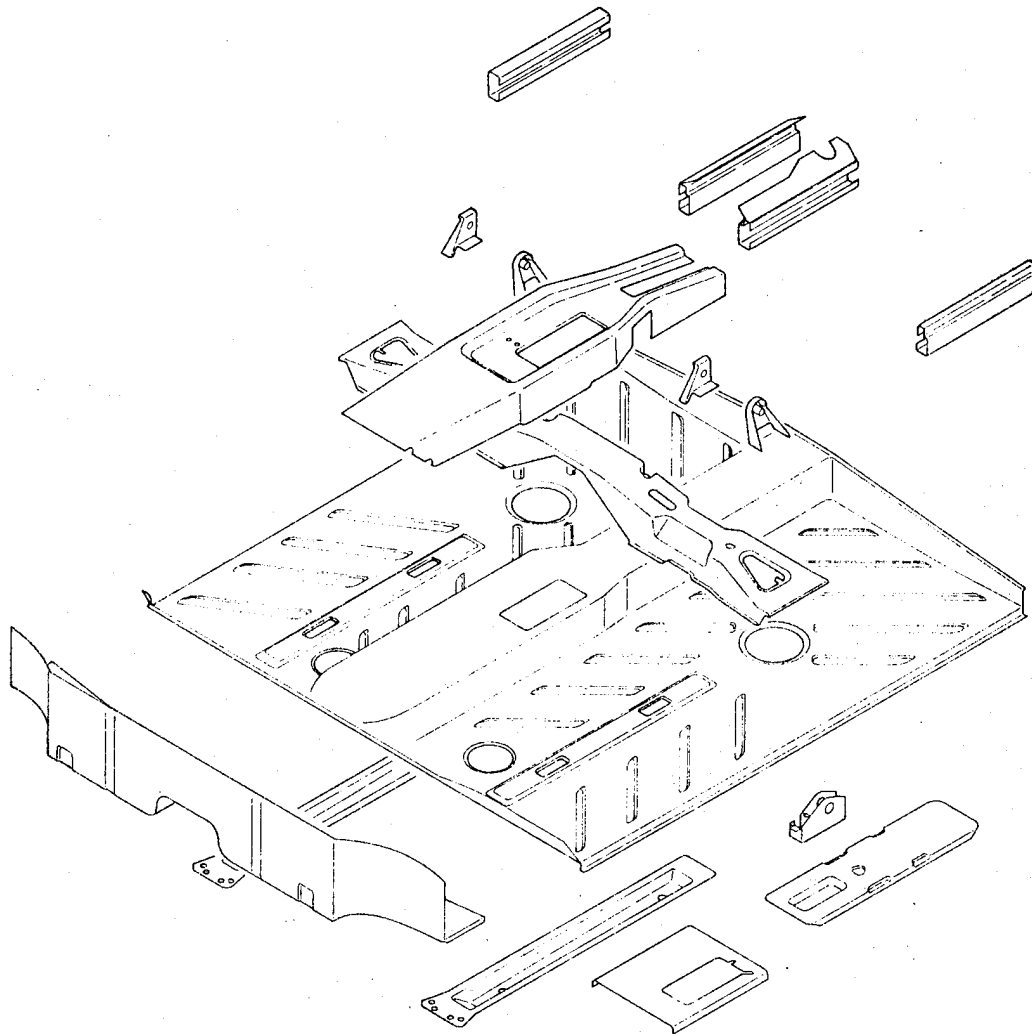
FIGURE 178   RABBIT – FLOOR – REAR
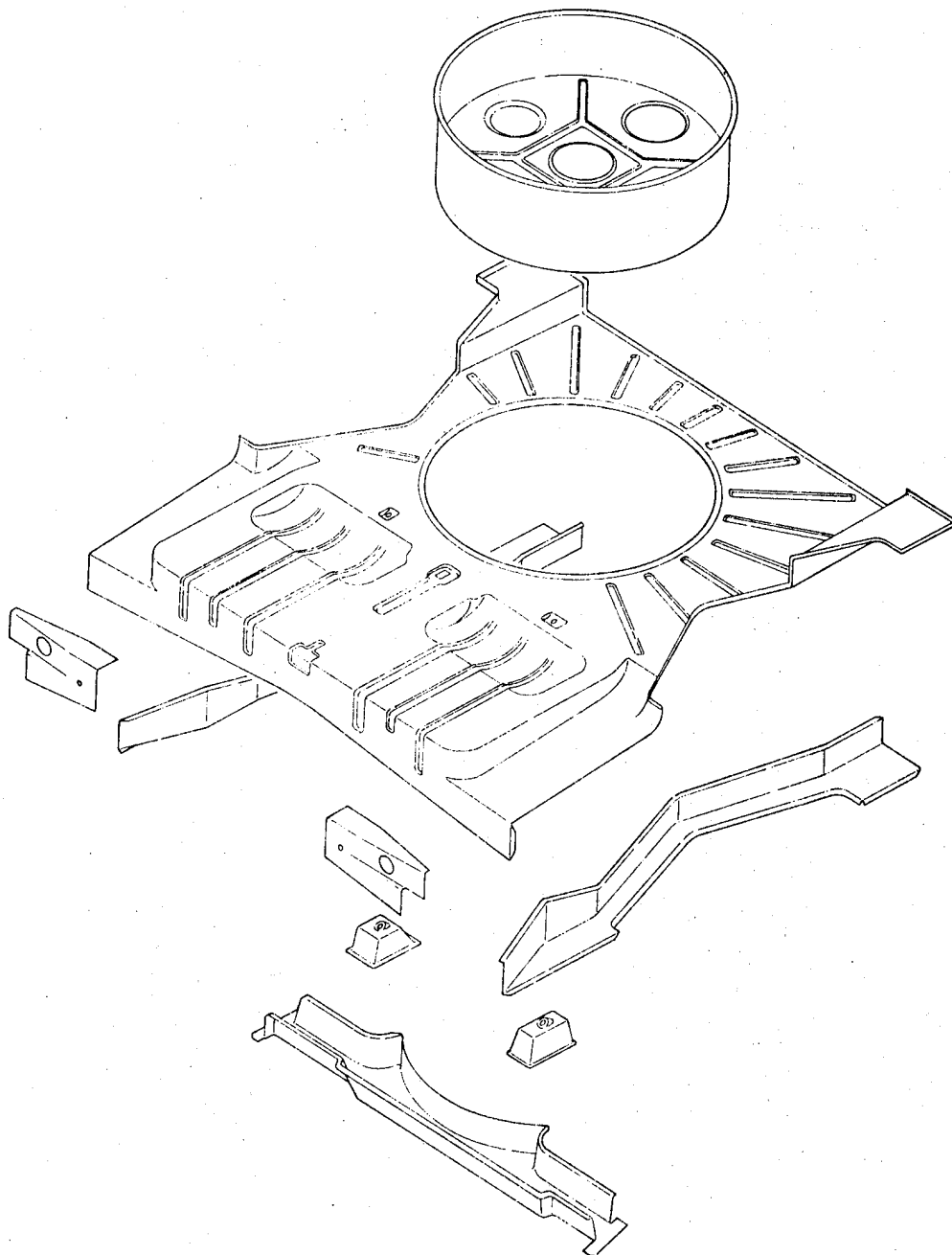
FIGURE 179   SECTIONS – FLOOR STRUCTURE

SECTION A-A

SECTION B-B

SECTION C-C

SECTION D-D

SECTION E-E

SECTION F-F

SECTION G-G

SECTION H-H

SECTION J-J

SECTION K-K

SECTION L-L

SECTION M-M

352
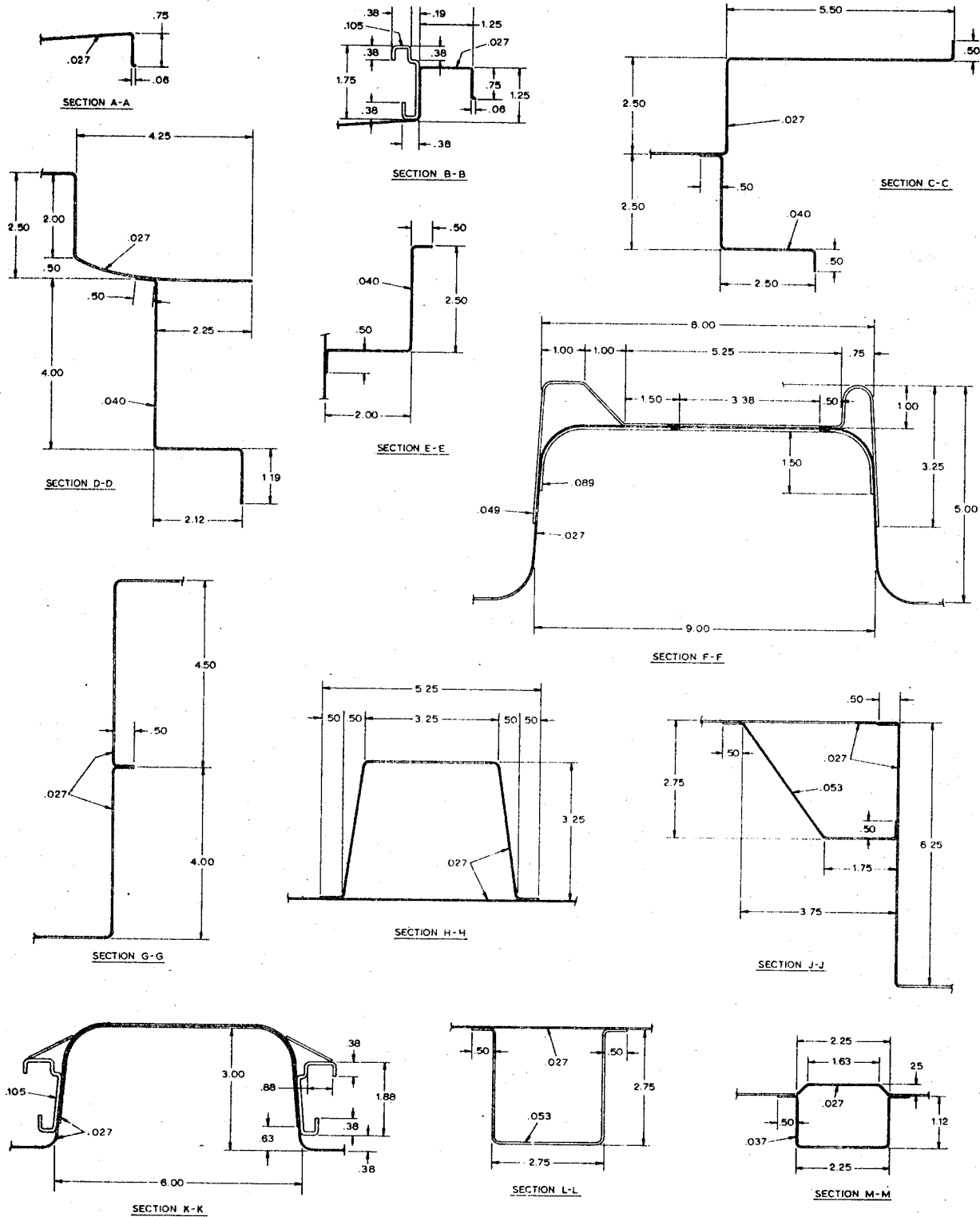
FIGURE 180   RABBIT – ROOF
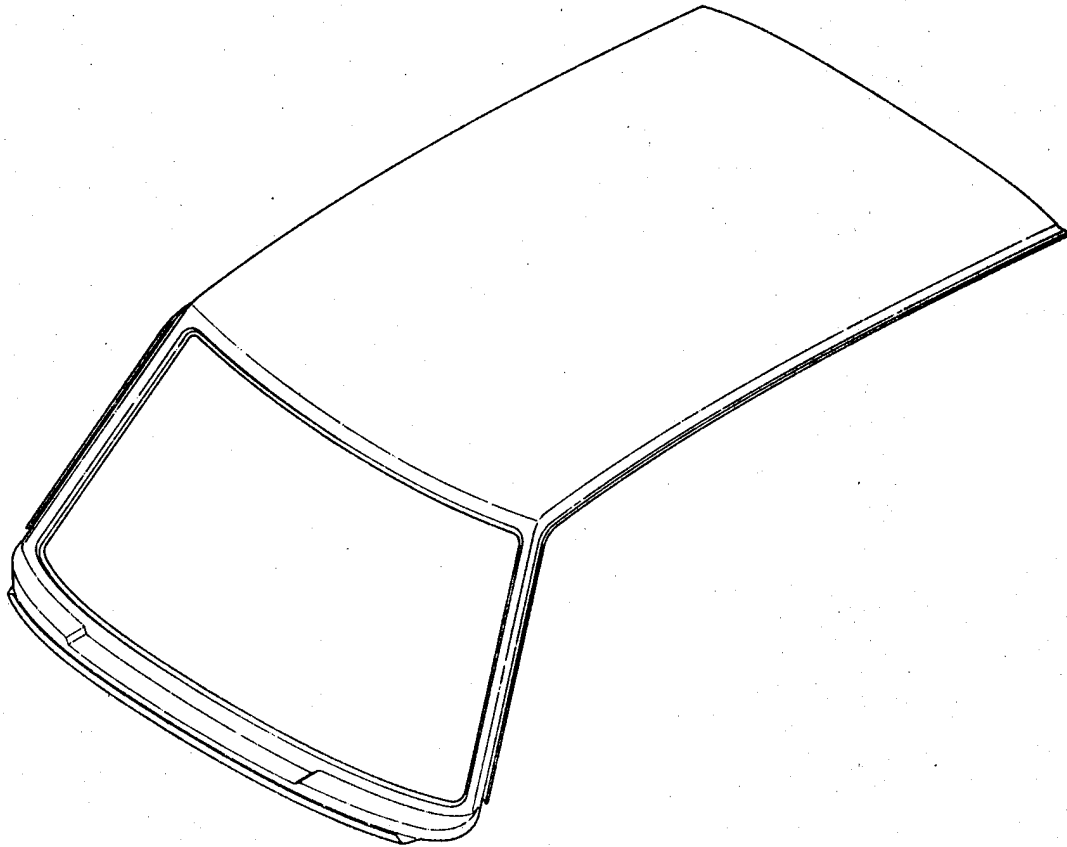
FIGURE 181   RABBIT – FIREWALL – SUSPENSION SUPPORT
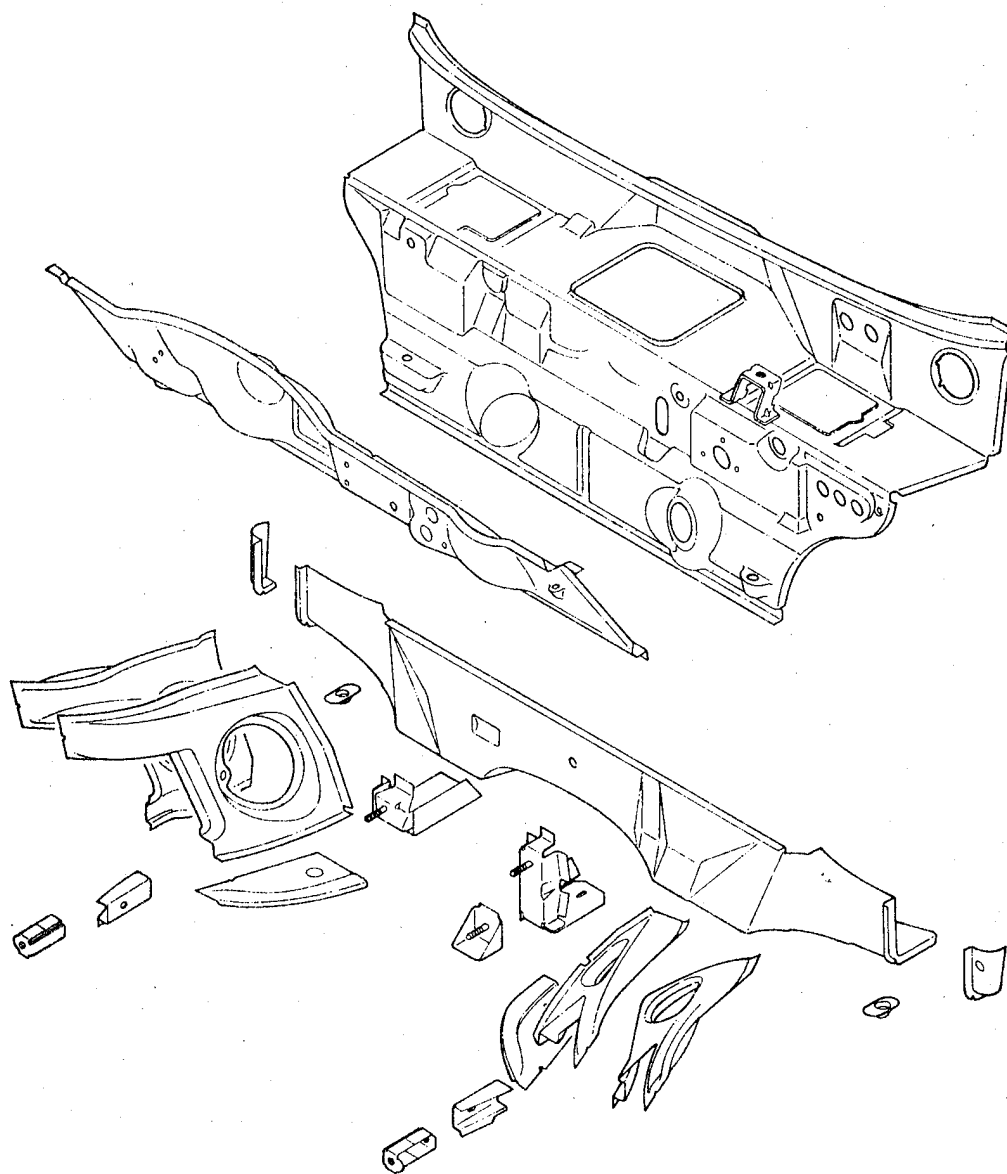
FIGURE 182   RABBIT – FENDER AND FRONT SILL
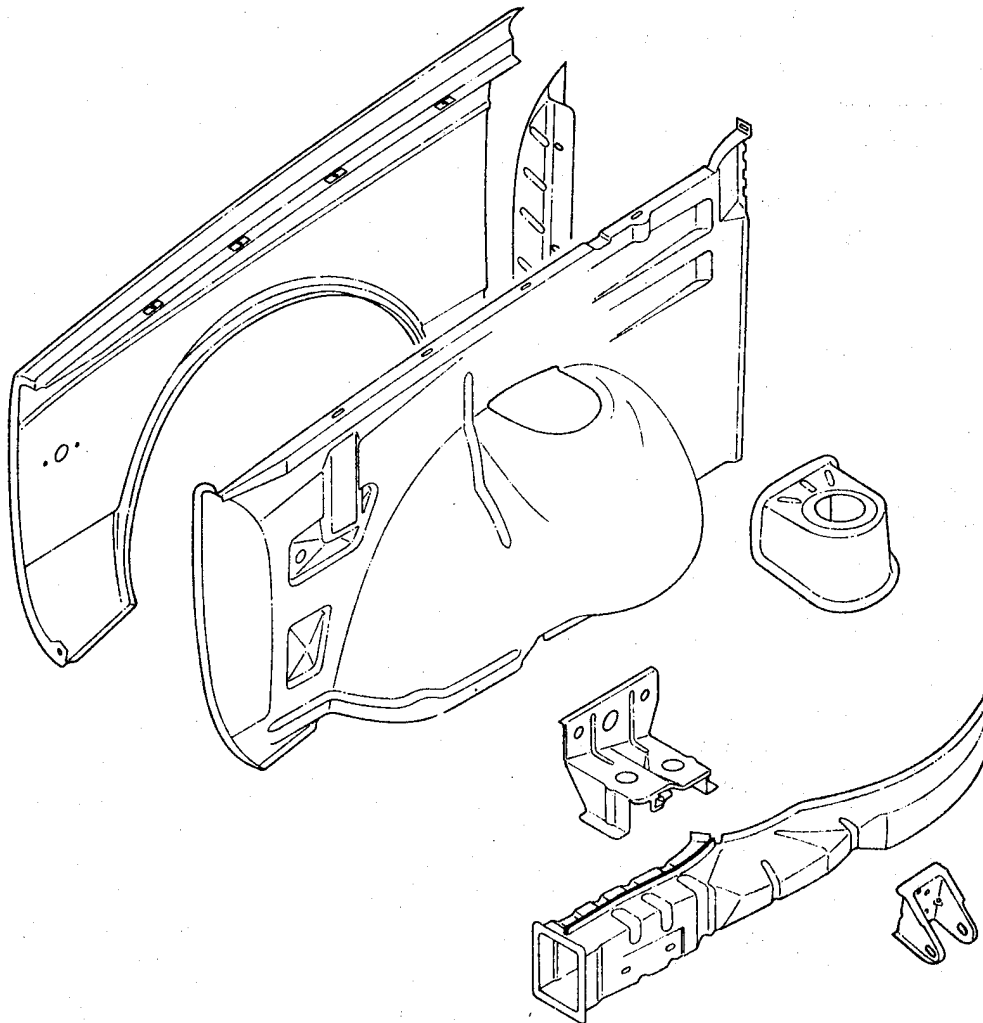
FIGURE 183   **RABBIT – RADIATOR SUPPORT**
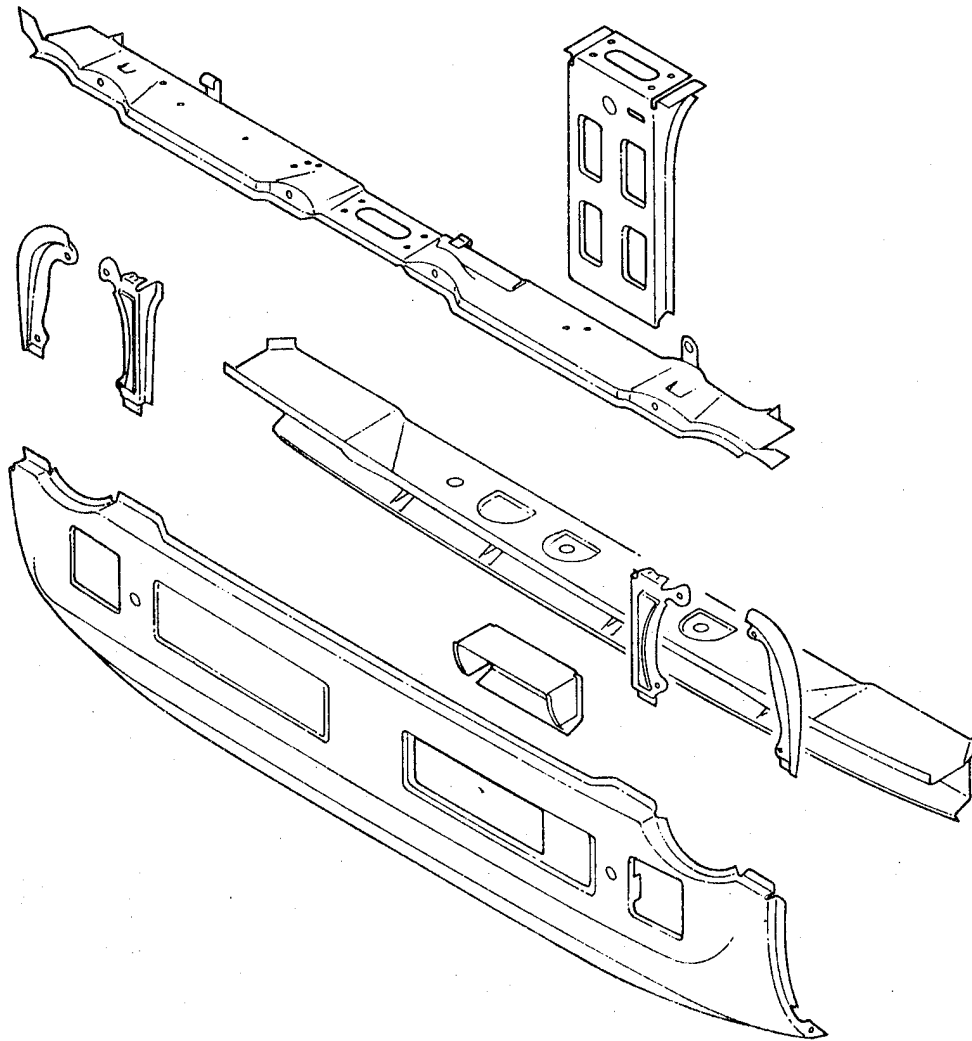
FIGURE 184   RABBIT – REAR CLOSE OFF PANEL
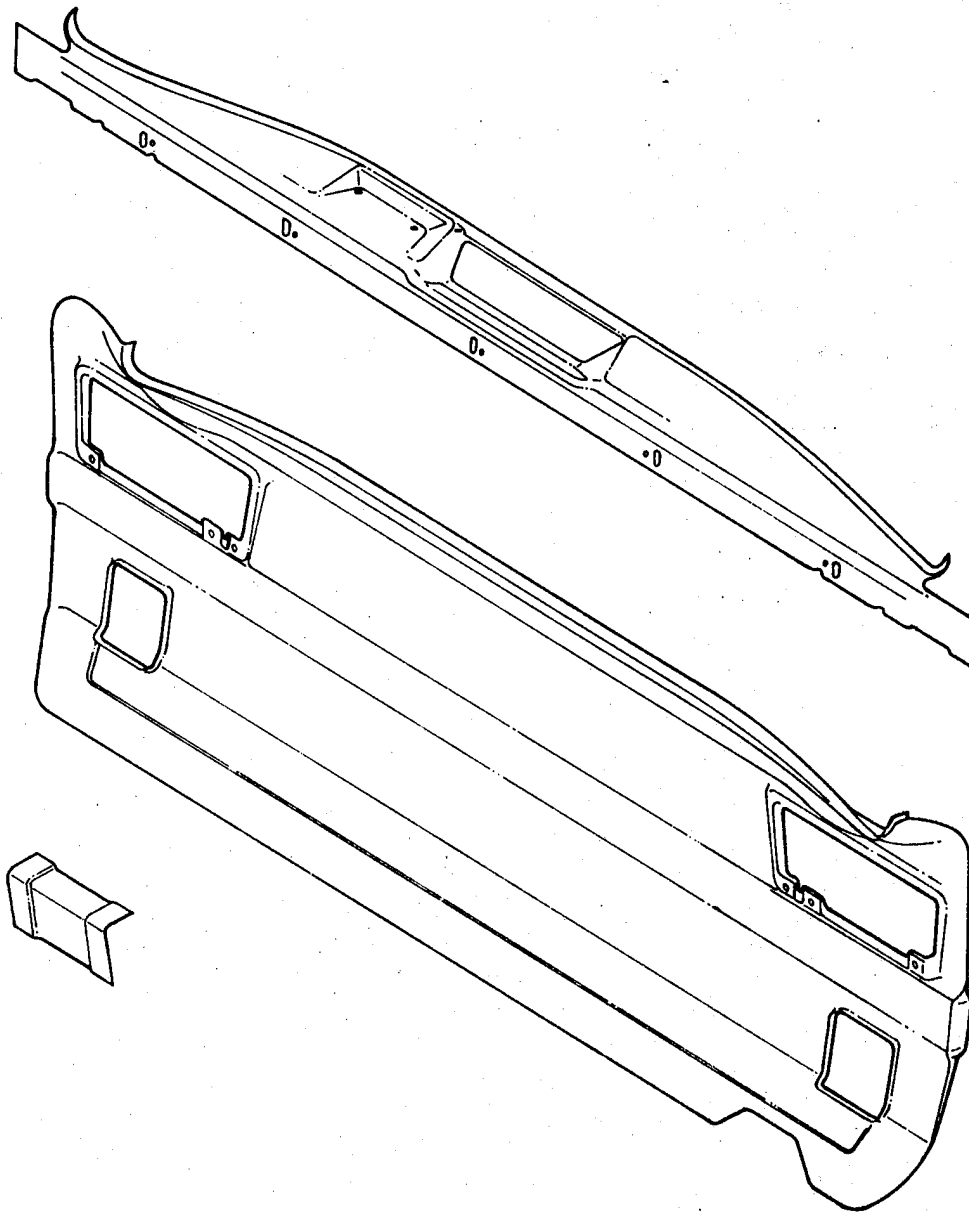
Using aluminum alloys in place of low carbon steel will also require changes in the number of resistance spot welds or the weld pattern. A low carbon steel, 0.040" thick, at 35,000 psi ultimate strength will develop an individual spot minimum weld strength of 1000 pounds. An aluminum alloy of the same strength and thickness will develop individual average spot strengths of 500 pounds. This data is taken from resistance spot weld charts shown in Tables 74 and 75. Doubling of the number of welds may be impossible without increasing the flange size and the entire joint area. Adhesive bonding in conjunction with resistance spot welding provides a big improvement over resistance spot welding alone. Using weld-through adhesives, which cure in the paint oven, the joint strengths can be increased considerably. The area of bonding can be determined from the overlap dimensions shown on the welding chart, Table 74. For an 0.040 inch thick material the joint overlap is 0.750 inches. For a 2000 psi shear strength adhesive, the adhesive joint has the possibility of 1500 psi per inch of joint. This is better than the welds alone in shear. Experience has shown however that the combination of the two joining processes are superior to either one alone, providing excellent shear, peel and fatigue strength. The adhesive is expensive, and is another cost which has to be included in comparisons.

It should also be pointed out that aluminum alloys should be cleaned to remove grease, oil, other preservatives and the oxide film. This cleaning has to be completed somewhere in the manufacturing process to provide consistant resistance spot weld strength and adhesive bonding strength and durability. Normally this is not done on low carbon steel which does not form a highly resistant oxide film, and lubricants are used sparingly during the stamping of steel.

A reinforced plastic Volkswagen structure could be fabricated by combining parts. It is anticipated that the side structure extending from the front radiator support to the rear close off panel could be made of two large moldings as shown in Figure 185. In the front, the fender would be a separate piece slightly reshaped to provide a stiffening close off at the "A" post. The design problem becomes one of integrating parts and providing means of assembly of the resulting parts.

A reinforcing sill and spring tower molding is shown in Figure 186. A detailed analysis would be required to determine the optimum orientation of the reinforcing fibers. Glass or Kevlar 49^{TM} are tentatively preferred over graphite to obtain higher impact resistance. Continuous oriented fiber would be desirably located from the end of the energy absorbing portion to the fire wall. They would also be desirable in the vertical direction through the spring tower. A metal plate may be required in the spring tower seat to prevent wear and degrading of the spring and shock absorber mounting.

358

TABLE 74: ALUMINUM SPOT WELDING CHART

Thinnest Outside Piece	Electrode Diameter	Net Electrode Force	Weld Time	Weld Strength (28-56 ksi)		Weld Spacing
T in.	in.	lbs.	Hz	Min. lbs.	Av. lbs.	Min. in.
0.032	5/8	500	6	250	350	1/2
0.040	5/8	600	8	375	500	1/2
0.050	3/4	700	8	500	650	5/8
0.063	3/4	800	10	700	850	5/8
0.071	3/4	900	10	800	1,000	3/4
0.080	7/8	1,000	10	950	1,150	3/4
0.090	7/8	1,100	12	1,100	1,400	7/8
0.100	7/8	1,250	15	1,250	1,650	1
0.125	7/8	1,400	15	1,700	2,200	1-1/4

TABLE 75: LOW CARBON STEEL SPOTWELDING CHART

Thickness of Thinnest Outside Piece "T" in.	Electrode Diameter (2-1/2" R. Dome) Inches	Net Electrode Force Pounds	Weld Time (60 C.P.S.) Cycles	Minimum Weld Strength Pounds	Minimum Weld Spacing To Inches 2T	3T
.010	3/8	200	4	175	1/4	1/4
.020	3/8	300	6	320	3/8	3/8
.030	3/8	450	8	600	1/2	3/4
.035	1/2	520	9	800	5/8	1
.040	1/2	600	10	1000	3/4	1
.050	5/8	750	13	1500	7/8	1-1/4
.062	5/8	950	15	2000	1	1-3/8
.078	5/8	1200	19	3000	1-1/4	1-5/8
.094	3/4	1450	22	4000	1-1/2	2
.109	3/4	1750	24	5000	1-5/8	2-1/4
.125	7/8	2200	27	6000	1-3/4	2-1/2

FIGURE 185   RABBIT – COMPOSITE SIDE STRUCTURE

FIGURE 186   RABBIT-COMPOSITE SILL AND SPRING TOWER
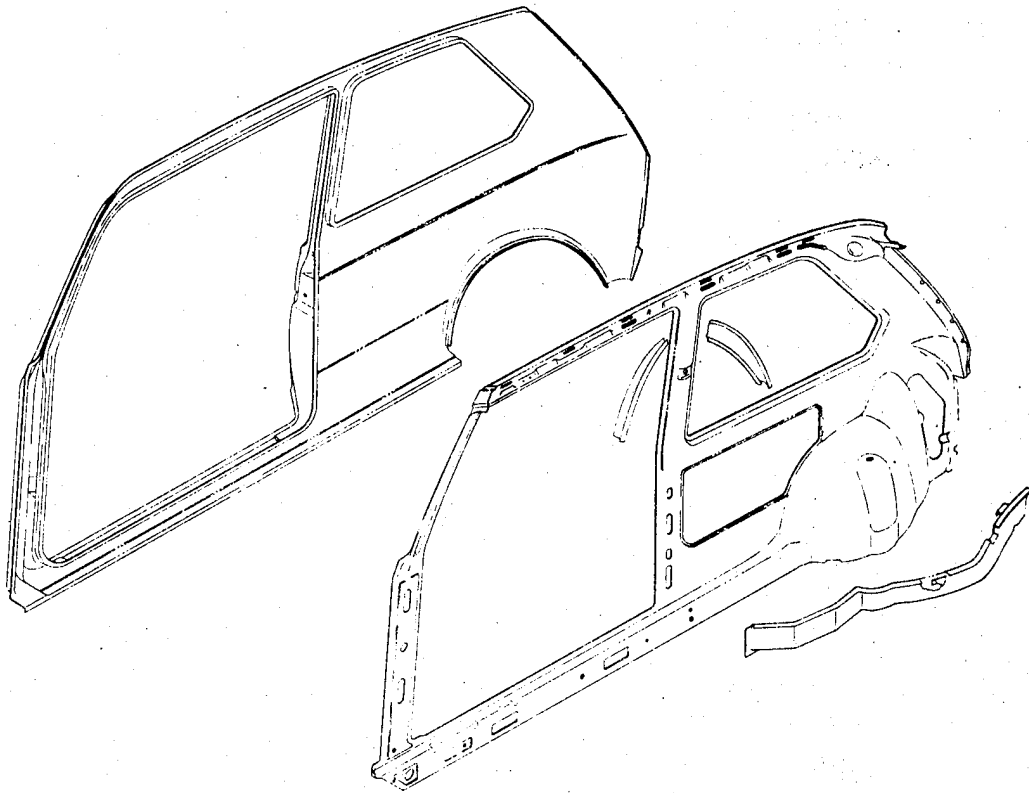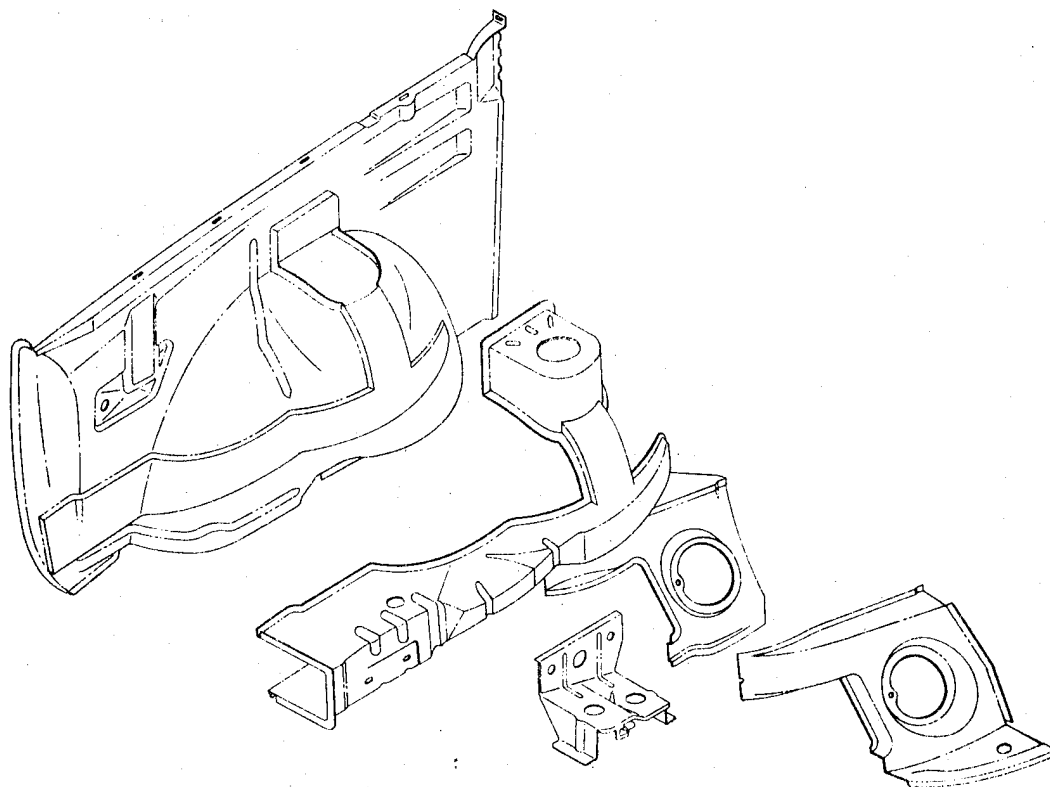
The motor mount can be rivet-bonded to the energy absorbing sill prior to mounting the sill onto the side structure. The reinforced plastic molding can be thickened locally if necessary, or an internal metallic back up pad can be used to support the engine mounting.

The Rabbit floor pan can be made of a reinforced plastic, 2 or 3 piece unit from the fire wall through to the rear close off panel. A single reinforcing molding will reinforce the front floor. Runners for the seats are feasible in nylon or remain metal. A conceptual drawing of the floor pan is shown in Figure 187.

As discussed in previous sections the strength of roof panels and reinforcements made of steel can be matched using reinforced composites. The roof deflection under load however requires a larger number of reinforcements in the case of the composites. Increasing the depth of the roof structure may also be required but results in a small decrease, less than 0.5 inches, in head room if the outer styling lines are maintained.

In the above general discussion of reinforced plastic the primary material in mind has been glass reinforced polyester. The material grade will vary as determined by analysis. In general the base material selection would be a 30% glass-polyester SMC with the glass in 1 inch chopped lengths. As required directional - continuous fibers can be applied to the molding although some care must be taken to be certain that fiber movement is not so large that the desired properties are not obtained. This in general requires that the amount of flow during molding be limited which in turn requires that the area of the mold covered by the charge be increased, approaching 100%. This does not mean that the oriented, continuous fibers cover the mold 100% but rather the combined charge. For example it is probably desirable to place long continuous fibers in the inner and outer roof moldings around the windshield opening and at the inner panel reinforcing ribs, Figure 188.

The directional continuous fibers have to be placed in the desired final position in the mold. The random fiber material cannot be placed such that as it is flowing to fill the mold it disturbs the directional fiber placement. One method of preventing this from occurring then is to have the chopped random fiber molding compound cover the entire mold face. A second method, which increases the mold cost slightly, would be to machine grooves in the inner mold half to locate the continuous fibers. With this half of the mold on the bottom, when in the press, the continuous fibers could be preplaced and the random fiber molding compound placed on top. How much flow could be tolerated with the random chopped fibers in this case is not known.

FIGURE 187   **RABBIT-COMPOSITE FLOOR**
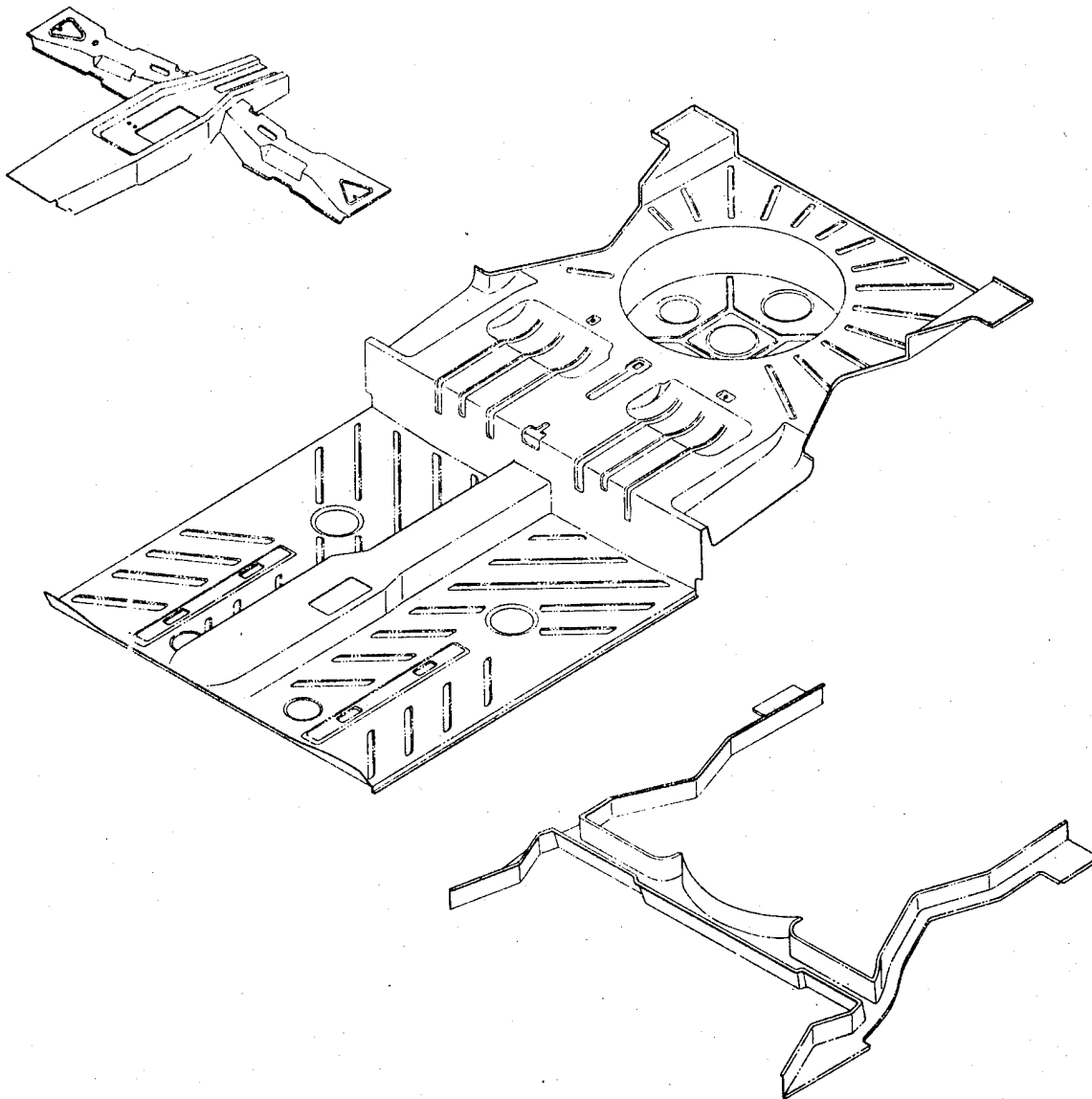
FIGURE 188   CONCEPT ORIENTED CONTINUOUS FIBER PLACEMENT

DIRECTIONAL,
CONTINUOUS
FIBERS
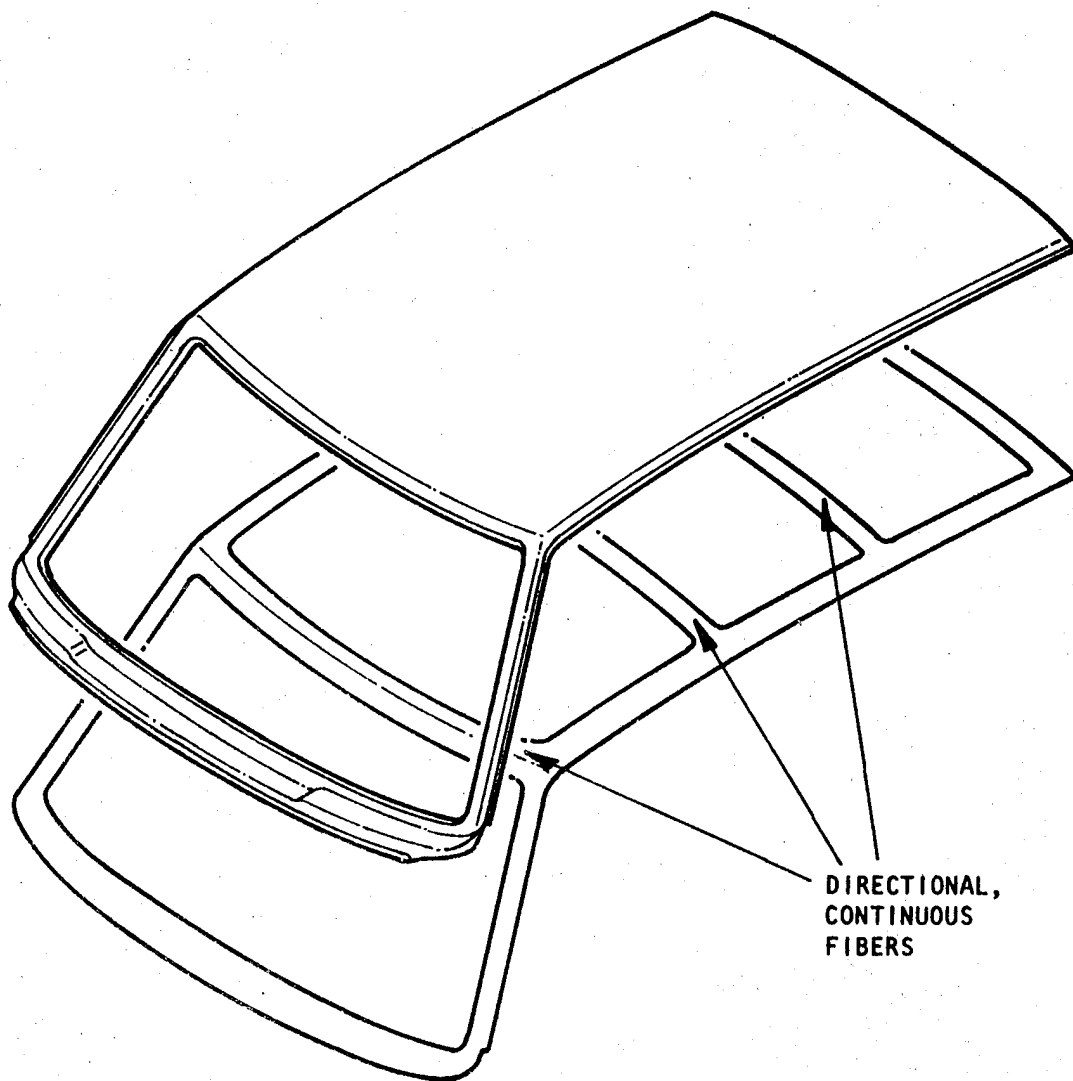
The joining of glass polyester systems can be accomplished by adhesives or adhesives and mechanical fasteners. The combination is preferred to prevent peeling in the joints with catastrophic failure. To eliminate the rivets, the joints can be designed such that there are always parts of the joint loaded in shear.

8.1 Analysis, Volkswagen Rabbit Body

A finite element model of the Rabbit was prepared as shown in Figure 189. The model consists of 181 nodes, 73 beams, 121 quadrilateral panels and 31 triangular panels. The model is a half model, symmetrical about the longitudinal axis. The 1 "g" static weight of 930# (steel) and 734# (aluminum) has been distributed to the nodes.

Five loading cases were run on the computer. Each case was analyzed for an all steel car and for an all aluminum structure. The five cases are listed below:

1. 1 "g" Vertical
2. 3.5 "g" Bump on Front Wheel
3. Braking 1 "g" Vert and 1 "g" Fwd
4. Cornering 1 "g" Vert and 0.7 "g" Lateral
5. Torsion 3.5 x Static at Outb'd Front Wheel

Shown on Figures 190 through 199 are the 3 most highly stressed beams and panels for each condition. The deflections of certain nodes are also shown.

In the case of static vertical loading, lower stresses and higher deflections are found in the aluminum vehicle. This is as expected due to the resulting lower vehicle weight and lower elastic modulus of the aluminum alloy.

A higher jouncing load at a front wheel, as shown in Figures 192 and 193, results in higher stresses in the front sills and adjacent front wheel housing (inner fender) panels. Roof deflections increase as might be expected.

Stresses and deflections produced by braking loads, Figures 194 and 195, emphasized similar panels and beams as the cornering loads. The stress levels, however, were considerably lower.

Cornering loads, Figures 196 and 197, produced the highest stresses in the front sill structure. These stresses are near the yield strength of either the steel or aluminum alloys. The loading is moderately higher than seen in actual service but does point out the similarity of the steel and aluminum structure.

Very high stresses and deflections are again encountered in the torsion loading condition. In this case the vertical load

FIGURE 189   RABBIT COMPUTER MODEL

367
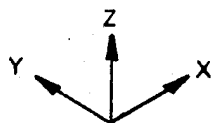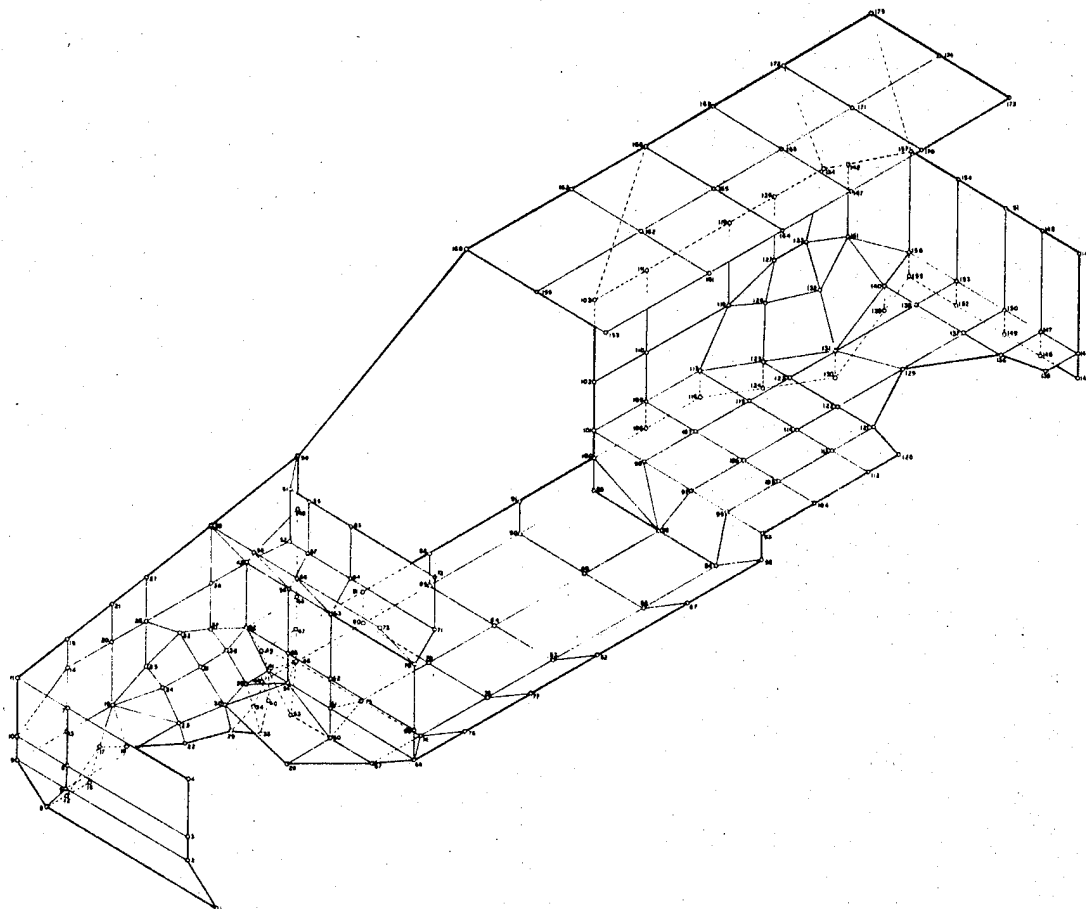
FIGURE 190   RABBIT 1"g" VERTICAL-STEEL

HIGH STRESS BEAMS

BEAM	STRESS
30-35	-9135,7765
116-124	-8790,8040
23-30	-6251,6936

DEFLECTIONS

NODE	X	Y	Z
173	-.001	0	-.136
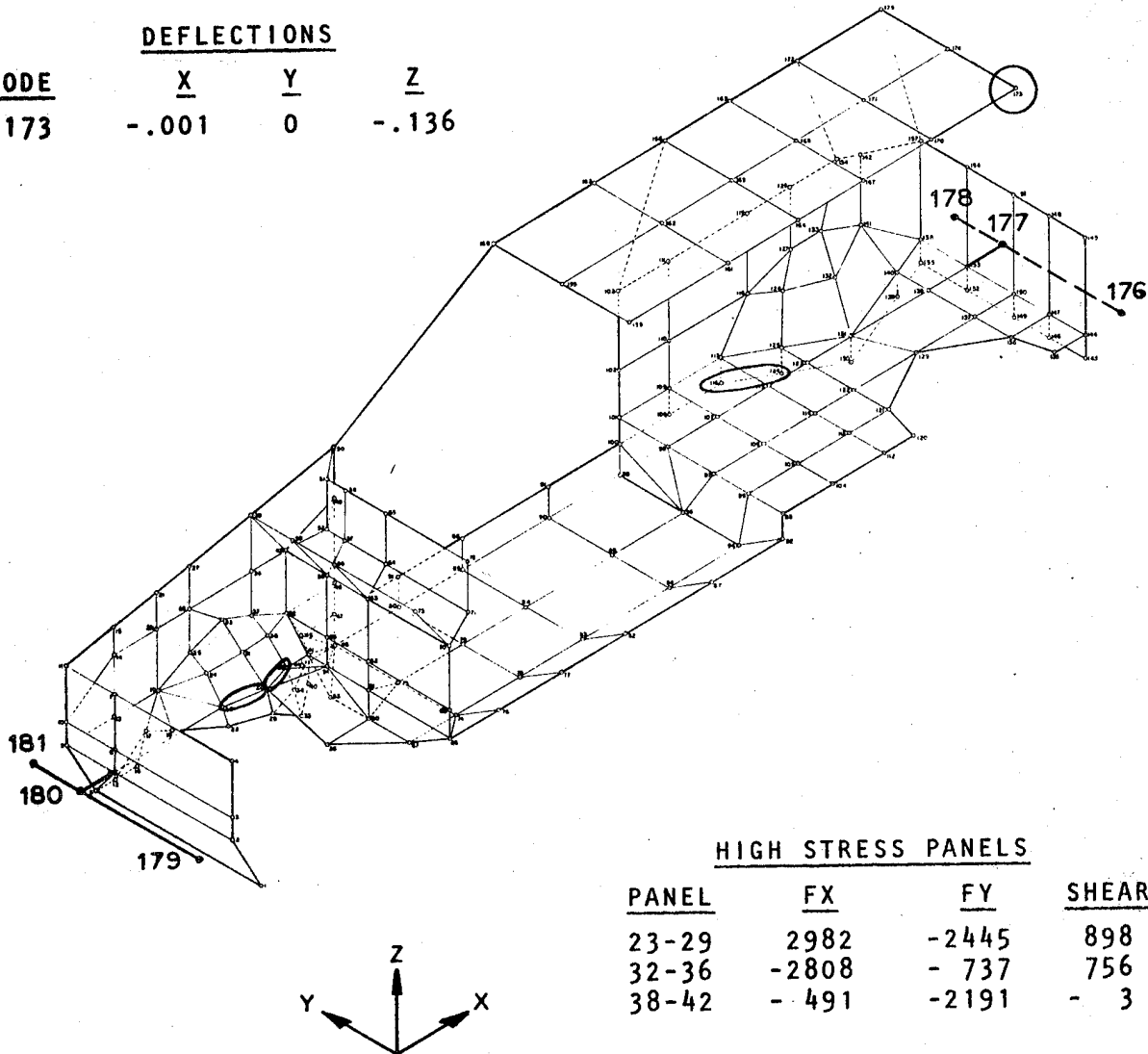
HIGH STRESS PANELS

PANEL	FX	FY	SHEAR
23-29	2982	-2445	898
32-36	-2808	- 737	756
38-42	- 491	-2191	- 3

368

FIGURE 191   RABBIT 1"g" VERTICAL-ALUMINUM

HIGH STRESS BEAMS

BEAM	STRESS
30-35	-7173,6717
116-124	-6165,5705
23-30	-4975,6022

DEFLECTIONS

NODE	X	Y	Z
173	-.004	0	-.167
174	-.004	0	-.112
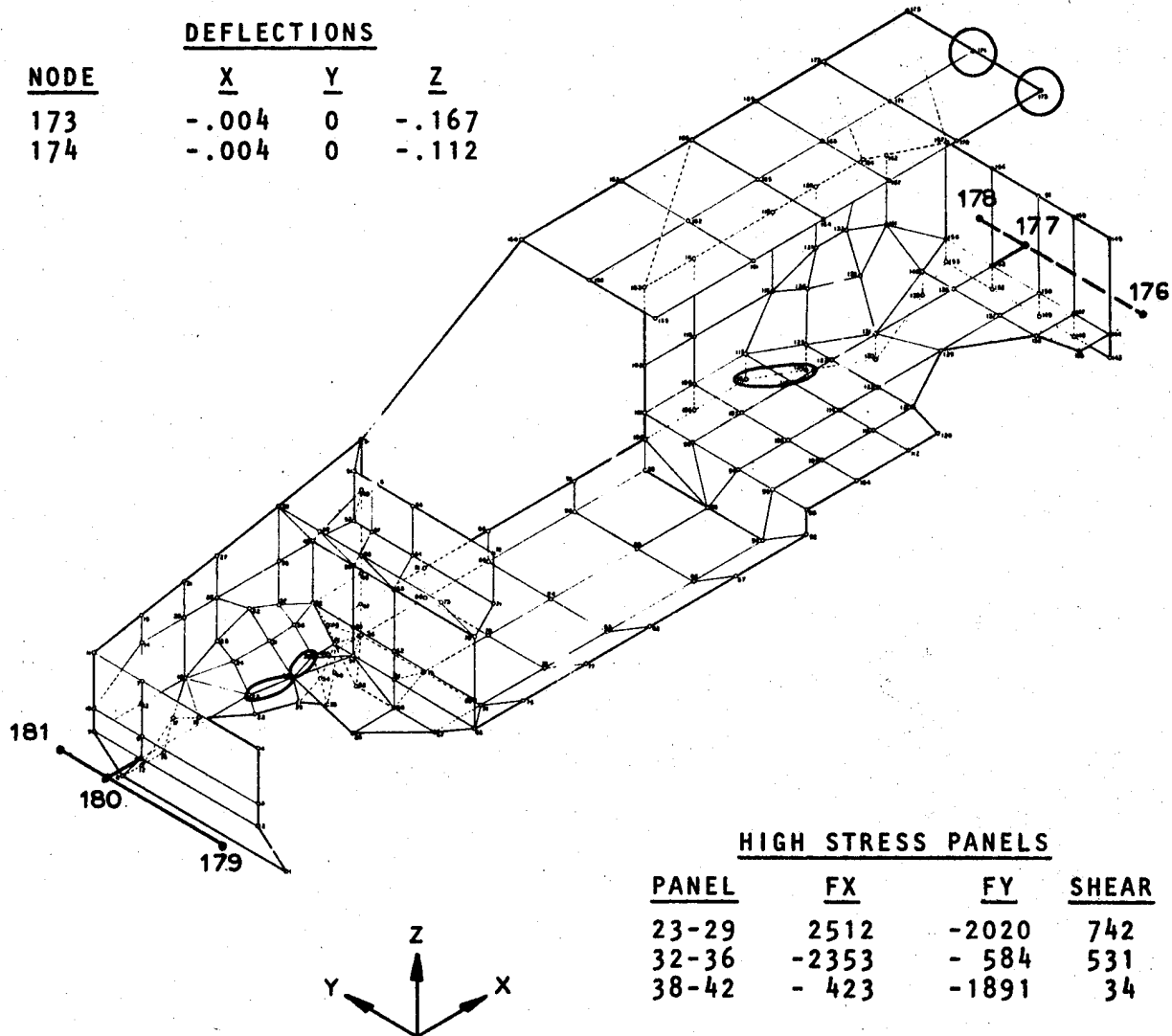
HIGH STRESS PANELS

PANEL	FX	FY	SHEAR
23-29	2512	-2020	742
32-36	-2353	- 584	531
38-42	- 423	-1891	34

369

FIGURE 192   RABBIT 3.5 "g" FRONT WHEEL BUMP-STEEL

HIGH STRESS BEAMS

BEAM	STRESS
30-35	-27805,2620
23-30	-19133,23399
5-6	-17136,13578

DEFLECTIONS

NODE	X	Y	Z
158	-.018	0	-.144
173	-.018	0	-.101
112	-.010	0	-.089
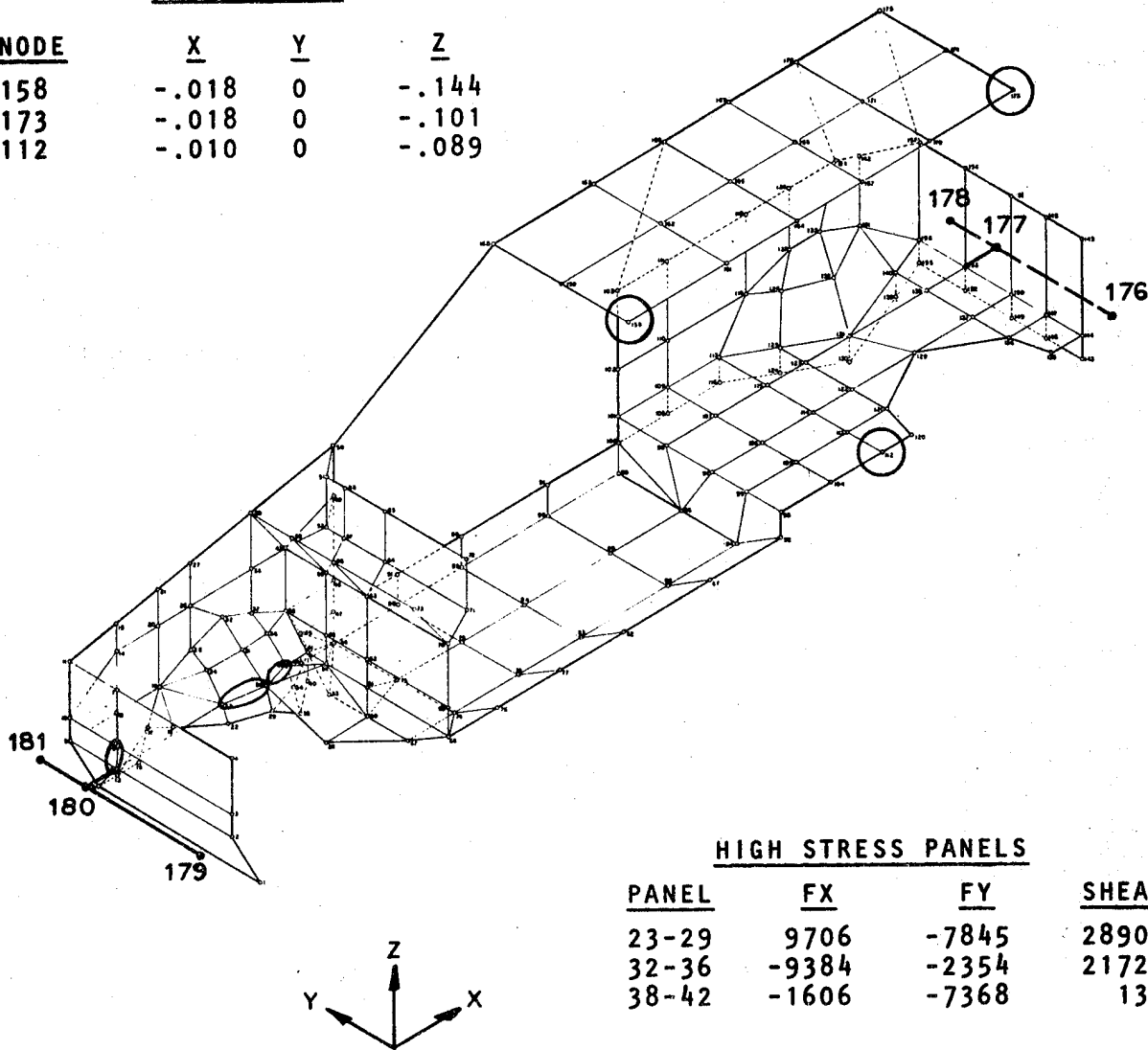
HIGH STRESS PANELS

PANEL	FX	FY	SHEAR
23-29	9706	-7845	2890
32-36	-9384	-2354	2172
38-42	-1606	-7368	13

FIGURE 193   **RABBIT 3.5 "g" FRONT WHEEL BUMP-ALUMINUM**

HIGH STRESS BEAMS

BEAM	STRESS
30-35	-25732,24018
23-30	-18016,21741
5-6	-17011,14081

DEFLECTIONS

NODE	X	Y	Z
158	-.043	0	-.170
173	-.043	0	-.126
112	-.019	0	-.073
4	-.041	0	-.149
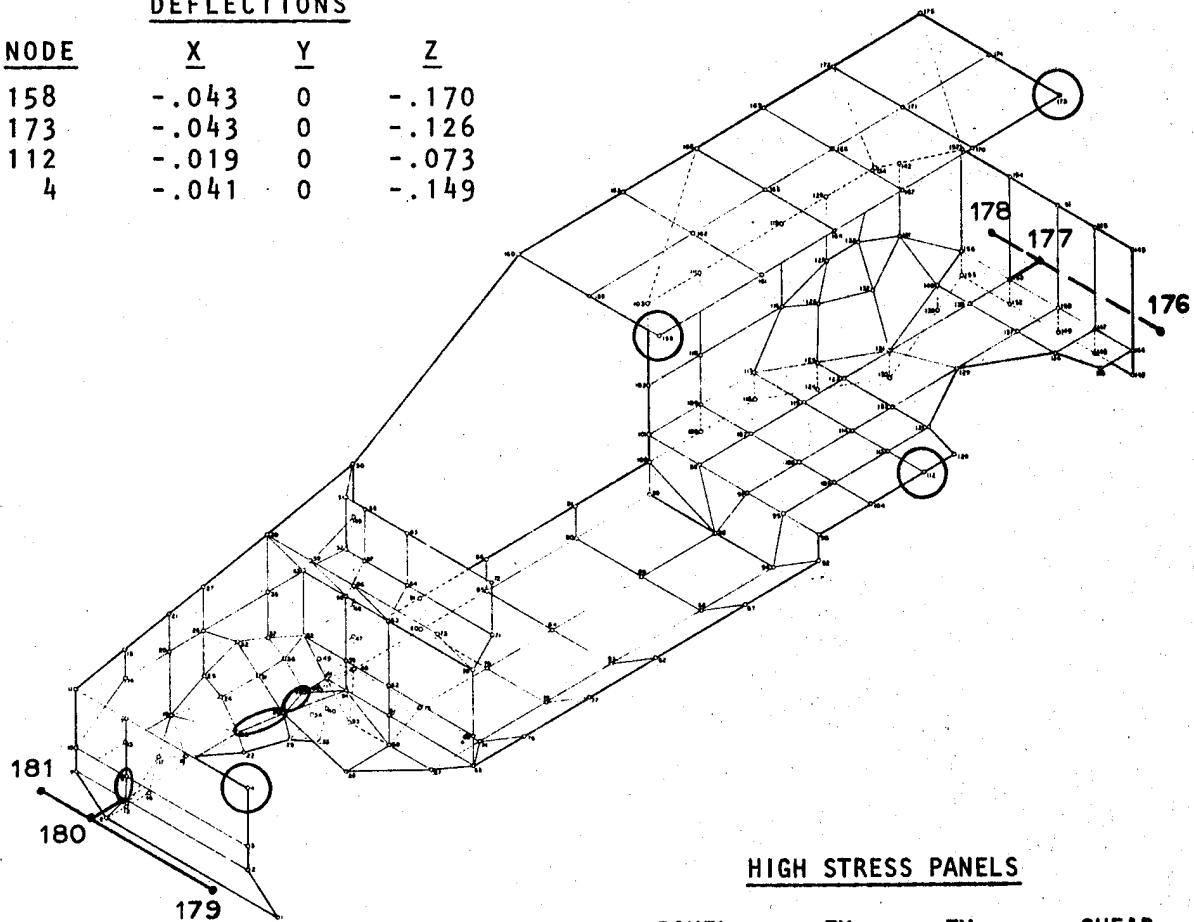
HIGH STRESS PANELS

PANEL	FX	FY	SHEAR
23-29	9194	-7291	2685
32-36	-8852	2101	1677
38-42	-1714	-7268	178
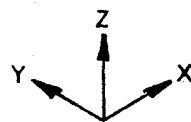
FIGURE 194   RABBIT BRAKING-STEEL

HIGH STRESS BEAMS

BEAM	STRESS
30-35	-9342,8760
116-24	-7896,9040
23-30	-5898,8631

DEFLECTIONS

NODE	X	Y	Z
173	-.008	0	-.126
72	-.114	0	-.002
112	-.001	0	-.073
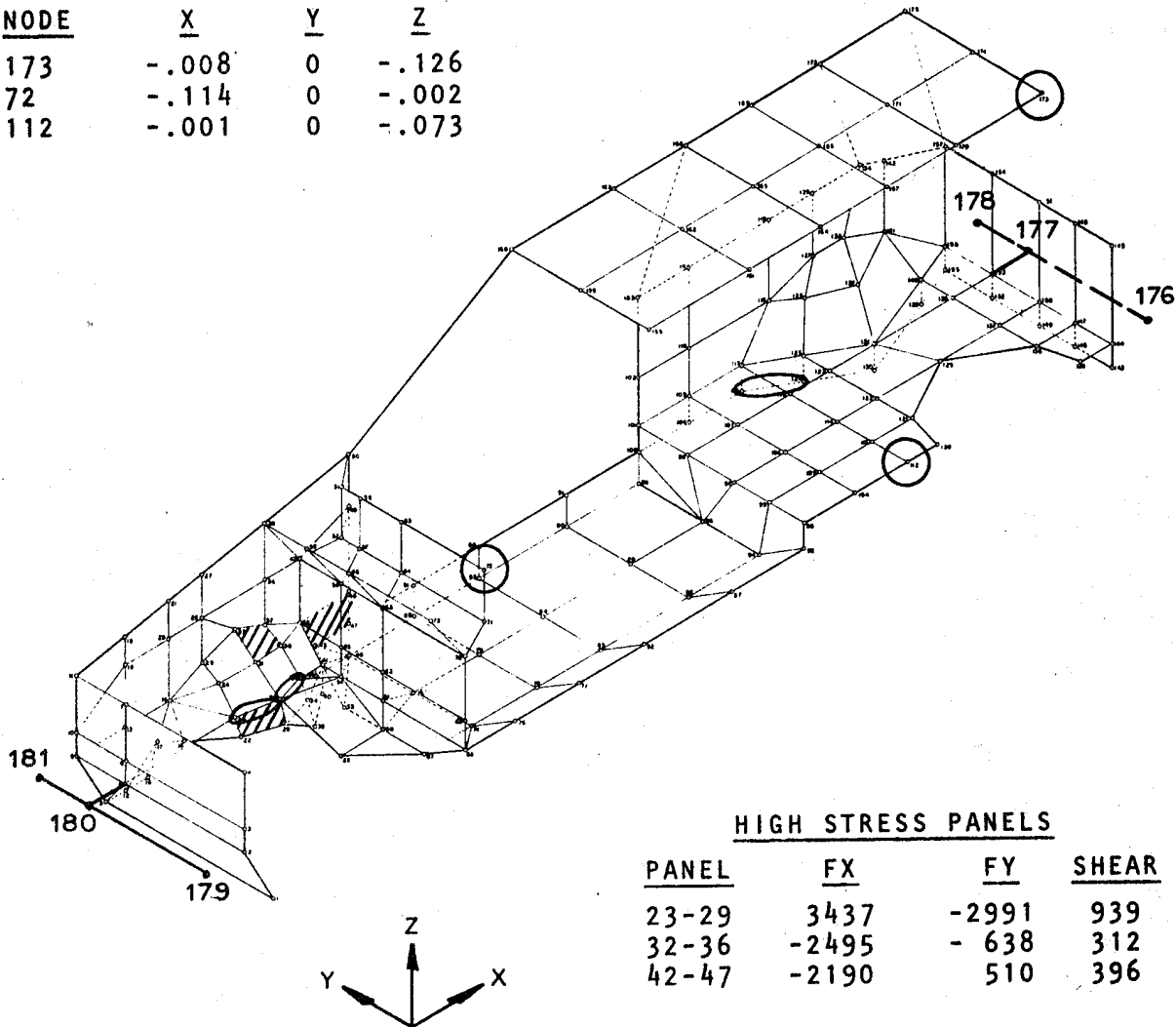
HIGH STRESS PANELS

PANEL	FX	FY	SHEAR
23-29	3437	-2991	939
32-36	-2495	- 638	312
42-47	-2190	510	396

FIGURE 195   **RABBIT BRAKING-ALUMINUM**

HIGH STRESS BEAMS

BEAM	STRESS
30-35	-6162,6178
23-30	-3876,5665
116-124	-4542,4333

DEFLECTIONS

NODE	X	Y	Z
173	-.008	0	-.151
72	-.166	0	-.002
112	0	0	-.049
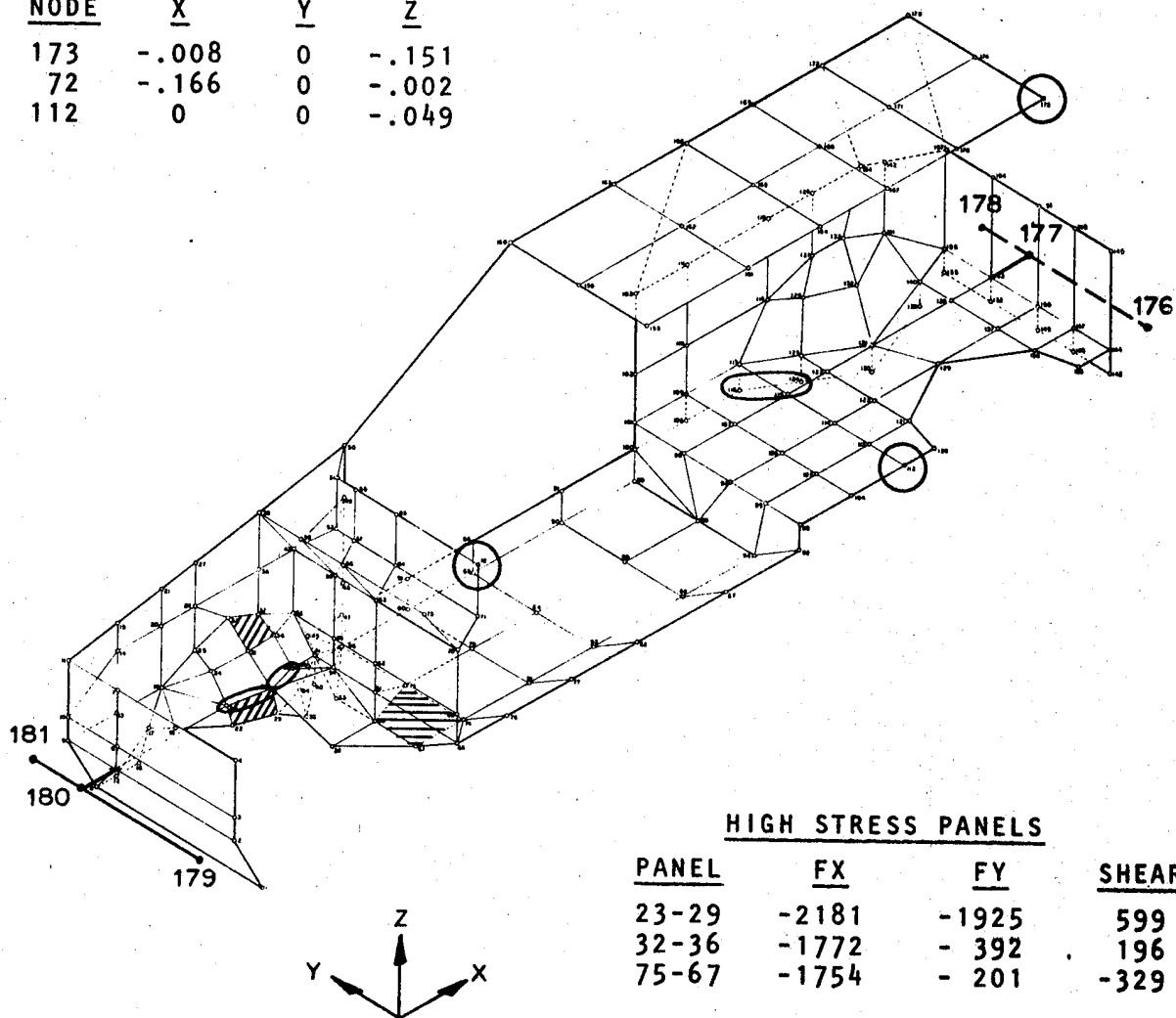
HIGH STRESS PANELS

PANEL	FX	FY	SHEAR
23-29	-2181	-1925	599
32-36	-1772	- 392	196
75-67	-1754	- 201	-329

373

FIGURE 196   **RABBIT CORNERING-STEEL**

HIGH STRESS BEAMS

BEAM	STRESS
30-35	-27732,25665
25-30	-23333,21602
116-124	-17053,15227

DEFLECTIONS

NODE	X	Y	Z
167	0	-.549	-.456
173	0	-.581	-.489
1	0	.298	-.612
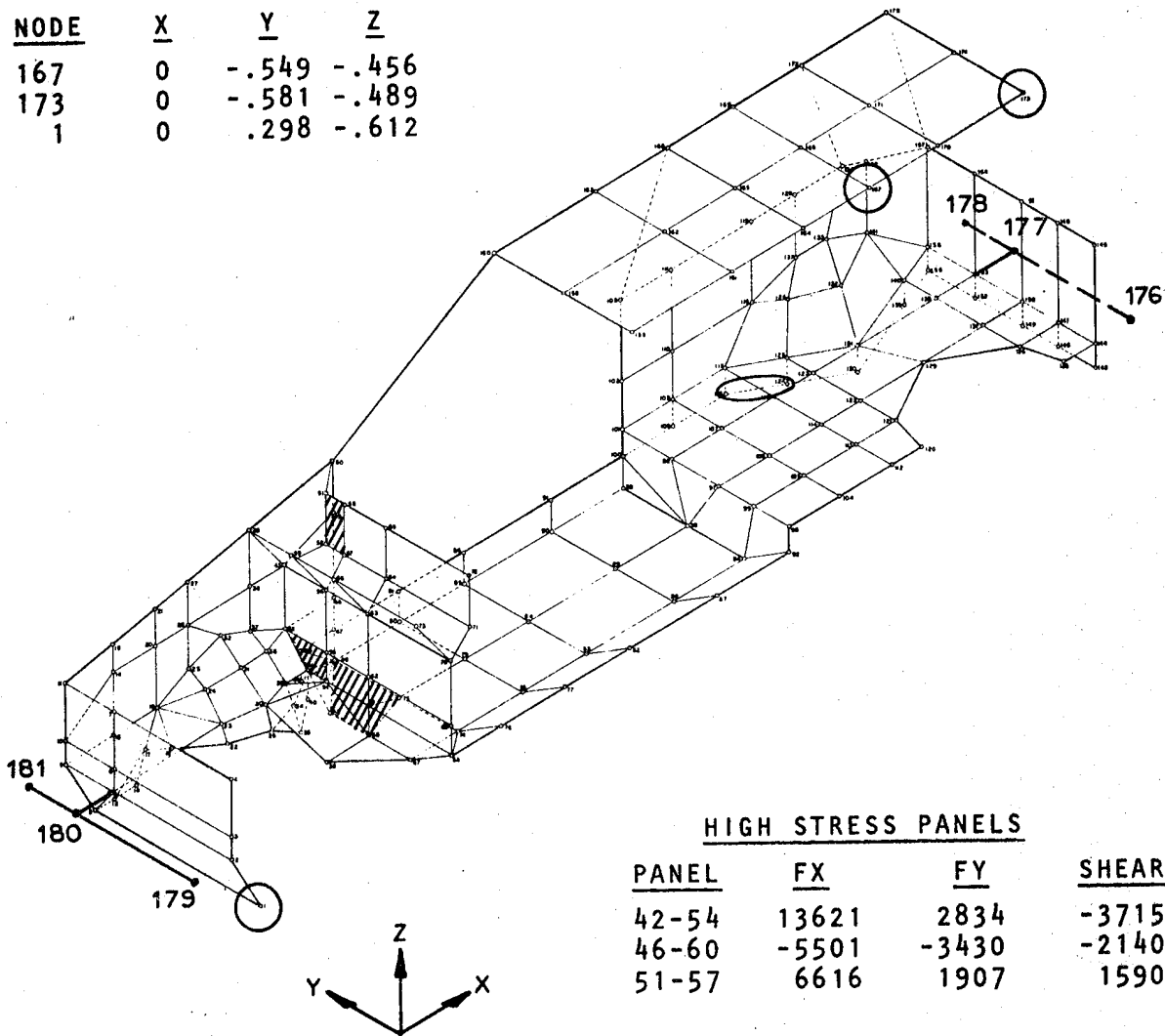
HIGH STRESS PANELS

PANEL	FX	FY	SHEAR
42-54	13621	2834	-3715
46-60	-5501	-3430	-2140
51-57	6616	1907	1590

FIGURE 197   RABBIT CORNERING-ALUMINUM

HIGH STRESS BEAMS

BEAM	STRESS
30-35	-23346,21765
23-30	-19814,18193
10-11	-16865,14210

DEFLECTIONS

NODE	X	Y	Z
167	0	-.550	-.363
173	0	-.551	-.389
1	0	.452	-1.05
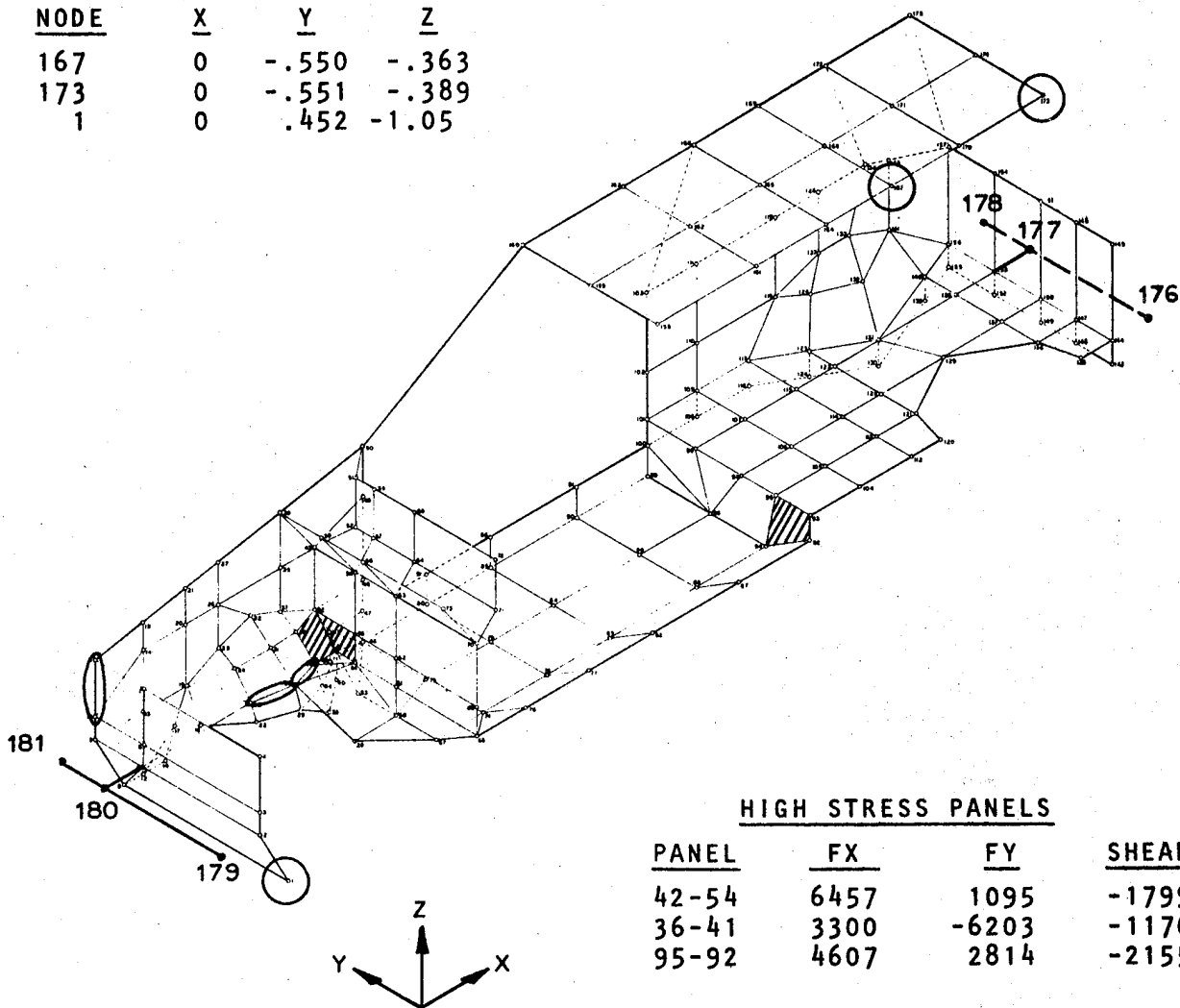
HIGH STRESS PANELS

PANEL	FX	FY	SHEAR
42-54	6457	1095	-1799
36-41	3300	-6203	-1176
95-92	4607	2814	-2155

375

FIGURE 198   RABBIT TORSION-STEEL

HIGH STRESS BEAMS

BEAM	STRESS
116-124	-46453,38502
175-157	-39447,40162
50-160	-30061,37278

DEFLECTIONS

NODE	X	Y	Z
11	-.009	.362	-.419
50	-.018	.423	-.363
175	-.033	.558	-.142
160	-.033	.468	-.332
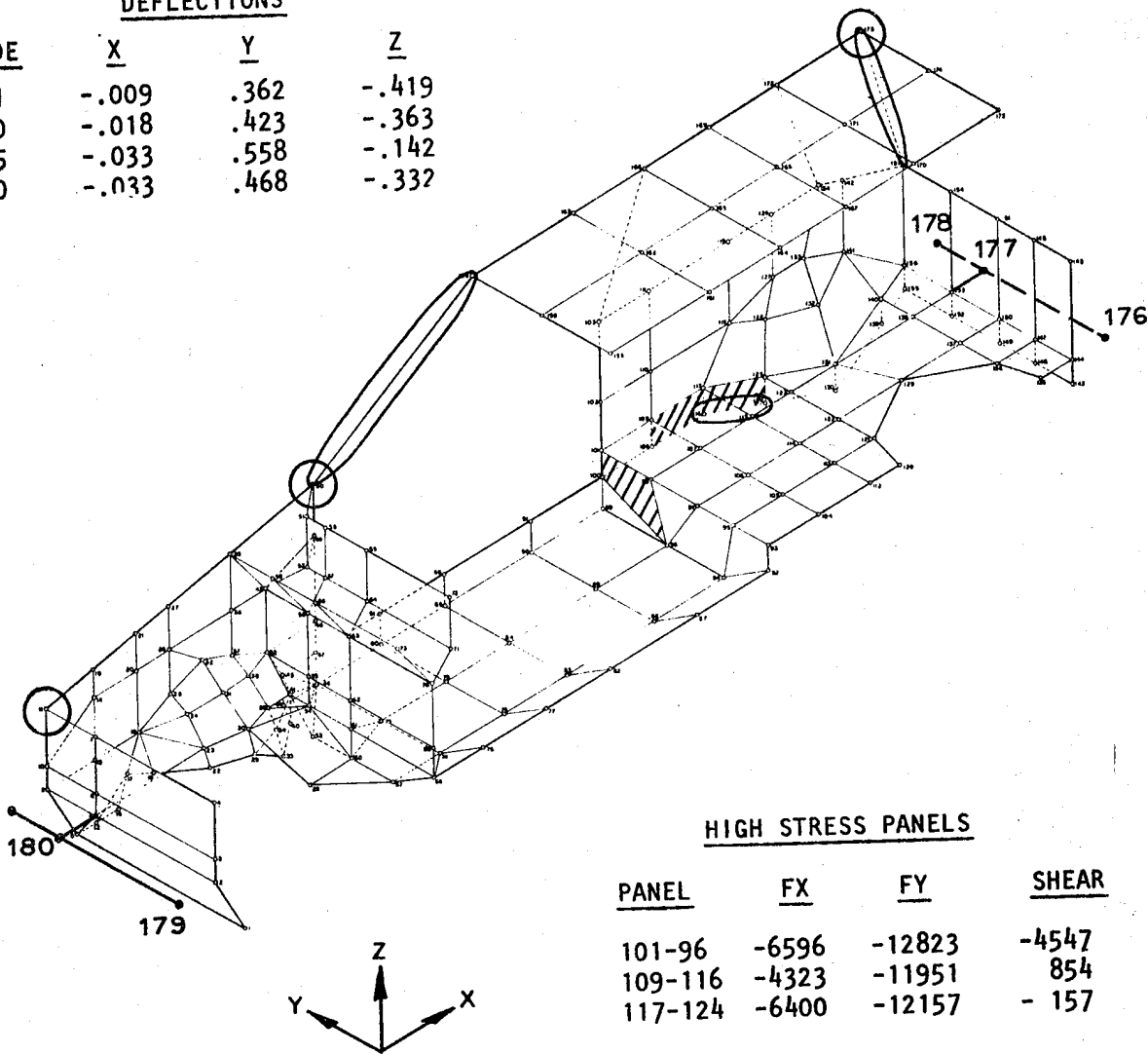
HIGH STRESS PANELS

PANEL	FX	FY	SHEAR
101-96	-6596	-12823	-4547
109-116	-4323	-11951	854
117-124	-6400	-12157	- 157

376

FIGURE 199   RABBIT TORSION-ALUMINUM

HIGH STRESS BEAMS

BEAM	STRESS
116-124	-35352,29439
175-157	-30352,31159
50-160	-24400,29974

DEFLECTIONS

NODE	X	Y	Z
11	-.025	.804	-.941
50	-.048	.937	-.802
175	-.074	1.24	-.314
160	-.074	1.039	-.741
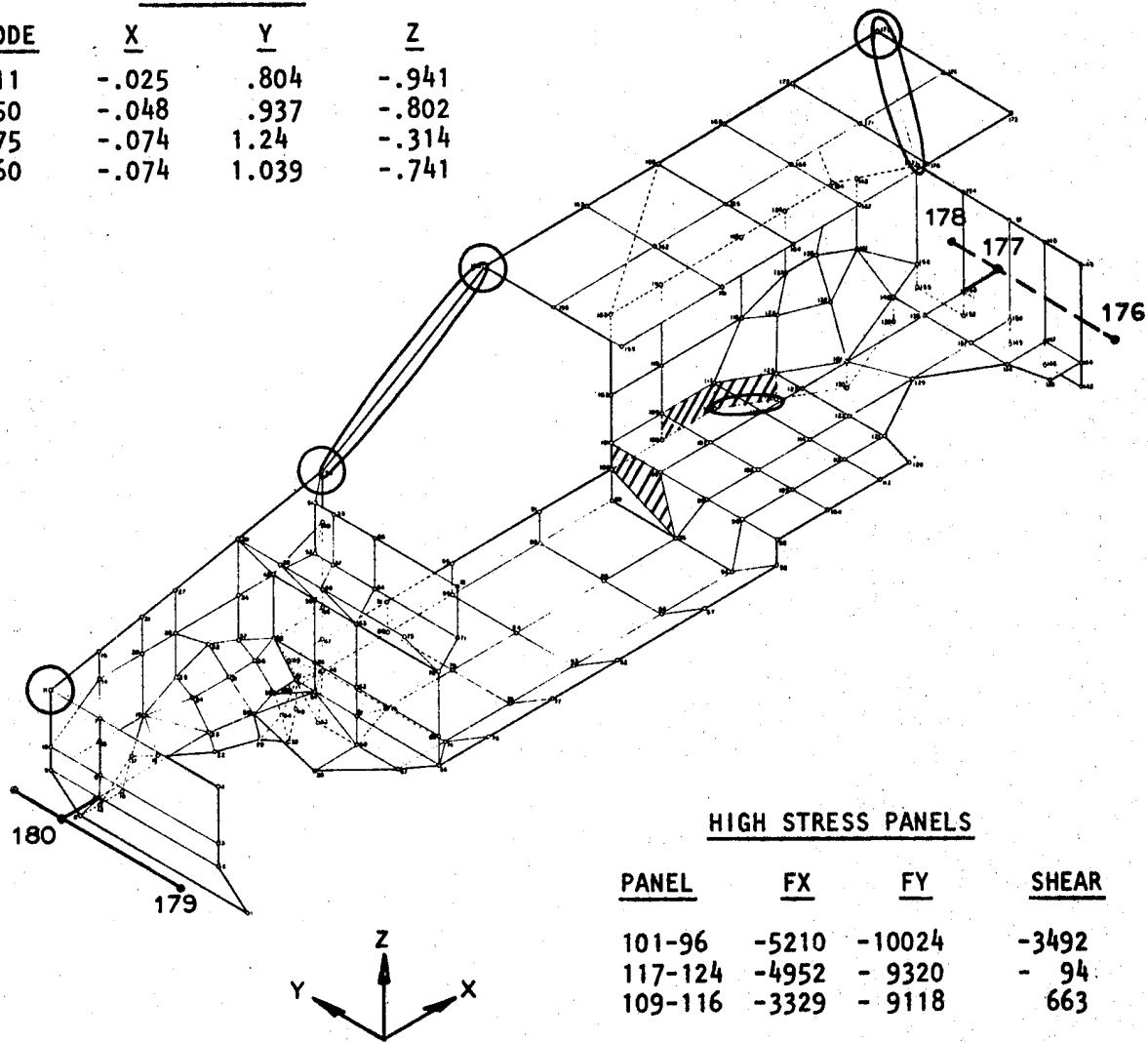
HIGH STRESS PANELS

PANEL	FX	FY	SHEAR
101-96	-5210	-10024	-3492
117-124	-4952	- 9320	- 94
109-116	-3329	- 9118	663

producing the twist is 3.5 times the static gravitational load as depicted in Figure 88. While these stresses are greater than the material yield strengths, the areas of potential failure agree with those found in testing.

8.2 Hood - Rabbit

Considerations of the Rabbit hood parallel those for the Impala hood. The primary requirements are appearance, stiffness and stability during high speed driving. The current Rabbit hood is shown in Figure 200. It is made of low carbon steel. The primary parts are the outer panel, inner panel, latches and hinge attachments. The Rabbit hood has two permanently positioned hooks welded to either side of the hood near the fire wall. Two matching eyes are welded to the inner fender wall. These are apparently provided to prevent the hood from shearing back toward the driver and passenger during a frontal collision.

Comparisons of several hood constructions are listed in Table 60 for the Impala. These comparisons are based on the calculated equal stiffness. The aluminum outer skin thickness could be kept the same by increasing the number of hat sections thereby reducing the unsupported area and resulting in a firmer feel to the outer panel. Similar consideration would be made for the Rabbit hood.

8.3 Side Doors

The side door structure for the Rabbit consists primarily of an inner and outer panel, an intrusion beam, and four reinforcements, Figure 201. Unlike the Impala doors, the window frame is integral with the lower panels. All parts appear to be made of low carbon steel, formed and resistance spot welded at assembly.

As discussed previously for the Impala door, the Rabbit doors must also withstand some minimum loading without distortion in an open position. Outer panel stiffness, or deflection, is determined by the intrusion beam. The doors must, of course, be capable of passing the FMVSS 214 static crush test. The limiting requirement would appear to be the side intrusion.

The door as shown in Figure 201 could be made from HSLA steels and aluminum alloys with a 10 to 50 percent weight reduction. Forming of the aluminum alloy panels without a redesign is questionable. To meet the current FMVSS 214 requirements a lower weight HSLA steel beam seems feasible as does an aluminum alloy beam. The reasoning is based on the belief that the bending and twisting resistance of "A" post and "B" post control the force deformation curve. While no actual static test data exists, observation of test results [101] on car to car dynamic and static tests lead to this conclusion. In fact, intrusion into the passenger compartment at a constant bullet vehicle weight and speed was most readily reduced by strengthening the "A" and "B" posts and using the lower side sill for support.

378

FIGURE 200   RABBIT – HOOD
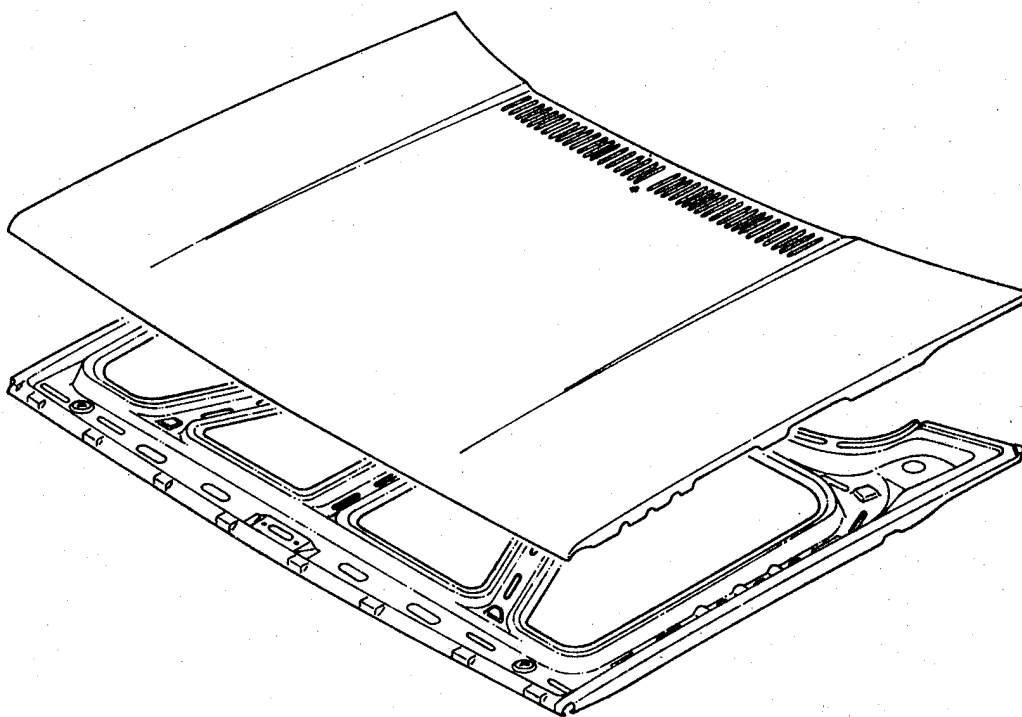
FIGURE 201   RABBIT – DOOR STRUCTURE
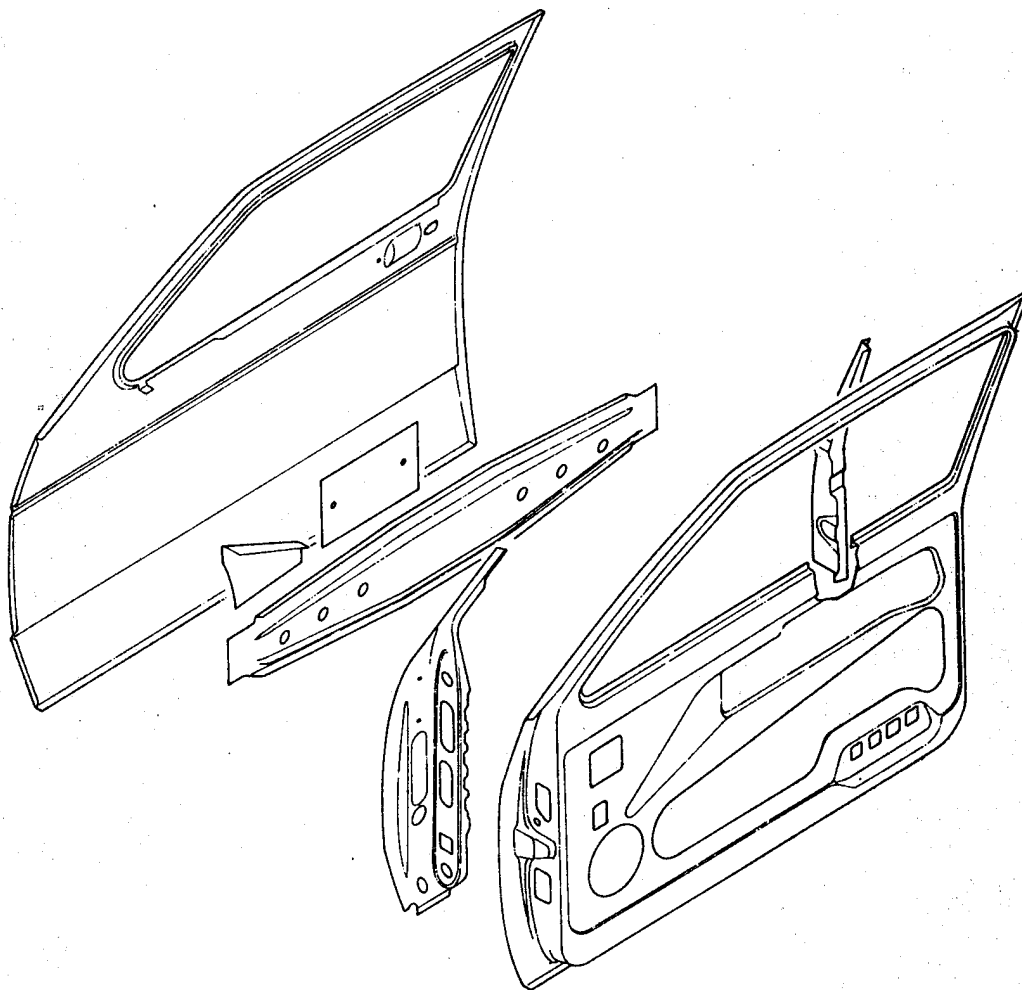
Composite doors can also be fabricated using the general configuration of the inner and outer metal panels. The inner panel could be thickened and reinforced by ribs at the latch and hinge areas as needed. The ribs would be parallel to the depth of the inner panel molding to permit removal from the mold. A composite anti intrusion beam such as that shown previously in Figures 79 and 80 can be used. Oriented continuous glass fibers provide sufficient strength. Chopped, high content glass fiber molding compound would be used for the end formations. The composite door structure would be made of 3 pieces and would be more cost competitive than one where the composite was substituted piece for piece.

8.4 Rear Door

The current rear door is shown in Figure 202 and it consists primarily of 2 sheet steel stampings. The two stampings, when assembled, provide a rigid window frame. For equal stiffness, an aluminum alloy or glass composite structure would be heavier than the steel and of no advantage. From a strength comparison the use of HSLA steel, aluminum alloy or composite would be weight effective. In these other materials there would be little change in the design except to permit manufacturing. The inner panel in the lock area would have to be modified to permit a molded composite to be removed from the tool.

8.5 Bumper System

The front and rear bumper system for the Rabbit, Figure 203 are the same, consisting of a steel bumper bar, EA devices and brackets. The weight is 37.38 pounds each or a total of 75 pounds per vehicle. Referring to Tables 46 and 47 and the associated sketches of foamed non-damageable systems, it would appear feasible to reduce weight and improve damageability using flexible foam and fascias. This is especially true for the 15 mph impact condition.

8.6 Cost Comparison

Those cost comparisons made for the Impala are applicable to the Rabbit structure. All applications of known alternate materials will result in an assembled vehicle cost increase, unless there is a sufficient opportunity to reduce labor costs through part integration.

The ratio of the direct material cost of an alternate material compared to carbon steel can be calculated based on design parameters. Using the price list of Table 65 the values listed in Table 76 were determined. Only in the case of the ultimate strength comparison is the direct material cost equal to or less than low carbon steel.

381

FIGURE 202   RABBIT – REAR DOOR
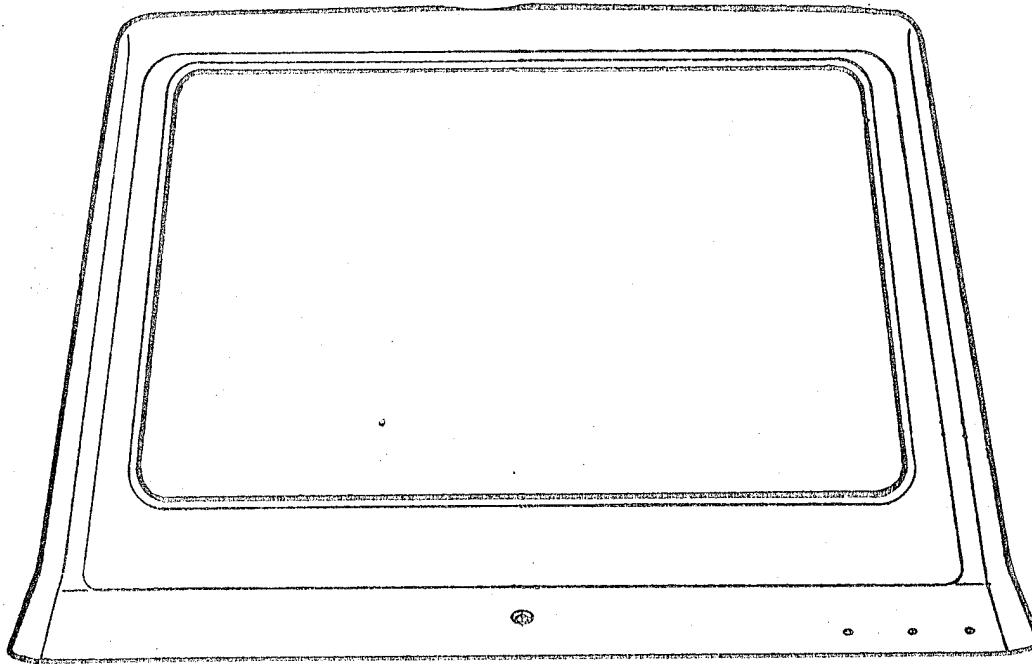
FIGURE 203   RABBIT — BUMPER SYSTEM
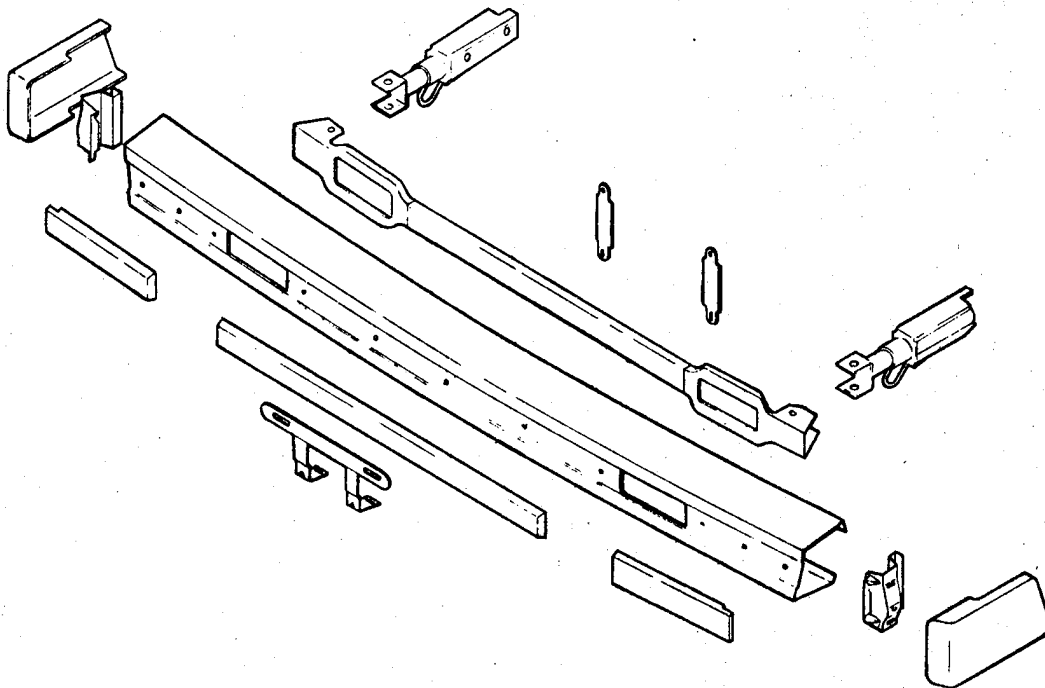
TABLE 76:   COST COMPARISON

$$F = \frac{\text{Direct Material Cost of Alternate Material Component}}{\text{Direct Material Cost of Low Carbon Steel Component}}$$

Design Parameter	Aluminum	HSLA	HMC	Graphite
Et^3	2.70	1.25	1.96	68.70
Et	5.61	1.25	11.91	134.10
σ_{ut}	1.0	0.47 to 1.25	0.48	7.38
Zf	2.65	1.08	1.38	21.29

E = Modulus of Elasticity

t = Thickness

σ_u = Ultimate Strength

f = Fatigue Strength

Z = Section Modulus

384

9.0 CRASHWORTHINESS - UNITIZED VEHICLES

9.1 Frontal Crashworthiness

There was no known available crashworthiness test data for the 1977 Volkswagen Rabbit at the time of this study nor was there any static crush data available. An impact simulation was completed, however, and the results compared to test data on a 1975 Rabbit. A 40 mph frontal impact was performed on the 1975 vehicle and was reported under DOT-HS-801-966 "Classification of Automobile Frontal Stiffness/Crashworthiness by Impact Testing", August 1976. This test result will form the basis for evaluating the simulation effort.

To obtain a first perspective of the magnitude of the kinetic energy and crush force-distances, calculations were made and the results have been tabulated below:

MPH	K.E. (ft. lbs.)	Crush Distance (in.)	Crush Force (lbs)
30	63,130	24	31,565
40	112,221	31.5	42,751
50	175,346	36	58,488

The Rabbit weighs 2100 pounds and the crush force is the average over the total crush distance.

The simulation model is shown in Figure 128 although the driveline force/deformation, S16, is eliminated because of the front wheel drive. The force/deformation curves for the firewall, S18, the radiator, S13 and the engine mounts, S15, were chosen to be the same as a 1975 Honda CVCC which had been statically crushed and whose test weight was similar to that of the Rabbit, Figures 204 through 206.

The force/deformation for the sheet metal, S14, forward frame (in this case the energy absorbing front side member box and surrounding structure), S11, and the aft portion of the frame (for the Rabbit this would primarily be the stub frame which supports the suspension members), S12, are the most critical for establishing the deceleration of the passenger compartment. An attempt to define the force/deformation response for these three members followed one of the efforts for the Impala where an ideal front end structure was assumed. Figure 207 presents the idealized force/deformation where it was assumed that F_{11} equals F_{12} and that the desired total dynamic crush would be 31.5 inches for a 40 mph frontal impact. Also used is the fact that the sheet metal should be capable for sustaining one-third of the total energy absorbed by the sum of the sheet metal and the front and rear portions of the frame. This assumption allows F_{14} of Figure 207 to be related to F_{11} and F_{12}. Following the procedure for the Impala,

FIGURE 204   ASSUMED RABBIT FIREWALL, S16

FIGURE 204   ASSUMED RABBIT FIREWALL, S16
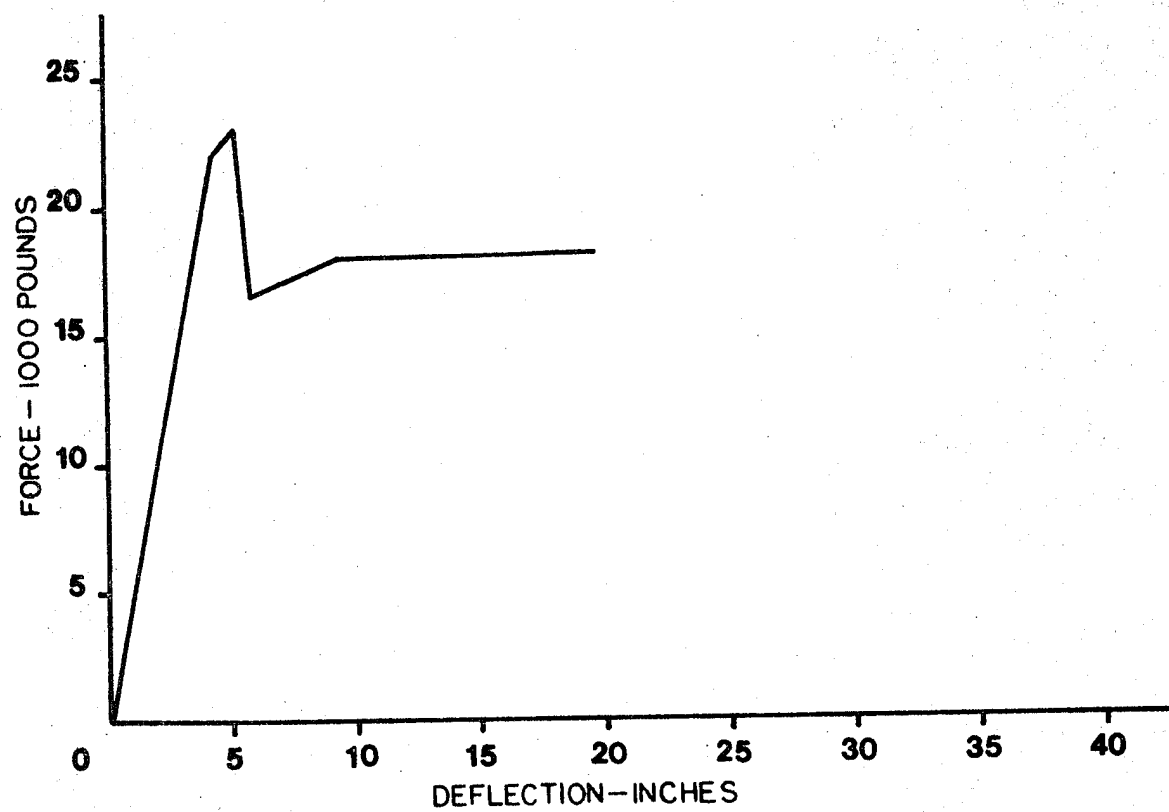
FIGURE 205   ASSUMED RABBIT RADIATOR, S13
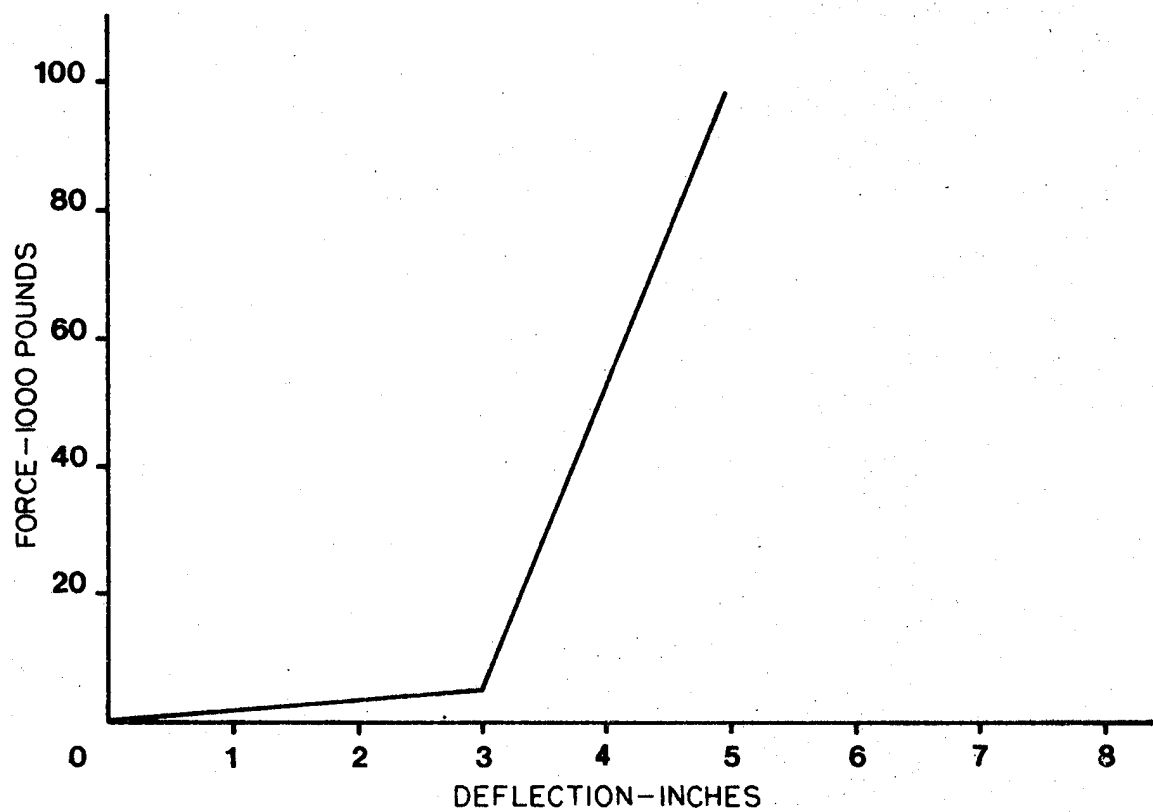
FIGURE 205   ASSUMED RABBIT RADIATOR, S13
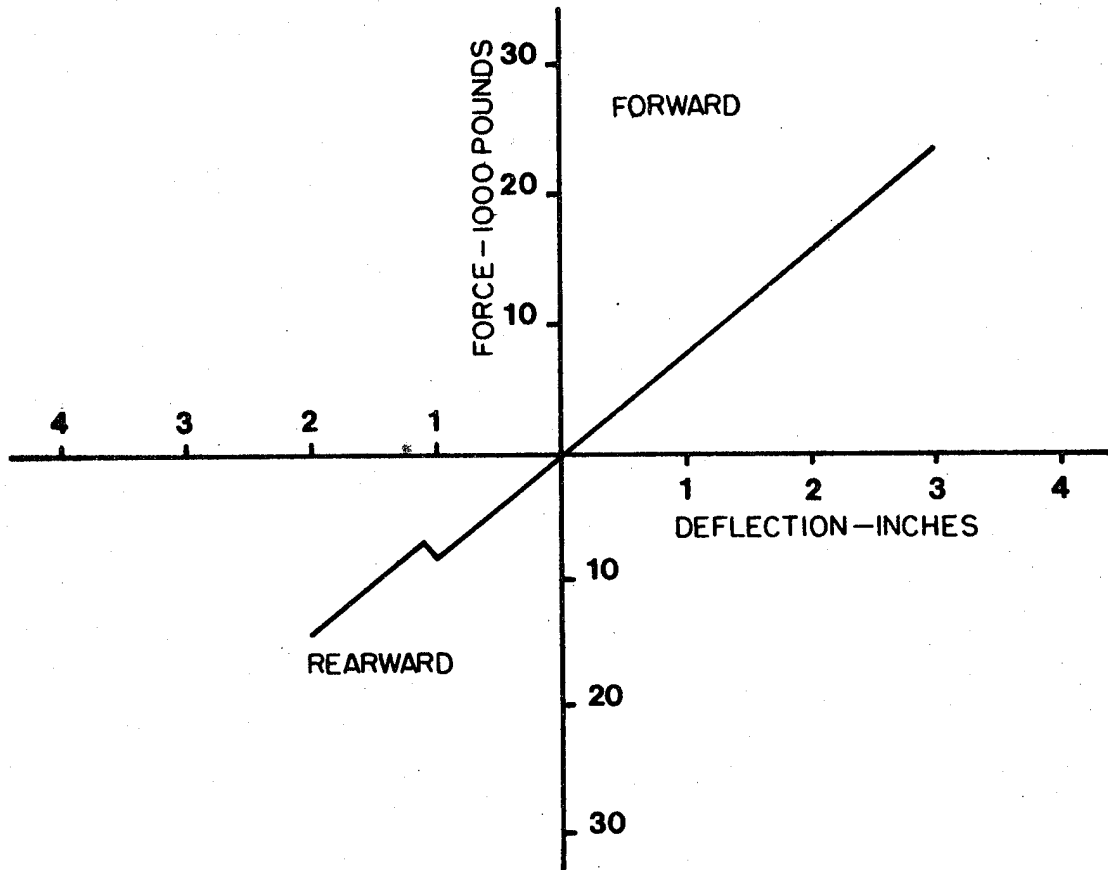
387

FIGURE 206   ASSUMED RABBIT ENGINE MOUNTS, S15

FIGURE 206   ASSUMED RABBIT ENGINE MOUNTS, S15

388

SHEET METAL

F_{14}

$ENERGY_{14} = 23.5 \; F_{14} \; IN-LBS$

.417   2.167

FORCE - POUNDS

100,000

FRONT OF FRAME

$ENERGY_{11} = (12.5 \; F_{11} + 100,000) \; IN-LBS$

.083   1.0   1.167

FORCE - POUNDS

REAR OF FRAME

F_{12}

$ENERGY_{12} = 24.5 \; F_{12} \; IN-LBS$

.083   2.083

FORCE - POUNDS

DEFLECTION - FEET

389
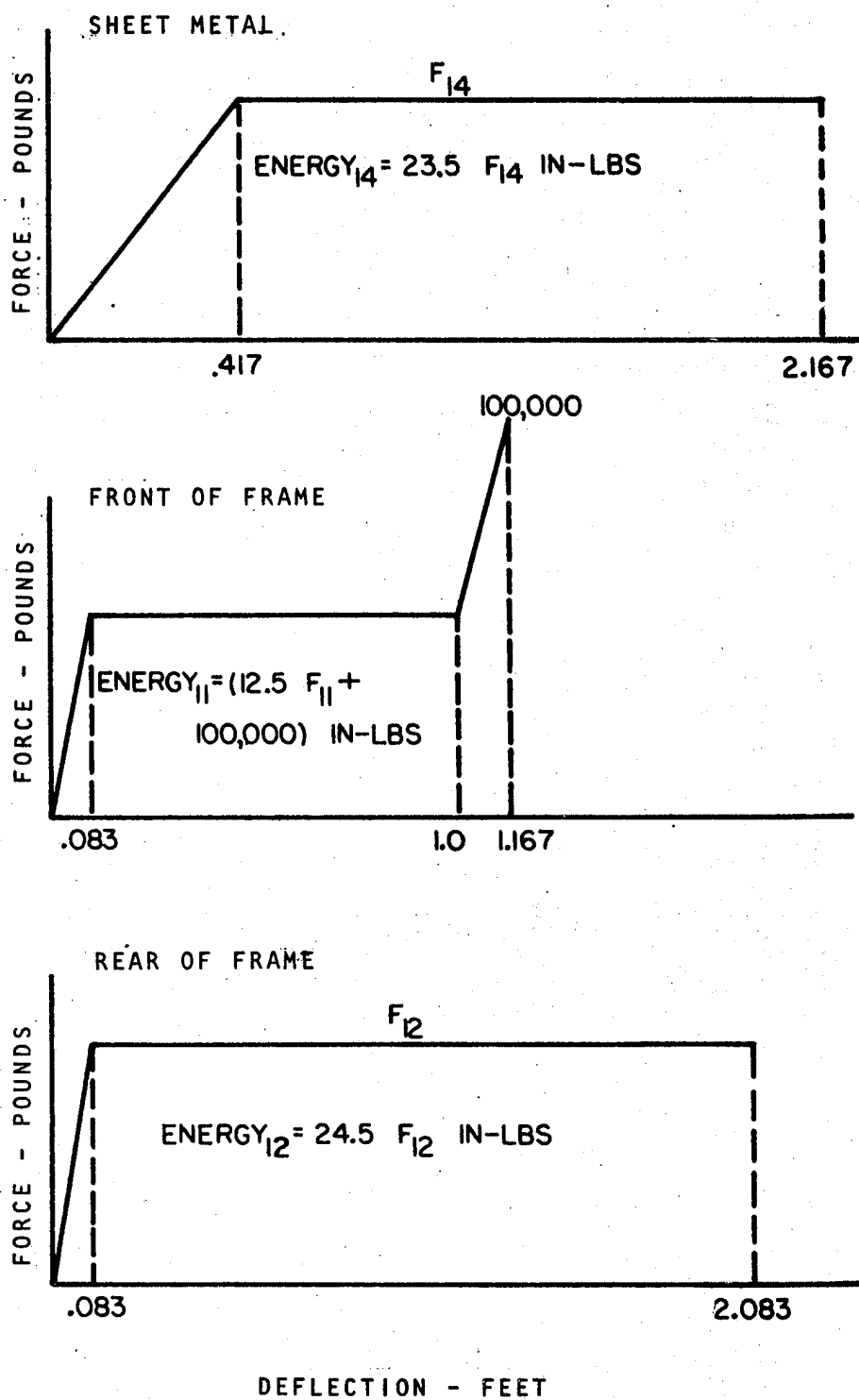
it was determined that:

$$F_{14} = 0.787 \ F_{11} + 2128, \ F_{11} = F_{12}$$

An iterative computer solution was required to obtain the value of F_{11} which would produce a total dynamic crush of 31.5 inches. A value of 16,000 pounds, using a logarithmic strain rate correction factor, was established. Therefore, the value of F_{12} was also 16,000 pounds and F_{14} was 14,700 pounds. In performing the computer analysis, the clearance shown in Figure 208 were used as well as the following weights: engine - 260 pounds, suspension - 178 pounds, bumper - 18 pounds, passenger compartment - 1404 pounds, and occupants - 280 pounds.

The results of the simulation for the passenger compartment is presented in Figure 209. The reasonable agreement between test and calculations would indicate that the Rabbit's structure, as related to sheet metal and front and rear frame sections, is close to matching the ideal assumptions of Figure 207. The large number of assumptions used for the simulation would, however, raise doubts regarding any conclusions.

The results of the simulation for the engine is presented in Figure 210. Poor correlation in both response shape and maximum deceleration levels is observed. The response shape was improved by increasing the "B" clearance of Figure 208 but the predicted peak was essentially unchanged. The peak value could be reduced by altering the assumed radiator force/deformation curve of Figure 205. Such a study was not performed because of the lack of static test data to compare the results of the study.

9.2   Alternate Materials in Frontal Structure

The Rabbit, unlike the Impala, has no separate frame. A sheet metal sill is attached to the wheel housing skirt and on the suspension supporting structure. This sill is corrugated and can be seen in the half vehicle drawings in Figure 174. The use of an aluminum alloy or HSLA steel with a resulting weight reduction appears feasible based on the data and test results discussed in Section 7.

Data available from other studies[86][102] on glass reinforced polyester energy absorption elements indicates these materials would also be satisfactory. As an example, a 6 inch diameter glass-polyester cylinder, 0.171 pounds per inch, has a crush resistance of 25,000 pounds. The corrugated sheet steel sill mentioned above has a calculated static crush resistance of less than 5820 pounds using the equation for P_m from Section 7. The corrugated steel sill weighs 0.272 pounds per inch. Using a strain rate factor of 1.8 the dynamic crush resistance of the steel sill is estimated at 10,476 pounds. A corrugated glass-polyester sill as shown in Figure 186 has been tested[102] on a study of a reinforced plastic electric

390

FIGURE 208   CLEARANCE INPUTS FOR COMPUTER SIMULATION
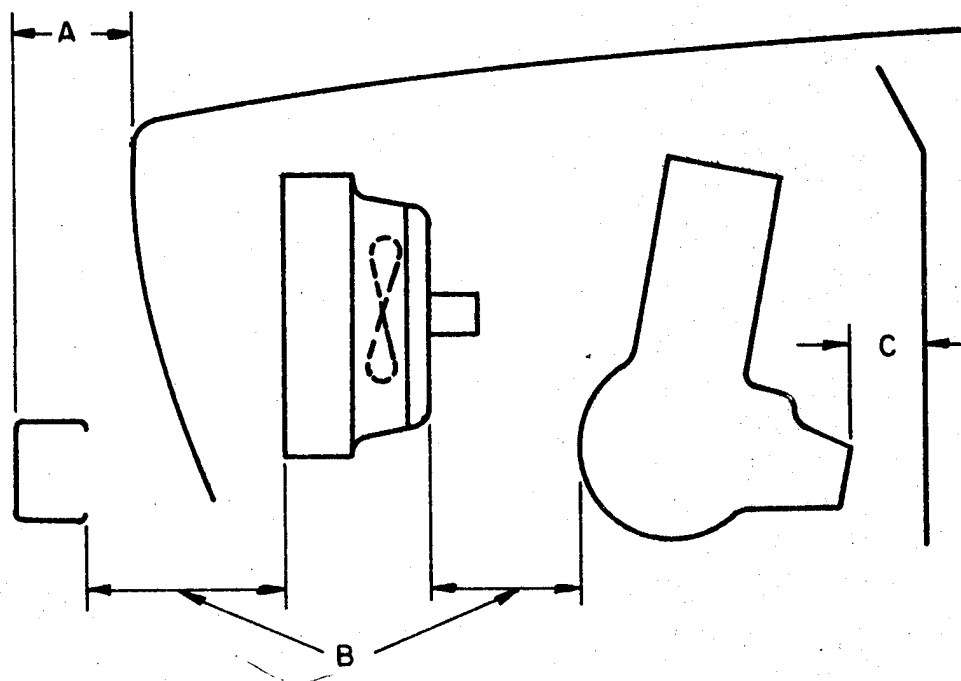
A: FRONT OF SHEET METAL TO BARRIER, 6.19 INCHES

B: BACK OF BUMPER TO ENGINE LESS THE RADIATOR 6.95 INCHES

C: REAR OF ENGINE/TRANSMISSION TO FIREWALL, 4.94 INCHES

FIGURE 209   COMPARISON OF PREDICTED AND MEASURED PASSENGER COMPARTMENT RESPONSE
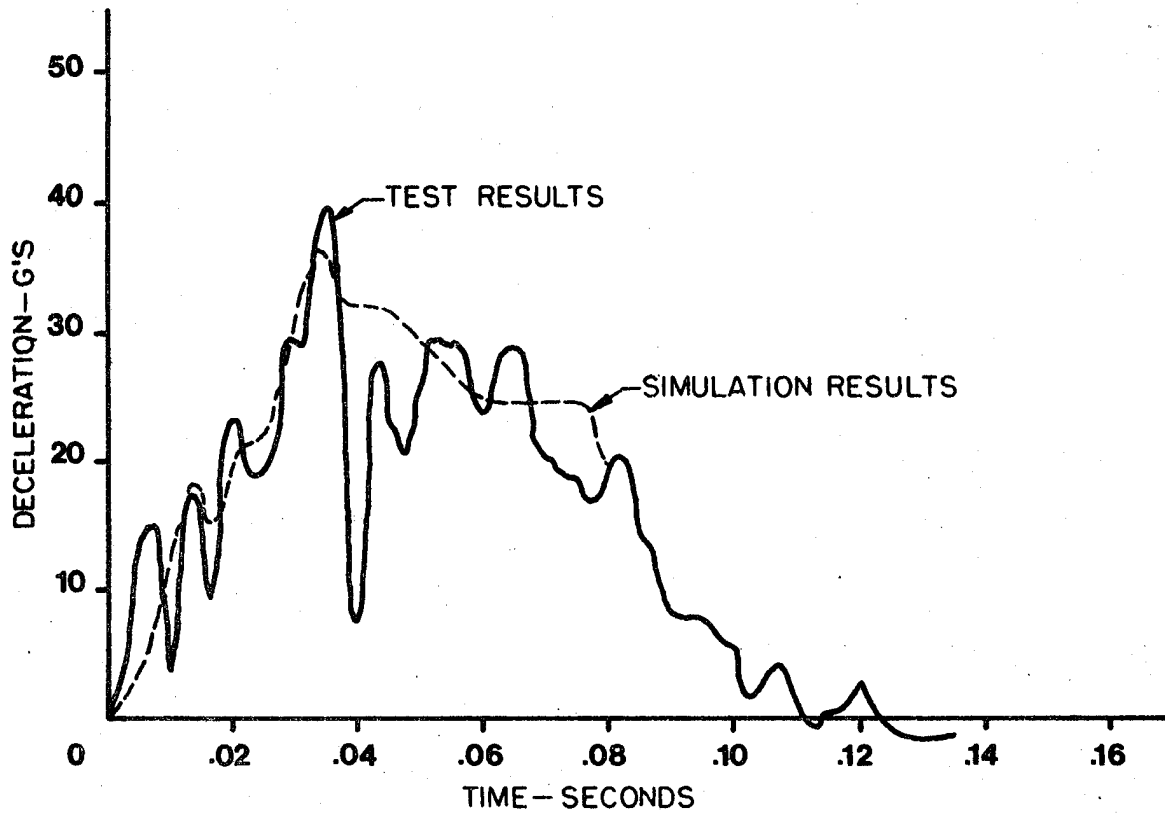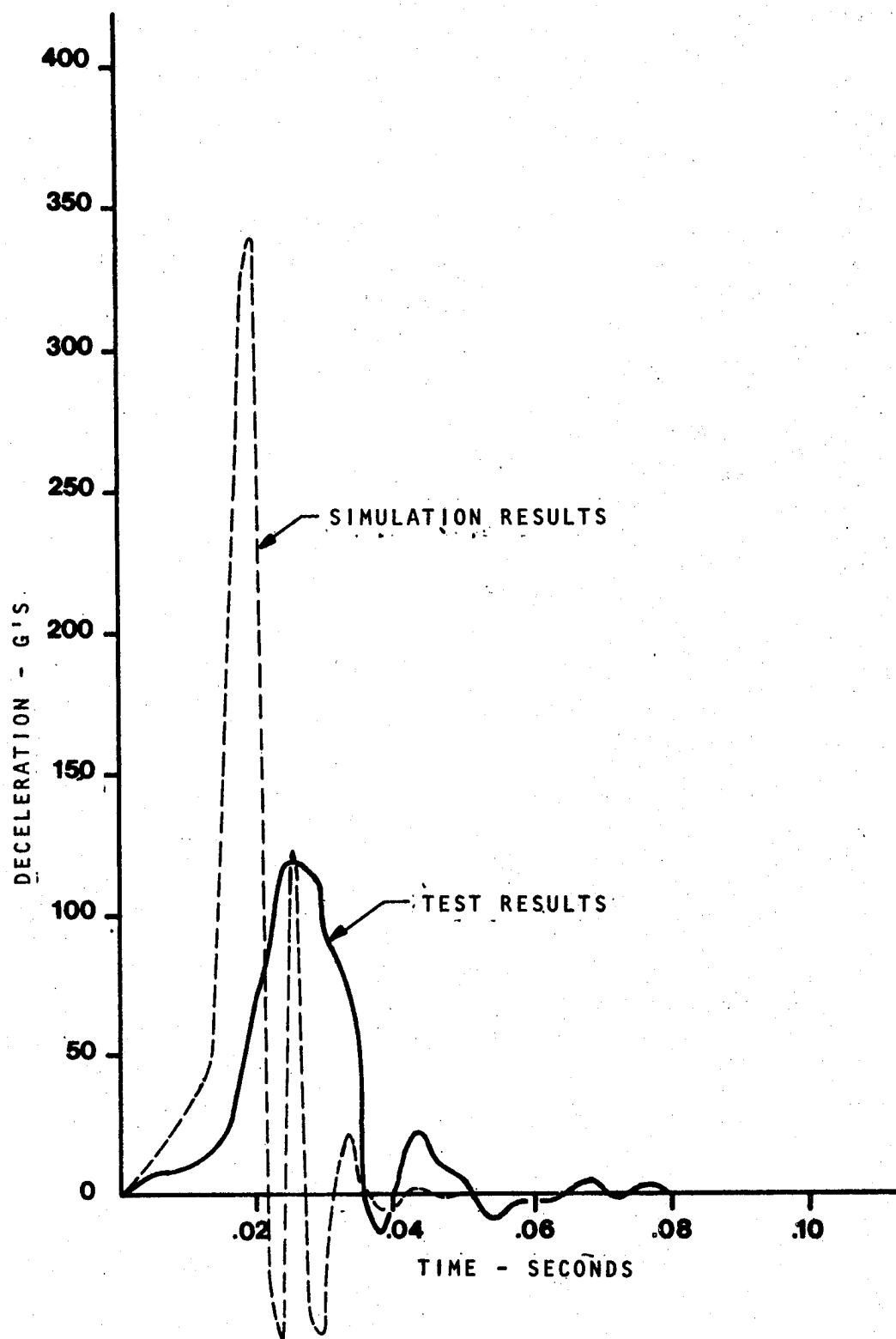
vehicle. An 8 inch by 9.5 inch corrugated composite sill filled with 2 pound per cubic foot rigid polyurethane foam has a crush resistance of 6500 pounds. This configuration, 0.351 pounds per inch, is not as efficient as the cylindrical element in terms of crush force per pound of structure.

It is readily apparent that the round crush element is more efficient than the corrugated rectangular element in glass-polyester. This would also be expected in other materials and this would indicate, on a crush force per pound efficiency basis alone, that a smaller, round cylinder of any material could provide a more efficient energy absorber. This is not completely true however since the size and shape is also determined by buckling resistance, bending resistance, and crush force density. Crush force density should be kept as low as possible or at least the energy absorbing components should not end up as "spears" which might attack a pedestrian or another vehicle.

Using data from the 6 inch diameter cylinder mentioned previously a desired crush force can be determined by scaling. For a 50 mph barrier crash the desired sill crush force is estimated to be 19,500 pounds. A 4.7 inch diameter cylinder at a 0.134 pound per inch weight will provide this desired crush force. This cylinder would be unfilled and the ramped force-deformation curves of Figure 207 could be obtained by varying the wall thickness of the front ends of the two cylinders. This reduced thickness permits low initial peak triggering as determined in a previous investigation [86].

9.3 Alternate Materials in Side Doors

The use of alternate materials in door panels and the intrusion beam as described in Section 8 is not expected to reduce the side intrusion characteristics of the Rabbit to any large degree. The reasoning is that, based on actual observations [101], the post and sill structure controls the force-deformation curve and energy absorption. The beam is believed to act more as a tension device rather than a bending device. Ductility or percent elongation of the material determined by static testing may not be an important requirement but rather the impact absorption values. Since the tensile strength and impact are potentially more important in future door designs then HSLA steels and continuous directional glass fiber composites become prime candidate materials. Aluminum alloys are also candidates but the need for heat treatment after fabrication to obtain this high strength reduces their cost competitiveness.

The use of composites with oriented continuous fibers in door beams, assembled to chopped random fiber composites requires new concepts to minimize molding labor costs. As an example, there are nine sheet steel parts in the Rabbit door, requiring press operations. To utilize composites on a direct substitution basis would require at least 12 times as much labor, and the number of parts must therefore be reduced to keep the cost somewhat competitive.

394

A design similar to that concept shown in Figures 70 and 165 for the Impala should be considered. Methods of attachment, mechanical and adhesive bonding, of the latch and hinges require an analysis and testing in static and dynamic conditions.

9.4 Summary

Based upon the considerations described in the use of alternate materials in vehicle structure it is believed that these materials can be used without degrading present levels of crashworthiness. Further work is certainly required because of the complexity of predicting passenger response in a crashing vehicle. While the structural response may be fairly well predicted, after testing by prescribed procedures, this does not mean passenger response is predictable. It is believed that alternate materials such as HSLA steels, aluminum alloys, and reinforced composites can be used in automotive structure without degrading the structural response to a collision. This cannot be done however on a gage to gage basis nor can it be necessarily done on a shape for shape basis. New concepts will probably be required for structure to obtain the greatest benefit on an energy absorbed per unit of weight.

10.0 VAN - WAGON STRUCTURAL CHARACTERISTICS

10.1 Weight Breakdown

A 1977 Dodge Sportswagon was purchased and disassembled to the point of all bolted on items. Welds were not destroyed and the vehicle was reassembled, after testing, for disposal.

Each part or subassembly was weighed. These weights are listed on Table 77. This vehicle is of a unitized construction having no separate frame. The front and rear bumper systems do not have intermediate energy absorber devices for low speed, non injury producing accidents. This vehicle, like other vans, light trucks and utility vehicles does not have anti-intrusion beams in the doors.

10.2 Structural Characteristics

The body in white, half view is shown in Figure 211. The front end assembly, under body assembly, right side assembly, left side assembly and roof are shown in Figures 212 through 216. The structure consists essentially of hat stiffened panels.

A front cross member, Figure 217 supports the engine and stabilizes the front steering and suspension. The front suspension consists of a pair of lower and upper control arms, coil springs and shock absorbers, Figure 218. The rear suspension, Figure 219, consists of two leaf springs and shock absorbers mounted to the axle and body in white. The leaf springs are mounted directly to the body.

The front doors, sliding door and rear cargo doors are shown in Figures 220, 221, and 222. The two cargo doors and two front doors are mirror images. As mentioned previously these doors on the van do not have anti-intrusion beams. The hood assembly shown in Figure 223 is made of two panels, inner and outer, similar to the Impala and Rabbit hoods.

A seat frame is shown in Figure 224. This is an intermediate seat which seats three, and is fairly easily removed or installed. Seats must withstand various static and impact loadings without failure of the frame, latches or anchorage. Such a test is outlined in SAE Standard 1879 B. Maximum deflections and failure loads are specified for various seat combinations. Bench type seats should not fail under a 12,375 inch pound loading. This requirement, combined with a maximum deflection of 2 inches under a 8250 inch pound loading requires a strong - high stiffness material. Due to packaging and comfort restraints, steels; and especially HSLA steels, are the most efficient of all the materials. For uncushioned seats molded plastics could be used; however this type seating is rarely found in vans or passenger vehicles.

TABLE 77: WEIGHT BREAKDOWN - 1977 DODGE SPORTSWAGON
MODEL B300 - 127" WHEELBASE
GVWR = 7700 Pounds

ALL WEIGHTS IN POUNDS

	Component Weight	Sub-Total	Total
SEATS			
Front R.H. Assembly	29.0		
Front L.H. Assembly	29.0		
Bench #1 Assembly	98.0		
Bench #2 Assembly	101.0		
Bench #3 Assembly	91.0		
			348.0
CARPET, PADS & MOLDINGS			
Carpets (all)	32.0		
Carpet Padding (3 pcs.)	51.0		
Carpet Molding Front Right	0.5		
Carpet Molding Front Left	0.5		
Carpet Molding Side Door Right	0.2		
Carpet Molding Side Door Left	0.2		
Carpet Molding Sliding Door (5 pcs.)	1.9		
Carpet Molding Seat Anchors (12 pcs.)	1.5		
			87.8
LINERS AND MOLDINGS			
Head			
Front Including Insulation	14.0		
Center Front Including Insulation	11.5		
Center Rear Including Insulation	12.0		
Rear Including Insulation	6.5		
		44.0	
Upper Side			
Over Front Door Right	0.3		
Over Front Door Left	0.3		
Over Sliding Door	0.7		
Over Rear Doors	1.4		
Over Side Windows Front Right	2.1		
Over Side Windows Front Left	9.0		
Over Side Windows Rear Left	8.0		
Over Side Windows Rear Right	8.0		
		29.8	

	Component Weight	Sub-Total	Total
Lower			
Left Front	7.0		
Left Rear	5.5		
Right Front	2.0		
Right Rear	5.5		
Rear Corner Left	1.4		
Rear Corner Right	1.6		
		23.0	
Moldings			
Headliner Joint (3 pcs.)	0.6		
Front Door Rear Post Right	0.4		
Front Door Rear Post Left	0.4		
		1.4	
			98.2

BOLT ON BODY COMPONENTS

	Component Weight	Sub-Total	Total
Outer Cowl	4.1		
Rear Bumper Bracket – Right	3.9		
Rear Bumper Bracket – Left	3.9		
Rear Bumper	24.0		
Front Bumper	36.0		
Grill Assembly	11.5		
Hood Assembly	21.0		
Engine Housing Cover	16.0		
Right Rear Cargo Door Ass'y with Glass	36.0		
Left Rear Cargo Door Ass'y with Glass	45.0		
Right Front Door Ass'y with Glass	65.5		
Left Front Door Ass'y with Glass	66.0		
Sliding Door Assembly	100.0		
Front Door Hinges – Upper (2)	3.4		
Front Door Hinges – Lower (2)	5.6		
Rear Cargo Door Hinges (4)	8.0		
Gasoline Tank & Bracket	26.4		
Front Cross Member	38.0		
			514.3

UNDER HOOD COMPONENT

	Component Weight	Sub-Total	Total
Engine			
Engine Block	475.0		
Starter Motor	25.0		
Engine Intake Manifold	57.0		
Exhaust Manifold (one side)	18.6		
Alternator	13.0		
Alternator Bracket	1.0		

	Component Weight	Sub-Total	Total
Distributer Head & Wires	3.9		
Heat Shield	1.0		
Fan Belts	0.4		
Dip Stick & Tube	0.3		
Hoses (4)	3.5		
Tubing (Oil)	0.2		
Air Cleaner Assembly	4.9		
Breather & Hose	0.6		
Misc. Bolts, Clamps, Brackets	1.4		
Oil Cooler Assembly	8.0	613.8	

Cooling, Air Conditioning, Heater

	Component Weight	Sub-Total	Total
Fan Assembly	6.2		
Air Conditioning Compressor & Hoses	39.0		
Fan Guard	2.0		
Expansion Tank Assembly	0.8		
Radiator Assembly	23.0		
Radiator Bracket	1.0		
Front Grill & Radiator Support Ass'y	13.0		
Blower & Motor Assembly	14.2		
Air Conditioning Cover Assembly	0.8		
Heater Core Assembly	30.8		
Duct	2.2	133.0	

	Component Weight	Sub-Total	Total
Battery	39.0	39.0	

Windshield Wiper Components

	Component Weight	Sub-Total	Total
Washer Reservoir	0.8		
Wiper Assembly (2)	1.2		
Wiper Motor Assembly	4.2	6.2	

Steering

	Component Weight	Sub-Total	Total
Steering Box Assembly	38.0		
Gearshift Linkage Assembly	2.6		
Steering Column Assembly	21.0		
Power Steering Pump Assembly	13.8	75.4	867.4

TRANSMISSION

	Component Weight	Sub-Total	Total
Linkage	1.3		
Driveshaft	21.0		
Transmission Support Assembly	8.0		

	Component Weight	Sub-Total	Total
Stiffening Rod	0.6		
Transmission Assembly	163.0		
			193.9

SUSPENSION & BRAKE SYSTEMS

	Component Weight	Sub-Total	Total
Wheels & Tires (5)	360.0		
Front Suspension Assembly Rods, Bushing, Ball Joints, Arms	145.0		
Front Shock Absorbers (2)	4.4		
Front Rotor (2)	76.0		
Caliper Disc Brakes Front (2)	26.0		
Front Springs (2)	29.0		
Rear Springs (2)	144.0		
Rear Shock Absorbers (2)	7.0		
Power Brake Booster & Master Cylinder Assembly	22.0		
Rear Axle & Suspension Assembly	317.0		
			1130.4

EXHAUST SYSTEM

	Component Weight	Sub-Total	Total
Pipes, Muffler	41.0		
			41.0

MISCELLANEOUS

	Component Weight	Sub-Total	Total
Headlights (2)	2.4		
Glove Box	0.6		
Glove Box Door Assembly	1.6		
Sun Visor Assembly Left	1.3		
Sun Visor Assembly Right	1.3		
Kick Panel Left Front Dash	2.2		
			9.4

TOTAL WEIGHT COMPONENTS - 3290.4 Pounds

The above components were removed from the purchased vehicle.

Weight of Vehicle as Purchased without Payload   4900.0

Weight of Components Removed from Vehicle   3290.0

Weight of Approximately 10 Gallons Gasoline
   Removed   58.7
                                                 _____
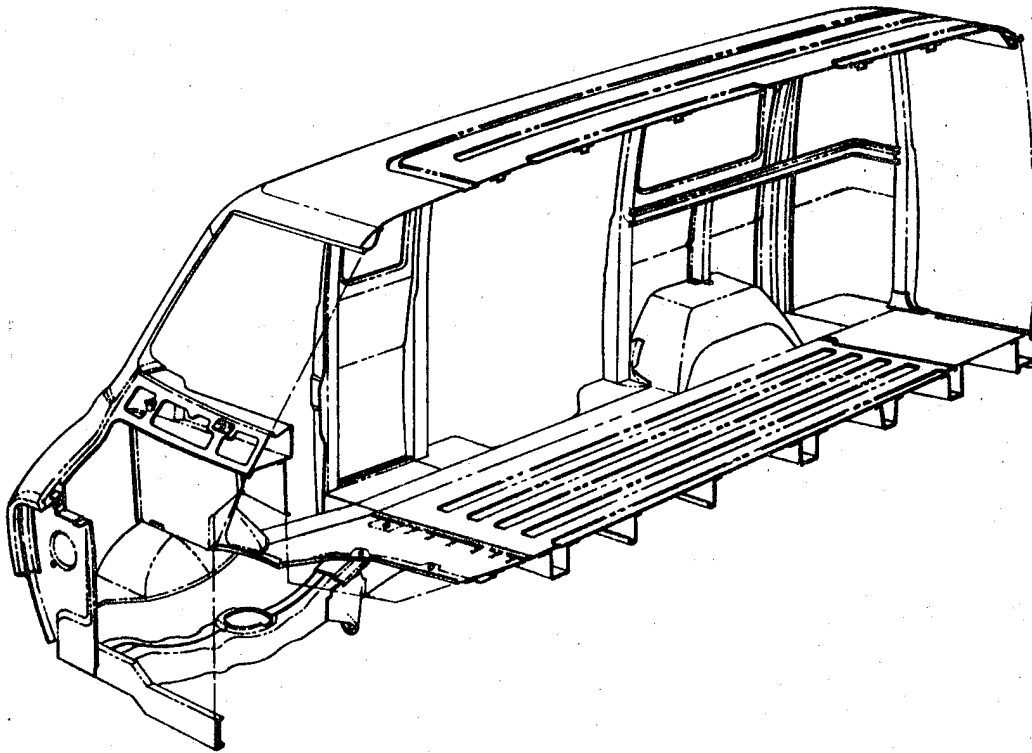Total Weight of Stripped Body   1550.9
                                                 ========

This weight includes glass as follows:

    Windshield   45.0
    2 Rear Quarter Windows   25.8
    2 Left Side Flipper Windows   14.5
    2 Front Side Windows   8.6
                                         _____
       Weight of Glass   93.9
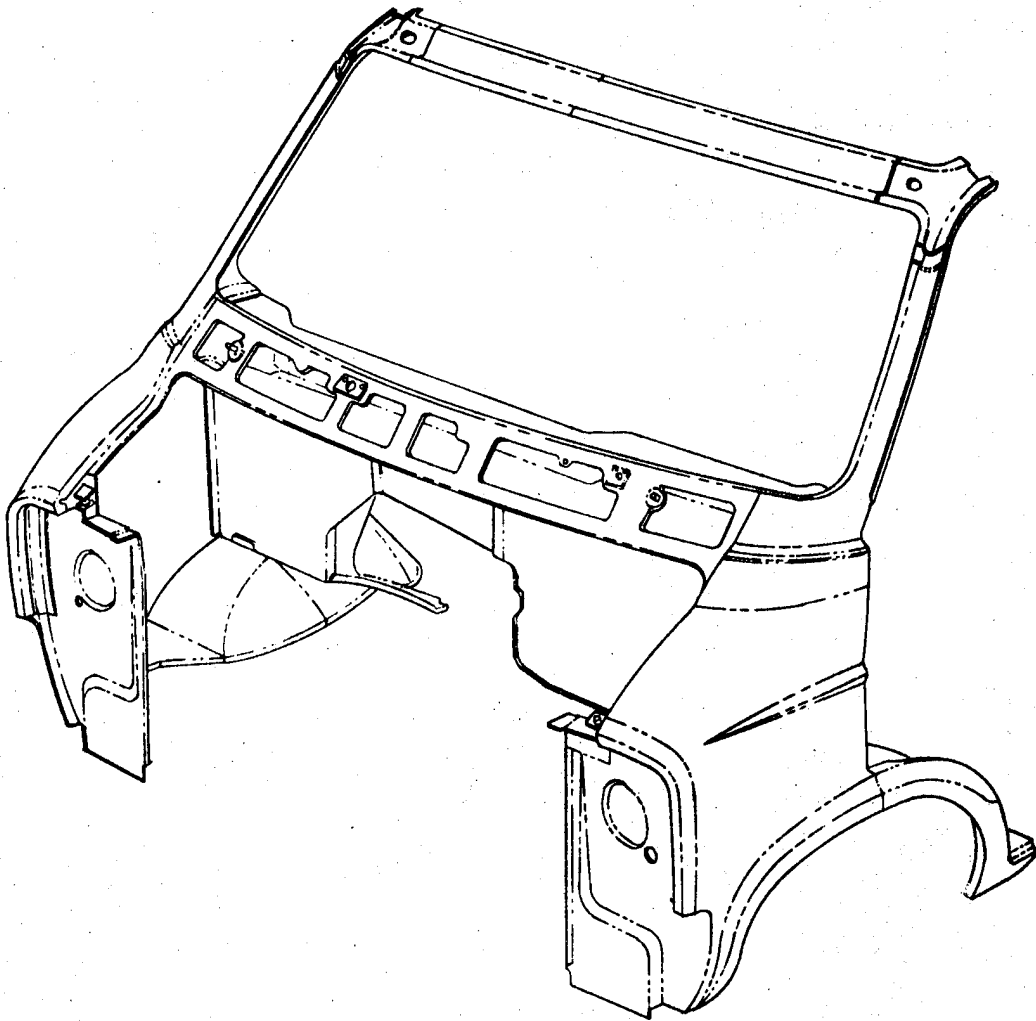 Estimated Wiring & Misc.   20.0
                                         _____
                                          113.9
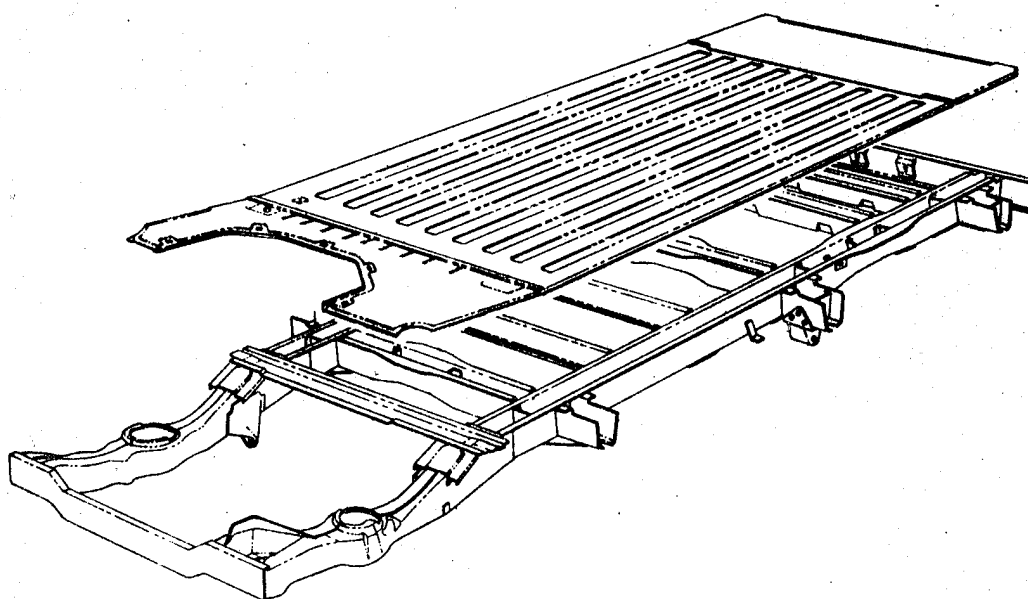

Structural Weight = 1550.9 - 113.9 = 1437 Pounds

FIGURE 211   VAN – UNITIZED BODY STRUCTURE

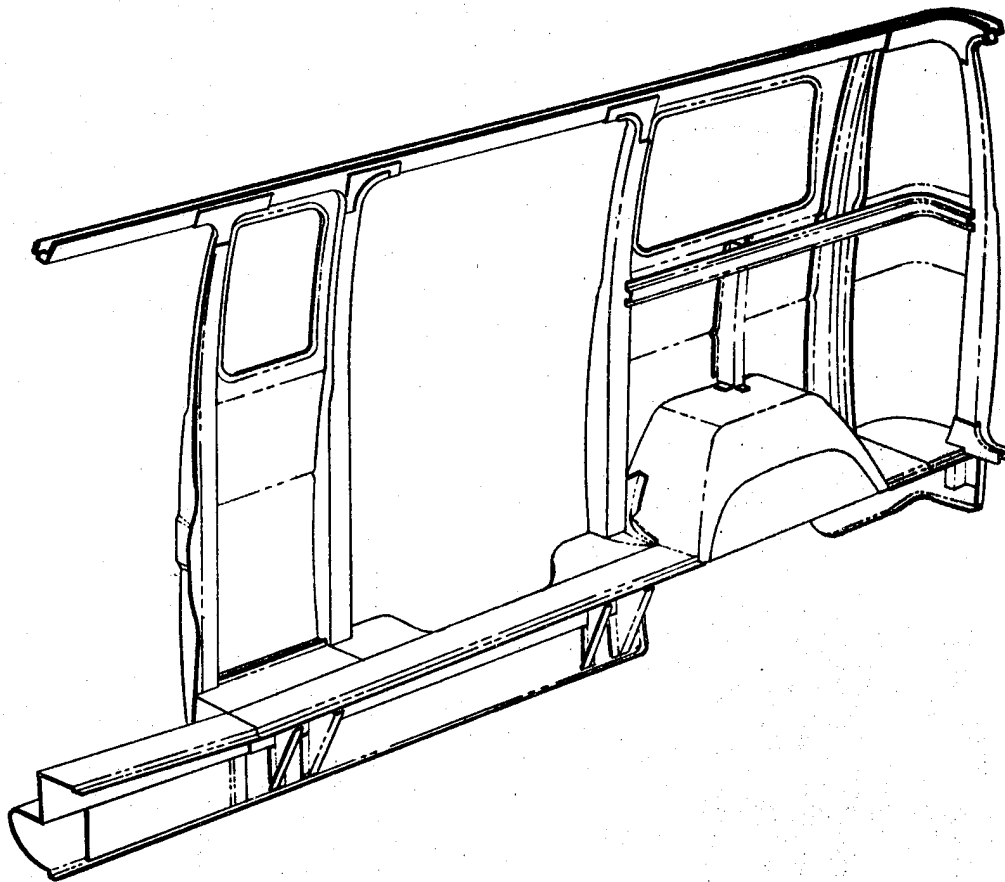FIGURE 212   VAN – FRONT END ASSEMBLY

FIGURE 213   VAN – FLOOR STRUCTURE
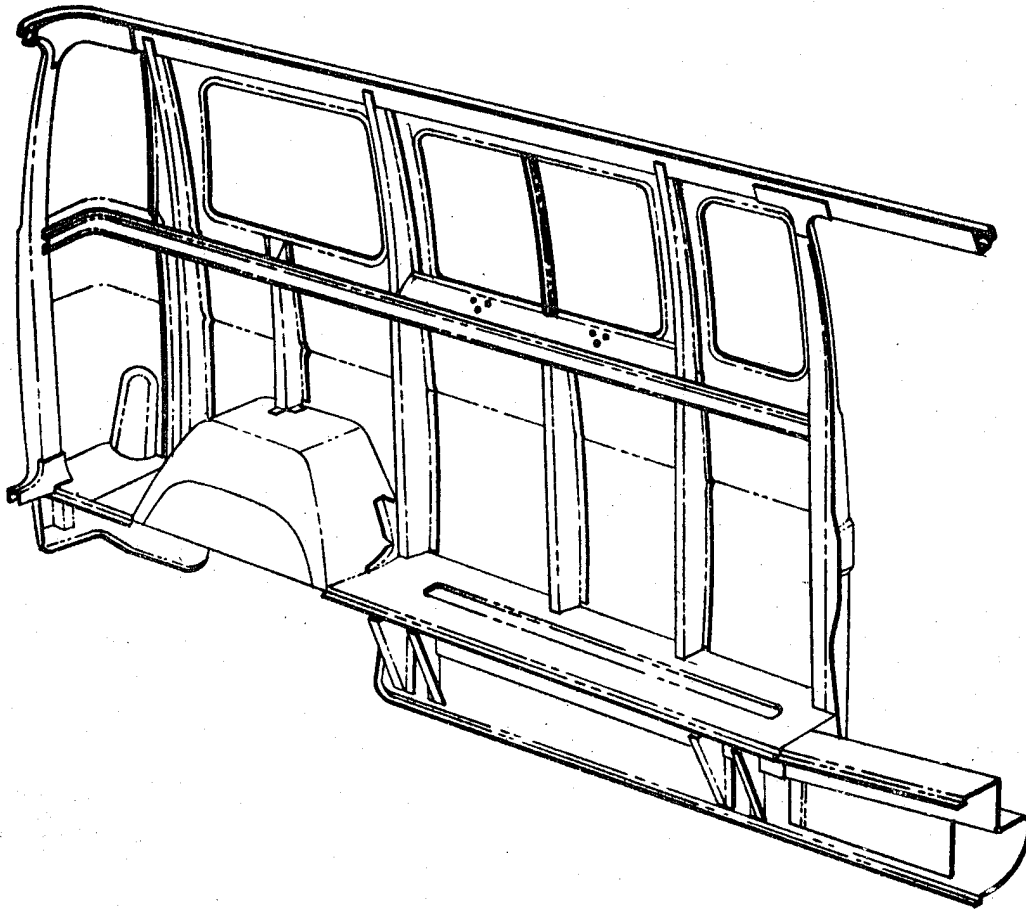
FIGURE 214   VAN – RIGHT SIDE ASSEMBLY

FIGURE 215   VAN – LEFT SIDE ASSEMBLY

FIGURE 216   VAN – ROOF ASSEMBLY
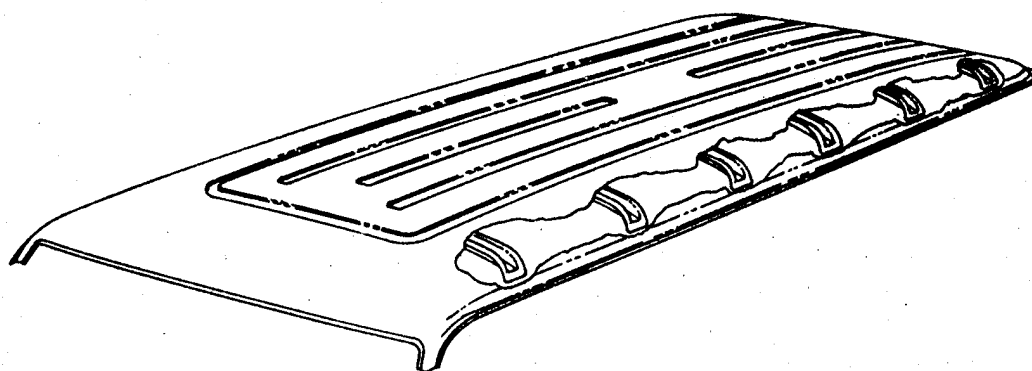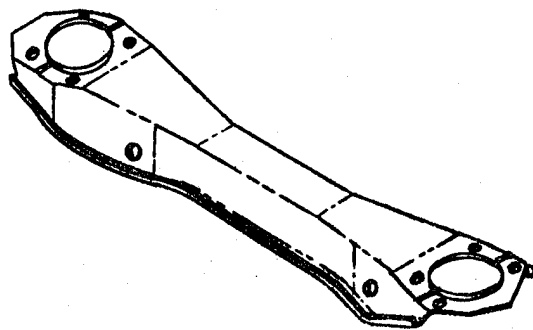
FIGURE 218   VAN-SUSPENSION-FRONT
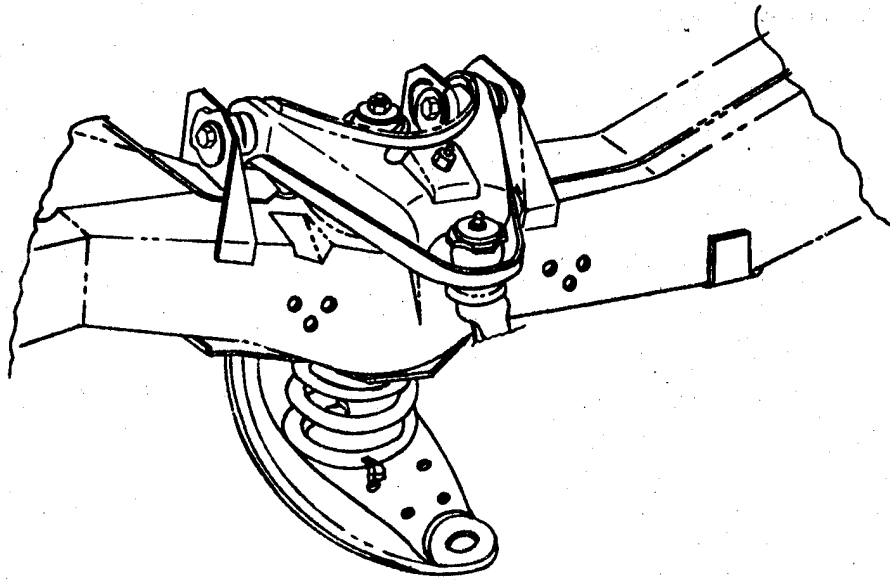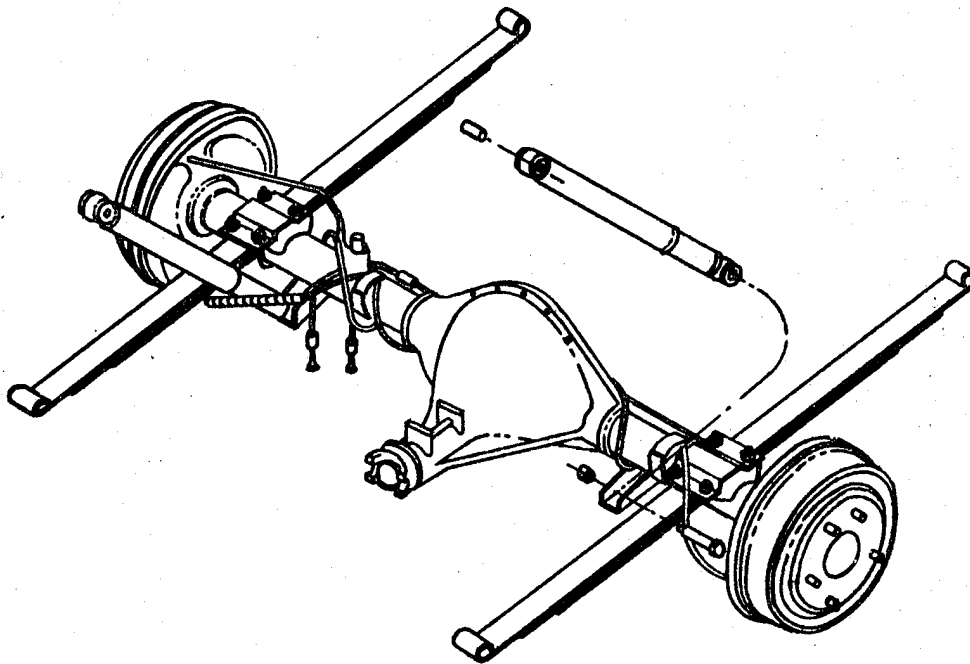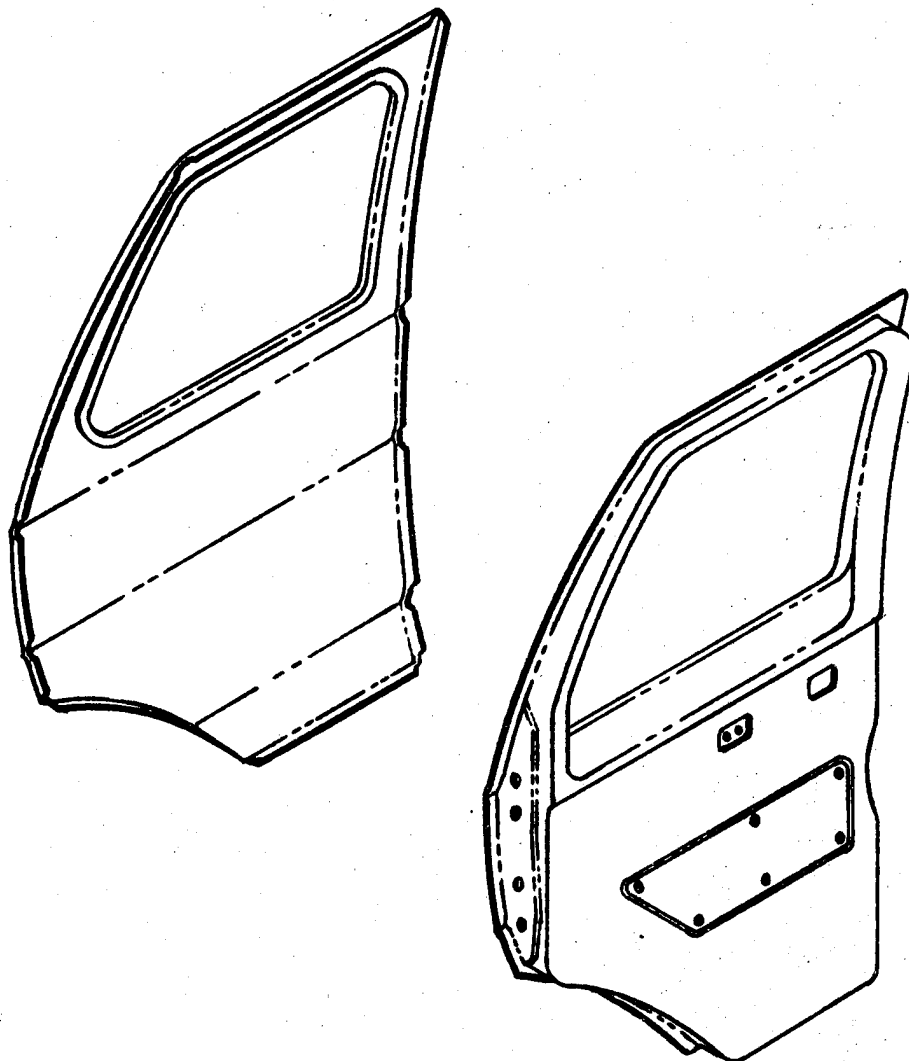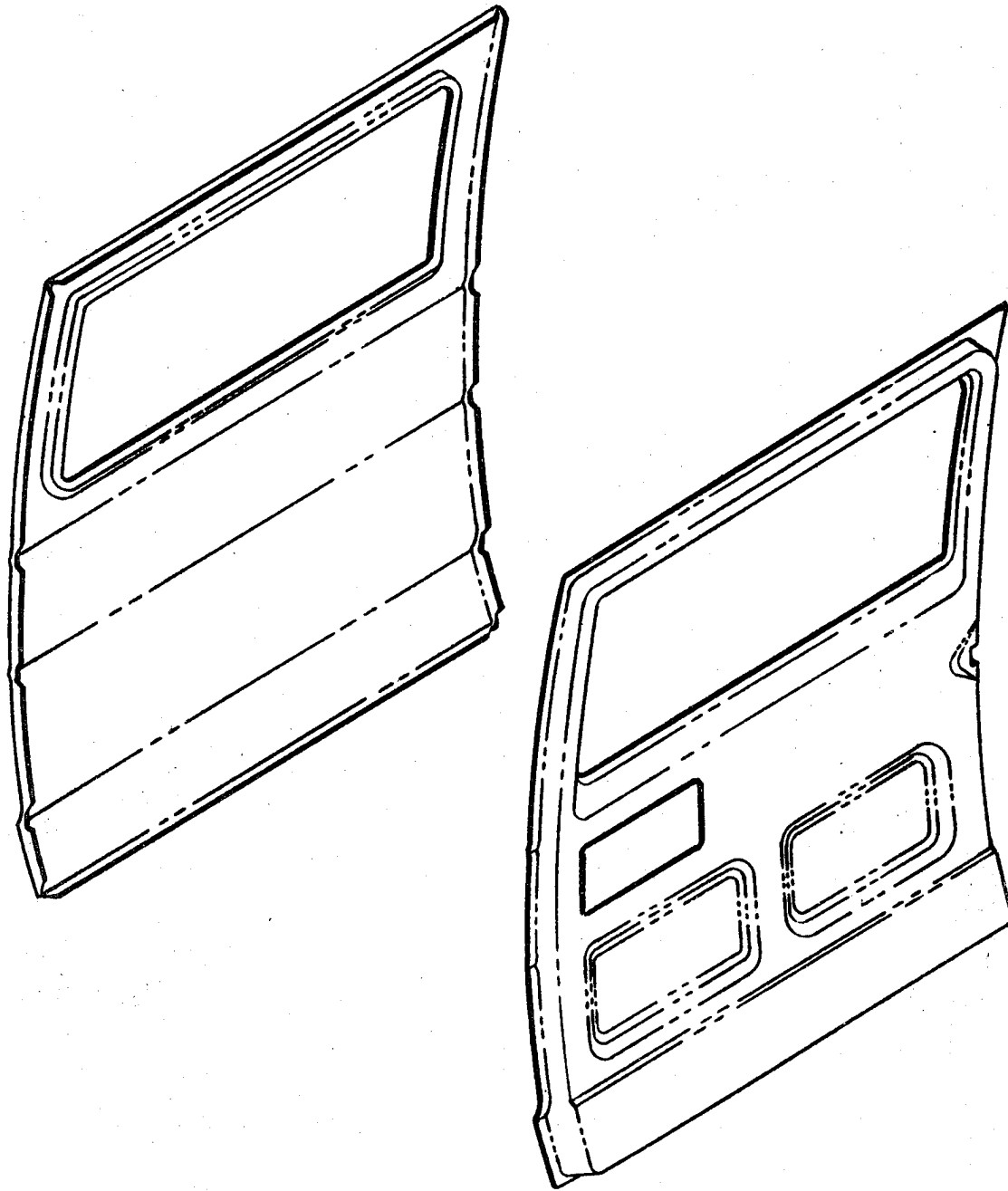
FIGURE 219   VAN-SUSPENSION-REAR

FIGURE 220   VAN – FRONT DOOR ASSEMBLY

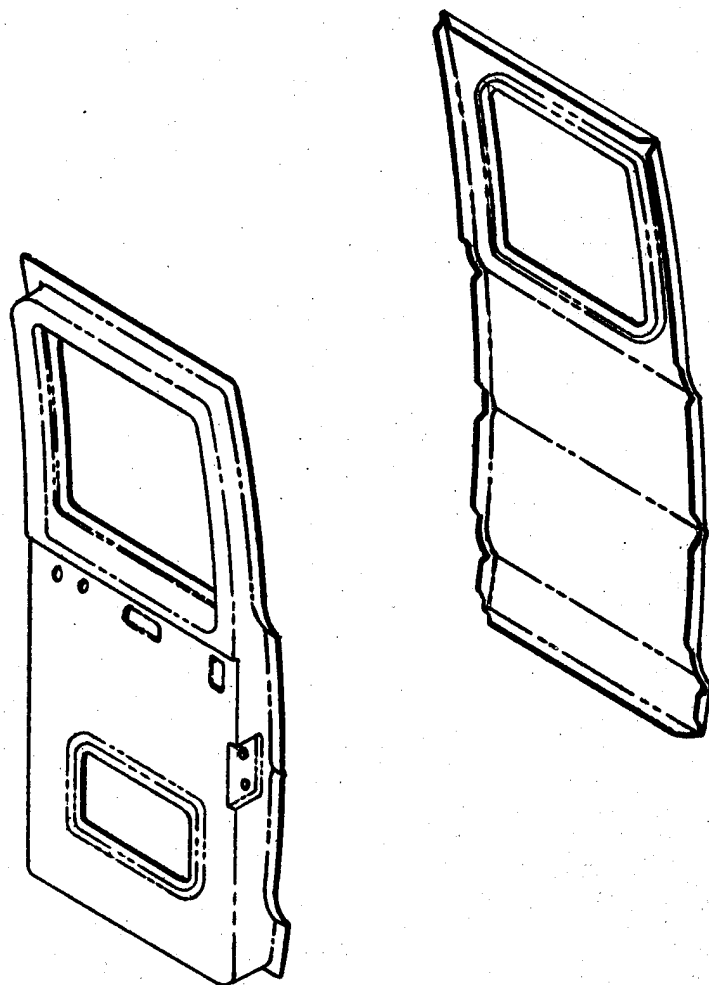**FIGURE 221   VAN – SLIDING DOOR ASSEMBLY**
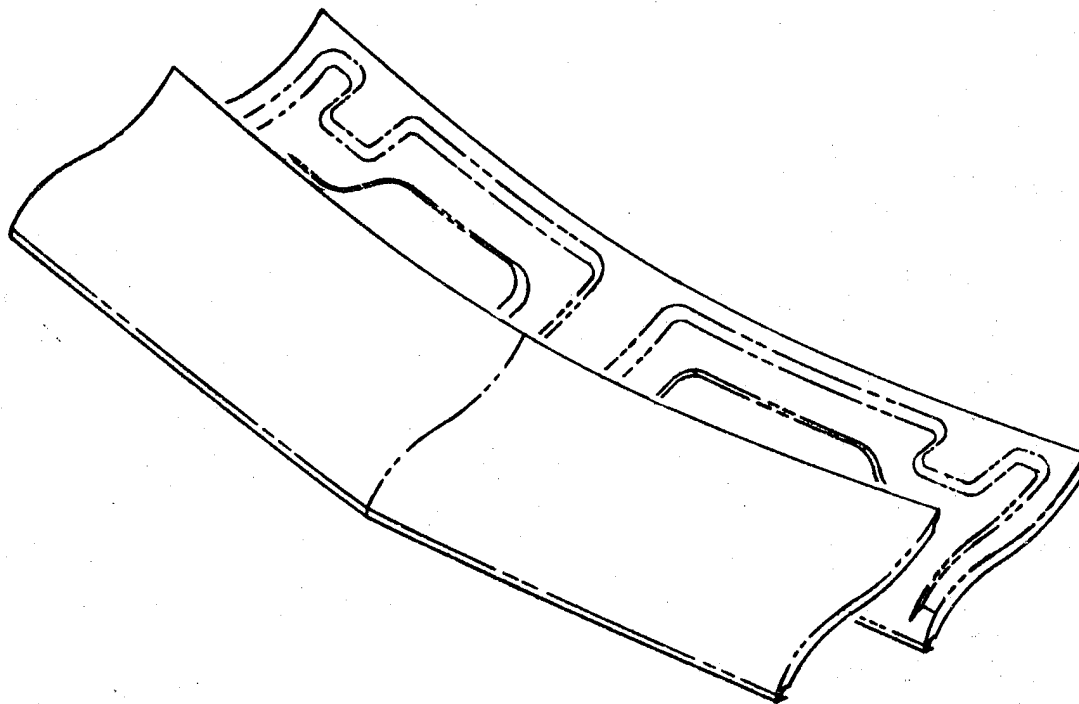
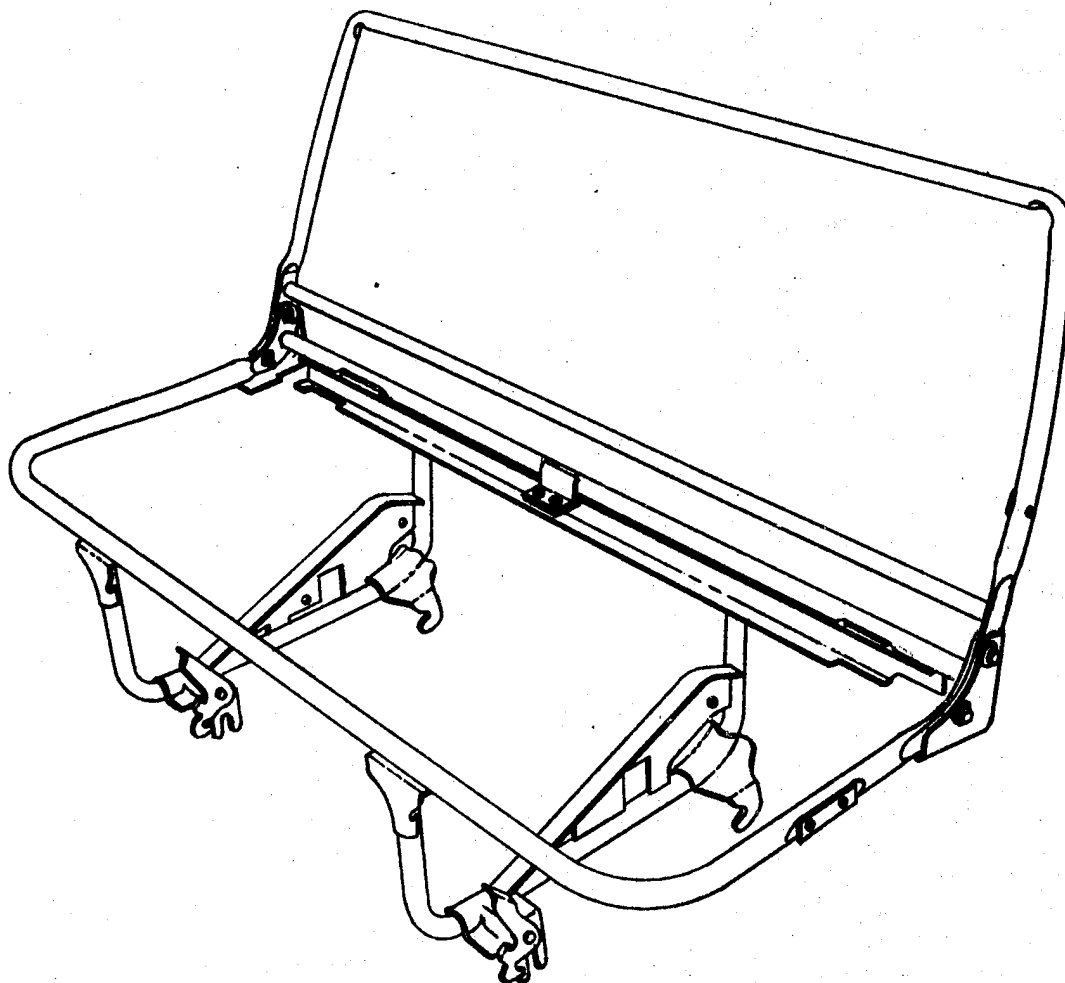FIGURE 222   VAN – RIGHT REAR CARGO DOOR

FIGURE 223   VAN-HOOD ASSEMBLY

FIGURE 224   VAN-SEAT STRUCTURE

10.3 Structural Analysis

Detail drawings were completed, for example Figures 225 and 227, to permit determination of the section properties. The section properties were determined by The Budd Program R-Sections, and corresponding typical computer plots are shown in Figures 226 and 228. Locations of the areas of the sections determined are shown in Figures 229 and 230. The resulting minimum and maximum moments of inertia are listed in Table 78 for these sections.

From the disassembled vehicle, the body in white was gaged and statically tested. For the bending case, dial gages were positioned as shown in Figure 231 . Actual X,Y,Z locations are listed in Table 79. The loading for the bending case is shown in Figure 232.

In the case of the torsion test the dial gages were repositioned as shown in Figure 233 and listed in Table 80. Two torsion tests were conducted. One test without any weight on the floor and one test with 1275 pounds applied to the floor. Static weights of 240 pounds and 500 pounds were applied to the front spring pockets. The rear frame was rigidly attached to support structure on the centerline of the rear wheels. The front cross member was supported on a knife edge. Up loads were applied to the left side spring pocket (looking aft) and down loads applied to the right spring pocket. The distance between the spring pockets was 38.75 inches which gives a torque of 9300 in-lbs. and 19375 in-lbs. Maximum deflection of 0.082 inches occurred at gage 20 without weight applied to the floor. Maximum deflection of 0.075 inches occurred at gage 21 with 1275 pounds applied to the floor.

A finite element model was prepared for analysis using The Budd Company Structural Analysis Program. The model is shown in Figure 234. The loading used for bending and torsion were examined and compared to the test results. In Figure 235 the deflections for the bending loads are plotted for various dial gages. The agreement with the calculated values is considered satisfactory. Results from the torsion test and computer model are listed in Table 81 .

The computer model was then used to determine maximum stresses and deflections encountered under the load cases shown below:

Case 1   1 "g" vertical
Case 2   3.5 "g" bump at front wheels
Case 3   braking, 1 "g" vertical and 1 "g" forward
Case 5   3.5 x static torsion at front wheel

The general conditions of loading are the same as used on the Impala and Rabbit, Figures 86 , 87 , 88 , and 89 . In the first group, the material considered was low carbon steel, the material of current construction.

FIGURE 225   SECTION 4 PILLAR FRONT-FRONT DOOR
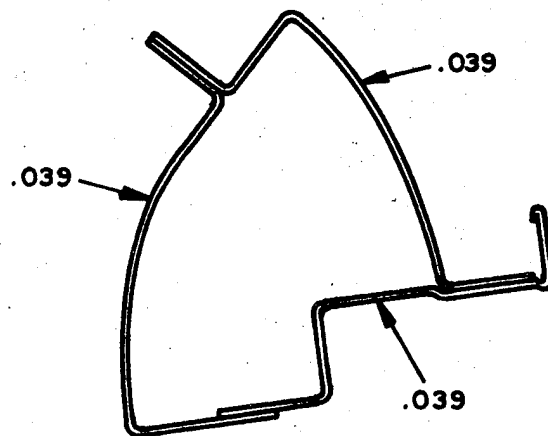
FIGURE 226   SECTION 4 COMPUTER PRINT
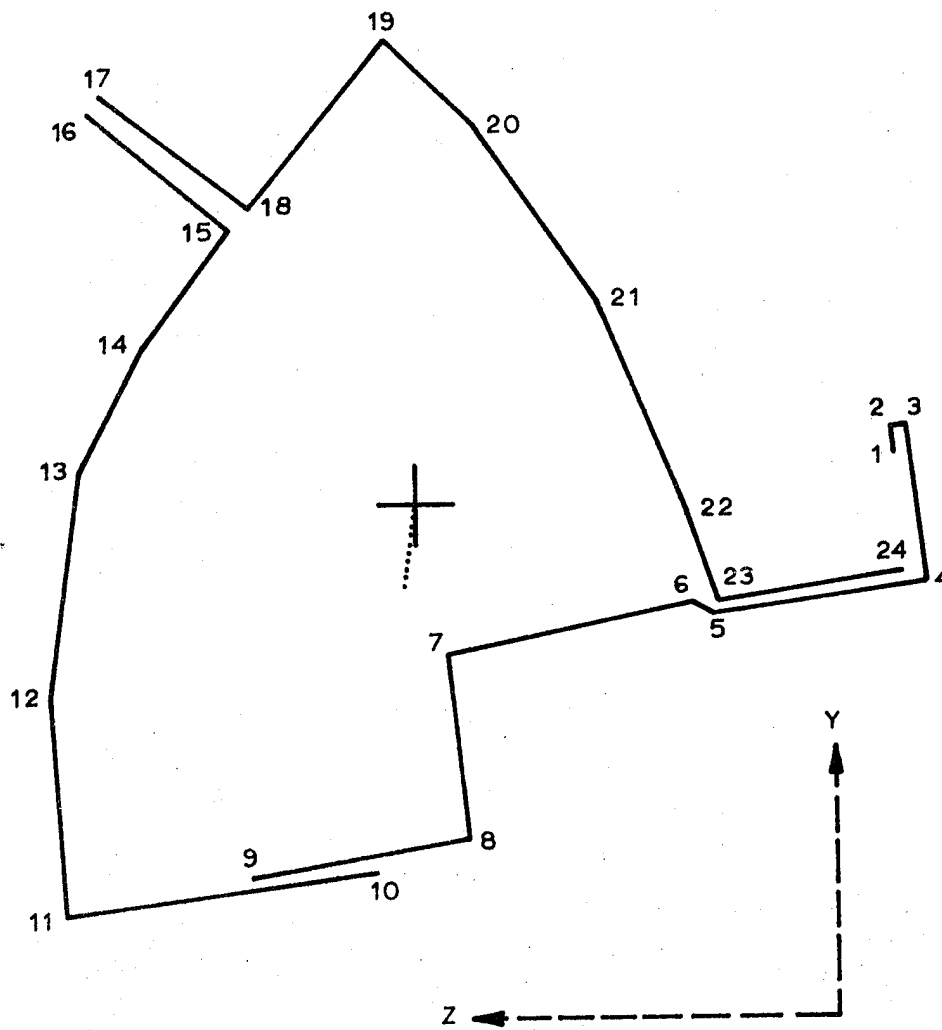
FIGURE 227   **SECTION 12 RAIL-SIDE**

.048

.115 NOM.
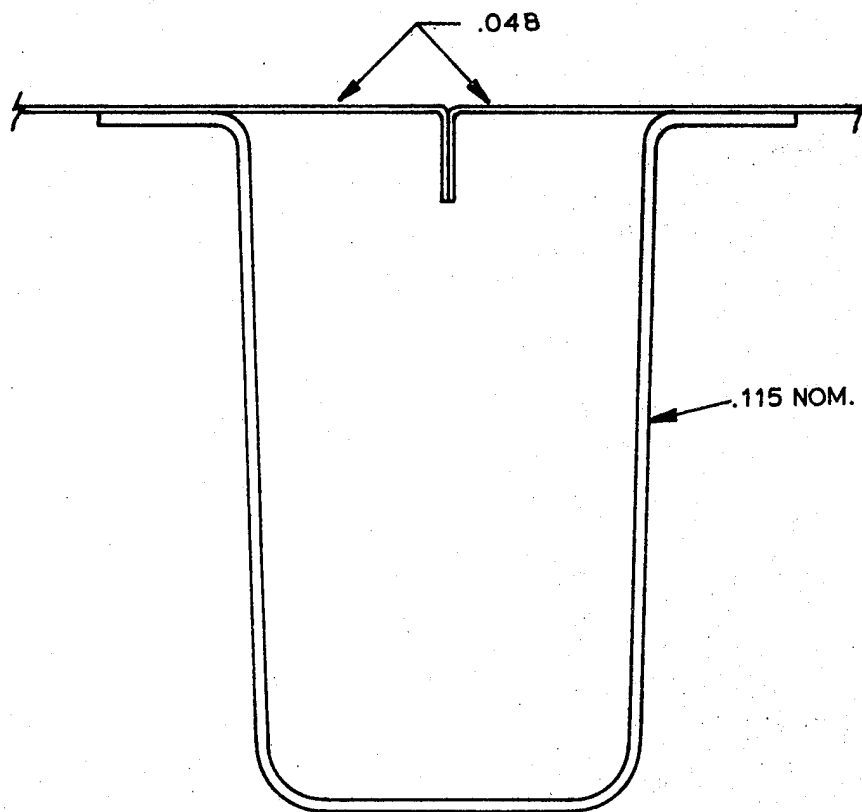
FIGURE 228 · **SECTION 12 COMPUTER PRINT**
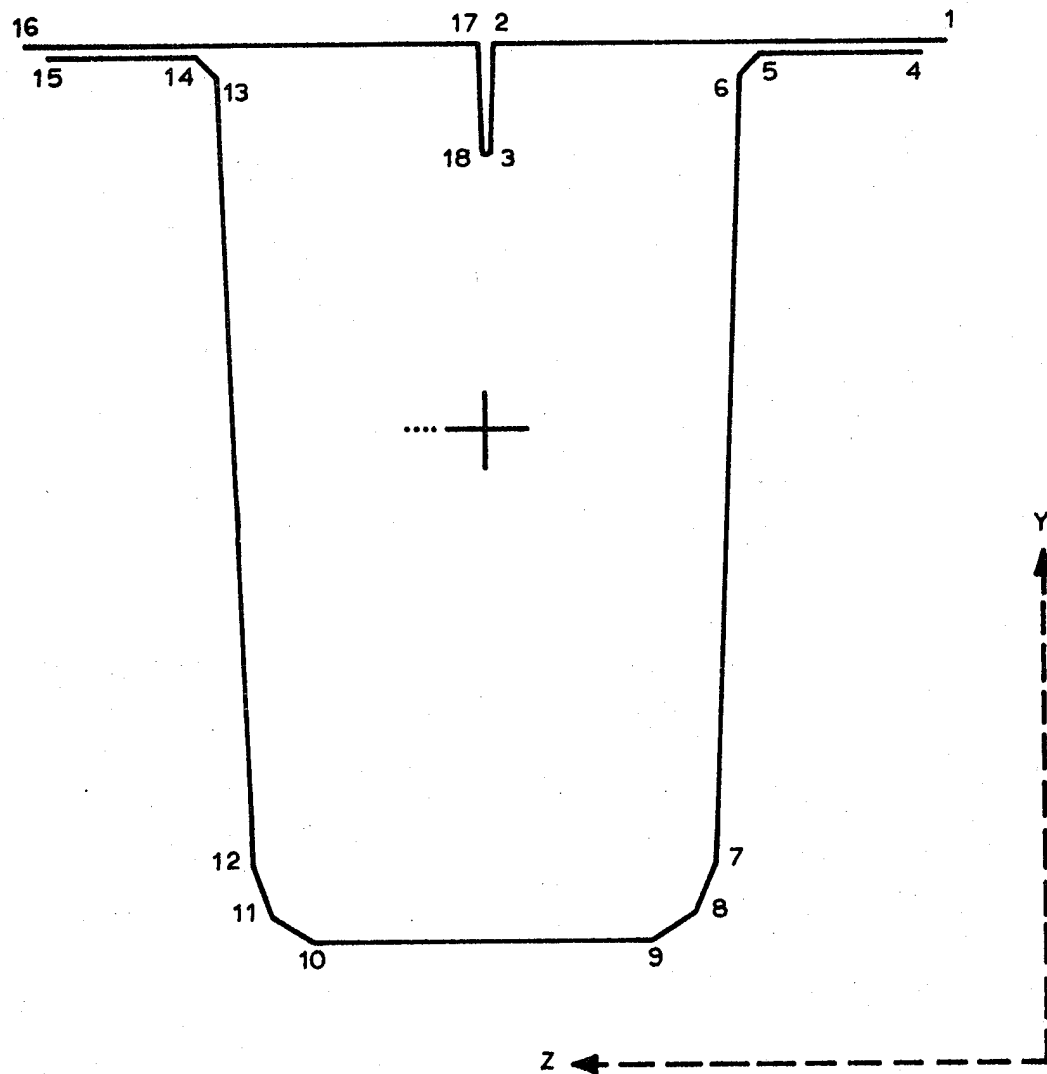
FIGURE 229   VAN – SECTION INDEX

PLAN VIEW

SIDE VIEW

REAR VIEW

FRONT VIEW
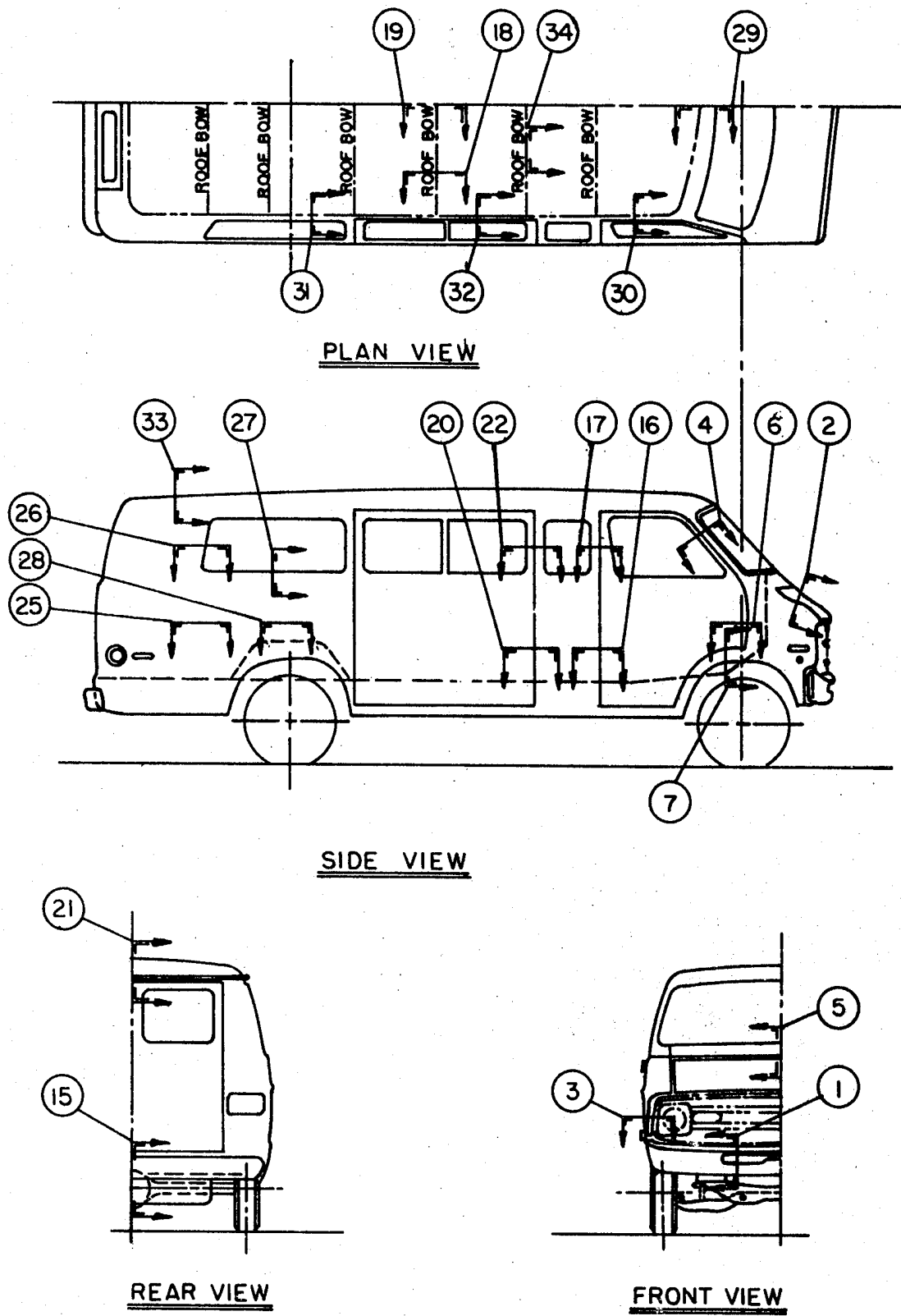
FIGURE 230   VAN – SECTION INDEX
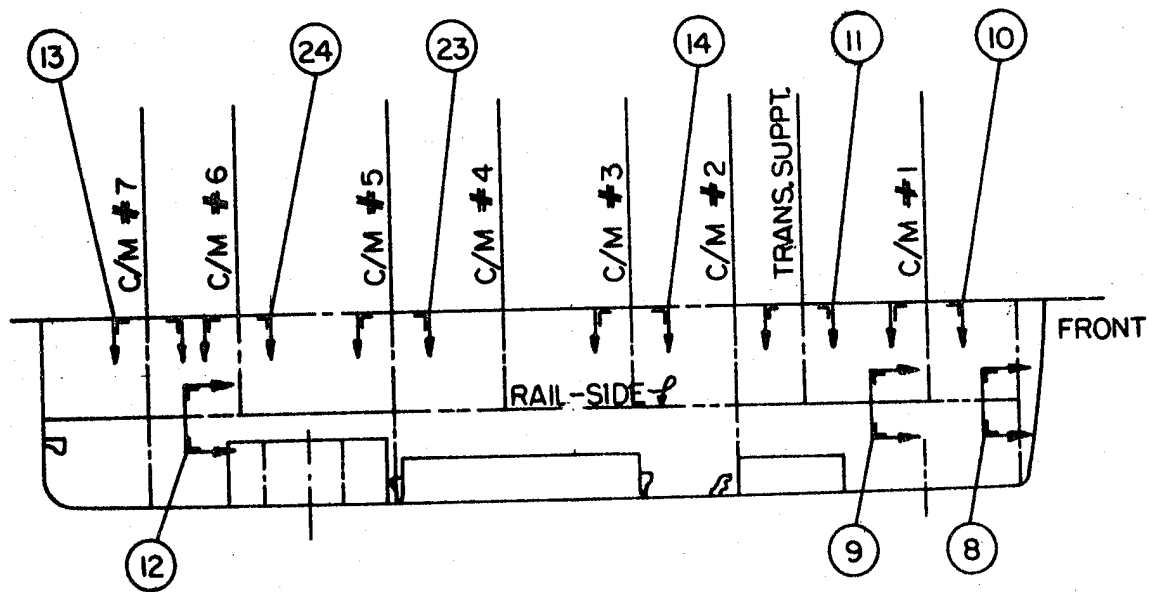
PLAN VIEW—FLOOR LEVEL

TABLE 78:   SECTION PROPERTIES OF VAN STRUCTURE

Section	I Min	I Max
1	0.6632	2.2318
2	0.0445	1.1802
3	0.1593	0.3559
4	0.1747	0.1905
5	3.2589	6.3372
6	0.1188	0.7076
7	1.0226	6.3791
8	4.5254	5.3399
9	2.5577	5.8269
10	6.7977	11.6908
11	0.0735	2.5122
12	5.3041	9.3162
13	2.7719	4.6600
14	0.1991	2.5702
15	5.2268	10.3761
16	0.3878	2.9230
17	0.0811	0.3572
18	0.0532	0.6373
19	0.0532	0.6373
20	0.4574	1.3827
21	0.1727	0.3378
22	0.1928	0.2881
23	4.7076	8.2323
24	3.3805	5.3830
25	0.3648	0.3720
26	0.1627	0.3491
27	0.0029	0.0646
28	0.2928	0.3110
29	0.0776	0.1077
30	0.1211	0.3158
31	0.1847	0.6831
32	0.2331	2.5405
33	0.1018	0.3669

FIGURE 231   **DIAL GAGE LOCATION-BENDING**
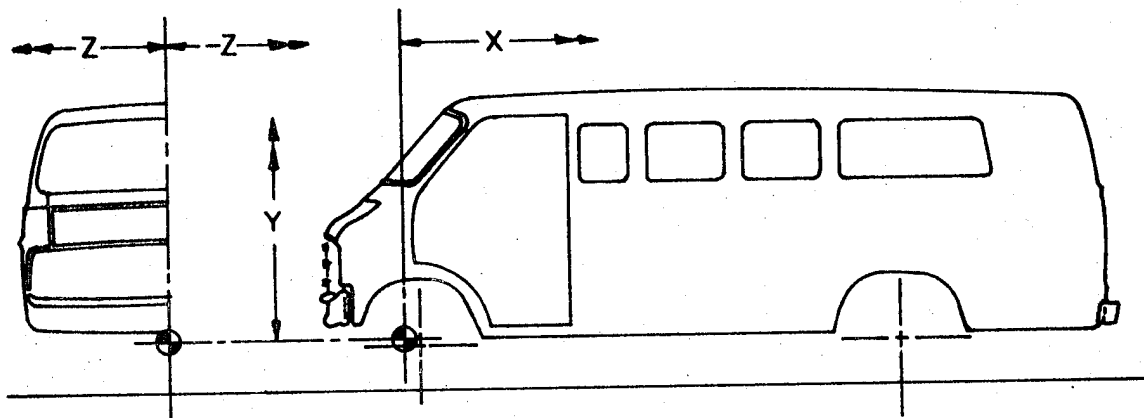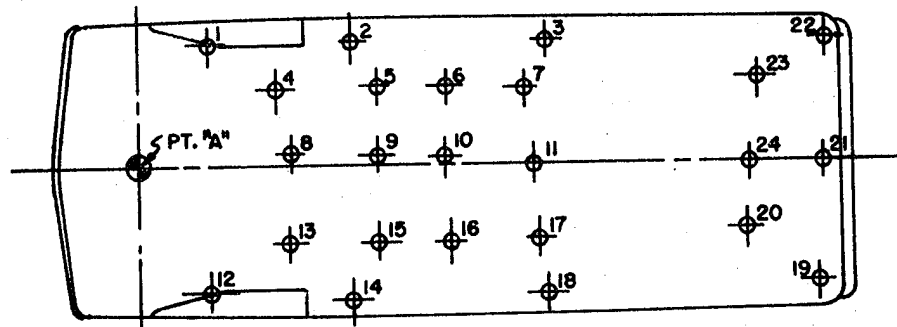
TABLE 79: DIAL GAGE LOCATION COORDINATES BENDING TEST

NO.	X	Y	Z
1	1.25	0.00	31.75
2	56.00	0.00	32.50
3	105.50	0.00	32.50
4	36.00	3.00	20.00
5	62.00	3.00	20.50
6	80.00	3.00	20.25
7	100.00	3.00	20.00
8	39.5	3.00	2.25
9	61.60	3.00	2.00
10	79.50	3.00	1.25
11	102.30	3.00	0.00
12	18.25	0.00	-31.75
13	39.00	3.00	-20.00
14	55.25	0.00	-34.00
15	62.00	3.00	-20.00
16	80.50	3.00	-20.00
17	103.50	3.00	-19.25
18	105.25	0.00	-33.00
19	175.75	0.00	-30.50
20	157.75	3.00	-17.75
21	177.05	3.00	0.00
22	177.75	0.00	32.00
23	160.50	3.00	21.50
24	158.55	3.00	0.00

FIGURE 232 **WEIGHT DISTRIBUTION-BENDING**
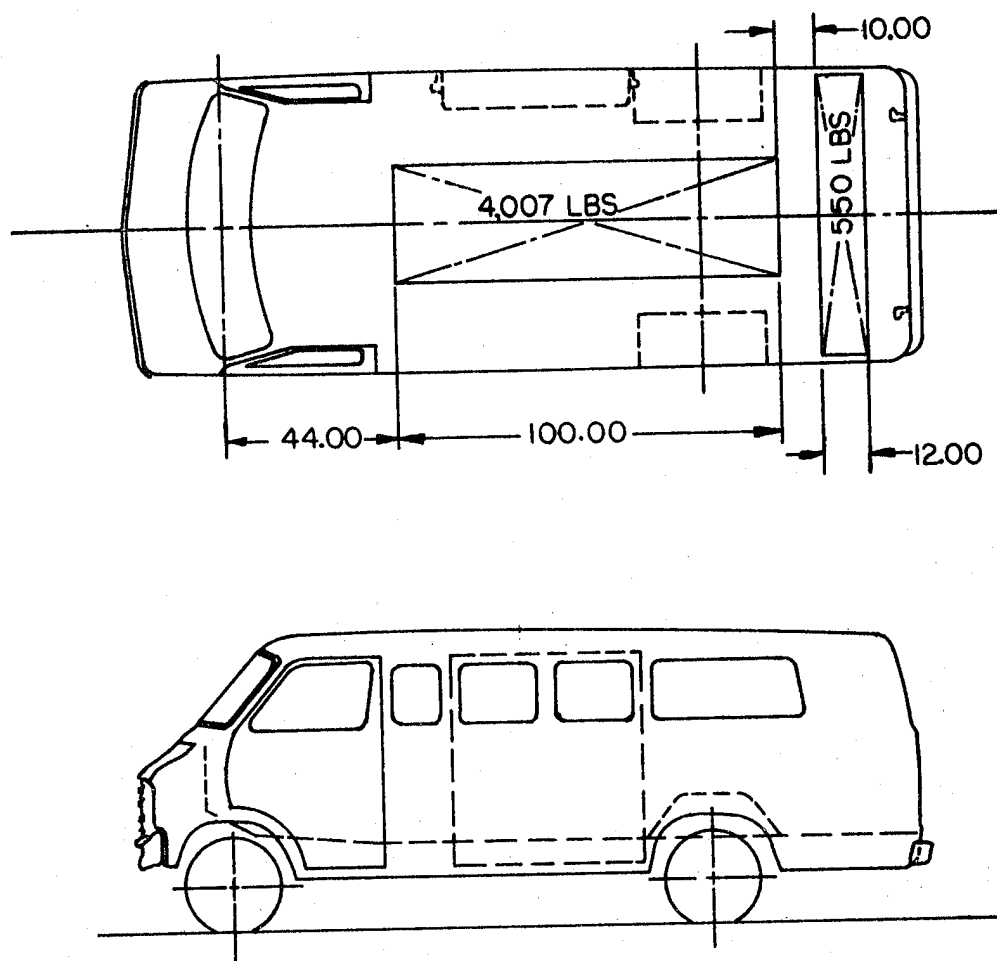
FIGURE 233   **DIAL GAGE LOCATION – TORSION**

427
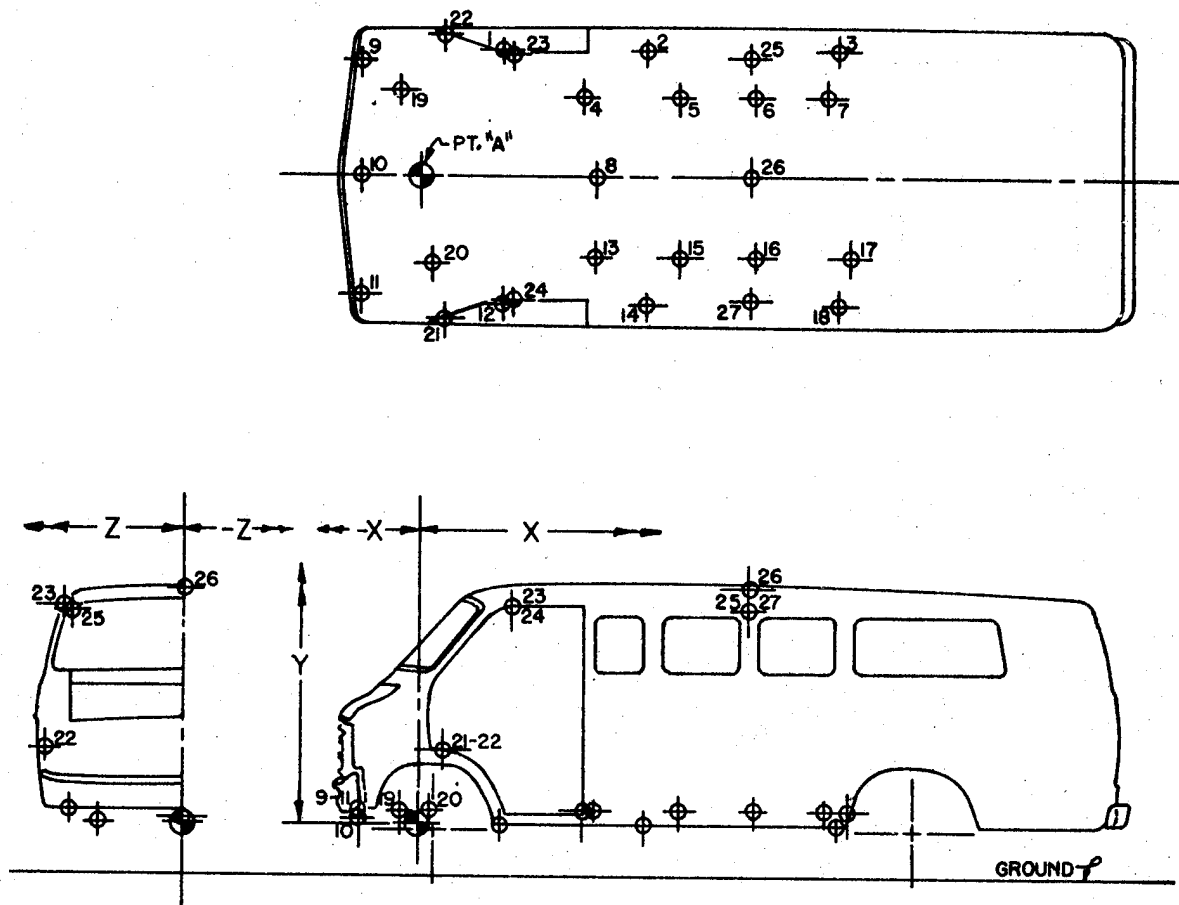
TABLE 80:   DIAL GAGE LOCATION COORDINATE TORSION TEST

NO.	X	Y	Z
1	22.00	0.00	31.00
2	59.00	0.00	31.00
3	109.00	0.00	31.00
4	42.00	3.00	20.00
5	66.50	3.00	20.00
6	85.00	3.00	20.00
7	106.00	3.00	20.00
8	45.00	3.00	0.00
9	-15.50	3.00	28.50
10	-15.50	1.00	0.00
11	-15.50	3.00	-28.50
12	22.00	0.00	-32.00
13	45.00	3.00	-20.00
14	59.00	0.00	-32.00
15	66.50	3.00	-20.00
16	85.00	3.00	-20.00
17	112.00	3.00	-20.00
18	108.00	0.00	-32.00
19	-5.00	3.00	22.00
20	3.00	3.00	-22.00
21	6.00	19.00	-36.00
22	6.00	19.00	36.00
23	24.00	55.00	31.00
24	24.00	55.00	-31.00
25	84.00	54.00	30.00
26	84.00	60.00	0.00
27	84.00	54.00	-30.00

FIGURE 234   VAN COMPUTER MODEL
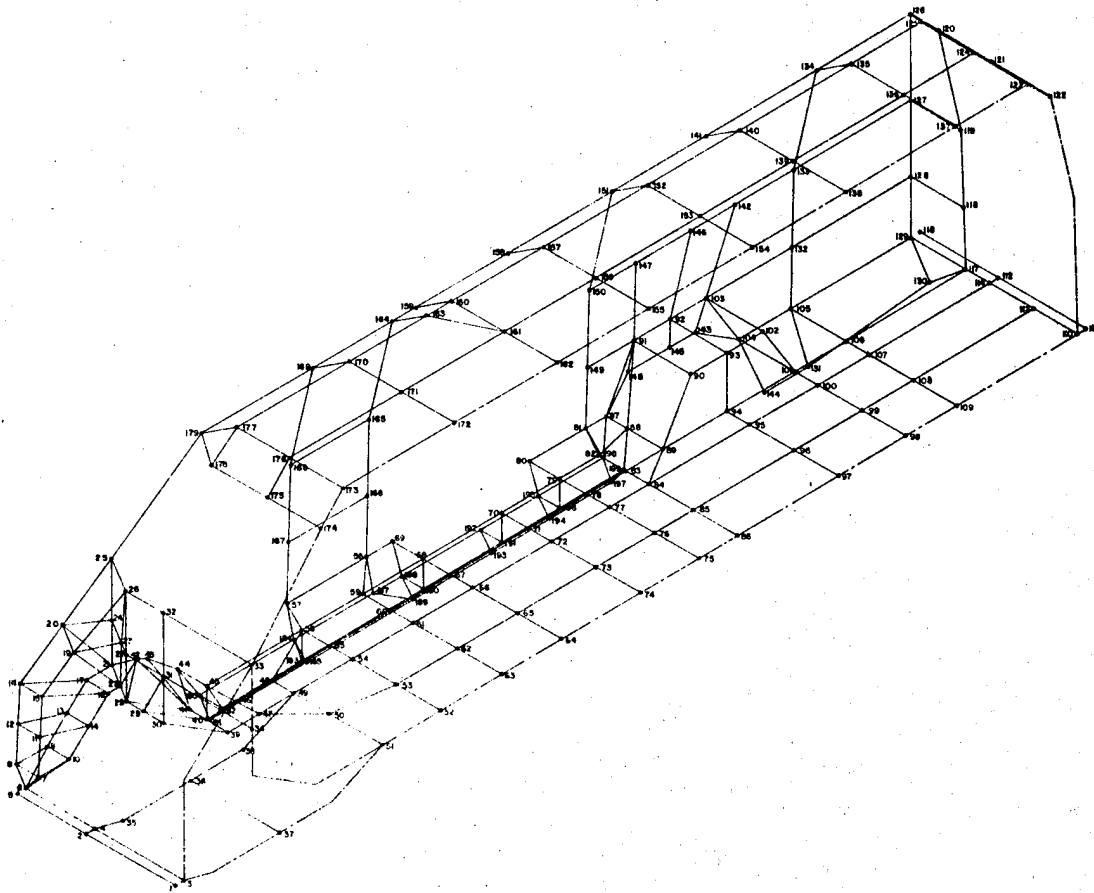
FIGURE 235   BENDING TEST RESULTS

BENDING TEST - ACTUAL TEST VS. COMPUTER MODEL
4557# APPLIED TO FLOOR OF VAN

NODE NO. ● MODEL DEFLECTIONS

GAGE NO. O TEST DEFLECTIONS
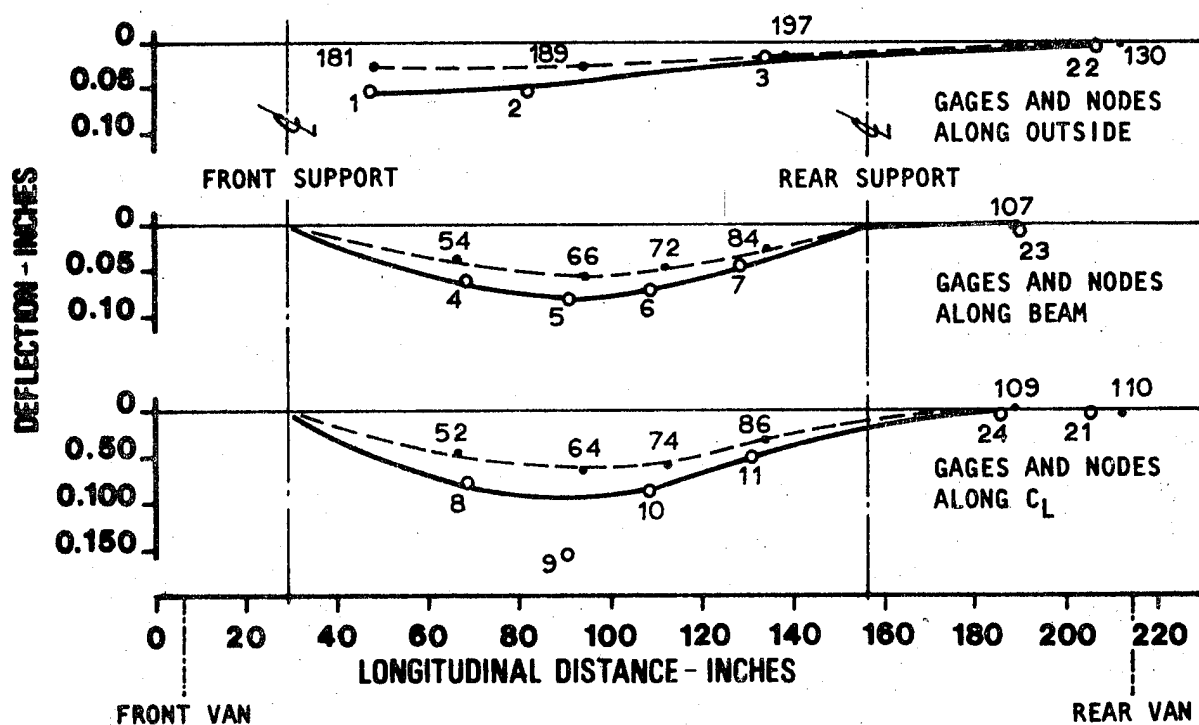
TABLE 81:   TORSION TEST – ACTUAL TEST VS COMPUTER MODEL

Node & Gage Location	Gage No.	Vertical Deflection (Inches)	Node	Vertical Deflection (Inches)
Vehicle	10 8 26	0.017 0.003 0.006	4 52 162	0.027 0.000 0.000
Outside Edge Lower Body	9 22 1 2 3	0.048 0.064 0.065 0.047 0.010	6 21 181 189 197	0.044 0.044 0.040 0.028 0.008
Along Beam	4 5 6 7	0.033 0.019 0.009 0.003	54 66 72 84	0.022 0.013 0.008 0.003
Roof	23 25 26	0.059 0.047 0.006	179 158 162	0.046 0.016 0.000

The Dodge B300 Sportswagon Finite Element Model consists of 196 nodes connected by beams and panels. There are 112 beams represented by 35 different cross sections. There are 141 quadrilateral panels and 30 triangular panels with material thicknesses varying from 0.033 to 0.070 inches. Floor panels are generally 0.049 inches thick and the side structure skins are 0.035 inches thick. The roof skin is 0.033 inches thick.

The model is only a half model of the vehicle and is symmetrical about the longitudinal center line.

The total weight of the steel finite element model is one half the vehicle weight, 2448.84 pounds. The structural weight, or stripped body weight, is 744.38 pounds for this half model. The weight difference is 1704.46 pounds which represents one half of the components removed from the body in white.

Beam weights and panel weights were calculated and divided equally to each corresponding node. Component weights were applied to those nodes which represented their mounting or attaching points.

In the aluminum model, the weight distribution was changed to represent the lower density. The total one half weight is reduced to 1843.73 pounds or an estimated optimum weight reduction of 1210 pounds per vehicle. The metal thickness remained the same as for steel and the section modulii were thus the same as for the steel.

A comparison of the steel and aluminum model results are shown in Figures 236, 237, 238 and 239. The high stresses found in the 3.5 g bump and in the torsion conditions are shown in Figures 236 and 237. As was expected the maximum stresses were found in the "A" post and roof region for the torsion case. In the bump case high stresses were also found in the front fender structure. The stresses found in the aluminum case were lower than those for the steel models. Deflections for the aluminum models were generally twice that for the steel case due to the combined affect of lower load and lower modulus. The deflection of the aluminum model under the torsion condition is shown in Figure 240.

The torsion finite element model case of 3.5 times static weight consists essentially of a 4284 pound load at the spring pocket. This is an extreme case and possibly higher than seen in actual service.

Since the finite element model deflections for the aluminum case were twice that of steel then for the actual test case, Figure 235 and Table 81, for an aluminum vehicle might be expected to be twice the values shown for steel. The results of these analysis would indicate in general that aluminum alloys cannot be substituted directly for steel.

FIGURE 236   VAN – CORNERING

XXXX STEEL STRESS
(XXXX) ALUMINUM STRESS

-13246PSI
(-9923)

A

25180PSI
(18870)

15766PSI
(11440)

16054PSI
(-15372)

16200PSI
(16066)

A - PANELS IN FRONT FENDER AREA ARE
    MOST HIGHLY STRESSED. MAXIMUM
    PRINCIPAL STRESS IS -8200PSI.
    (-6000)

433
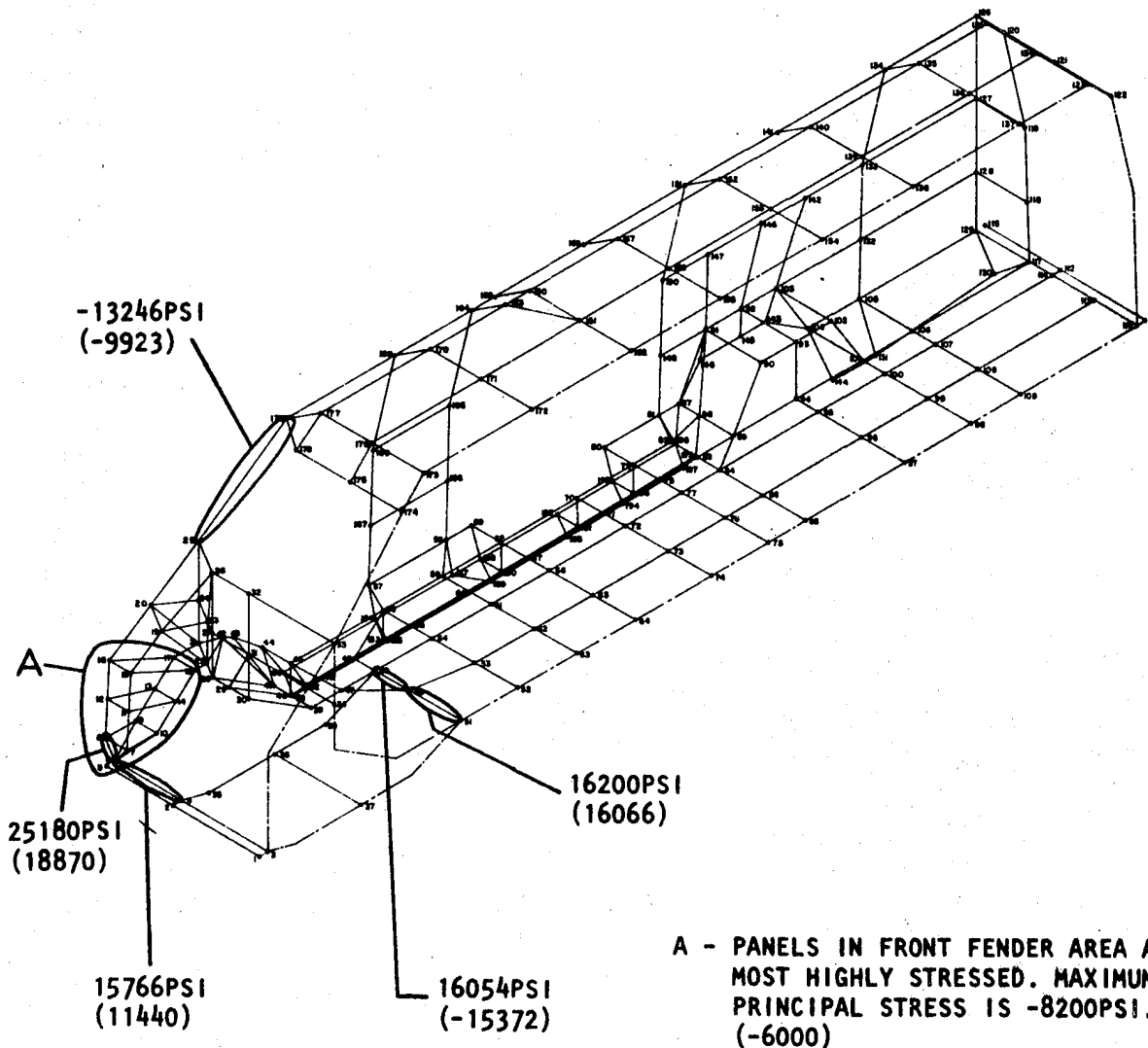
FIGURE 237   VAN — TORSION

XXX STEEL
(XXX) ALUMINUM

27860PSI
(19398)

-29414PSI
(23664)

40979PSI
(-28955)

-49920PSI
(-42680)

40033PSI
(28695)

1

3

2
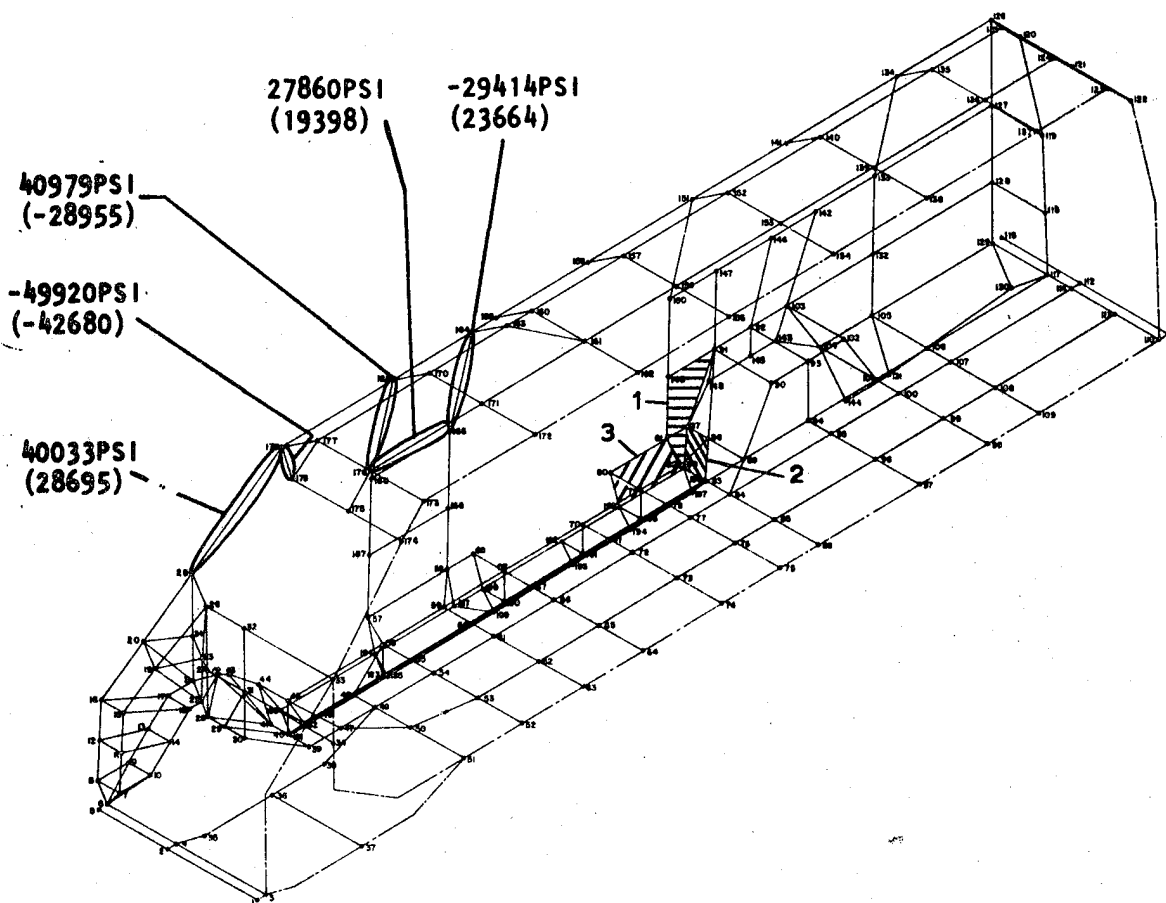
MAX PANEL STRESSES OCCURRED
IN WHEEL WELL AND SLIDING
DOOR AREA

(-12930)   1   -18600PSI PRINCIPAL STRESS

(-11800)   2   -17010PSI PRINCIPAL STRESS

(11090)   3   15704PSI PRINCIPAL STRESS

FIGURE 238   VAN – FRONT BUMP

XXX Steel
(XXX) Aluminum

-.081
(-.145)

-.080
(-.161)

-.164 (-.390)

-.137 (-.334)

-.105 (-.287)
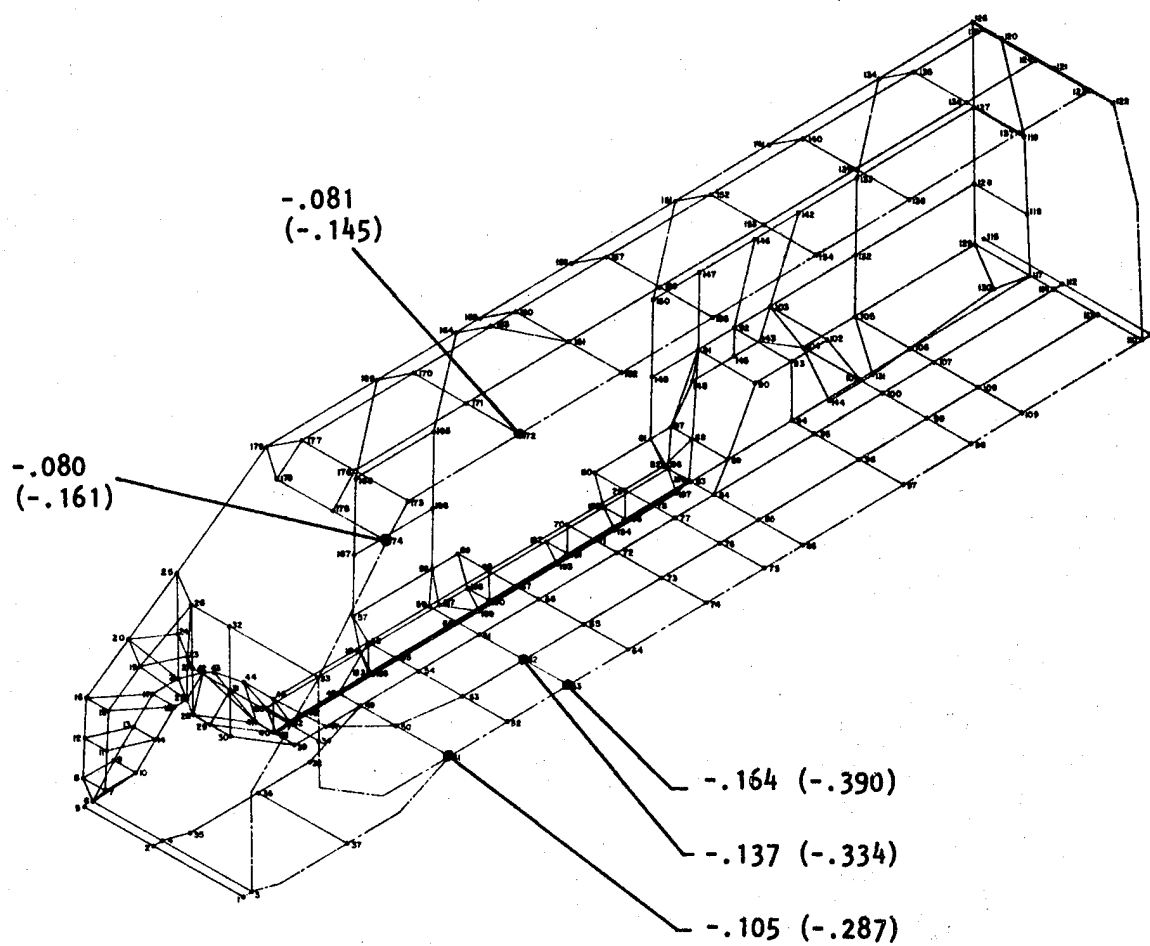
FIGURE 239   VAN – TORSION

XXX   STEEL
(XXX) ALUMINUM

.405
(8.11)

.430
(.861)

.399
(.801)

.373
(.743)

.354
(.704)

A stress analysis such as these do not predict the nature of cyclic dynamic loadings which might be encountered in service. Resonance or excessive vibrations may be encountered which would reduce the feasible weight reduction potential.

The use of aluminum alloys might be enhanced also by a more detailed analysis and variation of section properties of the floor for example to determine the benefit of stiffening it alone.

In the case of aluminum the higher stressed areas would also require a change in the joining procedure or a change in the joint itself. This is due to the lower joint strengths in aluminum alloys and the porr fatigue life.

One general concept for using reinforced composites such as the glass polyesters consists of replacing the steel side panels and roof with molded panels. This is similar in concept to a pick up truck with a removable box or camper cover. To provide adequate structural 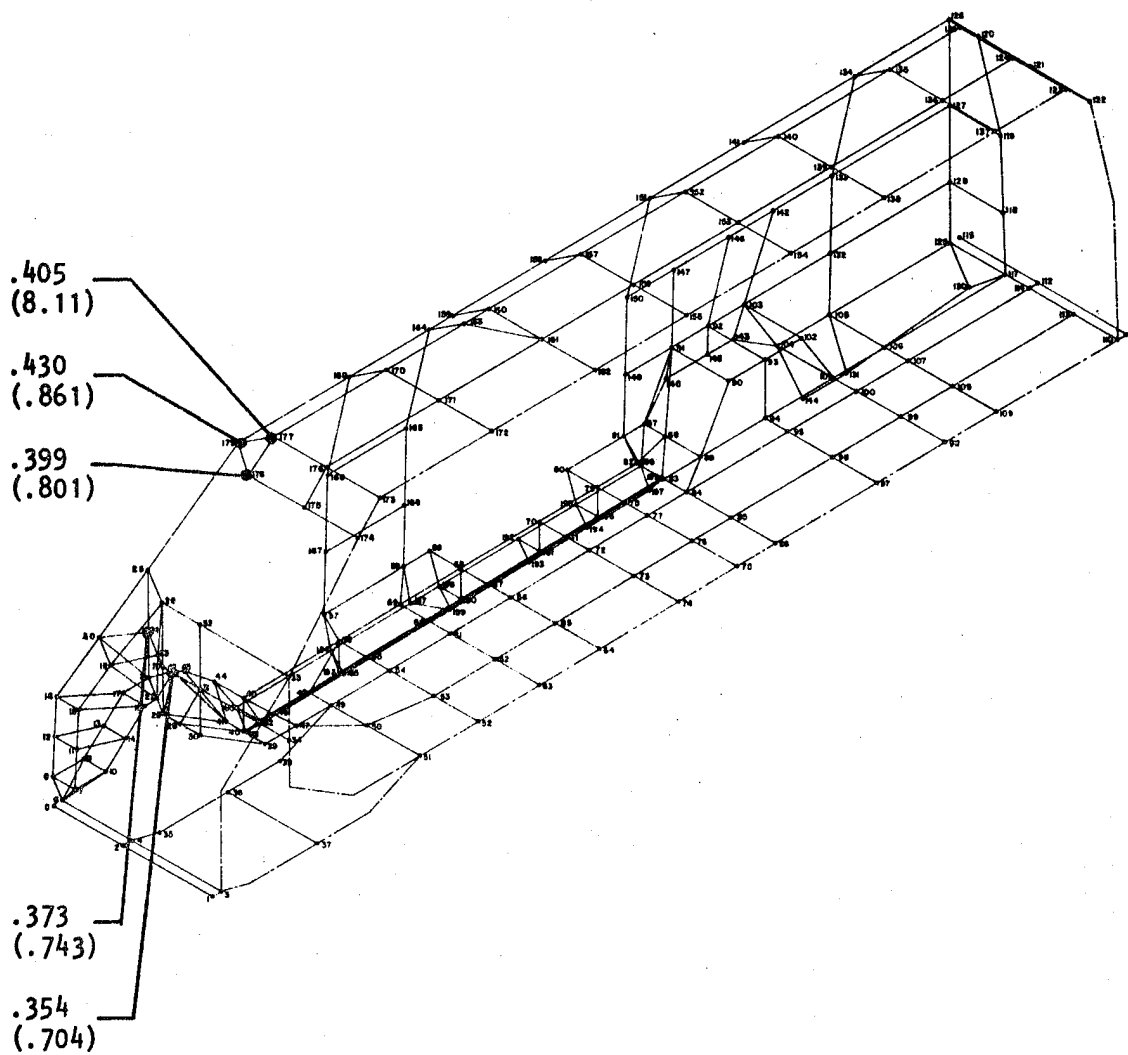stiffness and main ain as few pieces as possible the concepts of the roof and the right and left hand sides are shown in Figure 241, 242 and 243. To assure feasibility a number of joints were examined in detail and are shown in Figures 244 through 248.

The SMC composite upper sides and roofs were attached to the steel body at the window line in a finite element model. The composite thickness was 0.125 inches compared to the steel thickness of 0.033 inches. This is, in a sense, a zero weight reduction even if the internal headliner molding weights are incorporated into the inner SMC composite molding weights. Section properties were calculated for the composite roof and used in the model. While the resulting stresses were low, due to larger cross sections, the deflections were high in the composite panels although they were less than the aluminum panels. The results of this study were rather inconclusive except there was no weight reduction.

10.4 Space Frame Model

The Dodge van studied, and as pictured in Figures 211 through 216, could be described as a space frame or a bird cage with cover panels. Such a concept appears feasible. The lateral hat reinforcements in the roof are coordinated to essentially make connections with the side vertical reinforcements and the floor cross members. With some modifications these could be made into 6 hoops with interrupters at the windows. Longitudinal beams or sills could be provided at the four corners, roof to sides and sides to floor as they are now. Longitudinal stiffeners would be needed where the 2 main sills are now located. Thus the roof, 2 sides and maybe the floor panels could be replaced with alternate materials on the steel space frame. A sketch of what this space frame might look like is shown in Figure 249.

FIGURE 240   DEFLECTION OF ALUMINUM MODEL IN TORSION CASE
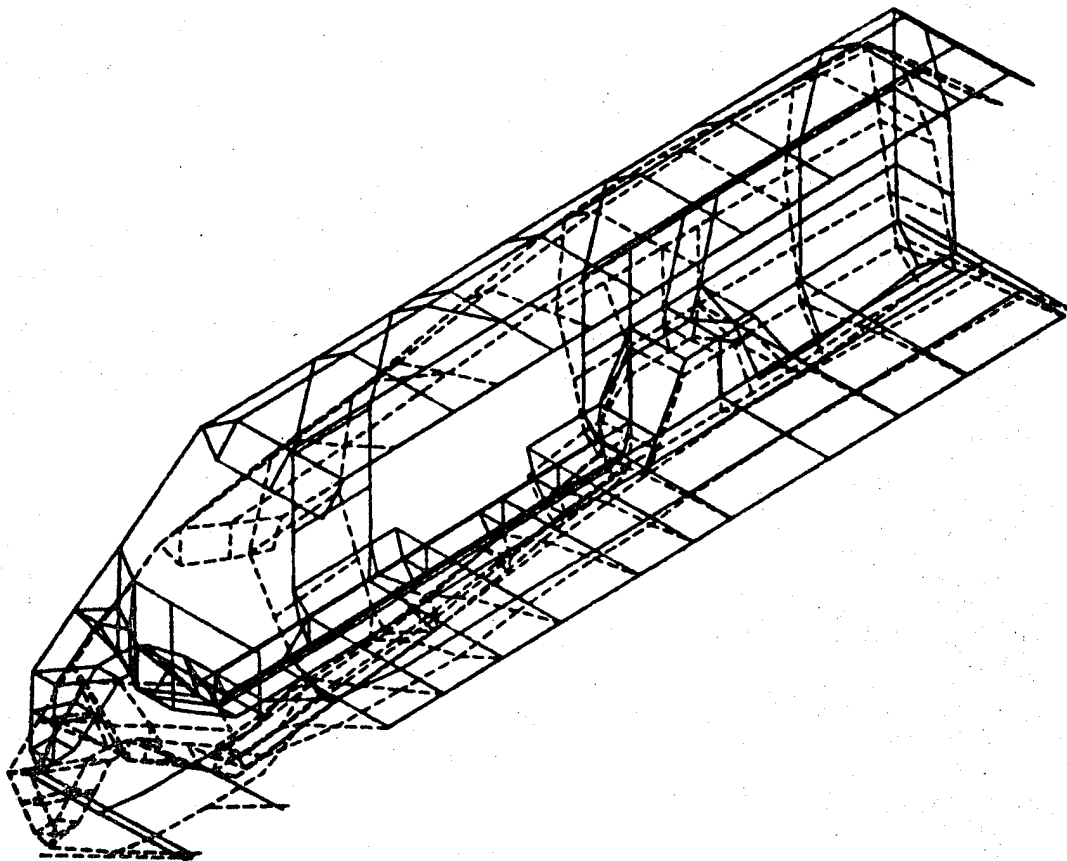
FIGURE 241   VAN – COMPOSITE ROOF
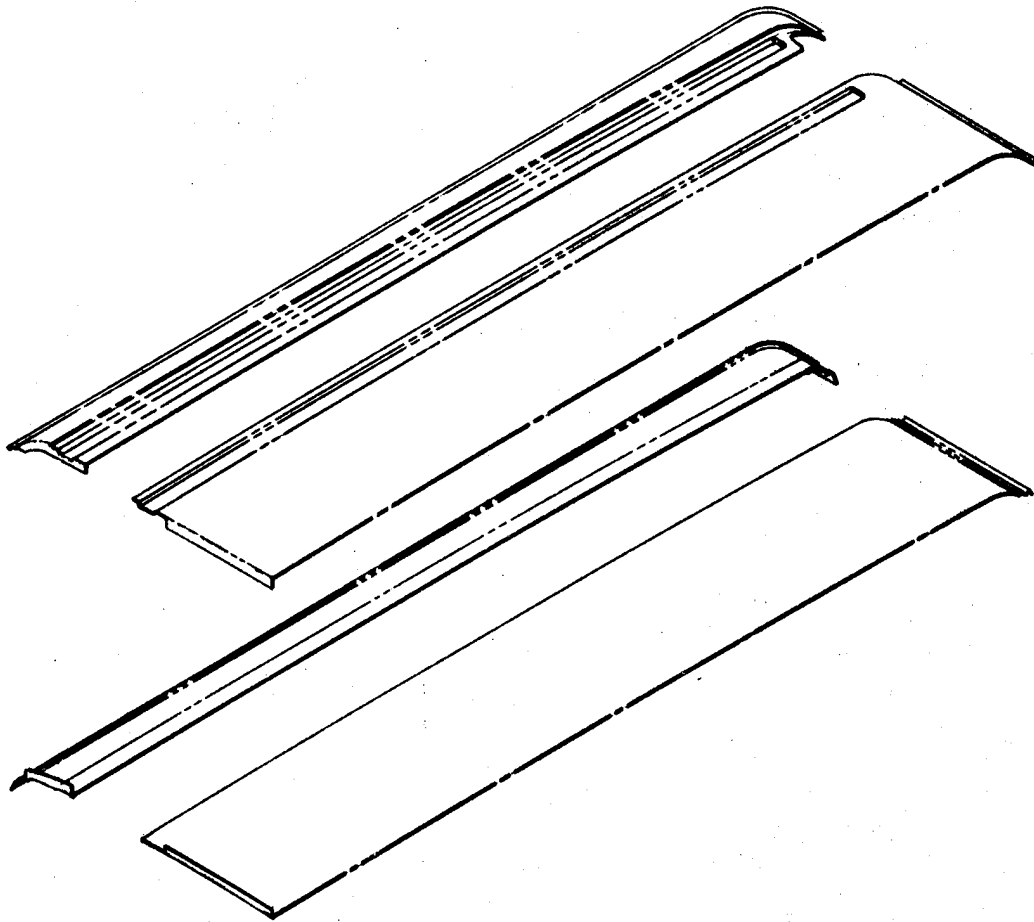
FIGURE 242   VAN – COMPOSITE SIDE ASSEMBLY – UPPER RIGHT
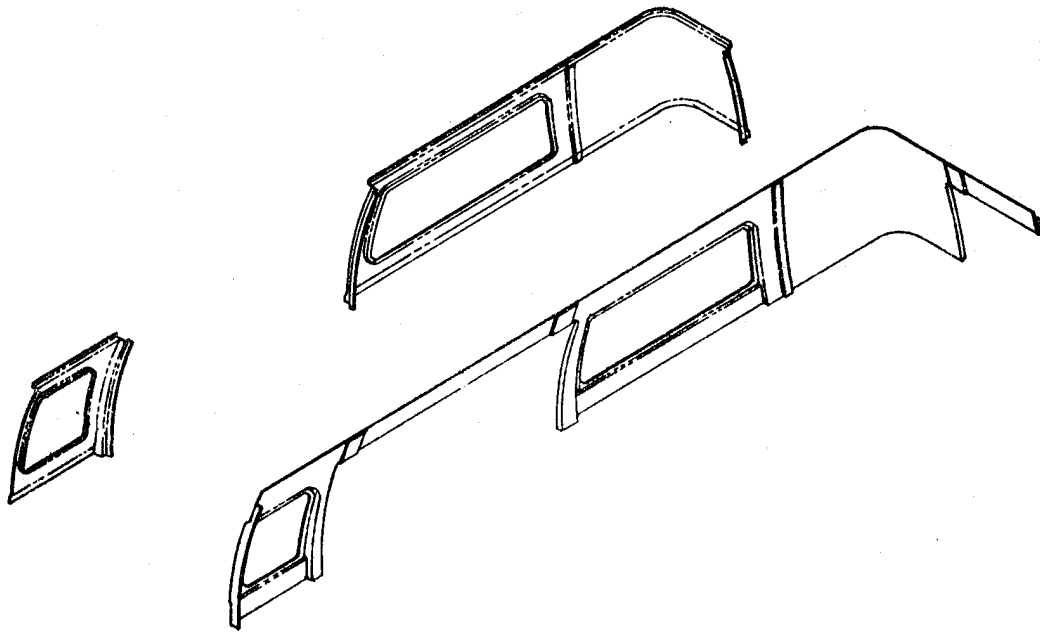
FIGURE 243   **VAN – COMPOSITE SIDE ASSEMBLY – UPPER LEFT**

FIGURE 244   VAN – COMPOSITE – METAL ROOF JOINT
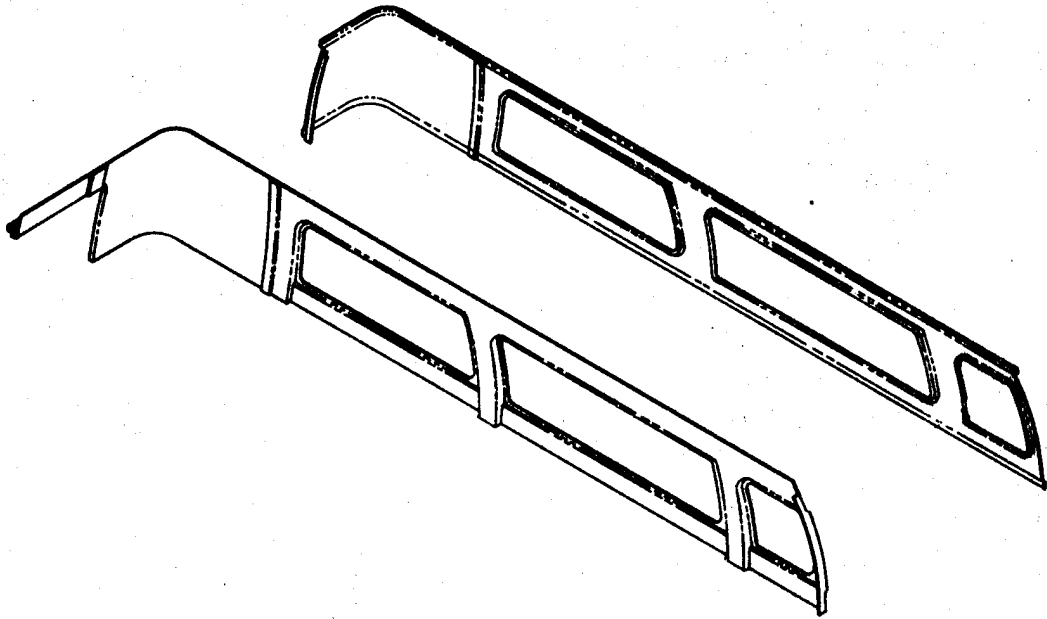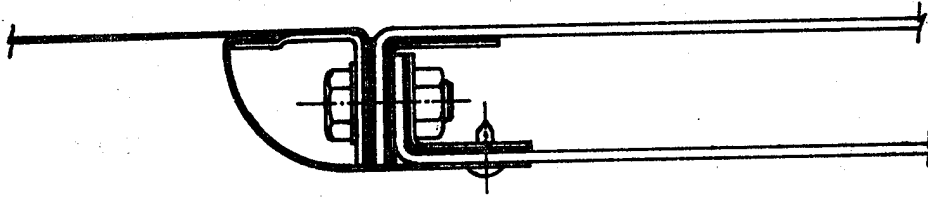
FIGURE 245   VAN – COMPOSITE ROOF BEAD AND JOINT
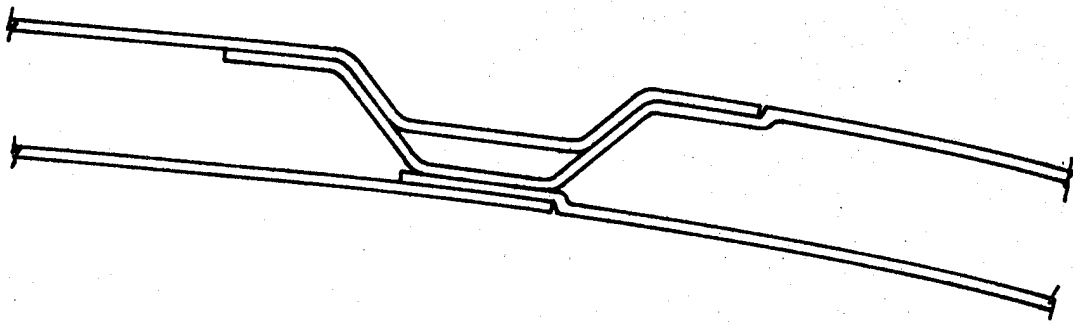
FIGURE 246   VAN – COMPOSITE ROOF TO SIDE JOINT
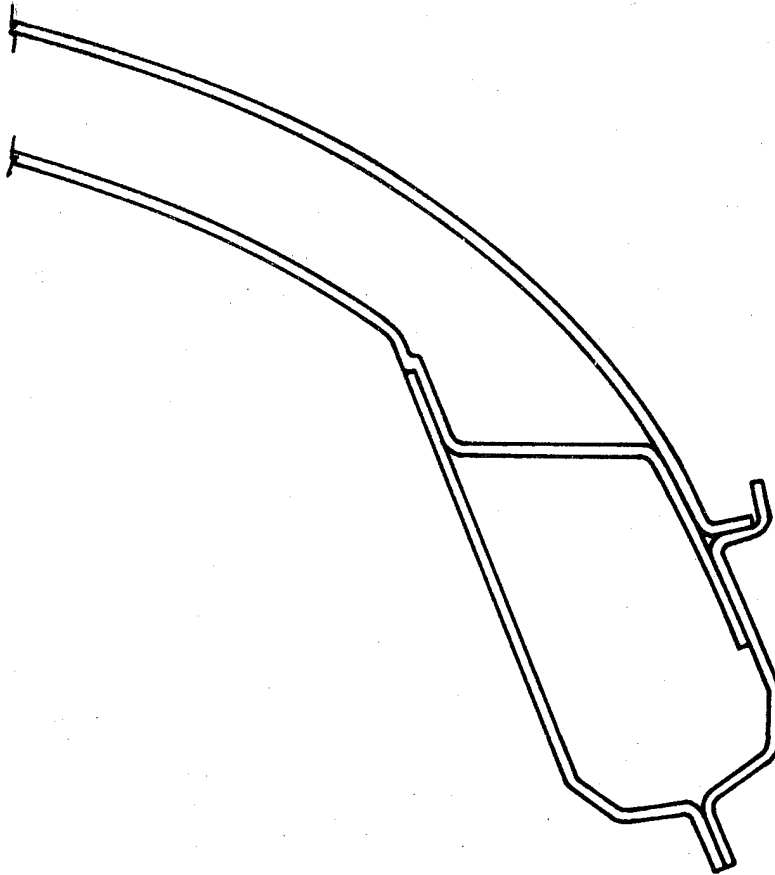
FIGURE 247   VAN – COMPOSITE ROOF TO REAR DOOR FRAME
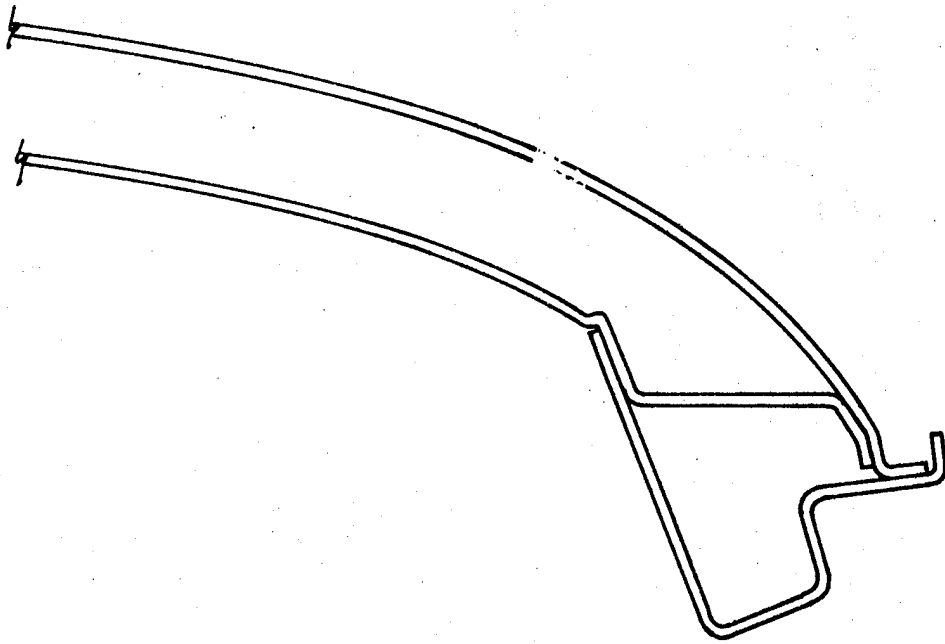
FIGURE 248   VAN – COMPOSITE ROOF TO SIDE DOOR
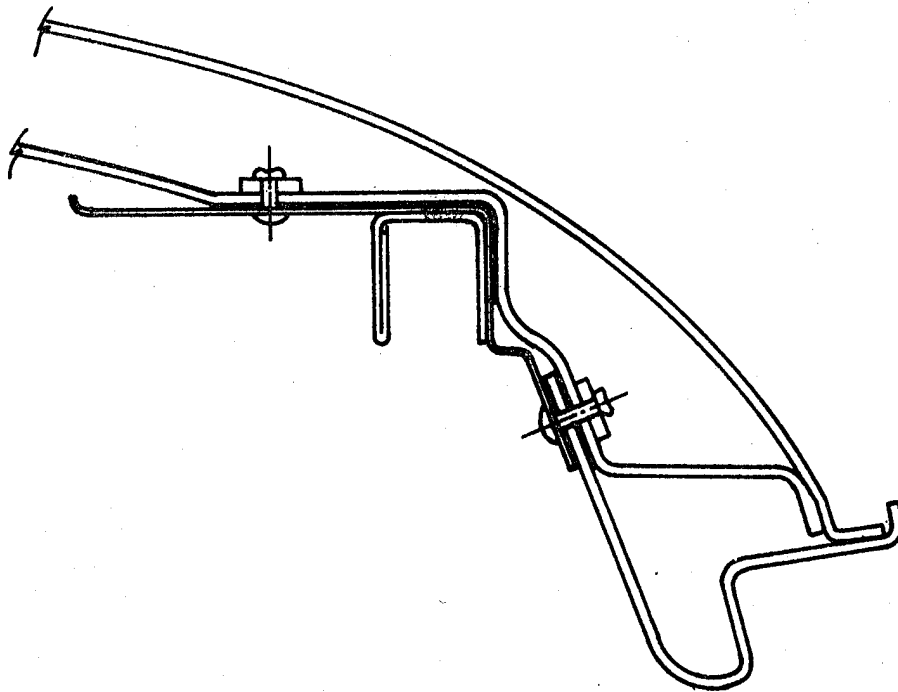
Panels for the roof, sides, back and floor could then be made from lower density and less strong or stiff materials. These attached to the space frame would provide a "dust cover" and would not be depended upon for structural strength. Materials such as soft formable aluminum alloys, reinforced thermoplastics such as Azdel™ of STX™ and unfilled thermoplastics might be used.

The weight reduction potential would be considerable for the roof and the side panels aft of the front doors. Using a material such as continuous fiber glass mat reinforced polypropylene (Azdel™) a weight reduction in these panels from 264 pounds in steel to 79 pounds in reinforced polypropylene might be obtained. The reinforced polypropylene has a density of 0.0468 pounds per cubic inch compared to 0.283 for steel. The reinforced polypropylene thickness would be 0.060 inches for stiffness and manufacturing reasons.

Such materials as the thermoplastic polypropylene may not be satisfactory for the applications such as floors due to scuffing or scraping by sharp objects. A steel surfacing sheet might be required or a replaceable protective plastic skin.

Other panel materials applied to this space frame could be thinner gage steels, aluminum alloys or reinforced thermoset polyesters.

Aluminum alloys of the same gage as the present steel would result in an estimated weight reduction of 171 pounds and a reinforced polyester would result in a 91 pound weight reduction. Since the panels are modular the panel materials might be mixed as desired or required.

Details of the joints and joining are yet to be solved. If the space frame is made of steel then aluminum panels can be bonded or resistance spot welded through bimetallic transition strips. Reinforced polyesters can be bonded to the steel with rivit assists. Transition strips of steel-polyurethane or polyethylene would be one method of joining the reinforced polypropylene to the steel frame. This has not been tried as far as can be determined in any production application. Several joint configurations are shown in Figure 250. These may be used by themselves or in combination, such as rivets and bonding.

10.5 Crashworthiness and Safety

A review of the discussions on materials and their effects on crashworthiness, Sections 7 and 9, and the van structure provides the basis for this review. The van as now designed would not suffer any loss of crashworthiness by the applications of aluminum alloys or HSLA steels. Considerations of design previously mentioned have to be considered to insure that the desired load-deflection characteristics are obtained.

447

FIGURE 249   VAN — SPACE FRAME BODY
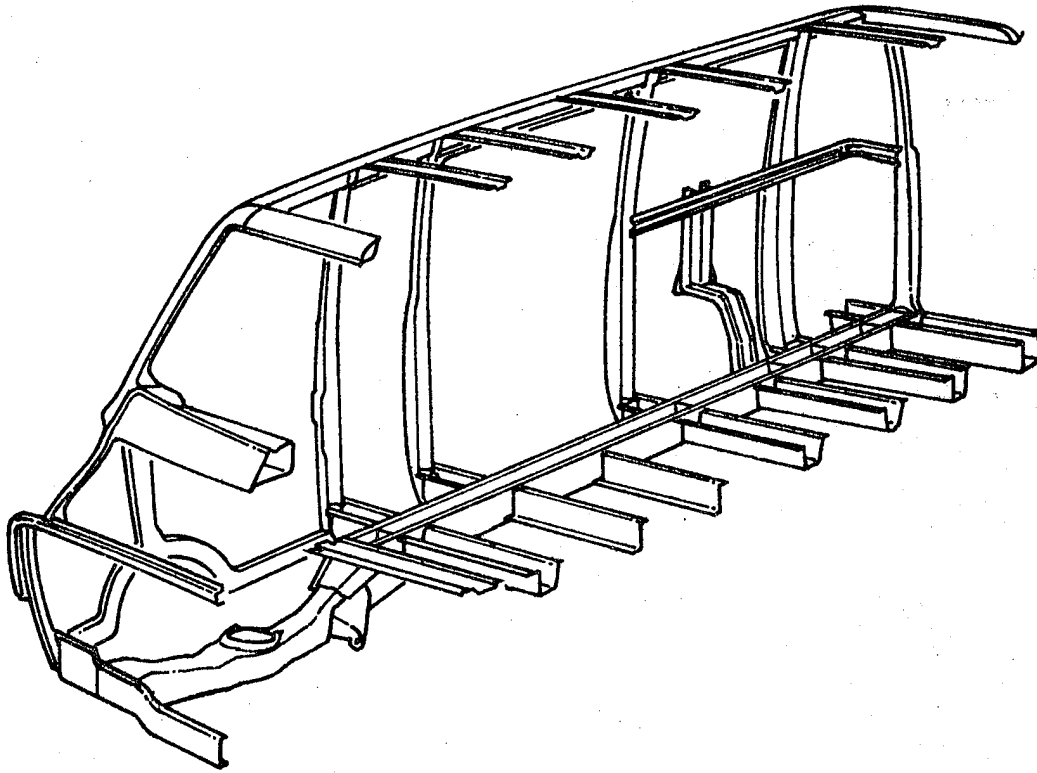
FIGURE 250   SPACE FRAME – PANEL JOINTS

RESISTANCE SPOT WELDED

STEEL OUTER PANEL

STEEL DOOR PILLAR

TRANSITION STRIP, WELDED

ALUMINUM OR THERMOPLASTIC OUTER SKIN

STEEL DOOR PILLAR

ADHESIVE BOND

ALUMINUM OR BONDABLE THERMOPLASTIC OR THERMOSET OUTER PANELS

STEEL DOOR PILLAR

MECHANICAL FASTENER

ALUMINUM THERMOPLASTIC OR THERMOSET OUTER PANEL

STEEL DOOR PILLAR

449
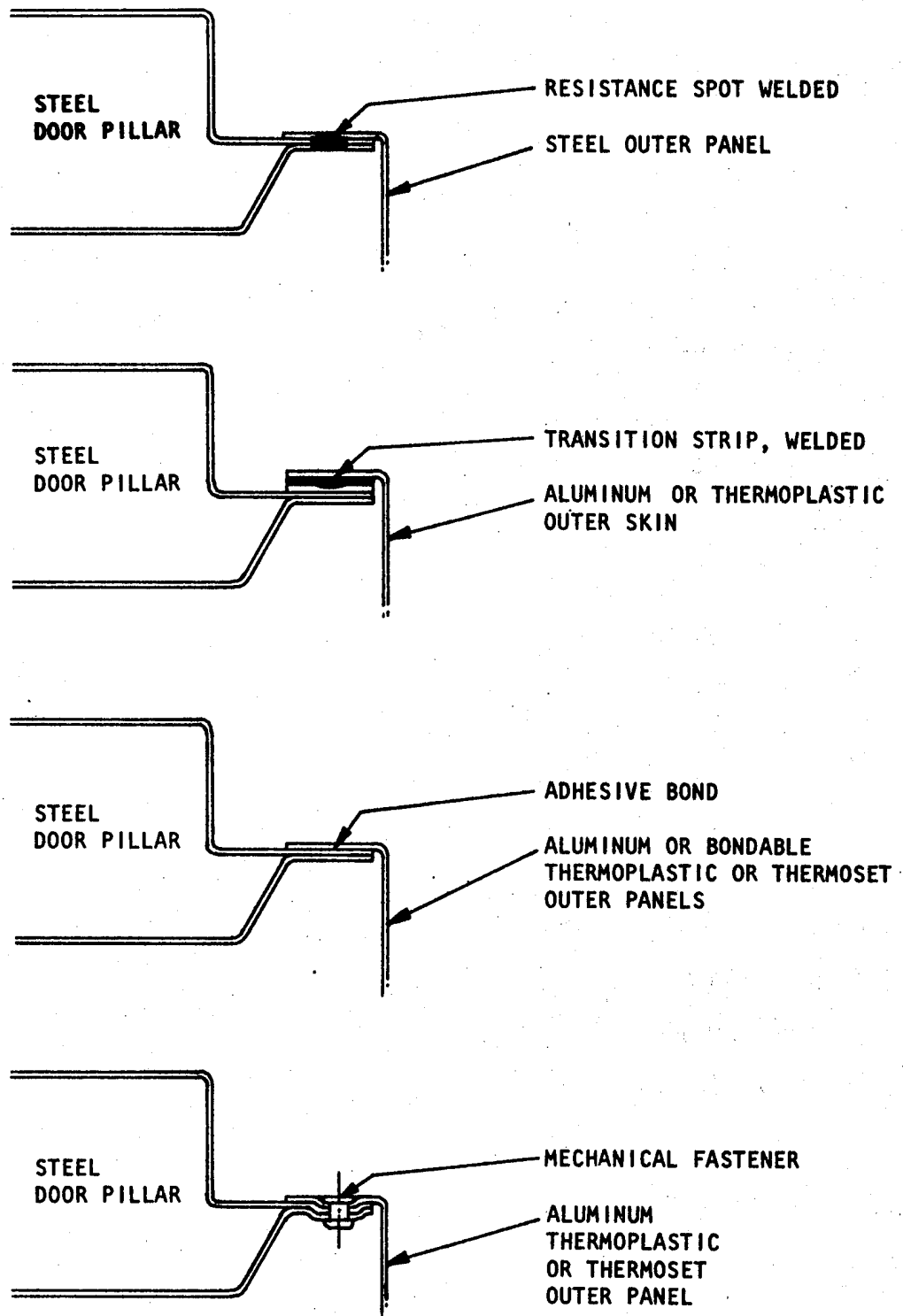
The van as currently designed and produced does not have to meet either the side intrusion nor the frontal barrier test requirements that are required of passenger cars. As these requirements are established it is believed that the use of alternate materials will not be restrictive.

10.6 Weight Reduction - Body in White

Weight reductions are hazardous to project for any vehicle without an intimate and complete knowledge of the design and durability test performance. Downsizing and performance reduction can only be accomplished with an accurate knowledge of the intended market and performance specifications. As an example, a reduction in sheet metal gage of any or all of the panels or reinforcing members can be easily suggested to reduce weight. Obviously a ten percent reduction in thickness would result in a ten percent reduction in weight, but would the reduced strength and rigidity be acceptable for the intended market?

Referring to Figure 106 the total manufacturing cost is determined in part by direct materials costs. A satisfactory cost-earnings ratio depends upon minimizing this direct material cost. Based on this reasoning it is expected that the metal thicknesses are currently at, or near a minimum. This minimum thickness may not necessarily be due to load carrying requirements, however, and in some instances may be specified to improve or meet a quality level in appearance.

In contrast to the above concept, material prices depend upon the quantity purchased and it may be advantageous to buy a larger quantity of a thicker gage than to buy a small quantity of two or more gages. In this instance the thickness purchased would be that required for the thickest application and other vehicles, or components, will become over designed.

Following in the same line of reasoning it is not unreasonable to envision that the direct labor costs of manufacturing various sizes of one object is greater than the loss in direct material costs if only one size is made. For example, front door hinges required for one vehicle may weigh 2.8 pounds and for another 2.6 pounds. The cost of resetting dies and assembly fixtures for a small number of hinges more than offset the material costs and the hinges become over weight.

Similarly, vehicles are designed for a volume and weight payload, and more weight efficient designs could be developed if a single objective was selected. The Dodge van studied has a cargo volume of 288 cubic feet and a payload of 3150 pounds without seats. A 3150 pound steel block, for example, is only 6.42 cubic feet in volume, requiring less than one fortieth of the available cargo volume.

Based on the above observations estimated weight reductions can be summarized for the Dodge van studied using the following guidelines:

1. Inner envelope cannot be reduced.
2. Outer envelope cannot be enlarged.
3. Total vehicle deflections cannot increase (IE constant).

Consider first the unitized body structure of Figure 211. It consists primarily of beams and panels as pointed out previously. The reinforcement weight can only be reduced by the application of carbon fiber composites, high modulus/density ratio, if the criteria stated previously are to be met. The reinforcement weight in steel is 466 pounds and the carbon fiber reinforcement weight would be 138 pounds, or a reduction of 328 pounds. This is an optimistic value which does not consider impact in collisions or jouncing.

The side and roof panels, using a space frame concept described in Section 10.4, could be made of a reinforced thermoplastic or an aluminum alloy with a resulting weight reduction of 180 pounds.

The floor panel now weighs an estimated 182 pounds in steel. This panel is made from 0.048 inch thick sheet and it is welded to the floor reinforcements. Continuing with the space frame concept this floor panel could be replaced with a steel-thermoplastic or an aluminum-thermoplastic sandwich laminate. These materials are under development by material suppliers currently, and still require considerable development, primarily in joining. A replacement material would consist typically of two skin sheets of carbon steel 0.012 inch thick with a 0.024 inch thick thermoplastic core. The successful application of this laminate floor panel would result in a 43% weight reduction or 78 pounds.

An alternate floor concept using a deep foam filled sandwich could be married to the remaining structure and provide an expected weight reduction. The two longitudinal side rails, Section Number 12 of Figure 230, have a combined moment of inertia of 18.64, Table 78. An equivalent double skin sandwich at five inches deep requires 0.020 inch skins, $I=AD^2$. Additional reinforcements, doublers or mounting pads would be required for such things as rear suspension mounting, gasoline tank attachments and exhaust system supports. The full floor weight to be replaced weighs 514 pounds now and this could be reduced by an estimated 70 to 80 pounds which is similar to reduction from the laminate space frame concept.

The frontal, cab-engine, portion of the body structure not yet considered constitutes another 152 pounds. Replacement of the current steel with another material in these areas is difficult unless it would be all aluminum or all molded glass polyester

composite. With these two materials, the weight reduction is considered to be negligible due to the stiffness requirements.

Hang on parts for the body include the five doors and hood. These are primarily steel inner and outer panels and operating mechanisms. An estimated weight reduction of 75 pounds is expected using either aluminum, laminate or composites.

Glass in the doors, sides and rear, replaced with scratch and haze free plastic when developed, could result in another 25 to 30 pounds reduction.

Seat structure as now built, although heavy, conforms to FMVSS207. A reduction of the seat frame weight does not appear feasible. If the seat comfort was reduced and the entire seat made from two reinforced plastic moldings, a weight reduction might be feasible, yet of a small amount.

The total estimated weight reduction of the unitized body and doors is 686 pounds with a carbon fiber space frame and 338 pounds with a steel space frame concept. The steel space frame concept is more conservative but does provide a safe, crashworthy structure. The use of carbon composites is suspect due to the impact loading generally encountered in normal use and in collisions. For this reason, although cost is also a factor, a steel space frame (cage-of-steel) is recommended.

The existing van weights have been listed as systems in Table 82 and the percentage of total weight calculated. These percentage values of systems have been compared to large passenger vehicles and utility vehicles and against data in the literature.[103,104] The percentage values agree surprisingly well and have been used in estimating a first van weight. The reduction in structure weight, 338 pounds, results in a new structure weight of 1807 pounds. Assuming this structure weight is 43.8% of total vehicle weight, new weights can be calculated as shown in Table 83. This results in a first vehicle new weight of 4125 pounds, a weight reduction of 775 pounds.

From methods of references 103 and 104, the reduction of required horsepower was determined and the reduction in engine weight and power train was estimated. This agreed well with the value obtained in Table 83.

Other vehicle weight reductions which might be obtained are found in the two rear springs and five wheels. Carbon fiber composites and hybrids of glass and carbon fibers have been proposed for springs and aluminum alloys for wheels. Based on experiences of other investigators, an estimated 75 pounds of the wheel weight can be reduced with aluminum alloys

452

TABLE 82: SYSTEM WEIGHT, DODGE MAXIWAGON

System	Weight	% Total
Powertrain	1159.8	23.66
Structure	2145.8	43.79
Suspension	626.4	12.78
Brakes	144.0	2.93
Steering	75.4	1.54
Tires, Wheels	360.0	7.34
Bumpers	79.3	1.63
Miscellaneous	309.3	6.30
	4900.0	

TABLE 83:   SYSTEM WEIGHTS, MODIFIED DODGE MAXIWAGON

System	Weight	% Total
Powertrain	976	23.66
Structure	1807	43.79
Suspension	527	12.78
Brakes	120	2.93
Steering	63	1.54
Tires, Wheels	302	7.34
Bumpers	67	1.63
Miscellaneous	260	6.30
	4125	

A new structure weight establishes 4125 pound vehicle weight. This in turn establishes remainder systems weights. Percentage established in Table 82.

454

and 75 pounds can be taken out of the rear springs using carbon-glass fiber hybrid composites.

Subtracting this last 150 pounds from the van weight of Table 83 results in a predicted 3975 pound weight for the maxiwagon or a reduction of 925 pounds.

11.0 ALUMINUM ALLOY DOOR DESIGN

11.1 Objective

In an effort to involve materials producers in this program and to obtain their latest thinking, sub contracts were invited. The Aluminum Company of America responded and performed a design study of the Impala front door.

The requirements for the front door were increased from those of FMVSS 214 to higher values. FMVSS 214 requires a maximum load of 7000 pounds within 18 inches of static crush and an average force of 3500 pounds over the first 12 inches of crush. These loads were increased to 60,000 pounds to be obtained in a six inch intrusion distance. This requirement is considerably more severe than FMVSS 214 and was specified based on a 15 to 20 g acceleration of the struck vehicle.

A second requirement concerned the doors contribution during a frontal collision. Based on the evaluation of the ideal sheet metal in Section 7, an estimated 20,000 force at the upper hinge area was expected in a 50 mph collision. A maximum permanent set of half inch was specified to permit door opening after a collision.

The aluminum concept is shown in Figure 251 where the intrusion beam has been sized to react the 60,000 pound side intrusion load by itself without benefit of the inner and outer panel. The lightest door intrusion beam design relies on reacting the 60,000 pound load by membrane tension and not by beam bending. Sufficient bending stiffness was included to carry the required longitudinal collision forces. Using the concept of membrane tension, very large loads are introduced into the "A" and "B" posts. To insure that the load can be transmitted to the posts the intrusion beam of Figure 251 was directly connected to the modified hinges and to the modified latch details of Figure 252. The "B" post hook is required to transmit the loads since the latch is not sufficient by itself.

A spring constant of 75,000 lbs/in. was established as required for the "A" and "B" posts to insure that the 7075-T6 intrusion beam does not yield in tension. An evaluation of the present steel "A" and "B" posts indicated that they are stiff enough but that they should be modified for strength requirements. In addition, for the rest of the automotive structure to adequately resist the 60,000 pounds, reinforcement of some structures and addition of others, as displayed in Figure 253, are required. One other study was conducted to see if part of the membrane load could be transferred to the sill area with an extension from the intrusion beam to the sill. The result of this study was that the additional vertical member would allow a significant portion of the load to be transferred to the sill but only if moment resisting connections could be designed at both ends of the new member. This approach was not developed because of the uncertainty of such a connection at the sill, especially during the crushing.

456

FIGURE 251   ALUMINUM DOOR BEAM CONCEPT

SECTION A-A
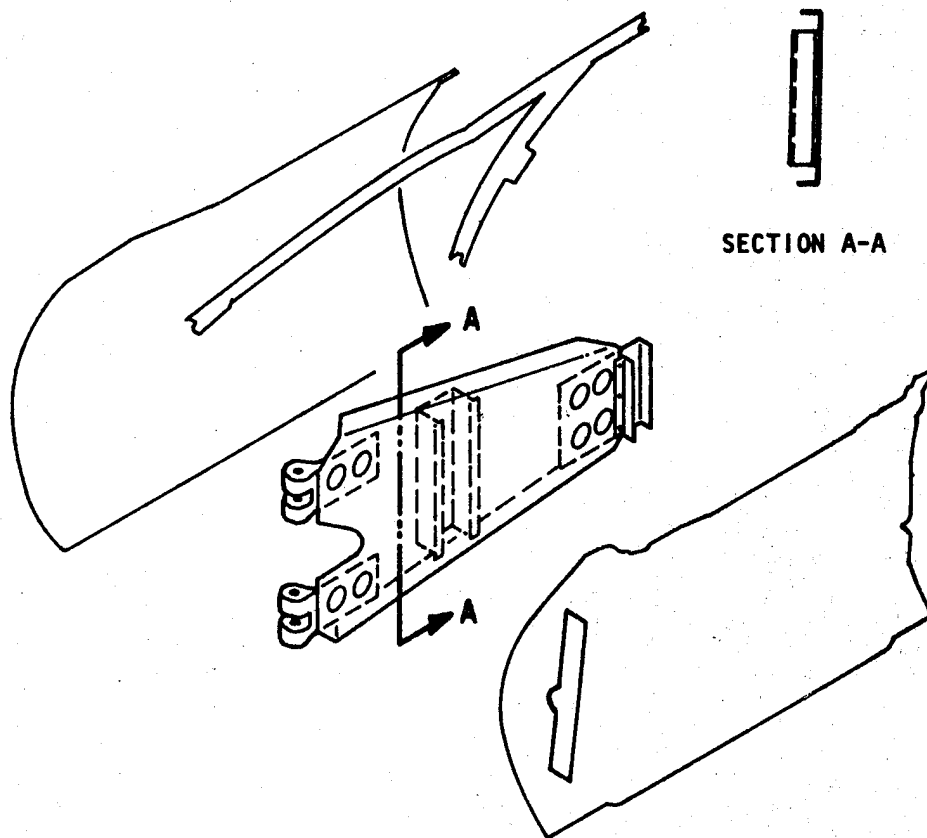
ALCOA CONCEPT FOR MODIFIED DOOR REQUIREMENTS

FIGURE 252   "B" POST HOOK DETAIL

LATCH

B POST

ALUMINUM INTRUSION BEAM

PRESENT INTRUSION BEAM

OUTER PANEL
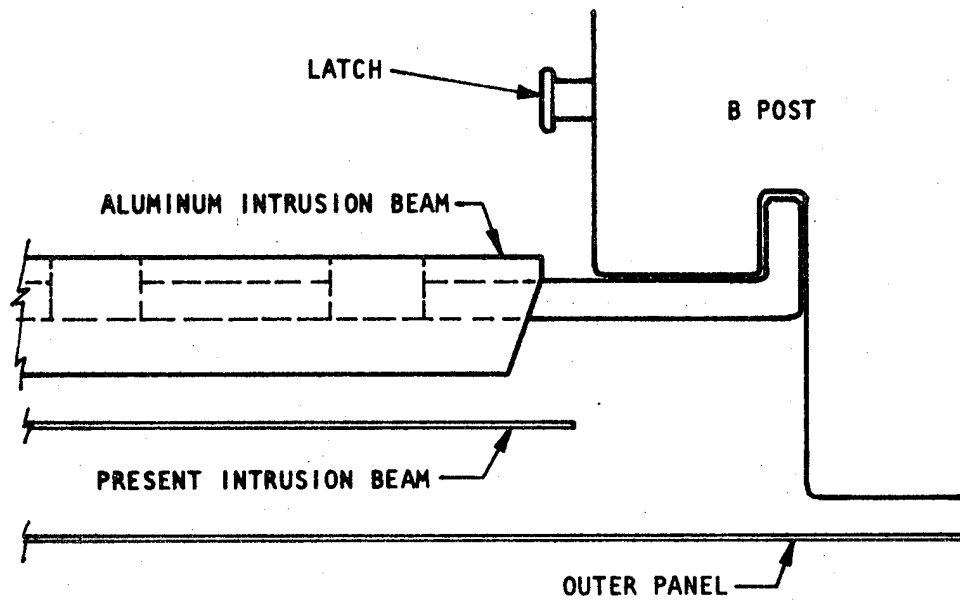
FIGURE 253   IDEALIZED FRAMEWORK FOR THE MODIFIED IMPALA

ADDITIONAL FRAMING

PRESENT MEMBERS
(REINFORCED)

C POST (REINFORCED)

FIRE WALL

20,000 POUNDS

A POST
(REINFORCED)

B POST (REINFORCED)

60,000 POUNDS

INTRUSION BEAM

SILL (REINFORCED)
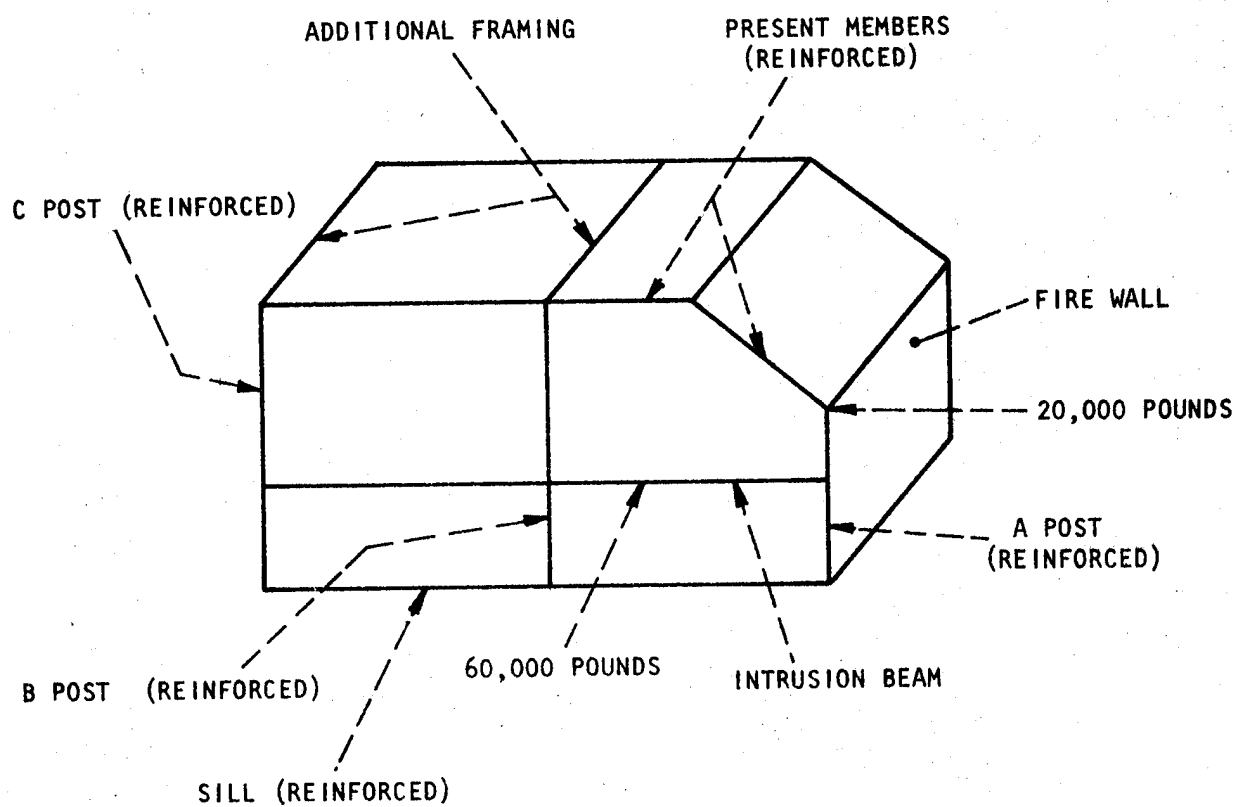
The predicted force/deformation of the intrusion beam, which has a spring constant resistance of 75,000 lbs/in. at each end, is shown in Figure 254. The maximum deflection of 4.7 in. from Figure 254 was intentionally made less than the 6 in. allowance to provide for fabrication tolerances and for the deformation of the steel framework.

Table 82 presents the weight and cost summary for the aluminum door. The design of Figure 251 is shown to be 76.6 pounds compared to the existing steel door weight of 72.5 pounds. Of the 76.6 pounds, 45.1 pounds is aluminum and 31.5 pounds consists of glass, trim, insulation, and steel mechanism parts which were not converted to aluminum. To meet the existing FMVSS 214 requirements the present steel door could be replaced by an aluminum door weighing 52.3 pounds. Therefore, the crashworthy aluminum door creates a penalty of 24.3 pounds above the weight required for an aluminum door to meet the existing standards. Additional undetermined weight would also be required to beef up the supporting steel framework of the car body.

From Table 82, Alcoa estimated the total net cost of the aluminum is $54.73 per door. This cost reflects an allowance for scrap recovery and also includes a 2-1/2% process scrap rate. Assuming a production of 400 doors per hour the incremental fabrication cost above the existing steel door is estimated to be $2.89 per door. In addition, special attention has to be taken when joining steel to aluminum parts to prevent galvanic corrosion problems. While the study recommends procedures to avoid this problem, no delta cost has been provided.

The energy requirements to produce, process, and fabricate only the aluminum portion of the door was discussed by Alcoa. The actual energy required will depend on the amount of recycled aluminum which can be included with new metal. In 1976, recycling of old aluminum scrap was only about 6.6 percent of the annual output. All of this scrap, at present, is used in casting operations. Therefore, if no old aluminum is to be recycled in estimating the energy requirements of the aluminum, a total of 6.26 to 6.67 x 10^6 Btu per door would be needed depending on fabrication energies assumed. If it becomes possible to economically remove contaminating elements so that recycled aluminum scrap could be used in rolled products then the energy requirement would be 4.01 to 4.42 x 10^6 Btu per door where 50 percent cycling was assumed.

FIGURE 254   CALCULATED RESPONSE OF INTRUSION BEAM TO 60,000 LOAD
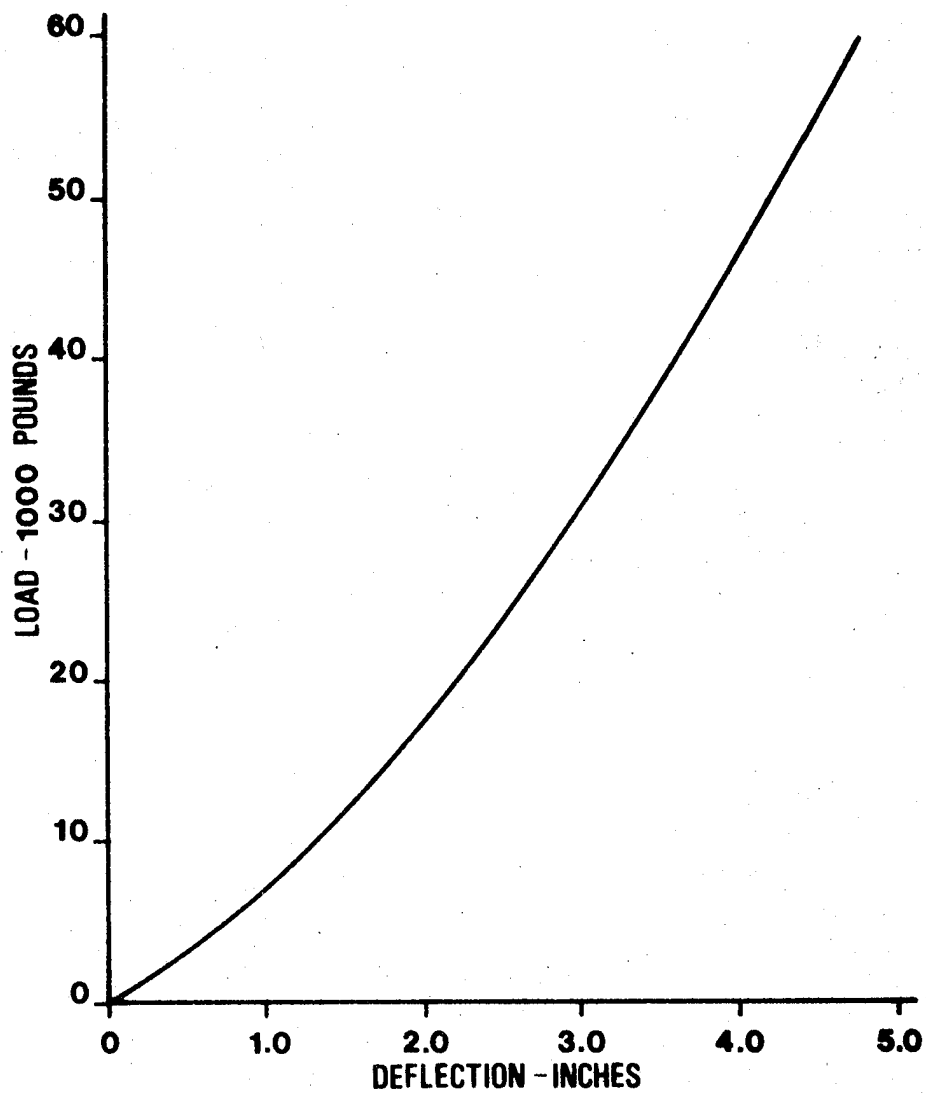
TABLE 84: SUMMARY – WEIGHT AND COST – ALUMINUM DOORS

	Wt. Lbs
1977 Steel Door, Complete with Hinges	72.5
Crashworthy Aluminum Door, Complete with Hinges	76.6
Difference	+ 4.1
1977 Steel Door, Without Beam & Hinges	62.0
Crashworthy Aluminum Door, Without Beam & Hinges	47.0
Difference	-15.0

Assuming present loading requirements could be met
with an aluminum beam at 50% of steel weight
(0.5 x 8.5 = 4.3) and same for hinges (0.5 x 2.0 - 1.0):

Indicated weight of aluminum door meeting   =52.3 [1]
present requirements: 47.0 + 4.3 + 1.0

Indicated weight savings over 1977 steel 72.5 - 52.3 =20.2

Indicated weight penalty to an aluminum door
associated with upgraded requirements is
76.6 - 52.3 (without regard to posts, etc.)   =24.3

For the Crashworthy aluminum door:

Aluminum Content	45.1
Total (Net) cost of aluminum mill products	$54.73
Estimated Incremental Fab Cost	$ 2.89

[1] Note: 31.5 lbs. of this weight is glass and steel
parts not converted to aluminum.

12.0 GRAPHITE FIBER COMPOSITE FRAME

A second subcontracted materials application study was offered to Hercules, Inc. The objective of Hercules' study was to evaluate the feasibility of using graphite fiber material to replace the portion of the Impala steel frame which is forward of the firewall. The static and fatigue loading was the same as for the existing steel frame but an additional requirement of being able to provide crush characteristics as measured by a force/deformation curve were also imposed. This criteria resulted from the ideal force/ deformation computer simulation study detailed in the Section 7 for a 50 mph frontal impact. The static force/deformation criteria for the portion of the frame forward of the suspension cross-member and the comperable curve for the frame section between the suspension cross-member and the firewall are given in Figure 255.

Both portions of Figure 255 correspond to a static condition for the steel frame, to which a velocity sensitive dynamic strain rate correction would be applied. The strain rate correction factors for composites are at present unknown while the factor for steel could range from 1.0 to 1.8 depending on the instantaneous velocity. To arrive at the appropriate force/deformation curve to apply to the composite design, Figure 255 should be altered to reflect some ratio of strain rate correction rates for the two materials. Since this ratio is presently unknown, it was decided to size the composite frame using the unmodified curves of Figure 255. While this approach may not be conservative, it will result in a methodology which can be applied when appropriate data becomes available.

This complex geometric shape and difficult packaging problem caused the composite design to duplicate the existing steel frame wherever possible. For this study it was decided to match axial stiffness and axial load carrying capability while maintaining the same geometric shape. The matching of the torsional stiffness could have also been included but it was not done to simplify the present evaluation.

It was established that for any cross section of the frame the axial modulus and axial strength would behave in a linear fashion as shown in Figure 256. The corresponding steel thicknesses, are, however, non-linear as seen in Figure 256. This figure formed the basis as a design curve for use in selecting acceptable material combinations.

A composite data base was compiled for the graphite, glass, and Kevlar fibers in a woven, unidirectional, and chopped form using an epoxy, polyester, or polyimide resin system. This data base covered static test results with much of the data sought being unavailable. None of the materials selected, by themselves and in any form or orientation, matched any part of the design curve of

463

STATIC/FORCE DEFORMATION FOR
FRAME SECTION BETWEEN BUMPER
AND SUSPENSION CROSS-MEMBER
WITH LOAD REACTED AT THE
CROSS-MEMBER.

FRAME
BOTTOMS
OUT

STATIC FORCE/DEFORMATION FOR
FRAME SECTION BETWEEN SUSPENSION
CROSS-MEMBER AND THE FIREWALL
WITH LOAD REACTED IN THE AREA
OF THE SILL.
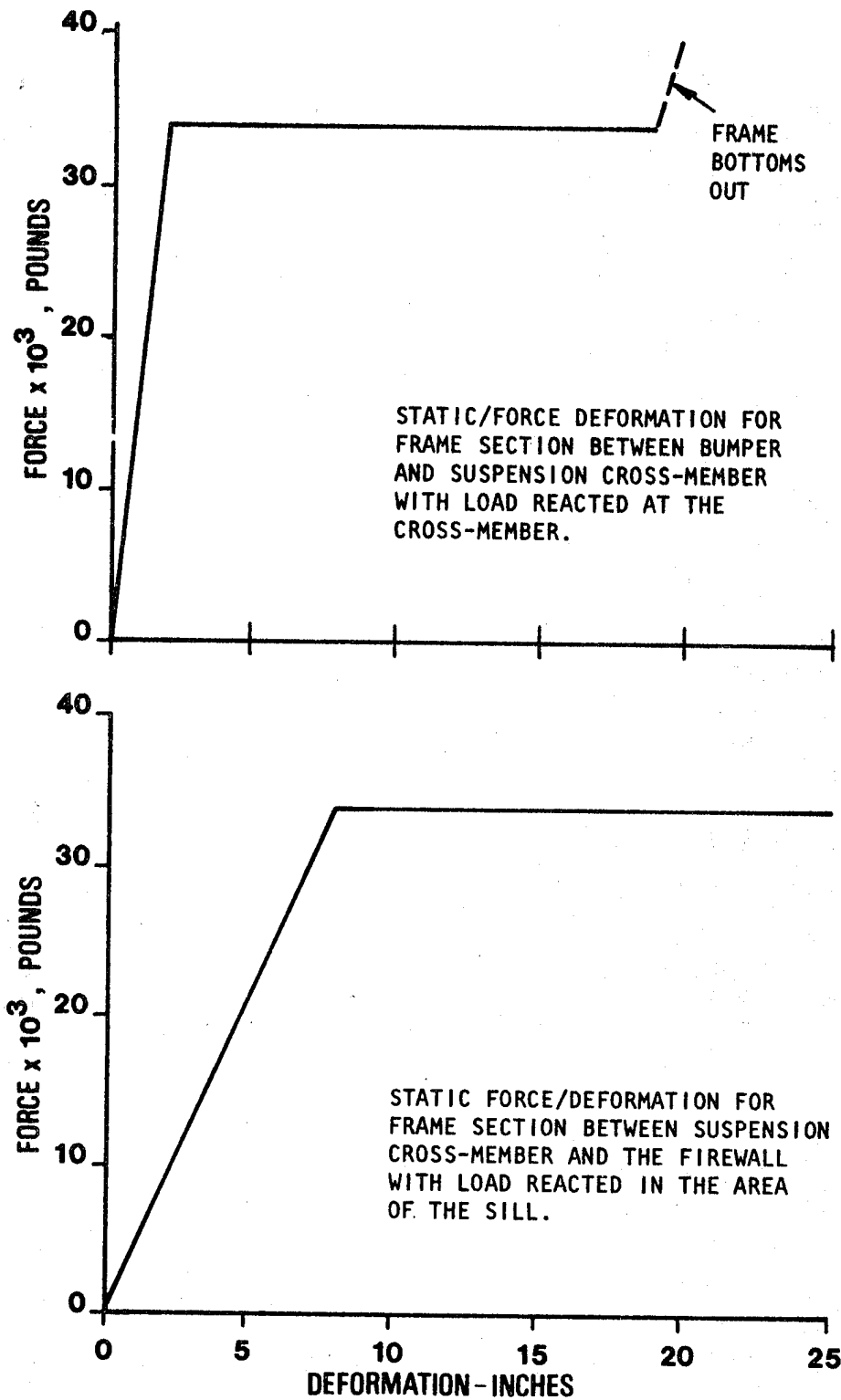
DEFORMATION - INCHES

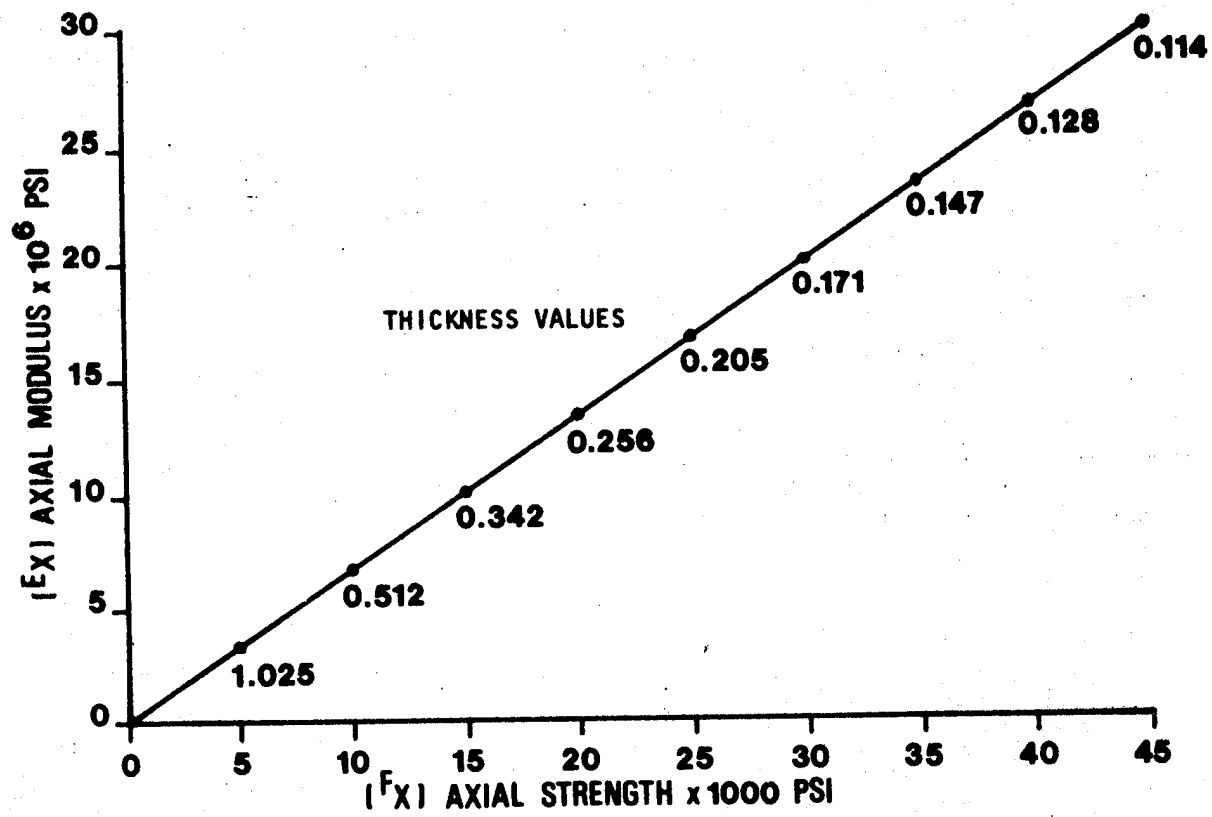**FIGURE 256   EI/FA DESIGN CURVE**

465

Figure 256 except for the very thick laminates which would not be acceptable.

The next effort involved evaluating a number of material combinations to see if they could be tailored to fit the design curve. While this approach does not necessarily insure the optimum design in terms of matching stiffness and strength at the minimum weight, it still should be at least close to it. Figure 257 gives the selected material combination, continuous HMS graphite at $\pm \theta$ layup angles and oriented short Kevlar fiber aligned at 0°. From Figure 257, $\pm$ 20 degrees for the HMS graphite yields the minimum frame weight while meeting the stiffness and load carrying requirements derived from the steel frame. The corresponding composite thickness was established to be 0.25 in. while the resulting composite torsional stiffness, GK, is approximately one half of the GK for the steel frame. If it was important to match GK then from Figure 257 another higher angle can be chosen for the HMS fibers which would cause a larger wall thickness and would result in a net increase in GK but still the axial stiffness and load carrying capability would match that of the steel. This would be one approach but to insure minimum weight, other material combinations should be checked.

With the selection of the composite material completed, the design of the front portion of the frame took the form of four (4) compression molded sections which are displayed in Figure 258. These sections are then bonded and riveted together.

The effort thus far has centered on the static, elastic response of a composite frame to match the elastic response of the baseline steel frame. The next effort involved modifying this basic 0.25 in. thick walled composite design to be able to absorb a required amount of energy. This was accomplished by selecting eight (8) sections of the steel beam and establishing the maximum steel stress at each section caused by the peak force of the imposed force/deformation curves of Figure 255. A corresponding composite thickness could then be calculated for this same applied load. To obtain a controlled collapse, however, the load was varied from 26,000 to 42,000 lbs. compared to the 34,000 lb. peak of Figure 255. The crushing is expected to be of a consecutive cell failure with the higher strain capable Kevlar holding the fractured cells together. The predicted force/deformation curves are shown in Figures 259 and 260. The failure mode assumed and the resulting force/deformation curve responses are only best guesses at present and there is no substantial justification to say that the dynamic (impact) response would be similar and testing is required to substantiate this estimate.

The weight for the composite redesigned portion of the frame is 66.93 lbs. which is approximately half the weight of 132.58 lbs. for the corresponding steel part. Of the 66.93 lbs. there are 48.11 lbs. of composite and 18.82 lbs. of steel members. The 18.82 lbs. consists of upper and lower control arms of 14.48 lbs., front

FIGURE 257   SELECTED MATERIAL FORMULATION
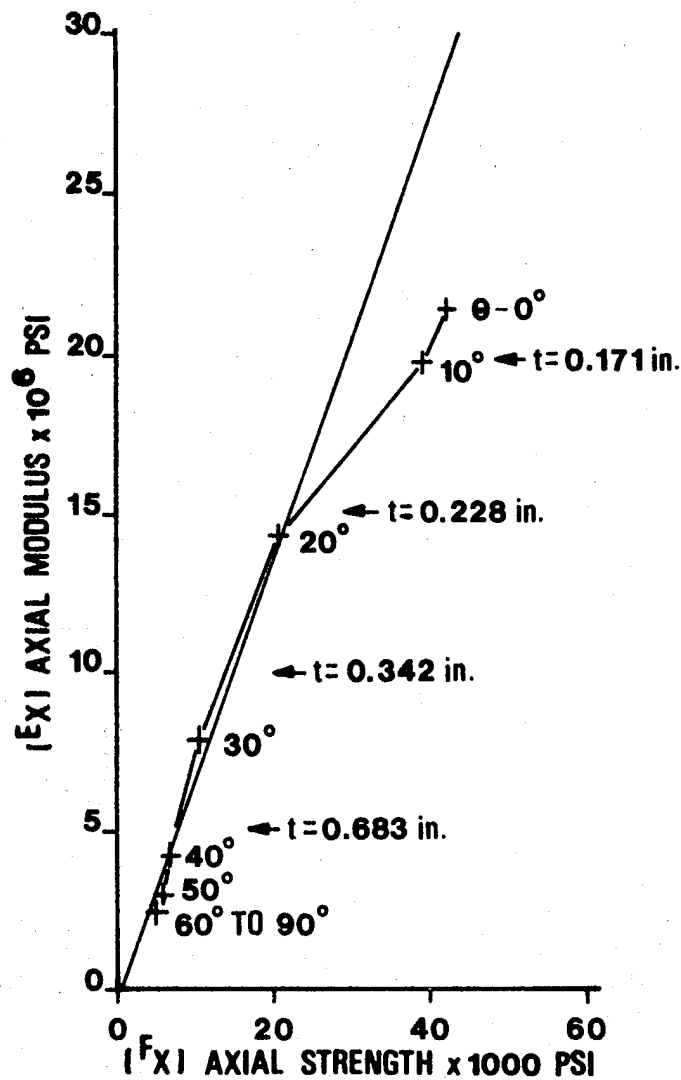
	HMS	KEVLAR
E_1	30×10^6 psi	4×10^6
E_2	1.5×10^6 psi	1×10^6
ν_{12}	0.28	0.30
G_{12}	0.8×10^6 psi	0.5×10^6
F_{1T}	100,000 psi	10,000 psi
F_{1c}	75,000 psi	8,000 psi
F_{2T}	3,000 psi	2,000 psi
F_{2c}	10,000 psi	2,000 psi
F_{12}	5,000 psi	2,000 psi
H_{1T}	.00333 in./in.	.00250 in./in.
H_{1c}	.00250 in./in.	.00200 in./in.
H_{2T}	.00200 in./in.	.00200 in./in.
H_{2c}	.00667 in./in.	.00200 in./in.
H_{12}	.00025 in./in.	.00400 in./in.
ρ	.05455 lb/in.^{3}	.04892 lb/in.^{3}

MATERIAL: A: HMS (CONTINUOUS)   LAY-UP: ($\pm\ \theta^A$, 0^B)

MATERIAL: B: SHORT KEVLAR FIBER
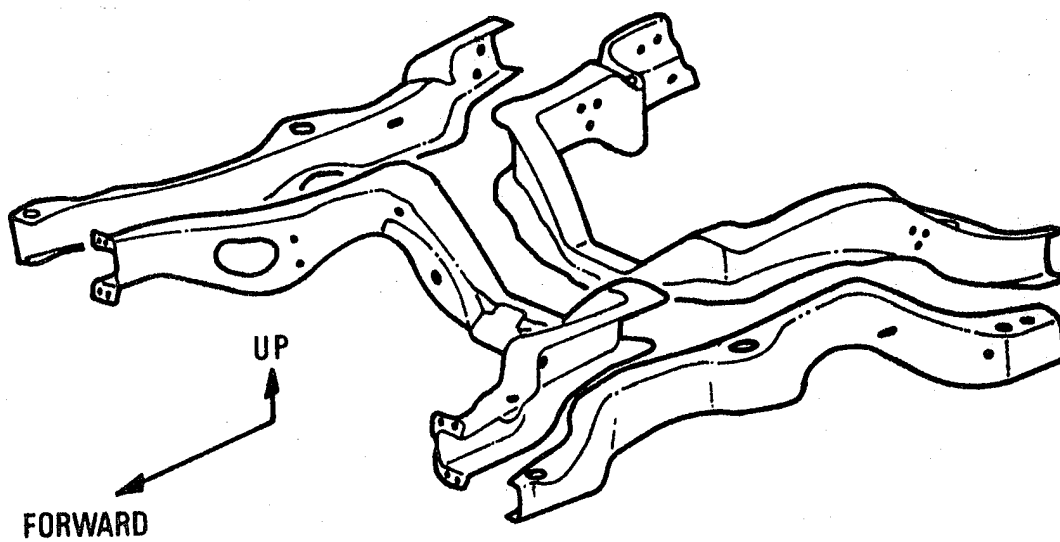
FIGURE 258   COMPOSITE DESIGNED FRAME (EXPLODED VIEW)

UP

FORWARD

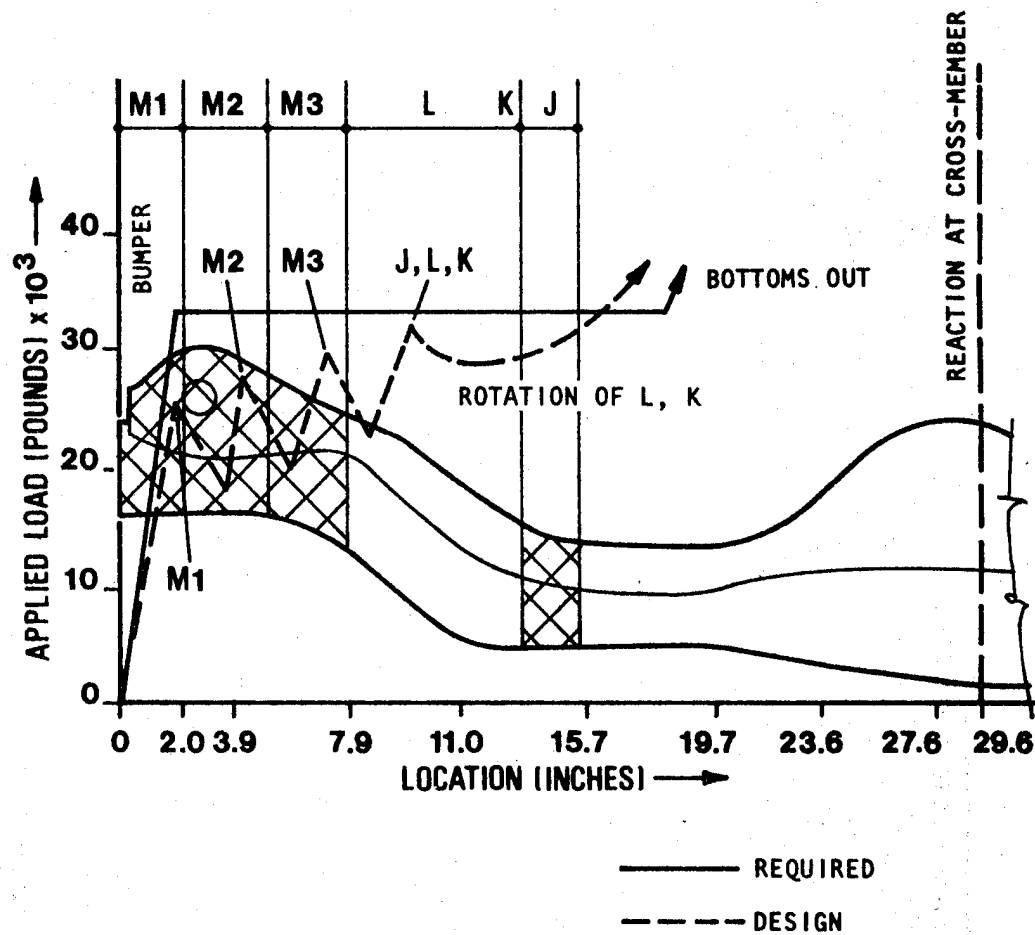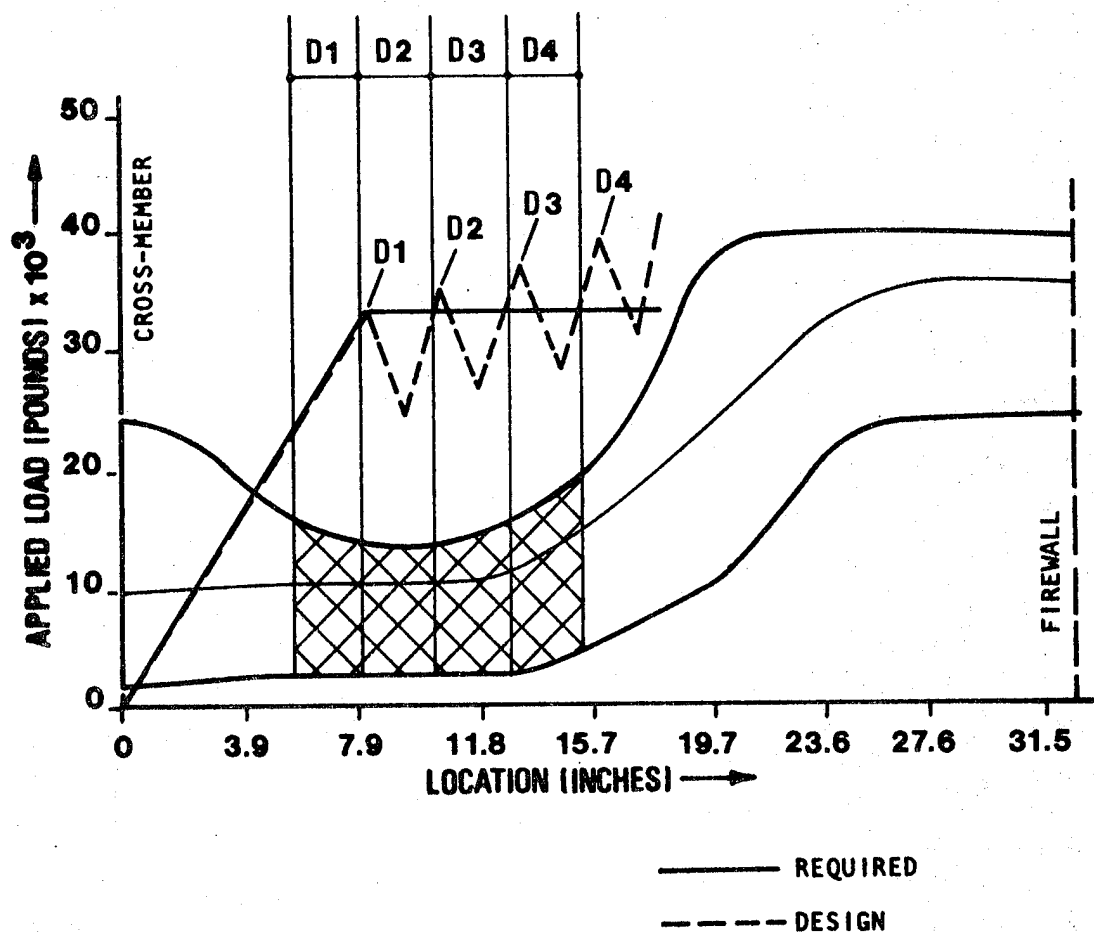**FIGURE 259**   **ENERGY ABSORBING CURVE FOR FORWARD AREA**

469

FIGURE 260   ENERGY ABSORBING CURVE FOR AFT AREA

470

cross-member skid plate of 2.65 lbs. and 1.69 lbs. of miscellaneous items. The approximate total energy required to manufacture the composite frame including the energy required to produce the component materials and a scrap factor is 3.66 x 10^6 Btu. These weights and required energies are for a composite frame which matches the axial stiffness and strength of the baseline steel frame but does not match the steel frames' torsional stiffness. If it did then the composite frame would in most probability have to gain material and hence weight so that some of the weight advantage over steel would be reduced.

It was estimated by Hercules, Inc. that for the 1985 time frame the total cost of the materials ($6.00/#) used in the fabrication of the composite frame portion would be $277.00. This includes a 2% scrap factor and a 1% line loss. For a production of from 2,000,000 to 5,000,000 million units the estimated labor per unit is 0.81 man/hours.

No effect of recycling the base material or of burning the discarded frame to derive energy was considered. In the case of scrap, some of the fiber is continuous and to maintain its strength and stiffness, it could not be reused. In terms of extracting energy by burning the composite material in a generating plant, there is hesitancy at this time to do this because of the potential problem of releasing graphite fiber which could short out electrical equipment. Hence the graphite frame was considered for burying at a cost of $1.41 per frame.

13.0 SUMMARY AND CONCLUSIONS

Candidate Materials

During the course of this investigation a most probable list of alternate candidate materials for future automotive structure has been examined. These materials were considered as groups of materials rather than individual compositions, such as: aluminum alloys and not 6061-T6. In some instances attention had to be focused on a particular alloy or composite formulation to show an effect or to report data.

Availability

A number of references were reviewed to determine if the raw ore or crude oil were available to provide the necessary quantities of mill product. The candidate materials selected were steels, plastics, aluminum alloys and fiber reinforced composites. Since the primary components of these candidate materials are iron, aluminum, silicon, oxygen and hydrocarbons and these components are the major constituents of the Earth's crust, it was concluded that there is no lack of raw materials. As the ore or crude hydrocarbons become less accessible, however, the energy and dollar cost of procurement will increase. Those materials requiring the least effort to obtain will be consumed first. To conserve energy, materials and possibly cost, conservation measures should be promoted at every instance. As an example, the use of alternate materials in automotive structure should be selected with the intent to recycle.

Mill Capacity

Refinery and mill capacity is marginal and will remain that way. The suppliers of ingot, bar or sheet will not provide capacity much greater than the current demand. New refinerys and mills require very large capital costs. Aluminum primary refining requires tremendous quantities of energy to reduce the oxides and the industry is in direct competition with all other business and residential demands on the supply of electric power. This one factor reduces the potential of aluminum applications in automotive structure.

Vehicle Designs

Passenger vehicles and light duty trucks and vans are currently body-on-frame or unibody construction. The candidate alternate materials can be used for all the components required to construct these structures, but each material has its advantages or disadvantages when compared to one another. The design criteria, material properties and packaging restraints must be reviewed for each case. Prior to a final material selection the safety, crashworthiness and durability in a service environment must also be considered. Manufacturing feasibility, material availability in the form desired and

472

a detailed cost analysis must then be completed to obtain a true evaluation of all materials. The material selection process is complex and may require several iterations before the process is complete.

State of the Art

Many alternate materials are currently being evaluated by the material suppliers, component suppliers to the automotive industry and the automobile producers themselves. These experiments and engineering studies are directed largely toward reducing vehicle weight and compliance with the Corporate Average Fuel Economy standards enacted by Congress.

Costs

Incorporation of the candidate alternate materials will in almost every case result in a vehicle cost increase. The direct material costs are the lowest with the existing material of construction, low carbon steel, and, of the suggested alternate materials, carbon (graphite) fiber reinforced plastic would result in the most expensive vehicle. The relative direct material costs are expected to remain at the same ratio in the future although carbon fiber prices could be reduced with increased production and aluminum prices may increase at a higher rate due to the intensive dependence on energy.

The direct labor costs to produce a vehicle are the lowest with low carbon steel and again are the highest for carbon fiber composites. Low carbon steel fabrication costs have the benefit of essentially sixty years of development. It is expected that the other materials will also benefit from an experience factor which will reduce but not eliminate the difference that is now found. Basic differences in properties would indicate that the candidate alternate materials will always be associated with a higher direct labor cost than low carbon steel.

CONCLUSIONS

1. Low carbon steel is and will remain the primary material of construction in future automotive structure based on the current cost projections. The use of HSLA steels will replace some applications of low carbon steel.

2. Vehicle first cost in dollars will increase, with the use of the candidate alternate materials.

3. Raw materials are available to permit the extensive application of aluminum alloys, HSLA steels, plastics, and glass or carbon fiber reinforced composites in future automotive structure.

4. Mill capacity is and will continue to remain marginal, on a supply-demand basis.

5. Vehicle durability comparable to that found with low carbon steel is achievable with the alternate materials with a weight reduction.

6. Crashworthiness, with reduced weight, can be maintained with alternate materials.

7. Front and rear end non-damageability can be improved with alternate materials, specifically elastomeric plastics, without a weight penalty.

8. Aluminum alloys and glass reinforced composites will continue to compete for hang on components. Aluminum alloys are more expensive but result in a greater weight reduction.

9. Plastics applications, as elastomeric materials, will increase for front and rear end non-damageable energy management up to 15 - 20 mph.

10. New process developments such as reaction injection molding (RIM) will increase plastics potential in exterior body panels where a combined weight reduction and cost effectiveness can be achieved.

11. New material developments in laminate or composite forms such as metal skin thermoplastic laminate and mixed fiber hybrid composites provide potential weight reductions at lower cost penalties, when combined with a steel space frame design.

474

14.0 RECOMMENDATIONS

Manufacturing Cost

Research and development effort should be continued or increased to reduce the manufacturing costs of applying alternate materials which will result in vehicle weight reduction. This includes simple detail programs as well as major efforts. Significant cost reductions could be achieved by:

a. Elimination of the cleaning costs and reduction of electrode costs during the resistance spot welding of aluminum alloys.

b. Reduction of the cycle time, and automatic press loading and unloading in the molding of fiber reinforced composites.

c. Development of automatic adhesive bonding of structural components at a rate comparable to resistance spot welding.

New manufacturing processes must be investigated to permit utilization of materials in a manner which exploits their best characteristics. The ability to press mold oriented fiber composites and obtain the desired orientation in the finished part would permit greater utilization of their high strength and stiffness. Similarily the ability to join dissimilar metals at high rates and obtain highly efficient joints would increase the designers ability to use lower density materials.

Material Properties

Additional effort should be assigned to the determination of material properties to permit utilization of alternate materials within a shorter time span. The utilization of equipment and personnel outside of the automotive and materials industries, such as universities, to develop statistical materials design data would reduce the time needed before a material is actually used.

Analysis

An improved knowledge of operating loads imposed on the vehicle and faster methods of modeling and analysis would permit a finer tuned vehicle and an expected lower weight. Finite element methods of analysis have made significant gains in recent years and further improvements would enhance vehicle structure performance.

Conservation

Effort should be directed toward the reduction of energy and dollar costs to produce primary metal products. A reduction in the secondary energy carrier, such as electricity, to refine aluminum ore would benefit all industries. This may not be feasible although the ability to use natural occuring minerals or chemicals in the refining process would be of considerable usefulness. Improved recycling of scrap metals and organic materials in all discarded wastes is another approach to the reduction of material and energy costs.

New Designs

New design concepts which will utilize existing material properties more fully should be sought. A particular design concept utilizing a steel space frame, with non structural closure panels, while not new, should be restudied in light of new low density aluminum alloys and plastic matrix materials, particularly for a van.

Crashworthiness

Tremendous progress has been obtained in the area of crashworthiness and safety and there is much more to be accomplished. Improvements in analysis and design techniques are required to reduce expensive test time and vehicle modifications which may not be beneficial to the passenger. A more complete knowledge of the energy absorption characteristics of alternate materials in vehicle configurations are required.

Health Hazard

Continuing investigations during the initial stages of material and manufacturing development must be maintained to identify and eliminate health hazards.